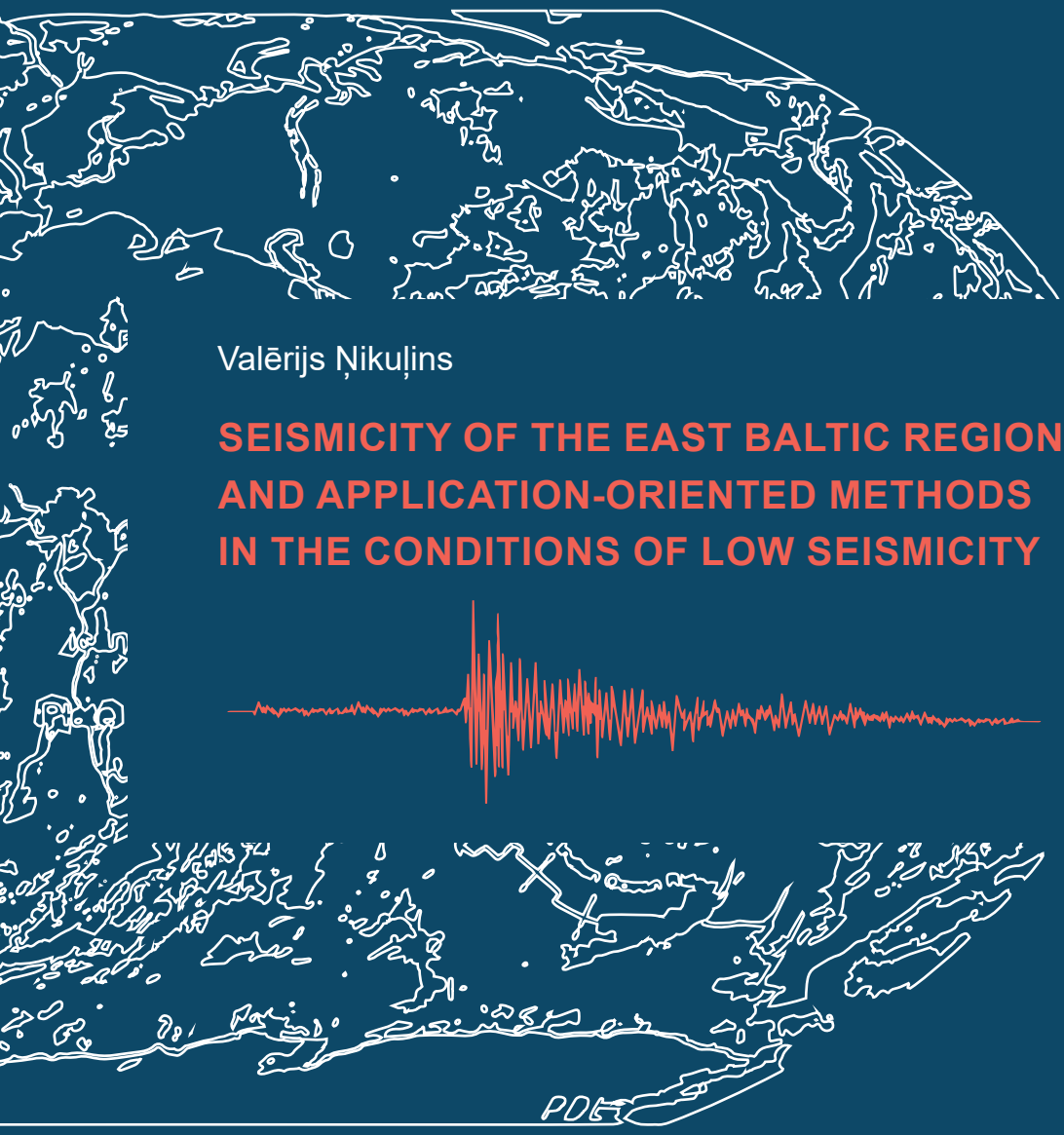

Valērijs Ņikuļins

SEISMICITY OF THE EAST BALTIC REGION AND APPLICATION-ORIENTED METHODS IN THE CONDITIONS OF LOW SEISMICITY

Valērijs Ņikuļins

SEISMICITY OF THE EAST BALTIC REGION AND APPLICATION-ORIENTED METHODS IN THE CONDITIONS OF LOW SEISMICITY

LU Akadēmiskais apgāds
2017

Ņikuļins Valērijs, 2017. *Seismicity of the East Baltic Region and application-oriented methods in the conditions of low seismicity.* Rīga: LU Akadēmiskais apgāds, pp. 292.

Monograph is dedicated to seismicity of the East Baltic region and its assessment. As the first study of its kind, it is published in English language to ensure accessibility of the facts and methodological solutions reflected in the book to the readership worldwide. Most of the factual material included in the study is published for the first time, and a particularly valuable contribution of the book includes the methodological techniques developed and approbated by the author for assessing seismicity of the territories. These are novelties that the author presents in a relatively simple language, providing explanations on the basis of traditional notions and seismic observation network data.
The book is intended for geologists and geophysicists, territorial planning specialists, builders, as well as other individuals, whom this edition will enable to become familiar with this specific knowledge regarding Latvia and its neighboring countries. This information is also important in extraction of mineral resources and planning thereof, where artificially induced seismic events are a factor with a significant environmental impact.

Monogrāfija ir veltīta Austrumbaltijas reģiona seismiskumam un tā novērtējumiem, tas ir pirmais šāds pētījums, tādēļ sagatavots angļu valodā, lai grāmatā atspoguļotais faktiskais materiāls un metodiskie risinājumi kļūtu pieejami plašam lasītāju lokam. Grāmatā ietvertā faktiskā materiāla lielākā daļa ir oriģināli un tiek publicēti pirmo reizi, un īpaši vērtīgu šo izdevumu izceļ autora paša izstrādātie un aprobētie metodiskie paņēmieni teritoriju seismiskuma izvērtēšanai. Tās ir novitātes, kuras autors pasniedz salīdzinoši vienkāršā valodā, skaidrojumus balstot uz tradicionāliem priekšstatiem un seismisko novērojumu tīklu datiem.
Grāmata paredzēta ģeologiem un ģeofiziķiem, tomēr vēl vairāk teritoriju plānotājiem, būvniekiem, kā arī citiem interesentiem, kam šādas zināšanas par Latviju un kaimiņzemēm ar šo izdevumu ir kļuvušas pieejamas. Svarīgi tas ir arī attiecībā uz derīgo izrakteņu ieguvi un tās plānošanu, kur mākslīgi ierosināti seismiskie notikumi ir nozīmīgs vidi ietekmējošs faktors.

Editor in Chief / Atbildīgais redaktors: *Dr. geol.* Valdis Segliņš

This publication was financially supported by the National Research Programme "ResProd" No. 2014.10-4/VPP-6/4.1 project "GEO"/ Izdevums tapis ar Valsts pētījumu programmas "ResProd" Nr. 2014.10-4/VPP-6/4 1. projekta "GEO" atbalstu.

Editor / Redaktore: Andra Damberga
Computer graphics and design / Datorgrafika un dizains: Paula Lore
Cover design / Vāka dizains: Paula Lore

ISBN 978-9934-18-300-3

CONTENT

The author expresses gratitude to the University of Latvia Vice-Rector, professor Valdis Seglins for the idea of writing this monograph, discussing its structure, and scientific management of the dissertation work, many sections of which have become a part of the monograph, Head of the project "GEO" of Latvian National Research Program "ResProd" Agnese Kukela for her organizational and technical support of the work.

In recognition of the former colleagues-seismologists, the author notes the contribution of Ukrainian and Russian seismologist Oleg Safronov, who participated in the creation of the first version of the Latvian seismic zoning of 1998, and Belarusian seismologist Alexander Boborykin, who after Bruno Doss continued the seismicity studies of the East Baltic region and prepared the corresponding catalogue of earthquakes.

The author also expresses his gratitude regarding Chief Scientific Officer of the Schmidt Institute of Physics of the Earth of the Russian Academy of Sciences, professor Andrey Nikonov, who greatly contributed to the seismic study of the East European Platform and the East-Baltic region, and also actualized and proposed solutions to a number of problematic macroseismic issues touched upon in the monograph.

INTRODUCTION

Traditionally, the purpose of seismology is to study earthquakes and the associated phenomena, which occur in earthquake-prone regions, where seismology is objectively an especially hot topic to ensure health and safety of people inhabiting those territories, as well as the safety of infrastructure, buildings, and structures located there.

In seismically quiet territories, like Archean and Proterozoic cratons, seismology, at the first sight, is nearly an exotic line of research. Until quite recently, seismic line of research did not look too relevant with respect to ancient Pre-Cambrian, Eastern European Craton (EEC), where the research territory – East Baltic Region (EBR) – is located. EBR occupies the north-western part of EEC including the southern slope of the Baltic Shield. EBR covers the East Baltic States – Estonia, Latvia, Lithuania, and the Kaliningrad Region of Russia. All of them occupy the territory of about 190.24 thousand km^2, with the total population of about 7.12 M. The studied territory is located within the following coordinates: 53.9°N – 59.7°N latitude, and 19.4°E – 29.6°E longitude.

In terms of seismic hazard, earthquakes taking place in EBR do not seem to be of any special interest, since the danger of their occurrence is highly unlikely. Little concern with seismology was related to a deep-rooted idea dating to XX century, according to which EBR is a non-seismic region, where no earthquakes actually take place. This was a typical insight in ancient platforms as territories with a "*state reposed in seismic terms*" [Рустанович, 1967].

However, the situation took a 180-degree turn with commencement of the Baltic Region's industrialization. Railways and industrial enterprises were built. At a later stage, the rate of industrialization did not subside, on the contrary, it stepped up at the expense of the development of hydropower engineering (in particular, Ķegums, Pļaviņas, Kaunas, Kroness, and Narva electric power plants) and nuclear power engineering (Ignalina); moreover, development of subsurface gas reservoirs (Inčukalns), as well as the burial disposal of hazardous waste, took place. All of those facilities had to be of reliable security, since the consequences of their possible damage and, all the more so – their destruction could bring about numerous human victims, inflict financial and physical damage, and have huge consequences and adverse effects on ecology.

Present-day earthquakes that took place on the island of Osmussaare (Estonia) in 1976 and the Kaliningrad Region of Russia in 2004 have become additional reasons making experts and the public change their views on EBR seismic safety precautions.

New data on the historical background of seismic intensity has appeared, attesting to the earthquakes that took place on EBR territory in 1616, 1670, 1821, 1857, 1881, etc.

The tremor intensity of historical and present-day earthquakes was rated as V– VII points according to MSK-64 scale. Moreover, new geological and geophysical data has been received, supported by results of seismotectonic, geodynamic, geological, geophysical and geodetic surveys which attested to the block structure of the Earth's crust, its dynamics, tectonic faults, and the availability of seismogenic areas. The accumulated data describing EBR seismic intensity had to be generalized, and some provisional results had to be summarized.

Human-induced impact can affect seismic activity quite seriously. It triggered the occurrence of new seismic phenomena – namely, the occurrence of induced earthquakes. Several man-caused factors for induced earthquakes have been known: 1) injection or extraction of technologically unfit waters or carbon dioxide CO_2 into wells; 2) changing water level in water-storage reservoirs; 3) coal mine and pit bounces; 4) hydrocarbon extraction and storage in underground natural "reservoirs"; 5) extraction of groundwaters; 6) production of geothermal energy; 7) reservoir hydraulic fracturing in process of shale gas production. With respect to EBR, the most relevant reasons for induced seismic activity can be factors 2, 4, and 5.

The man-induced factors certainly refers not only to platform territories. But, while human impact could not essentially affect the "reputation" of natural seismic activity, it is quite capable of competing with the latter on platform territories.

A comprehensive global analysis of all human-induced earthquakes [Foulger et al., 2017] shows that the leading role belongs to mining industry, which is associated with 37.4% of all cases of human-induced earthquakes.

The below-listed factors are rated next: water reservoir impoundment-induced earthquakes (23.3), conventional oil and gas production (15%), geothermal energy production (7.8%), waste fluid injection (5%), fracking (3.9%), nuclear explosion (3%), research experiments including geophysical surveys (1.8%), groundwater extraction (0.7%), carbon capture and storage (0.3%), and construction (0.3%).

Within the magnitude range from to induced earthquakes pertaining to the first two types of human-caused interference, i.e., those arising from mining industry and water reservoirs occur most frequently.

For example, with regard to the magnitude range some data is available describing 73 cases of mining-induced earthquakes and 67 cases of induced earthquakes caused by changing of water level in water reservoirs. [Foulger et al., 2017].

The development of energy engineering, especially, nuclear power engineering, on EBR territory, is the reason why focus more on seismicity problems and seismotectonic hazard, since some large atomic nuclear power plants such as Ignalina NPP and Leningrad NPP are located on the territory of EBR. Moreover, construction of at least two more NPP and the Baltic NPP in the Neman district of the Kaliningrad Region of Russia, as well as Belorussian NPP in the Ostrovets district of Belarus is scheduled.

Besides, construction of a new modern NPP by Lithuania, Latvia, Estonia, and Poland on the old site by 2018 is scheduled [*http://ru.euronews.com/2009/12/31/lithuania-to-close-its-only-nuclear-power-station*] – although this project will hardly ever be implemented.

Nuclear power plants are the most serious and susceptible industrial and ecologically hazardous facilities that require close attention, a comprehensive justification of the choice of construction site at the design and control stage, including the assessment of seismic hazard during the operation phase. Any damage inflicted on NPP entails unpredictable environmental disasters and huge material losses, not to mention the death of people. It was shown by the sad experience of Chernobyl in 1986 and Fukushima in 2008.

IAEA poses strict requirements to seismic safety – not only to NPP being designed but those already existing. Some special IAEA standards – for example, a safety guide titled "*Evaluation of seismic safety for the existing nuclear installation*" [Safety Guide No. NS-G-2.13] – claim for the assessment of seismic risk.

One of the provisions of this document (namely, paragraph 2.10) states that seismic safety assessment should be carried out if at least one of the following conditions exists: if an earthquake more than the projected earthquake can occur in the area of the nuclear power plant, or if new data appears attesting to the presence of seismogenic structures recently identified by seismological networks, or, in connection with the occurrence of earthquakes that affect the operation of nuclear power plants.

It is quite obvious that no new data can be obtained without carrying out seismological monitoring and special surveys in the field of geodynamics and seismotectonics. Taking IAEA requirements into consideration, an alarm system warning about an impending earthquake was developed around Ignalina NPP in 2000 [Wieland et al., 2000].

The possibility of the occurrence of induced earthquakes is not a single problem faced in process of investigation of seismicity on any territory. Another problem is connected with the investigation of historic seismicity. Historic seismicity research provides a new information on historic earthquakes; as a result of reassessment of their parameters (epicenter coordinates, earthquake center depth and tremor intensity), or, on the contrary, they make one exclude some seismic events from the category of tectonic earthquakes. With regard to EBR, in particular, the reasons for carrying out such reassessments are quite sufficient already [Никонов, 2013]. The data obtained within the instrumental observation period should also be reassessed – starting from the middle of the sixties of XX century. The point is that, due to the absence of a regional seismic network in EBR, the data from Scandinavian seismic networks was used. In this case however, some errors are possible, when identifying the genesis of seismic events.

A typical example of the underestimation of seismotectonic conditions in EBR is the current situation in the region of Pļaviņas impoundment. The construction of Pļaviņas hydroelectric power plant took place in 1961–1966. The studies by the agency (*Hydrostroy*) responsible for the construction of water power plants did not provide the assessment of geodynamic conditions of HPP surroundings. Only in process of construction, in 1962, investigations of crustal movements by using the method of high-precision levelling were initiated on a test site in the area of Pļaviņas impoundment.

The task posed was to study the character and the differentiation degree of the emerging present-day crustal movements and to identify the possibility of exercising an impact on these movements made by the additional load of the impoundment [Аболтыньш, 1969_*upm*; Аболтыньш, 1971_*upm*].

The leveling results for the period from 1963 to 1965/1966 only permitted to mark the tendency towards multidirectional shifts of the benchmarks located in the south-eastern and the north-eastern parts of the site. By the beginning of the 1970s, it became clear that the present-day movements recorded on the territory of the Pļaviņas test site are of differential character expressed in short-period oscillations.

It was stated that the change in the direction of present-day movements (semi-period) is 2–3 years, whereas the full period of oscillations is measured by the interval of up to 5–6 years [Аболтыньш, 1971_*upm*].

As a result, the research of present-day vertical crustal movements has allowed to discover the prerequisites for the existence of geodynamic adversity in the area of Pļaviņas HPP. Subsequently, those prerequisites were confirmed in process of analyzing the historic seismicity. In particular, according to remarks by B. Doss [Doss, 1909], historical earthquakes with epicentral intensity took place in the Koknese district in February, 1821 [Авотиня и др., 1988].

Only 15 years after the Pļaviņas HPP was commissioned, the Aizkraukle and the Piebalga tectonic faults forming graben structure were discovered in the impoundment area as a result of exploration works carried out to select spots for the disposal of non-cleanable industrial waste [Бебриш et al, 1985_*upm*]. It indicates that the hydroelectric dam of the Pļaviņas HPP was built exactly on the keystone fault discovered. At the same time, the Piebalga fault extends in the vicinity of the dam proper, while the Aizkraukle fault crosses the impoundment. The vertical displacement amplitude of the two fault edges relative to the crystalline basement surface reaches 50 m [Brangulis & Kanev, 2002].

The aforementioned example makes it clear that the geodynamic environment even on the territory of ancient platforms is far from "rosy" as it had been presented before. Seismotectonic and geodetic methods have allowed to discover features of geodynamic activity, namely: the availability of tectonic faults, short-period crustal pulsations, and historic earthquake focuses. As a result of neglecting the necessity of geodynamic investigations to be carried out within the framework of the front end engineering design works, Pļaviņas HPP was built into the zone of geodynamic risk. This was manifested by some adverse supergene processes associated with underwashing (suffosion).

An impetus to heighten seismologists' interest in EBR seismicity was the *Osmussaare* earthquake of magnitude 4.7 that took place on October 25, 1976. In terms of the possibility of earthquakes occurrence in EBR, the plot thickened even more when the Kaliningrad earthquakes took place on September 21, 2004, with the strongest shock magnitude 5.2 [Gregersen et al., 2007] and – VI ½ shock level in epicentral area [Nikonov et al., 2005] according to *EMS-98* scale.

Those earthquakes were so unexpected to seismologists, geologists, and geoscientists that the fact of their occurrence was even reflected in the title of a fundamental publication prepared by a working group based on scientific research of a large territory of the Baltic Sea States. It was given the following title: "*The exceptional earthquakes in Kaliningrad district, Russia on September 21, 2004*" [Gregersen et al., 2007].

Analysis of historical data for EBR territory showed that historical earthquakes not only did occur in the Baltic countries, but some of them even caused damage to the

walls and roofs of houses, and brought about cracks in the soil and stone walls [Doss, 1909]. The intensity of the strongest historical earthquakes was estimated as VI and even VII on the MSK-64 scale.

Thus, it is quite obvious that at first the *Osmussaare* and then the *Kaliningrad* earthquakes served as a powerful impetus to promote the development of seismic research in EBR, including the creation of a seismic stations network and the assessment of seismic hazard.

Therefore, the tasks of the monograph include the integration of the accumulated results of seismicity studies from the historical time to the present, the consideration of a number of methodological issues accompanying the conduct of these studies, as well as integration of geological, geophysical and geodetic data that may serve as prerequisites for seismicity. The author who has more than 20-year experience in carrying out seismologic studies in Latvia and EBR has used both his own research findings, as well as the results obtained by seismologists, geoscientists, and geologists of EBR and other regions with a stable continental crust.

Many processes running in the Earth's crust interior, as well as the process of laying the groundwork for the manifestation of seismicity may be understood better, if we compare the target of research with some other "exemplary", better-investigated objects.

Therefore, by way of comparison, North American lithospheric plate was chosen as an exemplary region. This was done for a few reasons. Firstly, the central place on the plate is occupied by North American craton (NAC), which has a stable continental crust; the structure is similar to East European craton (EEC) by formation and geological history.

Secondly, NAC and EEC in the Pleistocene have repeatedly undergone glaciation processes, alternating with interglacial epochs. During the Holocene isostatic equilibrium-leveling processes affected both cratons and played an important role in the geodynamics of the crust of both cratons.

Thirdly, the detail and the completeness of seismological and other geological studies with respect to NAC by far exceed any similar studies in territories of other platforms.

The end result of earthquake seismology is the information describing the place, magnitude, and periodicity of seismic impact – i.e., General Seismic Zoning Maps (GSZ) for large territories on a national scale, and seismic micro-zoning maps (SMZ) for agglomerations, individual local territories or sites used for construction of residential real estate properties, industrial and support facilities. Such maps provide information describing the specific spot where earthquakes may take place, and the degree of possibility, periodicity, and intensity of potential tectonic earthquakes. Furthermore, such maps allow one to minimize the risk of earthquakes by taking into account those recommendations in process of design of buildings and structures, or, when taking security measures to safeguard the already existing objects. Therefore, the review covers both the GSZ method and the newly appraised SMZ method that was tried on EBR territory just a short time ago. The timeliness of SMZ has enhanced significantly after the Kaliningrad earthquakes of 2004 and the plans for NPP construction in the Kaliningrad Region of Russia and in Belarus.

In the monograph considerable attention was paid to the issues related to identification of the genesis of seismic events. The point is that, with a low level of

natural seismicity associated with tectonic stresses materialization in the Earth's crust, there exist a large number of stationary, human-induced seismic sources in EBR.

Basically, those sources are associated with the extraction of mineral resources for building industry (gypsum, dolomite, and limestone) and for power industry (oil shale).

Mineral resources are extracted mainly in open quarries by an explosive method. In addition to stationary, human-made sources, there are a number of non-stationary sources, mainly in the Baltic Sea area. These sources are connected either with naval activities aimed at UXO clearance of the Baltic Sea to get rid of explosive objects left after World War II or even WW I, or, to geophysical work carried out in the Baltic Sea.

Some problems are faced in EBR, associated with the detecting of seismic events against the interference background and with the identification of genesis of seismic events.

These problems are associated with the fact that most of the human-induced events have a small magnitude, while the distance between EBR seismic stations is large and the seismic background noise is sufficiently high. Therefore, examples of the identification of the genesis of seismic events are considered based both on the results of our own and on the experience of other researchers, by applying new identification methods.

This line of research is as important as the revision of materials dedicated to historical EBR earthquakes, since, in both cases, errors may be made when identifying the genesis of a seismic event. Errors of that kind may essentially affect the results of seismic zoning, since false, pseudo-tectonic earthquakes may get into the earthquake catalogue. It is especially important with respect to historical earthquakes. Their number in EBR is quite small, but nevertheless they make for a significant value. Consequently, each pseudo-earthquake that erroneously got into the earthquake catalogue may distort the true picture.

However, the goal of the monograph goes beyond the issues of classic seismology, i.e., study of earthquakes and the phenomena associated therewith and the identification of the genesis of seismic events.

If we consider seismology in a broader sense, we can regard it as a source of information on the Earth structures including, in particular, the deep structure of the Earth. By using arrival times, amplitudes, and polarization of waves of different kinds (reflection and refracted signals), it can identify the Earth structures connected with their geologic composition [Astiz et al., 1996; Shearer, 2009]. Different-scale levels of seismological studies furnish researchers with valuable information both on the deep structure of the Earth and the near-surface structure thereof. In the first case it gives one an opportunity of a better understanding of the geodynamics of the inner part of the Earth, while in the second case it enables one to solve application geotechnical tasks and the tasks for civil engineering.

A considerable part of the monograph is focused on applied approaches used in seismology for civil engineering purposes (seismic soil properties, structural monitoring) and environmental protection measures (level of vibration emanating from human-induced sources, and identification of sources of surface waves).

At that, the methods considered can be applied not only in seismically active regions, but also in the regions like EBR featuring weak seismicity.

The main methods are based on ambient seismic noise (ASN). ASN consists of both natural microseisms, the main part of which consists of surface waves of Rayleigh and

Love, as well as of human-induced microseisms, or the so-called seismic tremor, the bulk of which is composed by body waves.

We have to emphasize two important advantages of the methods based on using seismic noise. Firstly, those are passive methods which do not claim for seismic signal generation but make use of natural or human-induced seismic noises. This allows to apply them in the context of agglomerations as environmentally-friendly methods.

Secondly, operational responsiveness and cost efficiency are among advantages of those methods, since test duration can be very short (up to 30 minutes per a measurement), while the material and financial investigation costs are relatively low.

Until recently, a factor hampering the development of methods based on investigation of ASN parameters has been lack of a number of conditions that are objectively necessary. Those conditions were connected with the availability of hardware, methodological and computational capabilities. Such capabilities appeared only recently. This enabled recording of new kinds of seismic signals received by continuous seismic data sets.

Thus, it became possible to study weak changes in the medium, to recognize very weak seismic sources among ASN. In fact, a new trend – ecological seismology – has emerged [Larose et al., 2015]. The subject matter of this direction is natural seismic vibrations, which are triggered by processes that occur either outside the solid Earth (cryosphere, hydrosphere, atmosphere and space), or due to changes in external parameters (temperature, hydrological regime), or, through human activity (man-made factors).

There emerges a possibility to study propagation of waves in solid Earth, caused by processes running in ambient medium (hydro-meteorological phenomena, temperature changes, and erosion processes), as well as studying natural seismic sources associated with external atmospheric phenomena (wind, storms) and hydrosphere (river noise, sea noise etc.)

Using ASN makes it possible to check human-induced perturbations in the medium (those caused by oil, gas, and geothermal energy production, extraction of natural resources, and urbanization processes), or check perturbations caused by changes in environmental parameters (hydrologic and temperature ones). Such investigations allow to obtain more information on ecological processes and to recognize the impact on ASN seismic wave parameters made by various environmental factors.

Among the examples are the state of tectonic stress, changes in rheology, fracturing, etc. At the same time, the whole set of signal characteristics, wave polarization, amplitude, and duration is used. These features help identify sources of ASN. Obtaining new knowledge about seismic sources helps to understand physical processes in a variety of natural objects.

From the viewpoint of applied methods, the target of research is geologic environment and the processes running therein, while the subject of applied research is seismic noise and its typical parameters, the study of which gives an opportunity of acquiring knowledge on the target of research.

The new line of research extends the potential of seismological method, which has currently obtained a "second wind". This monograph is a contribution to implementation and development of new seismological methods on the territory of the East Baltic Region.

1. EARTH'S SEISMICITY AND ITS CAUSES

1.1. Depth tectonic structure of Earth and geodynamic preconditions of seismicity

Seismic activity of the Earth is closely related to peculiar features of its deep geotectonic structure, the divisibility of the Earth's outer layers into constituent parts, i.e. into lithospheric plates, the type of boundaries between the lithospheric plates (*divergent* and *convergent*) and the nature of interaction between the lithospheric plates, i.e. geodynamic conditions. Thus, prior to considering the seismicity of the Earth, it becomes necessary to briefly characterize the main features of its geotectonic structure, which determine the preconditions of seismicity.

The lithosphere is the outer, solid part of the Earth. It consists of a solid crust and the upper part of the mantle up to the asthenosphere (Figure 1). In the asthenosphere, the velocities of seismic waves decrease, which witnesses a change in the physical mechanical properties, in particular, changes in ductility. The lithosphere has an average thickness of about 100 km. Its thickness depends on the age. The greater the age, the thicker the lithosphere.

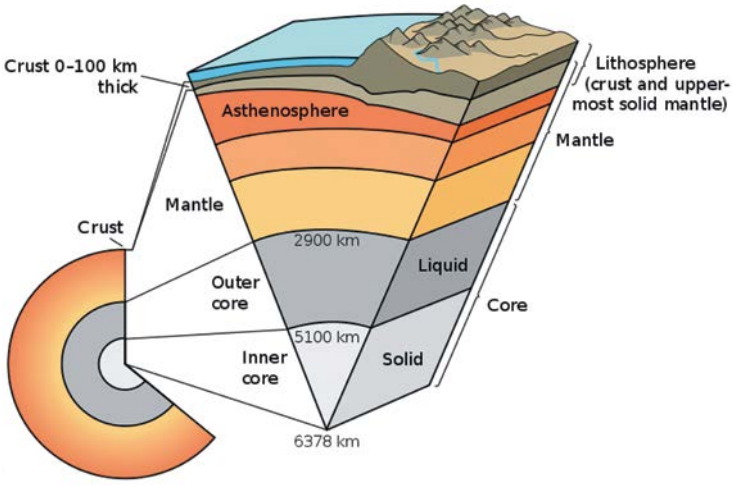

Figure 1. Internal structure of the Earth's interior

[*Wikipedia, https://upload.wikimedia.org/wikipedia/commons/thumb/8/8a/Earth-cutaway-schematic-english.svg/800px-Earth-cutaway-schematic-english.svg.png*]

In the lithosphere, the mobile areas (folded belts) and relatively stable platforms are distinguished. The lithosphere is sufficiently fragile, which is favorable for the occurrence of origins of tectonic earthquakes. This situation is typical, for example, to the subduction oceanic crust. The lithosphere is not monolithic, but fragmented and consists of separate lithospheric plates of different sizes (Figure 2). The lithospheric plates particularly play a leading role in geodynamic processes that manifest themselves on the surface of the Earth and in the upper part of the Earth's crust, and determine the degree of seismic activity.

The dynamics of lithospheric plates is considered within the framework of the theory of plate tectonics. This theory is related to the idea of movement of lithospheric blocks, which was first expressed by Alfred Lothar Wegener in the 1920s. From the very beginning of its emergence, it has not received general recognition. In the 1960s, as a result of studies of the relief and geology of the ocean floor, data was obtained that evidenced the processes of expansion (*spreading*) of the oceanic crust and immersion of some parts of the crust under the others (*subduction*). These discoveries served as the basis for appearance of the generally accepted concept of plate movement.

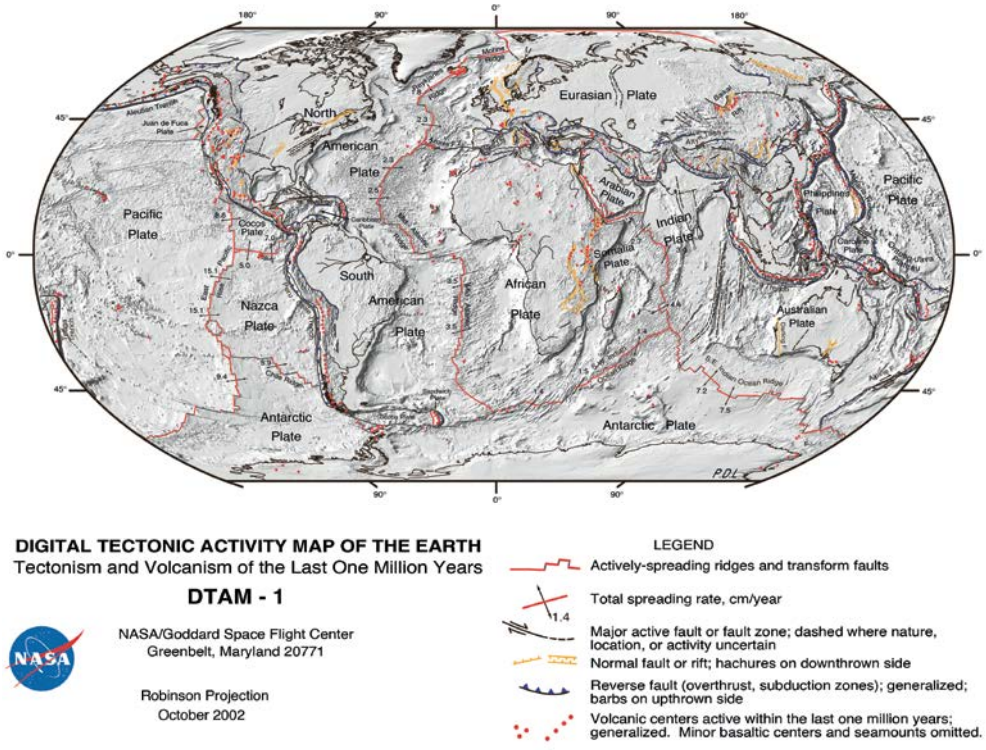

Figure 2. Digital map of tectonic activity of the Earth

[*Lowman P., Yates J, NASA Goddard Space Flight Center https://visibleearth.nasa.gov/view.php?id=88415*]

From the standpoint of plate tectonics, the Earth's crust consists of blocks being relatively integral – i.e., individual lithospheric plates that are located on a less viscous and hotter asthenosphere. Only the upper part of the entire volume of the Earth, that is, the lithospheric plates retain their rigidity on a scale of geological time, about 10^9 years. Geological rocks located beneath the lithospheric plates have a higher temperature, and therefore a solid creep process may occur there. The impact of external forces (convection currents) underlying the lithosphere leads to the event that the rocks "flow" on a scale of geological time. The temperature in the base of the lithosphere is approximately 1600 K (~ 1300°C). This is the temperature of transition to the solid state. Therefore, geological rocks located above this *isotherm* are rather cold and manifest themselves as a rigid material. Thus, the lithosphere can be defined as a part of the upper mantle enclosed between the Earth's surface and the isotherm with a certain temperature value. The greater the age of the lithosphere, the deeper this isotherm is located. The lithosphere thickness increases with the distance from the mid-oceanic ridge (Figure 3). At the same time, the cooling time of the lithospheric plate increases, as well.

The lithospheric plates are in continuous motion in relation to each other. They bend at the boundaries of the plates. The rigidity of the plates allows the transmission of elastic stresses over a long geological time. In fact, the plates are conductors of tectonic stresses. These stresses are transferred to the internal parts of the plate. This property of the plates is important as a driving mechanism of the plate tectonics. However, only the upper, the so-called elastic part of the lithosphere is sufficiently rigid, where the elastic stresses do not relax during time intervals of about 10^9 years [Turcotte & Schubert, 1985].

Horizontal displacement of tectonic plates is carried out due to the mantle thermos-gravitational flows, *convection*. The temperature difference between the inner regions of the Earth, which are heated to a very high temperature (the Earth's core temperature is about 5000°C), and temperature on the surface of the Earth creates the conditions for the occurrence of convective motion. The mechanism of convective motions is that the geological rocks heated in the depths of the Earth expand, their density decreases and they float, while cold and therefore heavier geological rocks are lowered. Thus, there is a transfer of heat (a consequence of the emergence of light-hot masses and immersion of heavy, colder masses), which goes on continuously, as a result of which the convective currents arise. Convective currents are closed by themselves. As a result

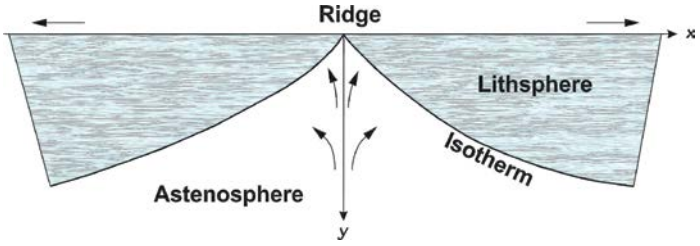

Figure 3. Scheme of separation of oceanic lithosphere

of self-regulation, they form stable convective cells, the flow direction in which is consistent with the directions of flows in neighbouring cells. In the upper part of the cell, the flow of substance takes place almost in the horizontal plane. This part of the flow carries the plates in horizontal direction with enormous force due to huge viscosity of the mantle substance.

In accordance with the concept of the plate tectonics, different types of interaction can exist on the plate contacts (Figure 4). In the expansion areas (mid-oceanic ridges and continental rifts), a new oceanic crust forms as a result of spreading ("*spreading*" of the seabed) and rifting (expansion of continental rifts). In subduction areas, the old oceanic crust is absorbed.

Areas of spreading of the ocean floor play an important role in geodynamics. The idea of the ocean floor expanding was proposed by Robert Sinclair Dietz [Dietz, 1961]. This allowed him, together with Harry Hammond Hess in 1962–1963 to put forward the hypothesis of spreading. According to this hypothesis, the mantle material, moving at a speed of 1 cm/year, is carried out under the mid-oceanic ridges due to the ascending branches of the convection cells. With a periodicity of 300–400 years, the ocean floor is renewed in the axial part of the ridges. The lithospheric plates move along the asthenosphere due to the high viscosity of mantle, convection currents.

The formation (spreading) and absorption (subduction) of the Earth's crust are confined to the boundaries of the lithospheric plates that move relative to each other. It is just at the boundaries of the lithospheric plates where an active geodynamic situation exists, the main seismically active zones are concentrated (Figure 2) and the strongest

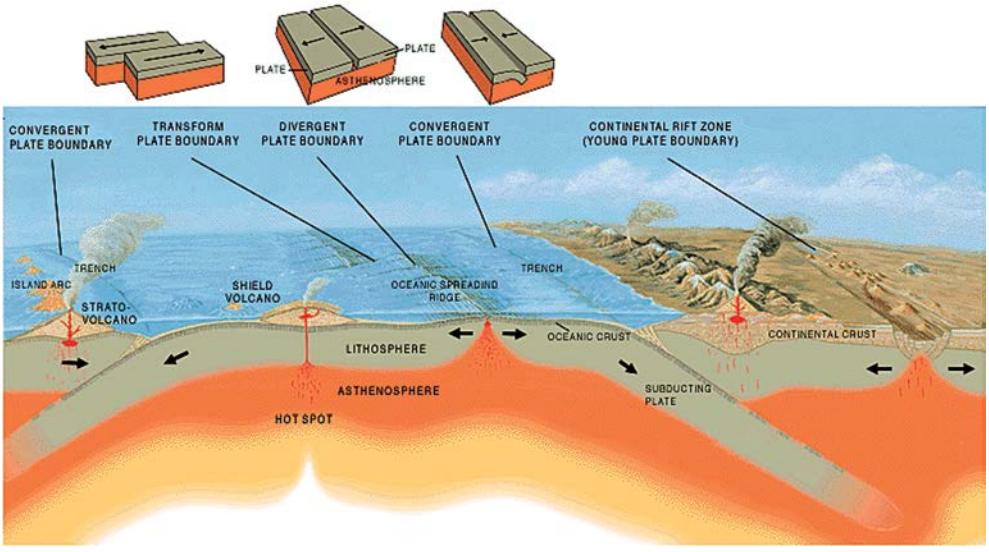

Figure 4. Classification of geotectonic processes according to the concept of plate tectonics

[*Vigil J.F., 1997_si. A cross section illustrating the main types of plates boundaries. https://pubs.usgs.gov/gip/earthq1/plate.html*]

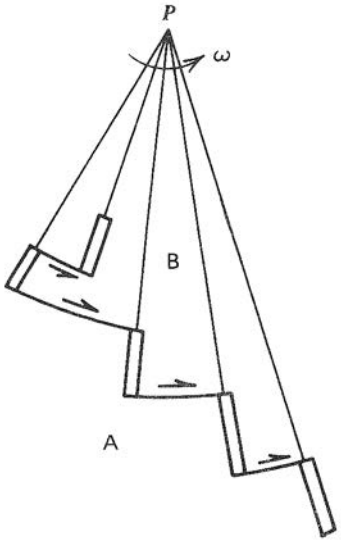

Figure 5. Counter-clockwise movement of plate B in relation to plate A

[Turcotte & Schubert, 1985]

Note: double lines are segments of the ridge; the arrows show the direction of movement on the transform faults

tectonic earthquakes occur (Figure 14). At present, more than 90% of the Earth's surface is covered by 8 largest lithospheric plates: Australian, Antarctic, African, Eurasian, Hindustan, Pacific, North American and South American (Figure 2). The geodynamic situation differs significantly at the boundaries of different lithospheric plates. This can be seen from the position of the rotation pole and the angular velocities of relative motion of adjacent surface plates.

The motion of the plate is a rotation with angular velocity ω relative to the pole of rotation P (Figure 5). The motion of two adjacent, rigid lithospheric plates can be characterized relying on Euler theorem. It says that any "straight line" (a section of an arc of a large circle) drawn on a sphere can be translated into any other, given position and determine the orientation on this sphere by rotating the straight line to a certain angle around the correspondingly chosen axis that passes through the center of the sphere. The plate can be moved over the sphere to any new position by rotating about an axis, which is uniquely determined by the initial and final position of the plate. The point of intersection of such axis with the Earth's surface is called the rotation pole [Turcotte & Schubert, 1985]. In Figure 5, individual segments of the ridge are located on the "meridians" that pass through the pole of rotation P while the transform faults are located on the "parallels" with the center in the pole of rotation.

Thus, the relative motion of two adjacent plates is completely determined by the coordinates of the rotation pole and the angular velocity of rotation ω. These parameters determine the active geodynamics. According to calculations based on the orientation of the ridge crests, band magnetic anomalies and transform faults, and also according

to the spreading rates determined from the width of the band magnetic anomalies and judged from the condition of the invariance of the Earth's surface area, these parameters were obtained (Table 1).

Table 1.

Position of rotation pole and angular velocities of relative motion of adjacent surface plates [Minster & Jordan, 1978]

Plates	Degrees north latitude	Degrees east longitude	ω, degree/million years
African – Eurasian	25.2	–21.2	0.10
Eurasian – North American	65.8	132.4	0.23
Indian – Eurasian	19.7	38.5	0.70
Eurasian – Pacific	60.8	–78.9	0.98
Indian – Pacific	60.7	–5.8	1.25
Cocos – North American	29.8	–121.3	1.49
Nazca – Pacific	56.6	–87.9	1.54
Cocos – Caribbean	23.6	–115.5	1.54
Cocos – Pacific	38.7	–107.4	2.21

The first of these plates rotates counter-clockwise relative to the second plate. The table shows how much the geodynamic activity, expressed in terms of the angular velocities ω of the relative motion with the participation of the Eurasian plate, is less than the corresponding angular velocities of the most geodynamically active boundaries of other plates.

Summing up the concept of plate tectonics, its main provisions can be formulated as follows:

1. The upper part of the Earth's surface is covered with a lithospheric layer, which is divided into fragile and plastic parts, i.e. the lithosphere and the asthenosphere. Lithospheric plates are considered as solid bodies.
2. The lithospheric plates move relative to each other. Motion of lithospheric plates can be represented as a rotation around the center of rotation of the lithospheric plate. The motion of the lithospheric plates is subject to Euler rotation theorem, which asserts that any motion of a solid body in three-dimensional space having a fixed point is a rotation of the body around some axis.
3. The main reason for motion of lithospheric plates is convection in the asthenosphere.
4. The entire lithospheric layer is divided into 8 large lithospheric plates, dozens of medium and many small lithospheric plates. Small lithospheric plates are located in buffer areas between large plates. There are the following large lithospheric plates: Australian, Antarctic, African, Eurasian, Hindustan, Pacific, North American and South American. Medium-size plates include Arabian, Cocos and Juan de Fuca.

5. Seismic, tectonic and volcanic activity is concentrated on plate boundaries.
6. There are three main types of relative displacements of lithospheric plates: 6.1) divergence, manifested in the form of rifting and spreading, 6.2) convergence, expressed as subduction and collision, 6.3) shear displacements along transform geological faults.
7. Spreading in the oceans is compensated by subduction and collision at their periphery. The radius and volume of the Earth remain constant.
8. The displacement of lithospheric plates is due to that they are captured by mantle convective currents caused by heat-gravitational flows. The temperature difference between the central parts of the Earth's interior and its surface is the source of energy of these mantle flows. The mantle mass heated in the central part of the Earth's interior expands and its density decreases, therefore it floats up. The colder and heavier masses of the Earth's interior plunge down. There takes place a process of heat transfer, which goes on continuously. As a result, the convective currents arise. These flows or circular currents are closed to themselves, forming stable convective cells. It is characteristic that in the upper part of the cell the movement of the mantle substance flow occurs almost in the horizontal plane. Just in this section the lithospheric plates are moved due to adhesion to the mantle substance having a huge viscosity.

The consequences of the dynamics of lithospheric plates are earthquakes, volcanic activity and mountain building. The bulk of dynamic processes of lithospheric plates is confined to their boundaries. This is the so-called interplate seismicity. Thus, the most dangerous seismic areas are located near the boundaries of tectonic plates.

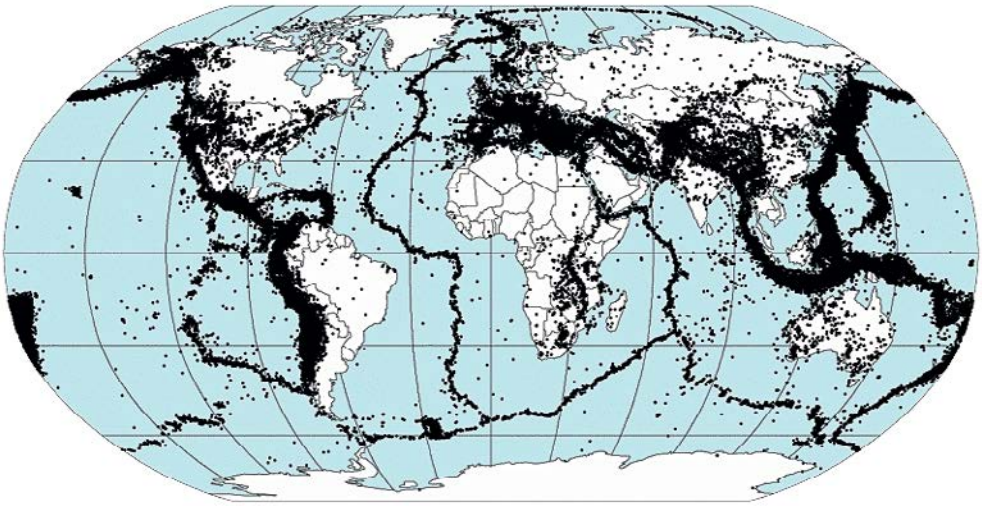

Figure 6. Global distribution of epicenters of earthquakes

[*NASA, DTAM project team, 1998_si. Preliminary determination of epicentres 358214 events, 1963–1998. http://denali.gsfc.nasa.gov/dtam/seismic/ ; https://commons.wikimedia.org/wiki/File:Quake_epicenters_1963-98.png*]

The boundaries of tectonic plates are traced in the form of a chain of earthquakes (Figure 6).

The upper part of the lithosphere is represented by the Earth's crust, which is the outer shell of the lithosphere. It is just this part of the lithosphere that is especially important for earthquake preparation processes. The most significant characteristic of the Earth's crust is its fragility and power. In 1909, the Croatian geophysicist and seismologist Andrija Mohorovičić discovered a seismic boundary, which was later called *the Mohorovicic (the Moho) discontinuity (boundary)*. The Moho boundary confines *the Earth's crust* from below and separates it from the upper mantle. Thickness of the Earth's crust is unstable. It varies from 5 km in the oceanic regions to 70 km in the mountain regions of the continental regions. On average, the effective thickness of the Earth's crust is about 35 km.

Thus, the prerequisites for seismicity are the active dynamics of lithospheric plates caused by convective mantle flows of substance. The main seismically active areas are located on the boundaries of lithospheric plates. Tectonic stresses from the boundaries of lithospheric plates are transmitted to the intracontinental parts, causing the intraplate seismicity.

1.2. Statistics of world earthquakes

An earthquake means rapid displacements of volumes of the geological environment, vibrations of the Earth's surface as a result of earth shocks. Some earthquakes can be caused by strong explosions, caving of vaults of underground cavities (mine workings, solutional caves). Small shocks can also be caused by the rise of lava during volcanic eruptions.

Most often, earthquakes (especially strong earthquakes) are caused by a rapid displacement of the Earth's crust section as a whole at the time of plastic (brittle) deformation of elastically stressed rocks in the earthquake focus. The earthquake focus is the area of the geological environment in which the potential deformation energy accumulates. Most foci of earthquakes occur near the Earth's surface.

The earthquake is a rapid transition of the potential energy accumulated in the rocks of the Earth's interior into the energy of oscillations of this very interior (seismic waves) as well as into the energy of the change in the structure of rocks in the origin of the earthquake. This transition occurs at the moment of exceeding the rock strength limit in the earthquake origin.

More than a million earthquakes occur all over the Earth each year, but most of them are so insignificant that they remain unnoticed.

Statistics show (Figure 7) that every year in the world there occurs one earthquake with magnitude of 8.0 or more, 14 earthquakes with magnitude from 7.0 to 7.9, 139 earthquakes with magnitude from 6 to 6.9, 1509 earthquakes with magnitude from 5.0 to 5.9 (this group also includes the Kaliningrad earthquake 2004). In addition, on the planet there are approximately 13,000 earthquakes with magnitude from 4.0 to 4.9, about 130,000 earthquakes with magnitude from 3.0 to 3.9 and about 1,300,000 earthquakes with magnitude from 2.0 to 2.9.

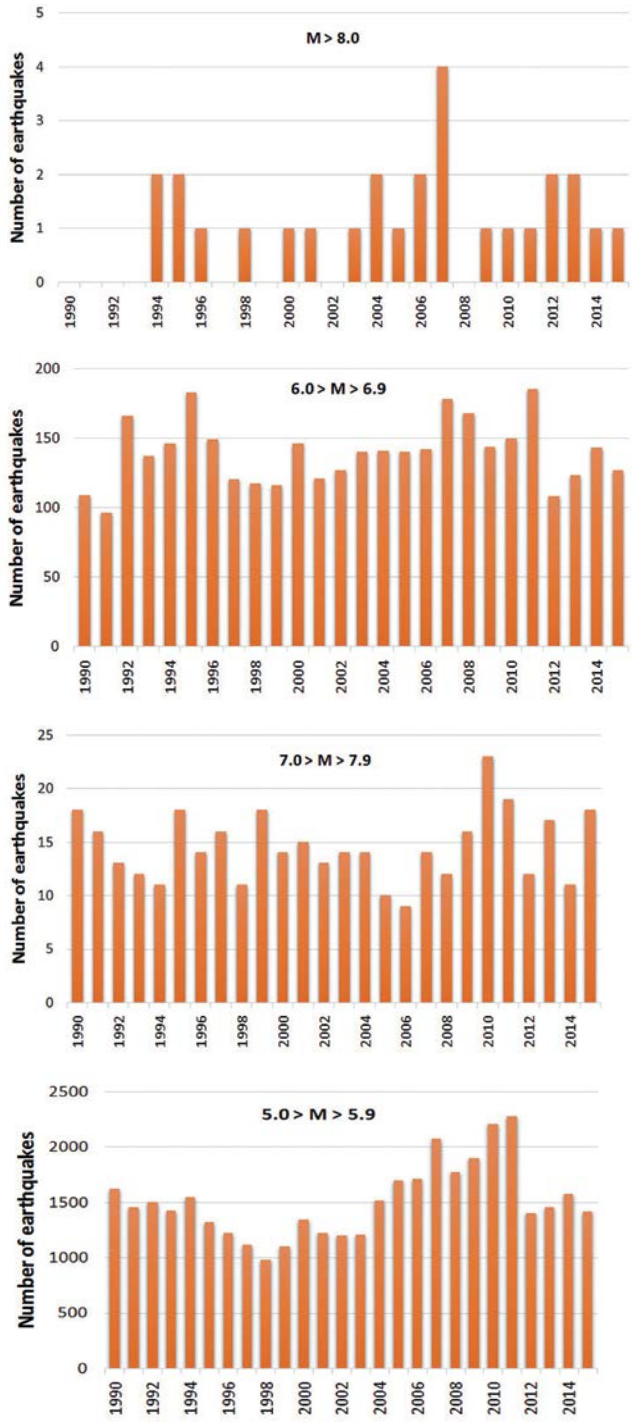

Figure 7. The number of world earthquakes with magnitudes from 5 to more than 8

Note: According to statistical data of USGS

If this interdependence is expressed in the form of a graph, an exponential dependence is obtained, according to which it can be possible to forecast the occurrence of the strongest earthquake, such as in Chile in 1960, once in about 9 years. As for weak earthquakes, we can expect about 12.5 million earthquakes with a magnitude of 1.5, about 126 million earthquakes with a magnitude of 0.5, about 1.27 billion earthquakes with a magnitude of –0.5 (negative magnitude), about 12.8 billion earthquakes with a magnitude of –1.5 (Figure 8). It is clear that the weaker the earthquakes, the more of them there are and the probability of their registration by seismic stations is lower. Therefore, a huge number of micro-earthquakes are not registered by seismic stations.

Statistics on weaker earthquakes are less reliable. This is due to the fact that the world network of seismic stations is distributed unevenly, while earthquakes frequently occur in remote and sparsely populated areas located at considerable distance from the stations. In such cases, weak earthquakes can remain unnoticed by seismic stations of the global network. Even the East Baltic region is not an exception in this respect. The stations of the *GEOFON* network, although existing here, are inter spaced by quite considerable distances (about 150–200 km). Therefore, seismic events, and consequently the earthquakes and especially micro-earthquakes with a magnitude below 1.0–1.5, can remain unnoticed. Moreover, even if a micro-earthquake was registered by one or two seismic stations, it may not be sufficient to reliably determine the earthquake epicenter. As a rule, it is expedient to use at least three stations for location of an earthquake.

At the same time, the energy contribution of all earthquakes with magnitudes 3.5 is low enough and does not exceed 0.25%. The contribution by earthquakes of smaller magnitudes is even lower. For example, for earthquakes with magnitude 2.5–0.08%, even less for earthquakes with magnitude 1.5–0.024% (Figure 9).

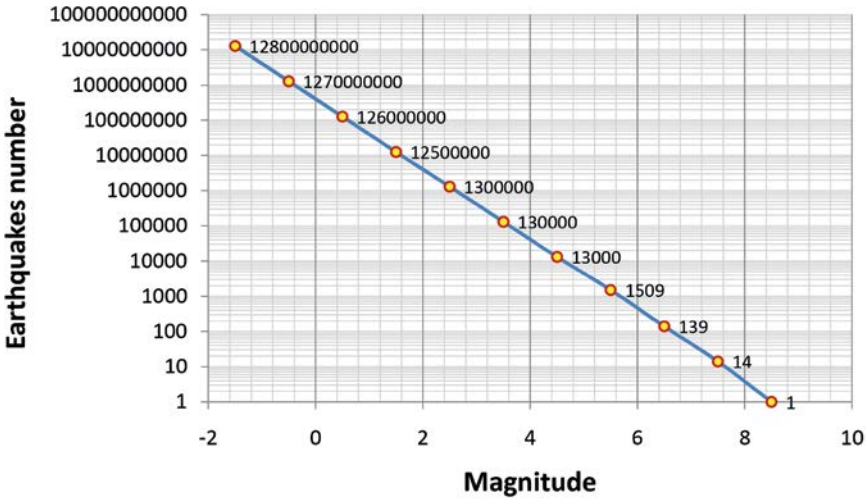

Figure 8. Average annual number of tectonic earthquakes worldwide

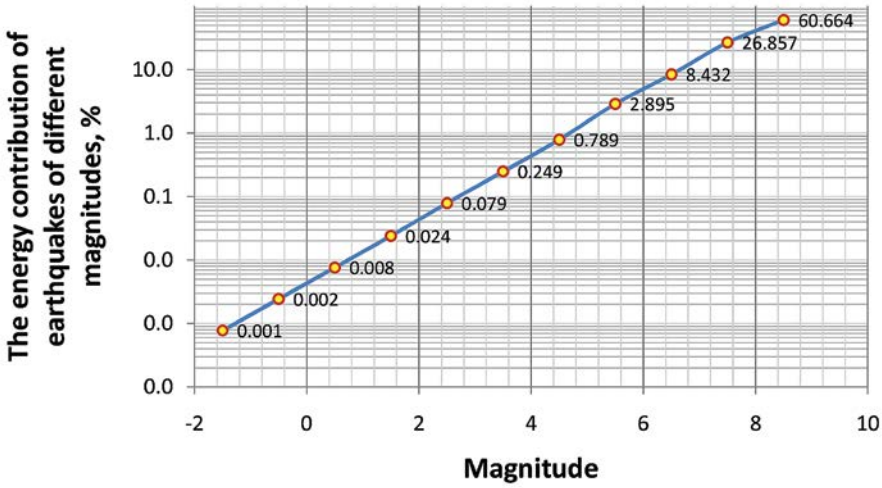

Figure 9. Energy contribution by earthquakes of different magnitudes to the total balance of seismic energy of tectonic earthquakes

The main energy contribution is made by earthquakes of magnitudes starting with 4.5 (0.8%). The maximum energy contribution is made by earthquakes within the magnitude range 7.0–7.9 (about 26.9%) and magnitudes exceeding 8.0 (about 60.7%).

Distribution of earthquakes within the time interval 1990 to 2015 (Figure 10) demonstrates that the number of earthquakes in different magnitude ranges is not uniform. The maximum number of earthquakes within the main magnitude ranges (5.0–5.9, 6.0–6.9, 7.0–7.9) were observed in 2010 and 2011 (Fig. 7).

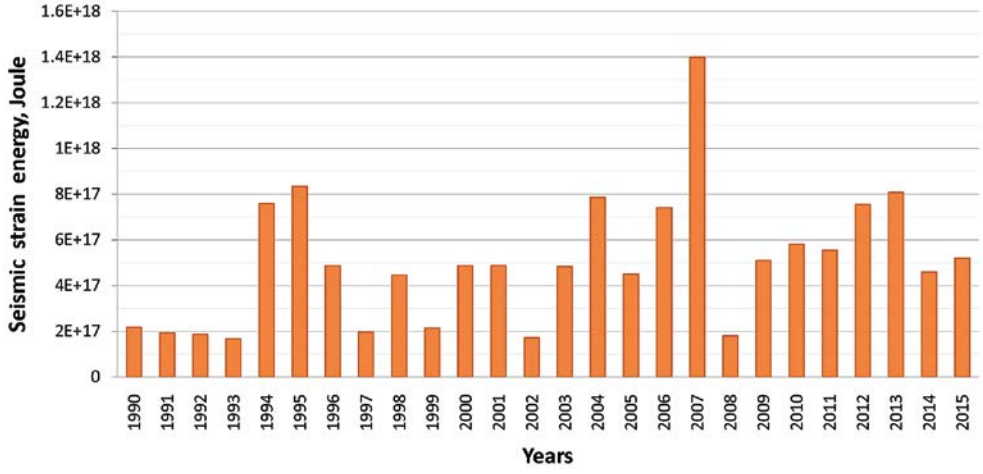

Figure 10. Global distribution of released seismic energy of deformation (Joule) during 1990–2015

An abnormally large amount of seismic energy (1.410^{18} Joules) was released in 2007 in the origins of tectonic earthquakes. This is almost 1.7 times more than in 1995, the year that ranks second in the number of seismic energy released in earthquakes. The level of released seismic energy in 2007 was higher than average – approximately 2.8 times average.

A certain difficulty is the study of historical earthquakes. Data on them were obtained on the basis of macroseismic studies, since instrumental observations appeared much later. Minimum requirements for the description of macroseismic information include data on the coordinates of the earthquake (latitude and longitude), the intensity of the shock, based on some widespread macroseismic scale, the name of the perception location, the identification code and the quality assessment. This set of minimum requirements allows to characterize the elementary cell of macroseismic information (*Macroseismic Data Points – MDP*). However, quite frequently the data on historical earthquakes does not contain a complete description of the parameters for *MDP* points (name of place, coordinates of location or intensity). It reduces the amount of reliable data. In addition, there are cases, when different authors report the same earthquake but within their own set of parameters for *MDP* points.

For example, Figure 11 shows the map [Albini et al., 2013], in which 432 historical earthquakes of total 994 earthquakes from the *GHEA* (*Global Historical Earthquake Archive*) catalogue are highlighted in red. Gray color shows the epicenters of earthquakes without any data on the parameters of *MDP* points.

Of 432 earthquakes shown on the map (Figure 11), some do not contain a complete set of *MDP* characteristics, or the information was taken from map, with an unclear quality of isoseismic data. All this leads to a decrease in the quantity of qualitative data. As a result, the number of reliable earthquakes was reduced to 292 (Figure 12). However, separate sets of MDP data were indicated for the same earthquake in 69 cases.

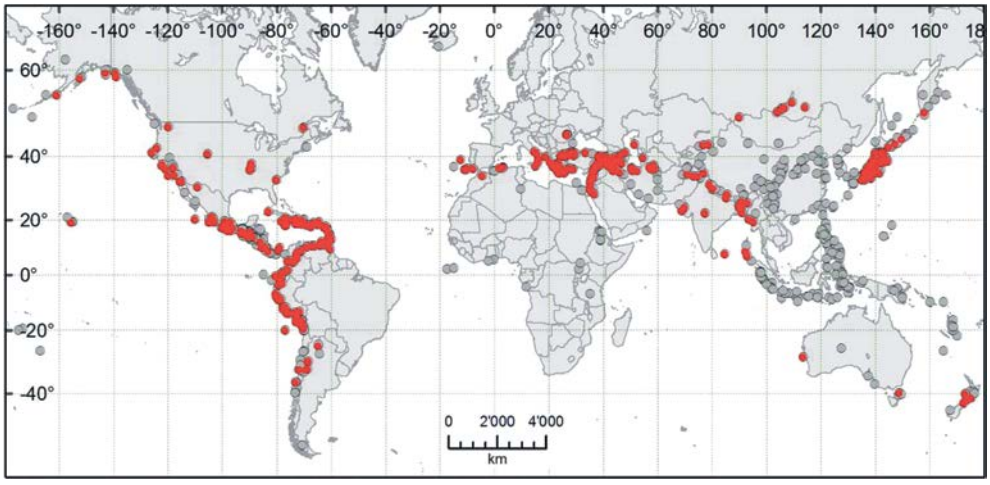

Figure 11. 492 world historical (1000 to 1903) earthquakes (red colour) from the GHEA catalogue, which are included in seismic statistics. Gray color shows events not having a complete set of parameters for MDP points [Albini et al., 2013]

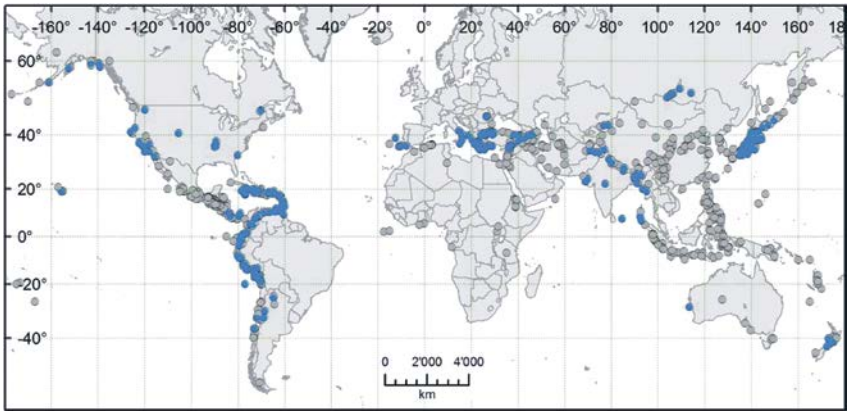

Figure 12. 292 world historical (1000 to 1903) earthquakes (blue colour) from the GHEA catalogue, which are suitable for use in seismic statistics [Albini et al., 2013]

Based on the data with the a full set of MDP parameters (Figure 12), the most dangerous seismic areas for the historical period 1000 to 1903 were the western coast of the North and South America, the Caribbean Sea area, the Euro-Mediterranean seismic belt extending from the Gibraltar Strait to the Caucasus, seismic belt stretching across Tajikistan, Afghanistan, Nepal, Bangladesh and Burma, as well as Japan, New Zealand. Taking into the *MDP* data with an incomplete set of characteristics, the seismically active belts also include the Middle East, Iran, Central China, Taiwan, the Philippines and Indonesia.

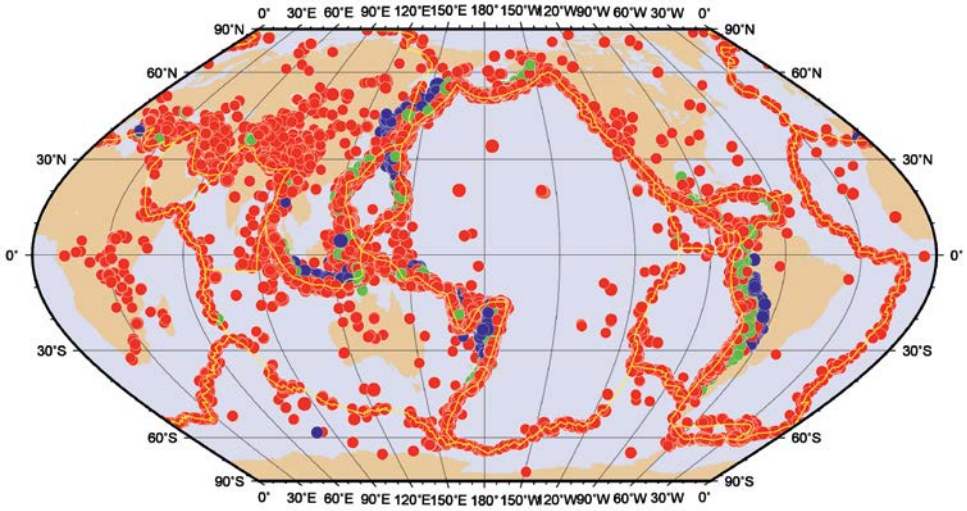

Figure 13. Distribution of world earthquakes with magnitudes from 4 to 9.1 within the period 1970 to 2017

Note: depth of hypocenters of earthquakes: red colour – 0 to 100 km; green color – 101 to 300 km, blue – 301 to 800 km, yellow lines – boundaries of tectonic plates

Epicenters of 20,000 strong earthquakes from the *IRIS* [IRIS Earthquake Browser] database for the period 1970 to 2017 are shown in Figure 13. The magnitude of earthquakes varies from 5.4 to 9.1.

Foci of earthquakes are grouped along the boundaries of tectonic plates. At the same time, it can be seen that a number of earthquakes occurred within the plates. For example, quite a lot of earthquakes occurred inside the Eurasian Plate. An example of intraplate seismicity is the New Madrid earthquakes. They occurred in 1811, 1812, 1865 and 1895. On 16 December 1811, the shock magnitude reached 7.9.

579 of the world's strongest earthquakes from the above list are shown in Figure 14. These earthquakes had a magnitude from 7.0 to 9.1. The majority of strong earthquakes occurred along the Aleutian Trench, the western coast of both Americas, on the eastern and northern border of the Australian Plate, on the western border of the Philippine Plate, at the southern boundary of the Sunda Plate.

Seismicity of the Earth is characterized by a certain zonality while the intensity of seismic processes is determined by the nature of the intraplate motions. Subduction zones are more intense sources of seismicity while spreading zones are characterized by more moderate earthquakes. The most seismically active plate is the Pacific Plate, to the boundaries of which most of the strong earthquakes of the world are confined. In the spreading zone of the Mid-Atlantic Ridge, strong earthquakes almost do not occur. There mainly occur moderate earthquakes (Figure 13), with magnitudes below 7.0.

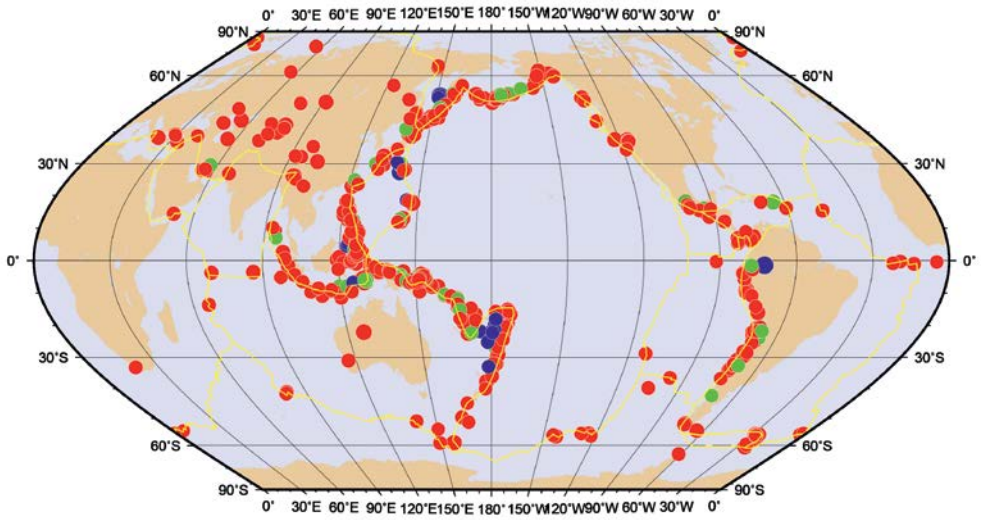

Figure 14. Distribution of world earthquakes with magnitudes 7 to 9.1 within the period 1970 to 2017

Legend: depth of hypocenters of earthquakes: red colour – from 0 to 100 km, green colour – from 101 to 300 km, blue colour – from 301 to 800 km, yellow lines – boundaries of tectonic plates; names of tectonic plates: 1 – Pacific, 2 – Eurasian, 3 – North American, 4 – South American, 5 – African, 6 – Australian, 7 – Arabian, 8 – Hindustan, 9 – Sunda, 10 – Philippine, 11 – Nazca, 12 – Cocos, 13 – Caribbean, 14 – Antarctic

2. SEISMICITY AND PREREQUISITES OF SEISMICITY OF STABLE CONTINENTAL REGIONS

The platforms occupy large areas of the continental crust and are characterized by relatively calm tectonic regimes. Platforms occupy about 45% of the surface of the continents. Within the platforms, the average thickness of the Earth's crust reaches 35–40 km. Thickness of the lithosphere within the ancient platforms is from 150 to 200 km, but can also reach 400 km. The platforms consist of two structural floors. The crystalline basement represents a more ancient structural floor and consists of strongly dislocated and metamorphosed rocks. Above it is located a platform cover – a younger, upper structural floor. The platform cover usually consists of unmetamorphosed, sedimentary rocks. Between the crystalline basement and the platform cover, there is usually a distinct boundary. Within the platforms, the non-metamorphosed sedimentary cover occupies significant areas. Its thickness is 3–5 km but sometimes reaches 10–12 km and even greater thickness in deep depressions.

In the evolutionary series of large elements of the Earth's crust and lithosphere, platforms, and the more the ancient ones, with the Archean and Paleozoic basements, follow the orogens. The platform regime is established after the platforms have passed the stage of cratonization and the stage of avlakogene and entered the stage of accumulation of the plate cover. A large sedimentary cover is formed on most of the EEP territory. However, the sedimentary cover is not ubiquitous on the platforms. Within the platforms there are areas, where the Precambrian crystalline, igneous and metamorphic rocks, i.e. shields emerge. They represent a tectonically stable territory. The age of the shields exceeds 570 million years but sometimes reaches 2 or even 3.5 billion years. After the Cambrian period, the shields are slightly exposed to tectonic processes.

Shields represent relatively flat areas of the Earth's surface, within which the processes of mountain formation, tectonic faults, geodynamic processes are significantly weakened in comparison with the geodynamic processes that occur outside their boundaries. The continental crust continued to form during the Proterozoic, but at a slower rate. Archean protocontinents collided with each other and with volcanic island arcs. There was a process of accumulation and formation of large continents. Significant internal spaces of the continents were isolated from the influence of magmatic activity associated with subduction, which occurred at the edges. The inner areas of the continents were

gradually cooled and strengthened until they became rigid and strong. Such area of cold, relatively stable continental crust was named a craton, i.e. areas of ancient platforms with Precambrian, metamorphosed basement. They became the most ancient "cores" of the continents and include the North American, South American, East European, African-Arabian, Siberian, Sino-Korean, Hindustan, Australian (Figure 15).

Within the limits of the ancient platforms – consistent, stable continental sections of the Earth's crust, the intensity of tectonic movements and seismic activity is much less than at the plate boundaries in the geosynclinal belts. The stable continental crust (SCR) consists of 7 areas: North and South America, Eurasia, Africa, India, China and Australia (Figure 16). Antarctica is not included due to the lack of sufficient seismic and geological data.

One of the main factors determining the level of seismicity of the territory is the tectonic movements. They are caused by deep forces and processes that affect the motion of substance and energy inside the Earth, i.e. by the geodynamics. The main elements of geodynamics are slow (tectonic creep) and rapid (earthquakes) tectonic motions. Slow and rapid motions manifest in different ways under different geological conditions. For example, the rate of deformation of the crust in the interior of the continents is usually much lower (less than 1 mm/year) than near the plate boundaries (3–16 cm/year). This affects the average time of recurrence of major earthquakes. According to paleoseismic studies and rates of deformation of the Earth's crust, the average time of recurrence of major earthquakes in continental areas may be of the order of thousands of years [Lee et al., 2007].

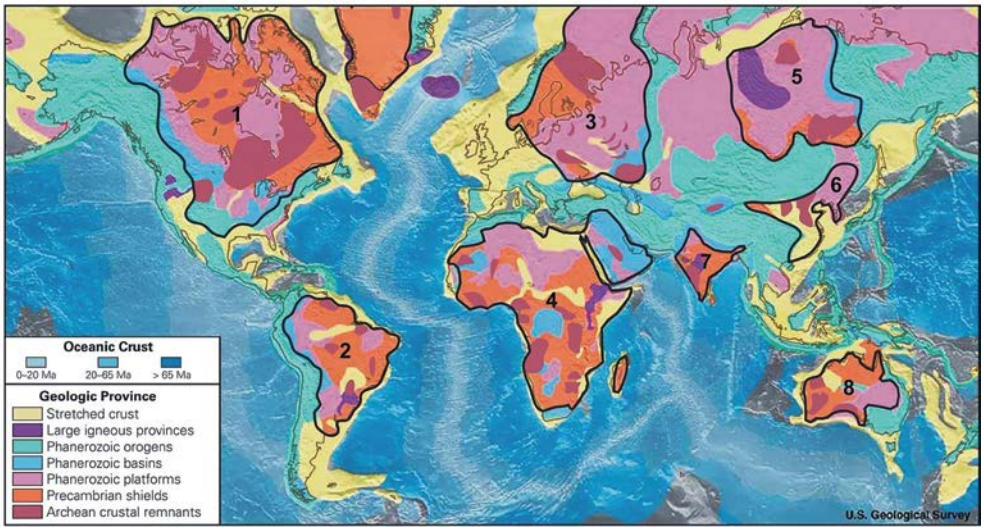

Figure 15. World geological provinces

[*https://commons.wikimedia.org/wiki/File:World_geologic_provinces.jpg*]

Denotations of platforms: 1 – North American; 2 – South American; 3 – East European; 4 – African-Arabian; 5 – Siberian; 6 – Sino-Korean; 7 – Hindustan; 8 – Australian

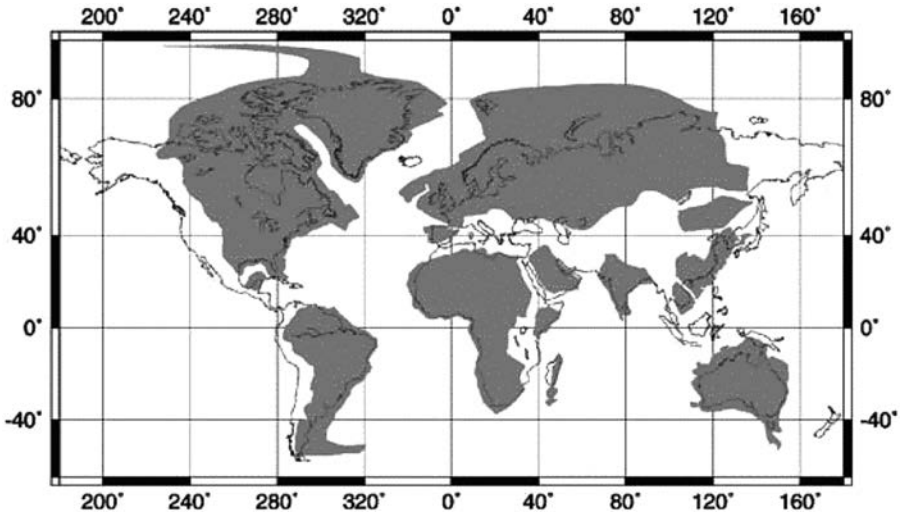

Figure 16. Stable continental regions – SCR
[*Saskia & Mooney, 2005*]

The origins of tectonic earthquakes are mainly confined to the boundaries of lithospheric plates. However, the strongest earthquakes occur practically only in the subduction areas and in the region of continental collision [Turcotte & Schubert, 1985]. Strong earthquakes far from lithospheric plates are rare, but nevertheless still occur. For example, the New Madrid earthquakes in the USA 16/12/1811, 23/01/1812 and 07/02/1812 had magnitudes from 7.3 to 8.0. The origins of these earthquakes are confined to the internal, continental rift. The region is referred to the New Madrid seismic area while the earthquakes occurred far from the boundaries of lithospheric plates, i.e. within the stable continental crust [Johnston et al., 1994].

The following chapters will consider the main geological elements of the intraplate regions of the stable continental crust where tectonic earthquakes can occur, as well as the seismicity characteristics within them.

2.1. Review of seismic geological conditions of stable continental crust

To understand the genetic relationship between geologic-tectonic structures located on the stable continental crust (SCR) and tectonic earthquakes, a classification of sources of intraplate seismicity was developed. According to a number of researchers [Schulte & Mooney, 2005], there exist 5 types of sources of intraplate seismicity: 1) rifting in the internal parts of the SCR (taphrogenes); 2) continental margins exposed to rifting; 3) crust not exposed to rifting; 4) possible intracontinental areas of the crust exposed to rifting; 5) margins that may have been exposed to rifting.

Statistical analysis covered crustal earthquakes with a magnitude $M \geq 4.5$ within the period 495 to 2003 (Figure 17). Taking into account the removal of non-tectonic earthquakes from the catalogue, 1221 tectonic events were used. Investigations of intraplate earthquakes showed [Schulte & Mooney, 2005] that the intraplate seismicity was distributed unevenly. On the background of diffused, scattered seismicity, there are several areas of its concentration. This is particularly true for internal rifts (*taphrogenes*).

27% of earthquakes belong to internal rifts, 25% to rift continental margins, 36% of earthquakes occurred inside the non-rift crust, and 12% of earthquakes were not determined as belonging to any particular structures. Thus, more than a half (52%) of intraplate earthquakes are associated with the rift cortex. The largest earthquakes ($M \geq 7.0$) arose mainly within the rifts (50%) and continental margins (43%) [Schulte & Mooney, 2005].

Inside 12 geological tectonic structures, 74% of plate earthquakes occurred and 98% of seismic moments were realized. The most important among them are the rift areas: Kutch Rift (India), Reelfoot Rift (USA), East China Taphrogene, huge rift clusters in central Africa and the centre of Western Europe.

A number of rift clusters are located in the centre of Western Europe (Figure 18), near the East European platform.

Since the Paleozoic, the region of Western Europe has undergone a large-scale expansion [Schulte & Mooney, 2005]. In the North Sea, in the northern part of Britain and in Ireland, the rift areas formed in Paleozoic predominate. On the mainland, the age of rifting is younger – Cenozoic.

The youngest rifting belongs to the British Rift Cluster [Sengör & Natalyin, 2001]. This rift cluster was formed within the period from Pliocene to Quaternary. It was included in the stable continental region (SCR) (Figure 18) according to Johnston et al [Johnston et al., 1994].

Other Cenozoic rifts in central Europe have an age not younger than Palaeogene and are therefore included in the SCR. The Rhine graben consists of two parts – the upper and the lower graben. It is one of few rifts in Europe where a high concentration of seismicity is noted. For example, it is known about 14 earthquakes with a magnitude not exceeding 5.6. The presence of large faults, salt deposits and small thickness of the Earth's crust (about 27 km) indicate that the centre of Western Europe experienced a significant thinning of the Earth's crust and the expansion was not limited to individual rifts. At the same time, seismic activity in Europe is not high. For example, from 495 to 2003 in the stable continental part of Western Europe there were 148 tectonic earthquakes with a magnitude 4.5.

The degree of detail and the scale of seismicity studies of the ancient platforms are quite different. One of the most explored areas of the stable continental crust is the North American Platform. There is an extensive network of seismic stations on its territory, which allowed to accumulate a significant amount of information on earthquakes and to assess the relationship of seismicity to the geological and tectonic structure. Since 1970, US research organizations have accumulated data on more than 40,000 earthquakes every year (with magnitudes starting from 1.0). Whereas, on the territory of the East European Platform the seismic network is a fairly sparse and

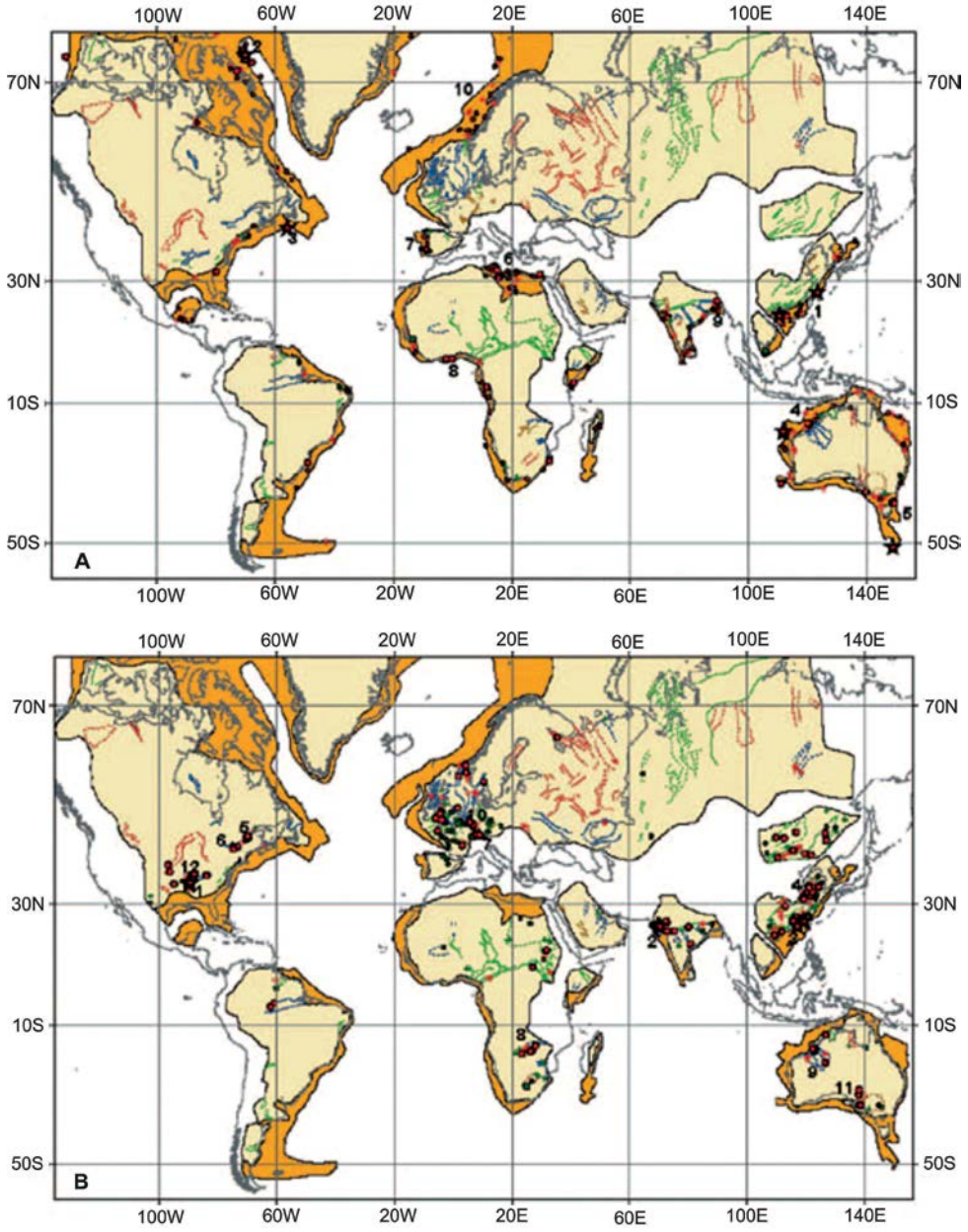

Notes: Extended margins are coloured orange; inner continental areas are coloured in yellow; rifts and taphrons are indicated by solid lines when the boundaries are clearly defined or by dotted lines when the boundaries are poorly defined. Precambrian rifts are marked in red, Paleozoic – in blue, Mesozoic – in green and Cenozoic in brown. The maps were constructed on the basis of the Exxon tectonic maps (Exxon Production Research Company, 1985) and the rift catalogue (Sengör & Natalyin, 2001). Red circles denote events that have occurred; green circles – events that can be associated with rift continental margins or internal rifts; blue circles denote events that occurred in the non-rift crust. Numbers indicate regions with concentrated seismicity

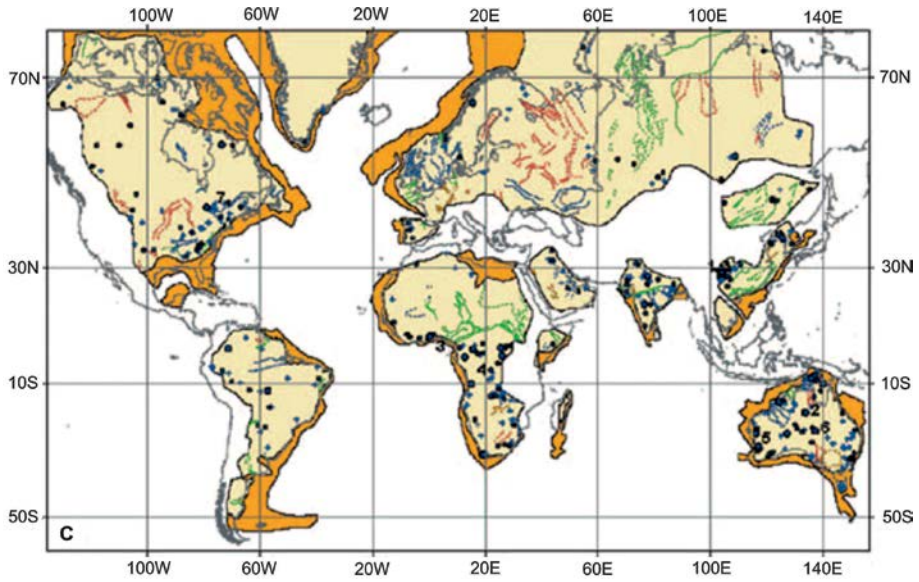

Figure 17. Intraplate earthquakes: a) in rift continental margins; b) in internal rifts /taphrons/; c) in unexpanded continental crust [Schulte & Mooney, 2005]

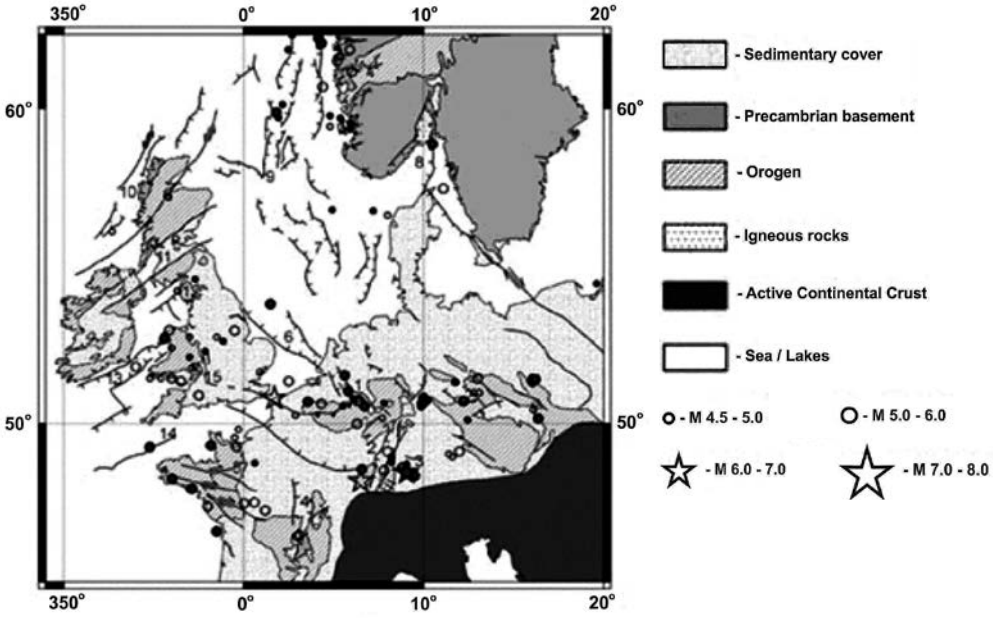

Figure 18. Simplified tectonic map of European region inside stable continental crust with epicenters of strong earthquakes [Schulte & Mooney, 2005]

Notes: Numbers on the map: 1 – Lower Rhine rift; 2 – Upper Rhine rift; 3 – Illies rift cluster; 4 – Limange rift; 5 – Brittany rift cluster; 6 – West Netherlands Sole Pit; 7 – Central graben; 8 – Oslo rift; 9 – Viking graben; 10 – Minches basin; 11 – Midland valley; 12 – Solway – Northumberland basin; 13 – North Celtic sea basin; 14 – Western Approaches basin; 15 – Worcester basin

therefore unrevised catalogue of earthquakes from ancient times to 2005 contains only about 350 earthquakes in the range of magnitudes from 2.5 to 6.3 [Маловичко и др., 2007]. Among these earthquakes, there are also seismic events of non-tectonic origin.

In Russia, which occupies a significant part of the Eurasian plate and most of the East European platform, the seismicity of the platform part has been investigated much worse. This is due to the fact that instrumental observations in Russia started in 1906 when registration began at the stations Ekaterinburg (11.10.1906) and Pulkovo (09.12.1906). However, these stations were equipped with long-period seismographs,

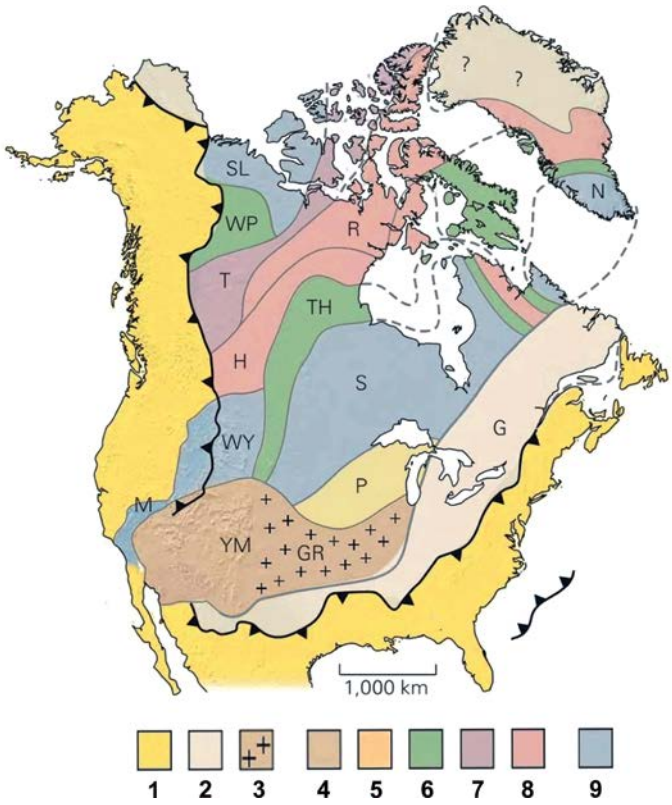

Figure 19. Layout of basement of the North American Platform

[*The North American craton …, 2015_si http://geologylearn.blogspot.com/2015/11/the-proterozoic-earth-in-transition.html*]

Legend: 1 – Phanerozoic orogen; 2 – collision orogen at the age of 1.1 billion years (G-Grenville); 3 – accreted crust covered with granite and rhyolite where the pattern shows GR – granite-rhyolite province; 4 – accreted crust of age from 1.6 to 1.7 billion years (YM – Yavapai and Mazatzal); 5 – accreted crust of the age of 1.8 billion years (P-Penokean); 6 – collisional orogen at the age of 1.8 billion years (TH – Trans-Hudson; WP – Wopmay); 7 – collisional orogen at the age of 1.9 billion years (T – Thelon), 8 – Archean rocks later deformed and metamorphosed in Proterozoic (H – Hearn; R – Rae); 9 – relict Archaean crust (WY – Wyoming; M – Mojave; S – Superior; N – Nain; SL – Slave)

which with their amplitude-frequency characteristics were intended for recording of distant and strong earthquakes. In addition, the stations were located far from each other, i.e. there was no network of seismological observations as an essential condition for the localization of regional earthquakes. The network of stations was supposed to be created only in seismically active areas. Only in early 20s of the 20th century the introduction of new equipment (seismograph of P.M. Nikiforov) began for registration of near earthquakes [Яновская, 2014]. It allowed to significantly increase the amount of information on earthquakes in seismically active regions. Although seismic networks were still located in the Caucasus, Central Asia, the Altai and the Far East, it nevertheless became possible to register strong earthquakes of the East European Platform. Thus, it can be considered that during the instrumental observation period in the territory of the East European Platform, about 250 earthquakes were registered (revised catalogue, removing the earthquakes of non-tectonic nature).

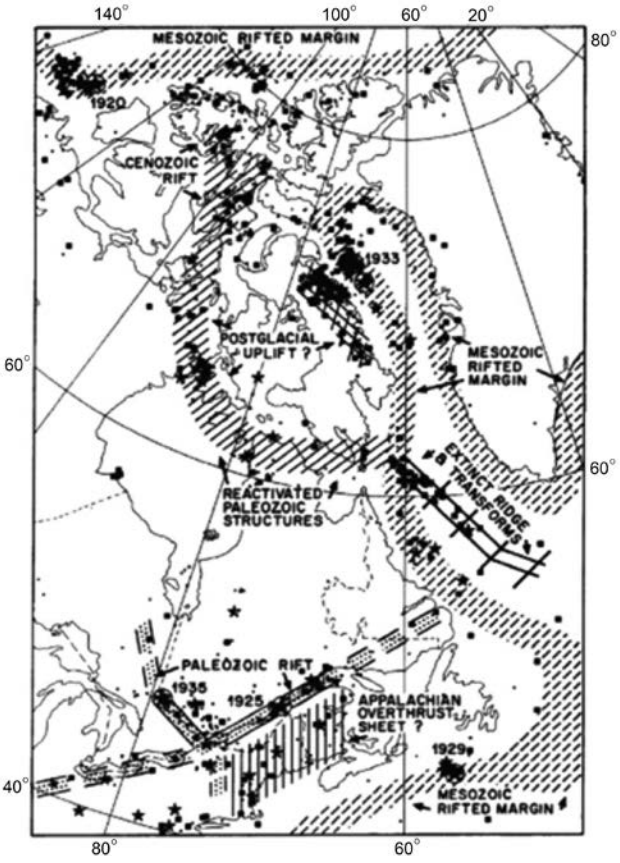

Figure 20. Earthquakes in eastern Canada (for M>3 since 1970, for M>4 since 1960, for M>5 since 1940, for M>6 since 1900), along with interpretation in connection with causes of seismicity [Adams & Basham, 1989]

The results of studies, materials and experience obtained in the study of seismicity in other platform territories with a stable continental crust are of undoubted interest for a better understanding of laws governing the development of seismic process on the East European Platform. Therefore, the following is a brief analysis of the most studied ancient North American Platform (NAP).

The North American Platform is one of the largest platform territories and occupies the central part of the North American continent. Its basement consists of rocks of the Archean, Lower and Middle Proterozoic age. Approximately 2/3 of the area of the North American Plate is occupied by a stable North American ***craton***. It consists of a series of geological tectonic belts and blocks combined together during the collisional and accretionary orogeny in the Precambrian time. Within the Canadian Shield, the basement of the platform crops out. The Canadian Shield has a extension to the north-east and occupies a part of the island of Greenland. From the west, south and southeast, the North American craton is framed by the Phanerozoic orogen (Figure 19).

The territory of the craton is predominantly aseismic. Nevertheless, there are several areas of increased seismicity. They are located both on the east coast and in the interior of the craton.

In the transit oceanic continental area of the east coast (Figure 20), two major earthquakes occurred in 1929 with a magnitude of 7.2 (Grand Banks), in 1933 with a magnitude of 7.3 (Baffin Bay) and several small earthquakes. These earthquakes could be associated with the reactivation of the Mesozoic rift faults that arose during the formation of the North Atlantic.

Inside the southern part of the North American craton, the seismicity is concentrated in five areas. Three areas – Ottawa River, Charlevoix and Lower St. Lawrence are located within the collisional orogen Grenville (Figure 19). Here the depth of the hypocenters of most earthquakes is within the range 5 to 25 km. According to some authors [Adams & Basham, 1989], the seismicity here is probably related to the reactivation of the rift fault system along St. Lawrence and Ottawa River. In the early Cretaceous period, traces of hot spots could be the cause of the fourth seismic area northward of Ottawa River, westward of Quebec. The fifth area of seismicity is located northward of the Appalachians. Here the Miramichi shallow earthquake occurred in 1982. This earthquake had a *thrust faulting* mechanism, as a result of which relatively young rocks were submerged under the older basement.

In the northern part of the craton, earthquakes occur on the island of Baffin, along the arc-shaped strip between the Boothia and the peninsula of Ungava, and also in the Sverdrup basin. Earthquakes in the area of the Baffin Island and Boothia-Ungava are spatially related to normal faults in the Cretaceous period, and also with a sharp gradient of motion during the post-glacial rise. It indicates that there could be a differential uplift located at the place of the existing faults. The earthquake in Sverdrup is a deformation under a thick layer of precipitation.

Earthquakes along the eastern continental margin are mainly associated with the faults of the Mesozoic rift formed during the opening of the Atlantic. In addition, the faults in the middle of the Labrador Sea are connected with the disappeared expansion of mountains and their transform faults. In some marginal structures extending within

the northern Baffin Bay, earthquakes could be partially associated with stress induced by deglaciation.

One of the reasons for seismicity may be disturbances in the isostatic equilibrium of the Earth's crust in areas that have been numerously subjected to glaciation and the formation of powerful ice sheets. After removal of the glacial load the isostatic equilibrium is restored, which is accompanied by uplift of the Earth's crust, redistribution of stresses within the crust and occurrence of earthquakes.

The last deglaciation took place in the interglacial period replacing the last quaternary glacial period, which ended approximately 12 thousand years ago. Quaternary glaciation or the modern glacial period, began 2.588 million years ago [Clayton et al., 2006i], in the Pleistocene glaciation, and is a series of glacial "events" separated by interglacial "events".

The process of the last deglaciation became a significant exogenous factor, which influenced the seismicity of continental spaces. Huge weight of the ice sheets covering the northern and southern continental areas facilitated the submersion of the Earth's crust into the asthenosphere, which disturbed its isostatic equilibrium. In this case, the cover glaciers appear and disappear faster than the isostatic equilibrium is established. That is why the process of restoration of isostatic equilibrium protracted for a long time. Up to now, the crust has not completely restored. This is evidenced, for example, by the model of modern change in masses due to the post-glacial recovery and the reloading of ocean basins by seawater (Figure 21).

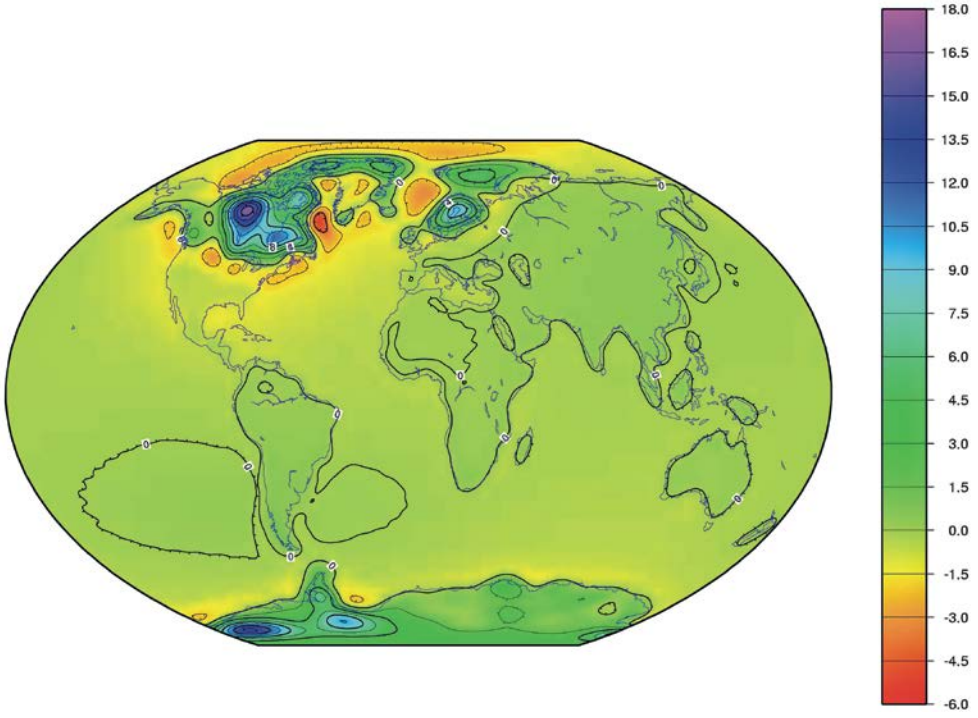

Figure 21. Rate of lithospheric uplift due to postglacial rebound. Vertical movements of the Earth's crust (mm/year) according to Paulson [Paulson, 2007_t]

A significant part of the North American Platform exposed to the effect of ice sheet is experiencing a rise up to the present time. The rate of uplift in accordance with model estimates [Paulson et al., 2007] is shown in Figure 21.

The model for the rate of the lithospheric uplift (Figure 21) shows the mass change associated with the postglacial rebound. It shows the change in the thickness of the equivalent water mass (in mm) during the year but not the magnitude itself of the change in the crust's movement up or down. The secular change in gravity demonstrates a significant positive anomaly over a large area (more than 3,000 km) near the Hudson Bay. This anomaly, both in area and in intensity, considerably exceeds the anomaly in Scandinavia. In the center of the anomaly located slightly westward of the Hudson Bay, the secular change in gravity is ~ 2.5 mcGal per year [Paulson et al., 2007]. On the map (Figure 21) it corresponds to the uplift rate of 16.5–18.0 mm/year.

Glacial loads create an additional vertical stress (about 20–30 MPa), which is counteracts the mantle and bending of the lithosphere. A number of tectonic faults that occurred after the glacial retreat are due to a change in the field of tectonic stresses in southeastern Canada. In particular, the tectonic faults that occurred during the last deglaciation period 9000 years ago indicate that the orientation of the main horizontal stress σ_H was almost perpendicular to the existing edge of the glacier. Today, the orientation of σ_H is directed from the northeast to the southwest, along the direction of extension of the Mid-Atlantic Ridge. It indicates that the stress of post-glacial recovery played an important role during the deglaciation period but then gradually lost its influence and today the tectonic stress became more dominant.

The assessment of the possibility of the glacial load influence on earthquakes in North America demonstrated that the glacial load was capable of initiating the paleo-earthquakes at the margin of a glacier near Charlevoix ($\varphi = 47.5°N$ and $\lambda = 70.1°W$) and in the Wabash Valley (and), outside the ice field. However, the glacial load outside the former glacier field would hardly have provoked large earthquakes, such as the earthquake in New Madrid (and) with a magnitude M = 8.0 [Wu & Johnston, 2000].

For a long time, a discussion was held among seismologists about the predominant role in the occurrence of earthquakes of directly tectonic causes or the post-glacial restoration of equilibrium. A number of researchers [Adams & Basham, 1989] believe that modern tectonic forces predominate over postglacial effects. In most cases, there was no evidence of strong effect of the past glaciation on the current seismicity model.

Thus, the main conclusion about the relationship between the seismicity and the process of deglaciation during the last glacial period in conditions of ancient, stable platforms, in particular the North American Platform, is that the completely unfinished deglaciation process has lost its predominant role in initiation of earthquakes. It became caused by other reasons and in particular by pressure from the northeast to southwest, from the Mid-Atlantic Ridge. It is just these tectonic forces that influence the modern geodynamic situation in the east of the North American Platform, i.e. on the stable continental crust.

To study the geodynamic conditions in the North American continent, modern methods of geodynamic monitoring are used. One of them is the study of slow

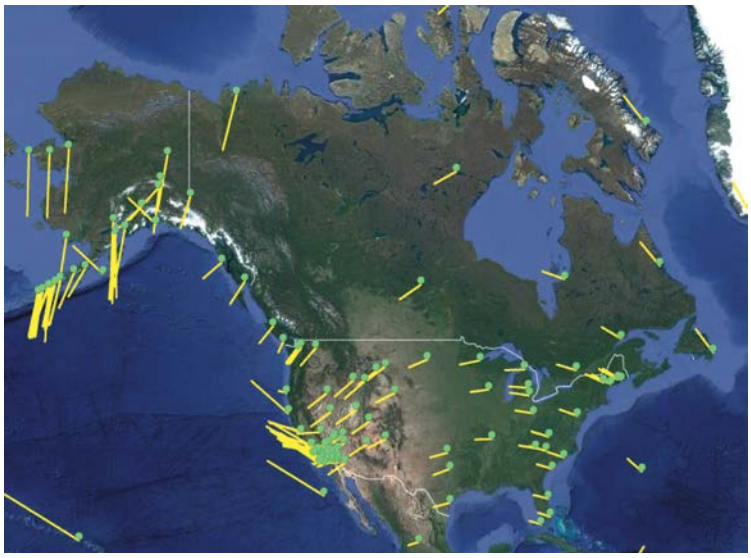

Figure 22. Vectors of modern horizontal speeds a GPS observation points

[*Jet Propulsion Laboratory, California Institute of Technology, https://sideshow.jpl.nasa.gov/post/series.html*]

movements of the Earth's crust using GPS technology. In the US territory, there exists one of the densest networks of GPS signal reception points (Figure 22).

GPS stations are not evenly distributed over the territory of the North American Platform. The density of GPS stations is much higher in the US than in Canada, which occupies most of the North American Platform. Nevertheless, even a rare network of GPS stations in the territory of Canada allows to have an idea of the current speeds of horizontal movements of the Earth's crust on the platform.

GPS system of Jet Propulsion Laboratory, California Institute of Technology, uses 30 satellites and collects data from more than 2,000 receivers. The data processing results demonstrate that the azimuth of the direction of the vectors of horizontal motions varies from east to west. The azimuth changes in the profile of the GPS points (Figure 23) located in the latitudinal band between the parallels 37.5° and 39.2°, as follows: it decreases from 288.3 ° (on the meridian 75.5°) to 240.6° (on the meridian 117.2°), and then sharply grows up to 299.2° (on the meridian 122.5°).

The sharp increase is explained by the fact that the profile of GPS points at this location crosses *a transform fault* that delimits the North American and Pacific plates. Along this fault, movement of the plates takes place.

In the east of North America, earthquake foci (within the period 1534 to 1971) are mainly confined to four geologic formation provinces: 1) the Phanerozoic orogen located along the eastern and southern coast of the USA; 2) the collisional orogen *Grinville*, which is a narrow area parallel to the previous one and located northwest of the Phanerozoic orogen, 3) accreted crust covered by granite and rhyolite of age 1.6– 1.7 billion years and 4) accreted crust 1.8 billion years of age.

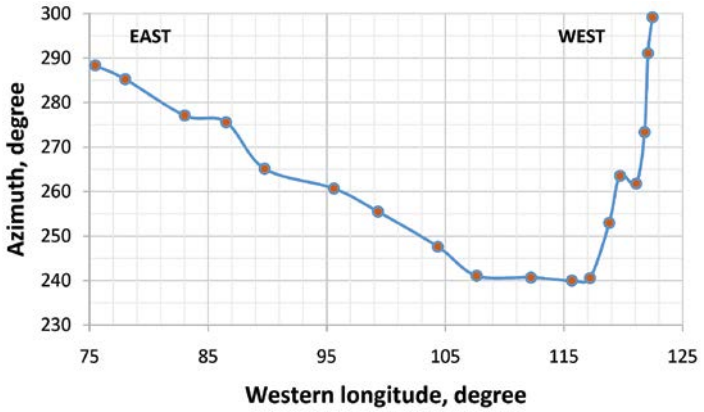

Figure 23. Change in azimuth of horizontal GPS reference travel vector along profile that crosses the North American continent from east to west.

The current seismicity of the North American Platform and the geological provinces framing it are shown in Figure 24. The sampling area was for the latitude from 30°N to 84°N and for longitude from 26°W to 155°W. The earthquake statistics for the 8-year period were used, from January 2000 to January 2008 for magnitudes above 1.0. The sampling was made from the catalogue of the North Carolina data center and seismic laboratory in Berkeley [Northern California Earthquake Data Center & Berkeley Seismological Laboratory_*i*].

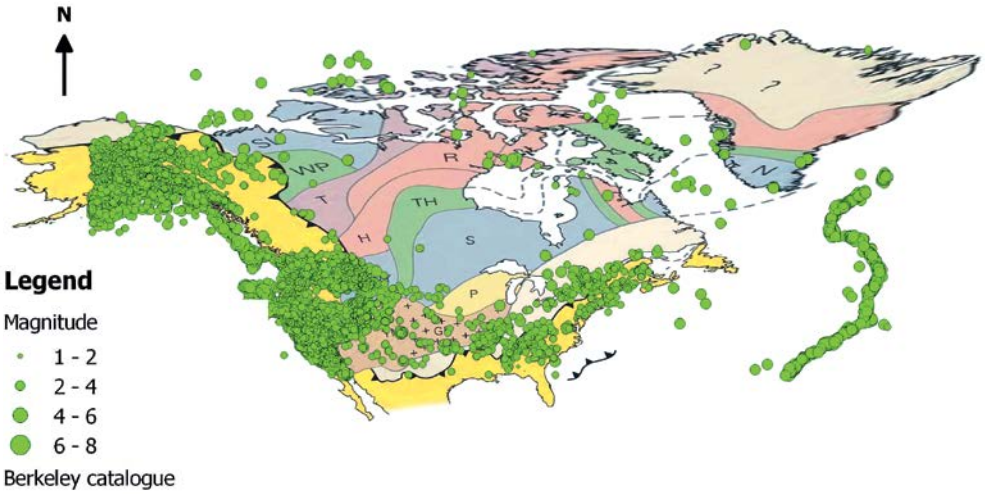

Figure 24. Seismicity of the North American Platform and its framing geological provinces

Note: earthquakes are only presented for the territory limited by coordinates: latitude – from 30°N to 84°N; longitude – from 26°W to 155°W. Designations of geological formations are similar to those shown in Figure 19

The platform area is characterized by a significantly lower seismic activity. Although weak earthquakes with magnitude 1.0–2.0 are recorded here, this is due to a much less dense network of seismic stations (1 station per 120 thousand km^2). In the US territory, the density of seismic network is significantly higher (about 1 station per 2,530 km^2).

2.2. Brief description of geotectonic conditions of the East European Platform and its individual elements

Geological structure and geodynamic potential in terms of geotectonic conditions are obvious indicators of seismicity. Knowledge of geotectonic conditions of the EEP is necessary for understanding the relationship of seismicity with deep geological structure, geodynamic conditions, tectonic structures of the basement and sedimentary cover.

The East European Platform (EEP) has a complex geometric shape (Figure 25). To the east, it borders the Hercynian folded Urals structure of a submeridional strike. At a latitude of about 60°, the boundary of the VEP turns to the northwest and extends along the Timan uplift area, near the Kanin Peninsula and the coast of the Kola Peninsula, the northern part of the Rybachiy Peninsula and Varangerhalvoya. In the western part of the Varangerhalvoya Peninsula, the platform boundary turns to the southwest. Further for about 1500 km the boundary passes along the edge of the Scandinavian Caledonides. To the south-west of the Baltic Shield, the EEP boundary is mixed. Most often it is led in a southeasterly direction along the Teisseyre-Tornquist Zone, from the southern coast of Norway to southern Sweden and further to the Swiętokrzyskie Mountains in Poland. Then the boundary runs along the northeastern side of the Precarpathian Trough. In the south, the EEP borders on the Scythian Plate, which encompasses the flat Crimea and Ciscaucasia. The southern boundary starts from the mouth of the Danube and goes in the submeridional direction to the east, crossing the northwestern part of the Black Sea and the central part of the Azov Sea. Further, it skirts the Rostov-Salsk High of the PreBaikal basement and the Hercynian structure of the Donbas, reaches the coast of the Caspian Sea and turns to the north, towards the southern end of the Predural edge trough. Within the East-European platform lies the East-Baltic region, occupying its northwestern part and adjoining the Baltic Sea from the east.

In the west, the EEP borders on the younger Western European Platform (WEP) formed from the Paleozoic folded basement and the Mesozoic-Cenozoic sedimentary cover. The boundary between these platforms is a marginal suture along the Teisseyre-Tornquist line, which is also defined as the Trans-European Suture Zone (TEZZ) separating the EEP from the WEP.

The total area of the EEP is about 5.5 million km$_2$. The EEP includes the Baltic and Ukrainian shields as well as the Russian plate, which occupies 2/3 of the EEP territory and completely defines its boundaries in the east and south. The boundaries of the EEP in some places are very conditional. However, if the region of the spread of the Paleozoic Plate cover is taken as the criterion for the boundary of the Russian Plate on the one hand while the position of the areas of manifestation of the Paleozoic and a younger

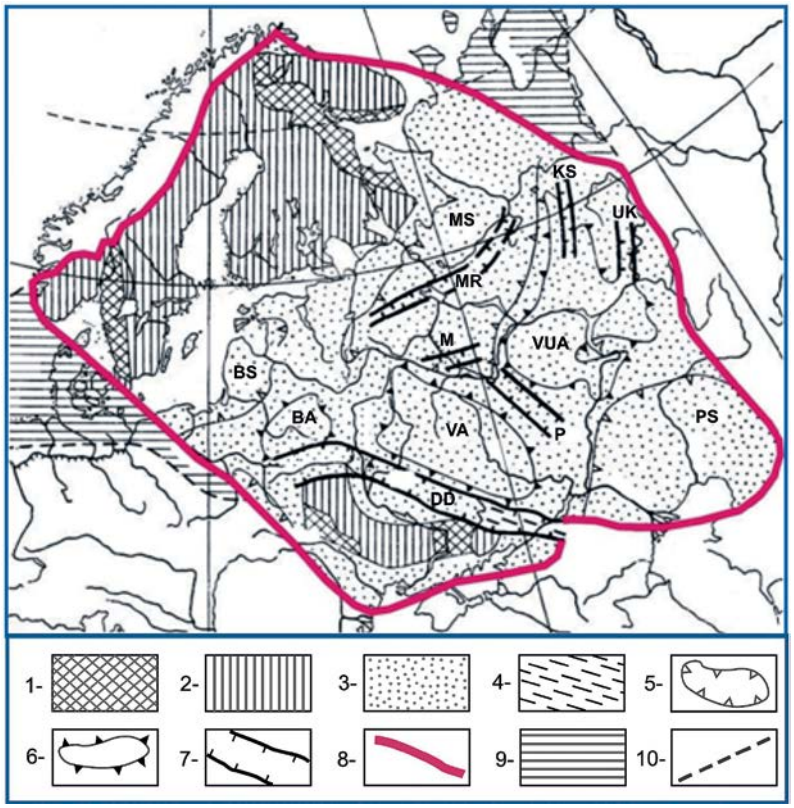

Figure 25. Tectonic structure of the East European Platform

[http://bse.sci-lib.com/article006811.html]

Legend: 1 – highs (outcrops to the surface) of the Archaean basement (>2,500 million years); 2 – highs (outcrops to the surface) of the Karelian foundation (> 1,600 million years); 3 – epi-Karelian cover; 4 – folded structure of Donbas; 5 – syneclises (BS – Baltic, MS – Moscow, PCS – Pre-Caspian); 6 – anteclises (BA – Byelorussian, VA – Voronezh, VUA – Volga-Ural); 7 – avlakogenes (UK – Verkhnekamsk, DD – Dneprovodonetsky, KS – Kazan-Sergievsky, M – Moscow, P – Pachelmsky, MR – Middle Russian); 8 – platform boundaries; 9 – areas with the Baikal folded foundation; 10 – boundaries of territories with the Baikal folded foundation

folding is taken on the other hand, then the southern boundary only of the plate in the northern Black Sea region cannot be strictly justified [Юдахин и др., 2003].

The crystalline basement plays a leading role from the point of view of the geological environment, in which important seismotectonic processes occur. Most foci of earthquakes are located inside the Earth's crust, at a depth of 1 to 10 km. Therefore, it seems important to consider the deep structure, the structure of the basement and the processes of its evolutionary formation, primarily geographically close to the East Baltic region. Since there is still no consensus on the structure of the East European basement, the next chapter will consider some of the most common points of view based primarily on deep seismic sounding.

2.2.1. Overview of evolutionary processes of the formation of East European Platform and main elements of its geological structure

Currently, more alternative points of view exist on the structure of the basement of the East European Platform.

In the earlier period of studying the structure of the EEP, in accordance with the views of a number of researchers [Павловский, 1965; Муратов, 1979] the most ancient protoplatform complex was singled out. It was formed during the creation and development of the folded metamorphosed base of ancient platforms. The oldest platform cover consists of the products of erosion of the Archaean crystalline basement. Within the EEP, the protoplatform cover has a limited spread on the slopes of the Baltic Shield, in the Ladoga Avlakogen, on the southern coast of the Kola Peninsula, in the northern part of the Volga-Urals anteclise, under the sedimentary cover of the Voronezh anteclise. In the structure of the protoplatform covers, two complexes are distinguished: the lower and the upper. They differ in the degree of dislocation and metamorphism [Муратов, 1979]. In addition to the protoplatform complex, the cataplatform complex and directly the plate complex are distinguished. The sedimentary cover of ancient EEP began to form from the upper Proterozoic [Муратов, 1979].

Yudakhin et al. [Юдахин и др., 2003] adhere to a similar position in the structuring of the Earth's crust. They also note two stages in the development of platforms. At the early stage, the structure of the basement was formed, and at the later stage the Riphean-Phanerozoic structural formation complex was created. In the last stage of development, a typical platform cover was formed, which covers large areas of the basement. In the Riphean-Phanerozoic complex, 6 structural floors are distinguished. The two lower structural floors correspond to the conditions for the development of mobile platforms (avlakogenic stage), and the next 4 floors – to the stage of the plate development. Avlakogenes were formed not simultaneously. The most ancient avlakogenes are located on the east of the platform.

According to Academician R.G. Garetsky [Гарецкий, 2007], within the EEP there exist all types of tectonic elements of ancient platforms (Figure 26). They include shields, plates, anteclises, syneclises, pericratonic subsidences, avlakogenes, etc. He considers several stages of evolutionary development of the crust. In the first three stages (Gothic (Early Riphean), Dalsland (Middle Riphean), Early Baikal (post-Riphean/Early Vendian)), a preplate (quasi-and cataplatform) cover was formed. Other stages of the crust evolution (Late Baikalian (Early Vendian/Early Cambrian), Caledonian, Hercynian, Cimmerian, Alpine) belong to the plate period of the EEP development.

Duration of the first three stages of the evolutionary development of the crust is estimated as follows: Gothic – 1,600–1,300 million years, Dalsland – 1, 300–900 million years, Early Baikal – 900–650 million years. During the Gothic period, there was a consolidation of the EEP in the form of a single rigid block and the formation of the Rodinia supercontinent [Garetsky et al., 2006]. The early pre-rift and rift regimes and the late post-rift regime are associated with the Dalsland stage. During the early Baikal stage, the Rodinia supercontinent was split. In the northeast and southwest of the EEP, the crust was stretched, which has led to the appearance of two diagonal rift systems. At

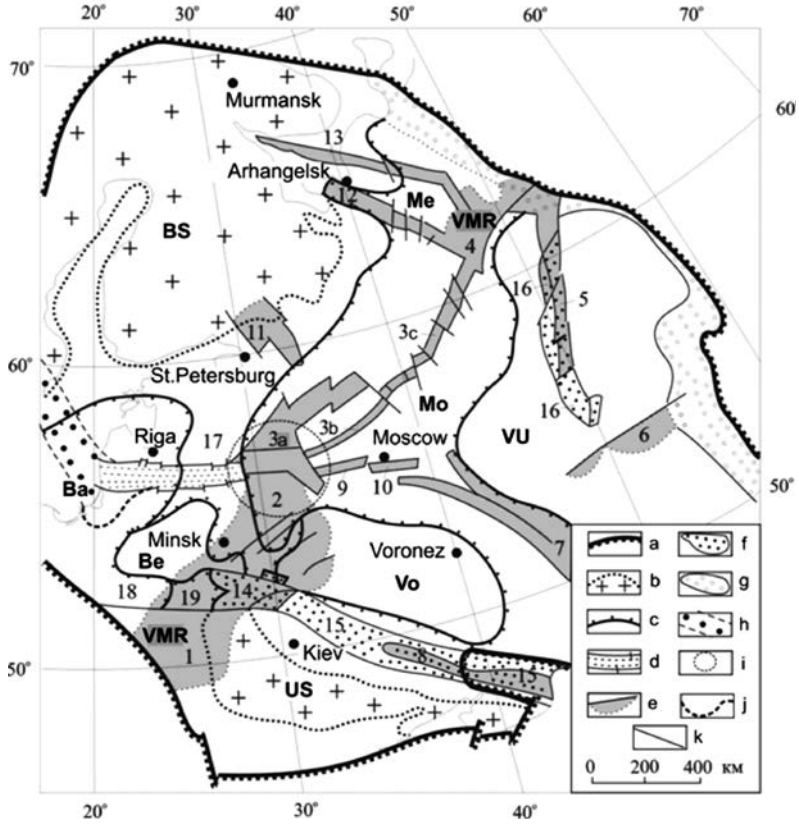

Figure 26. Scheme of main tectonic elements of the East European Platform [Garetsky, 2007]

Legend: a – boundary of the platform; b – shields (BS – Baltic, US – Ukrainian); c – anteclise and syneclise boundaries (anteclises: Be – Byelorussian, Vo – Voronezh, VU – Volga-Urals, syneclises: Ba – Baltic, Mo – Moscow, Me – Mezenskaya); d – Polotsk-Kurzeme fault belt; e – f – system of paleorifts: e – early (VMR – Volynian – Middle Russian system of troughs: 1 – Volynsky, 2 – Orshansky paleotroughs; Central Russian avlakogene: 3a – Kresttsovskaya (Valdai), 3b – Tverskaya, 3c – Sukhona branches; 4 – Yarenskaya depression; 5 – 8 – avlakogenes: 5 – Kazhimsky (Vyatka), 6 – Sernovodsko-Abdulinsky, 7 – Pachelmsky, 8 – Dneprovsky-Donetsk, 9–13 grabens: 9 – Gzhatsky, 10 – Moscow, 11 – Ladozhsky, 12 – Dvinsky, 13 – Leshukonsky; f – late (14 – Pripyatsky, 15 – Dnepro-Donetsk, 16 – Vyatka troughs); g – areas of pericratonic subsidences synchronous in development with early paleorifts; h – the Gothlandian belt; i – contour of the Slobodsky Late Proterozoic tectono-geodynamic knot; j – the complex southern boundary of the Klaipeda tectonic sigmoid; k – faults. 17–19 – structures: 17 – Latvian saddle, 18 – Podlasie-Brest depression, 19 – Polesskaya saddle

the beginning of the Early Baikal stage, the rift system of the northwestern strike was formed (Sernovodsko-Abdulinsky, Leshukonsky, Dvinsky, Pachelmsky paleorifts), and in the second half – the Volyn-Srednerussky transplatform rift belt of the northeasterly strike. It consists of three elements: the Volyn-Orsha trough, the Central Russian avlakogen and the Yarenskaya depression.

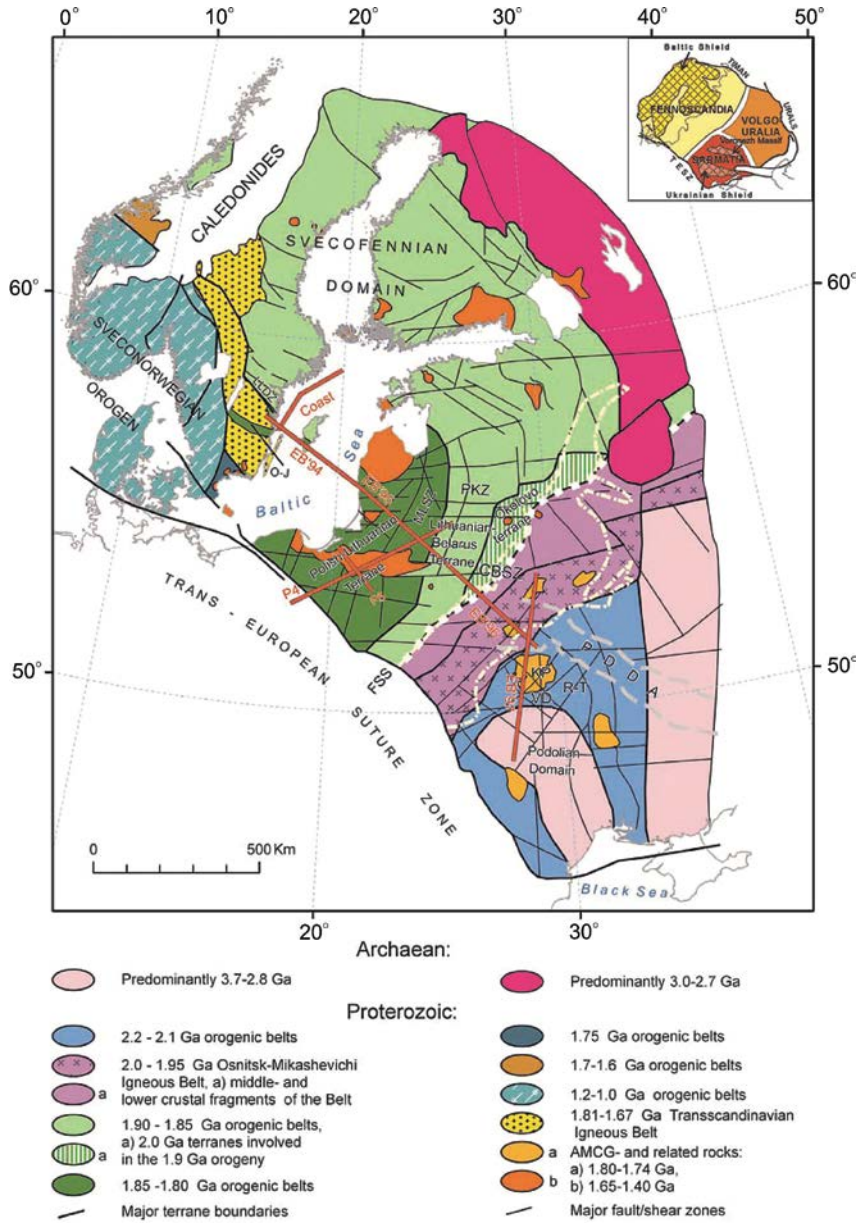

Figure 27. Main tectonic subdivisions of the crust in western part of the East European craton [Bogdanova et al., 2006a]

Designations: CBSZ – Central Byelorussian Sutural Zone; KP – Korosten pluton; LLDZ – Loftahammar-Linkoping deformation zone; MLSZ – Middle Lithuanian Sutural Zone; O-J – Oskarshamn-Jonkoping Belt; PDDA – Pripyat-Dnepro-Donetsk avlakogene; PKZ – Polotsk-Kurzeme fault zone. The dotted light line outlines the Volyn-Orsha avlakagen. The red lines show the position of the EUROBRIDGE profile (EB'94, EB'95, EB'96 and EB'97), COAST and POLONAISE (P4, P5) seismic profiles. The inset shows three segments of the East European craton [Bogdanova, 1993; Khain & Leonov, 1996]

According to the standpoint of Bogdanova et al. [Bogdanova, 1993; Gorbatschev, Bogdanova, 1993), three major segments of the Earth's crust are distinguished in the EEP: Fennoscandia, Sarmatia and Volga-Uralian (Figure 27).

These segments of the Earth's crust are separated by suture zones, i.e. deep root structures at the place of closure of the oceanic type basin. The age of the Sarmatian and Volga-Uralian segment of the Earth's crust is attributed to the Archaean. The Fennoscandian segment is formed by the Early Proterozoic crust. According to this view [Bogdanova et al., 2006a], the subduction of the Fennoscandian segment of the Earth's crust under the Sarmatian continent took place at the site of contact of Sarmatia and Fennoscandia. Between the Baltic and Ukrainian shields, there is located the Paleoproterozoic and juvenile crust, which has been formed by accretion plate-tectonic processes along the margins of the Archean and Early Paleoproterozoic cores of Fennoscandia and Sarmatia. The result of these processes was the formation of terrains – geological bodies delimited by faults and having a significant regional extent (Figures 27, 29): 1) Western Lithuanian granulite region (WLG), 2) Eastern Lithuanian-Latvian belt (EL), 3) Byelorussian-Baltic granulite belt (BBG) and 4) Central Byelorussian belt (CB). The boundaries between EL and WLG, EL and BBG are the fault systems of the submeridional strike in the vicinity of Jelgava and Valmiera.

Each terrain has its own stratigraphic, magmatic, metamorphic and structural features that determine its own tectonic history. Since the neighbouring terrains may have differences, it can witness their involvement in larger horizontal displacements. The terrains have an arcuate shape, mainly of the northeasterly strike. All the accumulated Paleoproterozoic terrains in the Baltic-Byelorussian region of Fennoscandia are younger than 2.0 Ga (2.0–1.9, 1.90–1.85 and 1.84–1.82 Ga), whereas in Sarmatia their age is greater than 2.2–2.1 and 2.0–1.95 Ga. Lithospheric deformation and magmatism of the age 1.50–1.45 Ga and Devonian rifting (splitting) were determined using the results of seismic sounding in the project of EUROBRIDGE and gravimetric models [Bogdanova et al., 2006].

In accordance with an alternative point of view [Буш и др., 2000; Аксаментова, 2004], a peculiar feature of the structure of the crystalline basement of the EEP is the submeridional orientation of the main structural elements as well as their symmetrical arrangement. The most ancient granulite and gneiss-amphibolite complexes predominate in the western and eastern geostructural areas of the EEP. They are separated by the younger Late Archean-Early Proterozoic granite-greenstone Karelian-Kursk-Krivoy Rog super-belt. The main difference between the western geostructural region and the eastern one is the deeper processing (transformation) of the basement in the first of them [Гарецкий, 2007].

As noted above, most intraplate earthquakes are confined to internal rifts and continental rift margins. Therefore, when characterizing the geotectonic conditions for the formation of EEP, we first of all pay attention to such structures.

According to Yudakhin et al. [Юдахин и др., 2003], the Baikal cycle played a leading role in the development of the paleoreefs (avlakogenes) of the EEP. During this period, a network of avlakogenes originated and began to develop. Later, at the plate

stage of development the avlakogenes practically did not appear. Only the existing ones experienced the activation of tectonic movements and inversion. The system of Riphean avlakogenes overlapped the ancient metamorphic base almost simultaneously with the appearance of the Late Proterozoic geosynclinal belts.

Considering the central part of the EEP, i.e. the Russian Plate located between the Baltic Shield in the north, the Ukrainian Shield in the South, the Pre-Ural Trough in the East, Yudakhin et al. [Юдахин и др., 2003] note the orientation of the avlakogenes in three dominant directions (northwest, northeast and meridional). In their opinion, the formation of avlakogenic structures proceeded from the north or northeast while the southwestern part of the platform was not crushed. According to these ideas, the buried Riphean avlakogenes, except the Middle Paleozoic Dnepro-Donetskiy, are assumed to be in the base of the Upper Paleozoic Oslo Graben and the Baltic syneclise. During the Hercynian stage of development of the Russian Plate (the stage of platform formation), tectonic movements were activated in the riftogenic areas. In the Devonian, opening of the Dnieper Graben took place, and the Pripyat Graben was developing in the Upper Devonian. In the Late Paleozoic and Early Permian, the tectonomagmatic activation process covered the southwestern part of the Baltic Shield where the paleoriftic structure of the Oslo graben was formed.

Milanovsky, Baluev et al. [http://atlantic.ginras.ru/education/russia/lecture_04.pdf] single out 20 avlakogenes (paleorifts) in the territory of the EEP. They are usually confined to the places of mobile belts of the preplatform stage or to major disturbances in the basement. Powerful thicknesses of sediments are concentrated in avlakogenic troughs, which are the sources of most fold systems on the platforms.

Most of the territory of the East European Platform is covered with a sedimentary cover. The exception is the Baltic and Ukrainian shields. Formation of the structure of the basement, and then of the Riphean-Phanerozoic structural formation complex, corresponds to the two stages of the crust evolution. The sedimentary cover of ancient EEP began to form since the Upper Proterozoic. A new understanding of the formation processes of the Earth's crust of the EEP, in particular the Paleoproterozoic processes of continental collision and crustal accretion between the main structural elements of the EEP – Fennoscandia and Sarmatia. In the process of subduction of Fennoscandia under the Sarmatian continent, the Paleoproterozoic and juvenile crust was formed, represented as a system of individual terrains, extended geological bodies confined by the faults. The system of avlakogenes – ancient paleorifts formed during the Baikal cycle, is located in the central part, in the east and south of the EEP. The Polotsk-Kurzeme belt of faults is the continuation of the sequence of structures forming the northeastern and central part of the Volyn-Middle Russian system of troughs. In the west, the Polotsk-Kurzeme belt of faults, crossing the Latvian Saddle and the Baltic Syneclise, passes into the Gotland belt.

After consideration of evolutionary processes that characterise formation of the East European Platform and the basic elements of its geological structure, it is expedient to proceed with the consideration of the deep geological structure of the western part of the EEP and the East-Baltic region, as a potential indicator of seismotectonic processes.

2.2.2. Deep geological structure of western part of the East European Platform

The deep geological structure allows to have an idea of the thickness of the Earth's crust, the morphology of the main interfaces in the Earth's crust and the Moho boundary between the crust and the upper mantle, and the velocities of propagation of seismic waves in the Earth's crust. As will be shown later (Chapter 5), some of these parameters can be considered as indicators of seismicity (the relief of the Moho surface, the boundary velocity of longitudinal seismic waves on the Moho surface), or as necessary intermediate data for estimating other probable seismicity indicators (depth anomalies of gravity force).

In the study of the deep geological structure of the East European Platform, the deep seismic sounding (DSS) method is of primary importance. Over the last 30 years, this method enabled to obtain new data on the deep geological structure of the Earth's crust of the northwestern part of the EEP and to significantly improve the understanding of conditions for the formation of a modern geological situation in the East Baltic region.

The first studies with deep seismic sounding (DSS) in the west of EEP were carried out along the DSS profile Sovetsk-Riga-Kohtla-Jarve in 1982–85 [Садов & Пензина, 1986_*upm*]. They made possible to obtain the first data on the deep geological structure of the East Baltic region and the seismic velocities in the depths of the crust [Анкудинов и др., 1991].

It was established that the Earth's crust of the East Baltic region consists of 3 parts (Figure 28): northern (PK 420-600), central (PK 170-420) and southern (PK 130- 170). The northern and southern parts are separated into separate blocks and have a minimum thickness of the Earth's crust of 46 and 40 km, respectively. The Moho surface is characterized by a calm character. In the central part of the section, the thickness of the crust increases

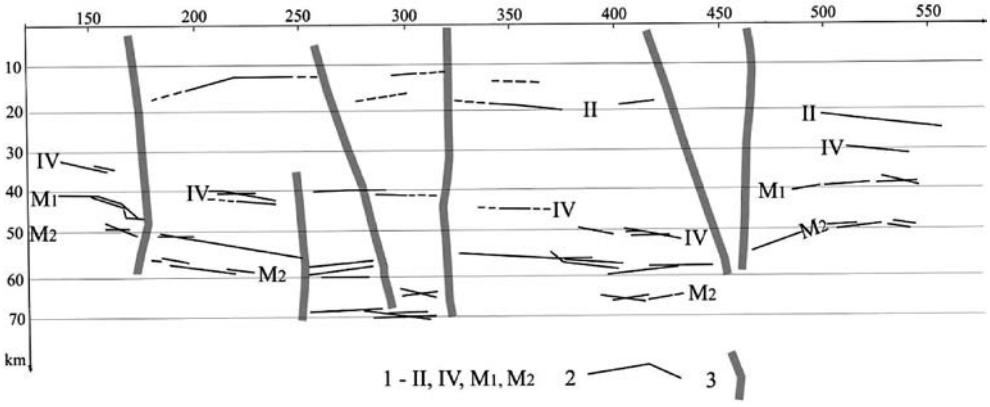

Figure 28. Crustal blocks in the East-Baltic region according to the data of DSS Sovetsk-Riga-Kohtla-Jarve [based on the materials of Садов & Пензина, 1986_upm]

Legend: 1 – indices of intracrustal boundaries II and IV, Mohorovicis boundary M1 and intramantle boundary M2; 2 – horizontal interfaces II, IV, M1 and M2; 3 – deep tectonic faults

significantly reaching its maximum (64 km) near the pikets PK 290-320. The bottom of the Earth's crust has a complex relief under the influence of tectonic disturbances that divide the central part into several blocks. As a result, on the profile Sovetsk-Riga-Kohtla-Jarve there are singled out 5 independent blocks: Northern, Riga, Kurzeme, Curonian and Neman.

Based on the apparent block divisibility of the Earth's crust (Figure 28), four regions were singled out, which correspond to different horizontally layered seismic models [Садов & Пензина, 1986_*ipm*]. For all models, the common is the presence of 5 layers corresponding to the number of wave groups recorded in the wave field. The upper, layer I with thickness of 0.6–2.0 km and boundary P-wave velocities = 2.6–3.0 km/s correspond to the sedimentary layer. The lower boundary of layer II is associated with the surface of the basaltic layer at the depth 14–22 km and the boundary velocity = 6.6–6.4 km/s. The third layer is characterized by thickness of 20–22 km. Its bottom coincides with the boundary IV and corresponds to the lower horizons of the basalt layer. At the boundary IV, the velocity = 7.2–7.5 km/s. The fourth layer is located between the boundary IV and M. Its thickness is variable, from 5 to 17 km. On the Moho boundary, the boundary velocity = 8.0–8.2 km/s. The fifth layer is located below

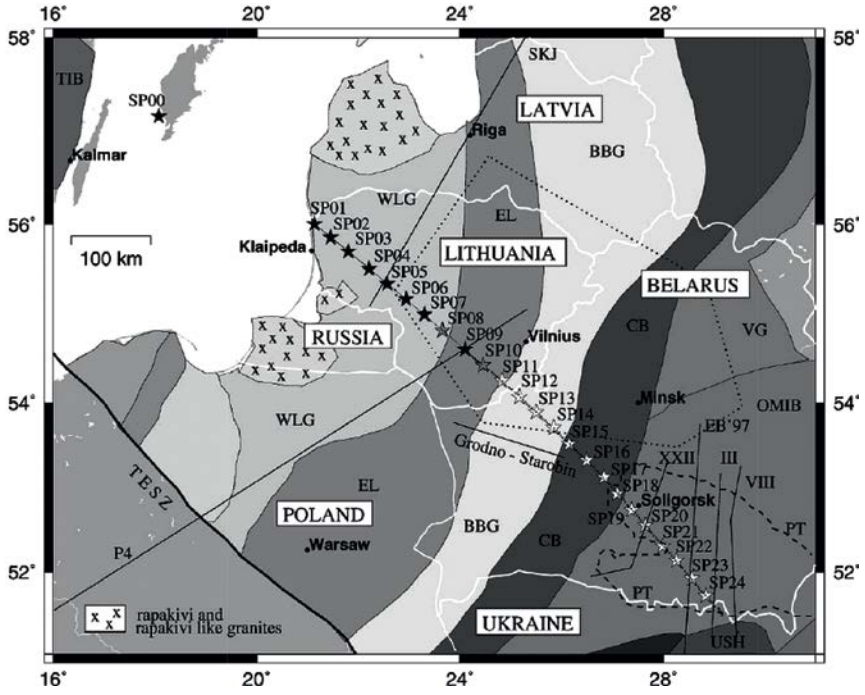

Figure 29. DSS profile of Eurobridge in the territory of Lithuania, Belarus and Ukraine

*Legend: geological structures: TEZS – craton boundary, TIB – TransScandinavian Igneous Belt, WLG – West Lithuanian Granulite domain, EL – East Lithuanian-Latvian Belt, BBG – Byelorussian-Baltic Granulite Belt, CB – Central Byelorussian Belt, VG – Vitebsk Granulite domain, OMIB – Osnitsk-Mikashevichi Igneous Belt; DSS profiles: P4 – Polonaise, SKJ – Sovetsk-Riga-Kohtla-Jarve; SP** – shotpoints on Eurobridge profile*

the Moho boundary, in the subcrustal layer. Its lower boundary is not traced. The layer velocities reach = 8.5 km/s.

Investigation of deep crustal structure of the East Baltic region was continued in the middle of the 1990s. During this period, new data was obtained on the deep geological structure of the southwestern part of the East European Craton (the term craton will be further used instead of the platform). Within the projects *Eurobridge* 1994/1997 and *Polonaise* 1997, deep structure studies were mainly based on the use of the DSS method (Figure 29).

The studies were of fundamental importance for a clearer understanding of the deep geological structure, the formation and development of large segments of the Earth's crust and geodynamic processes in the western and southwestern part of the East European Craton. The 1,500 km long DSS profile stretches from southwestern Fennoscandia to the Ukrainian Shield and crosses a number of large tectonic subdivisions of the Earth's crust – the terrains (Figure 29).

The main objective of the *EUROBRIDGE* project was to test the fundamental hypotheses about the formation of the East European Craton, with an emphasis on the study of the connection area between Fennoscandia and Sarmatia [Bogdanova et al., 2006a; Bogdanova et al., 2006b]. A new study demonstrated that the system of Neo-Mesoproterozoic reefs was superposed on previously unknown, Late Paleoproterozoic sutures. These sutures are located at the place where three independent segments of the Earth's crust (Fennoscandia, Sarmatia and Volga-Uralia) have collided, thus forming the East European Craton [Bogdanov 1993; Gorbachev and Bogdanova 1993; Bogdanova et al. 1996; Bogdanova et al. 2005].

According to the results of the *EUROBRIDGE* [Bogdanova et al., 2006a] project and geophysical modelling performed along the southwestern part of the craton, it is assumed that the Central Belarus Suture Zone (CBSZ) is a junction, buffer between two colliding segments of the Earth's crust – Fennoscandia and Sarmatia (Figure 30). The buffer is represented as a visibly deformed crust with the presence of a metamorphic crustal complex. 1.80–1.74 billion years ago (Ga) the post-collisional expansion and

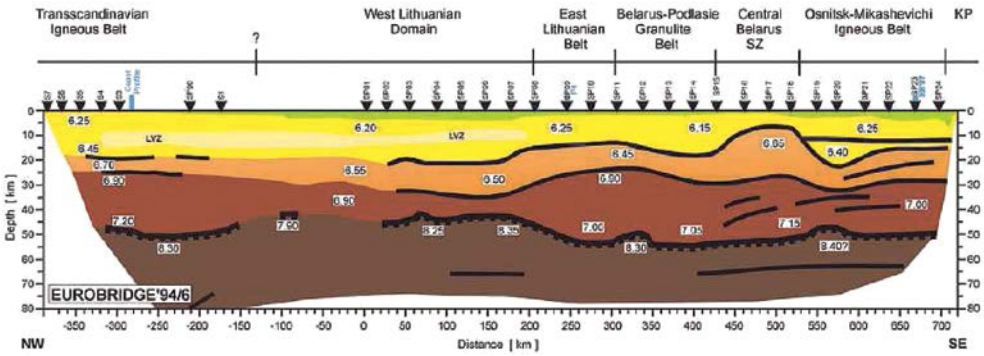

Figure 30. Model of crustal-mantle section along Eurobridge'94/96 profile [Bogdanova et al., 2006a]

magmatism affected a part of Sarmatia adjacent to the CBSZ and created a layer with a high velocity V_p = 6.65 km/s at the base of the crust (Figure 30).

Inside Sarmatia and in the Polish-Lithuanian part of Fennoscandia, there are located other individual suture terrains of different ages (West Lithuanian Domain – WLD, East Lithuanian Belt – ELB, Belarus-Podlasie Granulite Belt and Osnitsk-Mikashevichi Igneous Belt, respectively).

Retreats and unevenness of the Moho boundary and lateral changes in petrophysical properties and compositions in the upper mantle are interpreted as "petrified" Paleoproterozoic subduction and collision zones [Bogdanova et al., 2006]. This is especially true for the Central Belarus Suture Zone (CBSZ), between the Fennoscandian and Sarmatian terrains. The boundary between Fennoscandia and Sarmatia is determined by the main Minsk fault, which is superposed on the suture zone.

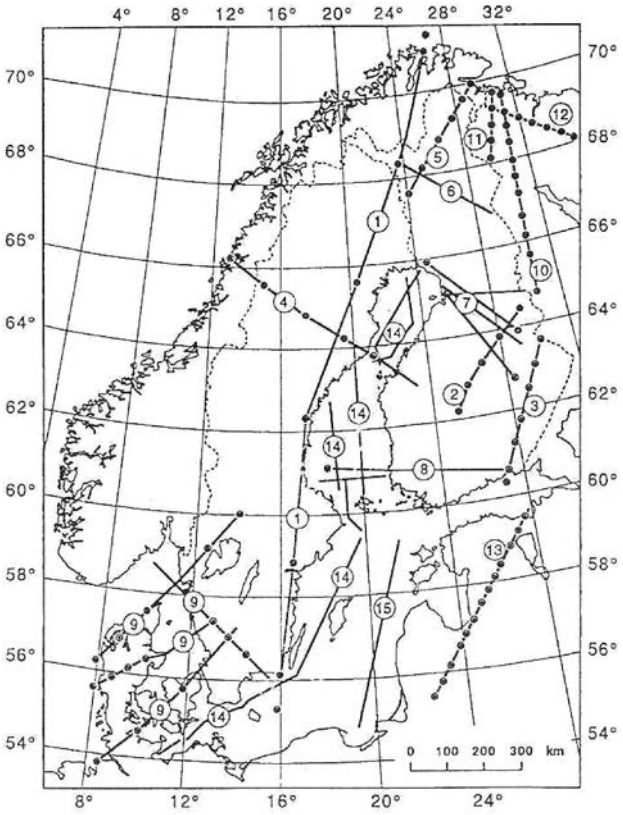

Figure 31. Seismic profiles by method of reflection and refraction at the Baltic Shield, in the Baltic Sea and in western part of the EEP [Ostrovsky et al., 1994]

Designation of seismic profiles: 1 – FENNOLORA; 2 – SVEKA; 3 – BALTIC; 4 – BLUE ROAD; 5 – POLAR; 6 – FINLAP; 7 – BOTHNIAN; 8 – SYLEN-PORVOO; 9 – EUGENO-S; 10 – PECHENGA-KOSTOMUKSHA; 11 – PECHENGA-LOVNO; 12 – NIKEL-UMBOZERO; 13 – SOVETSK-KOHTLA KARVE; 14 – BABEL; 15 – BALTIC SEA

In addition to the above profiles, other seismic studies were performed in the western and north-western (Baltic Sea) parts of the EEP and at the Baltic Shield [Ostrovsky et al., 1994]. The DSS profile of *BALTIC SEA* stretched from the Gdansk Gulf towards the coast of Finland and is located approximately 60–65 km from the coast of Latvia (Figure 31).

As a result of the studies, it was established that the depth of the Moho boundary in the Teisseyre-Tornquist zone varies intermittently from 30–35 km on the Paleozoic West European Platform up to 42–47 km on the Precambrian East European Platform [Ostrovsky et al., 1994]. However, the most important result of these studies was that, according to Ostrovsky et al., a depression at depth of 45 km was found in the central part of the *BALTIC SEA* profile. It is confined by 2–3 km steps and an uplift from both sides. Width of the depression is about 150 km (Figure 32). Similar depression can be traced at *FENNOLORA* and *BABEL* profiles. Velocities in the upper mantle vary from 7.8 km/s under depression to 8.1 km/s away from it. The P-wave velocities V_p are determined by a three-layer model with velocities 5.8 to 6.3 km/s, 6.3 to 6.7 km/s and 6.9 to 7.1 km/s. Velocities in the crust change laterally, reaching its minimum inside the central depression.

Surface of the Moho boundary in the considered part of the East Baltic region is located at average depth of 40–50 km (Figure 33) [Grad et al., 2009]. Depth of about

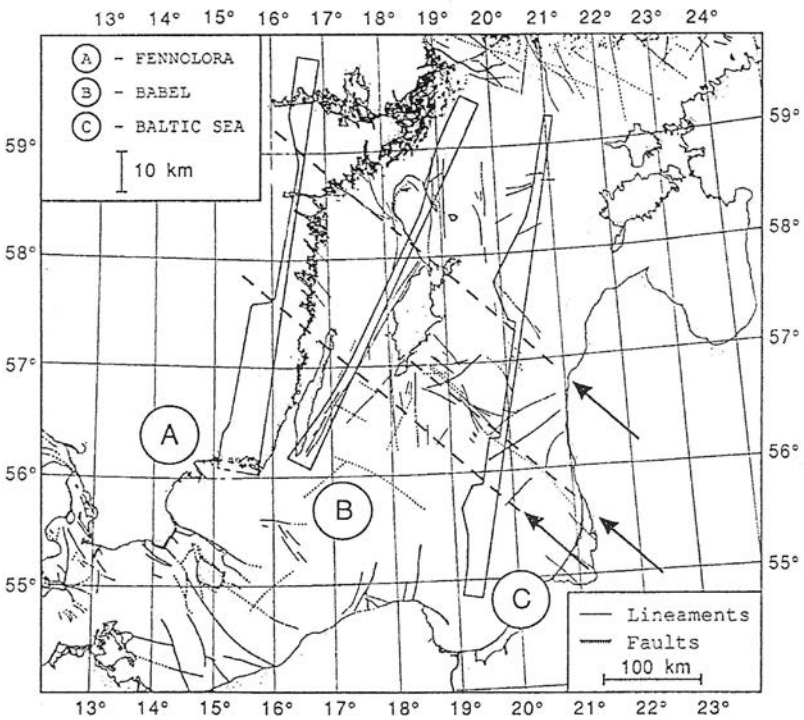

Figure 32. Comparison between the results of studying the Moho surface at profiles FENNOLORA, BABEL and BALTIC SEA [Ostrovsky et al., 1994]

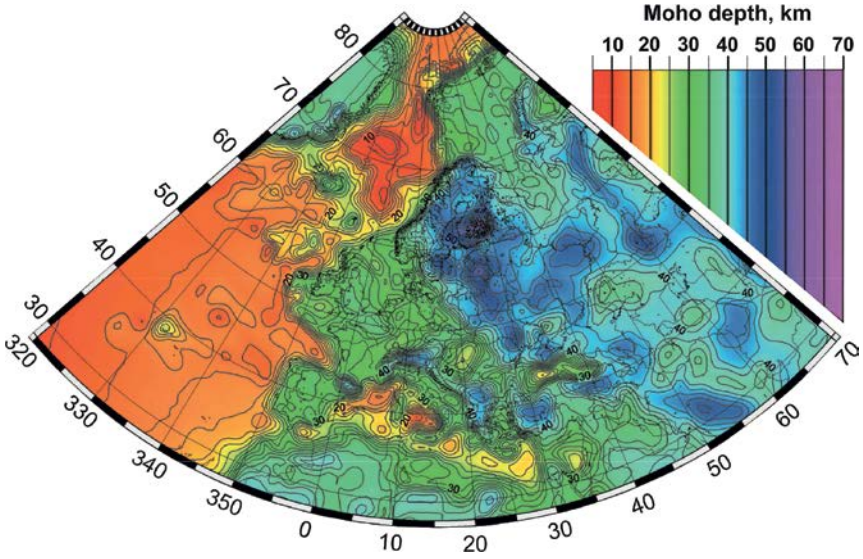

Figure 33. Map of depth of the Moho boundary in the European Plate [Grad, Tiira et al., 2007]

45 km is typical for the territory of Lithuania, western and eastern Latvia. In northern and central Estonia, depth of the Moho surface is about 40–45 km. In the Kaliningrad Region of Russia, depth of the Moho surface is slightly over 40 km. In the Leningrad Region of Russia it reaches 40–45 km. The deep structure of the St. Petersburg region has been studied in seismic works of Litvinenko et al. [Литвиненко и др., 1982]. In the central part of Latvia, thickness of the Earth's crust increases significantly, reaching its regional maximum of 64 km [Анкудинов и др., 1991].

The most important role from the standpoint of seismotectonic indicators is played by tectonic faults in the basement and sedimentary cover. A significant part of the faults in the basement and sedimentary cover of the East Baltic region was identified as a result of DSS (Deep seismic sounding) seismic reflection method and seismo-acoustic profiling in the Baltic Sea offshore area.

The main fault network was formed in the Paleozoic times and refers to the epochs of the post-Baikal, Caledonian and Hercynian tectogenesis. Major regional tectonic dislocations and zones of tectonic faults are the Liepāja-Riga-Pskov Rift Zone, which crosses the territory of Latvia from the southwest to the northeast. In the region of Valmiera, the area of tectonic faults turns to the east and then extends almost in the sub-latitudinal direction. On the border of Latvia, Lithuania and Belarus, a sublatitudinal Kurzeme-Polotsk zone of tectonic faults is distinguished [Каратаев и др., 1993]. This zone includes the Bauska fault, with which is associated one of the first historical earthquakes in the Baltic region in 1616.

In Estonia, the Pärnu-Tapa fault zone extends from the Gulf of Finland to Pärnu in northeast to south-west direction. In the Kaliningrad Region of Russia, the Pregolian fault zone extends southward of the Sembian Peninsula in the sublatitudinal direction.

The very peninsula is crossed by a diagonal fault system, while its western coast has a neotectonically active system of submeridional disturbances.

Thus, new data obtained with the use of geological and geophysical methods, and especially the DSS method, allowed to achieve a better understanding of the deep structure of the Earth's crust in the EEC, as well as the characteristics of potential seismicity indicators – the tectonic faults.

2.2.3. Assessment of geodynamic potential of the East Baltic Region

One of parameters characterizing the geodynamic potential is the isostatic equilibrium index. This is especially true for territories that have experienced a glacial load and subsequent recovery during the interglacial epochs. The DSS method provides a valuable information for assessment of physical properties of individual structural floors and analysis of isostatic state of the Earth's crust. Therefore, for the East Baltic region the assessments of isostatic state of the Earth's crust were performed based on the results of the DSS along the Sovetsk-Riga-Kohtla-Jarve profile.

For small spaces (length of the DSS profile Sovetsk-Riga-Kohtla-Jarve reached 600 km), it would be inexpedient to use the classical approach to assessment of isostatic state of the Earth's crust in the denser layer of the upper mantle, the asthenosphere. The explanation is that the short-wave relief is maintained mainly by the rigidity of the lithosphere while the longer-wave relief – by hydrostatic forces that act on the lithosphere pressed into the mantle [Turcotte & Schubert, 1985]. In other words, the isostasy is not local since sufficiently large blocks are in isostatic equilibrium (about 100 km for platforms [Артемьев, 1975]) and therefore in the classical approach (Pratt model) to the equilibrium estimate the isostatic equilibrium disturbances can be unnoticed for smaller in size blocks of the Earth's crust. Therefore, a method of estimating the isostatic index at the level of the Mohorovicic boundary was used, which is more suitable for studying the isostatic equilibrium disturbances of small-scale blocks of the Earth's crust. The essence of the method was that the Archimedean equilibrium of the Earth's crust confined from below by the Moho boundary (A-equilibrium) [Файтельсон, 1973] was considered, in contrast to the traditional isostatic equilibrium type when the pressure equalization occurs at some depth of compensation, i.e. at the level of the asthenosphere (P-equilibrium). A-equilibrium is the Archimedean equilibrium of the Earth's crust confined from below by the Moho boundary located above the upper mantle. With P-equilibrium, pressure equalization occurs at a certain depth of compensation, i.e. at the level of the asthenosphere, about 100 km.

The results of the DSS for studying the depth structure of the Earth's crust along the Sovetsk-Riga-Kohtla-Jarve profile [Анкудинов и др., 1991] made it possible to generalize the physical properties of the medium along structural floors, to create density models of the sedimentary cover, the crystalline basement, the lower part of the Earth's crust and test them when modelling the gravitational effects from various structural floors [Озолиня & Ковригин, 1986_*upr*]. One of the main results was that after exclusion ("subtraction") of the effects of the sedimentary cover and the basement, the hypsometric position of boundaries M1 and IV is mainly "displayed" in the residual gravitational field g_{res}.

The conditions of equilibrium of the Earth's crust at the level of the Moho boundary can be represented by the formula:

$$m_M - m_C = \Delta m \quad (1)$$

$$-\rho_m h_t + \sum \Delta\rho_{mi} H_i = \Delta m \quad (2)$$

$$-\rho_m h_t + \Delta\rho_{mw} H_w + \rho_{mS} H_S + \Delta\rho_{mg} H_g + \Delta\rho_{mb} H_b = \Delta m \quad (3)$$

here, m_M – mass of mantle displaced by the crust; m_C – mass of the crust; Δm – indicator of the crust A-disturbance disturbance; $h_t = h + T_0$; h – altitude of location; T_0 – assumed absolute depth to the mantle in the absence of load – the crust; $\Delta\rho_{mi} = \rho_m - \rho_i$; $\Delta\rho_{mw} = \rho_m - \rho_w$, where ρ_m, ρ_i, ρ_w, ρ_S, ρ_g, ρ_b – densities of the upper mantle (index), i – layer of water (w), precipitation (S), "granite" layer (g) and "basalt" layer (b), H_i, H_w, H_S, H_g, H_b – thicknesses of the Earth's crust layers.

Physical meaning of Δm is the difference in crustal and mantle masses per unit of area when in the vertical column of the geological substrate the mantle mass displaced by the crust (m_M) is not equal to the crustal mass (m_C) in accordance with equation 1.

The results of the estimation of the isostatic index Δm by the type of A-equilibrium were compared with the geological-geophysical and geodetic parameters along the Sovetsk-Riga-Kohtla-Jarve DSS profile (Figure 34) [Nikulin, 1997; Nikulin, 1999; Никулин, 2008b]: 1) the observed gravitational field Δg_B of the normalized level [Озолиня & Ковригин, 1986_*upm*]; 2) density of the heat flux Q [Zazimko & Sokurenko, 1994_*upm*]; 3) neotectonic vertical movements A_{Nm}, beginning with Rupelian [Garetsky et al., 1999]; 4) velocity of modern vertical motions V_{mvm} [Ковалевский и др., 1966_*upm*].

Analysis of the correlation of the isostasic index Δm with the indicated geological-geophysical and geodetic parameters showed that the strongest relationship was established between Δm and V_{mvm}. In this case, the correlation coefficient $CC_{\Delta m\&V mvm} = 0.8$. Although V_{mvm} was used only for the territory of Latvia, nevertheless the connection is quite expressive. The maximum of the isostatic index $\Delta m = 6.0$ kg/m^2 is noted on the section between pickets 390–400, which are located 5–10 km southwest of Cesis. Here the Ieriķi uplift is located, distinguished in the Hercynian structural complex. According to the results of the leveling performed during 1935–1965, it was just the geodetic benchmark of Ieriķi that moved with the maximum velocity among modern vertical movements observed in Latvia: $V_{mvm} = 3.5$ mm/year [Ковалевский и др., 1966_*f*]. The error in estimating the isostasic index $\varepsilon_{\Delta m}$ does not exceed ± 2.5 ÷ ± 3.0. Thus, the maximum value of the isostasic index coincides with the maximum value of velocity of modern vertical movements of the Earth's crust in the Ieriķi region. Moreover, here the maximum value of the total amplitudes of vertical neotectonic motions is located. Consequently, the uplift in the Ieriķi region takes place already for a long time, at least during the neotectonic stage (early *Oligocene* – *Quaternary*) estimated at 35–37 million years. Here is also located the local maximum of the heat flux density Q.

The multiple regression analysis has demonstrated that the closer relationship ($CC_{\Delta m\&(\Delta g B\_hor.grad + Q)} = 0.55$) is noted between Δm on one hand and the horizontal gradient Δg_B and Q on the other hand. The obtained multiple regression equation was used for the prediction of Δm from the given values of $\Delta g_{B\_hor.grad}$ and Q. It allowed to identify

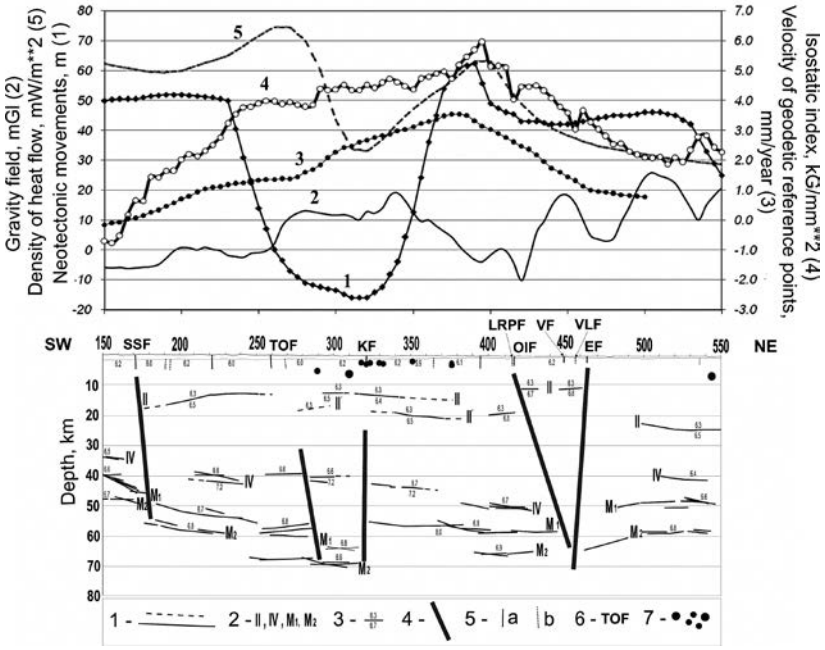

Figure 34. Deep structure of the Earth's crust and upper mantle in the East Baltic region and geological and geophysical parameters along DSS profile Sovetsk-Riga-Kohtla-Jarve [Никулин, 2008b]

Legend on the upper graph: 1 – summary amplitudes of neotectonic vertical movements in m, beginning with Rupelian; 2 – relative observed gravitational field, mGal; 3 – velocity of modern vertical movements of the Earth's crust, mm/year; 4 – isostatic index, kg/mm2; 5 – density of heat flow, mW/m2. Legend on the depth section: 1 – interfaces in the Earth's crust and upper mantle (confident and assumed); 2 – indices of interfaces in the Earth's crust and upper mantle; 3 – average (top) and boundary (bottom) velocities of longitudinal seismic waves, km/s; 4 – deep tectonic faults in the Earth's crust and upper mantle; 5 – tectonic faults penetrating (a) and non-penetrating (b) into the sedimentary cover; 6 – abbreviation of tectonic faults; 7 – hypocenters of earthquakes. Fault designations: SSF – South Šilalas; TOF – Taurages-Ogre; KF – Ķekava; LRPF – Liepāja-Riga-Pskov; OIF – Olaine-Inčukalns; VF – Valmiera; VLF – Valka; EF – Ērģeme

five abnormal regions with a positive value of the isostasic index ($\Delta m \geq +5.0$): 1. Bārta, 2. Dobele – Jaunbērze, 3. Kursenai – Joniskis, 4. Inčukalns, 5. Valmiera. Four sections with a negative value of the isostasic index ($\Delta m \leq -0.5$) were also identified: 6. Rucava – Telsiu, 7. Palanga – Kretinga, 8. Ziemupe, 9. Oglaine. Taking into consideration the error in estimation of the isostasic index, negative anomalies cannot be interpreted. For purposes of interpretation, the model proposed by Faytelson was used [Резанов, 1974].

The same directions of motion on the Earth's surface can be caused by different deep-seated processes. In order to determine the type of development of the crust (Figure 35) in each particular case, in addition to the sign of the crustal movement (uplift or lowering), it is necessary to know the magnitude and sign of the deviation of this section of the Earth's crust from the corresponding Archimedean equilibrium (Table 2).

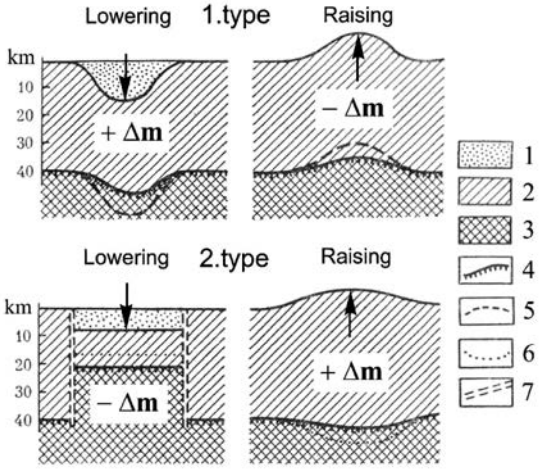

Figure 35. Types of development of the Earth's crust and direction of changes in its thickness

Legend: 1 – precipitation; 2 – consolidated crust; 3 – upper mantle; 4 – Moho boundary; 5 – supposed position of Moho boundary in case when an equivalent subsidence or uplift of Moho boundary corresponded to subsidence or rise on the Earth surface (type 1 of development); 6 – supposed position of Moho boundary in the event that the displacement of Moho boundary along a section (type 2 of development) were not accompanied by a counter-subsidence or rise of the entire crust; 7 – fault

Table 2.

Dependence of direction of leading processes on the type of crustal development

Type of development	Directionality of leading processes	Character of surfacial tectonic movements	Sign of Δm
I	Crustal subsidence	Warping	+
	Crustal recoil	Uplift	–
II	Crustal thinning from below	Warping	–
	Crustal thickening from below	Uplift	+

According to conditions of Table. 2, in the Ieriķi region where the maximum positive value of the isostasic index is noted, the crust thickens from below is in accordance with the II type of crustal development. In this case, the crust is characterized by a clearly expressed inverse relationship between the relief of the Moho boundary and the boundary of the Earth's surface. In Figure 30 it can be seen that this section corresponds to the thickness of the Earth's crust of about 58 to 59 km, which is generally larger than the average thickness of the Earth's crust estimated at 53–55 km. Thus, the Moho boundary is located at an excessive depth, i.e. deeper than necessary, which has led to a disturbance of isostatic equilibrium. The uplift of the Earth's surface in the area of Ieriķi seems to compensate for the deep processes of crust reconstruction.

Analysis of isostatic state of the Earth's crust is an important method for understanding the geodynamic development of the investigated territory. The initial

data for such analysis is primarily the data obtained on deep seismic sounding profiles, as well as other geological, geophysical and geodetic data. The complex of these data allows to identify the types of development of the Earth's crust. Identification of types of the Earth's crust allows to foresee the trend of development of geodynamic processes and therewith associated seismotectonic activation.

2.3. Basic characteristics of the EEP seismicity

The East European Platform relates to territories with a weak seismic activity. Since the study of seismicity on the platforms usually receiveslittle attention, then, as a rule, the earthquakes often turn out to be unexpected. Even the Kaliningrad earthquakes of 2004 were attributed to the category of *"exceptional earthquakes"* despite that in 1976 an earthquake with a magnitude of 4.7 already has occurred on the Osmussaar Island [Kondorskaya et al., 1988].

In the 16th–19th centuries, strong seismic events with intensity of tremors to grades VI–VIII are known [Ананьин, 1977; Special Earthquake Catalogue .., 1996].

The instrumental period of observations on the EEP began relatively recently. The most serious earthquakes relate to the historical period. Relatively weak earthquakes are recorded in the instrumental observation period. Therefore, they are rather widely represented in earthquake catalogues. However, this fact should not be misleading since weak earthquakes occurred of course also in the past but remained unnoticed due to small magnitude values, the absence of urbanized areas – the main source of information on seismic shocks and poorly developed means of communication, often even their absence, which did not allow the operative collection and analysis of information about earthquakes that have occurred.

Analysis of information on earthquakes of the East European Platform made it possible to identify and evaluate the seismic activity of its individual regions [Ананьин, 1968]. A peculiar feature of seismicity in the EEP is the dissociation of earthquake foci, i.e. the so-called background, diffuse seismicity. Nevertheless, three large areas of increased seismicity are distinguished. They include the south-eastern part of the Baltic Shield, the eastern part of the Voronezh Massif and the Ukrainian Shield, as well as the Middle Urals and the western piedmont of the Ural Mountains. The Middle Urals and the western piedmont of the Ural Mountains merge into a single transverse zone. Here, the maximum thickness of the EEP Earth's crust is observed.

Practically all foci of earthquakes are located in the Earth's crust. The intensity of tremors reaches VI–VII while the magnitude of earthquakes does not exceed 5. Most earthquakes have a small magnitude from 3 to 4. The depth of most earthquake foci is within 5 and 25 km. These include the Narva earthquake of 1881 (3–5 km), the Kupyansky earthquake of 1912 (5–10 km), the Tambov earthquake of 1954 (about 15 km), the Ladoga earthquake of 1927 (5–15 km). Only two earthquakes are known under the Earth's crust or on its boundary: an earthquake in the eastern part of Finland (1902, depth ~ 50 km) and an earthquake in the Sverdlovsk area (40 km) [Юдахин и др., 2003].

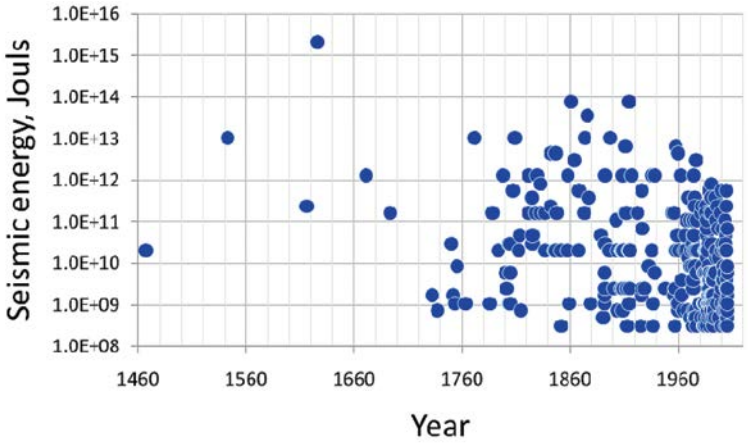

Figure 36. Seismic energy released in the East European Platform from 1467 to 2005

The diagram of seismic energy released in the territory of the East European Platform (Figure 36) demonstrates that the information on earthquakes is not uniform. In the historical period (until about 1800), information about earthquakes is negligible. For 331 years (from 1467 to 1798), there are only 18 known earthquakes. Over the period 1800 to 1948 (148 years) about 106 earthquakes are known to have occurred. And finally, over the period 1955 to 2005 (50 years), 245 earthquakes are known. Obviously, in this case it is difficult to estimate the change in seismic activity since the information has increased mainly due to the growth in the observational network of stations.

The strongest earthquakes with magnitude M > 5 and intensity of tremors in the epicenter $I_0 \geq 7$ were observed on the marginal parts of the EEP, in the Kandalakshsky Graben area (the Baltic Shield), the Ural Mountains and on the EEP boundary with Western Kazakhstan, the Caucasus, Crimea and the Carpathians [Аптикаев и др., 2012]. The strongest in the EEP earthquake in Kandalaksha in 1626 had a magnitude of 6.3 according to the Russian catalogue [Маловичко и др., 2007] and 5.1 in accordance with the FENCAT catalog. In the rest of the VEP territory earthquakes with M≤ 4.5–4.6 were observed.

According to Aptikayev et al. [Аптикаев и др., 2012], there is no strictly determined relationship between magnitude M and intensity in the epicenter I_0 for earthquakes of small magnitudes. It is asserted that in some local zones the impact of earthquakes on objects with low M values can be stronger than at higher values of M. As an example, earthquakes of 1910, 1911, 1939, 1991 in Tatarstan, Western Kazakhstan are mentioned with the ratio $I_0/M \sim 1.6–1.75$, while according to the Gutenberg-Richter formulas this ratio does not exceed 1.3 and the average value in the catalog of earthquakes on the EEP [Аптикаев и др., 2012] is ~ 1.2. It is stated that although the probability of an earthquake with M ≥ 6 in Moscow is not high, but the danger of notable seismic impacts with $I_0/ \geq 7$ is real.

Seismicity of the East European Platform and its framing territories is based on two catalogues (Figure 32).

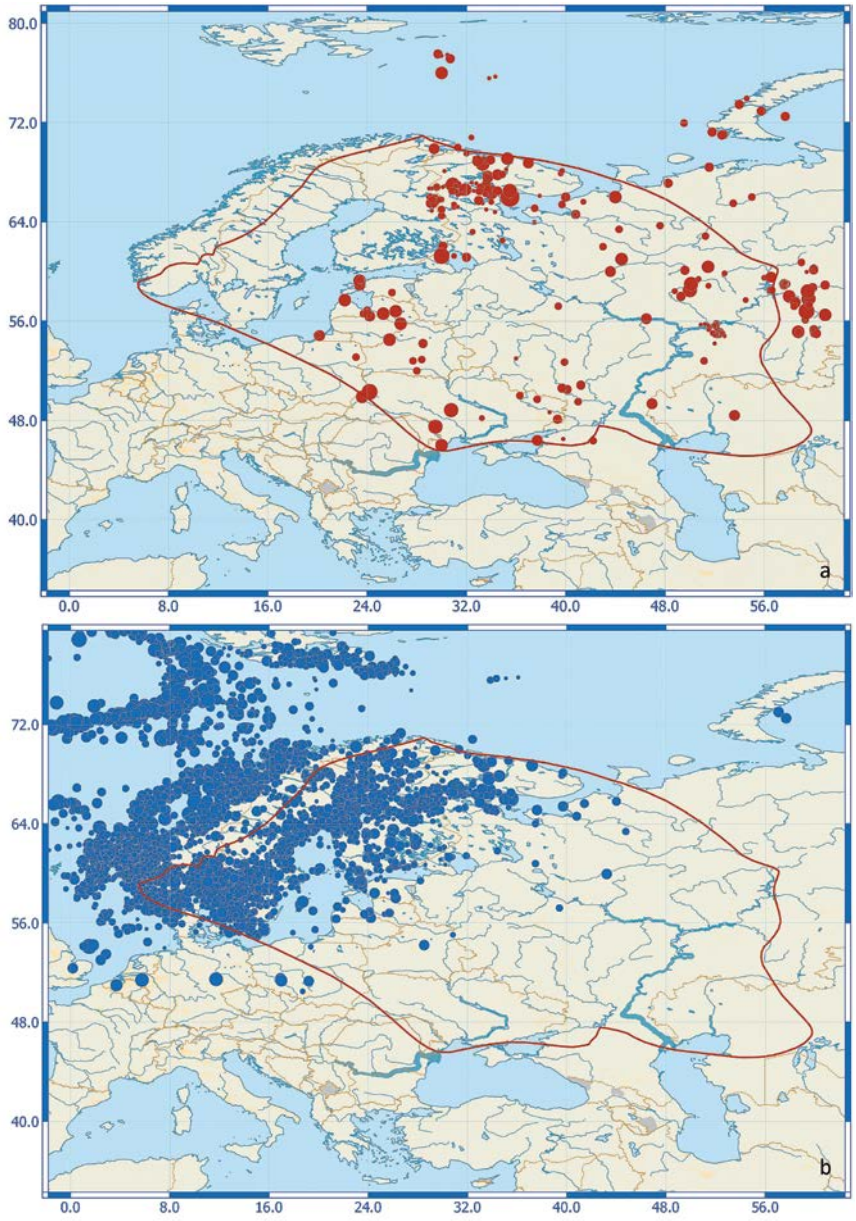

Figure 37. Seismicity of the East European Platform and its framing territories according to Russian catalogue of earthquakes (a) [Маловичко и др., 2007] and Catalogue of earthquakes in Northern Europe (b) [*University of Helsinki Institute of Seismology*]

Legend: red circles – earthquakes according to the catalogue of earthquakes of the East European Platform [Маловичко и др., 2007]; blue circles – earthquakes according to the catalogue of earthquakes in Northern Europe (Catalogue of earthquakes in Northern Europe 1375) of the Seismology Institute of Helsinki University; are shown only earthquakes for the East European platform and Northern Europe

FENCAT *(Catalog of earthquakes in Northern Europe 1375)* of the Seismology Institute of Helsinki University [*http://www.seismo.helsinki.fi/english/bulletins/catalog_northeurope.html*] includes 21,442 earthquakes that took place within the period 1375 to 2012 in the territory limited by the following coordinates: latitude 46.44° N to 85.82° N and longitude 24.96° W to 57.69° E. The magnitude range of earthquakes varied from –0.9 to 6.1. The range of focal depths varied from 0 to 197 km. In Figure 32, epicenters of earthquakes, from the Catalogue of earthquakes in Northern Europe (*FENCAT*), are shown in blue colour.

The consolidated catalogue of earthquakes in the territory of the East European Platform for the period from ancient times to 2005 [Маловичко и др., 2007] contains information on 372 earthquakes. However, several earthquakes raise doubts among the authors of the catalog [Маловичко и др., 2007] since seismic events of various genesis could be mistaken for earthquakes. Such seismic events include karst caving, pits, landslides, thunderstorms, seismic events that are questionable, or information about earthquakes not confirmed by other authors. As a result, 20 such seismic events are noted. All these dubious events were excluded from consideration. As a result, the EEP earthquake catalogue is represented by 352 tectonic earthquakes. Epicenters of earthquakes from Russian catalogue, are shown in red colour.

These earthquakes occurred within the period 1467 to 2005 in the territory confined by the following coordinates: latitude 46.0° N to 77.53° N and longitude 19.99° E to 60.9° E. The magnitude range of earthquakes varied from 2.5 to 6.3. The range of focal depths varied from 0 to 68 km. In Figure 32 they are shown in red.

First of all, attention is drawn to a much higher level of seismicity of the Baltic Shield in comparison with the rest of the territory of the East European Platform. Increased seismic activity is manifested, in particular: 1) along the coast of the Gulf of Bothnia, 2) in the southwest of Sweden (between Lillehammer and Malmö), 3) in the west of Norway (between Molde and Stavanger) and 4) on the Norwegian coast of the Norwegian Sea (between Molde and Tromsø). In the latter case, earthquakes are located already outside EEP.

Seismicity of the Baltic Shield is not uniform. The solution of the mechanisms of earthquake origins in Fennoscandia demonstrates that maximum compression is detected by analyzing the horizontal deviator stresses grouped in the NW-SE direction [Slunga & Norrman, 1984_*upm*; Gregersen et al., 1991]. This field of stresses is not affected even by significant heterogeneities in the Earth's crust of Fennoscandia region. Orientation of the maximum horizontal compression stress σ_H (Figure 38) is due to pressure from the North Atlantic Ridge.

Orientation of σ_H not inconsistent with the field of stresses arising from the postglaciation uplift after the last glaciation. In northern Scandinavia, large neotectonic faults have been discovered [Lagerback, 1988; Muir Wood, 1989], which are considered as indicators of large-scale displacements that occurred shortly after the end of the last glaciation [Lagerback, 1988]. Origins of Fennoscandian earthquakes are concentrated in specific areas of fragile and weakened crust.

The rest part of the East European Platform (without the Baltic Shield) is characterized by a relatively weak, scattered seismicity. From the standpoint of confinement of foci of

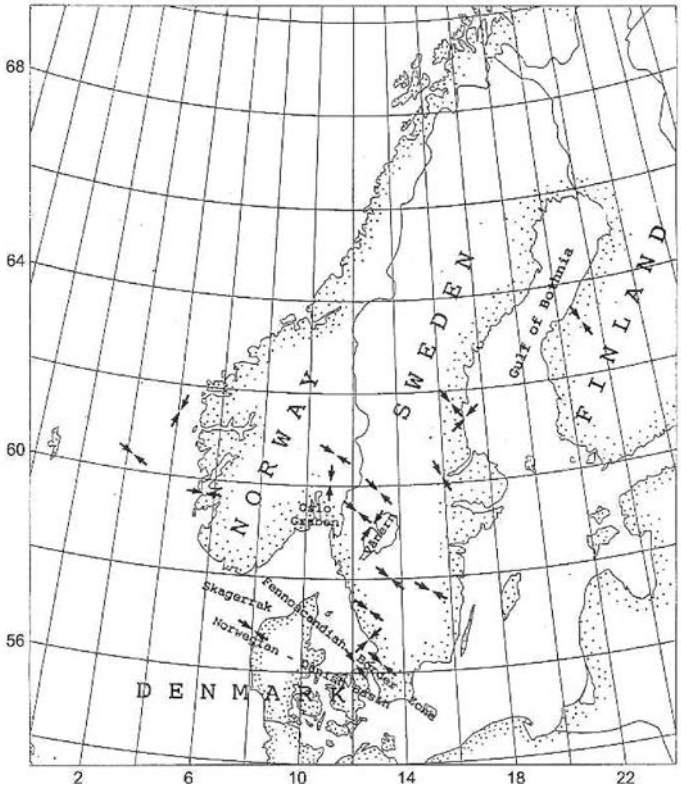

Figure 38. Orientation of generalized maximum horizontal compressive stresses [Gregersen et al., 1991]

earthquakes to the main tectonic elements of the EEP according to Garetsky [Гарецкий, 2007], the following features can be noted:

1. Concentration of foci of earthquakes in the area of the Sernovodsk-Abdulinsky avlakogen (Nizhnekamsk, Naberezhnye Chelny and especially in the area of Almetyevsk). However, these areas of seismic activity practically coincide with the areas of oil extraction. Consequently, these earthquakes belong to the category of induced seismicity.
2. Dissipated seismicity (8 earthquakes) is confined to the area of the Kazhimsky (Vyatka) avlakogene and to the Vyatka trough.
3. Dvinsky and Leshukovsky grabens (Arkhangelsk region) are characterized by insignificant seismicity.
4. Minor seismicity is noted in the southeast of the Voronezh anteclise.
5. Several earthquake foci are confined to the Dnieper-Donetsk avlakogene and the paleorift, as well as to the Pripyat paleorift, which forms a narrow strip stretching from the southeast to the northwest.

6. Two foci of earthquakes are confined to the Ukrainian Shield, and several foci of earthquakes are located along the southern boundary of the EEP, including the territory of Moldova.
7. An insignificant seismicity of the Ladoga graben can be noted, which is associated with three sources of earthquakes.
8. In the East Baltic region, several foci of earthquakes (Bauska, Jelgava, Koknese) are confined to the Polotsk-Kurzeme belt of faults.
9. Relative concentration of foci of earthquakes (5 foci) is noted on the west coast of Estonia, including the Osmussaar earthquakes of 1976. Earthquakes in Latvia (Irbene) and the Kaliningrad region of Russia are also associated with the coastal part of the Baltic Sea. Foci of earthquakes in the East Baltic region located in the coastal zone of the Baltic Sea can be associated with the depressive system of grabens formed by the Gdansk, East Gotland and Finnish grabens. At the edges of this depression system, large horizontal gradients of neotectonic movements are noted [Nikulin, 2007].

3. SEISMICITY OF THE EAST BALTIC REGION

From the standpoint of seismology, the seismicity of the northwest part of EEP, i.e., of the East Baltic Region – is of the largest concern to the Baltic States. The interest in seismicity occurred as early as in XIX century when the data describing historical earthquakes of the East Baltic Region was generalized [Мушкетов & Орлов, 1893; Doss, 1909]. In the Soviet period (the 1970s–early 19 90), certain attention was paid to seismic hazard assessment associated with the construction of Ignalina ANPP. However, those assessments were made mainly on the basis of geological, geophysical and geodetic data. The development of seismic methods as the principal source of seismicity data was initiated only at the present day – since the 1990s . This is due to urbanization process, the growth of population density, industrial potential, and the growth of power industry – including, in particular, nuclear power engineering. In this context, the risk of inflicting damage on civil, industrial, power, and ecologically destructive objects even by a relatively small earthquake with a small earthquake focus escalates significantly.

1.1. History of seismological studies in the East Baltic Region

Four periods may be highlighted in the history of seismological studies of the East Baltic Region. These periods differ in duration and in the subject matter of studies. The first period was the most extended, historical one that lasted from ancient times to the end of XIX century. Descriptions of the earthquakes that took place within that period are evidenced by various written sources, including ecclesiastic ones. Within the subsequent periods of development of seismological studies in the East Baltic Region, instrumental seismological observations were developed apart from the accumulation, collection, and analysis of earthquake data. At first, observations through long-period seismometric channels were exercised to record remote and strong earthquakes. Later, researchers started to introduce short-period and broadband channels to make records not only of remote events but regional and even local seismic ones (explosions) and earthquakes.

They commenced research to assess the seismotectonic situation, seismic hazard, and seismic risk in the study area. Thus, ever more information was made use of to carry out a seismological research. Geological and geophysical, geodynamic (crustal motions) and directly seismologic information was added to written sources. The information volume increased not only numerically but also in a qualitative sense.

1.1.1. Seismologic data collection period from the earliest times to the end of XIX century

The first period turned out to be the longest one. Within the entire period that lasted from ancient times to the end of XIX century, historical earthquakes mentioned in various sources like ancient clerical manuscripts and newspapers were spontaneously stated and described. For instance, in the work by Bruno Doss [Doss, 1909] a reference to an ancient manuscript [Mancelius, 1619] is given. A reference to *Bodeckerschen Chronik* is given, as well. In particular, a quotation from *Bodeckerschen Chronik* pointing to the date of tremor that happened near Bauska, was cited: *"Auch ist diese woche" – d.i. in der Woche des 28. Juni 1616 – "in Churland nach dem Bauske ein fross Erdbebend gehört worden"("Moreover, this week" – i.e., the week falling on June 28, 1616 – "a strong earthquake was perceived in Curland, behind Bauska").* Nevertheless, the above-mentioned time span is very important since the earthquakes documented by eyewitnesses of that time make a substantial contribution to the overall earthquake statistics of the region under study. Undoubtedly, a human element is present in the descriptions of historical earthquakes – for instance, this concerns the assessment of earthquake intensity. Nevertheless, the earthquakes recorded were all perceivable, since no instrumental observations took place at that time. Therefore, this information is of great importance.

1.1.2. Seismological studies until mid-70s of XX century

The second stage covers the period from the end of XIX century up to the mid-seventies of XX century. Within that period, generalization of historical data on tectonic earthquakes continued; moreover, the first earthquake catalogues were compiled [Мушкетов & Орлов, 1893; Doss, 1909]. Furthermore, instrumental observations in the Pulkovo observatory (Russia) were initiated – i.e., on the territory bordering on the East Baltic Region considered.

Figure 39. Karls Bruno Doss – Professor of the Riga Polytechnic School

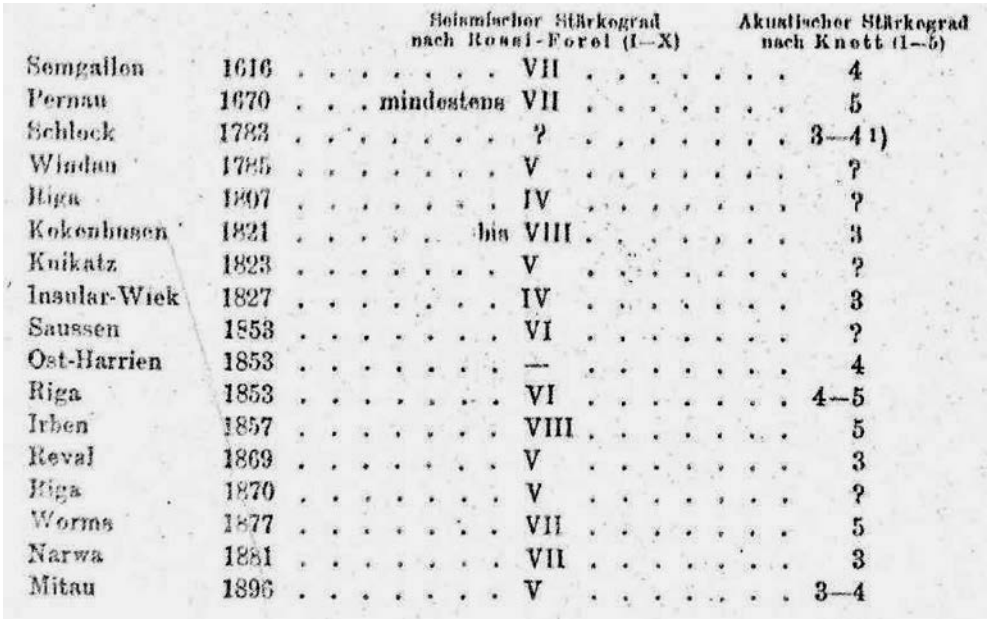

		Seismischer Stärkegrad nach Rossi-Forel (I—X)	Akustischer Stärkegrad nach Knott (1—5)
Semgallen	1616	VII	4
Pernau	1670	mindestens VII	5
Schlock	1783	?	3—4 1)
Windau	1785	V	?
Riga	1807	IV	?
Kokenhusen	1821	bis VIII	3
Knikatz	1823	V	?
Insular-Wiek	1827	IV	3
Saussen	1853	VI	?
Ost-Harrien	1853	—	4
Riga	1853	VI	4—5
Irben	1857	VIII	5
Reval	1869	V	3
Riga	1870	V	?
Worms	1877	VII	5
Narwa	1881	VII	3
Mitau	1896	V	3—4

Figure 40. The earthquakes of the East Baltic Province [Doss, 1909] according to Rossi-Forel intensity scale and Knott's acoustic scale

The epicentral intensity of the earthquake that took place in Koknese (Kokenhusen) and the Irbene Strait (Irben) was rated VIII according to Rossi-Forel scale (Figure 40). The intensity of the four other earthquakes in Semgallen (southern part of Latvia), Pernau and the Worms Island and Narva (Estonia) was rated VII according to Rossi-Forel scale.

A substantial contribution to the systematization of data describing historical earthquakes in the East Baltic Region was made by geologist, Professor of the Riga Polytechnic School Karls Bruno Doss (Figure 39) (1.11.1861–05.1919). He had compiled one of the first historical earthquake catalogues that took place in the East Baltic Region.

B. Doss has assessed the epicentral intensity of the earthquakes that had taken place in the East Baltic province, according to Rossi-Forel scale. The acoustic intensity according to Knott scale is also shown in Figure 40.

The epicentral intensity rate appraisals made by Bruno Doss seem to be too inflated (Figure 41). Later, the assessments of epicentral intensity of East Baltic earthquakes were made according to the International intensity scale MSK-64 [Авотиня и др., 1988] and were reduced at least by grade 1.

The first instrumental observations made in the Baltic Region were commenced at the Pulkovo seismograph station (Russia) that had been opened on December 9, 1906. The station was equipped with long-period seismographs.

The main contribution to the opening of seismograph stations and the beginning of seismological studies – not only in the East Baltic Region but in the entire Russia – was made by a Russian physicist, Academician of Russian Academy of Sciences, Member of Royal Society of London – Boris Borisovich Golyzin (Figure 42) (18.02.1862–4.05.1916).

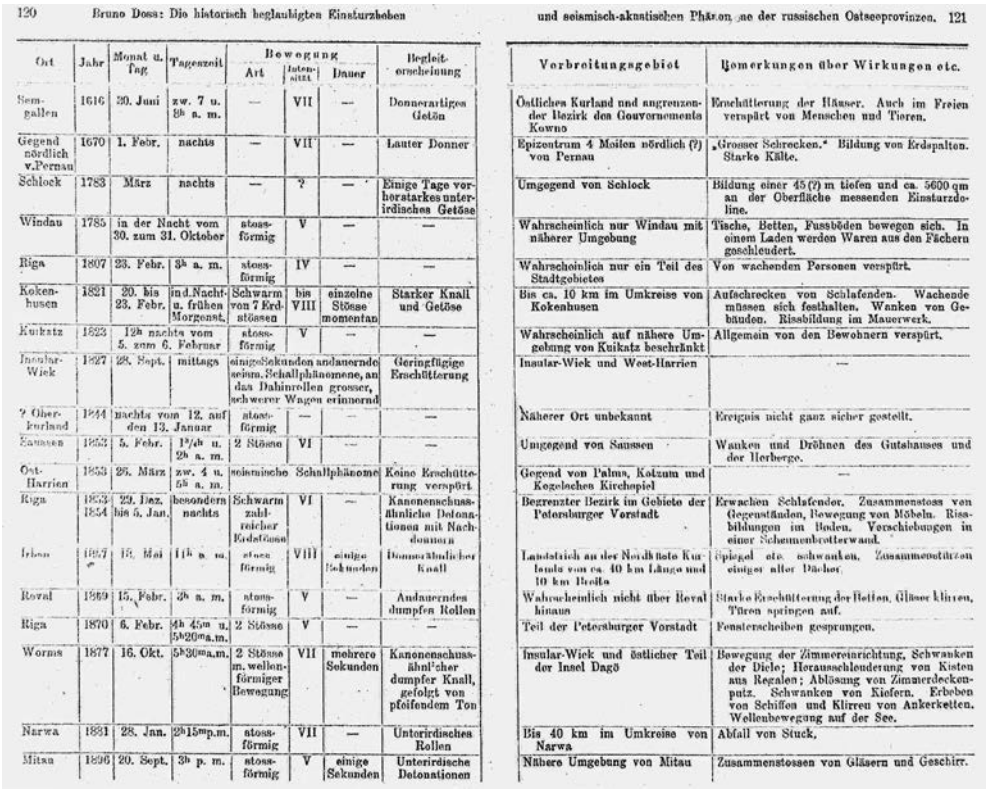

120 Bruno Doss: Die historisch beglaubigten Einsturzbeben

Ort	Jahr	Monat u. Tag	Tageszeit	Bewegung Art	Bewegung Intensität	Bewegung Dauer	Begleiterscheinung
Semgallen	1616	20. Juni	zw. 7 u. 8h a. m.	—	VII	—	Donnerartiges Getön
Gegend nördlich v. Pernau	1670	1. Febr.	nachts	—	VII	—	Lauter Donner
Schlock	1783	März	nachts	—	?	—	Einige Tage vorher starkes unterirdisches Getöse
Windau	1785	in der Nacht vom 30. zum 31. Oktober		stossförmig	V	—	—
Riga	1807	23. Febr.	3h a. m.	stossförmig	IV	—	—
Kokenhusen	1821	20. bis 23. Febr.	in d. Nacht- u. frühen Morgenst.	Schwarm von 7 Erdstössen	bis VIII	einzelne Stösse momentan	Starker Knall und Getöse
Kuikatz	1823	12h nachts vom 5. zum 6. Februar		stossförmig	V	—	—
Insular-Wiek	1827	28. Sept.	mittags	einige Sekunden andauernde seism. Schallphänomene, an das Dahinrollen grosser, schwerer Wagen erinnernd			Geringfügige Erschütterung
? Oberkurland	1844	nachts vom 12. auf den 13. Januar		stossförmig	—	—	—
Saussen	1853	5. Febr.	1h/4h u. 2h a. m.	2 Stösse	VI	—	—
Ost-Harrien	1853	26. März	zw. 4 u. 5h a. m.	seismische Schallphänome			Keine Erschütterung verspürt
Riga	1853/1854	29. Dez. bis 5. Jan.	besonders nachts	Schwarm zahlreicher Erdstösse	VI	—	Kanonenschussähnliche Detonationen mit Nachdonnern
Irben	1857	13. Mai	11h a. m.	stossförmig	VIII	einige Sekunden	Donnerähnlicher Knall
Reval	1869	15. Febr.	3h a. m.	stossförmig	V	—	Andauerndes dumpfes Rollen
Riga	1870	6. Febr.	4h 45m u. 5h20m a.m.	2 Stösse	V	—	—
Worms	1877	16. Okt.	5h30m a.m.	2 Stösse m. wellenförmiger Bewegung	VII	mehrere Sekunden	Kanonenschussähnl²scher dumpfer Knall, gefolgt von pfeifendem Ton
Narwa	1881	28. Jan.	2h15m p.m.	stossförmig	VII	—	Unterirdisches Rollen
Mitau	1896	20. Sept.	3h p. m.	stossförmig	V	einige Sekunden	Unterirdische Detonationen

und seismisch-akustischen Phänomene der russischen Ostseeprovinzen. 121

Verbreitungsgebiet	Bemerkungen über Wirkungen etc.
Östliches Kurland und angrenzender Bezirk des Gouvernements Kowno	Erschütterung der Häuser. Auch im Freien verspürt von Menschen und Tieren.
Epizentrum 4 Meilen nördlich (?) von Pernau	„Grosser Schrecken." Bildung von Erdspalten. Starke Kälte.
Umgegend von Schlock	Bildung einer 45 (?) m tiefen und ca. 5600 qm an der Oberfläche messenden Einsturzdoline.
Wahrscheinlich nur Windau mit näherer Umgebung	Tische, Betten, Fussböden bewegen sich. In einem Laden werden Waren aus den Fächern geschleudert.
Wahrscheinlich nur ein Teil des Stadtgebietes	Von wachenden Personen verspürt.
Bis ca. 10 km im Umkreise von Kokenhusen	Aufschrecken von Schlafenden. Wachende müssen sich festhalten. Wanken von Gebäuden. Rissbildung im Mauerwerk.
Wahrscheinlich auf nähere Umgebung von Kuikatz beschränkt	Allgemein von den Bewohnern verspürt.
Insular-Wiek und West-Harrien	—
Näherer Ort unbekannt	Ereignis nicht ganz sicher gestellt.
Umgegend von Saussen	Wanken und Dröhnen des Gutshauses und der Herberge.
Gegend von Palms, Kolzum und Kegelschen Kirchspiel	—
Begrenzter Bezirk im Gebiete der Petersburger Vorstadt	Erwachen Schlafender. Zusammenstoss von Gegenständen, Bewegung von Möbeln. Rissbildungen im Boden. Verschiebungen in einer Schemenbrotterwand.
Landstrich an der Nordküste Kurlands von ca. 40 km Länge und 10 km Breite	Spiegel etc. schwanken. Zusammenstürzen einiger alter Dächer.
Wahrscheinlich nicht über Reval hinaus	Starke Erschütterung der Betten, Gläser klirren, Türen springen auf.
Teil der Petersburger Vorstadt	Fensterscheiben gesprungen.
Insular-Wiek und östlicher Teil der Insel Dagö	Bewegung der Zimmereinrichtung, Schwanken der Diele; Herausschleuderung von Kisten aus Regalen; Ablösung von Zimmerdeckenputz. Schwanken von Kiefern. Erheben von Schiffen und Klirren von Ankerketten. Wellenbewegung auf der See.
Bis 40 km im Umkreise von Narwa	Abfall von Stuck.
Nähere Umgebung von Mitau	Zusammenstossen von Gläsern und Geschirr.

Figure 41. The earthquake catalogue of the East Baltic Province from 1616 to 1896 [Doss, 1909]

B.B. Golyzin has developed the theory of conceptionally new seismographs using galvanometric method of registration (Figure 43). He had designed an electromagnetic seismometer and subsequently organized the manufacture of instruments of that kind in 1906. Those seismographs recorded ground movements with the necessary sweep of seismic records, thereby providing a qualitative (for his time) and quantitative estimate of remote earthquakes.

The first-ever seismic station in the East Baltic Region was developed by Mr. Golyzin in the University of Tartu (Estonia) in XIX century.

In 1925, Golyzin-Wilip seismographs (jointly designed by Golyzin and Johann Wilip) had been manufactured by H. Meising enterprise "*Werkstatt Für Wissenschaftliche Instrumente*" in Tartu, Estonia. 25 equipment units of that kind (one vertical and two horizontal ones) were sent out to 22 largest seismic stations of the world by their order [Heinloo, 2006]. A Golyzin-Wilip seismograph was installed on the Tartu seismic station in 1931. It operated until the beginning of World War II. J. Wilip was the Head of the seismic station.

In 1909, Professor Bruno Doss had prepared the first integrating seismic-geological map of the East Baltic Province [Doss, 1909] (Figure 44) where isoseists of sensible

Figure 42. Boris Borisovich Golyzin – a Russian physicist, Academician of Russian Academy of Sciences, Member of Royal Society of London, one of the founders of seismology, geophysicist, inventor of electromagnetic seismometer

earthquakes of the East Baltic Regions were shown. Moreover, the age of geological deposits and their lithological composition was designated.

Bruno Doss tried to find a definite association between earthquakes and weather conditions. That is why sample information on air temperature and atmospheric pressure is given in some of his works. However, no comprehensive data on weather conditions is presented in his works. Perhaps, that is the reason why he failed to find out a precise correlation between weather conditions and the origin of earthquakes. A comprehensive analysis of changes in winter temperatures, carried out in December 1908 showed convincingly that the earthquakes that had taken place on EBR in winter that year were associated with abrupt changes in winter temperatures and a sufficiently large humidity of soil. Actually, the conditions under which frost earthquakes take place have occurred. That was repeatedly emphasized by Professor Andrey Nikonov in his research works [Никонов, 2010; Никонов, 2013].

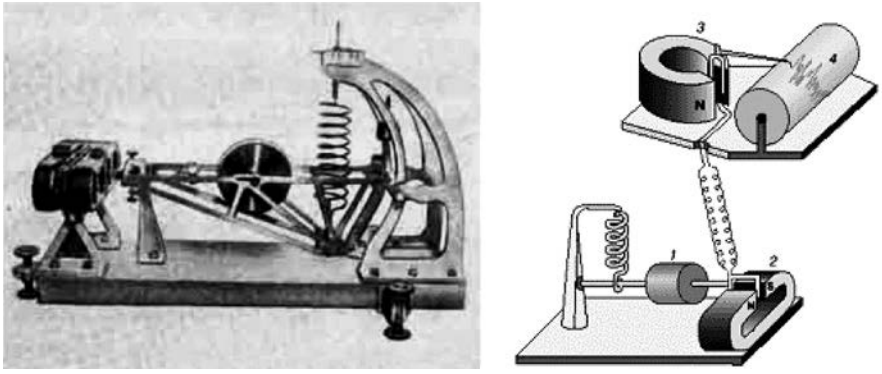

Figure 43. Electromagnetic seismometer by B.B. Golyzin (left) and seismometric channel providing galvanometric records made on photosensitive paper (on the right).

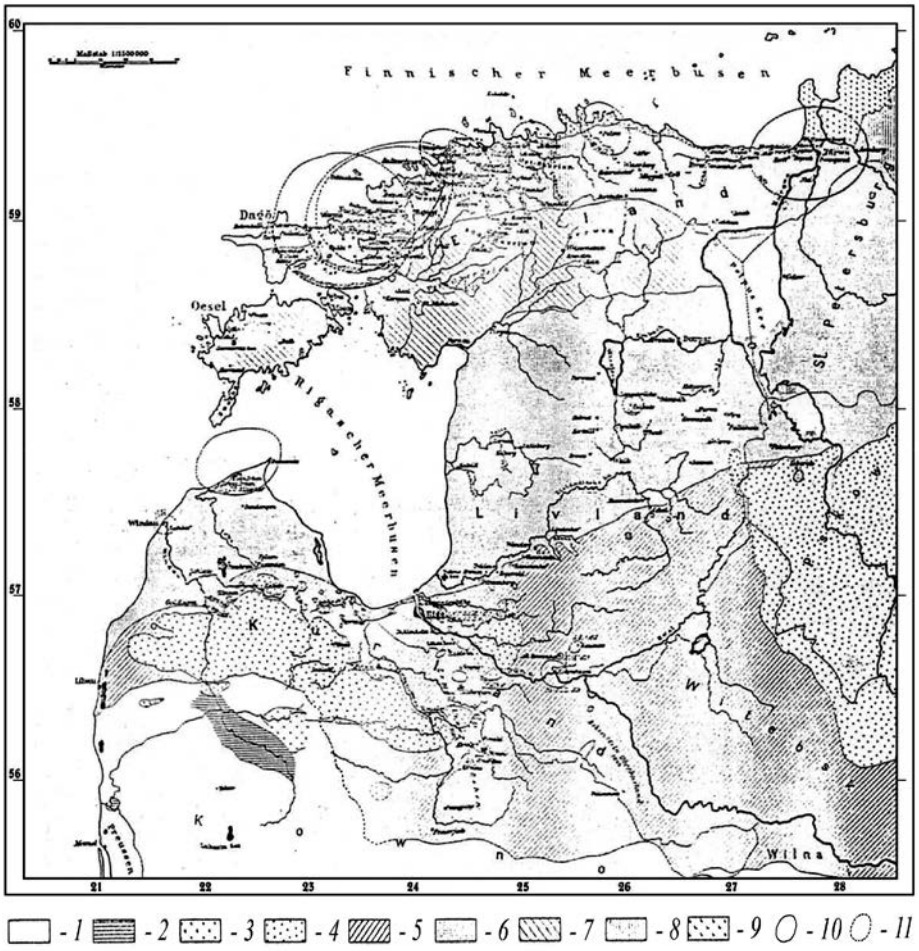

Figure 44. Seismologic map of the East Baltic Province according to B. Doss [Doss, 1909]

Designation of the age of geological deposits: 1 – quaternary deposits; 2 – Jura; 3 – Permian deposits; 4 – Upper Devonian sandstone, clay, and dolomite; 5 – Middle Devonian dolomite; 6 – Middle Devonian sandstone; 7 – Upper Silurian limestone and dolomite; 8 – Low Silurian limestone; 9 – limestone and Cambrian Clay; 10 – steady line of seismic shocks similar intensity; 11 – assumed line of similar intensity of seismic shocks

1.1.3. Seismological studies from mid-70s of XX century to 2004

The third stage of development of seismological studies covers the period from the 1970s to 2004. The stage began on October 25, 1976 when tectonic earthquakes took place on Osmussaar Island in Estonia. The magnitude of the main Earth shock reached 4.7 with epicentral intensity VI within epicentral area as according to the MSK-64 scale [Kondorskaya et al., 1988].

The instrumental observations initiated on seismic stations in the East Baltic Region and Belarus for the record of remote and strong earthquakes should be referred to the same period. In particular, seismic stations equipped with long-period seismographs SD-1 (СД-1) were developed in the 60s of the last century in Baldone (Latvia) – on the territory of the radio-astrophysical observatory operated by Academy of Sciences of Latvia. The same units were deployed of the territory of the radiological sciences laboratory owned by the Institute of physics and mathematics under the Academy of Sciences of Lithuania. Those stations, in conjunction with the Belarussian seismic station *Pleschenitsi* formed a triangular network. With the aid of the network, observations of surface waves generated by remote and strong earthquakes were carried out to study the deep-seated geologic structures of the Earth's crust and the upper mantle [Хотько, 1974].

However, long-period seismographs were incapable of detecting any regional earthquakes since their bandwidth was adjusted to recording low frequencies generated by remote earthquakes.

A notable contribution to the development of seismic stations in the East Baltic Region was made by Alexander Mikhailovich Boborykin and Anatoly Petrovich Yemelyanov – Belarussian geologists, geo scientists and seismologists, acting as managers of the field trial seismological team for the seismology department of the Institute of Geophysics and Geochemistry under the Academy of Sciences of Belarussian SSR. It was just Boborykin who turned his attention to a possible association of earthquakes with the tectonic structure of Latvia – having published a corresponding article dedicated to the subject [Боборыкин, 1988].

Since the beginning of the 1960s, seismic observations have begun to develop in Belarus. In 1963, the Minsk seismic station (Pleschenitsy) was opened. The station was equipped with broadband and long-period seismometers SSM-SKD and SSM-SCM. The recording range for SKD is from 0.5 to 50–60 seconds. The seismometer made it possible to record oscillation amplitudes from 10^{-3} to 5 mm. SM seismometers had a recording range from 0.2 to 10–15 seconds and allowed one to make a record of signals with the amplitudes from 10^{-3} to 5 mm [Аранович и др., 1974]. These stations were intended for recording remote earthquakes.

Early in the 80s of the last century, three seismic stations were already operating in Belarus – particularly, those in Minsk (Pleschenitsy), Gomel, and Naroch. At that, the Minsk station pertained to base stations of Class 1 covered by the Uniform System of Seismic Observations (USSO) used in USSR. The Gomel (1982) and the Naroch (1989) stations were equipped with SKM geophones. Those seismic instruments allowed one to record seismic waves within the range from 0.1 to 3 seconds and record signals with the amplitudes from 10^{-5} to 1 mm [Аранович и др., 1974].

The creation of short-period stations in the East Baltic Region – in particular, in Estonia (Tallinn) and Lithuania (Suginčiai) – refers to the same period.

The first seismograph station in Latvia was created in the 1970s by the Moscow University in Baldone, on the territory of astrophysical observatory of Academy of Sciences of Latvia. The station was equipped with long-period seismograph SD-1 and

was intended for registration of strong, remote earthquakes. Early in the 1990s, the station ceased to work due to the lack of funding.

In 1989, Research and production association for Marine engineering geology (RPA Morgeo) of the USSR – the former parent enterprise for geologic and geophysical studies in the offshore zones of the USSR – posed the task of preparing a geologic and economic justification of seismological monitoring in Latvia. This work was finished in 1991 [Никулин, 1991_*um*].

In 1992, Research and manufacturing association "*Jūras inženierģeoloģija*" ("Marine engineering geology") (Director: Romanov, Deputy Director for science: Y. Bezrodnikh) supported by the Geology Department of Latvia (A. Freimanis) acquired a set of seismological equipment manufactured by Institute of Physics of the Earth under the Academy of Sciences of the USSR. In 1993, *SSK* (short-period seismic station) station was deployed on the territory of a special design bureau "*Jūras inženierģeoloģija*" ("Marine engineering geology") in Babīte (the Riga region), where experimental observations were carried out in the course of a year.

In 1994, the *SSK* station was installed for permanent seismic registration at *"Čiekuri"* farmstead in the Valmiera region of Latvia. Later the station was named *"Skujas"*. The seismic receivers were located in a bunker, at a depth of about 1 meter from the Earth's surface, on a dense sandy-clay soil. Since 1994, the *Skujas* seismic station has registered more than 2900 seismic events, including more than 1400 distant and 550 regional seismic events. 630 seismic events could not be identified as any known seismic event or an earthquake.

Before 2000, only *SSK* analogue seismic recording system operated on the station. Ink recording on paper tapes was exercised. The tape unfolding velocity was 120 mm/ min. In 2001, a digital recorder *GBV-316* manufactured by *GeoSIG* (Switzerland) was installed in parallel with the analogue seismic recording system. Accumulation of seismological data was in *GRSSEI* format, under control of *SeisLog* programme worked out by the Bergen University (Norway) [Urtheim et al., 2001]. The analysis and processing of seismological data were carried out by using *SEISAN* software package [Ottemöller et al., 2016] developed by the Bergen University.

In other countries of the East Baltic Region, seismic stations operated, as well; as a rule, they were short-period ones but they all were not integrated into a single centre for collection, processing, and generalization of regional seismological information. The information was accumulated on each station separately, and the stations lacked a hot link for data exchange. As a rule, photographic, thermal, and conventional paper tapes were used as data carriers. Lack of a unified network of seismological observations for monitoring regional seismic events could not allow one to locate and identify the parameters of seismic events and tectonic earthquakes (origin time, epicentre coordinates, focal depth, and magnitude) in the East Baltic Region. The seismograph stations rather acted as alarm warning devices signaling about the occurrence of something like an earthquake or explosion. An exception is the Ignalina local seismic network created in 2000. The task of the Ignalina local network was to alarm out regional earthquakes that had taken place, with the view of taking prompt actions at

nuclear power plants to prevent losses inflicted by seismic waves generated by possible earthquakes.

Apart from the development of instrumental seismological observations, studies associated with the assessment of seismic hazard are carried out for the East Baltic Region – both in the framework of All-Union projects (USSR) and regional projects.

The first-ever formal normative map of the general (small-scale) seismic zoning of the entire territory of the former USSR was published in 1937 by G.P. Gorshkov. This map triggered the process of regular mapping of seismic hazard, as the basis that regulates the design and construction in the seismically active regions of the USSR.

In the late 1940s, a new approach to seismic hazard assessment methods took shape; a concept of seismic hazard assessment, consisting of two stages, was accepted. At the first stage, the actual and the potential source zones are highlighted, while at the second stage, the expected seismic shocks on the Earth's surface are calculated. Actually, all the compilers of the subsequent seismic zoning maps stuck exactly to that paradigm: in 1957 (editors: S.V. Medvedev, B.A. Petrushevsky), in 1968 (editor: S.V. Medvedev), and in 1978 (editor: M.A. Sadovsky).

On the seismic zoning map compiled in 1978, the Baltic Region, as well as the major part of the USSR territory, were attributed to grade V zone (Figure 45).

However, V.I. Ulomov – the leading seismologist of O.Y. Schmidt Institute of Physics of the Earth, Dr. Sci. in Physics and Mathematics of the Russian Academy of Sciences, believes that the OSR-78 map failed to furnish one with an adequate assessment of

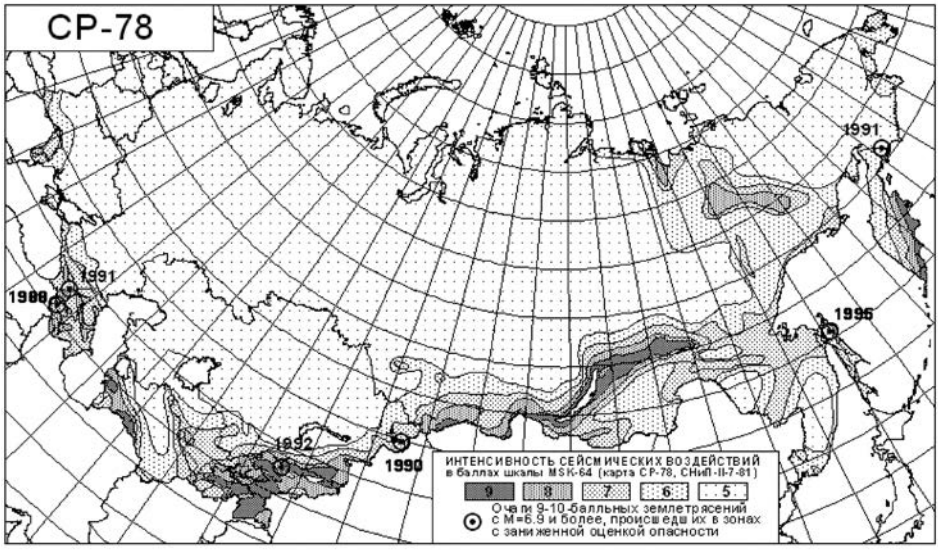

Figure 45. General Seismic Zoning Map OSR-78 for the territory of the former USSR and epicentres of strong earthquakes that took place within zones with an underscored estimate of seismic hazard

(from left to right: Spitak, 1988; Racha-Java, 1991; Suusamyr, 1992; Zaisan, 1990, Khailino, 1991; Neftegorsk, 1995) http://lib.znate.ru/docs/index-38430.html

seismic hazard, since the authors of the map-1978 and all the subsequent maps adhered to deterministic approach, not taking into account the peculiarities of seismic setting of the regions [Уломов, 2013_*si*].

At the International Symposium on Geodesy and Geophysics that was held in Vancouver (Canada) in 1987, the problem of studying the tectonic activity and seismicity of ancient platforms was attributed to major problems that had to be solved in XX century already. It was noted that the added complexity of construction of civilian properties and, especially, of ecologically hazardous structures, in the context of cost and materials cut, may result in serious consequences [Гарецкий & Боборыкин, 1989].

Efforts were made in USSR to follow those recommendations. In USSR, the frequency of mapping with regard to General Seismic Zoning Maps was 10 years approximately. Such a time space was quite substantiated, since a new volume of seismological information was accumulating during that time, and new methodological approaches to the assessment of seismic hazard were introduced. Moreover, temporal schemes of seismic zoning were also created, which were necessary for the design of facilities of special importance. In 1987, a temporary scheme for the seismic zoning of the East European Platform was prepared at the Hydroproject Research Institute [Уломов & Шумилина, 1999]. On the seismic zoning map issued in 1987, source zones with the epicentral intensity up to VII points on the MSK-64 scale were already highlighted in the Baltic region (Figure 46).

The results of seismic zoning in the East Baltic region after 1991 are discussed in Chapter 5.

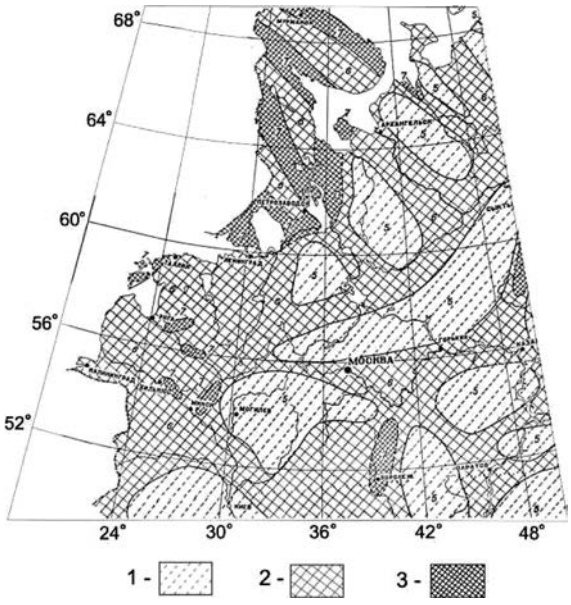

Figure 46. Map of seismic zoning for the European part of the USSR at a scale
1:5000000 [Уломов & Шумилина, 1999; author of the map – Владимиров;]
Legend: 1–5 points on the scale of MSK-64; 2–6 points; 3–7 points

1.1.4. Current stage of seismological studies in the East Baltic Region

The present-day – the fourth stage of the development of seismological studies in East Baltic Region is connected with the Kaliningrad earthquakes that took place on September 21, 2004. Those earthquakes were the strongest among those ones that had ever taken place on EBR territory. The first and the second shock magnitude had reached 5.0 and 5.2, respectively [Gregersen, 2007]. The epicentral intensity was VI ½ on the EMS-98 scale [Nikonov et al, 2005].

After the Kaliningrad earthquakes, considerable efforts were made to develop a network of seismological observations in the countries of East Baltic Region.

Figure 47. Slītere seismic station

Notes: 1 – general view of the territory of Slītere beacon, where the station is installed; 2 – the upper part of the tool-equipped compartment; 3 – the outdoor room where the computer is installed; 4 – ADC and SeisComp installed inside the compartment; 5 – STS-2 seismometer without the outer jacket; 6 – STS-2 seismometer with the outer jacket.

Since 2004, creation of modern seismic stations has begun in East Baltic region. They were included into a single international seismic network *GEOFON* with the centre in *GeoForschungZentrum* (*GFZ*), Potsdam, Germany [http://geofon.gfz-potsdam.de/].

The first *TRTE* station (Tartu) was established in 1996 in Estonia. Thereby, the seismological research traditions initiated at Tartu University in the previous historical period, were continued. In 2005, two stations were installed in Estonia at the same time. One of them was *MTSE* (Matsalu) – in the western part of Estonia, while the other – SRPE (Suurupi) in the north, near Tallinn. The availability of three stations made it possible to locate seismic events with a seismic network of their own.

On October 25, 2006, SLIT station (Slītere) was installed. This date is remarkable because exactly 30 years ago a perceivable earthquake took place on Osmussaar Island in Estonia that played an important role in the development of seismological studies in East Baltic Region.

Siting of the *Slītere* seismic station was quite a challenge, since soil conditions predominant in Latvia and on the major part of EBR territory are characterized by friable quaternary deposits and a high level of subsoil water. The quaternary overburden

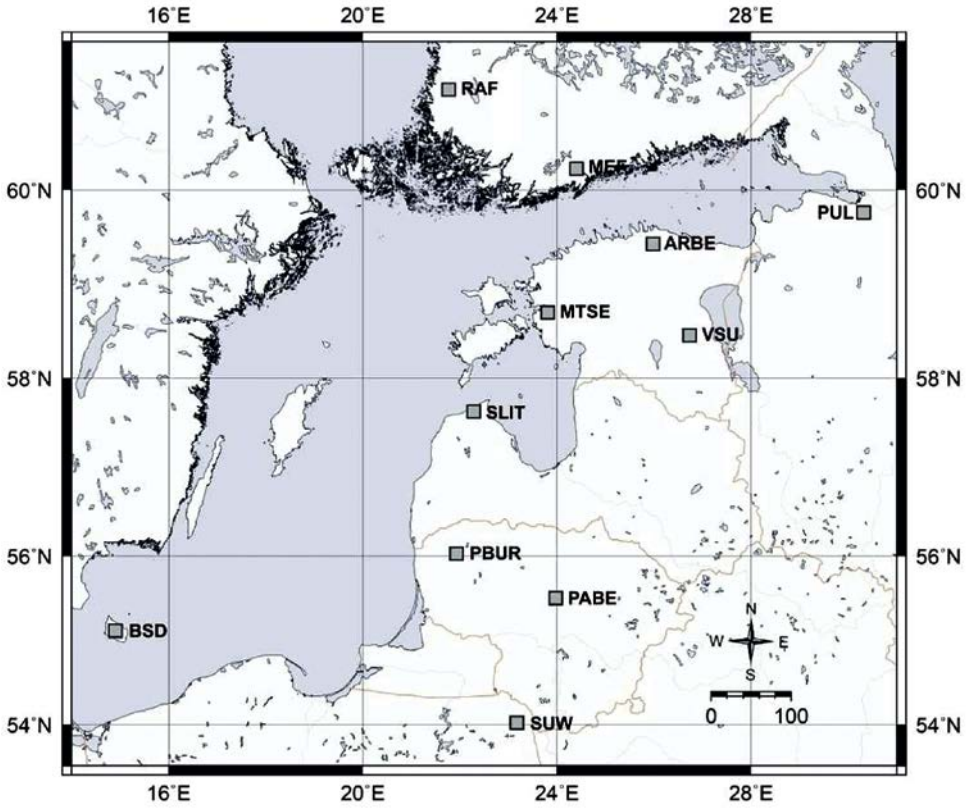

Figure 48. BAVSEN – the Baltic virtual seismic network

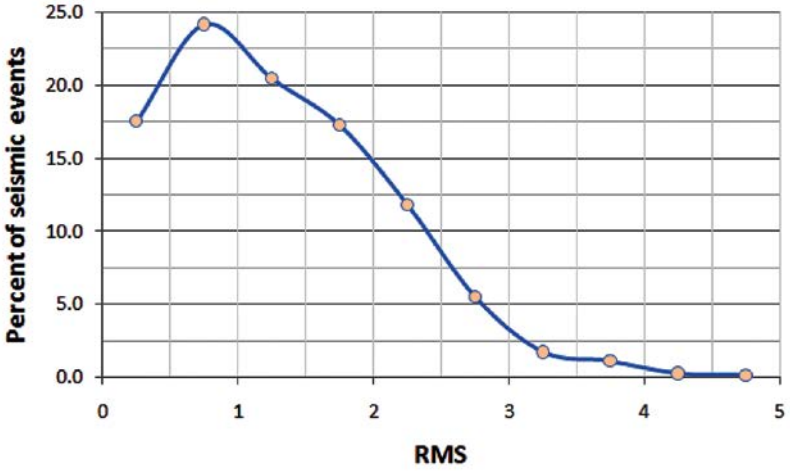

Figure 49. *RMS* for seismic events recorded by the BAVSEN network

thickness is variable. The maximum thickness (310 m) is associated with trench cuts in Pre-Quaternary deposits. Quaternary deposits are represented mainly by ice-laid formations containing glaciofluvial, interglacial, and interstadial deposits inside [Брангулис и др., 1984].

Such conditions are unfavorable since they substantially influence the parameters of approaching seismic waves – in particular, polarization – by distorting them. Therefore, in order to reduce the ambient seismic noise, a 6.5 m of depth compartment equipped with tools was dug. At the bottom of the bin, a concrete-fabricated pedestal was made with a number of sensors mounted thereon (Figure 47). The concrete pedestal rests directly on morainic deposits of dense siltstone.

Taking part in the GEOFON network allowed to receive data from the neighbouring seismic stations located both in the East Baltic Region and in the southern Fennoscandia. Thus, the so-called Baltic virtual seismic network (BAVSEN) was established, which currently includes 11 seismic stations (Figure 48).

The distances between the BAVSEN network stations exceed 200 km. Moreover, a considerable background noise at the seismic stations located at the southern slope of the Baltic Shield (VSU, MTSE, ARBE) and in the Masurian Belorussian anteclise (SUW) hampers the first arrivals of P-waves considerably. Only the stations located in Southern Fennoscandia (MEF, RAF) feature a lower background noise.

The seismic monitoring quality (namely, positioning accuracy and seismic network sensitivity) can be assessed mainly by (*Root mean square*) and the value of minimal registered magnitude of seismic events M_{min}.

The analysis shows that, given the stated network density, *RMS* = 0.75 sec (Figure 49) is encountered most frequently, while M_{min} = 1.25 (Figure 50).

RMS and M_{min} values have been defined with respect to the regional seismic events that took place on the area of the East Baltic Region (Lat = 53.9N – 59.7N; Lon = 19.4E – 29.6E) within the time span from 2008 to 2017. The general number of

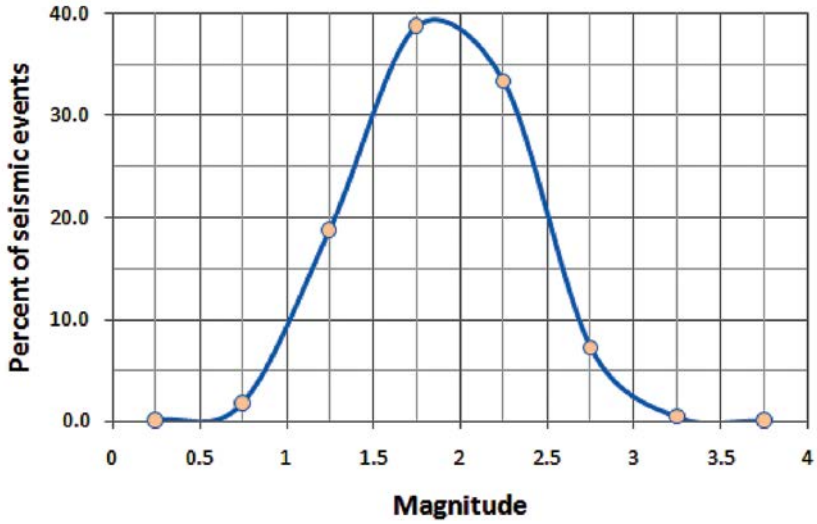

Figure 50. Distribution of magnitudes of seismic events recorded by the BAVSEN network

seismic events for *RMS* is 4790 while for magnitude distribution, it is 4674. The reduction in the number of seismic events for magnitude values exceeding 2.0 is explained by the fact that mainly explosions made in industrial open pits and the Baltic Sea waters are recorded. Their power is limited to a defined level.

Within the same period, investigations associated with the preparation of a seismic risk map of Latvia were carried out [Nikulin, 2011]. The investigations had been carried out by order of the Ministry of Economic Affairs of Latvia. Those investigations will be considered in detail in the next chapters.

1.2. Historical earthquakes in the East Baltic region

The historical earthquakes of the East Baltic region refer to all the earthquakes that had taken place before the regional instrumental observations were commenced in the Baltic Sea Region. The beginning of instrumental observations can be dated back to the mid-fifties of XX century when the first short-period seismic stations, integrated into national networks, have been installed on the territory of Finland and Sweden.

Thus, the period of historical earthquakes of the East Baltic region begins from times immemorial and ceases in the mid-50s of XX century.

The major contribution into the investigations of the historical earthquakes in the East Baltic Region was made by Bruno Doss – a geologist, Professor of the Riga Polytechnical School. The main line of research that B. Doss adhered to was geology. He was engaged in research for geology, petrography, and mineralogy. Since no detailed delegation of geoscience tasks existed among scientists in XIX century, Mr. Doss was

also engaged in seismological investigations and greatly contributed to the earthquake studies in the East Baltic Region.

B. Doss made use of archive materials, clerical manuscripts, and newspaper reports, implementing a sort of macroseismic investigations. Investigation of historical earthquakes is with a hint of subjective estimates from researchers (seismologists) who, in turn, relied on reports from eyewitnesses or, on information presented by authors of ancient manuscripts.

Therefore, before macroseismic information on ancient earthquakes is embodied into the form of a catalogue, it passes through a chain of carriers of that information, namely: the eyewitness – the person who had captured the information in a newspaper or manuscript – the seismologist preparing the catalogue. It was exactly the chain that B. Doss could make use of to investigate historical earthquakes before 1898–1900, since only at that time he started working in the Riga Polytechnical School. Actually, he could use eyewitnesses' accounts only with respect to the earthquakes of 1908 that were perceived in many places of the East Baltic Region and the subsequent earthquakes that took place before 1912.

Now, let us consider the main macroseismic characteristics of perceivable strong historical earthquakes that have taken place in the East Baltic Region. The historical earthquakes are presented in the Earthquake Catalogue for the East Baltic Region (see Annex 1).

3.2.1. Earthquakes in East Prussia in 1302 and 1328

Traditionally, the first known earthquake in the East Prussia was deemed to be the one in Bauska that took place on June 30, 2016. However, after the Kaliningrad earthquakes in September, 2004 there was a considerable surge in interest with respect to the historic seismicity investigations in that region. In his address pronounced at the International Conference in Vilnius in 2007, Andrey Nikonov, the leading expert in the field of macroseismic and tectonic investigations of O.Y. Schmidt Institute of Physics of the Earth, Professor, Dr. Sci. in Geology and Mineralogy, have reported about new data on historical earthquakes of the East Baltic Region [Nikonov, 2007].

According to this data, 4 earthquakes with the epicentral intensity up to VII took place in August and December 1302 in East Prussia. In 1238, an earthquake took place in the central part of Lithuania – with the epicentral intensity of about VII, as well. The main sources of that information were two memorials [Peter, 1997; David, 1813]. The author of a medieval chronicle, Peter from Duisburg (XV c.) wrote about *"a horrible trembling*" of the Earth, so that old houses were about to collapse in Memelburg (the present-day Klaipeda). The fact took place in 1328 [Nikonov, 2015_*si*].

3.2.2. Bauska earthquake of 30 June 1616

The Bauska earthquake is the best-known among those earthquakes that took place in the territory of the East Baltic Region. It occurred on June 30, 1616. A reference to the earthquake can be found in the church records by a preacher, Georgius Mancelius

(*Georg Manzel*) [Doss, 1909]. *Bodeckerschen Chronik* contains an entry attesting to the fact that people in Kurland had perceived a strong earthquake. In many places of the Duchy of Zemgale on particular, Wollhof (Valle) and Kovno (Kaunas) – a tremor was perceived.

Meanwhile, Valle is located at a distance of 17–19 km from the Bauska tectonic fault, which has east-west trending. The Bauska fault is a downthrow with the lowered Southern wall. The amplitude over the fault surface is fluctuating from 70 to 150 m. The Bauska fault penetrates into basement rocks, the Caledonian and the Hercynian structural complexes [*Брангулис и др*., 1984].

Here is the description of the earthquake [Doss, 1909]: "*A crash resembling a thunder. The tremor was perceived in the east of Kurzeme and in the Kovno area (Kaunas). Houses were trembling. People and animals in the open perceived a tremor of the Earth's surface*".

Kaunas is located at a distance of 159 km from the earthquake focus. At the same time, according to the data published in the historical earthquake catalogue for Belarus and the Baltics [Авотиня и др., 1988], the focus was located within the urban area of Bauska (Lat = 56.4N; Lon = 24.2E). However, tectonic maps issued late in the 1980s did not have any reliable referencing. A new Latvian system of coordinates – *LKS-92* – was introduced in 1992. Taking into account the new coordinate system, tectonic maps of Latvia were subsequently compiled [Brangulis & Kanevs, 2002], where tectonic faults have a referencing to the geodetic grid. Based on those maps, it is more expedient to associate the seismic origin of the Bauska earthquake either with the Bauska fault (Lat = 56.3N; Lon = 24.3E) or with the boundary between the Baltic tectonic depression (syneclise) and the Latvian saddle, where the city of Valle is actually located (Lat = 56.5N; Lon = 24.8E).

3.2.3. Koknese earthquakes of 1821

The Koknese earthquakes of 1821 occurred in the vicinity of Koknese (Kokenhusen). Bruno Doss reports [Doss, 1909] that several tremors had occurred from February 20 to 23, 1821. In particular, grade VII are mentioned. Sleeping people awoke from the tremors. Those who were in a waking state could hardly restrain themselves on their feet. The buildings were swinging. Cracks in the plaster formed on the walls. There are even reports on a series of earthquakes, among which the strongest ones were assessed as VII points on the MSK-64 scale [Авотиня и др., 1988].

The maximum epicentral intensity reached grade VIII on the Rossi-Forel scale. The Rossi-Forel scale covers the range from I to X grade. Bruno Doss makes his estimates on the basis of three sources, two of which (Rambdamm and Dörptschen) are anonymous, while the third source is the pastor G. Lienig of Kokenhusen (Koknese). In assessing the intensity of earthquakes in the Baltic region, Boborykin AM [Авотиня и др., 1988] estimated the intensity of the main shock in Koknese at grade VII on the MSK-64 scale. The grade VIII on the Rossi-Forel scale correspond to grade VII on the MSK-64 scale [Levret & Mohammadioun, 1984]

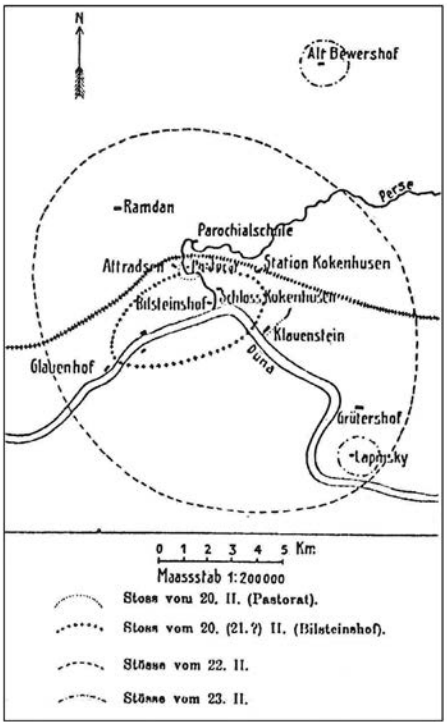

Figure 51. Isoseismic line scheme of the Koknese earthquake [Doss, 1909]

The strongest shock as of 22.02.1821 took place early in the morning. The shock was perceived mainly by those people who were sleeping or light sleeping at the moment. The *isoseismal line* covering the largest shaking area corresponds to the strongest shock (Figure 51).

The perceptibility threshold corresponds to II–III points [EMS-98], with its size along the major axis 15.8 km, along the minor axis – 10.3 km. The perceptibility area (of the ellipse) is about 511 km^2. Presuming that the isoseist of the strongest shock corresponds to III point-intensity, we may assess M_S based on the dependence between the perceptibility area and the magnitude [Muir Wood & Woo, 1987]:

$$Ms = 0{,}69 \cdot log(A_{III}) + 0{,}0006 \cdot A_{III} + 0{,}95 \quad (4)$$

The focal (hypocentral) depth can be assessed based on the formula of the regional macroseismic equation elaborated for the East Baltic shield: [Assinovskaya & Nikonov, 1998]:

$$I_0 = 1{,}36 \cdot M_S - 2{,}7 \cdot \lg(h) + 3{,}36 \quad (5)$$

In this case, the magnitude of the strongest Koknese earthquake is 2.8, while the focal depth of the Koknese earthquake is 1.2–2.7 km.

At present, there is lack of consensus between individual seismicity researchers of Scandinavia and the Baltic Region on the issue of the genesis of Koknese earthquakes of 1821. The essence of the controversies is that, according to the viewpoint of Professor Andrew Nikonov [Никонов, 1995; Никонов, 1996; Никонов, 2010], non-tectonic earthquakes – i.e., earthquakes not caused by tectonic movements – might have existed

on the East European Platform in the past. Frost phenomena or dolines (karst holes) could have been the sources of non-tectonic earthquakes. Frost phenomena occurred in winter, when certain conditions invoking ice cracking on rivers might exist, or frozen ground was cracking. Karstic phenomena occurred in a number of EEP, including the East Baltic Region. Consequently, non-tectonic phenomena were mistaken for tectonic earthquakes in some cases. Such phenomena did take place of course. However, not all of the similar phenomena that took place in winter or in the regions characterized by developed Karstic processes should be classified as non-tectonic ones.

It should be noted that some definite prerequisites, allowing to consider those earthquakes as those of tectonic nature, exist in the region of the Koknese historical earthquakes of 1821.

The prerequisites are based on such indicators as morphological traits. In particular, this applies to the case of geological outcrops lying on the Earth surface. In this context, the waterfall through the Pērse River is especially noteworthy.

The waterfall may originate due to a tectonic fault or cracks on the Earth's surface [National Geographic, Waterfall_*si*]. These geologic tectonic factors may be initial prerequisites triggering erosion advancing of geological stones in the waterfall region.

It is characteristic that the elliptical major axis of the isoseismic line ("*Stoss von 20. 21(?) II.Bilsteinshof"*), extending through Bilsteinhof (the present-day Bilstiņi) is oriented actually at right angle relative to the Pērse River (Figure 52). This means that the focus was also located at right angle relative to the Pērse River bed – i.e., in the same way as the river-crossing waterfall axis is oriented. The probability of this ellipse-shaped isoseismal line being associated with a doline (karst hole) is minimal.

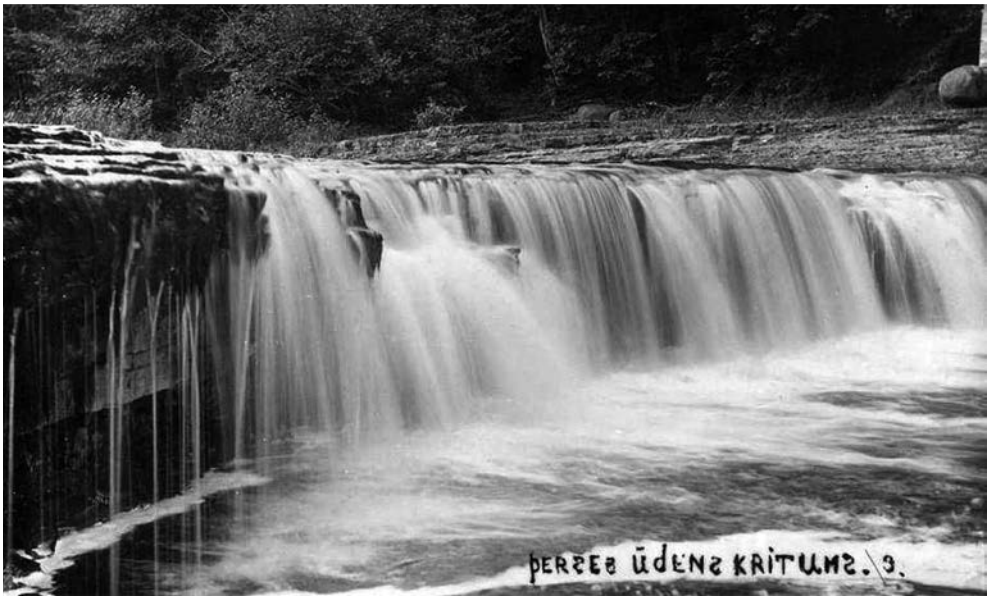

Figure 52. Waterfall on Pērse River in the Koknese region

Another sign of tectonism may be an uplift, which is located in the Koknese region [Barangulis & Kanevs, 2002]. The uplift stands out against the Hercynian structural complex. Signs of tectonism are confirmed by the current vertical movement velocity variations [Аболтиньш, 1969_*upm*] on the Koknese-Sece profile (located 1 km to the south of Koknese]. For example, the velocity variation reached 2.5 mm per a year between the benchmarks 0022 (in the *Bilstini* district) and 0038 (on the left bank of Daugava River), with the distance between them being about 1 km. After the reservoir filling – i.e., within the period 1965–1968 – the benchmark 27 (in the estuary of Pērse River) was ascending at a speed = 3.6 mm/per year, whereas, prior to the reservoir filling, the benchmark had actually zero speed of present-day vertical movements. Therefore, there is a number of morphological (the waterfall), tectonic (the Koknese uplift) and deformational (the present-day vertical movements) prerequisites attesting to the existence of some separate crustal blocks in this district, which are moving with different velocities. Those crustal blocks are demarcated by faults, which are probably associated with the earthquakes of 1821.

The Koknese earthquakes have been included into such reputable catalogues as *Catalog of earthquakes in Northern Europe* (http://www.seismo.helsinki.fi/english/bulletins/catalog_northeurope.html) issued by the Institute of Seismology under the Helsinki University, or, the Earthquake Catalogue for the East European Platform [Маловичко и др., 2007].

3.2.4. Irbene earthquake of 18 May 1857

The focus of the Irbene earthquake that took place on May 18, 1857 was located in the northern part of the Kurzeme peninsula (Lat = 57.7N; Lon = 22.0E). Throughout the entire neighborhood of Lielirbe – Mazirbe – Kolka people perceived vibrations making mirrors and table plates fall down. The roofs of old buildings collapsed. A thunder-like roar was heard [Avotina et al., 1988]. The epicentral intensity of the earthquake is assessed at VI on the MSK-4 scale.

It should be noted that the northwestern coast of Kurzeme – from Miķeļtornis to Kolka, which is about 40 km-long – actually extends along a direct line. This landscape feature should be associated with the lineament area highlighted by Belorussian geologists and geoscientists [Айзберг и др., 1997]. The Irbene seismogenic area is associated with this particular structure [Safronovs & Nikulins, 1999].

3.2.5. Narva earthquake of 1881

In 1881, a VI-epicentral intensity earthquake on the MSK-64 scale took place in Narva and Ivan City. The earthquake provoked clatter of crockery, peeling of plaster, and breaking glasses. An underground boom was heard [Мушкетов & Орлов, 1893; Doss, 1909; Doss, 1898]. For example, in a study by Mushketov and Orlov [Мушкетов & Орлов, 1893] is given macroseismic description of this earthquake: «on January 16 (28), 1881, at about 2:15 pm light vibrations with an underground noise lasted 3 or 4 s in Narva and Ivangorod. This earthquake was felt at a distance of 13 km to the west

of Narva, 21 km to the east, l5 km south and 10 km to the north. In addition, by the way, at the station Korf and Lagena and Repnik m*anor estates, plaster fell from walls and many windows were broken. In the Lagena manor an underground noise was heard*».

Professor Nikonov shows the tectonic nature of this earthquake, in contrast to the karst nature, and attaches great importance to this earthquake in assessment the seismic hazard for strategically important facilities in Russia [Nikonov, 2011].

3.2.6. Sesmic shocks in December 1908 in the East Baltic Region

Seismic shocks recorded in December 1908 (Figure 53) hold a special place among the historical earthquakes of the East Baltic Region. They took place in EBR right after a powerful, disastrous earthquake that took place in Messina (Italy) on December 28, 1908 (the magnitude M*w* = 7.5). The earthquake took place at 05:20 local time.

After the earthquake, a 13 m-high tsunami wave was generated in the Mediterranean Sea [Messina earthquake and tsunami of 1908*i*]. In the epicentral area of Messina earthquake, the epicentral intensity had reached X–XI on the Mercalli – Cancani – Sieberg (MCS) scale [Risk Management Solution, Inc., 2008], which is equivalent to X– XI points on the MSK-64 scale. From 70 to 2000 thousand people perished.

Seismic shocks that occurred in EBR after Messina earthquake had a number of special features, which are ambiguously assessed even up to the present day. Thereby, the genesis of those seismic shocks in December 1908 perceived on EBR is still uncertain. The seismic shocks in question have a number of peculiarities, as follows.

Firstly, the shocks were perceived on a large EBR area (25–30 thousand km^2). In particular, they were perceived in communities of Belarus and Latvia: 1) in the Bystrica village (Belarus), 2) in the Gudogay residential settlement of the Ostrovets district (the Serzhanty isolated farmstead (Belarus); 3) 3 (three) shocks were registered in Riga at different times; 4) in Madona (Latvia); 6) in the Daugavpils region: Krāslava, Ilūkste,

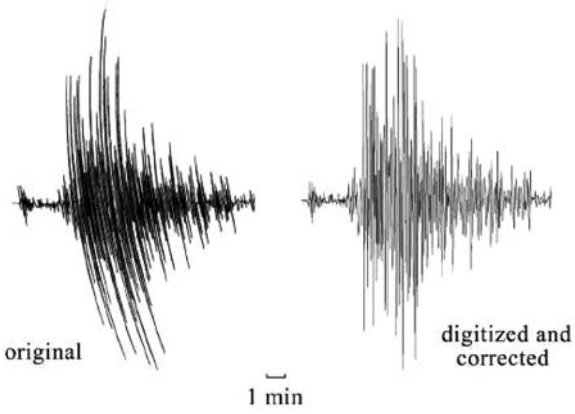

Figure 53. Seismic record of Messina earthquake as of December 28, 1908 made by Wiechert seismograph weighing 1200 kg, in Plauen, Germany (left) and the corresponding digitized and corrected signal (right) [Pino et al., 2009]

Daugavpils, Medumi, – as well as on the territory of Lithuania, close to the Latvian border; 7) in Valmiera [Авотиня и др., 1988].

The intensity of those shocks is different. For instance, the shock intensity in Riga was assessed as grade IV–VI, whereas in Gudogai and the Daugavpils area – as grade VII [Авотиня и др., 1988].

Secondly, the seismic shocks in question, or their consequences, were registered within a long time: from the moment of the occurrence of Messina earthquake (Bystrica) to several days (Valmiera), but in most cases, they were registered within 3 days – from December 28 to December 31, 1908.

Third, according to some estimates [Авотиня и др., 1988], the strongest shock intensity reached grade VII on the MSK-64 scale. From the impact of some strong shocks, the following macroseismic manifestations were observed: 1) cracks on the ground (Bystrica); 2) a crack from Āgenskalns to Baloži (Riga); 3) cracks in the church building and on the ground – with a width of ½ to 1 ¼ in. (Madona); 4) a 3–4 inches-wide crack through the fields and meadows, as well as a crack in the foundation of a house (the Daugavpils district); 5) through cracks (bracits) in the walls of a single-storey building – from the foundation to the ceiling (Valmiera). In the latter case, cracks appeared after a few days; however, nothing is reported about people's sensations.

Relative to the genesis of those earthquakes, there is some ambiguity in the estimates. In particular, according to the viewpoint of Professor Andrew Nikonov, the earthquakes of 1908 could be of frost nature. Such phenomena were repeatedly noted on EEP, in Siberia and Scandinavia [Nikonov, 2010]. Those seismic phenomena have a name of their own – *cryoseisms*.

Such a frost shock-generating mechanism implies that the earth in winter is first saturated with water – especially, it applies to the subsurface soil layer. Subsequently, with a precipitate drop in the temperature, the waterlogged grounds are freezing quickly. This results in ice expansion. The hard ice is cracking with an acoustic sound that can shake a house. These phenomena affect the ground which is a few feet-thick (1 feet = 0.3048 m). As a rule, such *cryoseisms* have a limited, local manifestation. The soil-freezing process leads to an increase in explosive stress, which may result in the formation of soil ruptures. Ruptures of such kind may be accompanied by loud sounds reminding shooting [http://frostquake.org/]. During the season 2014–2015, there circulated a lot of reports on cryoseims connected with the cold winter [http://frostquake.org/cryoseisms-reported-in-tennessee/]. However, the strength of the most powerful cryoseism is estimated by magnitude 1.5 [Freaky 'frost quakes'…_*si*]. These phenomena were also reported in England and Canada in wintertime.

One of the typical features of a cryoseism is lack of a snow cover, although there are some exceptions as well. Cryoseisms may occur not immediately but even some time later after the temperature drop (in a few days).

Information on 12 (twelve) cryoseisms has been collected in the North-East of the USA, in Maine. The collected data covered the period from 2000 to 2017 [http://www.maine.gov/dacf/mgs/hazards/earthquakes/quake-cryolist.htm]. According to that information, cryoseims occurred on the second and even on the sixth date after the temperature drop. The consequences of the cryoseims were quite impressive.

For example, at 3 a.m. February 2003, a 21 m (70 feet)-long crack appeared on the concrete floor in the basement of a house. This fact took place in the city of Philips. It is characteristic that the seismic network of New England did not record any seismic activity. This is of small surprise since cryoseims normally occur in the upper layer of the ground, where the major seismic energy absorption takes place.

The distribution of winter temperatures recorded throughout December, 1908 was analyzed based on the input values, data taken from logbooks run at meteorological stations, the observation site *"Marine House"* in Riga and the meteorological station in Dvinsk (Daugavpils). The surveillance sample rate was 3 times a day: at 07.00 a.m., 13.00 p.m., and 21.00 p.m.

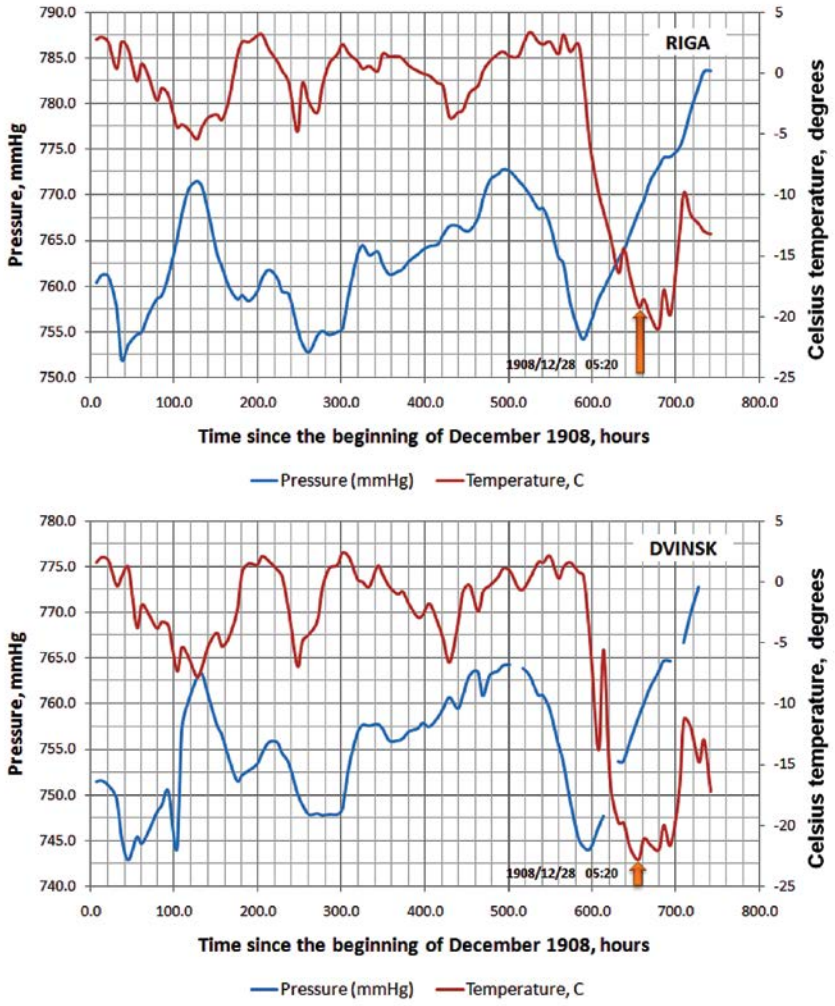

Figure 54. Pressure and temperature variation in December 1908, recorded at meteorological stations in Riga (above) and Dvinsk (below)

Immediately at the moment of Messina earthquake on December 28, 1908 (05.20) the air temperature in Riga had reached almost minimal value –19°C, while the temperature in Dvinsk had reached exactly the minimal value –22.8°C (Figure 54).

The first shocks were perceived either at the same time as in Messina or within three subsequent days – i.e., up to December 31, 1908 inclusive. But at that time, air temperature started to rise and the conditions favourable for frost phenomena occurrence worsened. It is characteristic that shocks were perceived even after the temperature started rising – although it was low enough anyway (–9. 8° C in Riga and –11.3°C in Dvinsk).

Thus, seismic shocks not associated with tectonic earthquakes but with frost phenomena – *cryoseims* – were perceived in December 1908 on an extensive EBR territory. Moreover, a database audit is necessary for those EBR earthquakes that took place in winter. The situation can be elucidated by the archive data on meteorological conditions of that time. The exclusion of those false tectonic earthquakes from the EBR earthquake catalogue may scale down EBR seismicity characteristics – in particular, reduce their alleged seismic activity. Nevertheless, no matter how sad it is to admit that, it is so. On top of everything else, earthquake statistics is deprived of its essential part. We must admit that Professor Andrew Nikonov, who was the first to raise the issue of EEP frost phenomena, was right.

Still, those seismic events are still available in some EEP catalogues – as, for example, the Earthquake Catalogue for Eastern European Platform (Institute of Physics of the Earth under the Russian Academy of Sciences (IPE RAS).

1.3. Present-day earthquakes of East Baltic Region

Present-day earthquakes of the East Baltic Region have been instrumentally recorded by regional seismic stations of Scandinavia, Eastern Europe, or the East Baltic Region. The beginning of the instrumental observation period refers to mid-1960s (since 1965)) [Mantyniemi et al., 2004]. Although the first seismographs were installed in Scandinavia (*Uppsala,* Sweden) and *Bergen* (Norway) in 1905–1906, their low sensitivity, frequency-response characteristics and lack of a regular survey grid did not allow one to record any regional earthquakes in the East Baltic Region (EBR).

The present-day notable earthquakes in EBR include, in particular, the Osmussaare earthquake of 1976 in Estonia and the Kaliningrad earthquakes of 2004 in the Kaliningrad Region of Russia – with the intensity VI–VI ½. The other earthquakes in EBR had insignificant magnitudes, but some of them were perceivable anyway. The earthquakes that took place in 1987 in Estonia, in the vicinity of the Lake Võrtsjärv, were stated only based in macroseismic information, since no seismic stations network that could locate earthquake hypocenters was not yet available in EBR at the time.

The present-day earthquakes in EBR were instrumentally recorded by regional seismic grids, while the reconnaissance of earthquake epicentral areas enabled researchers to plot earthquake isoseist maps. It is characteristic that that there were certain discrepancies between the instrumental results of specifying earthquake

hypocentres (especially, this applies to the Kaliningrad earthquake of 2004) and the macroseismic results. Information on the strongest EBR earthquakes that took place in 1976 and 2004 is given below.

3.3.1. Osmussaare earthquakes of 1976

In the autumn of 1976, earthquakes took place on the Osmussaare Island in Estonia, which was quite unexpected to geologists. The first and the strongest shock took place on October 25, 1976. The earthquake magnitude was 4.7 while the epicentral intensity was 7.0 ± 0.5 [Nikonov et al., 2002; Kondorskaya et al., 1988]. After the main shock, a few more aftershocks took place within the period from October 25 to November 22, 1976. The main shock was recorded by seismic stations of Finland (KEF, SUF, KAF, PRV, PKK NUR), whereas the aftershocks were also recorded by a seismic array which was jump-started by the Schmidt Institute of Physics of the Earth in the epicentral area. In particular, the mobile team used "*The Earth*" stations [Bulin et al., 1980]. Within the epicentral area, macroseismic data was collected that subsequently made it possible to plot an isoseist card of the main shock of the Osmussaare earthquake.

On the earthquake record (Figure 55) high-frequency oscillations with frequencies $f > 10–50$ Hz and large amplitudes can be observed. The seismogram analysis has shown an abnormally high portion of high-frequency oscillations at the source emission for P-waves spectra.

The earthquake was perceived on a large territory on both sides of the Gulf of Finland. The shock level was different for different directions. In the northeasterly

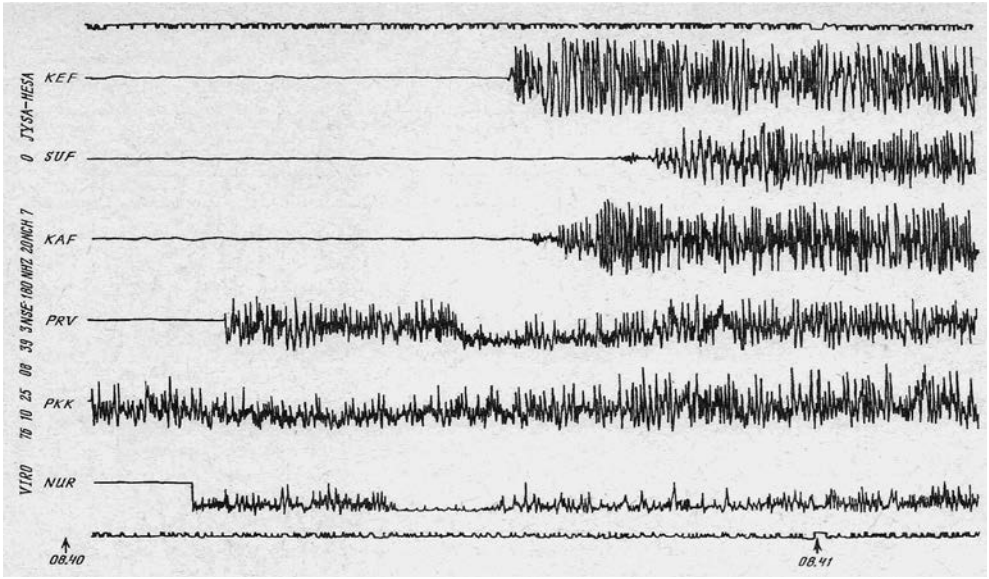

Figure 55. Records of Osmussaare earthquake of October 25, 1976 by seismic stations of Finland KEF, SUF, KAF, PRV, PKK, NUR [Kondorskaya et al., 1988]

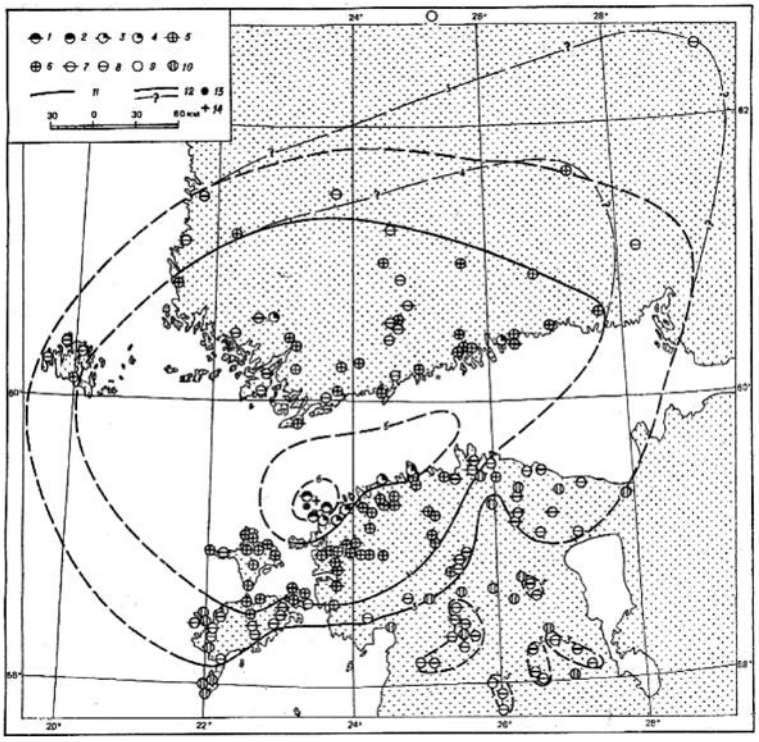

Figure 56. Input macroseismic data of Osmussaare earthquake of October 25, 1976 (08:40) [Kondorskaya et al., 1988]

Intensity designation: 1) 6–7 points; 2) 6 points; 3) 5–6 points; 4) 5 points; 5) 4–5 points; 6) 4 points; 7) 3–4 points; 8) 3 points; 9) 2 points; 10) not perceived; 11) actual isoseists; 12) hypothetic isoseists; 13) the focus according to instrumental data; 14) macroseismic focus

and northwesterly directions, the shocks were perceived at longer distances than in southwesterly and southeasterly directions (Figure 56). This may attest to inhomogeneity and anisotropy in the Earth's crust of the East Baltic Region.

The attenuation of the oscillations strength turned out to be less pronounced than it was expected [Kondorskaya et al., 1988]. For the earthquake in question, the macroseismic magnitude can be estimated from the correlation as follows:

$$M = 2{,}5 + \lg S \qquad (6)$$

where – perception area in km^2.

The parameters of the main shock of the Osmussaare earthquake are presented in Table 3.

4 (four) aftershocks took place after the main shock; they were recorded by the mobile group of "Earth" stations within the epicentral area. The aftershock analysis has shown that the epicentres of all the aftershocks were located at the same place as the main shock was. In the aftershocks spectra, high frequencies (8–15 Hz)

Table 3.

The main parameters of the Osmussaare earthquake as of October1976 [Kondorskaya et al., 1988]

Instrumental data						
Time, GMT	Lat	Lon	H, km	MLH	MPV	Source of information
08:39:44.7 ± 0.41	59.20 ± 0.037	23.58 ± 0.088	10	-	4.4	ISC Bulletin, 1978
08:39:45.0 ± 2.0	59.26 ± 0.15	23.39 ± 0.15	10 ± 10	4.3 ± 0.5	4.7 ± 0.7	Kondorskaya, Shebalin, 1982
08:39:46.2	59.35	23.22	-	4.9	-	Korhonen, Ahjos, 1984
	59.36	23.34	12			Slunga, 1981
Macroseismic data						
Time, GMT	Lat	Lon	H, km	I	M	Source of information
08:39:44.7 ± 0.41	59.3	23.5	15	7	4.7	Ananyin, Bulin, 1980
08:39:45.0 ± 2.0	-	-	10* 8**	6 – 7 ± 5		Kondorskaya, Shebalin, 1982
08:39:46.2	-	-	18	6.5	4.9	Korhonen, Ahjos, 1984
			16			Korhonen, 1977

Notes: MPV and MLH – magnitudes of surface waves for the vertical and the horizontal components, respectively; I – shock intensity in the epicentre; M – macroseismic magnitude;
** – depth calculated based on the character of intensity attenuation;*
*** – depth calculated based on epicentral intensity and MLH magnitude*

predominate. The aftershocks' magnitude was within the interval 3.0–3.5. The position of the epicenter of Osmussaare earthquake, specified based on instrumental data, actually coincides with the epicenter position specified based on macroseismic data (Figure 56). The parameters of aftershocks of the Osmussaare earthquake are presented in Table 4.

From the seismotectonic standpoint, the earthquake focus is located at a depth of 10–13 km in a granite-metamorphic stratum, in the vicinity of a seismic horizon where some changes in elastic and magnetic properties of the substance and in the formation density have developed [Ананьин и др., 1980]. The epicentral area is located on the territory characterized by a small power of the sedimentary cover (100–150 m). The velocity of the uplift of geologic highs and crustal elevations is estimated at 3 mm/per year.

Table 4.

The main parameters of the aftershocks from Osmussare earthquake of 25 October 1976 [Kondorskaya et al., 1988]

No.	Date	Time, GMT	Lat	Lon	H, km	M	Source of information:
1	25.10.1976	09:07	59.3 ± 0.1	23.5 ± 0.1	-	3.5	Ananyin et al., 1980 (macroseismic data)
		08:50	59.3	23.3	-	3.5	Korhonen, Ahjos, 1984.
2	25.10.1976	09:10	59.3 ± 0.1	23.5 ± 0.1	-	3.0	Ananyin et al., 1980 (macroseismic data)
		09:10	59.3	23.3	-	3.0	Korhonen, Ahjos, 1984.
3	8.11.1976	10:17:07 ± 0.5	59.33 ± 0.02	23.47 ± 0.02	0 – 13	3.5	Ananyin et al., 1980; Bulin, Vidr, 1980 (instrumental data from temporal seismic stations at an epicentral distance some 20 to 50 km).
		10:17:05	59.6	23.4	-	3.5	Korhonen, Ahjos, 1984.
4	22.11.1976	15:13:42.5 ± 0.5	59.33 ± 0.02	23.42 ± 0.02	13 ± 2	-	Ananyin et al., 1980; Bulin, Vidr, 1980 (instrumental data from temporal seismic stations at an epicentral distance some 20 to 50 km).
		15:14:43	59.3	23.4			Korhonen, Ahjos, 1984.

The deep-seated Paldiski-Pskov tectonic area (PPTA) identified on the basis of geophysical data [Побул & Сильдвээ, 1975] is crossing the epicentral area of Osmussaare earthquake. PPTA was the active border of a fault block in the early Paleozoic. Later, the orientation of the active border of the area was changed, and the elevation of the Northern Estonia (the Gulf of Finland) relative to the Southern Estonia was stated. During the non-tectonic period, the block slipping in the Paleozoic sedimentary cover of Estonia (and, apparently – the one in the basement) was developing along the faults oriented in NE-SW direction (Figure 57).

A narrow fault extends in the north – north-easterly direction through the epicentral area of Osmussaare earthquake [Sviridov, 1981]. The fact of its existence and its activity after the early Paleozoic period was confirmed in the Central Baltics, while it was also found in the northwestern part of the Hiiumaa Island. Satellite data attests to the existence of a large lineament extending across the bottom of the Gulf of Finland in the east – north-easterly direction [Lahtinen, 1984].

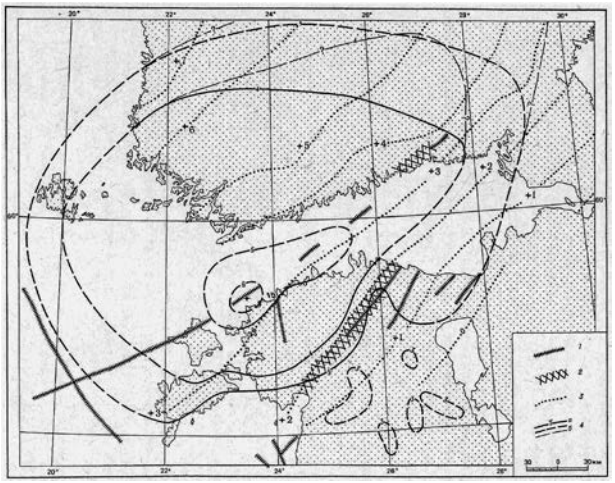

Figure 57. Seismotectonic scheme of the South East of Fennoscandia [Kondorskaya et al., 1988]

Designations: 1 – the basement fault and the fault in Paleozoic formation; 2 – the contrast vertical movement areas of the Holocene surface and the present-day surface; 3 – contour lines of the present-day uplift (elevation) (mm/year); 4 – isoseismic lines of the earthquake as of October 25, 1976: a – actual, b –assumed

3.3.2. Kaliningrad earthquakes of 2004

The earthquakes that took place on September 21 in the Kaliningrad Region of Russia were quite unexpected to seismologists, since they happened at a region characterized by a low seismicity level. Such a "surprise" happened in EBR for the second time in 28 years – i.e., after the Osmussaare earthquake in Estonia. The moment magnitude M*w* of the first two Kaliningrad earthquakes was estimated at 5.0 and 5.2, respectively. The second Kaliningrad earthquake with = 5.2 was the strongest one among all of the known EBR earthquakes. The earthquakes were recorded by many seismic stations of Scandinavia and Eastern Europe (Figure 59). The earthquake-entailed consequences were as follows: one person died from a heart attack and 20 people were hurt severely by falling objects, while about 2100 buildings were damaged (Figure 58). The total amount of damage constituted M 5.3 USD [Nikonov et al., 2005].

The earthquake took place at north-west of the ancient East European Platform – not far from the Tornquist – Teisseyre boundary separating the platform form the younger West-European Platform.

The shocks generated by the earthquake were perceived at distances up to 800 km. Westwards and southwards, the shock propagation is bounded by Tornquist – Teisseyrezone – i.e., by the south-western edge of EEC (Figure 60). The shock intensity at the earthquake epicentres was estimated at 6.0 ± 0.5 and 6.5 ± 0.5 for the first and the second shocks, respectively [Nikonov et al., 2005]. According to macroseismic data, 5 (five) aftershocks have occurred after the two initial shocks (see the Table), which took place on September 21 and 22, 2004 [Nikonov, 2007].

Figure 58. Consequences of the Kaliningrad earthquakes as of September 21, 2004 in the Kaliningrad Region of Russia [Nikonov et al., 2005]

Designations: 1 – fragment of the main fracture in the soil, in the vicinity of Veselovka residential settlement; 2 – collapsed plaster on the ceiling of the first floor of the school in Svetliy residential settlement; 3 – typical damage of chimneys (the Kosmodemyansky village); 4 – railway bed deformation on the 67th kilometer near the city of Svetlogorsk

Figure 59. Position of epicenters of Kaliningrad earthquakes that took place on September 21 on the Sambiysky Peninsula (Samland) in the Kaliningrad Region of Russia

Designation: red and white triangles – seismic stations, Tornquist-Teisseyre zone – the boundary between East European Platform and West European platform

According to instrumental data, the hypocentres of the first two earthquakes (the strongest ones) were located at a depth of 16–20 km [Gregersen et al., 2007]. The macroseismic depths of the hypocentres (10–19 km) are in reasonably good agreement with the corresponding instrumental data.

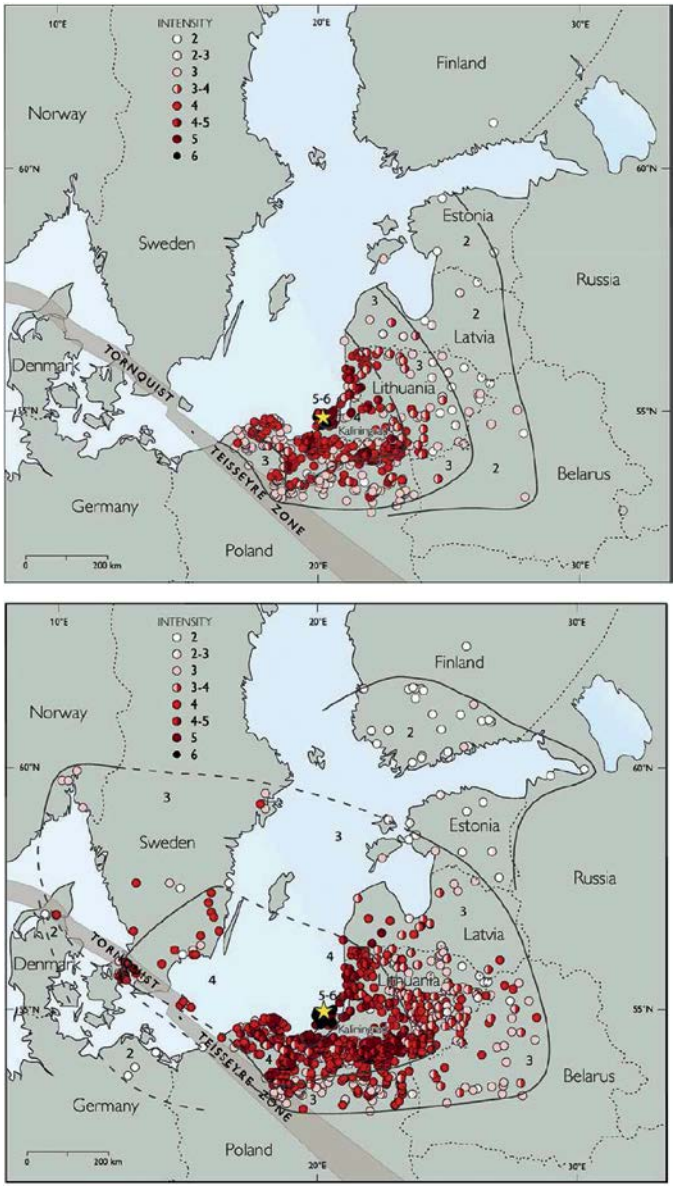

Figure 60. Generalized macroseismic map of shock intensity of the Kaliningrad earthquakes as of September 21, 2004 – for the first shock with = 5.0 (11:05) and for the second shock with = 5.2 (13:32) [Gregersen et al., 2007]

Explanations of the earthquake source mechanism have been received with respect to the two Kaliningrad shocks that were the first to take place. The source mechanism of the earthquakes was defined as the right lateral strike slip from west-north-west direction up to the east-southeast direction. To the best of our knowledge with regard to tectonic stresses, it is assumed that the key reason for the earthquakes was the absolute plate movement [Gregersen et al., 2007]. The movement is caused by the pressure from the Atlantic divergent plate boundary lying between Eurasian and North American Plates.

Analysis of historical earthquakes has shown that 5 earthquakes took place in the region of the above-mentioned earthquakes within the period from 1302 to 1328. The shock intensity of the historic earthquakes is estimated at 5–7 [Nikonov, 2007].

In 2004, two seismic stations included into *GEOFON* network with the centre in *GFZ Potsdam* were operated on EBR. The records of the two strongest Kaliningrad earthquakes (September 21, 2004) are shown in Figure 61. It should be pointed out that the third earthquake took place at 13:36 p.m. – right after the second earthquake that happened at 13.32. All of those earthquakes have been recorded and they were perceived by the people.

The results of the location of earthquake hypocentres are presented in Table 4. The magnitude average value was not specified, since various agencies used magnitude of different types. Most of the locations have been received by using a fixed depth of 10 km; therefore, there is no point of specifying the average value of hypocenter depth. Location parameters of the Kaliningrad earthquakes of September 21, 2004 are presented in Table 5.

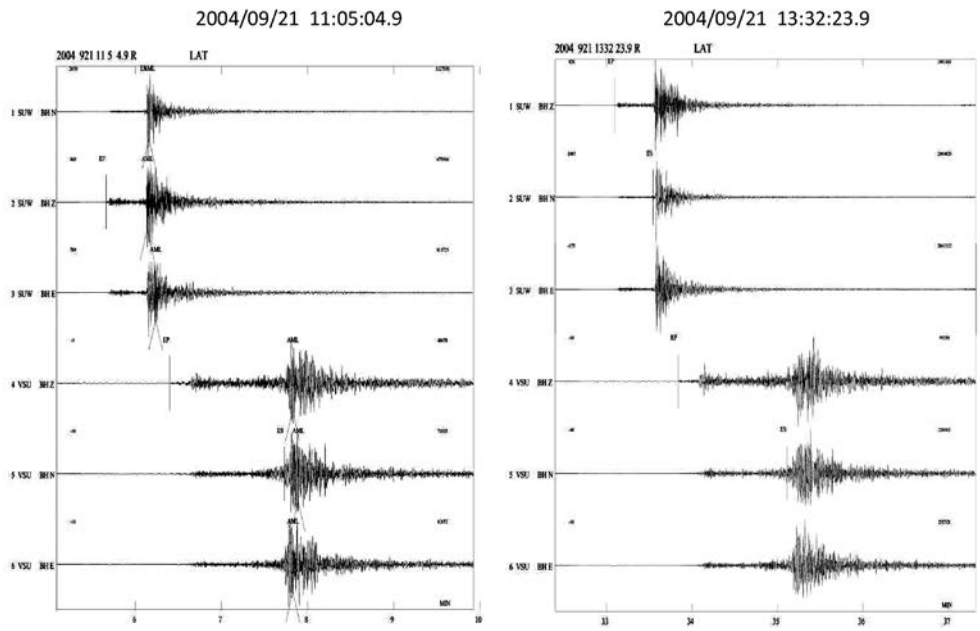

Figure 61. The Kaliningrad earthquakes seismograms of 21 September 2004 (11.05 – left; 13:32 – right) recorded at Suwalki (SUW) and Vasula (VSU) stations

Table 5.

Location parameters of the Kaliningrad earthquakes of September 21, 2004

Earthquake of 2004/09/21, 11:05:03.9							
ID	**Agency and model**	**Time, UTC**	**Lat, N**	**Lon, E**	**H, km**	**Magnitude type**	**M**
1	IGF IASP	11:05:01.8	55.14	19.88	10 fix	M_W	
2	IGF AK135	11:05:04.5	55.00	20.05	10 fix	M_W	
3	EMSC	11:05:04.3	54.91	20.08	10 fix	M_{mb}	4.4
4	ORFEUS	11:05:08.7	54.8	19.7	10 fix		
5	NEIC	11:05:03.2	54.858	19.980	4.1	M_{mb}	4.8
6	ASS	11:05:04.6	54.85	20.04	6.6		
7	GSRAS	11:05:05.0	54.84	20.13	21	M_S	4.1
8	MOS	11:05:02.0	54.843	20.024	10 fix		
9	ISC	11:05:03.0	54.83	20.04	10 fix		
0	IGF PROB	11:05:01.6 ± 1.4	54.924 ± 0.021	20.120 ± 0.050	16.0 ± 9.3	M_W	
11	UHIS	11:05:04.8	54.774	20.040	10	M_L	4.8
12	IRIS	11:05:01.0	54.86	20.07	10		4.8
13	NORD CAT	11:05:06.5	54.738	19.819	15	M_L	4.1
*	Average value	11:05:03.9	54.874	19.998			
Earthquake of 2004/09/21, 13:32:30.8							
ID	**Agency and model**	**Time, UTC**	**Lat, N**	**Lon, E**	**H, km**	**Magnitude type**	**M**
1	IGF IASP	13:32:33.6	54.79	20.14	10 fix	M_W	
2	IGF AK135	13:32:32.5	54.86	20.13	10 fix	M_W	
3	EMSC	13:32:30.8	54.89	20.18	10 fix	M_{mb}	5.0
4	ORFEUS	13:32:29.2	54.8	19.9	10 fix		
5	NEIC	13:32:30.8	54.841	19.912	10	M_{mb}	4.9
6	ASS	13:32:30.8	54.88	20.05	8.4		
7	GSRAS	13:32:31.3	54.84	20.17	17	M_S	4.3
8	MOS	13:32:28.3	54.896	20.185	10 fix		
9	ISC	13:32:28.58	54.82	19.96	10 fix		
0	IGF PROB	13:32:31.0 ± 1.3	54.876 ± 0.021	20.120 ± 0.055	20.0 ± 10.1	M_W	
11	UHIS	13:32:31.9	54.834	20.025	10	M_L	5.0
12	IRIS	13:32:28.0	54.83	19.97	10		4.9
13	NORD CAT	13:32:33.2	54.754	19.792	15	M_L	5.2
*	Average value	13:32:30.8	54.839	20.041			

Earthquakes of 2004/09/21, 13:36:38.8							
ID	**Agency and model**	**Time, UTC**	**Lat, N**	**Lon, E**	**H, km**	**Magnitude type**	**M**
7	GSRAS	13:36:33.8	54.87	19.99	0.5 ± 3	M_S	3.0
12	IRIS	13:36:48	54.47	21.26	10		4.0
13	NORD CAT	13:36:34.7	54.759	19.776	15.4	M_L	4.0
*	Average value	13:36:38.8	54.7	20.342			

Note: IGF IASP – Institute of Geophysics, Polish Academy of Sciences &velocity model IASP91(International Association of Seismology and Physics of the Earth's Interior); IGF AK135 – Institute of Geophysics, Polish Academy of Sciences &velocity model AK135; EMSC – European Mediterranean Seismological Centre; ORFEUS – Observatories & Research Facilities for European Seismology; NEIC – National Earthquake Information Center (USGS – United States Geological Survey); ASS – based on the location findings obtained by B. A. Assinovskaya – the leading seismologist of the Pulkovo observatory (Russia); GSRAS – Geophysical Survey of Russian Academy of Sciences; MOS – Moscow data center; ISC – International Seismological Centre; IGF PROB – Institute of Geophysics, Polish Academy of Sciences &velocity model PROB; UHIS – University of Helsinki Institute of Seismology; NORD CAT – Nordic catalogue of SNSN (Sweden National Seismological Network); – moment magnitude; – local magnitude; – surface wave magnitude; – body wave magnitude; fix – the determination of hypocenter depth was carried out by using fixed depth of 10 km

The location results for the first two Kaliningrad earthquakes (Figure 62) show that there exist some substantial divergences with regard to hypocentre determination by different agencies that have used different types of models for seismic wave propagation velocities through media.

For example, as one can see on the left Figure 47, the location results with the AK135 model used by IGF turned out to be more effective as compared to IASP model. As regards the AK 135 model, the first earthquake epicenter has deviated insignificantly

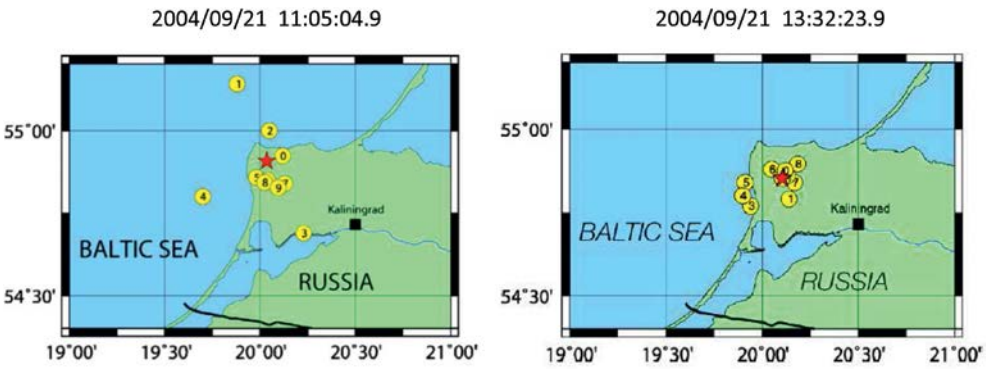

Figure 62. Results of instrumental location of the first two Kaliningrad earthquakes at 11:05:03.9 (left) and at 13:32:30.8 (right) [Gregersen et al., 2007]

Note: the figure inside the epicentres corresponds to the identifier (ID) in Table 5

from the general compact group of location results. With respect to the second earthquake with a larger magnitude, the scatter in location results is less pronounced. The location results for UHIS, IRIS and NORD CAT are not shown in Figure 62 since they are included into Table 4 in addition to the results previously published [Gregersen et al., 2007].

For the third earthquake, some limited data is available, because the earthquake magnitude was less than that of the first two earthquakes.

For the first time in EBR, an explanation of the earthquake focal mechanism of the two Kaliningrad earthquakes was obtained. Three seismological centres have found a solution for the second shock – the strongest one – by using moment tensor inversion, whereas IGF has found a solution for the first two shocks (Table 6) with the aid of the place of fracture solution and moment tensor inversion.

Table 6.

Parameters of the Kaliningrad earthquake focus mechanism

Parameter	IGF f.p.	IGF – Event 1	IGF – Event 2	Harvard	INGV	ETHZ
Seismic moment 10^{16}N m	–	0.57	2.13	1.40	1.20	1.38
Nodal plane A strike	211	202.0	204.7	205	211	206
Nodal plane A dip	88	89.2	84.3	78	81	86
Nodal plane B strike	301	111.7	113.4	297	300	294
Nodal plane B dip	82	73.7	77.3	80	81	64

Note: all the data refers to the second shock (13:32:30.8) except for IGF definitions of the two earthquakes; all the solutions for the nodal plane B are alike if the moment tensor solutions are used; the component not associated with the shear for all the moment tensor solutions is lower than 5%; IGF – Institute of Geophysics, Polish Academy of Sciences; f.p. – fault plane; Harvard – Harvard University; INGV-Mednet; ETHZ – Swiss Seismological Service

Out of the two nodal planes, plane B is considered as a more realistic candidate for the fault plane. Plane A is rather an auxiliary plane. It is confirmed by the fact that the plane B is almost parallel to the Tornquist-Teisseyre area. Another indirect indicator is lack of the proof of any earthquake having actually taken place along the direction of plane. The third indicator is the extremely high amplitudes of S-waves recorded southeast of SUW and north-west to BLEU. Those amplitudes could be caused by a fracture along the fault passing in this direction.

The earthquake focal mechanism for Kaliningrad earthquakes of 2004 (Figure 63) was determined by the International Mediterranean Seismological Data Centre INGV – *Mednet*, Seismological Data Service of Switzerland – ETHZ, Harvard University and Institute of Geophysics under the Academy of Sciences of Poland (IGF). The parameters of the sources – i.e., the first two earthquakes – are assessed based on instrumental data (Table 7).

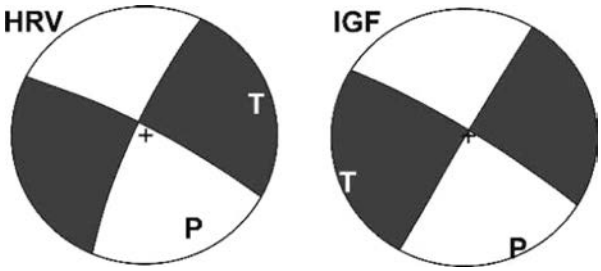

Figure 63. Source mechanism diagrams according to the Harvard University (HRV) and Institute of Geophysics, Polish Academy of Sciences (IGF) moment tensor solutions of the second, bigger Kaliningrad earthquake of September 21, 2004.

Table 7.

Source parameters of the September 21, 2004 Kaliningrad earthquakes [Gregersen et al., 2007]

Parameter	Event 1	Event 2
Seismic moment, N m	5.0×10^{16}	7.2×10^{16}
Magnitude,	5.04 ± 0.15	5.22 ± 0.15
P wave corner frequency, Hz	1.3 ± 0.4	1.3 ± 0.5
S wave corner frequency, Hz	1.1 ± 0.4	1.1 ± 0.5
Source radius, m	962 ± 360	945 ± 336
Stress drop, MPa	24.6	37.4
Apparent stress, MPa	4.2	11.9
Average displacement, cm	38.0	57.1
Seismic energy, J	4.3×10^{12}	2.2×10^{13}

According to macroseismic and seismotectonic data [Никонов, 2006], the fracture (fractures) activation planes have azimuths as follows: 190° ± 10° for the first shock, 95° ± 10° for the second shock, and 190° ± 10° for the third shock. The tilt angle is equal to 90° ± 10°, 80° ± 10°, and 90° ± 10°, respectively.

The fault planes inclination parameters (Table 6) specified based on instrumental data and the macroseismic and seismotectonic data closely agree with each other. The lines of strike of those planes diverge within the limits 15°–20°, given that the solutions for nodal planes A and B are taken into account. However, the main differences obtained from macroseismic and structural tectonic data from the solutions based on instrumental data consist in the fact that, according to macroseismic data, the earthquake foci are located under the seabed, near the western and northern coasts of the Sambian Peninsula (Figure 64) but not on the adjacent land as it follows from the instrumental data. The second difference consists in the fact that, according to macroseismic data, the focus of the first earthquake is in the meridian plane but not in the inverse-latitudinal plane as suggested by the instrumental data.

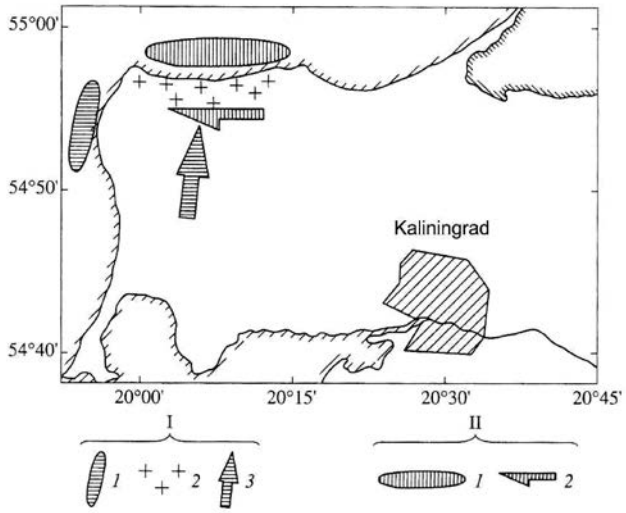

Figure 64. Position of the focus projections of the first (I) and the second (II) shocks of Kaliningrad earthquake as of September 21, 2004 according to macroseismic and seismotectonic data [Никонов, 2006]

Legend: I – the first shock: 1 – focus projection, 2 – the region wherein the first shock was perceived as a vertical one; 3 – the direction of relative movement of continental block displacement (the Sambian Peninsula); II – the second shock: 1 – focus projection, 2 – the direction of relative movement of continental block displacement (the Sambian Peninsula)

According to the foci mechanisms assessment results obtained with the aid of instrumental and macroseismic methods, the earthquakes occurred at a compression from the northwest to southeast direction (macroseismic) or, from the west-northwest to east-southeast direction (the instrumental method). It is exactly in these directions that the predominant tectonic stress is the pressure exercised on a part of the spreading zone in North Atlantic.

3.3.3. Review of contemporary, small earthquakes of the East Baltic Region

Within the instrumental observation period, a few earthquakes with a small magnitude took place in the East Baltic Region. Most of them took place on the territory of Estonia. The characteristics and the description of the earthquakes is given below.

The Osmussaare earthquakes of 1987

Some earthquakes took place in the neighbourhood of the Lake Võrtsjärv in Estonia – in April and July 1987. Those earthquakes could well have been registered, since instrumental observations were already carried out at that time in Finland. For instance, they could have been registered at the stations: Nurmijarvi (NUR, Porkkala (PKK), Porvoo (PRV) and Helsinki (HEL), which are located on the south of Finland,

in the vicinity of the Baltic Sea coast. However, no data on instrumental records is available. Those three earthquakes were perceived by people, the more so that they took place either late in the evening or early in the morning (Table 7.) The epicentral intensity was assessed at III–VI on the MSK-64 scale [Sildvee, 1988; Nikonov & Sildvee, 1991; Nikonov, 1992; Авотиня и др., 1988; Боборыкин и др., 1993]. The parameters of earthquakes in the area of Lake Võrtsjärv are presented in Table 8.

Table 8.

The Võrtsjärv earthquakes of 1987

Date	Time	Epicentre	I_0	Macroseismic characteristics
1987/04/07–08	At night – between 11 p.m. and 01in the morning	The Lake Võrtsjärv, Estonia	III–IV	The shocks were perceived mostly by those people who were sleeping
1987/04/08	23:21	The northern part of the Lake Võrtsjärv	III–VI	Sleeping people woke up. Windows and crockery were rattling, while the floors and the walls of wooden houses were creaking and dogs barking.
1987/07/05	02	The northern part of the Lake Võrtsjärv	III	The shocks were perceived mostly by those people who were sleeping

The historical data attests to the fact that some earthquakes already took place in the Lake Võrtsjärv area – namely, in 1823 and 1909 in Kuigatsi, to the South of the Lake Võrtsjärv, and in Viljandi – to the West of the Lake Võrtsjärv. The epicentral intensity reached III–V on the MSK-64 scale.

Earthquake of 12 November 2016 in the Lake Võrtsjärv area

On November 12, 2016, a 2.5 magnitude earthquake took place in the Lake Võrtsjärv area. The earthquake was registered by many stations included into *BAVSEN* network, which are part of *GEOFON* network, with the centre in *GFS Potsdam,* and by stations of Scandinavia. The earthquake record made by the *BAVSEN* network stations is shown in Figure 65.

The records of the earthquake produced by MEF and SLIT stations show (Figure 66) the degree of impact from the sedimentary mantle. Those stations are actually located at an equal distance from the earthquake hypocentre – namely, 228 km (MEF) and 238 km (SLIT), respectively.

Whereas the wave pattern at the MEF station, which located a crystalline basement is simple enough, and the first P-wave is surely identified (Figure 51). This does not apply to the SLIT station, which sits on 1 a km-deep sediment stratum, the upper part of which is composed of quaternary deposits.

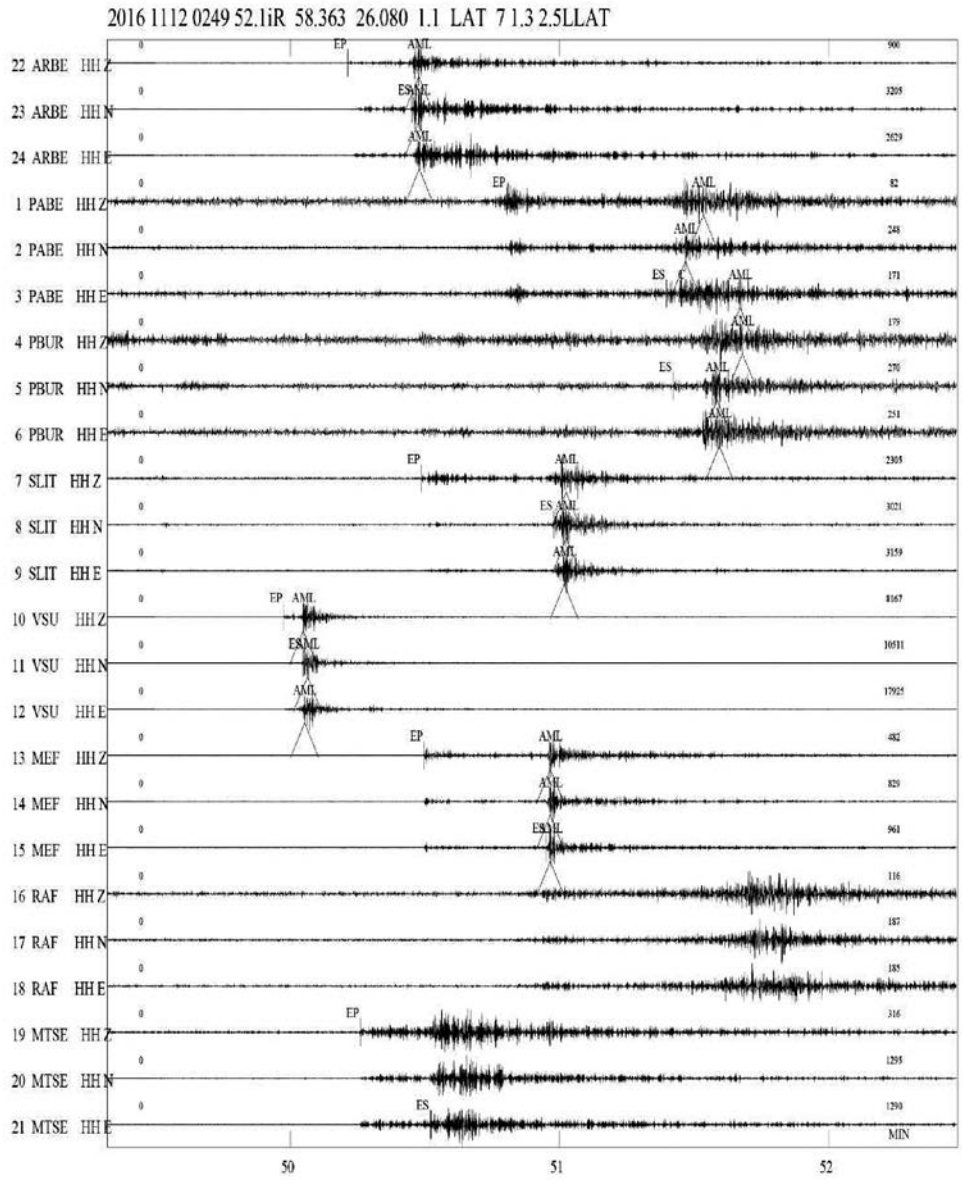

Figure 65. The earthquake in Estonia, in the Lake Võrtsjärv area, on November 12, 2016

Two groups of P-waves are highlighted at the SLIT station. The first group of P* waves even runs ahead of the arrival time of P-wave arrival to the MEF station – despite the fact that the distance to SLIT station is by 10 km longer than that to the MEF station. It seems more reliable to consider the first body wave as a group of P-waves that were second to arrive to the SLIT station (P without an index). Therefore, P-wave

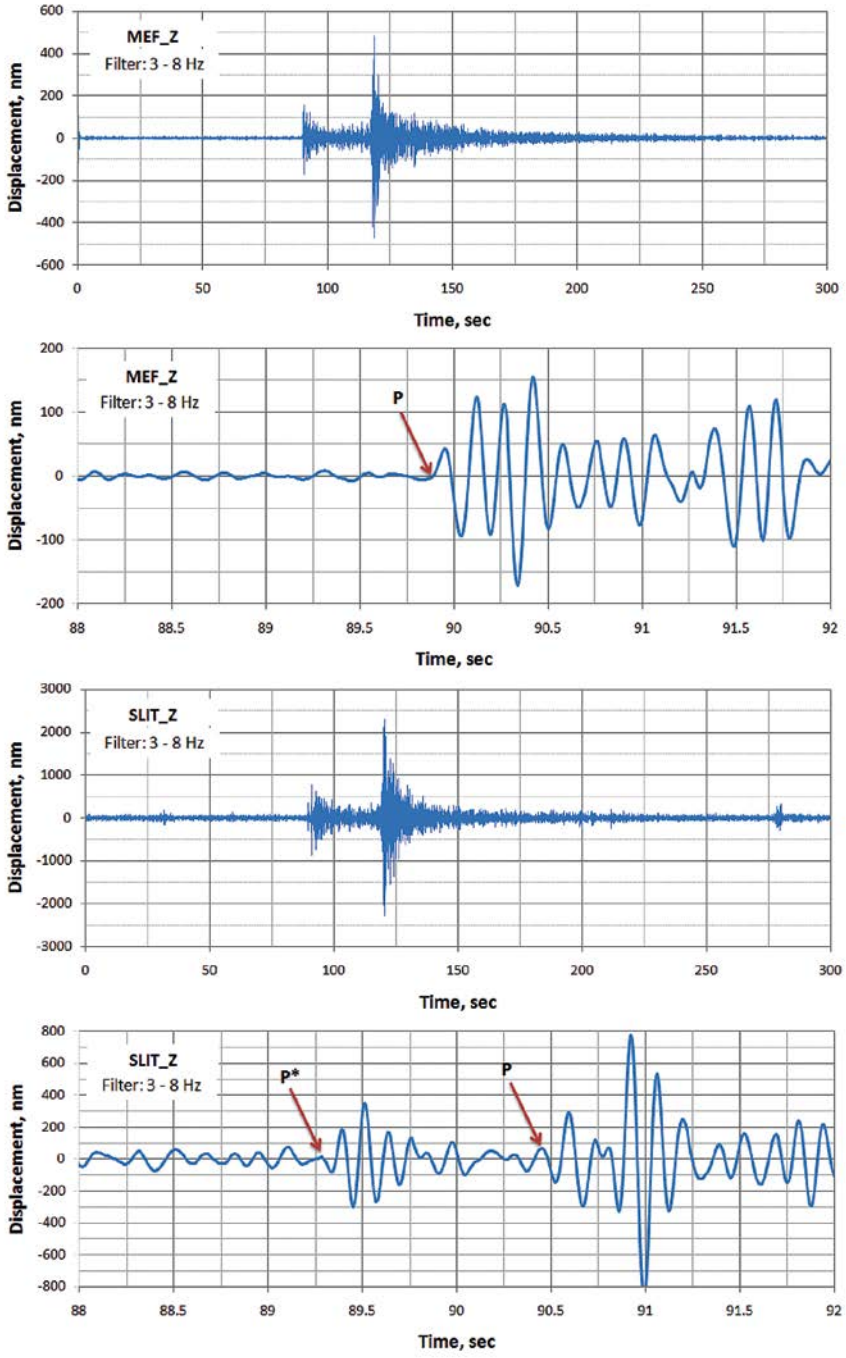

Figure 66. Records of the earthquake as of November 12, 2016 at MEF and SLIT stations, and fragments of records of P-waves arrival.

Notes: Displacements are presented in nm (nanometer) Z-component is indicated. Filtration band: 3–8 Hz

identification ambiguity is quite obvious with regard to the station, which sits on a thick stratum of sediments.

An additional problem is associated with a higher background noise level at the SLIT station. At the MEF station, the first P-wave amplitude relative to middle microseism level ratio *(SNR – seismic noise ratio)* is equal to about 8–10, whereas at the SLIT station, this ratio drops approximately to 5.

From the tectonic standpoint, the foci of the Võrtsjärv earthquakes may be connected with the Paldiski-Pskov deep-seated fault zone extending within a crystalline basement [Nikulins, 2017]. The zone width is about 15 km (Figure 67). The zone was shaped at the early Proterozoic age [Пуура, 1979]. The northeastern edge of the zone extends to the Gulf of Finland and further to the Osmussaare Island where tectonic earthquakes with the maximum magnitude 4.7 took place in 1976. According to the research findings obtained by Mindel [Mindel, 1994], two sublatitudinal fault zones are presumably located on the northeastern edge of the Lake Võrtsjärv. Their length is 15 km (the northern fault) and 24 km (the southern fault) accordingly, while the distance between the faults is about 10 km (Figure 67).

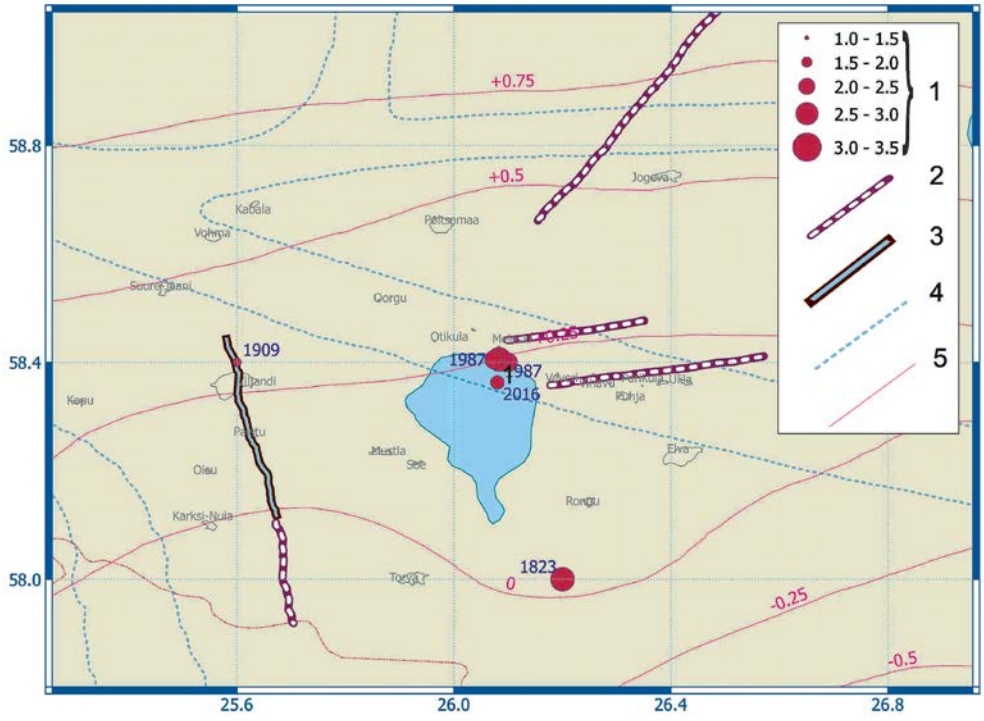

Figure 67. Seismotectonic situation of the Võrtsjärv area in Estonia

Legend: 1 – epicenters of tectonic earthquakes; 2 – assumed fault zones; 3 – fault zones in a crystalline basement and sedimentary cover, based on drilling data [Вяхер, 1983; Туулинг, 1990]; 4 – deep-seated fracture zones, located in a crystalline basement according to geophysical data [Побул&Сильдвээ, 1975]; 5 – velocities of modern vertical movements of the Earth crust, mm/year

Based on the solution for the earthquake mechanisms of the Southern Sweden [Slunga et al., 1984] and the Kaliningrad earthquakes of 2004 [Wiejacz & Debski, 2005; Gregersen et al., 2007], we can assume tha t the principal axis of tectonic stress is oriented towards from the north-east – to the south-west at azimuth of 136°–161°.

Taking into account dislocations with a break of continuity – with a strike azimuth about 71°–74°, it is fair to assume that the adjustment movement in the earthquake focus was caused by a right-lateral strike-slip.

Thus, the area of the Võrtsjärv region and its neighbourhood is a relatively active seismic zone in the context of the ancient East European Platform. The earthquake focus of 2016 is associated with an assumed tectonic zone formed by a number of east-west trending faults in the Paldiski-Pskov fault zone located in a crystalline basement. [Nikulins, 2017].

The complete list of the present-day and historical earthquakes of the East Baltic Region is to be found in Annex 1.

4. TECHNOGENIC SEISMICITY AND TECTONIC EARTHQUAKE IDENTIFICATION METHODS IN THE EAST BALTIC REGION

There is a variety of natural and human-induced sources that generate seismic waves. Oscillations of seismic waves arise due to elastic deformation. They can propagate through geological medium, water or over their surface in the form of single pulses or continuous oscillations. The energy of seismic sources has a huge range of frequencies and amplitudes. Two main types of seismic sources are natural and technogenic seismic events (Figure 68), i.e. seismic events due to human activities. Natural seismic events include tectonic earthquakes, volcanic tremor and volcanic earthquakes, falling rocks, destruction of karst cavities, frost damage (crioseisms), and storm microseisms. Technogenic seismic events include a large group of phenomena: controlled seismic sources (explosions, vibrations), earthquakes induced by changes in the water level in the reservoir, earthquakes induced by mountain impacts in coal and ore mines, rock collapse, injection and extraction of water into wells, injection of carbon dioxide into wells, production and storage of hydrocarbons in underground natural reservoirs, extraction of groundwater, generation of geothermal energy, hydraulic fracturing of seams during extraction of shale gas, aerodynamic shocks arising from mechanical action of air shock wave, which is formed when the aircraft reaches supersonic speed moving in the atmosphere, technogenic noises (industrial, transport, pile driving at construction sites, etc.).

Indeed, not all types of natural and anthropogenic sources exist in the East Baltic Region (EBR). The general scheme of natural and anthropogenic sources for the East Baltic Region is shown in Figure 68. The group of manmade sources includes both existing sources and those that may potentially appear in the future in the EBR. For example, induced seismicity caused by pumping or pumping out the liquid industrial wastes in the wells, induced seismicity caused by hydrocarbon production, underground storage of hydrocarbons. Induced seismicity caused by the collapse of rocks in coalmines, ore mines and quarries can already occur today in the EBR.

Technogenic seismicity is a consequence of various physical-mechanical processes caused by human activity. In the EBR, technogenic seismic sources on the land can be explosions in industrial quarries, mines, ice explosions on rivers to prevent the formation of ice jams, explosions during geophysical investigations by deep seismic sounding, explosions during seismic exploration works, downhole geophysical surveys,

including VSP (vertical seismic profiling), accidental emergency anthropogenic explosions (for example, on a gas pipeline), aerodynamic shocks occurring at the time the aircraft reaches supersonic speed and other physical-mechanical types of impact on solid and liquid medium. In addition, modern seismic exploration technology is based on use of non-explosive seismic sources – powerful seismic vibrators.

The sources of technogenic seismicity at sea may be explosions in the destruction of explosive objects left in the Baltic Sea after World War II or even World War I, explosions conducted during naval exercises in the Baltic Sea area, as well as the pulsed sources for excitation of seismic waves during geophysical works on the sea (the method of continuous seismoacoustic profiling), technogenic explosions on gas pipelines laid along the seabed.

Among the technogenic seismic sources, stationary and random ones can be distinguished. Stationary seismic sources are confined to industrial quarries, in which minerals and raw materials are extracted with the use of explosions. Random seismic sources are typical for the Baltic Sea. Time of action of stationary technogenic seismic

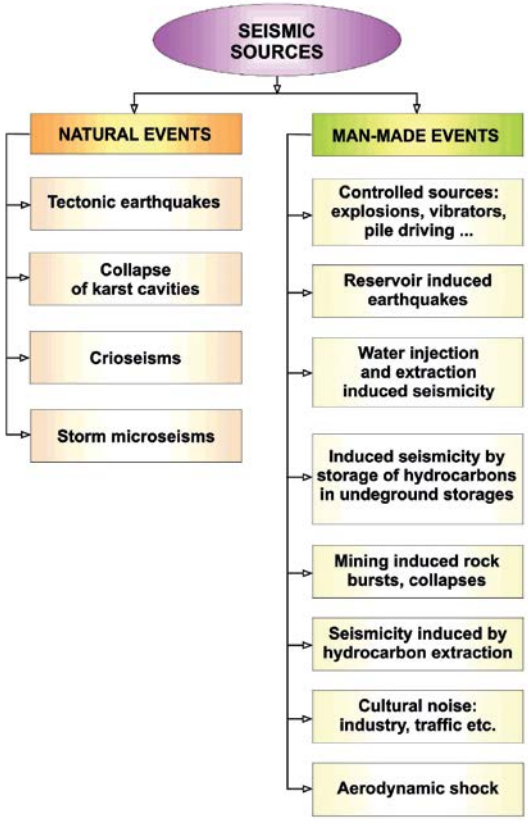

Figure 68. Schematic classification of existing natural and technogenic processes, as well as predicted technogenic processes in the East Baltic Region as a result of which seismic waves may arise

sources as a rule is within the working day and working week. On the contrary, random seismic sources can act practically at any time of the day and days of the week.

Technogenic seismic sources seriously impede the identification of natural tectonic earthquakes. The difficulty lies in the fact that there are very few tectonic earthquakes in the East Baltic Region and they need to be highlighted against the backdrop of a huge number of technogenic seismic events. Technogenic seismic events (as a rule, explosions in quarries) have turned into a kind of background of interferences, among which it is necessary to recognize rare and weak tectonic earthquakes. The magnitude of tectonic earthquakes in the East Baltic Region is very often low (less than 2.0). In addition, it is difficult for them to single out the onset of the first P-waves. The difficulty of singling out the first P-waves against the background of ambient seismic noise significantly decreases the possibility to identify and determine the type of a seismic event.

Special methods are used to separate tectonic earthquakes from technogenic seismic events. Some of these methods will be discussed in this chapter.

Some methodical techniques of separating the tectonic earthquakes from technogenic seismic phenomena are based on the use of special algorithms that allow filtering out the anthropogenic seismic events. It is achieved by analyzing the distribution of seismic events in time and space. For example, one of these *Exfilter* programs (from the *SEISAN* package) takes into account the location of the seismic source, time of its action (within the time of the working day) and a certain time of the year, magnitude below a certain threshold, depth not exceeding a certain value (e.g. 30 m). However, such logical filters are not effective if non-stationary seismic sources in the Baltic Sea are considered, since they can arise at any time of the day and days of the week.

At the same time, technogenic seismic sources are not only an interfering factor complicating the identification of tectonic earthquakes, but they can be useful in solving a number of special problems. For example, studies on the prediction of earthquakes involved also variations of parameters (kinematic and dynamic) of seismic waves (the method of seismic survey), which propagate through the region of earthquake preparation, [Мячкин и др., 1975; Мячкин, 1978; Добровольский, 2004]. In recent decades, methods based on recording of ambient seismic noise have been developed. Here, two areas of research can be noted. In the first case, the ambient seismic noise is used to study the internal structure (for example, the HVSR method). In the second case, the ambient seismic noise is used to study natural seismic sources.

Until now, the main types of regional seismic sources in the EBR are tectonic earthquakes and man-made explosions. Therefore, just these types of sources will be considered for understanding of their distinctive features, formation mechanisms, etc.

4.1. Models, mechanisms of seismic sources and tectonic regimes

The main place among all regional seismic sources of the East Baltic Region is occupied by tectonic earthquakes and technogenic explosions in quarries and in the water area of the Baltic Sea. To solve the main practical problem – recognition of

tectonic earthquakes among a large number of manmade explosions, it is necessary to consider models, the mechanism of seismic sources and earthquake-related tectonic regimes.

4.1.1. Focal mechanism of tectonic earthquake

The main natural seismic source is a tectonic earthquake. The physical model of a tectonic earthquake differs significantly from the physical model of an explosion. First of all, this difference relates to the nature of deformations, the speed of processes in the source and the formation of certain types of seismic waves. Consider the fundamental model of an earthquake.

The tectonic earthquake represents a more complicated deformation process than the explosion. It occurs when a brittle part of the Earth's crust is affected by a stress that exceeds its tensile strength. Usually such disruption occurs along a previously existing fault, but it can also occur (break up) in a continuous rock massif. The earthquake (tectonic) is characterized primarily by the action of tectonic forces and stresses, as well as the direction of the source. The source of the earthquake is connected with the plane of the tectonic fault S_α, along which the fault sides slip when the tectonic force exceeds the coupling strength of the fault sides. The simplest source of an earthquake can be represented in the form shown in Figure 69.

Tectonic forces F act on the side of the block of the Earth's crust, oriented perpendicularly to the action of force (Figure 69). The block of the Earth's crust is presented in the form of a square. The normal stress σ resulting from the action of the force on the face of the square, i.e. the tectonic block, is defined, as follows:

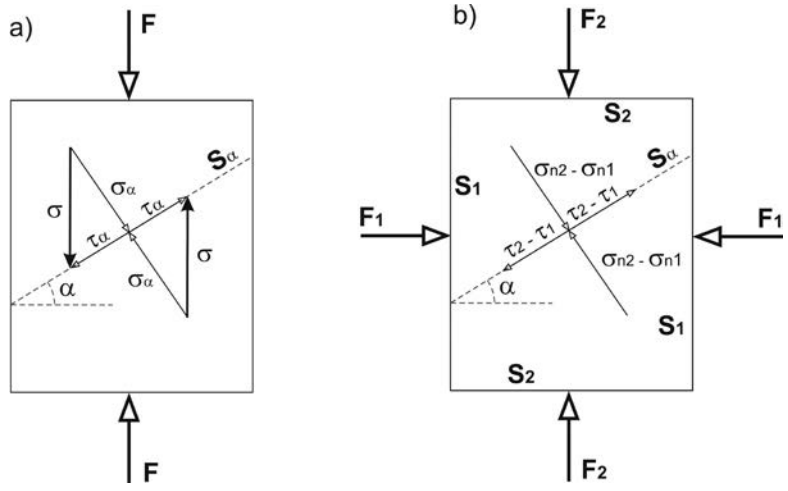

Figure 69. Stress state components in a tectonic block in case of uniaxial (a) and biaxial (b) compression.

$$\sigma = F / S \tag{7}$$

The tangential stress τ in this case is absent.

The plane of the tectonic fault S_α is located inside the block of the Earth's crust. It is oriented at an angle α to the sides of the tectonic block. In this case, on the sloping cross-section the values of normal σ_n and tangential stress τ will be different. The values of these stresses will depend on the angle α of the orientation of the fault plane S_α in relation to the plane normally oriented against the tectonic force vector. The dimensions of the fault plane S_α can be expressed in the following form:

$$S_\alpha = S / cos\alpha \tag{8}$$

Normal and tangential forces and stresses (respectively, and) acting on the area will be expressed as:

$$F_{n\alpha} = F \cdot cos\alpha \tag{9}$$

$$F_{\tau\alpha} = F \cdot sin\alpha \tag{10}$$

$$\sigma_\alpha = F_{n\alpha} / S_\alpha = \sigma \cdot cos^2\alpha \tag{11}$$

$$\tau_\alpha = F_{\tau\alpha} / S_\alpha = \sigma \cdot cos\alpha \cdot sin\alpha = (\sigma / 2) \cdot sin2\alpha \tag{12}$$

It follows from here that on areas perpendicular to F force vector the tangential stresses are equal to zero. If angle $\alpha = 45°$, then the tangential stresses are maximal and equal to $\tau_{max} = \sigma / 2$. Normal stresses σ will decrease from maximal values σ_{max} to 0 with increasing angle of orientation of the plane of the fault S_α to the plane S normally oriented to the action of external force F.

In case, when two forces F_1 and F_2 are acting applied to the sides of the tectonic block (Figure 69), the superposition (summing) of normal and tangential stresses will take place on the plane of the tectonic fault S_α.

$$\sigma_\alpha = \sigma_1^n + \sigma_2^n = \sigma_1 \cdot cos^2\alpha + \sigma_2 \cdot \cos(90 - \alpha) \cdot \cos\alpha = \sigma_1 \cdot cos^2\alpha + \sigma_2 \cdot sin^2\alpha =$$

$$(\sigma_1 + \sigma_2)/2 + [(\sigma_1 + \sigma_2)/2] \cdot cos2\alpha \tag{13}$$

$$\tau_\alpha = (\sigma_1/2) \cdot sin2\alpha - (\sigma_2 / 2) \cdot \sin(2\alpha - 180) = [(\sigma_1 - \sigma_2)/2] \cdot sin2\alpha \tag{14}$$

If both forces F_1 and F_2 are compressing, then the maximum tangential stress will be equal to $\tau_{max} = (\sigma_1 - \sigma_2)/2$. If one of the forces is compressing while the other one is tensile, then the maximum tangential stress will be equal to $\tau_{max} = (\sigma_1 + \sigma_2)/2$. In second case, the probability of formation of both shear fractures and rupture cracks increases. This is due to that a significant stretching takes place along one of the axes. It is known [*http://www.drillings.ru/svoystva*] that the tear strength of rocks is several times lower than the shear strength of rocks. Table 9 gives the limits of strength of limestone, dolomite, fine-grained and medium-grained granite.

As shown in Table 9, tensile (rupture) strength of rocks is lower than shear stress while shear stress is lower than the compression strength. Laboratory studies show that the uniform consolidate rocks can be destructed at volume deformation about 10^{-2}–10^{-3}, i.e. when volume varies within 0.1% and 1%. Shear deformations about 10^{-4} or less can cause the faulting of a solid brittle rock [Borman et al., 2002]. Strength of the rocks decreases if they have been already disturbed as a result of previous stages of seismotectonic activity.

Table 9.

Limits of strength of rocks in compression, shearing and stretching

Rocks	Compressive strength (10^5Pa)	Shear stress (10^5Pa)	Tensile strength (10^5Pa)
Limestone	1030 – 1640	95 – 192	91
Dolomite	1620	118	69
Fine-grained granite	1660	198	120
Medium-grained granite	2592	220	143

Length of the seismogenerating part of the faults can reach tens and even hundreds of kilometres, and the shift is several meters or even tens of meters. For example, for the Kaliningrad earthquakes of 2004, i.e. for the strongest earthquakes in the East Baltic Region, the values of these parameters vary from 962 ± 360 to 945 ± 336 m (radius of source) and from 38.0 to 57.1 cm (average displacement) [Gregersen et al., 2007].

4.1.2. Tectonic regimes

According to modern concepts of seismology and fracture mechanics, the focus of a tectonic earthquake can be defined as a dynamically moving disruption of the continuous material of the Earth, which arises under the influence of stresses accumulated during the shear tectonic deformations (Мячкин, 1978). Thus, one of the main, specific characteristics of the focus of a tectonic earthquake is its linearity, extent and type of movement, since it is confined to a tectonic fault site with a certain mechanism of movement.

The mechanism of the focus of a tectonic earthquake is associated with certain types of tectonic regimes. Each tectonic regime has its own, certain set of main stresses, the character of motion and deformation. The main parameters of the tectonic fault include *Strike, Dip, Rake* (Figure 70). These parameters are sufficient to describe the kinematics of tectonic motion.

Strike is defined as a fault with a vertical or inclined displacement (crack, rupture), along which propagation the fault wings are offset relative to each other. The right and left shifts are distinguished. Looking at the side shift, perpendicularly to the displacement, the farther wing in the right shift is shifted to the right, and in the left shift to the left. The shift is characterized by the angle between the direction to the north and the direction of the displacement line on the Earth's surface, i.e. the azimuth. The strike angle is measured clockwise relative to the north ($0° \le \varphi_S \le 360°$) and lies in the horizontal plane. The azimuth of the shift shown in Figure 70 is approximately 20°–25°.

Dip is the drop of the plane of the displacement. *Dip* is the angle between the horizon line and the plane of the displacement (crack, rupture). *Dip* can vary from 0° to 90° and lies in the vertical plane.

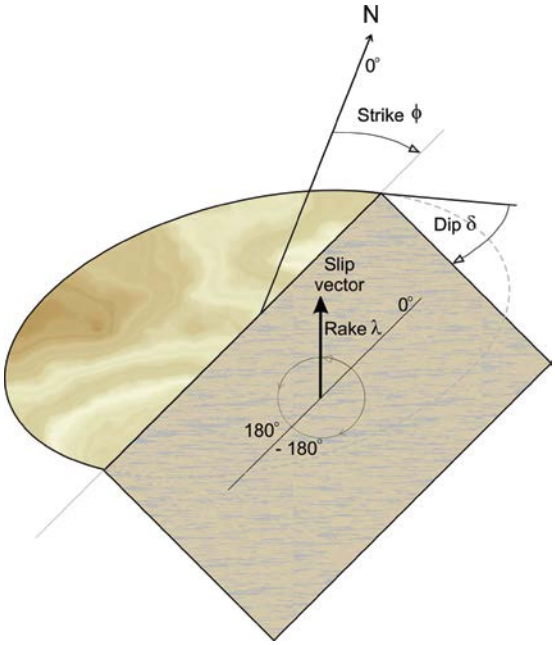

Figure 70. Main parameters of tectonic fault

Rake is the angle λ, which describes the displacement of the hanging block relative to the base. *Rake* change range: $-180° \le \lambda \le 180°$. If $\lambda = 0°$, it corresponds to slippage in the direction of shift. In this case, the thrust effect is manifested (see below). If $\lambda > 0°$, then this means moving up of the hanging block. If $\lambda < 0$ °, then this means a downward motion of the hanging block. In this case, there is a normal mechanism – a reset. *Rake* lies in the plane of the displacement.

Any mechanism of the source of the tectonic earthquake can be referred to a respective type of tectonic regimes (Figure 71).

A normal fault (designation NF) or a throw is a tectonic regime in which the following conditions for the correlation of the main tectonic stresses are satisfied: *SV*> *SH* > *Sh*. Vertical tectonic stress is dominant. The stress acting along the throw line (*SH*) exceeds the stress acting perpendicular to the throw line (*Sh*).

A normal fracture may have a strike-slip component. In this case, a separate tectonic regime (NS) is singled out. The dominant stress is still the vertical stress SV, but the relationship between the horizontal stresses will depend on the predominance of one or another component of the motion.

In case the horizontal component of the tectonic stress is dominant, a separate tectonic regime (SS) is singled out. In this case, the following condition is satisfied for the relationship between the main tectonic stresses: *SH*> *SV*> *Sh*.

A tectonic regime opposite to the shift is a thrust with some strike-slip component (TS). In this case, the main tectonic stress SH prevails, which is parallel to the horizontal plane.

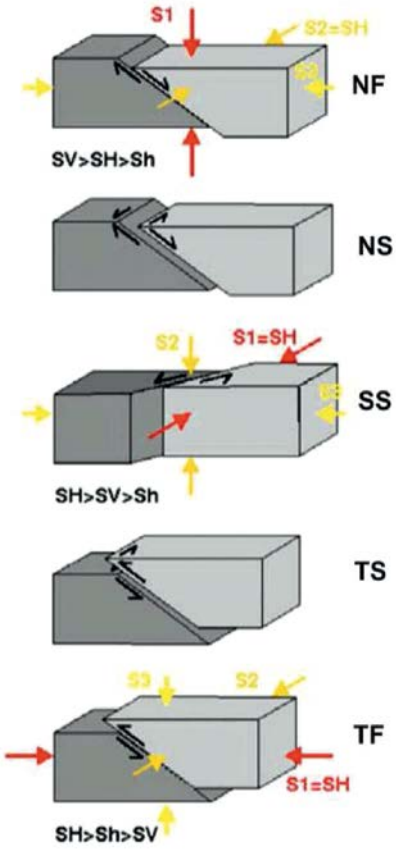

Figure 71. Diagram of main tectonic regimes and their corresponding orientation of major stress axes [Anderson, 1951; Zoback, 1992]

Legend:

Tectonic regimes:

NF – normal faulting; NS – Predominately normal faulting with strike-slip component; SS – strike-slip faulting (includes minor normal or thrust component); TS – predominately thrust faulting with a strike-slip component; TF – thrust faulting

Axes of main tectonic stresses:

SH – maximum horizontal tectonic stress

Sh – secondary horizontal tectonic stress

SV – vertical tectonic stress

S1 – main maximal tectonic stress

S2 – average tectonic stress

S3 – minimum tectonic stress

In the absence of the strike-slip component, there is a pure thrust (TF), for which the condition is satisfied: $SH > Sh > SV$.

Thus, using the above 5 tectonic regimes allows to characterize different mechanisms of earthquake foci.

4.1.3. Seismic moment tensor

The plane of the tectonic fault is determined with by means of a seismic moment tensor (SMT), which can be represented as elementary sources of a double pair and a source approximating the expansion centre (explosion) [Kikuchi & Kanamori, 1991]. The SMT contains sufficiently large information about the source (its energy and mechanism), which can be obtained from observations of seismic signals if the wavelengths are much larger than the source dimensions [Костров, 1975]. The SMT is of great importance not only in the analysis of the focal kinematics for individual strong earthquakes, but it is also important for solving problems associated with the reconstruction of the stress-deformed state of the Earth's interior by the seismological data. The SMT parameters are needed for better assessments of seismic hazard.

The SMT can be represented as a linear combination of = 6 elementary moment tensors (Figure 72):

$$M_{kj} = \sum_{n=1}^{N_e} a_n M_n \tag{15}$$

where tensors of the elementary seismic moment M_n assume the following values:

$$M_1: \begin{bmatrix} 0 & 1 & 0 \\ 1 & 0 & 0 \\ 0 & 0 & 0 \end{bmatrix}; \quad M_2: \begin{bmatrix} 1 & 0 & 0 \\ 0 & -1 & 0 \\ 0 & 0 & 1 \end{bmatrix}; \quad M_3: \begin{bmatrix} 0 & 0 & 0 \\ 0 & 0 & 1 \\ 0 & 1 & 0 \end{bmatrix}$$
$$M_4: \begin{bmatrix} 0 & 0 & 1 \\ 0 & 0 & 0 \\ 1 & 0 & 0 \end{bmatrix}; \quad M_5: \begin{bmatrix} -1 & 0 & 0 \\ 0 & 0 & 0 \\ 0 & 0 & 1 \end{bmatrix}; \quad M_6: \begin{bmatrix} 1 & 0 & 0 \\ 0 & 1 & 0 \\ 0 & 0 & 1 \end{bmatrix} \tag{16}$$

M_1 and M_2 represent pure strike slip faults (SS tectonic regime); M_3 and M_4 represent dip slip faults on vertical planes striking N-S and E-W, respectively (case for normal fault NF and fault of thrust type TF, if dip = 90°); M_5 represents 45° dip slip fault (case for normal fault NF and fault of thrust type TF, if dip = 45°); M_6 – represents an isotropic source radiating energy equally into all direction (i.e., an explosion).

M_6 is an isotropic source, which equally emits energy in all directions. This tensor of elementary seismic moment corresponds to the model of the expansion center, which is characteristic for explosions. Significantly rare is an explosion directed towards the center (implosion). As an example, Figure 73 shows the implosion of the Big Sandy Cooling Tower at the American Electric Power station in September 2016.

In case of a point source, the displacement at station located on the Earth's surface can be expressed as a combination of time-dependent elements of the moment tensor [Jost & Herrmann, 1989]. Here it is supposed that these elements of the moment tensor are also dependent on time, being convolved with the derivatives of the Green's functions in relation to the spatial coordinate:

$$u_s(x, t) = M_{kj}(\xi, t) * G_{sk,j}(x, \xi, t) \tag{17}$$

where,

$u_s(x, t)$ – s – component of ground displacement in position x and at time t;

M_{kj} – 2nd order components symmetrical to the seismic moment tensor M;

$G_{sk,j}(t)$ – derivative of the Green's function in relation to the coordinate of the source ξ_j;

x – vector denoting the position of a station with coordinates x_1, x_2, x_3 corresponding to the north, east and downward movement;

ξ – vector denoting the position of a point source with coordinates ξ_1, ξ_2, ξ_3 corresponding to the north, east and downward movement;

* – symbol indicating that the time-dependent elements of the moment tensor $M_{kj}(\xi, t)$ are convolved with the derivative of the Green's functions $G_{sk,j}(x, \xi, t)$ in relation to the spatial coordinate j.

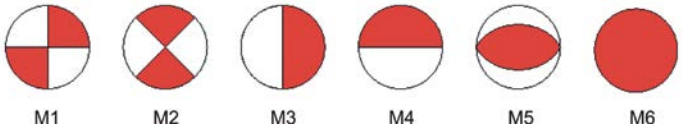

Figure 72. Elementary moment tensors used in inversion of full moment tensor

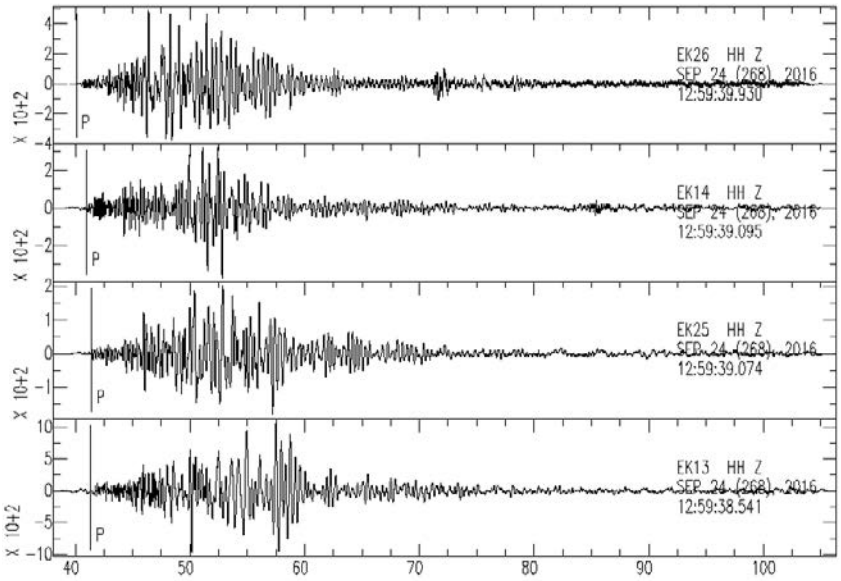

Figure 73. Implosion of the Big Sandy Cooling Tower at the American Electric Power station in September 2016

Derivative of the Green's function can be expressed by means of nine generalized pairs (Figure 74).

For the double pair source, the Cartesian components of the moment tensor can be expressed via the strike angle , dip angle and rake angle of the strike displacement source (in the fault plane) and the scalar of the seismic moment [Aki & Richard, 1980]:

$$M_{xx} = -M_0(sin\delta\ cos\lambda\ sin2\phi + sin2\delta\ sin\lambda\ sin^2\phi \quad (18)$$

$$M_{xy} = M_0(sin\delta\ cos\lambda\ cos2\phi + 0.5\ sin2\delta\ sin\lambda\ sin2\phi \quad (19)$$

$$M_{xz} = -M_0(cos\delta\ cos\lambda\ cos\phi + cos2\delta\ sin\lambda\ sin\phi \quad (20)$$

$$M_{yy} = M_0(sin\delta\ cos\lambda\ sin2\phi - sin2\delta\ sin\lambda\ cos^2\phi \quad (21)$$

$$M_{yz} = -M_0(cos\delta\ cos\lambda\ sin\phi - cos2\delta\ sin\lambda\ cos\phi \quad (22)$$

$$M_{zz} = M_0\ sin2\delta\ sin\lambda \quad (23)$$

More detailed information on the seismic moment tensor can be found in several well-known sources [Aki & Richard, 1980; Костров, 1975; Jost & Herrmann, 1989; Borman et al., 2002].

4.1.4. Model of explosion

The following factors are typical of explosions caused by the chemical transformation of explosives: reaction exothermicity, high process speed, gas formation. The exothermicity of the reaction is due to the release of heat, the heating of gaseous products and their expansion. High speed of the process is the most characteristic sign of the explosion,

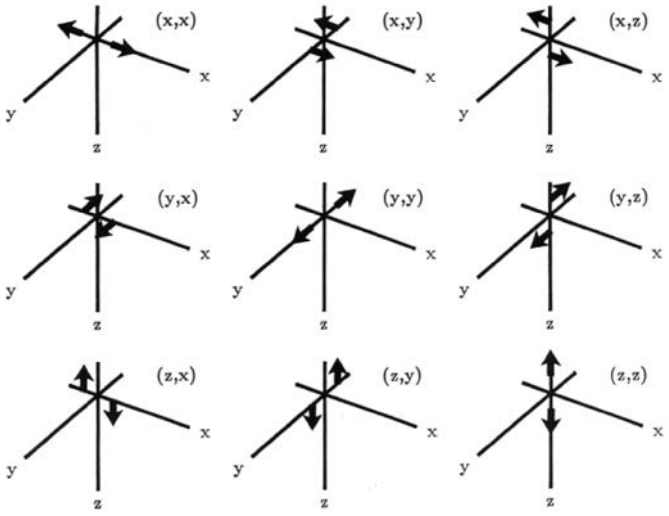

Figure 74. Nine generalized pairs representing the derivative of the Green's function [Jost & Herrmann, 1989]

which distinguishes it from ordinary chemical reactions. Transition to the final products of explosion occurs during 1/100000 second or even quicker. Notwithstanding that in terms of the total amount of energy related to equal weight amounts even the richest in energy explosives do not exceed conventional combustibles, in case of explosion, an incomparably higher volume concentration or density of energy is achieved (Баум и др., 1975). Gas formation is the result of a chemical reaction, leading to high pressures that cause a destructive effect. Upon explosion of 1 litre of TNT 1180 litres of gaseous products are formed, and in explosion of 1 litre of nitro-glycerine – 1105 litres.

The greatest interest is represented by explosions at large distances in solid and liquid media, i.e. in quarries or in an aquatic, usually marine environment. Distances are considered large if they at least 10 times exceed the radius of the charge. In the East Baltic Region, explosions are recorded at much greater distances. In this case, it can be assumed that seismic waves propagate in an elastic medium to which Hooke's laws apply.

Analytical model for the function of a seismic source of an underground explosion can be considered as an instantaneous increase in time, with a finite increase in time, with a steady state and without a steady state.

The characteristic of the explosion model can be represented in the form of a simple point source in a homogeneous medium – the spherical centre of expansion (Подъяпольский, 1966), the most typical case of the description of an explosion:

$$\int_V RF_R dV = -\frac{3}{4}\frac{V_P^2}{V_S^2}\oint_S R\tau_{RR} dS \tag{24}$$

where, R – radius of the considered sphere; F_R– function of the source, set by means of spherical coordinate system; dV – infinitely small volume of area occupied by spherical

source; V_P – propagation velocity of body (longitudinal) waves; V_S – propagation velocity of shear (transversal) waves; τ_{RR} – stress component in spherical coordinate system; dS – infinitely small element of surface confining the spherical source; integral $\oint$ – means contour integration.

In the ideal case, i.e. homogeneous medium and spherical charge, there exists a spherical symmetry of the explosion model and only radial longitudinal seismic waves are formed. At the same time, real conditions are characterized by the presence of layers with different density and propagation velocity of seismic waves in them. Therefore in real conditions, in addition to the longitudinal (body) wave, transversal (shear) waves are also formed, but much weaker than the longitudinal waves.

Amplitude A and the visible oscillation period T of the longitudinal wave at a point sufficiently remote from the source of the explosion depend on the weight of the charge and expressed as:

$$A = K_1 \cdot Q^m \tag{25}$$

$$T = K_2 \cdot Q^n \tag{26}$$

where K_1 and K_2 – proportionality coefficients, Q – charge of explosive, m and n – constant values.

Theoretical calculations for the case of a homogeneous elastic space show [Гурвич, 1970] that m ~ 2/3, and n ~ 1/3. The experimental data indicates the dependence of the constant values on the explosion conditions, charge weight and other factors. Nonlinear dependence of the amplitude on the charge weight is most frequently observed.

As a result of the development of blasting technology, it is now possible to control the mechanical action of the explosion. It is achieved by dosing the energy of the explosion, by choosing the type of explosive and the mass of the charge, by distributing the charge at internal points of the medium, using such factors as the shape of the charge, depth of its placement, mutual arrangement of the charge systems, choice of the explosion initiation points, sequence of detonation and deceleration intervals between individual stages (groups) of explosion.

4.2. Technogenic seismicity in East Baltic Region

The main types of regional seismic sources in the East Baltic Region are manmade explosions and, to a much lesser extent, tectonic earthquakes. Technogenic seismicity is caused by the development of deposits of natural resources with the use of explosive methods of extraction. The main importance of mineral resources of the EBR is for the construction industry, agriculture and power industry. The most important natural resources of EBR, for the extraction of which explosive technologies are used, are oil shale, dolomite, limestone and gypsum deposits.

Combustible shale is a solid fossil, organomineral sedimentary rock of carbonate-clayey, clayey, less often silica composition. Contains from 20% to 70% of organic matter (kerogen), insoluble in organic solvents. The genetic basis of kerogen is an organic mass of sapropelite character, which can have sapropelic, humus or mixed origin. Thermal decomposition of the organic constituent of oil shales produces a significant amount

of resin (shale oil), which is similar in composition to oil. The unique composition of the organic matter of oil shale makes it possible to obtain a wide range of chemical products.

Oil shales occupy an important place in the energy sector of a number of countries. Shale slates are usually called shale, clayey rocks, which contain combustible organic substances having an ash content of 30–40%. Calorific value of combustible shales is 1,500 – 3,000 calories. A peculiar feature of oil shales is the possibility of their processing into fuel – oil, gasoline, as well as the production of shale oil and shale gas from them.

Shale mining is carried out both in open pit mining and in underground mining – in mines. The depth of open development is 15–20 m, and of the underground one – 20 to 60 m. Thickness of an industrial deposit is usually 2–3 m. The oil shale is produced by drilling and blasting method. The main oil shale deposits are located in northeastern Estonia, as well as in the neighbouring Pskov Region of Russia. In the structure of the energy balance of Estonia, shale accounts for more than 50%.

Dolomites are a sedimentary carbonate rock. It contains 95% and more of a dolomite mineral. Chemical composition of dolomite: $CaCO_3 \cdot MgCO_3$. CaO – 30,4%, MgO – 21,7%, CO_2 – 47,9%. The contents of CaO and MgO often fluctuate within a small range. A number of dolomite deposits are located in Latvia and Lithuania. Dolomite is the most common type of mineral raw materials in the East Baltic Region, the extraction of which is conducted by the explosive method.

Limestone is a sedimentary rock of organic, and sometimes of chemogenic origin. Mainly, it consists of calcium carbonate ($CaCO_3$) in the form of calcium crystals of various sizes. A limestone species is the shell limestone. Under metamorphism, the limestone is recrystallized and the marble appears. Limestone is used in construction, including road construction, in production of concrete, metallurgy, etc. One limestone deposit is located in Kumas, Latvia.

Gypsum is a mineral belonging to the class of sulphates. In composition, it is calcium sulphate hydrate $CaSO_4 \cdot 2H_2O$. Gypsum is found in shelves sedimentary rocks in the form of scaly, fibrous or dense fine-grained masses. It can also exist in the form of colourless or white crystals, which are sometimes coloured in brown, blue, yellow or even red. Salaspils gypsum deposit is located in Latvia.

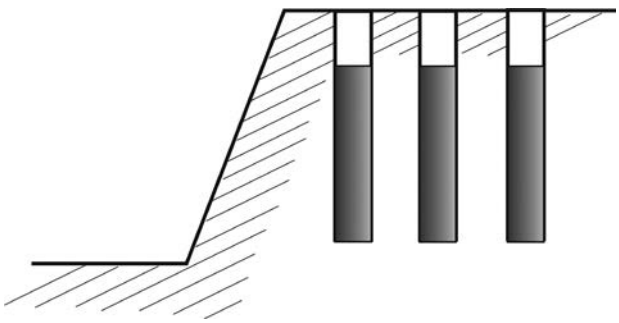

Figure 75. Arrangement of vertical blast holes on the bench

There are different methods of blasting operations: method of borehole charges, method of blasthole charges, method of chambered blasthole and chambered borehole charges, method of chamber charges, method of small-chamber charges (coyotes), method of external charges (dobies).

For the extraction of the above-mentioned natural resources in the EBR, the methods of borehole charges are most often used for loosening the rock in open quarries. In this case, vertical or inclined wells are bored in a rock mass, with a diameter about 100 mm (102 mm) and average depth about 10 m.

The most common use is the multi-row arrangement of wells, i.e. there are several rows of wells on the bench. A typical example of wells layout is shown in Figure 75. Before the commencement of drilling and blasting operations, the upper unproductive part of geological deposits is removed from the area. It is most often the Quaternary sediments. Thickness of this layer depends on the specific deposit. In the dolomite quarries in Latvia, thickness of the unproductive layer is 2–3 m.

Short-delayed blasting of borehole charges is used. Interval of deceleration between explosions depends on the physical and technical properties of rocks and is found

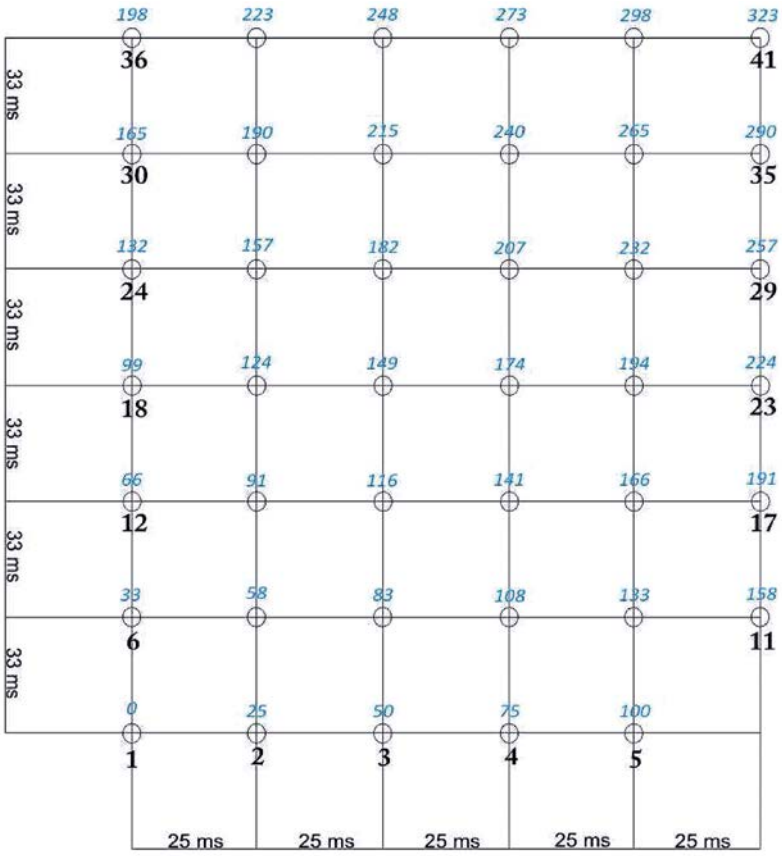

Figure 76. Explosion pattern in the dolomite quarry *Varpas* (Latvia)

experimentally, in the range 20 to 50 ms. In case of multi-row arrangement of wells, a variety of blasting schemes are used. The essence of these schemes is to create by explosion of the first charges the additional open surface, which facilitates the effect of charges of subsequent explosions. In addition, explosions of the first series of charges along the contour of the explosion area of the mass can create a fragmented screen (slit), which reduces the destruction of rock outside the contoured section and reduces the seismic impact of explosion. Cracks can also be closed in the mass, which ensures a better energy distribution and crushing during the explosion.

A multi-row short-delayed blasting of borehole charges is widespread, which provides higher technical and economic indices of blasting operations than with instantaneous, single-row blasting.

The detonators are connected according to certain schemes. An example of such explosion pattern in the dolomite quarry *Varpas* (Latvia) is shown in Figure 76.

The main criteria to be guided in performance of blasting operations with short-delayed blasting are the following: 1) to ensure the reliability of detonation transmission

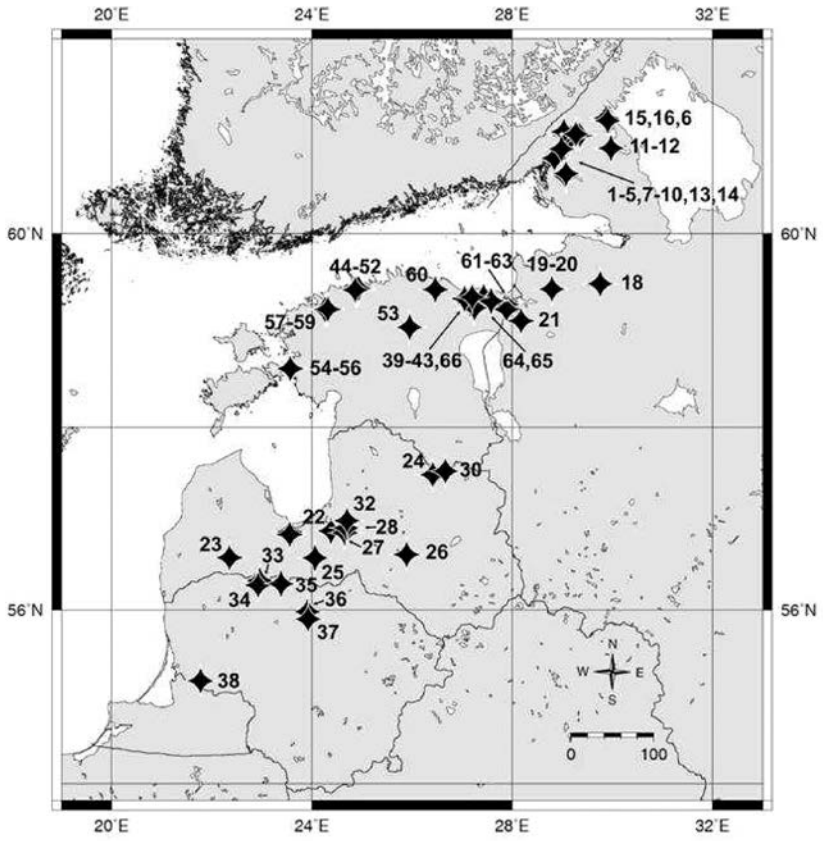

Figure 77. Quarries of the Baltic Region where blasting operations are carried out

Legend: asteroids – careers in which blasting operations are carried out, quarry and mine numbers correspond to data in Table 10

throughout the network; 2) to ensure a high intensity of crushing; 3) to form the rock crushing into necessary sizes; 4) to ensure minimum destruction in the depth of the mass; 5) to create a minimum seismic effect of the explosion on surrounding structures and objects.

The explosion pattern shown in Figure 76 consists of 7 rows, comprising a total of 41 wells. The charge in each well is 25.125 kg in TNT equivalent. The delay between explosions is 25 ms, and between the rows – 33 ms. As a result, a series of explosions occurs with a certain slowdown between the wells. Such technique reduces the seismic effect, but solves the main problem – it allows to shatter the productive layer.

In the territory of the East Baltic Region, there are more than 50 quarries and mines, where blasting operations are performed (Figure 77).

In Estonia, explosions are carried out in 23 open quarries and 5 mines. In Latvia, there are 11 quarries where explosive work has were or may be carried out. In Lithuania, there are 6 quarries in which explosions are made. In Pskov and Leningrad Region of Russia, there are more than 21 quarries where blasting operations can be carried out. Many quarries and mines where blasting operations are carried out are located on the Kola Peninsula and in Scandinavia. With the help of the *BAVSEN* seismic observation system existing in the EBR, it is difficult to single out the explosions that occur in Scandinavia (Finland, northern Sweden) and the Kola Peninsula. Exceptions are explosions in the Leningrad, Pskov regions of Russia and partly in southern Sweden. Table 10 presents the characteristics of the EBR quarries, as well as the nearest regions of Russia (Leningrad and Pskov), in which blasting operations may occur. Some of these explosions are recorded by the *BAVSEN* network.

Table 10.

Characteristics of quarries in the EBR, including Leningrad and Pskov Region of Russia

№	Name of quarry	City, region	Mineral resource	Mass of explosive, kg	Lat	Lon
1	DIM	Russia, Leningrad district			60.975	29.350
2	ERK	Russia, Leningrad district			60.748	28.844
3	KKU	Russia, Leningrad district			60.950	29.168
4	KKNM	Russia, Leningrad district			60.969	29.054
5	PRU1	Russia, Leningrad district			60.997	29.018
6	PRU2	Russia, Leningrad district			61.007	29.033
7	GKU1	Russia, Leningrad district			60.570	29.068

8	GKU2	Russia, Leningrad district			60.591	29.083
9	GKU3	Russia, Leningrad district			60.596	29.078
10	VOZR1	Russia, Leningrad district			60.838	28.985
11	VOZR2	Russia, Leningrad district			60.848	29.985
12	VOZR3	Russia, Leningrad district			60.846	29.974
13	PETR	Russia, Leningrad district			60.984	29.271
14	KUZ1	Russia, Leningrad district			60.984	29.271
15	KUZ2	Russia, Leningrad district			61.14	29.878
16	KUZ3	Russia, Leningrad district			61.114	29.907
17	BOX	Russia, Leningrad district			59.486	33.897
18	ELIZ	Russia, Leningrad district			59.492	29.756
19	ALEX	Russia, Leningrad district			59.438	28.795
20	SLAN	Russia, Leningrad district			59.438	28.795
21	PIK	Russia, Leningrad district			59.112	28.176
22	Open pit «Salaspils»	Latvia, Riga district	Gypsum	0.1–0.9	56.879	24.382
23	Open pit «Kumas»	Latvia, Saldus district	Limestone	4.5 and more	56.584	22.358
24	Open pit «Darzciems»	Latvia, Alūksnes district	Dolomite	1.5 and more	57.490	26.416
25	Open pit «Iecava»	Latvia, Jelgava district	Dolomite		56.581	24.064
26	Open pit «Aiviekste»	Latvia, Jēkabpils district	Dolomite	4.5–6.0	56.618	25.892
27	Open pit «Kranciems»	Latvia, Ogre district	Dolomite	around 5.0	56.858	24.660
28	Open pit «Turkalne»	Latvia, Riga district	Dolomite	3.5 and more	56.911	24.687

29	Open pit «Kalnciems II»	Latvia, Jelgava district	Dolomite	5.5andmore	56.867	23.561
30	Open pit «Ape»	Latvia, Alūksnes district	Dolomite		57.529	26.665
31	Open pit «Kalnciems»	Latvia, Jelgava district	Dolomite	5.5andmore	56.841	23.560
32	Open pit «Gaitini»	Latvia, Riga district	Dolomite		56.991	24.704
33	Open pit «Karpenai»	Lithuania, Siauliai district	Limestone		56.329	22.959
34	Open pit «Menciai»	Lithuania, Siauliai district	Limestone		56.278	22.930
35	Open pit «Skaitgirys»	Lithuania, Siauliai district	Dolomite		56.294	23.386
36	Open pit «Petrasiunai II»	Lithuania, Siauliai district	Dolomite	69–6382	55.982	23.913
37	Open pit «Klovainiai»	Lithuania, Siauliai district	Dolomite		55.900	23.928
38	Open pit «Stoniskiai»	Lithuania, Tauragė district	Siliceous marl		55.197	21.779
39	Mine «Estonia»	Estonia, Ida-Virumaa district	Oil shale		59.237	27.231
40	Mine «Ojamaa»	Estonia, Ida-Virumaa district	Oil shale		59.289	27.156
41	Mine «Sompa»	Estonia, Ida-Virumaa district	Oil shale		59.317	27.192
42	Mine «Tammiku»	Estonia, Ida-Virumaa district	Oil shale		59.358	27.431
43	Mine «Viru»	Estonia, Ida-Virumaa district	Oil shale		59.247	27.248
44	Open pit «Vao KMIN-039»	Estonia, Tallinn district	Oil shale		59.434	24.876
45	Open pit «Vao II KMIN-035»	Estonia, Tallinn district	Oil shale		59.428	24.898
46	Open pit «Tondi-Vao KMIN-061»	Estonia, Tallinn district	Oil shale		59.429	24.903
47	Open pit «Vao-Lagedi KMIN-085»	Estonia, Tallinn district	Oil shale		59.436	24.913
48	Open pit «Loo»	Estonia, Tallinn district	Oil shale		59.440	24.947
49	Open pit «13»	Estonia, Tallinn district	Oil shale		59.445	24.932

50	Open pit «Vao III KMIN-101»	Estonia, Tallinn district	Oil shale		59.431	24.869
51	Open pit «Karinu II»	Estonia, Tallinn district	Oil shale		59.048	25.944
52	Open pit «Karinu»	Estonia, Tallinn district	Oil shale		59.047	25.953
53	Open pit «Louna-Aru»	Estonia, Laane-Viruma district	Oil shale		59.435	26.466
54	Open pit «Kurevere»	Estonia, Laanemaa district	Oil shale		58.628	23.557
55	Open pit «Iiosa»	Estonia, Laanemaa district	Oil shale		58.619	23.568
56	Open pit «Nordkalk AS Kurevere»	Estonia, Laanemaa district	Oil shale		58.617	23.571
57	Open pit «Vasalemaa»	Estonia, Tallinn district	Oil shale		59.234	24.303
58	Open pit «Vasalemaa I»	Estonia, Tallinn district	Oil shale		59.229	24.262
59	Open pit «Nordkalk AS Vasavere»	Estonia, Tallinn district	Oil shale		59.232	24.318
60	Open pit «Aidu»	Estonia, Ida-Virumaa district	Oil shale		59.340	27.050
61	Open pit «Narva 1»	Estonia, Ida-Virumaa district	Oil shale		59.281	27.884
62	Open pit «Narva 2»	Estonia, Ida-Virumaa district	Oil shale		59.231	27.889
63	Open pit «Narva II»	Estonia, Ida-Virumaa district	Oil shale		59.232	27.889
64	Open pit «Sirgala»	Estonia, Ida-Virumaa district	Oil shale		59.325	27.579
65	Open pit «Sirgala II»	Estonia, Ida-Virumaa district	Oil shale		59.317	27.579
66	Open pit «Vanakula»	Estonia, Ida-Virumaa district	Oil shale		59.355	27.202

A large number of technogenic seismic sources causes mass explosions in the territory of the East-Baltic Region. Figure 78 depicts the seismic events localized by the virtual network of BAVSEN for the period from January 2008 to November 2017. These seismic events are predominantly technogenic in nature, especially in the territory of the EBR. In particular, seismic events concentrated in the north-east of Estonia, in the

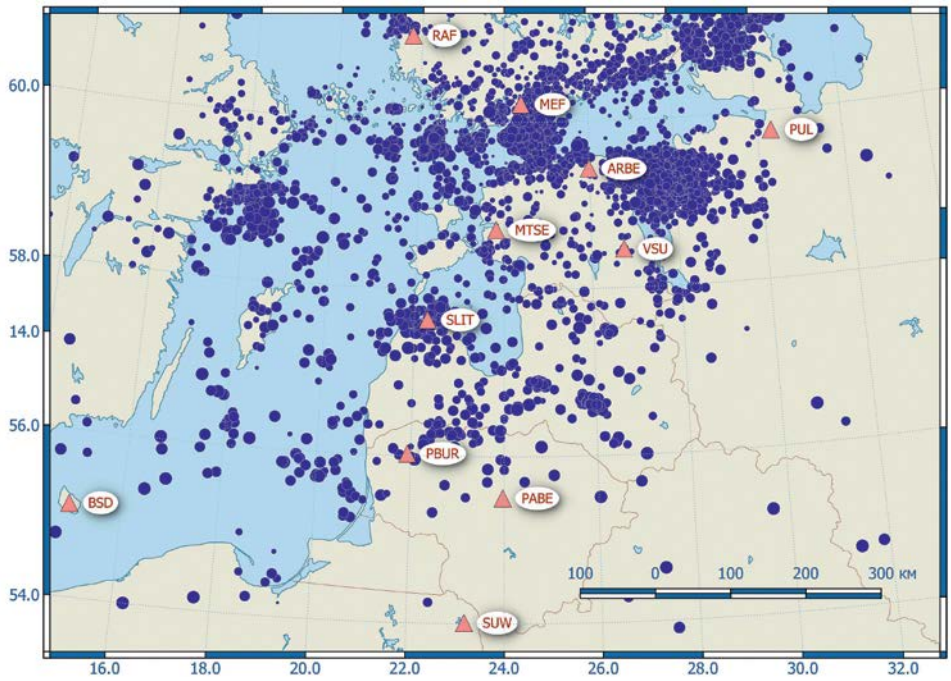

Figure 78. Seismic events in the East-Baltic region based on localization results by BAVSEN network from January 2008 to November 2017

Gulf of Finland and the Irbene Strait are caused by technogenic seismic events, i.e. explosions in quarries and in the water area of the Baltic Sea.

The prevalence of technogenic seismicity is witnessed by the distribution of seismic events by the time of day (Figure 79). The overwhelming majority of seismic events in the EBR occurs during the daytime, within working hours 8 to 14 GMT (Global Mean Time). Depending on winter or summer time, it corresponds to 10–16 hours in winter 11–17 hours in summer. Figure 80 shows distribution of seismic events for the EBR (ϕ = *53.9°N – 59.7°N;* λ = *19.4°E – 29.6°E*) by the time of day within the period January 2008 to May 2016 according to data of BAVSEN network.

90.9% of seismic events occur at a time interval between 8 and 14 hours (GMT). With a high probability, these seismic events have a technogenic nature caused by human activity. Only a small number of seismic events (9.1%) occurred outside the working hours. Although in some cases, events that occurred before 8 (7) and after 14 (15) can also relate to technogenic events. This accounts for about another 2.7%.

Of course, tectonic earthquakes can occur at any time of the day. On the other hand as already noted, non-stationary seismic sources in the Baltic Sea can act at any time of the day and day of the week. Therefore, the time of occurrence of seismic events cannot be the only criterion for identifying their nature.

As for the available information on the position of stationary seismic sources (quarries), although it is useful for identification, but it does not always allow to

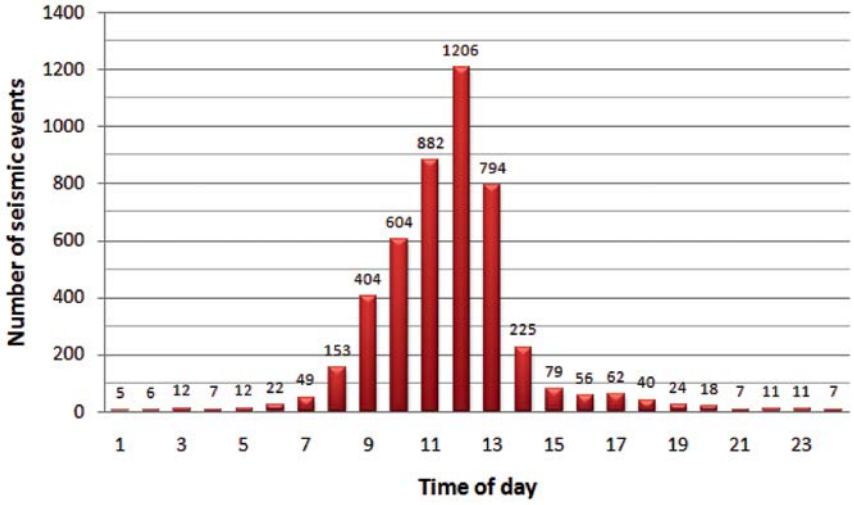

Figure 79. Distribution of seismic events by time of day in the East Baltic Region for the period January 2008 to May 2016 according to data of BAVSEN network

Note: 1) sampling area: ϕ = 53.9°N – 59.7°N; λ = 19.4°E – 29.6°E;
2) number of seismic events: 4696

confidently determine the type of a seismic event. The matter is that when locating a seismic event, there is an error in determining its location. The error increases with decreasing magnitude of the seismic event, i.e. for weak seismic events it is greater than for strong ones. This is due to the fact that for a confident location it is necessary to single out on the seismograms the arrival of the first P-waves or at least one P-wave. Since the ambient seismic noise has a sufficiently high level at many seismic stations of the *BAVSEN* network located in the EBR, this condition is not always satisfied. Therefore, the arrival of the P-wave is determined uncertainly and the error can be so great that the epicentre of the explosion turns out to be located far from the quarry in which the explosion took place.

Technogenic seismic sources are unevenly located on the territory of the EBR. They are mainly confined to deposits of mineral raw materials for the construction industry and energy: oil shale, dolomite, limestone and gypsum.

Now we consider the technogenic seismicity in some regions of the East Baltic Region – Estonia, Latvia, Lithuania.

4.2.1. Technogenic seismicity of Estonia

The main mineral resource of Estonia is fuel shale. In Estonia, there are approx. 5 billion tons of oil shale, of which about 1.4 billion tons are recognized as suitable for production (active reserve), and most often they are located in the thickness of limestone deposits. Estonia produces almost 70 percent of its world volume. Production of oil shale can make Estonia maximally independent in the field of energy supply.

In addition, production of oil shale has become a significant factor in influencing the world oil prices.

Until now, three well-proven methods have been used in the production of oil shale: 1) drilling and blasting operations, 2) semi-selective mining with rippers, bulldozers and excavators, and 3) open development as a fully selective mining method. Open technology has clear advantages. Leading oil shale producers in Estonia, *Kiviõli Keemiatööstuse* (*Kiviõli*) and *Eesti Energia Mining*, mainly use *Wirtgen* surface miners. Nevertheless, drill and blasting works still occupy a significant place in the oil shale extraction in Estonia.

Estonia is the leader among countries of the East Baltic Region in terms of the number and power of explosions used to extract mineral resources. Production of oil shale is carried out in 23 open quarries and in 5 mines (Figure 80). The mass of the explosive can reach 10–16 tons. Powerful explosions in Estonia are recorded at stations of the EBR and southern Scandinavia. Several explosions occur daily. Within a year their number reaches several thousands. The main sources of technogenic seismicity in Estonia are located in the northeast, in areas Kohtla-Jarve, Kohtla-Nõmme, Mustanina, Aidu and others.

Figure 81 shows a seismogram of a typical explosion in a quarry for oil shale mining, in the northeast of Estonia, near Mustanina. Most reliably the first longitudinal P-waves are recorded at stations located in Scandinavia: MEF and RAF, as well as at Estonian station MTSE. At other stations of the *BAVSEN* network, it is only possible to single out the S-wave against the background of interferences whereas the P-wave is difficult to be confidently identified.

Statistics on explosions in the northeast of Estonia is quite representative. Therefore the characteristics of these explosions are considered in more detail. For example, consider the characteristics of the eight explosions in the northeast of Estonia in January

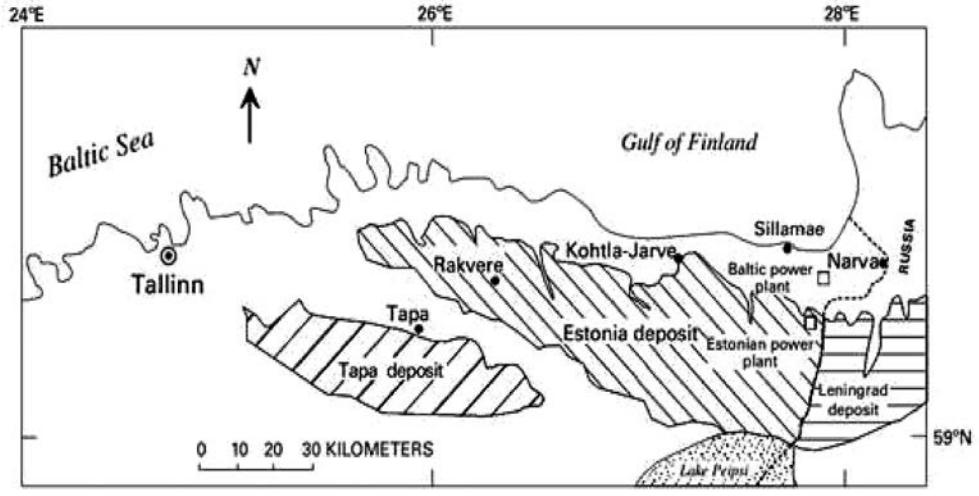

Figure 80. Location of oil shale deposits in the Baltic Basin in the north of Estonia and in Russia

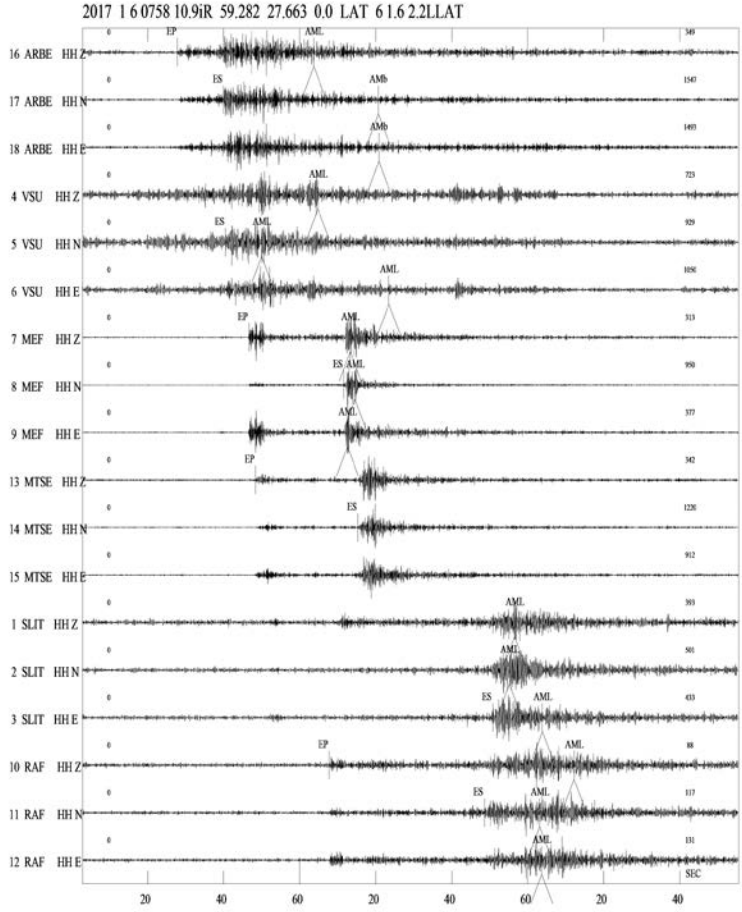

Figure 81. Explosion in a quarry near Mustanina, in the northeast of Estonia on 6 January 2017 (07:58:11 GMT), recorded at the stations of BAVSEN network

Table 11.

Parameters of explosions in the northeast of Estonia

Nr.	Date	Orig. Time	Latitude	Longitude	Depth, km	Mag
1	2017/01/06	07:58:10.0	59.265	27.925	0.0	1.9
2	2017/01/06	09:15:37.1	59.264	27.850	0.0	1.9
3	2017/01/06	11:42:39.2	59.277	27.710	0.0	1.7
4	2017/01/13	12:21:16.3	59.276	27.683	0.0	1.9
5	2017/01/14	11:25:14.1	59.223	27.717	0.0	1.9
6	2017/01/18	12:01:30.1	59.235	27.710	0.0	1.8
7	2017/01/19	12:27:16.9	59.219	27.703	0.0	1.9
8	2017/01/20	11:40:06.0	59.248	27.859	0.0	1.8

2017. These explosions occurred in about the same place. Parameters of those explosions are presented in Table 11, and the position of epicenters is shown in Figure 82.

Information on explosions to be analyzed is based on data from the Institute of Seismology of Helsinki University. Distances from seismic stations to the nearest epicenters of explosions in the indicated group are as follows: for ARBE 190 km, for VSU 137 km, for MEF 381 km, for SLIT 629 km, for RAF 687 km.

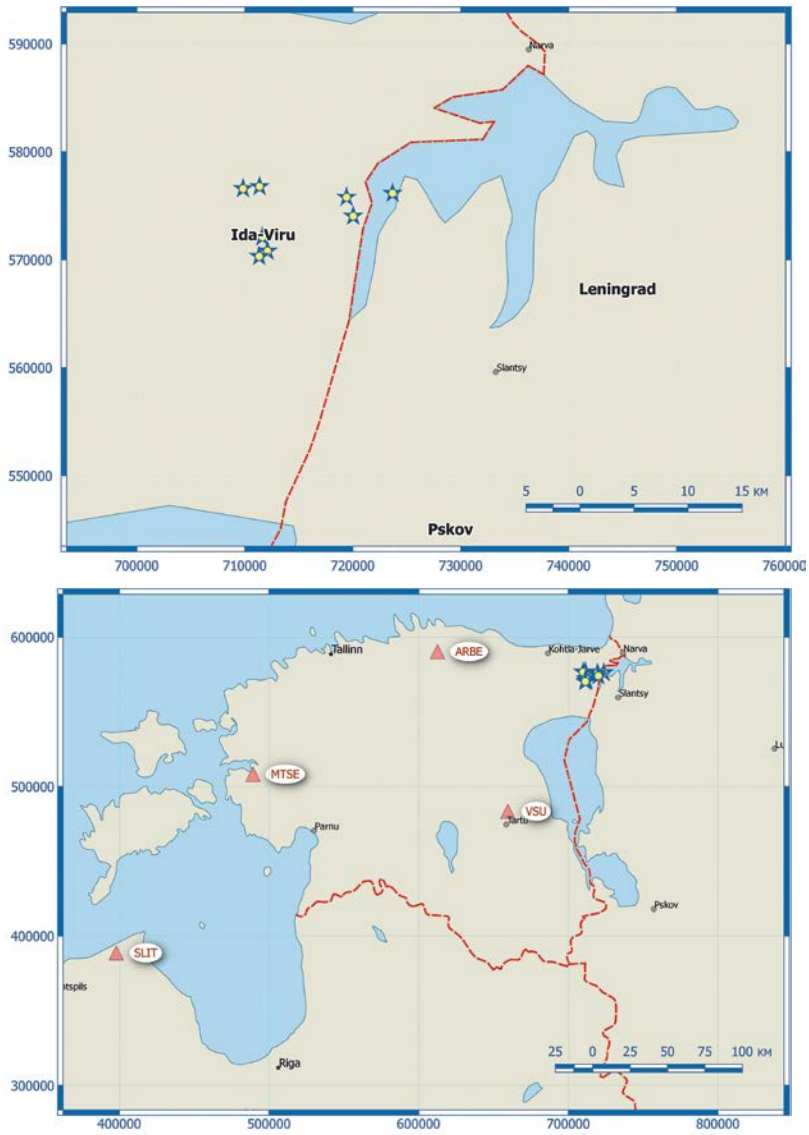

Figure 82. Stations of BAVSEN network in the East Baltic Region and epicenters of explosions in the northeast of Estonia

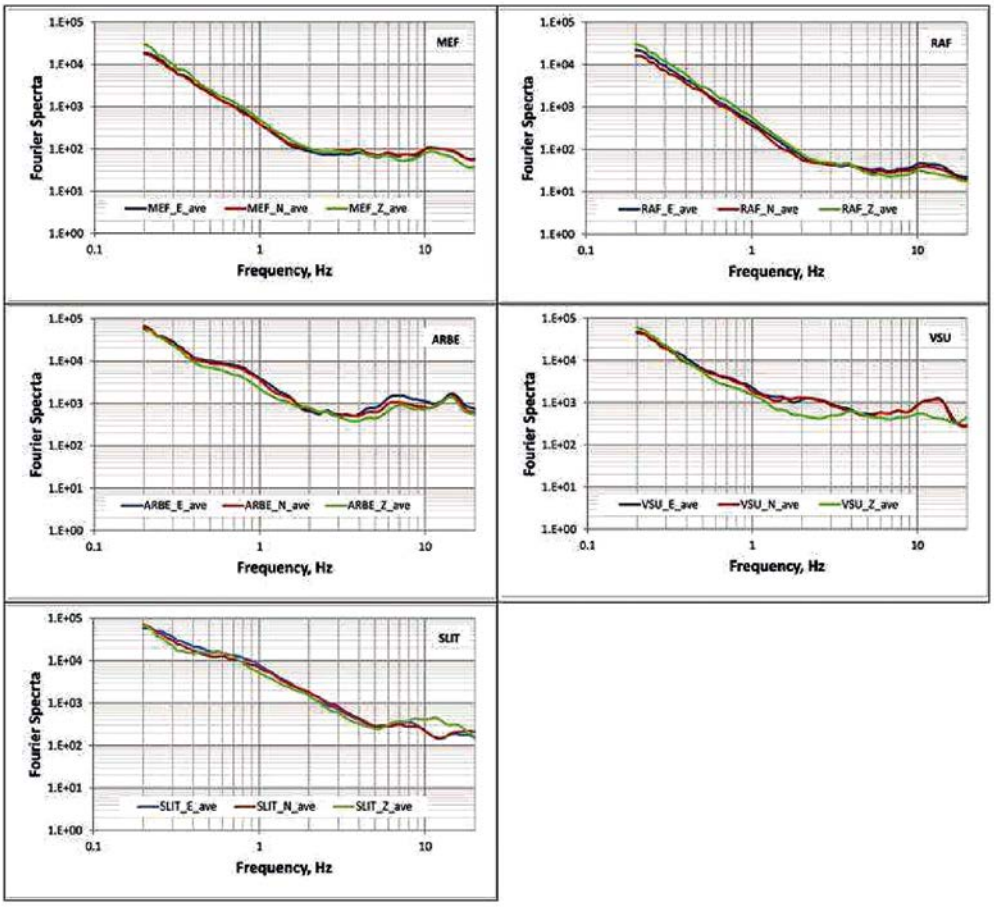

Figure 83. Averaged Fourier spectra according to records of BAVSEN network seismic stations for explosions in the northeast of Estonia

First of all, for a number of explosions the Fourier spectra were determined, which are shown in Figure 83. Fourier spectra for explosions in the northeast of Estonia are obtained for the frequency range Δf = 0.2 – 20.0 Hz. The spectral curve consists of two branches. The left branch of the Fourier spectra is characterized by a monotonous decrease in the spectral amplitude from = 0.2 Hz to about = 2 Hz. An exception is SLIT station, for which the decrease in the spectral amplitudes occurs up to a frequency of = 5 Hz. The right branch of the Fourier spectra is characterized either by a flat segment with a slight rise after = 10 Hz for MEF and RAF stations, or by a quasi-planar portion with variations in the spectral amplitudes for ARBE, VSU and SLIT stations. The spectra of ARBE and VSU have a local maximum of the spectral amplitude at frequencies = 13.8 – 14.9 Hz, and the amplitude of the Fourier spectra for the vertical component Z is less than for the horizontal components E and N. This is especially noticeable for VSU station. At SLIT station, the amplitude of the Fourier spectrum

on the Z component is larger than that on the horizontal components N and E at a frequency = 11.4 Hz.

Comparison of the Fourier spectra for SLIT and RAF stations located approximately at equal distance from the epicenters of explosions shows the resonance effect of the sedimentary cover on the spectral level at SLIT station.

4.2.2. Technogenic seismicity of Latvia

Prior to the crisis in 2008, the largest company carrying out blasting operations in Latvia's quarries was *Sprādziens*. It performed works in 8 quarries in Latvia: Aiviekste, Kumas, Kranciems, Dārzciems, Kalnciems, Tūrkalne, Gaitiņi, Saurieši. *Sprādziens* carry out most of explosive works and most powerful explosions in Latvia. These explosions were recorded by the *NORSAR* network, by network of the Institute of Seismology of University of Helsinki (UHIS) and the Baltic Virtual Seismic Network *BASEN*.

The scale of blasting works is evidenced by the following facts: 1) in 2000, 277 explosions were carried out in Latvia while the total amount of explosives exceeded 441 tons in TNT equivalent; 2) in 2002 and 2003 *Sprādziens* performed 558 explosions in 8 quarries of Latvia.

The mass of the explosive in TNT equivalent even for one quarry varied in a fairly wide range. This is due to the fact that besides the main industrial explosions, the auxiliary methodical explosions were carried out to select the optimal parameters of the blasting.

At present time apart from *Sprādziens*, several other companies are operating in the field of blasting operations (*Dinamix, Balrock, Mark Invest*). In addition to explosions in industrial quarries, they sometimes perform technical explosions to ensure the safety of HPPs on the Daugava River (Figure 84), to demolish old multistorey buildings, chimneys

Figure 84. Ice blasting on Daugava River near Pļaviņas HPP

or water towers. Decision to blast the ice cover on the rivers is made depending on the ice situation.

Seismogram of a typical explosion in one of the most active technogenic sources, Aiviekste quarry, is shown in Figure 85. Explosions in Aiviekste quarry are powerful enough. The total mass of explosives can reach 5–6 tons. However, due to the grouping of wells and specific methods of blasting (delays between blasting stages), even these explosions are sometimes difficult to be singled out against the background noise. Despite rather large local magnitude of 2.5, the first P-wave arrivals are difficult to be distinguish at RAF, MEF, ARBE, VSU stations (Figure 85).

Information about explosions carry out in the territory of Latvia was obtained mainly from the firm *Sprādziens* and partly from the firm *Dinamix*. The information included the date and time of the explosion to the accuracy of minutes, as well as the location of the quarry and the mass of the explosive. Since the exact time of blasting was not known

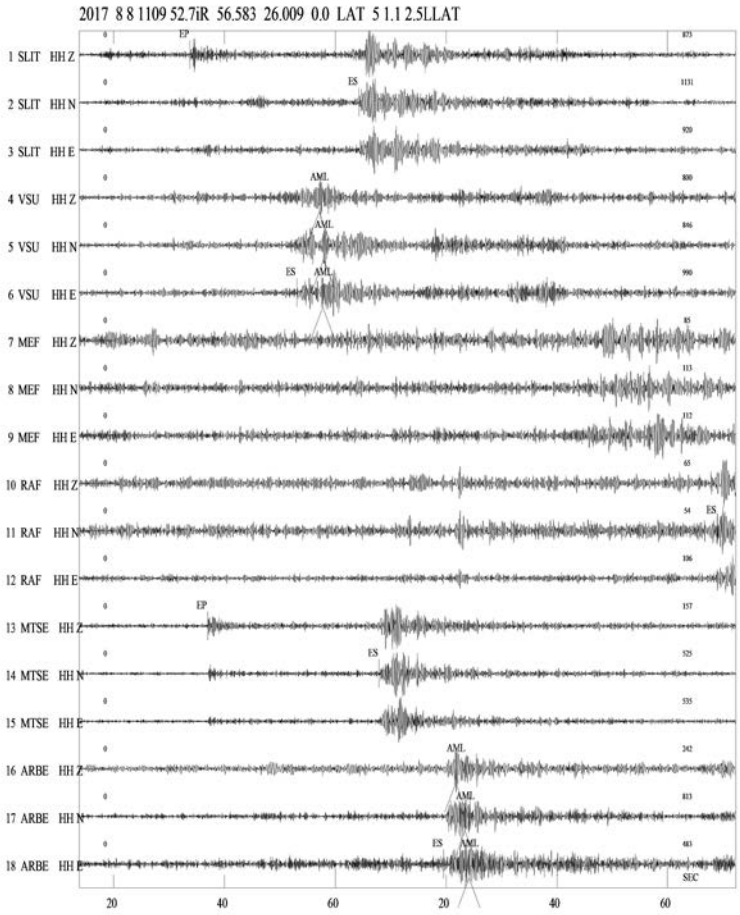

Figure 85. Explosion in Aiviekste quarry (Latvia) on 08 August 2017 (11:09:52 GMT), recorded by stations of BAVSEN network

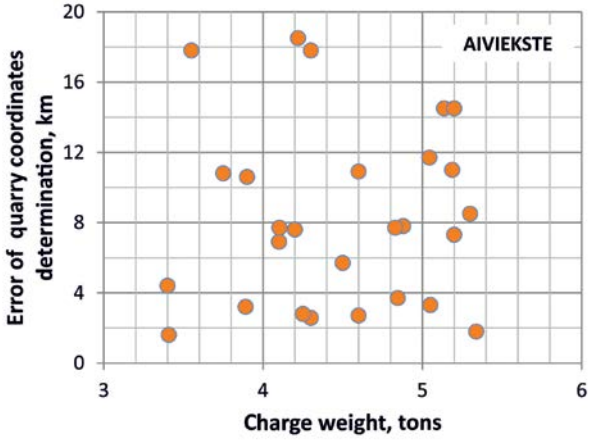

Figure 86. Relationship between mass of explosive charge and error in determination of quarry coordinates

to within seconds and fractions of a second, we are speaking about relatively calibrated explosions. The complete information about calibrated explosions in addition to above mentioned parameters includes the moment of the explosion occurrence with accuracy of fractions of a second, the exact coordinates of the epicenter of the explosion in the quarry.

More detailed information about explosions Aiviekste quarry allowed to analyse a number of parameters. In particular, the dependence between the mass of explosive W_{explo} and the error of location of the explosion ε_{coord} (Figure 86).

No correlation was found between W_{explo} and ε_{coord}. In this case, the blasting patterns, parameters of wells with charges were not taken into account, i.e. the source directionality was not studied. Range of ε_{coord} is within 1.6 and 18.5 km for stations of *BAVSEN* network. W_{explo} varied within 3.4 and 5.42 t. Also connection was not found between the explosive charge weight W_{explo} and the local magnitude *ML* (Figure 87).

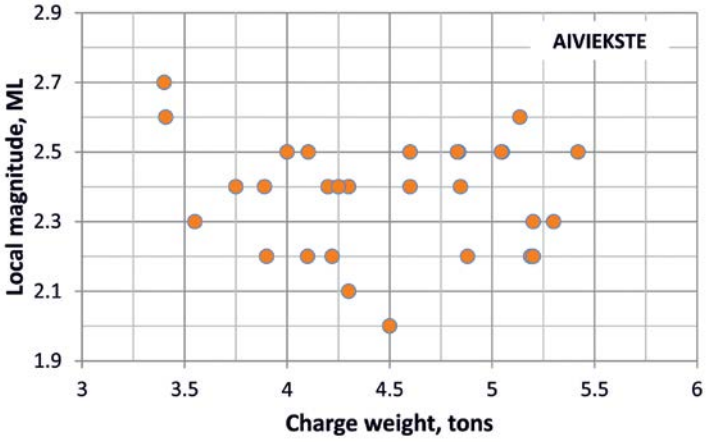

Figure 87. Relationship between explosive charge weight and local magnitude

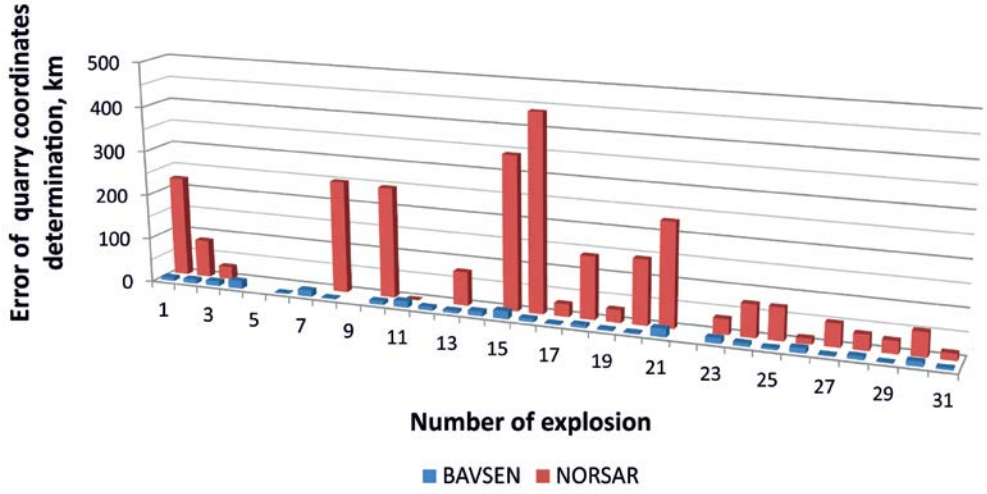

Figure 88. Quality of location of explosions in Aiviekste quarry (Latvia), using seismic networks NORSAR and BAVSEN

Nevertheless, this information helped to assess the quality of location of explosions using different models of seismic wave propagation velocities in the geological environment.

To locate regional seismic events in the Baltic Region using *BAVSEN*, several models of seismic wave velocities were used: *iasp91*, *Fennoscandia*, *UHIS* (University of Helsinki, Institute of Seismology) and own model *baltic07*.

Global international model *iasp91* does not take into account regional peculiarities and is mainly used to locate distant earthquakes. Models *Fennoscandia* and *UHIS* are more effective for Scandinavia and the southern slope of the Baltic Shield (Estonia). In particular, these models are used when locating explosions in northeastern Estonia. Model *baltic07* was developed based on the results of deep seismic sounding (DSS) 1986, using the Sovetsk – Riga – Kohtla-Jarve profile [Садов & Пензина, 1986]. The model is more effective for location of seismic events in the territory of Latvia and directly adjacent neighbouring territories.

The quality of location of explosions in Aiviekste quarry using *BAVSEN* network is significantly better than of location using *NORSAR* data (GBF bulletin). The error in determining the coordinates of the quarry according to *BAVSEN* data was 1.6–18.5 km while according to *NORSAR* (GBF bulletin) – 12.5 to 439 km (Figure 88).

4.2.3. Technogenic seismicity of Lithuania

The number of quarries where explosions are performed in Lithuania is not big. Number of explosions in Lithuanian industrial quarries also is relatively small. Explosions are carried out in an open way (Figure 89). The stations of the BAVSEN network record a small number of explosions in the territory of Lithuania.

Figure 89. Explosion in one of quarries of Lithuania

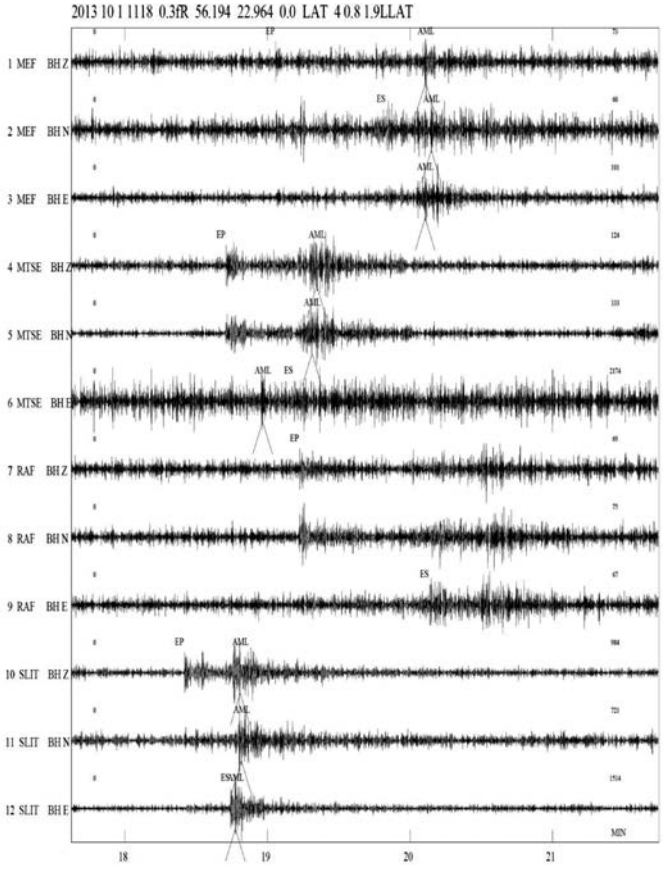

Figure 90. Explosion in a career in the north of Lithuania on 01 October 2013 (11:18:00 GMT)

In two quarries (Karpenai and Menciai) limestone is mined. In three quarries (Skaitgirys, Petrasiunai II and Klovainiai), dolomite is mined. In one quarry (Stoniskiai) they extracted a marl rock. However, in this career the blasting is no longer being done.

The dolomite base in Lithuania is found in many geological systems, but of practical importance are those located near the surface in the northern part of Lithuania in the Pļaviņas formation of the Upper Devonian, in formations of Istras, Stipinai, Kruoja or Žagare. The best dolomite is believed to be the one in the formation of Stipinai [Gasiuniene, 1998].

Only for the two explosions it was possible to estimate the error in determining the coordinates of the quarry. For these explosions with partially known parameters in Klovainiai and Karpenai, the errors in determining the coordinates of the career ε_{coord} are practically the same and equal to 7.3 km. A typical example of an explosion in a Lithuanian quarry is shown in Figure 90.

Stations SLIT and MTSE are closest to the epicenter of the explosion, at a distance of 165 and 285 km, respectively. Both types of seismic waves P and S are confidently singled out for these stations. At two other stations, these waves are also identified, although the S-wave less confidently.

4.2.4. Technogenic seismicity of the Baltic Sea

Technogenic seismicity in the Baltic Sea is mainly associated with various naval activities and geophysical operations. Naval activities include both military exercises and activities of mine clearance of the Baltic Sea aquatic area from explosive items that remained after World War II and even I. Geophysical work is usually carried out along certain profiles. Use of explosions at sea is prohibited in order to preserve fauna. Therefore, the source of excitation can be electric spark sources, gas-fired installations or pneumatic emitters. Unlike explosions, these sources excite waves where the amplitude and pressure in the front of the shock wave are less than in conventional explosions. Geophysical work is carried out on separate profiles (tacks), as well as in certain areas of marine testing grounds.

Figure 91 shows mainly marine seismic events that occurred in 1982, 1988, 2013– 2015. Information about three events in 1982, 1988 is taken from the *Catalog of earthquakes in Northern Europe* (Institute of Seismology University of Helsinki). Data for 2013–2015 are based on the results of location of *BAVSEN* network.

Attention is drawn by a group of 10 seismic events having occurred in the gas pipeline route area (= 56.0°N – 56.4°N; = 17.9°E – 18.3°E) on 06 August 2013. Magnitude of these events varied within 1.7 and 2.4. The events took place in the daytime within 12:21 and 15:17 (GMT). The second stage (branch) of the Nord Stream gas pipeline was put into operation on 08 October 2012. Seismic events in the pipeline area occurred after its commissioning. Therefore, these seismic events at least are not connected with the laying of the second stage of the gas pipeline.

On average, the events occurred after every 19–20 minutes. Such a short-term, regular and dense sequence of events in a weakly active region clearly witnesses the

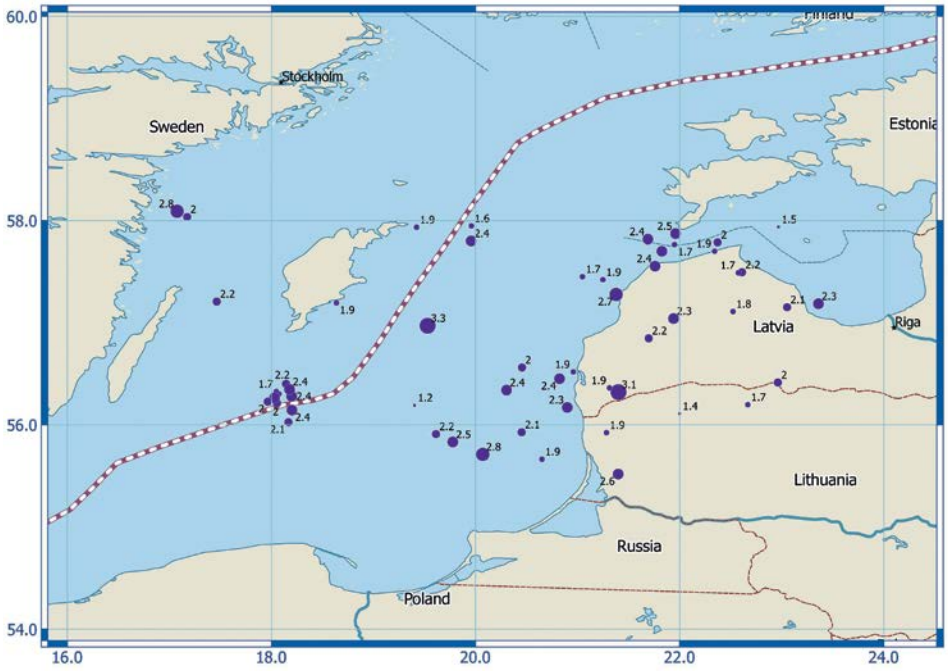

Figure 91. Seismic events in the Baltic Sea aquatic area in 1982, 1988, 2013–2015

Legend: circles - epicenters of seismic events with magnitude values; line (white and violet strips) – Nord Stream gas pipeline route from Vyborg (Russia) to Greifswald (Germany)

technogenic nature of these events. However, the exact cause of the occurrence of these events could not be clarified.

If onshore technogenic seismic events occur mainly during daylight working hours, then in the Baltic Sea they can occur at any time of the day, and even on any day of the

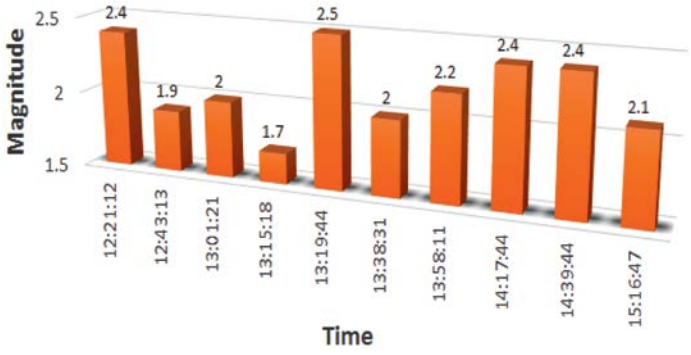

Figure 92. Time sequence of seismic events on 06 August 6 2013 in the Baltic Sea, in the area of the Nord Stream pipeline route

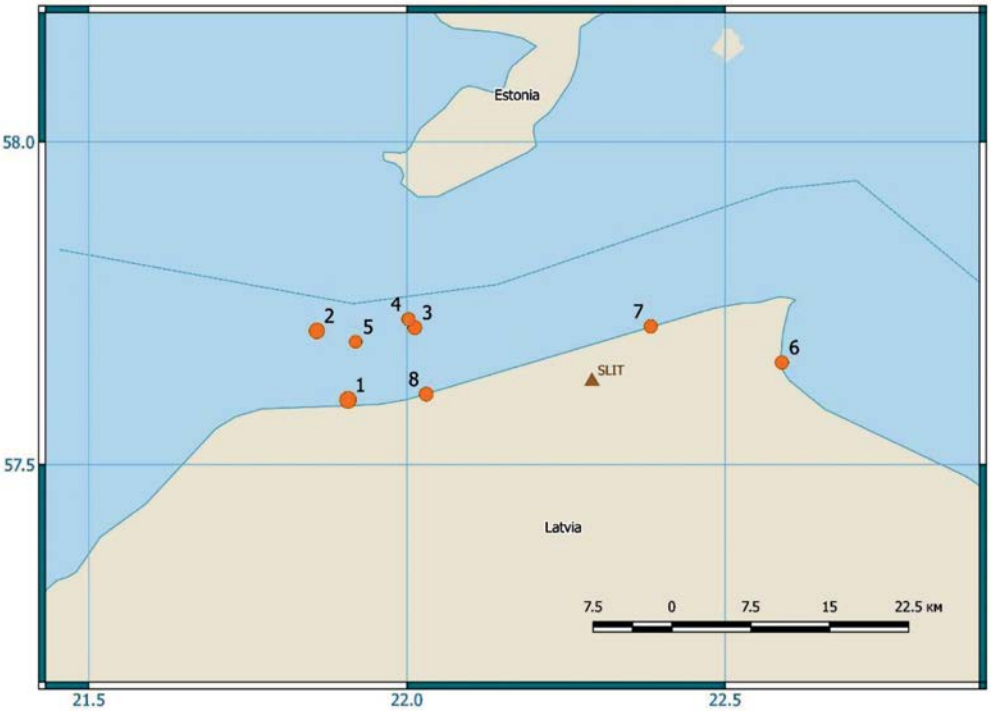

Figure 93. Series of explosions in the Irbene Strait (Kurzeme, Latvia) in April 2012 recorded by BAVSEN seismic network

Note: numbers at the epicenters indicate the sequence number of the explosion

week. A typical example is the performance of naval activities in the Baltic Sea aquatic area for the destruction of explosive objects of World War II and even World War I.

As a rule, in the process of carrying out such measures not one seismic event occurs but a whole series of successive seismic events, i.e. explosions. For example, Figure 93 shows a series of 8 sea explosions during the period 18 to 26 April 2012 in the Irbene Strait. The range of magnitudes of explosions varied from 1.9 to 2.6. Ordinal numbers of the explosions are indicated by digits. Seismic events occurred early in the morning (06:02 GMT) and late at night (19:44 GMT). Moreover, three of these seismic events occurred even on weekends, 21 and 22 April 2012. This series of seismic events was associated with naval activities in the Irbene Strait.

The seismogram of the most powerful explosion (ML = 2.6) from this series is shown in Figure 94. The nearest seismic station SLIT is located 26 km from the epicenter of the explosion. The most distant RAF station is located 370 km from the epicenter of the explosion.

Thus, explosions in the water area of the Baltic Sea occur at any time and are usually characterized by a continuous series. Marine explosions are generally better recorded, the first P-wave, as a rule, is well-identified.

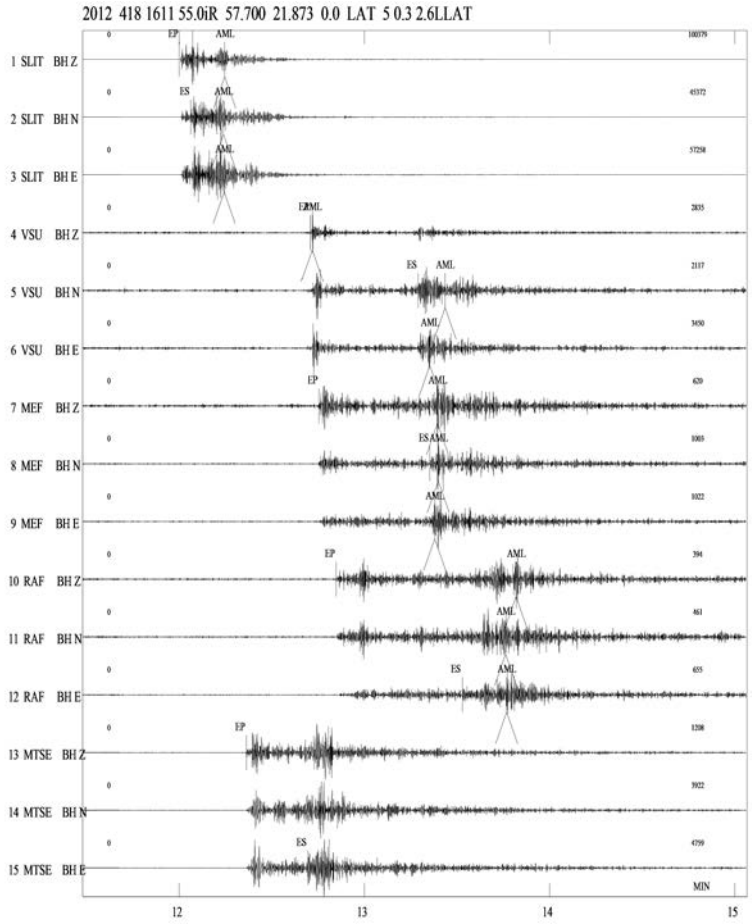

Figure 94. Seismic record of a sea explosion that took place on April, 2012 in the Irbene Strait near Kurzeme, Latvia

Note: EP – P-body wave onset; ES – shear S-wave onset. 3–8 Hz filter was used. Stations: SLIT – Slītere, VSU – Vasula, MEF – Metsahovi, RAF – Laitila, MTSE – Matsalu

4.3. Practical methods for tectonic earthquake identification

A major problem of the time-lapse seismology is to identify the genesis of a seismic event. The identification of tectonic earthquakes makes it possible to collect information necessary for the assessment of seismic hazard and seismic risk, obtain earthquake seismograms that can be used for applied purposes like seismic micro-zoning (SMZ) and the assessment of soil, buildings and structures' response to natural earthquake effect.

What are the key reasons hampering the identification of tectonic earthquakes in the East Baltic Region?

First of all, an earthquake is quite a rare occurrence in the East Baltic Region in general. Within the period of instrumental observations, i.e., in the 1970s, strong

earthquakes took place only in 1976 – on the Osmussaare Island in Estonia and in 2004 – in the Kaliningrad Region of Russia. As far as small earthquakes are concerned, there are very few of them, too. The seismic activity of platform territories is low. Due to long distances separating the BAVSEN network stations, it is quite difficult to detect, localize, and identify small earthquakes. The average distance between the closest seismic stations within the BAVSEN network is about 170 km, while the seismic grid density is 1 (one) station per 31707 km^2. Such network parameters allow one to detect and localize earthquakes starting from about 1.25 magnitudes [Ņikuļins, 2017f]. For reference, the seismic stations network of Sweden includes more than 65 broadband seismic stations (1 station per 6884 km^2) and features a favorable geologic setting (it sits on a crystalline basement), which makes it quite possible to highlight, localize, and specify the parameters of 0.5-magnitude earthquakes and even smaller ones.

Secondly, intensive macroseisms make it difficult identification of small earthquakes. A high level of ambient seismic noise implies a mixture of natural, seismic, and human-induced noise (tremor). Natural seismic noise is mostly associated with storm-generated microseisms forming in the Atlantic Ocean, offshore microseisms occurring in the Baltic Sea, and the local weather conditions. Tremor is due to human-induced activities. The main sources of the long-term and continuous vibration are metropolitan cities (point sources or poles) and traffic arteries (linear sources). As far as the latter ones are concerned, railway tracks and tram lines operating under urban conditions are of a particular importance. Rail traffic is the most intensive human-induced source.

Thirdly, the unfavourable geologic settings of the near-surface section adversely affect the wave pattern. Seismic energy scattering over local inhomogeneities takes place. Most of the BAVSEN network stations sit on sedimentary deposits represented by soft and water saturated soils. So, polarization analysis of seismic waves is hindered. As regards the stations sitting on thick sediment layers, the wave pattern is made more complicated and the first P-wave picking is hindered.

The sedimentary cover thickness increases from north to south – from the Southern slope of the Baltic Shield (tectonic depression) to the south, towards the Mazurian – Belorussian Anteclise.

The ambient seismic noise and the geologic setting affect the effective sensitivity, i.e., signal-to-noise ratio (*Seismic Noise Ratio*). At the MEF station for example, = 8 – 10, whereas on the SLIT station, ~ 5. The seismic resolution of the BAVSEN network is limited by a high level of ambient seismic noise, unfavorable geologic setting of the near-surface section, small magnitudes of tectonic earthquakes and long distances between the seismic stations. To reduce the influence of human-induced seismic noise, some stations have been deliberately deployed in underground bins.

However, this only partially improves waves recordings. The BAVSEN network seismic stations located on the Baltic Syneclise (SLIT, PABE, and PBUR) or, on the Mazurian – Belorussian Anteclise are installed in bins located at different depth. The same applies to the stations deployed on the southern slope of the Baltic Shield, in Estonia (VSU). For example, the SLIT station geophone is located on dense moraine deposits – at the depth 6.5 m from the Earth's surface. The sensors of PABE and PBUR stations are located at depths of 5 and 3 m respectively, while those of the SUW

stations – at a depth of 2 m, and those of VSU station – at a depth of 3 m. The sensors of MTSE and ARBE stations are located on dense superficial deposits. However, the microseism level at those stations cannot be found satisfactory.

In the fourth place, quite a lot of human-induced explosions take place in EBR – both in industrial quarries and in the Baltic Sea waters. The coordinates of the quarries are well known. However, an error is usually made in process of determination of the epicenter; as a result, the epicenter coordinates deviate from the quarry's actual position.

Information on explosions in quarries is provided only by some enterprises carrying out blasting operations. Sometimes the quarries where explosions are carried out are associated with tectonic faults. Earthquake focuses are associated with tectonic faults as well. This creates some additional problems in identifying tectonic earthquakes.

Problems related to small earthquake identification are not unique. This issue us quite relevant with respect to territories featuring low natural seismicity – i.e., platform territories. For instance, some resembling problems refer to the Eastern part of the USA [Kim et al., 1993].

The principal models for a tectonic earthquake and a chemical explosion, considered in Chapter 4.1, allow one to make a theoretical assumption of the existence of some essential discriminants and differences. The following refers to those discriminants: 1) spectral characteristics of earthquakes and explosions (Fourier spectra); 2) amplitude ratio *P/S* (*P/Lg*) of seismic waves or their spectra; 3) time frequency analysis of earthquakes and explosions; 4) complexity index being the correlation of integral power of S- and P-waves, and a number of other principal discriminants.

Chapter 4.3 will be dedicated to practical methods of identification of tectonic earthquakes.

4.3.1. Spectral characteristics of earthquakes and explosions (Fourier spectra)

Spectral representation of signals is a tool traditionally used for the amplitude-frequency and the phase-shift analysis of seismic records. Impulse spectra depend on many factors and therefore may be used to characterize impulses. To characterize seismic responses from explosions and earthquakes, a mathematical operation called *Fourier transformation (FT)* is often used in seismological practice. FT is used as a method for signal decomposition – i.e., frequency and amplitude-based separation of signals.

At that, a transition from time domain to frequency domain is taking place. *FT* is a suitable method to describe the initial function (waveform) frequency decomposition into simple components –harmonic vibrations of different frequencies.

Seismic signalis determined as time-varying function, i.e. as. The complex spectrum of direct Fourier transformation is given by mathematical expression:

$$X(\omega) = \frac{1}{2\pi}\int_{-\infty}^{\infty} x(t)e^{-i\omega t}dt \qquad (27)$$

where $X(\omega)$ is Fourier spectrum; $\omega = 2\pi f$ – angular frequency.

Inverse Fourier transformation is given by the expression:

$$x(t)(t) = \int_{-\infty}^{\infty} X(\omega) e^{i\omega t} d\omega \tag{28}$$

where $x(t)$ – the initial function in space-and-time; $\omega = 2\pi f$ – angular frequency.

The periodic function of time $x\ (t)$ with the period T may be presented as an infinite trigonometric series:

$$x(t) = a_0 + 2\sum_{k=1}^{\infty}[a_k \cos(\frac{2\pi kt}{T}) + b_k \sin(\frac{2\pi kt}{T})] \tag{29}$$

where

$$a_k = \frac{1}{T}\int_0^T x(t)\cos(\frac{2\pi kt}{T})dt\ ,\ k \geq 0 \tag{30}$$

$$b_k = \frac{1}{T}\int_0^T x(t)\sin(\frac{2\pi kt}{T})dt\ ,\ k \geq 1 \tag{31}$$

The full description of the subject relating to Fourier transformation can be found in professional literature [Bracewell, 1978; Lighthill, 1962].

To promote the speed of arithmetic operations, *the Fast Fourier Transform* (DFT) algorithm is applied when using discrete Fourier transformation. As an example illustrating the transformation of a time series into a spectrum (Figure 95), let us use a picture provided by FEMA (Federal Emergency Management Agency) [FEMA 451, 2007].

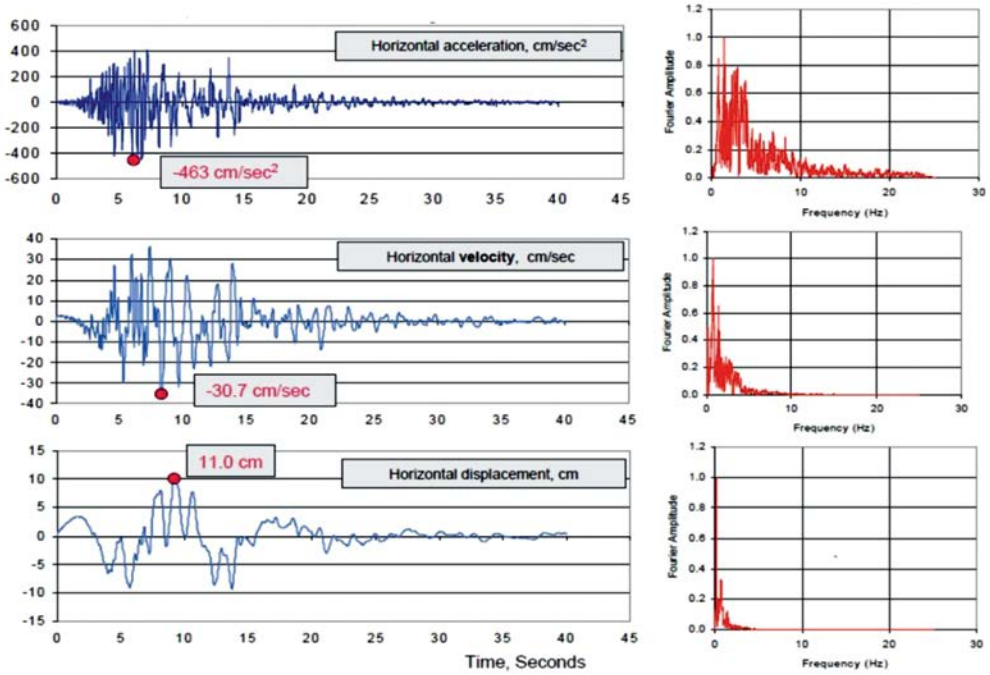

Figure 95. Results of acceleration, velocity and displacement time series transformation (from top to bottom) into Fourier spectra [FEMA 451, 2007]

Notes: top left – time series of horizontal accelerations of soil, on the left centre: time series of soil horizontal velocities; bottom left: time series of soil horizontal displacement; on the right – the corresponding Fourier spectra for soil accelerations, velocities, and displacements

It is apparent that the bandwidth of frequencies obtained as a result of Fourier transformation is getting narrow. The widest bandwidth is stated at accelerations, while the narrowest one – at displacements.

Spectral characteristics of regional earthquakes, on the one side, and explosions – on the other side may differ fundamentally from each other, since seismic waves occurring in the source have different shaping mechanisms. As against tectonic earthquakes, the process-running time within the source of explosion and the peak displacement level achievement time (Figure 96) is by far shorter (milliseconds as against seconds and even minutes for earthquakes) and more impulsive [Borman et al., 2002]. I.e., this is in reference to time values of the order of milliseconds – as against seconds and even minutes for earthquakes. Respectively, given identical magnitudes, an explosion excites higher-frequency oscillations than an earthquake does.

The first movement at an explosion produces a homogeneous expansion effect in all directions while the tectonic earthquake produces first motions of different amplitude and polarity in different directions. This difference can be used for the identification of process type within seismic source, i.e., can be used as a discriminant between explosions and tectonic earthquakes.

Step function depicted on the right side of the diagram may correspond to an earthquake with infinite velocity of crack propagation. In actual life however, the crack propagation velocity, i.e., the tectonic fault ripping velocity – is bounded. This velocity is substantially lower than the propagation velocity of the S-wave [Borman et al., 2002].

The speed of the process running within the earthquake source can be assessed given that the solution for the earthquake source is available and the corresponding parameters have been found: stress drop $\Delta\sigma$, the seismic moment M_0, and source radius r. The interrelation between those parameters is given by the Keilis-Borok formula [Keilis-Borok, 1959]:

$$\Delta\sigma = \mu \frac{7\pi}{16} \bar{u} = \frac{7}{16} \frac{M_0}{r^3} \tag{32}$$

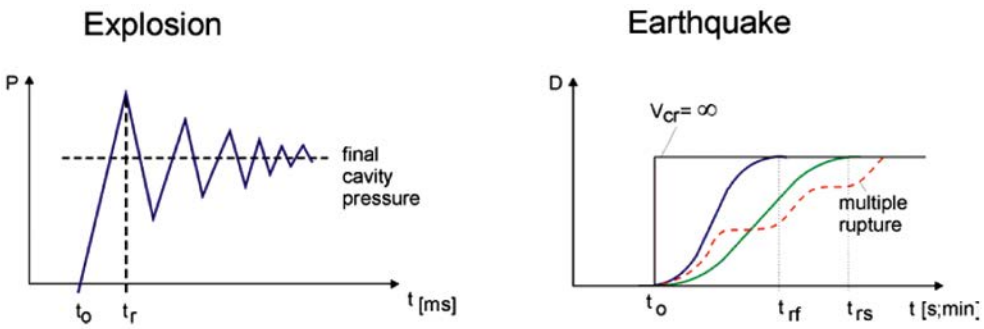

Figure 96. Schematic representation of different seismic sources [Borman et al., 2002]

Legend: P – pressure in explosion chamber; D – fault displacement; t0 –the event origin time; tr – pressure P build up time or, peak value passage time for the fault D; trf – fast fracture build up time; trs – slow fracture build up time

where $\Delta\sigma$ – fault stress; μ – impedance; $\overline{u}$ – mean displacement value; M_0 – seismic moment of the source; r – source radius.

Hence, by estimating the crack propagation velocity in the earthquake focus as $0.6 \cdot v_S$ – $0.9 \cdot v_S$, the time of tectonic fault can be obtained. Based on the data on strong earthquakes (magnitude M_w change from 7.8 to 9.1), collected worldwide within the period from 1963 to 1977 [Borman et al., 2002], – the time of tectonic fault *"rupture"* changes from about 77 to 227 seconds.

Finding the solution for the earthquake focus, as well as the assessment of parameters including the tectonic fault rupture velocity, is possible with respect to strong earthquakes, provided that a dense network of seismic observations surrounding the earthquake source is available. In EBR, the solution for the earthquake source mechanism was obtained only with respect to the two Kaliningrad earthquakes that took place on September 21, 2004, with 5.0 and 5.2 magnitudes. For small earthquakes, obtaining a solution for the mechanism of the earthquake foci in EBR is almost impossible because of amplitude limitations and the widely-spaced seismic network.

The application of spectral method for the discrimination between explosions and earthquakes is based on the fact that explosions do not generate S-waves. Anyway, if S-waves still occur, this happens either due to the explosion source asymmetry or with a change of the wave type on the horizon boundaries (converted waves). Therefore, with respect to explosions, P-waves spectrum level should be higher than S-waves spectrum level, while it should be vice versa with respect to earthquakes.

Let us consider Fourier spectra for a typical small earthquake that took place on November 12, 2016 in the Lake Võrtsjärv neighborhood (Figure 97).

With respect to Fourier spectra, the following analysis parameters were used: 1) length of the seismic signal = 4.0 sec; 2) time windows length = 1.0 sec; 3) frequency range: = 1 ÷ 20 Hz; 4) frequency sampling = 100 Hz. The selection of the seismic signal length was due to the fact that the difference between *P*- and *S*-wave constituted about 4.2 sec for the closest VSU station.

The main distinctive feature of Fourier spectra is the prevalence of S-wave spectral level over P-wave spectral level . For the most reliable stations (VSU, MEF and RAF) decreases from 5–6 (VSU) to 1.7–2.3 (RAF).

With the increasing distance, this correlation decreases. The higher correlation value has been recorded for the closest VSU station. Another peculiarity is that the frequencies of P-wave spectra are higher than the frequencies of S-wave spectra. As a rule, Fourier spectrum level on the vertical component is less than that on horizontal components – both with respect to *P*- and *S*-waves. The only exception is the SLIT station, where the Fourier spectrum level for the vertical component is higher than spectrum level for horizontal components.

The predominance of S_H for horizontal components may be due to the fact that a horizontal movement of NS type or, at least, of SS type (Figure 71) could be dominating in mechanism of earthquake in the Lake Võrtsjärv region.

Seismic event of unknown genesis occurred on June 12, 2015 (08:18:26 GMT) in the northern outskirt of Couronian Lagoon, on the territory of Lithuania. The Fourier spectrum for this event is shown in Figure 98.

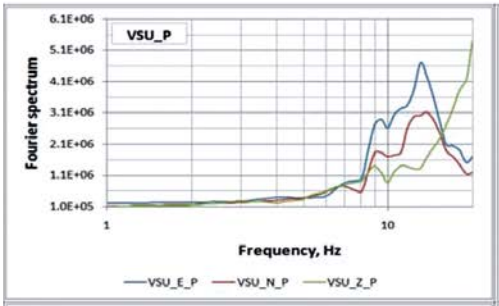
VSU_P
Fourier spectrum
6.1E+06
5.1E+06
4.1E+06
3.1E+06
2.1E+06
1.1E+06
1.0E+05
1
10
Frequency, Hz
VSU_E_P
VSU_N_P
VSU_Z_P

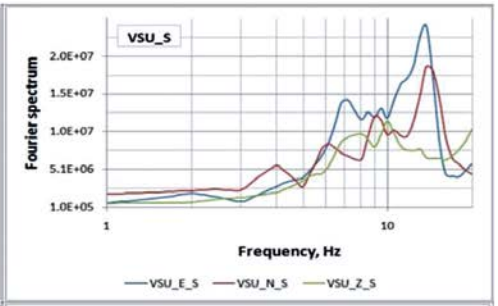
VSU_S
Fourier spectrum
2.0E+07
1.5E+07
1.0E+07
5.1E+06
1.0E+05
1
10
Frequency, Hz
VSU_E_S
VSU_N_S
VSU_Z_S

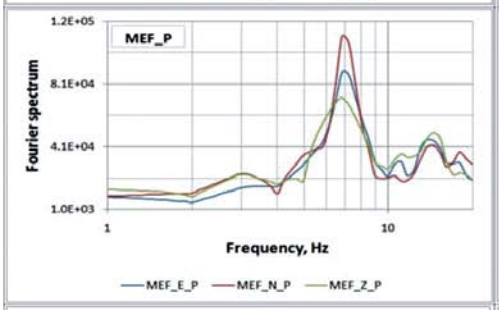
MEF_P
Fourier spectrum
1.2E+05
8.1E+04
4.1E+04
1.0E+03
1
10
Frequency, Hz
MEF_E_P
MEF_N_P
MEF_Z_P

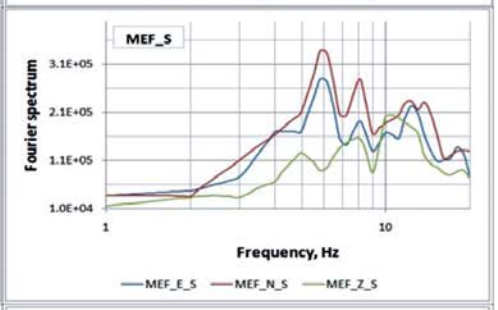
MEF_S
Fourier spectrum
3.1E+05
2.1E+05
1.1E+05
1.0E+04
1
10
Frequency, Hz
MEF_E_S
MEF_N_S
MEF_Z_S

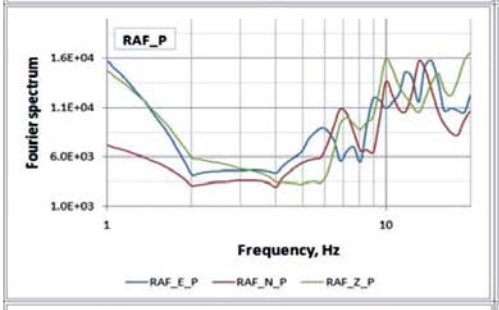
RAF_P
Fourier spectrum
1.6E+04
1.1E+04
6.0E+03
1.0E+03
1
10
Frequency, Hz
RAF_E_P
RAF_N_P
RAF_Z_P

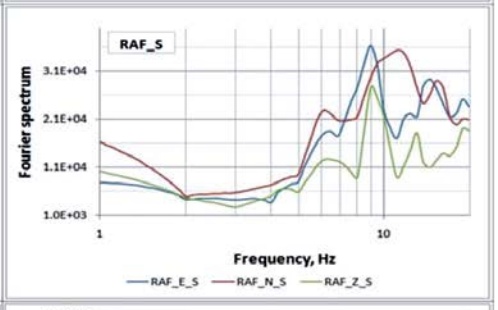
RAF_S
Fourier spectrum
3.1E+04
2.1E+04
1.1E+04
1.0E+03
1
10
Frequency, Hz
RAF_E_S
RAF_N_S
RAF_Z_S

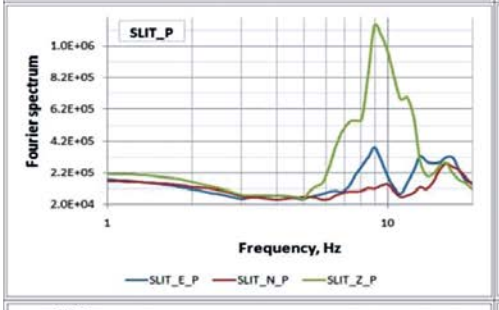
SLIT_P
Fourier spectrum
1.0E+06
8.2E+05
6.2E+05
4.2E+05
2.2E+05
2.0E+04
1
10
Frequency, Hz
SLIT_E_P
SLIT_N_P
SLIT_Z_P

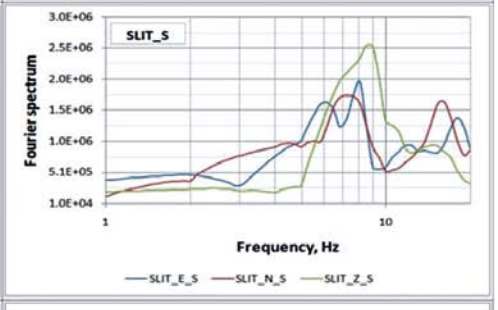
SLIT_S
Fourier spectrum
3.0E+06
2.5E+06
2.0E+06
1.5E+06
1.0E+06
5.1E+05
1.0E+04
1
10
Frequency, Hz
SLIT_E_S
SLIT_N_S
SLIT_Z_S

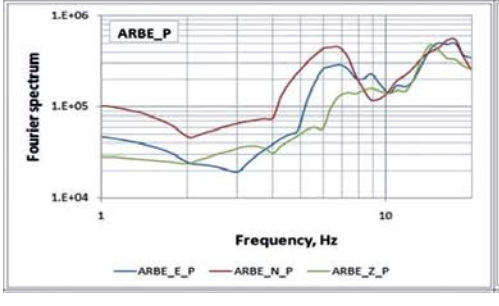
ARBE_P
Fourier spectrum
1.E+06
1.E+05
1.E+04
1
10
Frequency, Hz
ARBE_E_P
ARBE_N_P
ARBE_Z_P

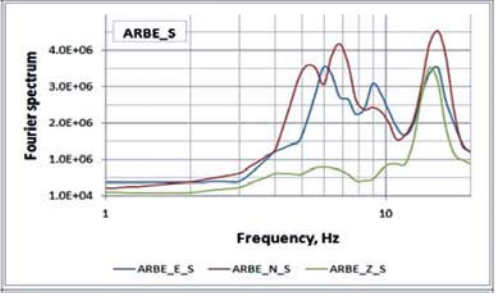
ARBE_S
Fourier spectrum
4.0E+06
3.0E+06
2.0E+06
1.0E+06
1.0E+04
1
10
Frequency, Hz
ARBE_E_S
ARBE_N_S
ARBE_Z_S

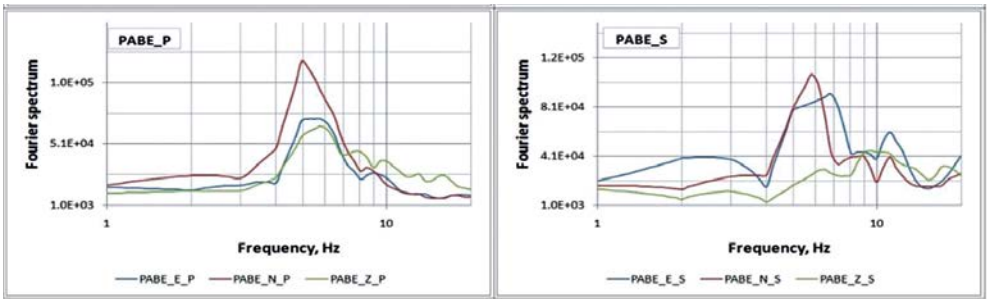

Figure 97. Fourier spectra for the earthquake as of November 12, 2016 in the Lake Võrtsjärv neighborhood (Estonia)

This region of Lithuania is characterized by total lack of industrial quarries wherein explosions might have been set off. For Fourier spectra, the following parameters of analysis were used: 1) length of the seismic signal = 10.0 sec.; 2) time windows length = 1.0 sec.; 3) frequency range: = 0.5 ÷ 10 Hz.

The spectral peaks frequencies are associated with 6–7 Hz. They scarcely change for *P*- and *S*-waves. As a rule, spectral level for *P*- and *S*- waves on the vertical component does not exceed spectral level on horizontal components.

For comparison, consider the spectra of typical explosions in the open-cast mines of the northeast of Estonia. The Fourier spectrum for these explosions is shown in Figure 99.

The seismic event of an unknown genesis in the Curonian Lagoon was recorded by the BH* channel, while an earthquake in the area of Lake Võrtsjärv and a typical explosion in the northeast of Estonia were registered by channel HH*. The sample rate of the BH* channel is 20 Hz, whereas the sample rate of the channel HH* is 100 Hz. Accordingly, the channels have different frequency bands. Nevertheless, it is noteworthy that the maxima of the spectra of the event of an unknown genesis are in the low-frequency range 6–7 Hz (Figure 98). The rise in spectral characteristics begins at 4–5 Hz. The spectral characteristic of a typical explosion in the northeast of Estonia is characterized by the fact that the maxima of the spectra are in the range 12–15 Hz, and the rise in the frequency response starts from 8–10 Hz (Figure 99). For an earthquake in the Lake Võrtsjärv area, the maximum frequency response is also predominantly in the low-frequency range, i.e. in the range of 5 to 9 Hz, with the exception of the VSU station located closest to the epicenter of earthquake (Figure 97).

Thus, there is more similarity between a seismic event of unknown genesis and an earthquake in the Lake Võrtsjärv area than between a seismic event of unknown genesis and a typical explosion in the northeast of Estonia. Therefore, with a certain probability, we can assume that the seismic event on June 12, 2015 in the Curonian Gulf has a tectonic nature.

Based on the records received at the MEF station (Figure 100), the Fourier spectra relating to 10 explosions that took place at the north-east of Estonia were summarized. Sources of the explosions in the north-east of Estonia were located within a narrow

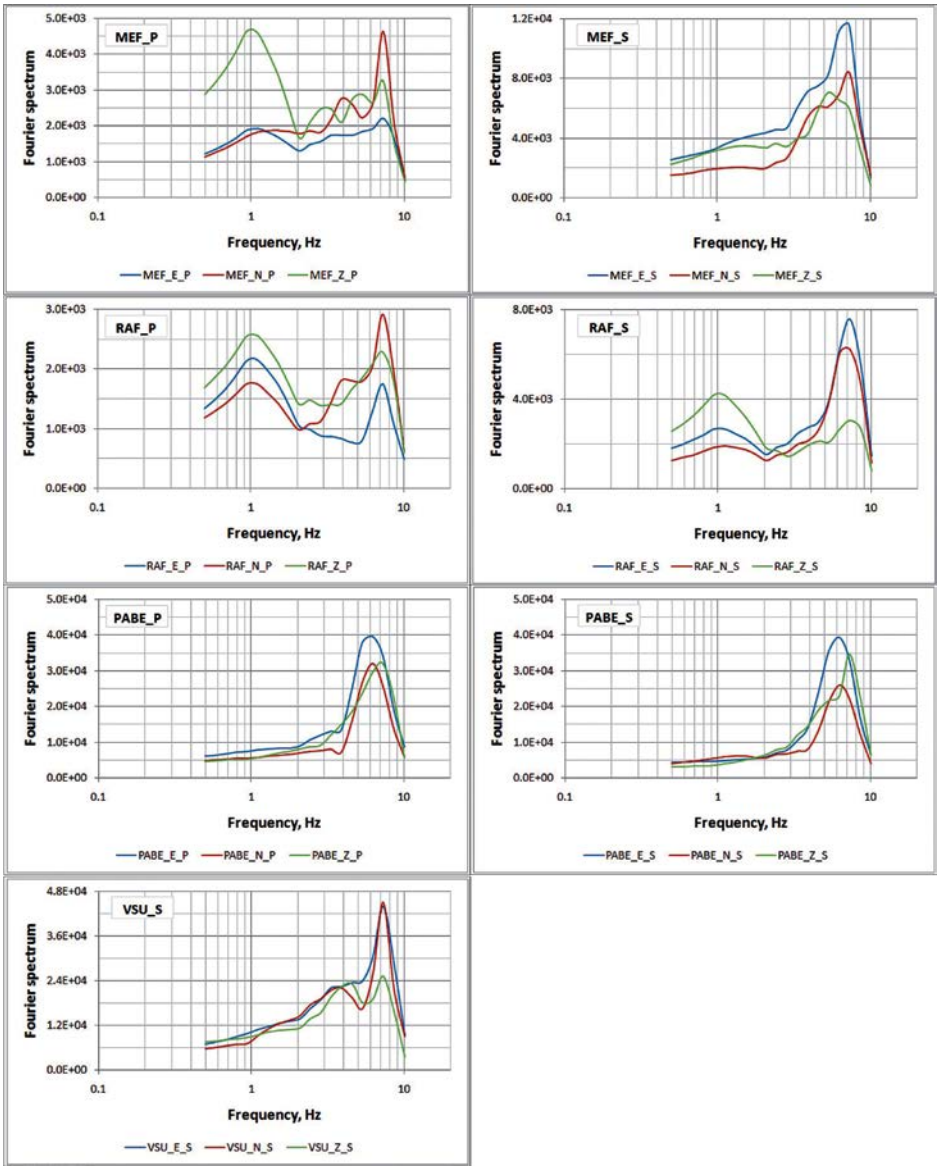

Figure 98. Fourier spectra of a seismic event of unknown origin that took place on June 12, 2015 in the area of the northern edge of Couronian lagoon, on the territory of Lithuania

azimuth section 11.5° (from 113.1°to 124.6°), i.e., seismic waves were propagating along close directions.

The results of spectral analysis show that, in the group of P-waves (MEF_P), the maximum spectrum level is characteristic for E-W component. The spectrum level of the vertical Z component is higher than that of the horizontal N-S component.

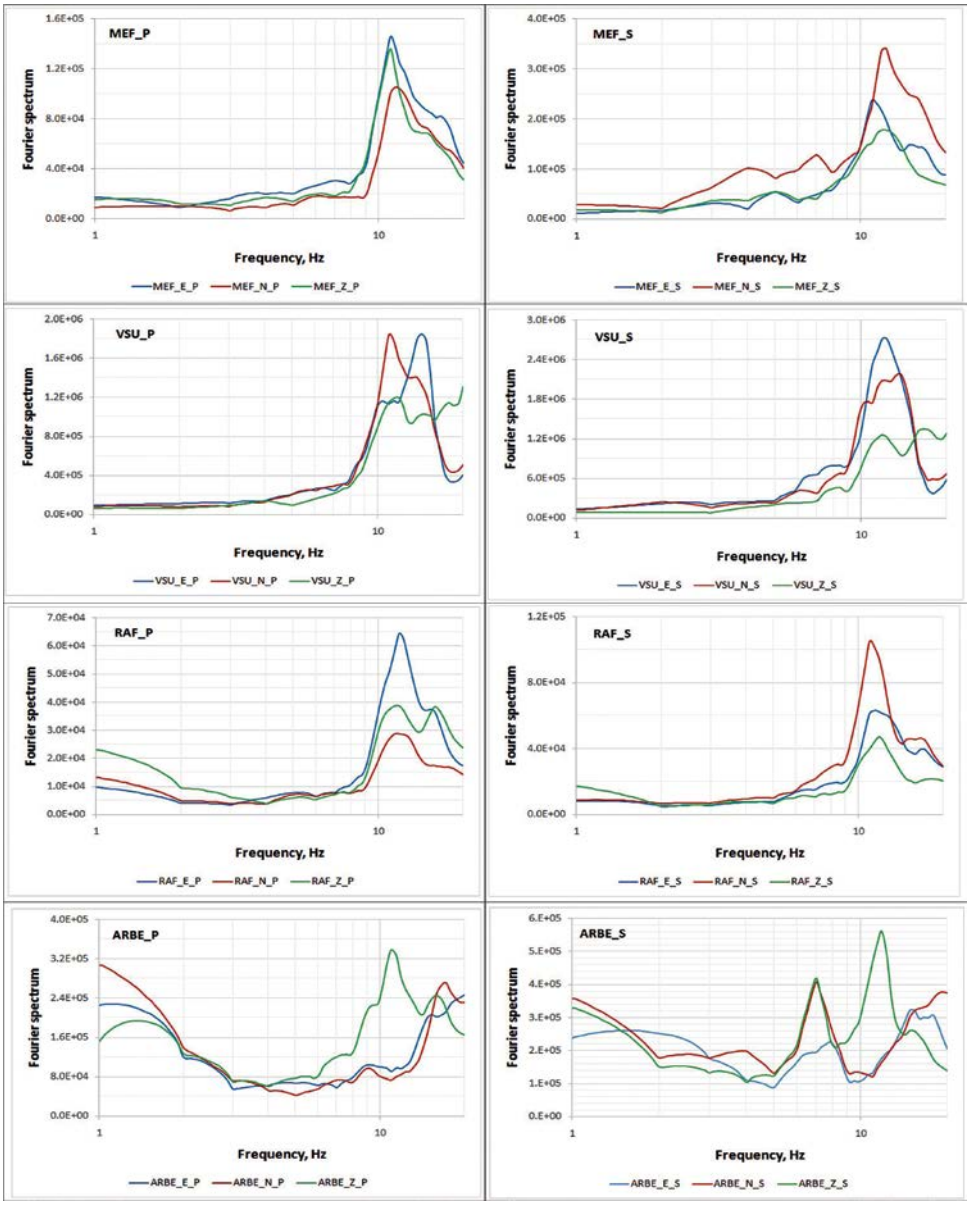

Figure 99. Fourier spectra for a typical explosion in the north-west of Estonia, obtained according to BAVSEN network stations records

In the group of S-waves (MEF_S), the maximum spectrum level is characteristic for the N-S component, while the minimum spectrum level is characteristic for the Z component.

The total spectra for explosions (Figure 100) show that the S-waves spectrum level is broader than the P-waves spectrum level. The major difference between analysed

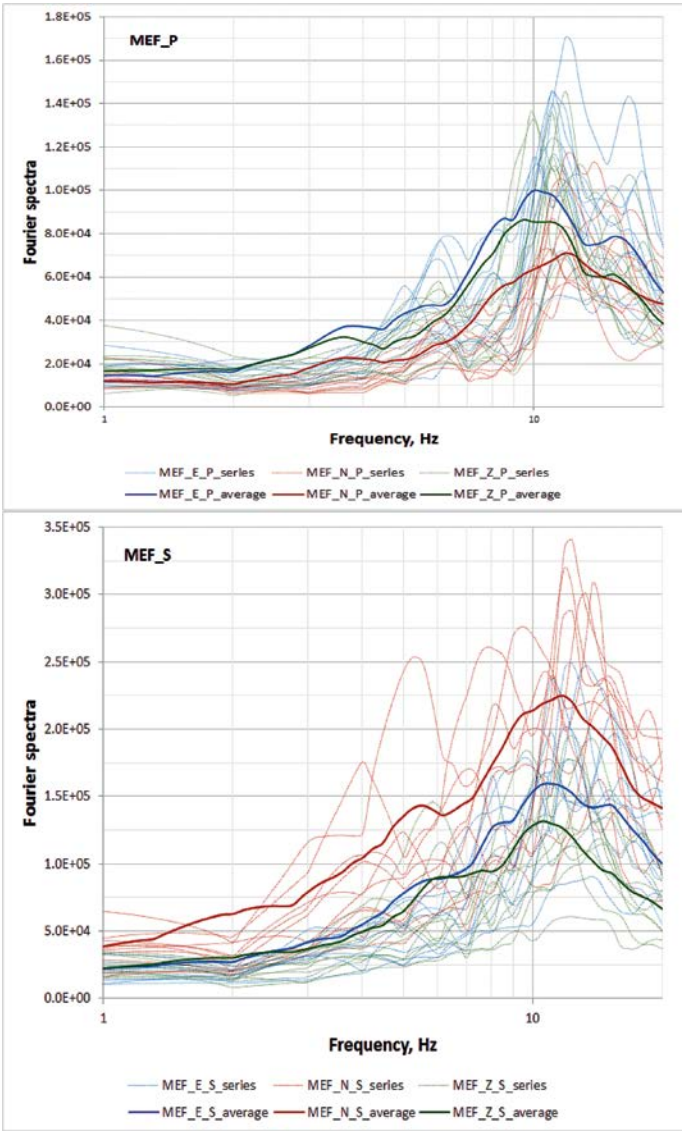

Figure 100. Fourier spectra of explosions that took place in the north-east of Estonia in 2016, received according to MEF station records

spectra of earthquake near the Lake Võrtsjärv and the explosion spectra is more a higher-frequency content of the explosion spectra as against the earthquake ones.

For P- and S-waves, the explosion spectra are normally higher than 10 Hz (Figure 100), whereas the frequency of the earthquake spectra is less than 10 Hz (Figure 97). Therefore, 10 Hz frequency may be regarded as some potential discriminator.

To provide a reliable identification of a seismic event type, some other additional discriminants should be used, which will be considered further.

4.3.2. Waves amplitudes ratio or spectra ratio P/S (P/Lg)

P-wave amplitude to S-wave (Lg-wave) amplitude ratio or waves amplitudes spectra ratio, is considered to be one of the promising discriminants to differentiate between earthquakes and explosions. As a rule, the numerator of this amplitude or spectral ratio is the amplitude of a body (longitudinal) *P*-wave, whereas the denominator is the amplitude of a shear wave, or, the amplitude of some other type of wave.

For example, the amplitudes spectra ratio *P/Lg* was used as a discriminant for earthquakes and explosions recorded in the eastern part of the USA [Kim et al., 1993]. As the first wave, direct *Pg*-waves were used (Figure 101). Small-magnitude earthquakes and some explosions comparable to them in magnitudes and lying within the epicentral distance range from 10 to 610 km were analyzed. It was found that the average spectral ratios *Pg/Lg* within the band width 1–25 Hz were equal to 0.5 for the earthquakes and 1.25 for the explosions. It was observed that, within the 5–25 Hz frequency range, higher explosion-invoked frequencies are more typical to *Pg*-waves then to *Lg*-waves. Within the 1–10 Hz frequency range, the discriminant *Pg/Lg* is less effective.

According to other sources [Bennet & Murphy, 1986], the discriminant *Pg/Lg* s higher for earthquakes than for explosions. Nevertheless, the discriminant researchers in the eastern part of the USA [Kim et al., 1993] believe that their conclusions hold true for regional distances and the frequencies up to 20 Hz, i.e., for high-frequency discriminant *Pg/Lg.* This discriminant features a certain dependence on near-shot conditions (the shot point is located within the deposits characterized by low propagation velocities). To minimize the source-induced discriminant fluctuations and the wave propagation routes, the network average ratio *Pg/Lg*s should be used.

In simplified form, the Earth's crust model consists of two layers: the upper and the lower crust separated from each other by Conrad discontinuity. A similar Earth's crust model with radiation lines and the main crustal phases of regional earthquake-induced seismic waves is shown in Figure 101.

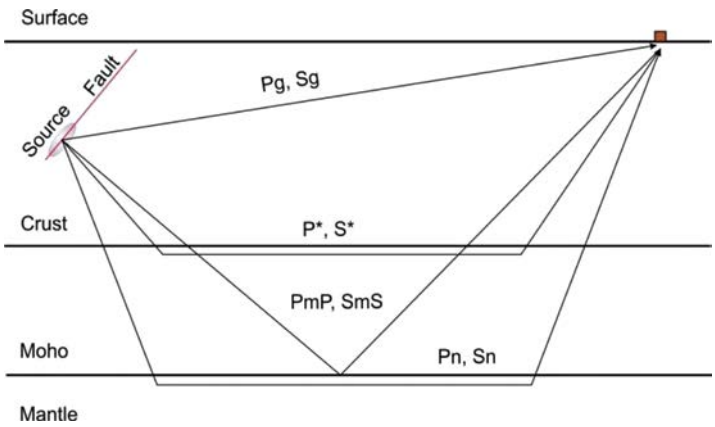

Figure 101. Simplified Earth's crust model with main types of regional earthquake-induced seismic waves

The main crustal phases of seismic waves are shown with respect to regional distances to 1500 km. approximately. *Pg*- and *Sg*-waves are direct upward waves emanating from the source in the upper part of the Earth's crust. *P**- and *S**-waves are those ones refracting at Conrad discontinuity. *PmP*- and *SmS*-waves are those ones reflecting from Moho discontinuity, which separates the Earth's crust from the upper mantle. *Pn*- and *Sn*-waves are the waves refracted at Moho discontinuity. Seismic wave *Lg* is a group of waves observed at large regional distances. It is generated by a superposition of multiple reverberation S-waves in process of exchange between *S* and *P* or, between *P* and *S*. The maximum energy of such waves corresponds to waves propagating with a wave group velocity of about 3.5 km/sec.

The essence of the amplitude ratio-based method is that seismic records are passed through filters in the first instance. Subsequently, signal amplitude for definite bandwidths is calculated. In case of a three-component record, the amplitude is calculated as:

$$A = \sqrt{A_X^2 + A_Y^2 + A_Z^2} \tag{33}$$

where, A_X, A_Y, A_Z are amplitudes on three channels of seismic record.

To assess the P/S amplitude ratio levels with respect to the main groups of seismic events in EBR – i.e., earthquakes and explosions –records of explosions that took place in the north-east of Estonia were used, as well as the records of the only regional earthquake reliably registered – that in the Lake Võrtsjärv neighborhood, on November 12, 2016 (Table 12).

Table 12.

Parameters of the earthquake in the Lake Võrtsjärv neighborhood and the explosions in the north-east of Estonia

Date	Time, GMT	Lat	Lon	H, km	Mag	Epicentre	Event's type
2016/11/01	11:36:15	59.149	28.044	0.0	1.7	NE of Estonia	Explosion
2016/11/02	12:27:28	59.200	27.781	0.0	1.9	NE of Estonia	Explosion
2016/11/03	10:11:01	59.272	27.774	0.0	2.2	NE of Estonia	Explosion
2016/11/04	09:42:13	59.170	27.878	0.0	2.1	NE of Estonia	Explosion
2016/11/05	09:19:51	59.265	27.633	0.0	2.2	NE of Estonia	Explosion
2016/11/08	12:09:07	59.198	28.162	0.0	2.1	NE of Estonia	Explosion
2016/11/09	11:35:20	59.138	28.019	0.0	1.9	NE of Estonia	Explosion
2016/11/10	11:58:49	59.164	27.989	0.0	1.9	NE of Estonia	Explosion
2016/11/12	02:49:52	58.378	26.081	1.2	2.5	Lake Võrtsjärv, Estonia	Earthquake

The P/S amplitude ratio for the earthquake ($A_{\frac{P}{S}}^{EQ}$) is lower than P/S amplitude ratio for the explosions ($A_{\frac{P}{S}}^{EXP}$) (Figure 102). The amplitude ratios $A_{\frac{P}{S}}^{EQ} \leq 0.4$ for the earthquake

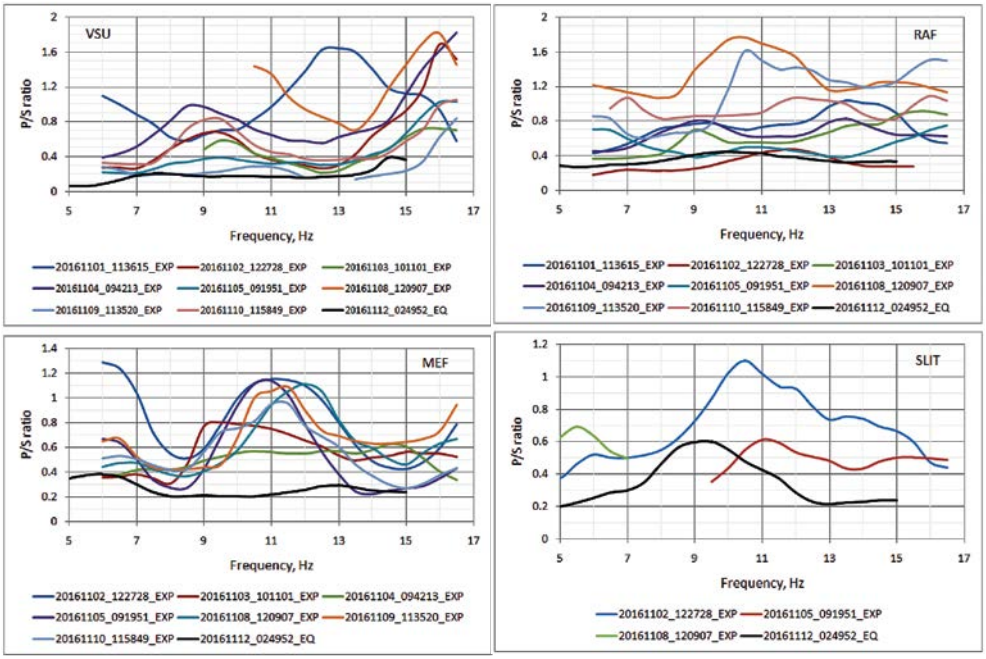

Figure 102. P/S amplitude ratios received according to BAVSEN network stations' records of explosions in the north-east of Estonia and the earthquake in the Lake Võrtsjärv neighborhood

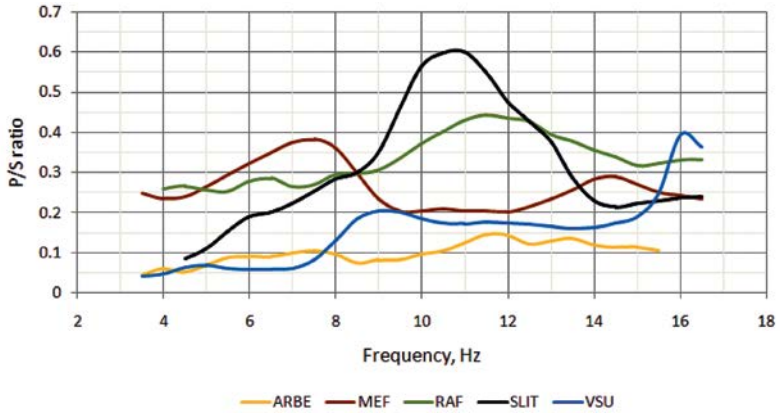

Figure 103. Amplitude P/S ratios for the earthquake of 2016/11/12 (02:49:52 GMT) in the Vyrtsyarv Lake neighborhood

were recorded at three stations (VSU, MEF and RAF). An exception is the SLIT station, for which, $A^{EQ_P}_{S_{max}}$ ~ 0.6. The difference in amplitude ratios is most reliably observed at the MEF station. For some explosions is equal or close to $A^{EQ}_{\frac{P}{S}}$. For example, $A^{EXP}_{\frac{P}{S}}$ for

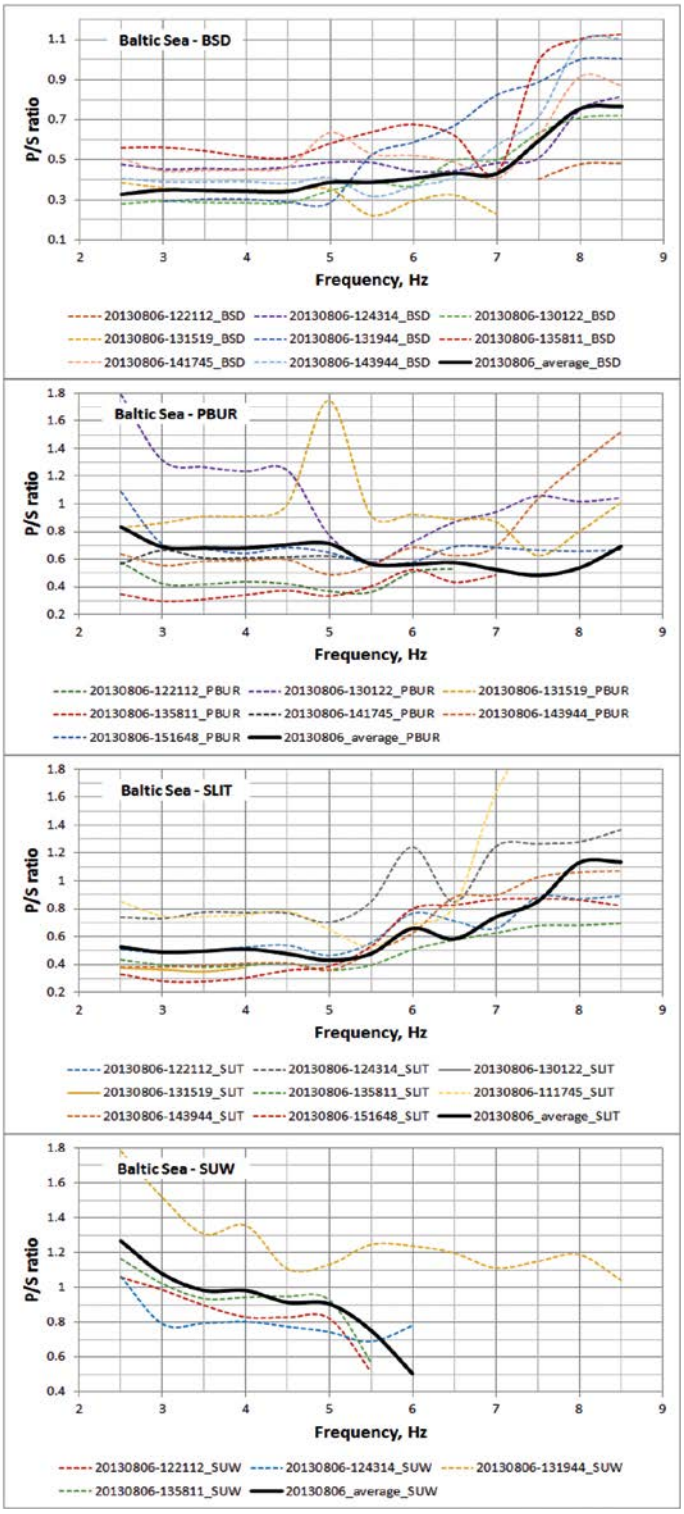

Figure 104.
P/S amplitude ratios obtained based on records made by BAVSEN network stations, with respect to explosions in the Baltic Sea

the explosion recorded 2016/11/09 (11:35:20) on the VSU station, and for the explosion recorded 2016/11/02 (12:27:28) on the RAF station. Some substantial variations $A^{EXP}_{\frac{P}{S}}$ could be observed with respect to explosions.

The amplitude ratios are affected by the distance from the hypocentre and by geological environment. Therefore, the level of amplitude ratios varies from station to station – both for the explosions and the earthquakes. Figure 103 shows the variation of for different seismic stations.

With the exception of the station SLIT, the P/S spectral ratios do not exceed 0.45 for the earthquake in the Lake Võrtsjärv area.

Amplitude ratio variations are typical for explosions in the Baltic Sea as well, although they are smoothed out to a greater extent (Figure 104). The explosions subject to analysis were recorded on seismic stations BSD, PBUR, SLIT, and SUW.

Thus, the amplitude ratios $A_{p/s}$ are not an absolutely reliable criterion for identifying a regional earthquake and explosions in the northeast of Estonia. Similar conclusions are contained in publications on the analysis of amplitude ratios in the Arctic region [Асминг и др., 2010; Ringdal et al., 2002]. However, in combination with other discriminants, the amplitude ratios will allow more reliable identification of the type of seismic event. It would seem that the amplitude ratio parameter P/S equal to 0.45 (Figure 87) can be accepted as a potential discriminator to discriminate between earthquakes and explosions. At 0.45, it is more reasonable to consider a seismic event to be an earthquake than an explosion; this holds true with respect to the majority of the seismic stations. Yet, this parameter is expediently used only in conjunction with other discriminators.

4.3.3. Time frequency analysis of earthquakes and explosions

Fourier spectra (i.e., Fourier transformation of signals) used in the previous sections, are based on the transformation in one-dimensional space and frequency domain. However, Fourier spectra have a number of shortcomings that limit the informative nature of the analysis of non-stationary signals and practically do not allow one to analyze their features. This leads to a *"blurring"* of signal features (breaks, steps, peaks, etc.) within the frequency domain throughout the entire frequency range of the spectrum.

The Fourier transform reflects only the most general (global) information about the frequencies of the signal under investigation; it fails to provide an insight into the local properties of the signal – for example, when during time fast variations of its spectral composition occur. For instance, the Fourier transformation does not distinguish between a stationary signal with the sum of two sinusoids from a non-stationary signal with two successive sinusoids having the same frequencies, since the spectral ratios are calculated by integrating over the whole interval within which the signal is specified. Finally, the Fourier transformation is incapable of analyzing the frequency characteristics of the signal at arbitrary instants of time.

This impasse may be partially overcome by Short-Time Fourier transform with a window function moving in a signal. As a result of the windowing (Short-Time

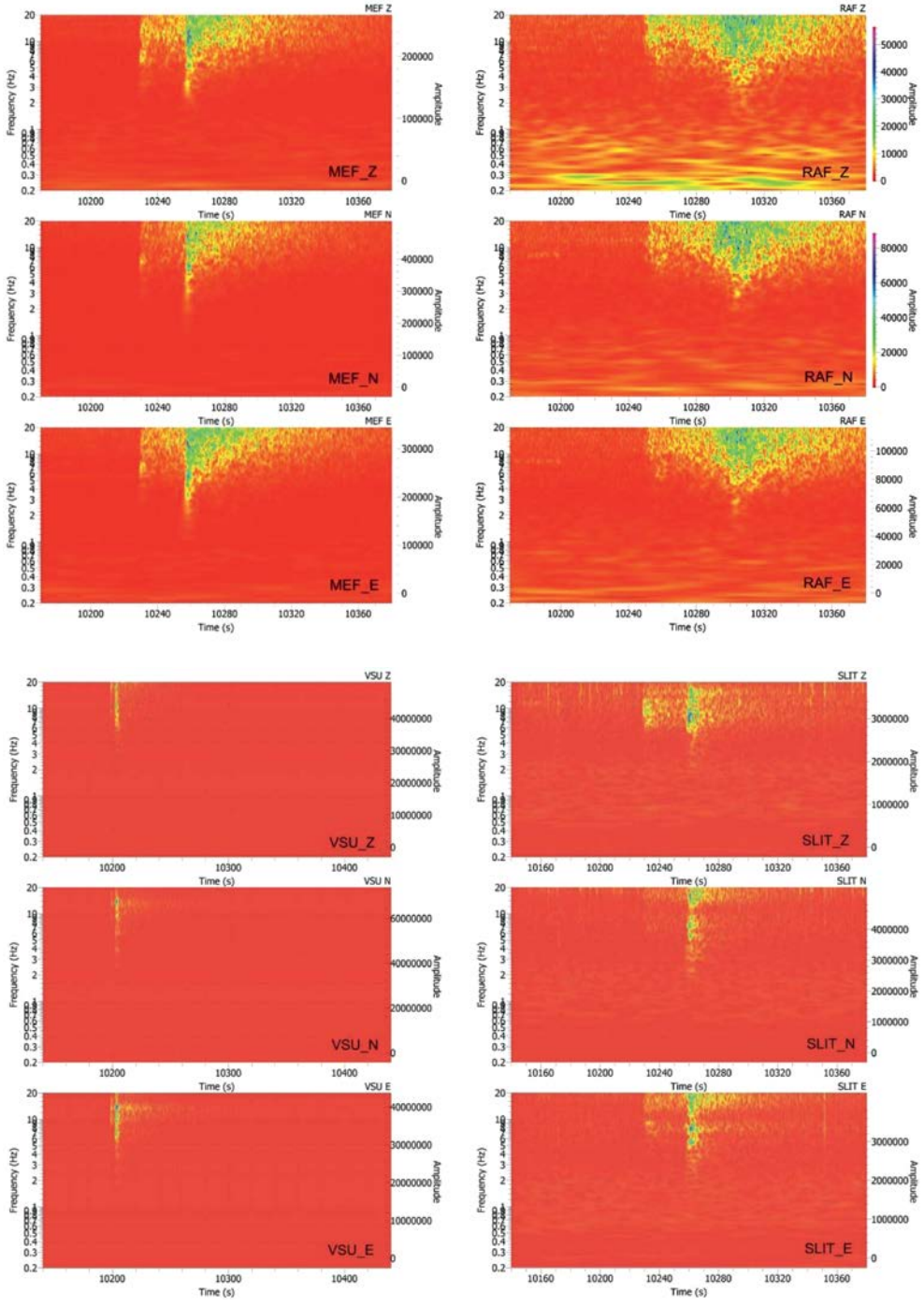
MEF Z
MEF_Z
MEF N
MEF_N
MEF E
MEF_E
RAF Z
RAF_Z
RAF N
RAF_N
RAF E
RAF_E
VSU Z
VSU_Z
VSU N
VSU_N
VSU E
VSU_E
SLIT Z
SLIT_Z
SLIT N
SLIT_N
SLIT E
SLIT_E
Frequency (Hz)
Time (s)
Amplitude

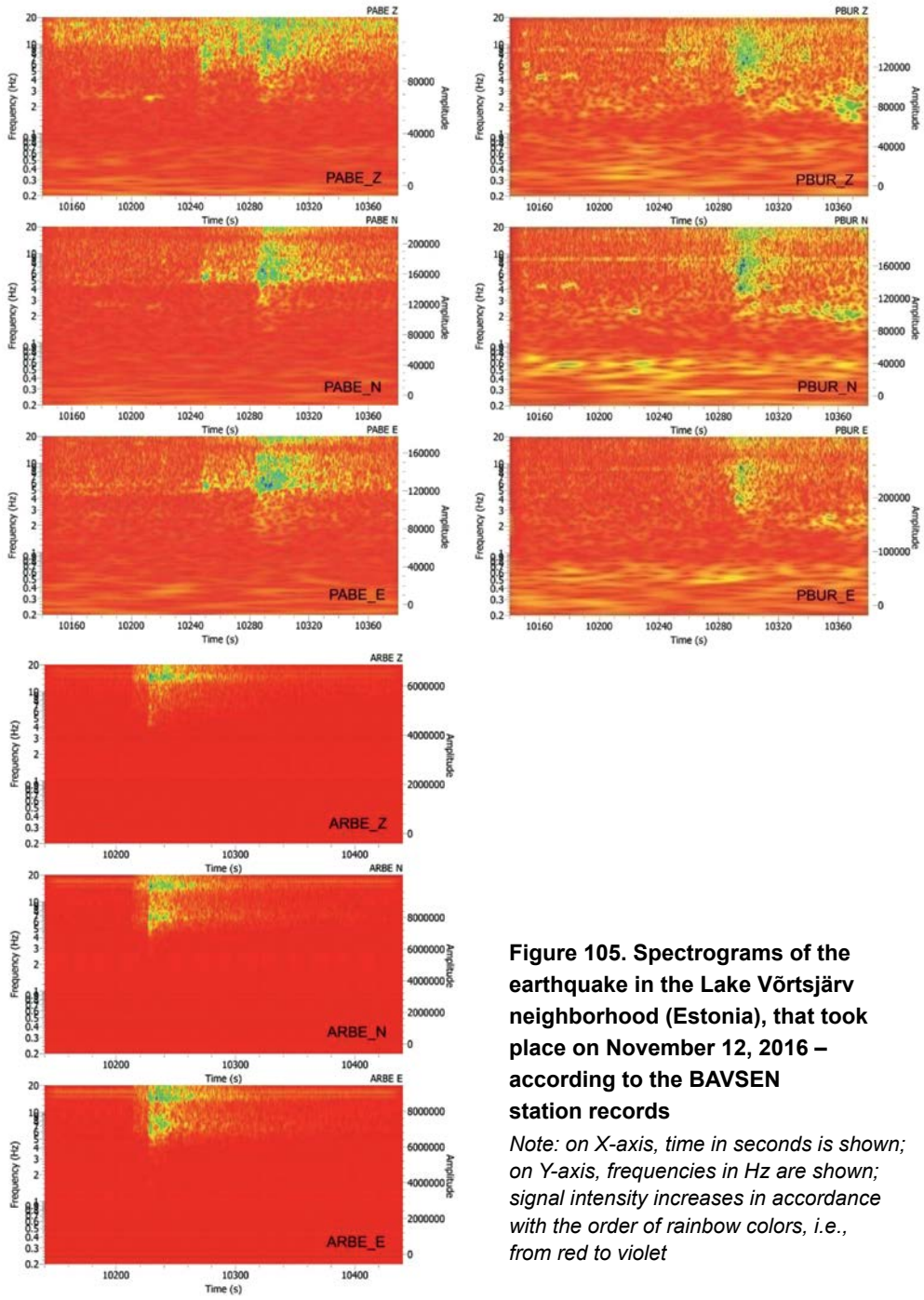

Figure 105. Spectrograms of the earthquake in the Lake Võrtsjärv neighborhood (Estonia), that took place on November 12, 2016 – according to the BAVSEN station records

Note: on X-axis, time in seconds is shown; on Y-axis, frequencies in Hz are shown; signal intensity increases in accordance with the order of rainbow colors, i.e., from red to violet

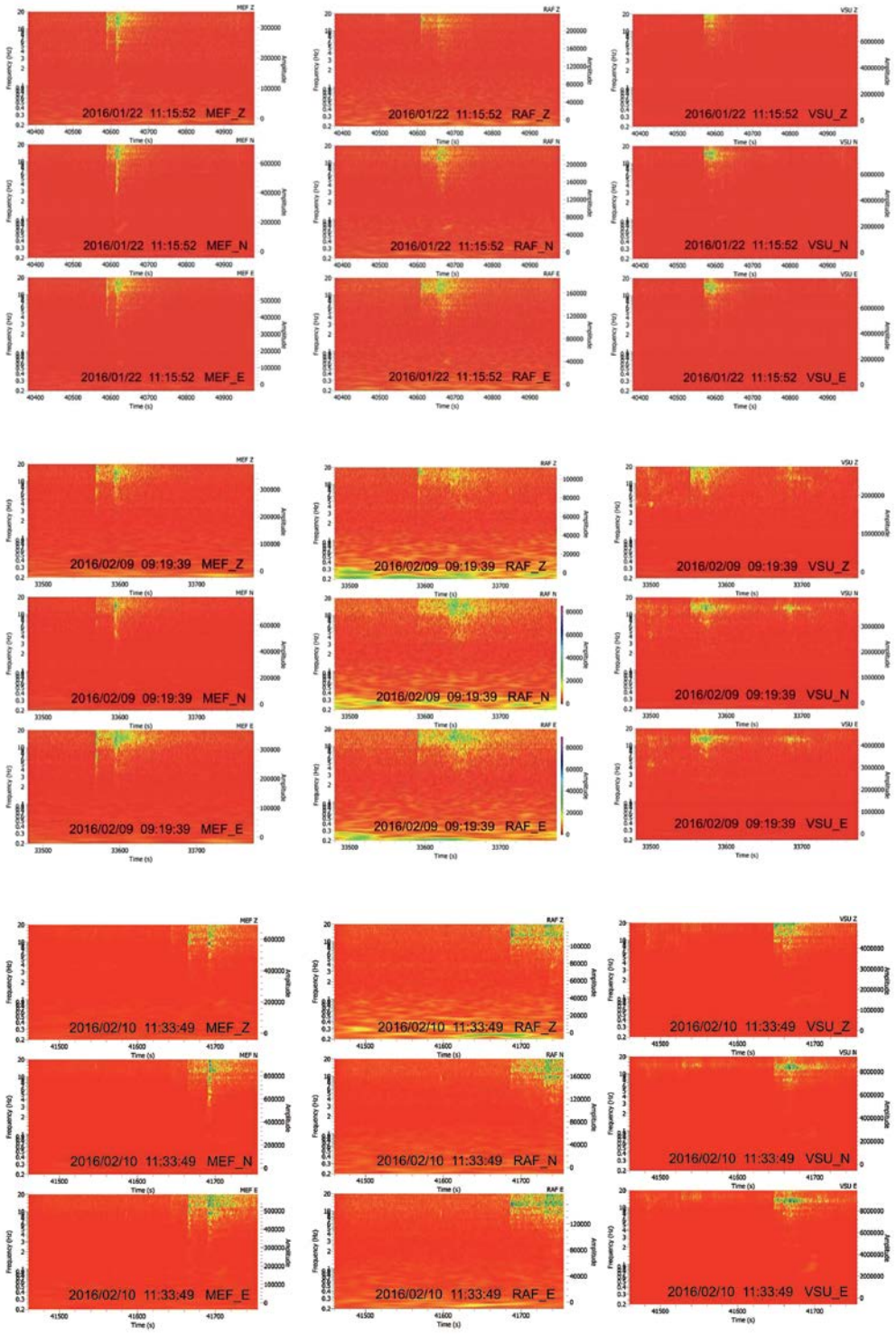
2016/01/22 11:15:52 MEF_Z
2016/01/22 11:15:52 RAF_Z
2016/01/22 11:15:52 VSU_Z
2016/01/22 11:15:52 MEF_N
2016/01/22 11:15:52 RAF_N
2016/01/22 11:15:52 VSU_N
2016/01/22 11:15:52 MEF_E
2016/01/22 11:15:52 RAF_E
2016/01/22 11:15:52 VSU_E
2016/02/09 09:19:39 MEF_Z
2016/02/09 09:19:39 RAF_Z
2016/02/09 09:19:39 VSU_Z
2016/02/09 09:19:39 MEF_N
2016/02/09 09:19:39 RAF_N
2016/02/09 09:19:39 VSU_N
2016/02/09 09:19:39 MEF_E
2016/02/09 09:19:39 RAF_E
2016/02/09 09:19:39 VSU_E
2016/02/10 11:33:49 MEF_Z
2016/02/10 11:33:49 RAF_Z
2016/02/10 11:33:49 VSU_Z
2016/02/10 11:33:49 MEF_N
2016/02/10 11:33:49 RAF_N
2016/02/10 11:33:49 VSU_N
2016/02/10 11:33:49 MEF_E
2016/02/10 11:33:49 RAF_E
2016/02/10 11:33:49 VSU_E

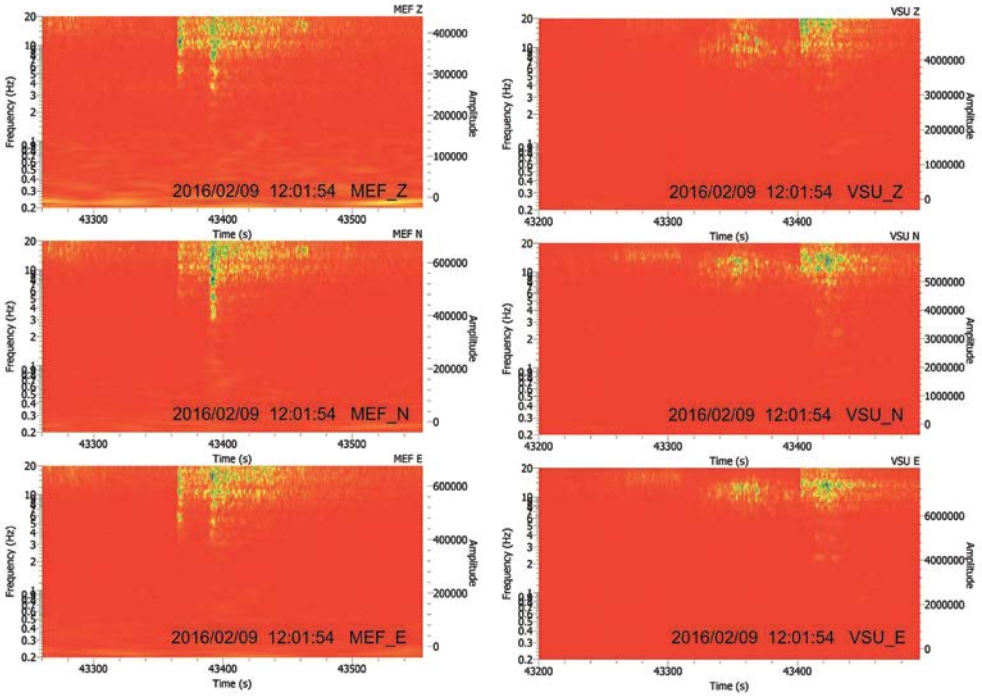

Figure 106. Spectrograms of explosions made in quarries in the northeast of Estonia

Note: on X-axis, time in seconds is shown; on Y-axis, frequencies in Hz are shown; signal intensity increases according to the order of rainbow colors, i.e., from red to violet

Fourier transform), a family of spectra is formed, which makes it possible to display a change in signal spectrum over individual sections of the moving window.

The resolution ability of the Short-Time Fourier transform depends on the width of the window function and is inversely proportional to frequency discrimination power. Given that the width of the window function is equal to b, the frequency discrimination power is dependent on the value $\Delta\omega = 2\pi/b$. Respectively, with the necessary frequency resolution $\Delta\omega$ value the width of the window function should be equal to $b = \frac{2\pi}{\Delta\omega}$.

A more effective instrument for analyzing signals is *wavelet* analysis (*wavelet*). Wavelet may be regarded as the functions holding intermediate position between harmonic and impulse functions. They should be localized both in the time and in the frequency domain of mapping. Signal analysis carried out both in the time and the frequency domains simultaneously – i.e., the wavelet analysis – is widely used in seismological practice.

Now, let us consider a spectral-time presentation of: the earthquake that took place in the Lake Võrtsjärv neighborhood, the explosions in the northeast of Estonia, and the seismic event of an unknown origin in the region of Couronian Lagoon – by using wavelet analysis, namely – the Morlet wavelet convolution method.

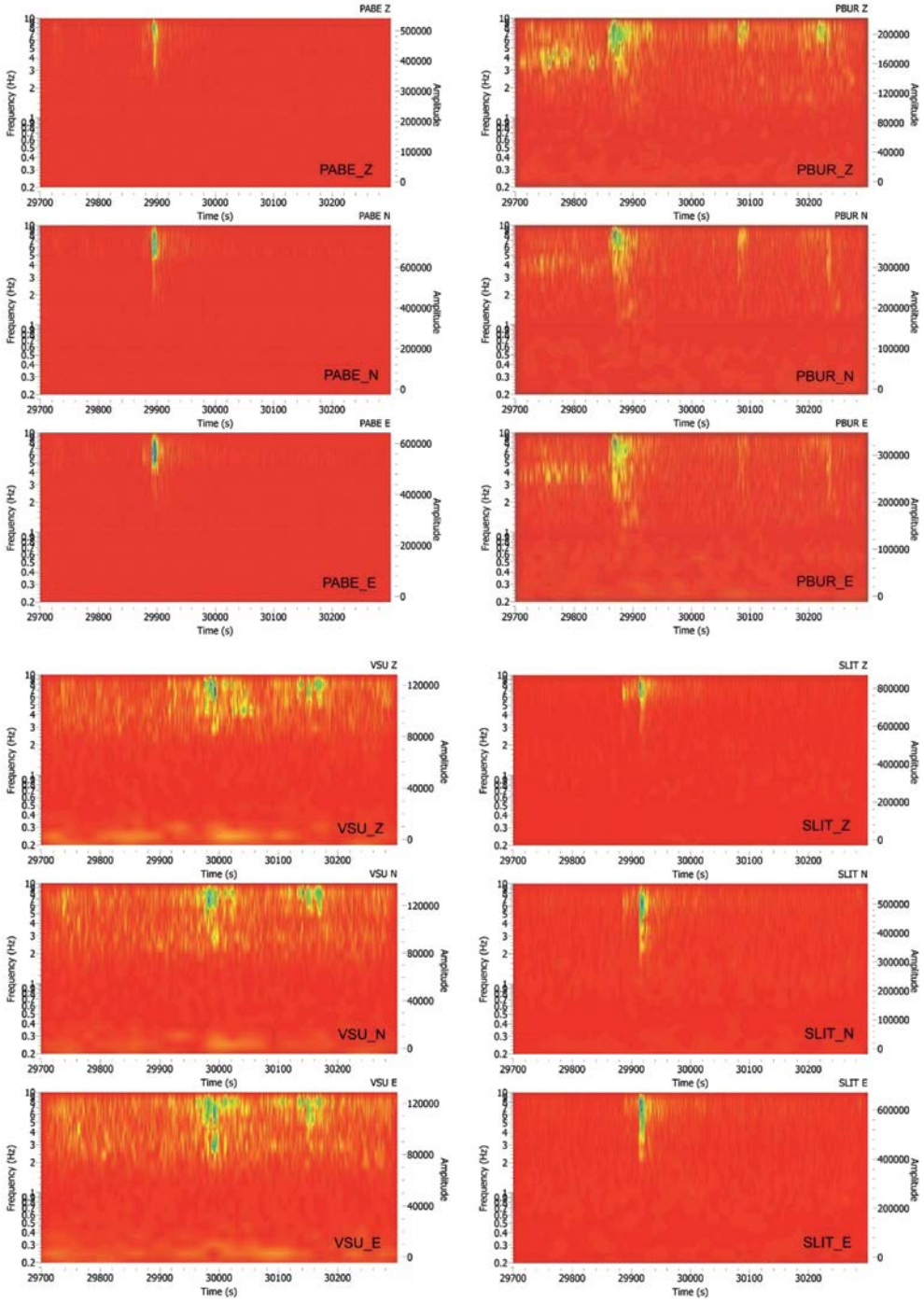
PABE Z
PABE_Z
PABE N
PABE_N
PABE E
PABE_E
PBUR Z
PBUR_Z
PBUR N
PBUR_N
PBUR E
PBUR_E
VSU Z
VSU_Z
VSU N
VSU_N
VSU E
VSU_E
SLIT Z
SLIT_Z
SLIT N
SLIT_N
SLIT E
SLIT_E
Frequency (Hz)
Time (s)
Amplitude

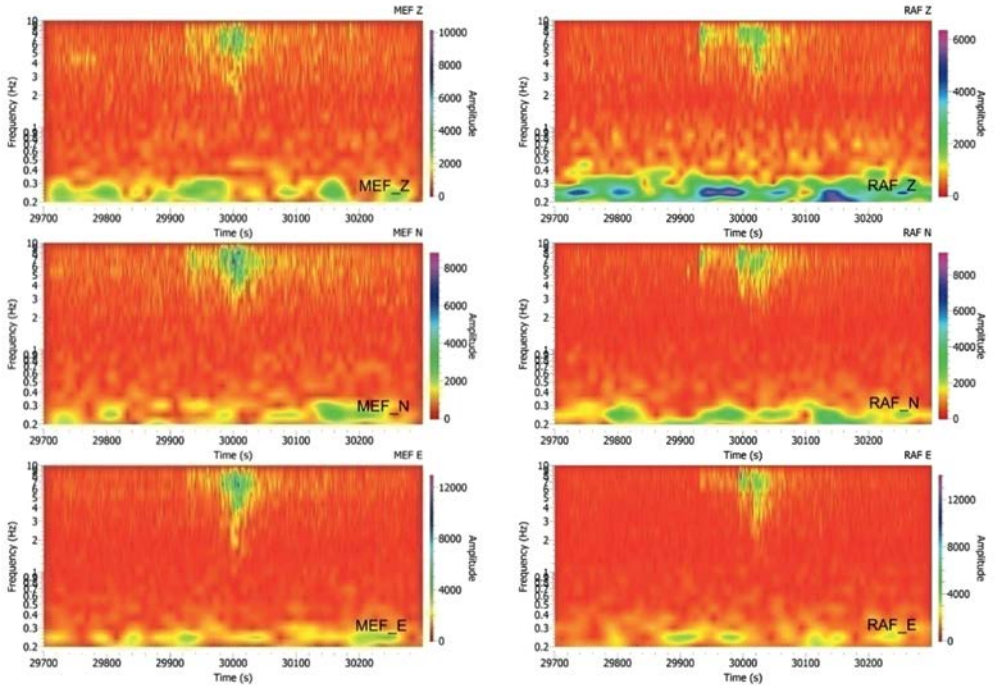

Figure 107. Spectrograms of a seismic event of unknown origin that took place on June 12, 2015 in the region of Couronian Lagoon (Lithuania)

Note: on X-axis, time in seconds is shown; on Y-axis, frequencies in Hz are shown; signal intensity increases in accordance with the order of rainbow colors, i.e., from red to violet

The spectral-time (wavelet) analysis for Võrtsjärv earthquake was carried out with the input parameters as follows: frequency range Δf = 0.20 – 20 Hz, sample rate f_{sr} = 100 Hz, wavelet parameters: m = 10.0, fi = 1.0 Hz, ΔT = 3.01975, ΔF = 0.0263523. The results of the wavelet analysis in the two-dimensional time-frequency domain are shown in Figure 105.

At the VSU station, which is the closest to the earthquake hypocentre, only one narrow band which corresponds to *S*-waves stands out within the frequency range 5–6 to 20 Hz (the higher frequency of the analysis). With the increasing epicentral distance, the first *P*-wave is identified more explicitly on those stations which are located on the Baltic Shield (namely, MEF and RAF stations), while the spectral contents within the interval between *P*- and *S*-wave onsets increases.

MEF and SLIT stations are located approximately at the same epicentral distances (228 and 239 km respectively). However, P-wave is much better highlighted on the spectrogram of the MEF station located on the crystalline basement of the Baltic Shield – as against the SLIT station located on the sedimentary cover of the Baltic Syneclise, where the upper part of the section is represented by Quaternary deposits. Due to numerous reflections from the boundaries, seismic waves interfere at the top of the section, resulting in a significant absorption of *P*-wave energy that is approaching the SLIT station.

To compare the time-frequency contents, spectrograms of explosions made in quarries in the northeast of Estonia are shown in Figure 106. The following parameters of

spectral-time (wavelet) analysis has been used: frequency range Δf = 0.20–20.0 Hz, sample rate f_{sr} = 100 Hz, wavelet parameters: m = 10.0, fi = 1.0 Hz, ΔT = 3.01975, ΔF = 0.0263523.

Explosion spectrograms are presented with respect to three seismic stations (MEF, RAF, and VSU), which were characterized by a satisfactory *signal-to-noise ratio* . For the rest of the stations – in particular, the SLIT station and, all the more so – the PABE and the PBUR stations – seismic noise level was much higher, obstructing any reliable identification of *P*-wave on records and any usage of seismic records for wavelet analysis. Comparing the records made at MEF station, which reflected both the earthquake in the Lake Võrtsjärv neighborhood and the explosions in the northeast of Estonia, it can be noted that the earthquake frequency band for the *P*-wave (on components Z and EW) was narrower than that for the S-wave, while for explosions, the frequency bands (on the same components) are comparable. Thus, the MEF station can be regarded as an expert station, with more expressive and pronounced characteristics for the earthquake and the explosion frequency bands – especially on the Z and E-W components.

A spectral-time analysis was also carried out for a seismic event of an unknown origin that took place on June 12, 2015 in the region of Couronian Lagoon (Lithuania) (Figure 107). The following parameters were used for the spectral-time (wavelet) analysis: frequency range: Δf = 0.20 – 10.0 Hz, sample rate: f_{sr} = 20 Hz, and wavelet parameters: m = 10.0, fi = 1.0 Hz, ΔT = 3.01975, ΔF = 0.0263523. Thus, in this case there was a narrower frequency band and detail. Nevertheless, this did not affect the overall appearance of the spectrogram.

The epicentral distance to the MEF station in that case reached 553 km– i.e., it was by far longer than the distance to the earthquake epicenter. Therefore, the spectrograms compared were those received on the basis of records made by the SLIT station which was located practically in same distance from the earthquake (239 km) and the seismic event of unknown origin (241 km).

The comparison shows that in both cases (the earthquake and the seismic event of unknown origin) the frequency bands for P-wave are narrower than those for S-wave. This is stated on all the components. The spectrogram of the seismic event of unknown origin contains only a trace of P-wave which can be observed. On the contrary, on the explosion spectrogram, P-wave is clearly defined. It is fair to assume very likely that the seismic event of unknown origin that took place on June 12, 2015 in the neighborhood of Couronian Lagoon (Lithuania) looks more like an earthquake than an explosion. In this case, spectrum width of P-wave was considered as a relative discriminant. Some additional criteria to confirm the above version more unambiguously should be used.

The quantitative estimation of the potential discriminant based on spectral-time analysis is problematic. This discriminant can be assessed at the qualitative level.

4.3.4. Complexity index as method of estimation of integral power ratio of S and P-waves

A more complicated parameter for distinguishing tectonic earthquakes from human-induced explosions may be the so-called *complexity. Complexity* is seismogram-depicted integral power ratio for the selected time windows, which are specified by time

marks . Symbolically, this parameter can be expressed by the formula, as follows [Arai & Yosida, 2004]:

$$C = \int_{t_1}^{t_2} a^2(t)dt \,/\, \int_{t_0}^{t_1} a^2(t)dt \quad (34)$$

where *a* is signal amplitude.

Integration limits are specified by the time marks , which depend on epicentral distance and which are selected experimentally. Actually, time windows are applied with respect to P- and S-wave group. corresponds to the moment of *P*-wave onset to the station. In particular, with respect to the earthquake in the Lake Võrtsjärv neighborhood, the time slot specifies the *P*-waves group and it cannot exceed 4 sec. with regard to the VSU station, because that station was the most closely located to the earthquake hypocentre. The time slot specifies *S*-wave group.

The complexity index C should have a higher value for earthquakes, since the amplitude of the earthquake-generated *S*-waves is normally higher than the amplitude of *P*-waves. The complexity index C is calculated by using the *MatLab* mathematical tools. The complexity indices *C* for the earthquake of November 12, 2016 in the Lake Võrtsjärv neighborhood are presented in Table 13. The sampling duration for the earthquake-generated *P*- and *S*-waves is = 4.0 sec., while the one for explosions is 10.0 sec.

Table 13.

Complexity indices for the tectonic earthquake in the Lake Võrtsjärv neighborhood and the explosions in quarries in the northeast of Estonia

Date	Time	Station	Δ, km	I_S	I_P	$C = I_S/I_P$	ML
Earthquake in the area of Lake Võrtsjärv							
2016/11/12	02:49:52.0	VSU	39.3	1.2151022	8.2781021	1.47	2.4
-	-	SLIT	239	1.8501018	4.6671017	4.04	-
-	-	MEF	226	8.5271018	1.0851018	7.86	-
-	-	RAF	381	8.1351017	3.5031016	23.23	-
Explosions in quarries in the northeast of Estonia							
2016/01/21	12:18:42	MEF	239	2.0221008	3.2841008	0.62	1.9
2016/01/26	09:52:13	MEF	233	1.8661007	3.7581007	0.50	1.8
2016/02/09	09:19:40	MEF	213	9.4791007	1.0631008	0.89	1.9
2016/02/09	12:03:05	MEF	204	2.0781007	5.0001007	0.42	2.2
2016/02/10	11:33:49	MEF	238	2.1931007	1.4731007	1.49	2.2
2016/02/12	07:58:10	MEF	227	1.8101007	9.1561006	1.98	2.1
2016/02/17	12:37:31	MEF	229	9.0911007	4.4941007	2.02	2.3
2016/02/22	18:59:37	MEF	234	2.1841007	5.1841006	4.21	2.4
2016/11/02	12:27:28.8	VSU	104	9.2701007	1.7211007	5.39	1.9

Legend: – epicentral distance; I_S *– S-waves power integral;* I_P *– P-waves power integral;* C *– complexity index; ML – magnitude*

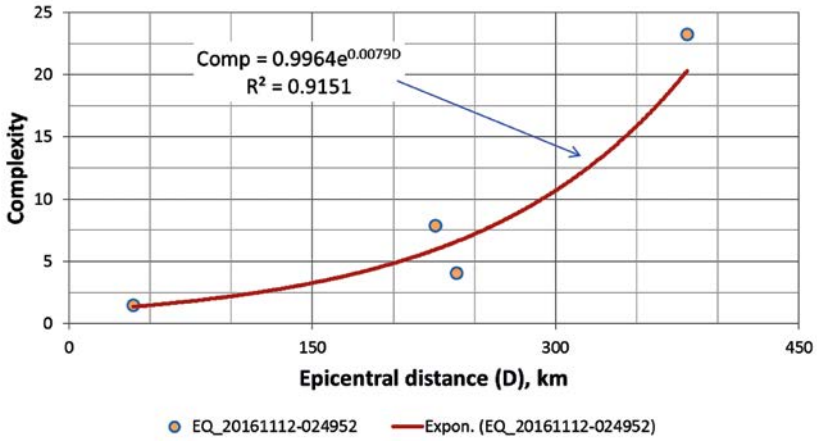

Figure 108. Change in complexity index subject to epicentral distance

For the earthquake in the Lake Võrtsjärv area, the complexity index increases with the increase in the epicentral distance (Figure 108). The PABE station is out of scope due to unsatisfactory wave-recording conditions. For the earthquake, the complexity parameter varies from 1.5 (VSU) to 23.2 (RAF), and epicentral distances – from 39 to 381 km.

As follows from the spectral-temporal analysis (Section 4.3.4), the frequency bands for P- and S-waves of the earthquake differ more strongly than the frequency bands for explosions. As regards the RAF station, the value of the complexity index C of the earthquake in the Lake Võrtsjärv neighborhood is greater than that for the explosions in the northeast of Estonia. In the case of earthquake, the complexity index C increases with distance (Figure 94). This is due to the fact that the energy of the longitudinal P-waves decays faster than the energy of the shear S-waves. The complexity index for explosions is unsteady and it can exceed unity. This means that the P-wave power integral is smaller than S-wave power integral. This is probably due to the asymmetry of the sources of explosion in the northeast of Estonia, or, with change of wave type on boundaries of geological layers.

Therefore, the complexity index should be investigated and specified for different epicentral distances. The increase in that parameter with the increasing distance is typical for the Võrtsjärv earthquake. The complexity index as a single discriminator may not allow one to recognize the type of a seismic event. It is necessary to additionally use a set of discriminants.

4.3.5. SOM method for discrimination between earthquakes and explosions

The methods tried in sections 4.3.1–4.3.4 with greater or lesser efficiency, allow to investigate the type of a seismic event. However, each method alone cannot provide for a reliable identification of seismic event. Therefore, the complex, joint use of all the potential discriminators is necessary.

The task is to highlight groups of similar objects selected from a set of data (seismic events as objects), i.e., to highlight clusters (earthquakes, explosions, or events of unknown type as classes). Clustering implies the allocation of objects by indefinite classes – unlike classification, which implies the allocation of objects by the classes known in advance. Clustering allows to group objects, and, subsequently, identify clusters as a result of a meaningful interpretation. Problems of such type are solved using self-organizing, neural networks of Kohonen [Кохонен, 2008]. The method is called the self-organized map of Kohonen (*SOM – Self Organized Map*). The Kohonen map is a computational method, which is intended, first of all, for solving problems like clustering, visualization, and also for analyzing data from high-dimensional space – i.e. multidimensional data. The *SOM* method is used for data mining throughout data sets. This is based on the fact that the dimension of the original space is reduced to a space of smaller dimensions, usually up to two-dimensional space. The topology of space, i.e., continuity, remains unchanged.

A self-organizing map consists of components called nodes, or neurons. Individual neurons form a neural network. An artificial neural network is a mathematical model based on the principle of organizing and functioning of biological neural networks, i.e., a network of nerve cells (ganglion cells) of a living organism.

An individual neuron in the network may be presented as a simple processor, whose functions are the reception and transmission of signals to other processors. Such a network of "processors", i.e., neurons acting collectively, is capable of solving challenging problems.

The number of neurons (properties of the object *) is specified based on analysis of the process structure. Each node is described by two vectors: weight vector *m* having dimensions similar to the input data, and vector *r* representing the coordinates of the node on the map.

The *Kohonen* map is visually displayed by using rectangular or hexagonal cells. The hexagonal shape is used more often, since in this case, the distances between the centers of adjacent cells are the same. This improves the correctness of the visualization of the map. The structure of the *SOM* looks as follows (Figure 109): there are two layers – the

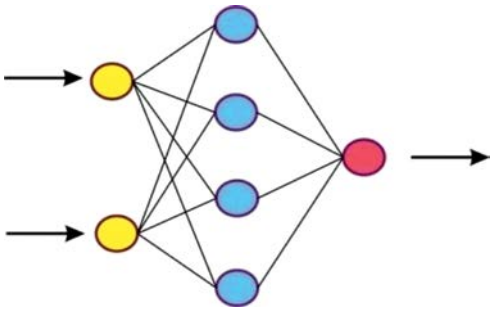

Figure 109. Diagram of a simple neural network

Legend: input neurons are designated by yellow; latent neurons are designated by blue; the output neuron is designated by red

input layer of neurons (the distributive one) and the output layer of neurons (the *Kohonen* layer). Neurons of the 2nd layer are arranged in the form of a two-dimensional lattice. The lattice can be a square, or a hexagon. Each neuron of the 1st layer is connected to each neuron of the 2nd layer. The number of neurons in the input layer is equal to the dimension of the original space. The neurons of the Kohonen layer (the 2nd layer) are also called cluster elements. Self-organizing map (Kohonen map) is an "unsupervised" neural network. From the mathematical standpoint, neural network's unsupervised learning process is a multi-parameter task of nonlinear optimization. Its essence lies in finding a coupling ratio between neurons. More details on *SOM* ideology can be found in professional literature [Kohonen, 2012].

Since SOM solves such complex problems of high and non-linear character as feature extraction, the method is applied in seismological practice for the recognition of nuclear explosions and tectonic earthquakes. Various discriminants are used as input parameters. For example, for discriminating between earthquakes and nuclear explosions, five discriminants (input vectors) were used: scalar seismic moment , local magnitude *Ml* and source parameter (constant level), (spectral corner frequency), (high-frequency spectral slope) [Allamehzadeh, 2003].

However, those discriminants are relevant only with respect to large-magnitude seismic events. A "shortage" of such events is observed in the East Baltic Region. Therefore, the above-enumerated discriminators can be used, namely – Fourier spectra, amplitude P/S ratios, spectral-time characteristics, the complexity index and other parameters.

SOM allows researcher to map the space input data to the output level by using the learning algorithm. This is achieved by the fact that the *SOM* creates a vector quantizer by adjusting the weights from common input nodes to M output nodes located on a two-dimensional grid (space). The *SOM* method creates a special clustering. With the aid of a neural network, input data (samples) are organized into different clusters, while the clusters themselves – into one- or multidimensional space in accordance with the similarity of the clusters themselves.

Neural nodes are tied with many local connections. The weights between the input and the output nodes are preset by initial, small, stochastic values. The distance between the input and all the nodes is calculated as follows:

$$d_j = \sum_{j=0}^{N-1}(x_j(t) - w_{ij}(t))^2 \tag{35}$$

where d – distance between the input and each output of j node for the time t; w_{ij} – weight from input node i to output node j for the time t.

Then, the output node with the minimal distance is selected, and the new weights renewal takes place:

$$w_{ij}(t+1) = w_{ij}(t) + \eta(t)(x_i(t) - w_{ij}(t)) \tag{36}$$

The equation member $\eta(t)$ is a growth factor $0 \le \eta \le 1$, decreasing in time.

Due to a small representativity of regional tectonic earthquakes in the Baltic Region, no reliable and effective discriminants have been specified to date. In the case of a sufficient volume of statistical data, the SOM method may turn out to be a promising tool for the identification of tectonic earthquakes in the East Baltic Region.

4.3.6. Nuclear Test Explosion Control in the context of seismic event type identification. An example of identification of nuclear explosion in the North Korea on September 3, 2017 by the BAVSEN seismic network

The identification of seismic events is of particular importance and practical significance in connection with the necessity of recognizing nuclear explosions. This trend in seismology is developing in connection with the Comprehensive Nuclear Test Ban Treaty (CTBT), which was adopted by the 50th session of the UN General Assembly on September 10, 1996 and opened for signature on September 24, 1996. The CTBT treaty complements the previous Treaty Banning Nuclear Weapon Tests in the Atmosphere, Outer Space and Under Water, adopted in 1963.

After the CTBT treaty was adopted, the international Preparatory Commission for the Comprehensive Nuclear-Test-Ban Treaty Organization – (CTBTO) was established.

Within the framework of this agency, an international monitoring system has been established, which includes 50 main and 120 auxiliary seismic stations, 11 hydroacoustic (hydrophone) stations for tracking acoustic waves in the oceans, 60 infra-acoustic stations that use microbarographs to detect very low-frequency sound waves, 80 radionuclide stations using samplers for the detection of specific isotopes that are

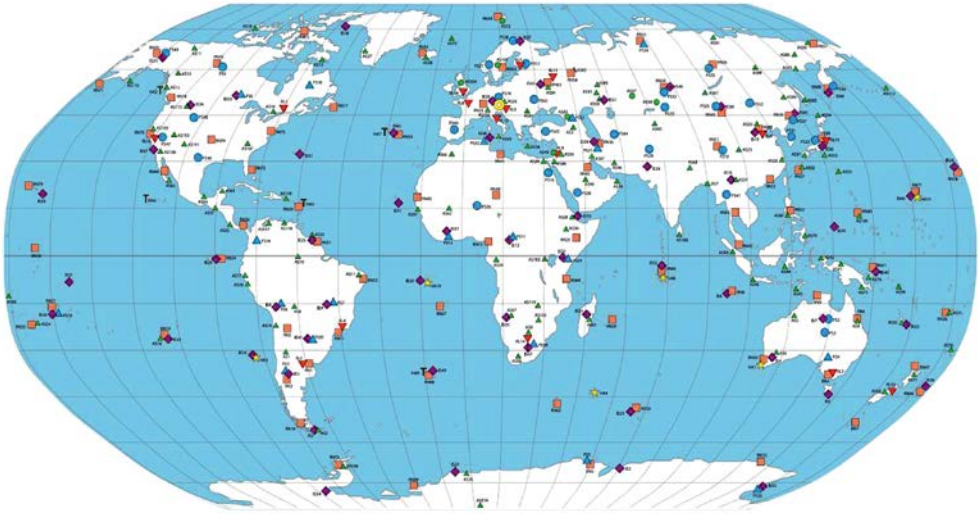

Figure 110. International monitoring system operating within the framework of CTBTO [CTBTO Preparatory Commission, 2003]

Legend: initial seismic groups (PS) – the blue circlet; initial three-component seismic stations (PS) – the blue triangle; auxiliary seismic groups (AS) – the green circlet; auxiliary three-component seismic stations (AS)–the green triangle; hydroacoustic (hydrophone) stations (HA)–the yellow asterisk; hydroacoustic (T-phase) stations (HA) – the T-shaped icon; SAM survey stations (IS) – the rhomb; radionuclide stations (RN) – the pink square; radionuclide laboratories (RL) – the red, upside triangle; International Data Centre CTBTO PreCom, Vienna – the yellow circlet with a wide point

formed predominantly by nuclear or thermo-nuclear explosions, and 16 radionuclide laboratories for analyzing samples received from radionuclide stations (Figure 110).

Thus, CTBTO operates a broad international monitoring network, wherein seismological methods play one of the key roles in the detection of nuclear explosions and the provision of rapid online information.

The main tasks of the seismic monitoring system are: 1) detection of seismic waves generated by a nuclear explosion against the background noise, and 2) positioning of underground nuclear explosions. The seismic method is effective for detecting an alleged nuclear explosion, since seismic waves rapidly propagate in the bowels of the Earth and can be recorded just in a few minutes after the seismic event took place. The data transmitted from the international network of seismic monitoring stations to the International Data Center allows one to determine the location of the alleged underground nuclear explosion and the exact coordinates of the area to which the inspection team will be sent. The international monitoring system components nearest to the East Baltic Region are located in: Finland (PS17, PL7), Sweden (AS101, RN63), Norway (PS27, PS28, IS37) and Russia (AS84, IS43, RN61, RL13). Obviously, the density and the location of the international monitoring network stations operating within the framework of CTBTO depends on the position of the proving grounds where nuclear weapons may be tested.

The seismic stations included into the international monitoring system unite 4 varieties of seismic tools: the primary seismic arrays (groups), the primary, three-component seismic stations, the auxiliary seismic arrays, and the auxiliary, three-component seismic stations.

The difference between the primary and the auxiliary seismic stations and groups is that the data from the primary seismic stations or sets comes to the International Data Centre in Vienna almost on a real-time basis, whereas the data from the auxiliary seismic stations and sets comes to the Centre upon requests.

Seismic arrays are a system of interconnected seismometers located in the form of a certain geometric figure (like for example, cross, circle, rectangle, "L"-shaped, etc.) in a limited area. Such a compact arrangement is necessary in order to increase the array's sensitivity to the detection of seismic events (explosions or earthquakes).Seismic arrays differ from the local seismic network mainly by the methods used for data analysis.

Seismic array data is received with the aid of dedicated technologies for digital signal processing – as, for example, plotting a directivity graph.

Technologies of that kind allow one to suppress noises and increase *Signal-to-noise ratio* (*SNR*). *SNR* is a standard which makes it possible to compare between the signal proper and the noise level.

Seismic arrays were developed exactly with the aim of improving the detection of nuclear explosions. At present, seismic arrays are used in the International seismic observations network not only for monitoring earthquakes and nuclear explosions but for solving other problems, as well. For instance, they are used for the detection of microseism sources, the investigation of microseism genesis, and for the detection and monitoring volcanic tremor.

The nearest seismic arrays are located in Scandinavia. One of the first seismic arrays – the Norwegian Seismic Array (NORSAR) was created in 1968 in Kjeller (Norway). The

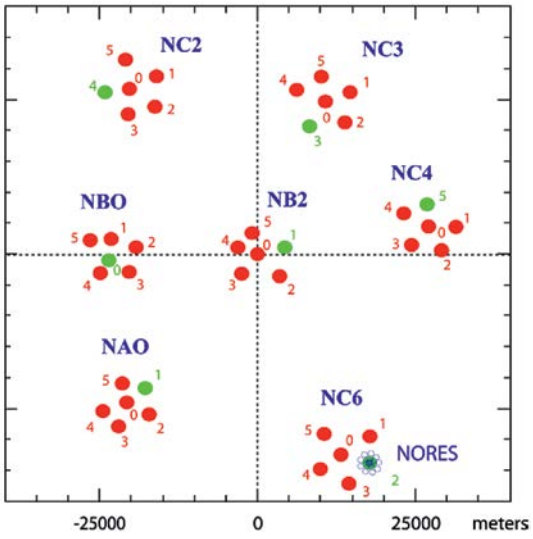

Figure 111. Configuration of a large-aperture NORSAR seismic array and a small-aperture, miniature NORES array

array has a large aperture with the diameter 100 km. The array was originally intended to detect earthquakes and nuclear explosions. Since 1999, the array is used for non-commercial research activities.

A miniature, small-aperture array is located within a large NORSAR array. The length of the square side where NORES is located is 2 km. Within the NORES boundaries, 21 (twenty-one) observation point equipped with vertically installed, short-period sensors is located as well as 3 observation points equipped with 3-component, short-period sensors, plus one more central observation point equipped with three-component, short-period, and long-period sensors.

The NORES array is a part of a large NORSAR array; at the same time however, it can be used as an independent, experimental miniature array – in particular, for testing and assessment of the array and equipment configuration.

An example of nuclear explosion identification in North Korea on September 3, 2017, where the BAVSEN network stations were used

North Korea still remains the main testing ground where nuclear weapon tests are carried out up to date. According to data presented by seismological agencies (Incorporated Research for Seismology – IRIS), 6 nuclear weapon tests have taken place within the period from 2006 to 2017 in North Korea (Table 14).

The main feature of the nuclear tests being conducted is a constant increase in the explosion power. As a result, the nuclear explosion power in 2017 was 1000 times higher than the nuclear explosion power in 2006. To show the possibilities of recognizing nuclear explosions by the BAVSEN network, it was necessary to select the explosions from the ones indicated in Table 12, so that they could be confidently and reliably

Table 14.

Characteristics of nuclear explosions made in North Korea according to data from IRIS [IRIS_i]

Nr.	Date	Time	Lat	Lon	H, km	Magnitude's type	Magnitude
1	2006/10/09	01:35:28	41.294	129.094	0.0	Mb	4.3
2	2009/05/25	00:54:43	41.303	129.037	0.0	Mb	4.7
3	2013/02/12	02:57:51	41.299	129.004	0.0	Mb	5.1
4	2016/01/06	01:30:01	41.300	129.047	0.0	Mb	5.1
5	2016/09/09	00:30:01	41.287	129.078	0.0	mb	5.3
6	2017/09/03	03:30:01	41.343	129.036	0.0	Mb	6.3

recorded in the East-Baltic region. Since the first explosions were by far weaker than the last one, it was quite difficult to highlight records of those explosions against the background noise. Therefore, the only actual explosion as the "candidate" turned out to be the last explosion as of September 3, 2017. On the other hand, it was necessary to select earthquakes of similar magnitudes, the epicenters of which would be located in the Far East Region (eastern China, southern and central Japan, Taiwan). As a result, the Taiwan 6.2-magnitude earthquake as of October 2016 was found. The parameters of comparable events are shown in Table 15.

Table 15.

Parameters of seismic events used for nuclear explosion identification

Date	Time	Lat	Lon	H, km	Type	Mag	Agency	Event's type
2016/04/14	15:03:48	32.66	130.84	10.0		6.0	EMSC	Earthquake
2016/04/14	15:04:19	38.852	131.923	15.0	MS	6.7	LEGMC	Earthquake
2016/10/06	15:51:59	22.63	121.43	14.0		5.8	IRIS	Earthquake
2016/10/06	15:52:03	24.099	122.112	7.3	MS	6.2	LEGMC	Earthquake
2017/09/03	03:30:01	41.343	129.036	0.0	Mb	6.3	IRIS	Nuclear explosion
2017/09/03	03:29:30	38.893	133.166	14.7	MS	5.7	LEGMC	Nuclear explosion

Note: EMSC – European Mediterranean Seismological Centre; IRIS – Incorporated Research Institution for Seismology; LEGMC – Latvian Environment, Geology and Meteorology Centre

Coordinates of hypocentres of remote seismic events (like powerful explosions and magnitude 5.5 earthquakes as a rule) are specified by the BAVSEN network with a greater error than the location results presented by international seismic agencies (EMSC, IRIS,

USGS etc.). This is accounted for by the geometric position of the BAVSEN network stations relative to the hypocentres of the above-mentioned events, and by the number of stations engaged in the hypocentre localization. In particular, the azimuthal angle of the 8 (eight) BAVSEN network stations with respect to the epicentre of the explosion as of 2017/09/03 does not exceed 2.1°. For comparison, IRIS had determined the coordinates of the North Korean explosion as according to data received from 145 stations – for the azimuthal angle ~ 360°. Moreover, a number of stations in Japan, Russia, China, and South Korea was actually located around the explosion epicentre. Nevertheless, even USGS calls this event very cautiously a *"possible explosion"*. This presumption is additionally substantiated by the fact that this possible explosion is located close to the place where the North Korea used to explode nuclear charges in the past time [North Korea explosion_*i*].

Thus, the main task was to assess the possibilities of the BAVSEN network – first of all, in terms of nuclear explosion identification capabilities. As discriminators, different types of spectra were used.

Fourier spectra

The Fourier spectra (Figure 112) were evaluated with respect to 90-minute records. The analysis window length was $\Delta\omega$ = 60 sec. The frequency range of the analysis was Δf = 0.02–20.0 Hz, and the frequency sampling f_{samp} = 100 Hz.

Thus, spectral analysis covered many types of seismic waves, ranging from high-frequency ones, which, as a rule are of local genesis, and to low-frequency surface waves. We have failed to highlight any substantial differences of the Fourier spectra under study, generated by a nuclear explosion, from the Fourier spectra of an earthquake. One can only note a slight increase in the level of the earthquake spectra as against the explosion spectra. Therefore, Fourier spectra practically do not allow us to single out any characteristic features of a nuclear explosion.

Spectrum Rotate

The spectrum rotate displays the Fourier amplitude/frequency ratio (amplitude spectra) in the horizontal plane. The spectrum rotate depends on the direction (azimuth) from which seismic wav130

es approach. By using this type of spectrum, it is possible to assess the redistribution of *E*-energy in the horizontal plane. The results of the analysis are presented within the range from 0°to 180°and from 180°to 360°, which correspond to the range from 0° to 180°. On the graphs of the spectrum rotate, 0°corresponds to the northward direction, while 90° – to the eastward direction. The input parameters for the spectrum rotate are similar to those for conventional Fourier amplitude spectrum (see above).

The most substantial differences (Figure 113) between the rotation spectra of the nuclear explosion and the earthquake (can be noted only at some seismic stations of the BAVSEN network (namely, RAF and VSU). The difference lies in the fact that the maximum energy in the rotation spectrum of the earthquake is distributed at several frequencies – unlike the energy distribution character in the spectrum rotate for the nuclear explosion.

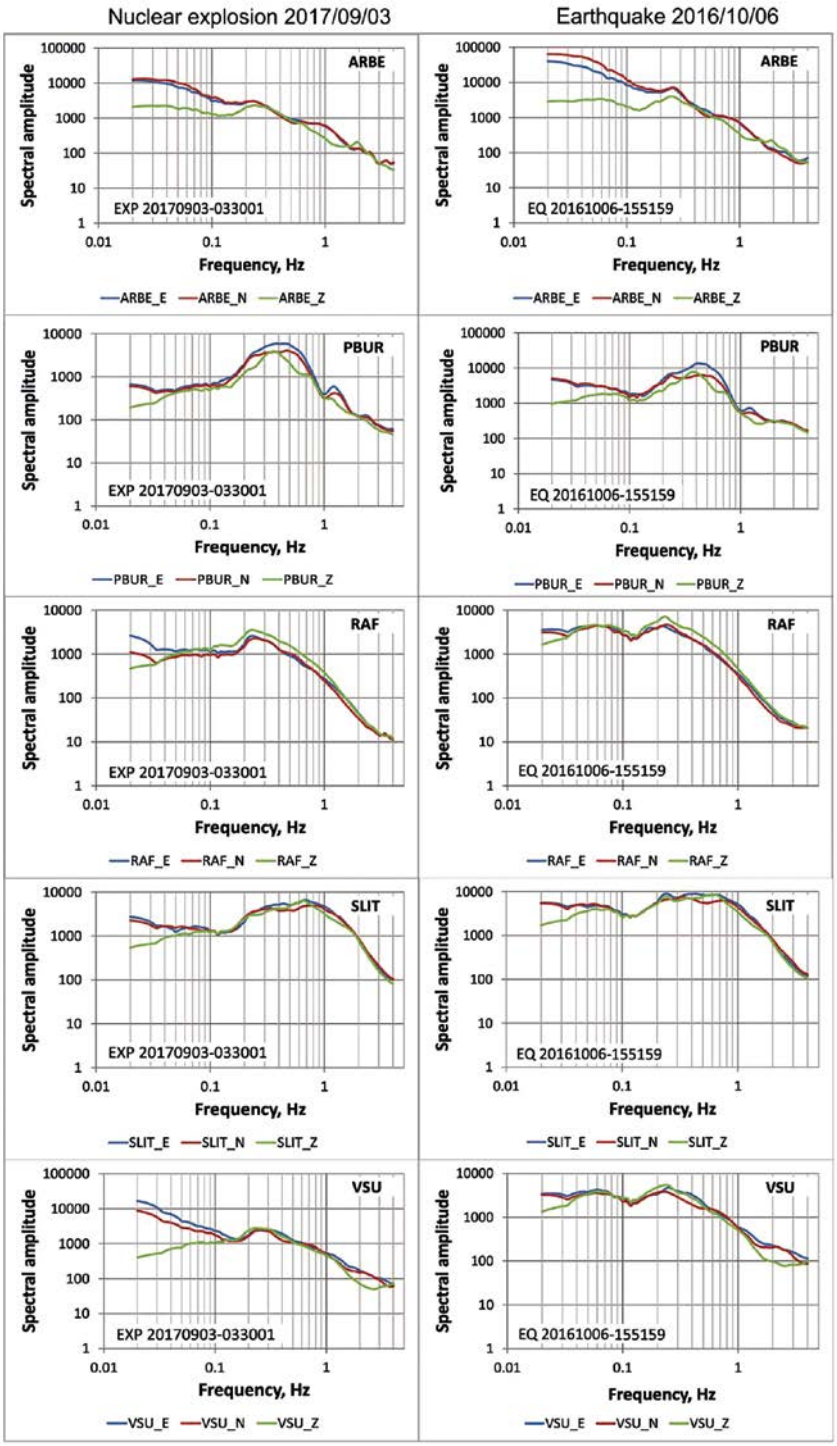

Figure 112. Fourier spectra for the Taiwan earthquakes of October 6, 2016 and the North Korean nuclear explosion as of September 3, 2017

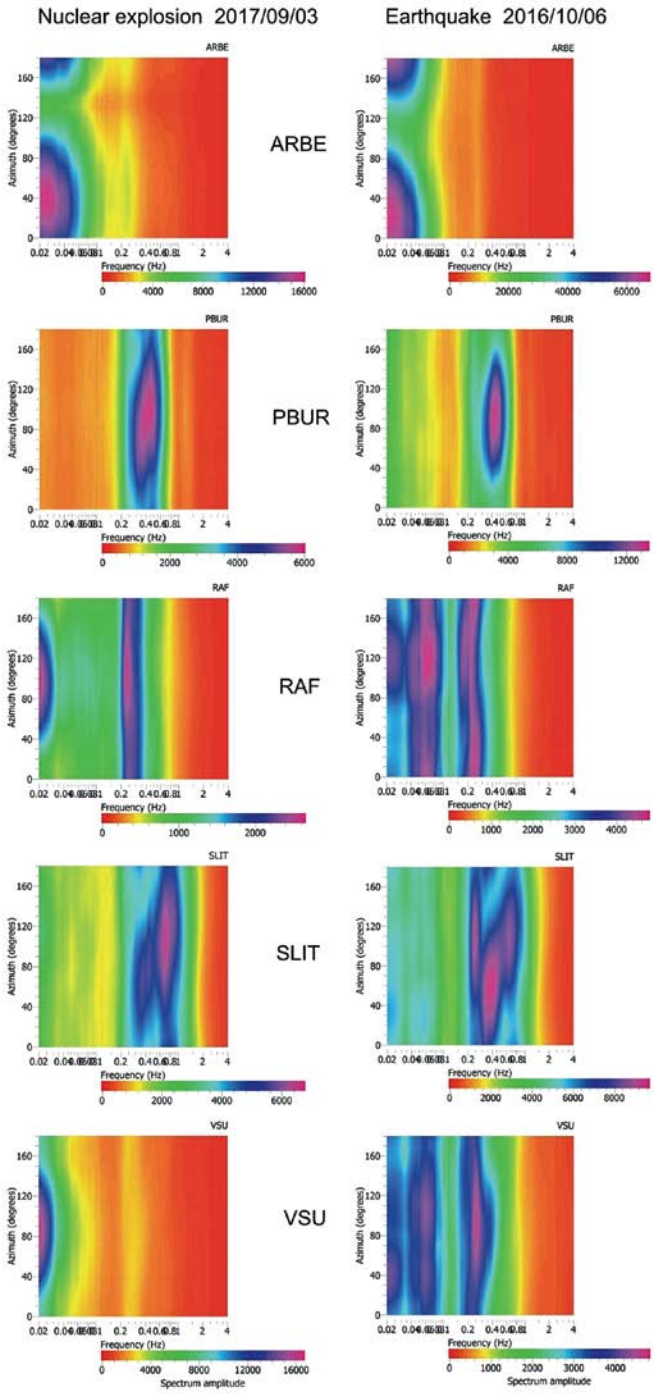

Figure 113. The results of spectrum rotate analysis with regard to the North Korean nuclear explosion as of September 3, 2017 and the Taiwan earthquake as of October 6, 2016

In particular, if we analyze the distribution of the maximum energy for all azimuthal directions, we can note some specific features. The maximum energy in the rotation spectrum of the earthquake recorded at the RAF station is distributed within two frequency ranges: $f_{\Delta 1}$ ~ 0.15–0.3 Hz and $f_{\Delta 2}$ ~ 0.4–0.8Hz, whereas, with respect to the explosion, is concentrated only within the bandwidth $f_{\Delta 1}$ ~ 0.2–0.35 Hz. The maximum energy within the earthquake-generated rotation spectrum recorded at the VSU station is also distributed within two frequency ranges $f_{\Delta 1}$ ~ 0.15–0.3 Hz and $f_{\Delta 2}$ ~ 0.4–0.8 Hz, whereas, with regard to the explosion, is absent within the specified frequency bands.

Thus, the specific feature of the maximum energy distribution within the rotation spectrum with respect to REF and VSU stations can be considered as a provisional indicator of nuclear explosion identification. At the same time however, some additional studies of the maximum energy parameter are necessary within the rotation spectrum – with regard to the earthquakes that took place in the region of Japan, Taiwan, and the East China.

Spectral analysis to determine the moment, source radius, and stress drop

The important potential discriminants for explosion identification can be the parameters of the focus of a regional seismic event – in particular, the earthquake moment (M_0), local magnitude *Ml,* and source parameters as follows: Ω (constant level), f_0 (spectral corner frequency) *s* (high-frequency spectral slope) [Allamehzadeh, 2003].

For a remote seismic event, the seismic source radius (R_S), stress drop (σ_{drop}) and moment magnitude (M_W) can also be considered as potential discriminants.

With regard to the explosion as of September 3, 2017 and the two earthquakes as of October 9, 2006 and April 14, 2016, a calculation of spectral parameters was made based on records by RAF and VSU stations.

The RAF station sits on a crystalline basement of Scandinavia, while the VSU station – on quaternary deposits (60 m) of the Southern slope of the Baltic Shield. The window (interval) length as from the P-wave onset (arrival) was 20 minutes. The results are presented in Table 16.

Table 16.

Spectral parameters of nuclear explosion and tectonic earthquakes

Station & components	RAF_Z	RAF_N	RAF_E	VSU_Z	VSU_N	VSU_E
Explosion 2017/09/03 03:30:01 M = 6.3						
M_0	18.14	17.96	18.04	18.49	18.58	18.69
ST	4.0	4.3	3.5	16.3	17.1	19.6
OM	3.9	3.7	3.8	4.3	4.3	4.5
f_0	0.219	0.258	0.227	0.267	0.253	0.244
R	11.5	9.8	11.1	9.4	9.9	10.3
M_W	6.043	5.920	5.969	6.274	6.335	6.406

Earthquake 2016/10/06 15:52:03 M = 5.8						
M_0	18.61	18.54	18.59	18.93	18.82	18.90
ST	19.8	16.7	15.9	39.3	30.2	43.3
OM	4.5	4.4	4.4	4.8	4.7	4.8
f_0	0.235	0.235	0.223	0.231	0.231	0.244
R	9.7	9.7	10.2	9.9	9.9	9.3
M_W	6.355	6.304	6.339	6.569	6.493	6.549
Earthquake 2016/04/14 15:06:22 M = 6.0						
M_0	18.95	18.86	18.89	19.33	19.32	19.31
ST	33.8	35.9	31.2	95.3	99.2	77.7
OM	4.7	4.6	4.6	5.1	5.0	5.0
f_0	0.239	0.262	0.244	0.253	0.258	0.239
R	10.5	9.6	10.3	9.9	9.8	10.5
M_W	6.580	6.518	6.541	6.832	6.828	6.821

*Notes: – log of moment, unit Newton*m; ST – stress drop in bars; OM – log spectral level (nm-sec); – corner frequency (Hz); R – source radius (km); – moment magnitude; RAF_Z, RAF_N, RAF_E – components of recording RAF seismic station; VSU_Z, VSU_N, VSU_E – components of recording VSU seismic station*

An example of the amplitude spectrum parameters for Z-component of the RAF station is shown in Figure 114. The earthquake and the explosion spectra are shown in conjunction with the spectra of the ambient seismic noise.

Some difference in the spectrum envelope shape can be discerned. For earthquakes, at the frequencies exceeding corner frequency , the spectrum is characterized by a smooth slope – up to the moment when a rise at the frequency 3.2 Hz begins. With regard to the explosion, a "sag" in the form of a spectrum envelope can be observed at the frequency 1.0 Hz. A rise of the envelope in the right part of the spectra is probably associated with high-frequency regional seismic noise.

The distance from the RAF station to the earthquake –2017/10/06 epicentre is by 20.6% greater, and to the earthquake – 2016/04/13 epicentre – by 13.2% greater than the distance to the epicentre of the explosion of 2016/09/03 (6910 km). The azimuthal alignment between the direction "station – explosion" and the directions "station – earthquakes epicentres" is narrow enough.

All of these facts entitle us to assume that the way length between the sources and the RAF station has a little impact on the envelope of spectrum; instead, the main impact is from the very source proper – i.e., the earthquake focus or the source of the explosion. The explosion source is located close to the surface; therefore, displacement amplitude attenuation for a definite part of the spectrum (between 1 and 10 Hz) is larger than the displacement amplitude attenuation of the same part of the spectrum generated by the earthquakes. The earthquake hypocentre depth is 10 and 14 km respectively, i.e., the

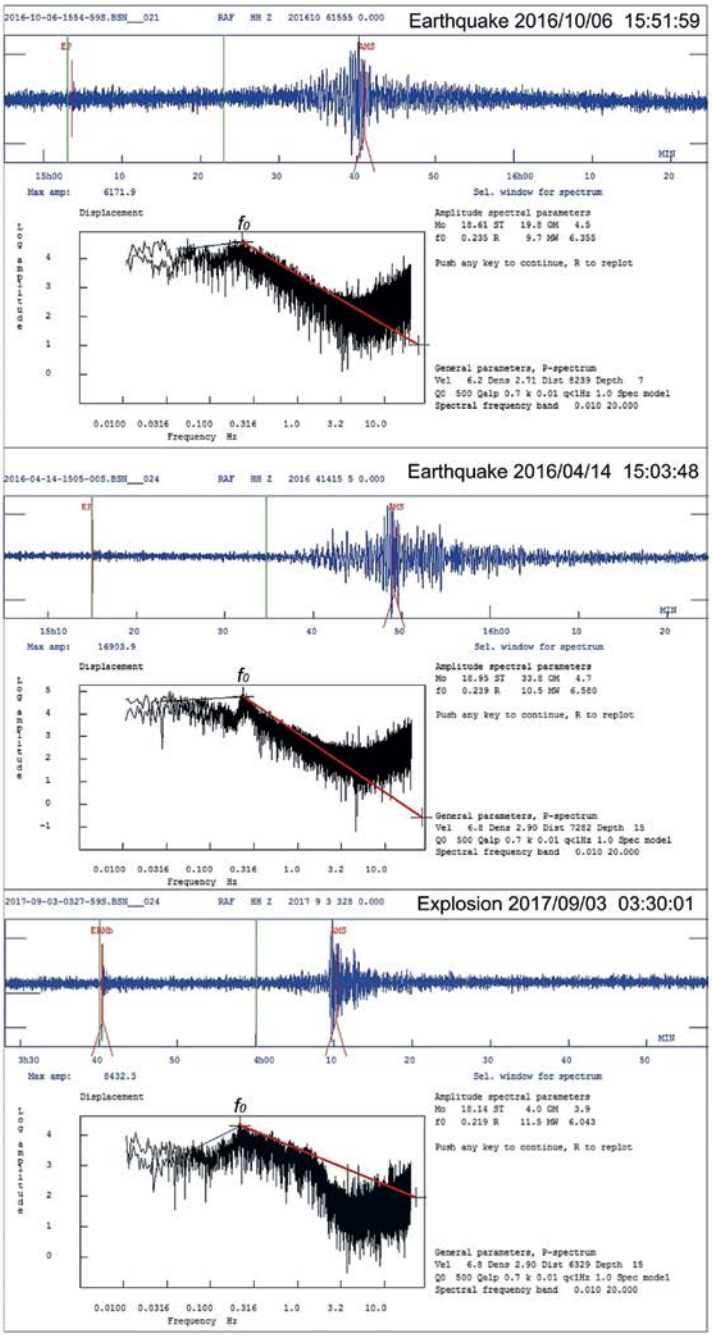

Figure 114. Amplitude spectra of the earthquakes as of April 14, 2016, October 6, 2016 and the explosion as of September 3, 2017 for Z-component of the RAF station

Legend: vertical red line on the right designates the moment of P-wave onset to the RAF station; the analyzed section is confined by green vertical lines on the seismogram; the red line on the spectrum shows the spectrum tilt;– corner frequency

earthquakes foci are located inside the Earth's crust. This means that, in the case of an explosion, the sedimentary cover can be regarded as a filter absorbing the energy of seismic vibrations of a definite frequency. It is exactly what is reflected in the amplitude spectrum of the explosion.

Thus, the spectrum envelope shape can be regarded as a certain promising symptom making it possible to discriminate between a remote explosion and a tectonic earthquake.

5. APPLICATION OF SEISMOLOGICAL METHODS IN CONDITIONS OF LOW SEISMICITY

Seismology as a section of geophysics is designed to study the causes of the formation, preparation and implementation of tectonic earthquakes and their consequences. The main directions of seismology are oriented to the study of physical and mechanical processes in the source of the earthquake, the generation and propagation of different types of seismic waves near the origin and in the far area. The seismic process is characterized by a combination of earthquakes in space and time. It is caused by dynamic rearrangements of the structure of the geological environment, the emergence of maxima of stress fields. Seismically active regions are characterized by increased velocity gradients of movements of the Earth's crust, rates of energy dissipation at various levels of the hierarchical series of heterogeneity [Садовский & Писаренко, 1991].

Supply of energy from outside into the system violates its energy strength. Reaching a certain *"energy strength"* of the mass, the system becomes unstable [Ризниченко & Артамонов, 1975]. Predicting its behaviour is difficult. Nevertheless, seismology should identify the causal and stochastic regularities of earthquake occurrence. Practical importance of seismology lies in the long-term identification of earthquake occurrence sites, the assessment of their strength and the period of recurrence.

In aseismic regions, the processes of dissipation and relaxation of accumulated energy are realized due to tectonic creep, friction of individual environmental blocks. Since any real geological environment consists of different-scale blocks, the fundamental property of the material world manifests itself in it, namely, the process of self-organization of the geophysical environment occurs, regardless of seismic activity of the region (seismically active regions or aseismic regions). This is expressed in the polymodality of distribution of the parts of matter of this medium according to size [Садовский & Писаренко, 1991]. In particular, the interrelation between the dimensions of its heterogeneity L, their energy saturation E and the characteristic time of the self-organization processes T is expressed by the following approximate relations:

$$L \sim \sqrt[3]{E} \tag{37}$$

$$T \sim \sqrt[3]{E} \tag{38}$$

The main classical tasks of seismological research are seismological monitoring and accumulation of statistical information on seismic manifestations, identification of tectonic earthquakes among different types of seismic processes, estimation of seismic

events, seismotectonic zoning, identification of seismic energy-generating structures and assessment of their parameters (seismically active tectonic disturbances, maximum possible magnitude of earthquakes, seismic activity, depth of earthquake foci), seismic zoning. At a more practical, applied level, seismic microzoning is carried out to solve engineering seismological problems.

Seismological methods have acquired a special significance in the age of scientific-technical and industrial revolution, transition from manual labour to machine labour, starting from the eighteenth century, the time of development of urbanization processes and the increase in manmade impact on the natural environment and ecology. The explanation is that many industrial facilities, functioning of energy complexes, construction of buildings and structures, transport traffic and "life" of agglomerations are connected with cyclic processes environmental impact. Cyclic processes are caused by operation of hydro turbines, turbines and generators of nuclear power plants, intensive traffic, operation of industrial units, mechanisms, implementation of construction activities (piling in the ground) in agglomerations. Cyclic processes promote the appearance in solid materials of a phenomenon called *fatigue* [Horii et al., 1992]. The phenomenon of material fatigue leads to the loss of its strength, damage [Karib & Hojatkashani, 2013] and even destruction.

Technogenic load on the environment has led to emergence of previously unknown processes: excited earthquakes and induced seismicity. This is especially characteristic of districts where water storages, dams are located [Carder, 1945; Simpson et al., 1988; Talwani, 1997; Gupta, 2002, etc.], of underground storages of hydrocarbons are created [Massonnat & Roland, 1997]. The induced seismicity can arise as a result of deep water injection in the oil industry, for hydraulic fracturing of seams, and also by pumping liquid wastes into deep wells for disposal [Hough & Morgan, 2015; Ellsworth, 2013].

As a result of people migration, its continuous dynamics, and trade development, the intensification of passenger and cargo traffic takes place. Human-induced load from industrial, power and transport facilities is accompanied by an increase in the intensity of human-induced seismic noise (tremor), vibration and their negative impact on the habitat, soils, buildings and structures. A phenomenon such as vibrational erosion of the Earth is revealed [Капустян, 2000], associated with the effect of weak signals on the rocks. For example, under influence of vibration from the Leningrad NPP, there was a change in the filtration capacity of the geological medium. As a result, areas that radiated (reemitted) the vibration in the medium were not subjected to water saturation.

In addition to traditional manmade sources, such as main transport routes, dams and artificial water storages, quarries, ore mines, coalmines where extraction of minerals is carried out by explosive method, there are also energy complexes with powerful electric machines that radiate into the ground a seismic energy from mechanical vibration in HPP, TPP, pumps in NPPs.

Technogenic seismic noise (tremor) mainly occupies the frequency range above 1 Hz. From the physical point of view, it is due to the generation from technogenic sources of mainly body waves and partially surface waves. Analysis of seismic noise power data [Brune & Oliver, 1959] in the 1950's made it possible to detect the existence of "quiet", "medium" and "noisy" areas on the Earth in terms of the seismic noise intensity. Studies

of seismic noise after 50 years demonstrated that the seismic noise in "noisy" places remained at the same level while where there were no obvious sources of interference, the power increased and approached the maximum level within the 1950s [Капустян, 2002_*t*]. Thus, the number of "quiet" places on the Earth has reduced significantly. It may be the result of the spread of the technological sphere throughout the planet and long-range propagation of seismic energy processed by the geological environment.

Investigation of the integral characteristics of ambient seismic noise and vibration, individual components of seismic noise, primarily shear S-waves, surface Rayleigh and Love waves, is becoming an effective tool for diagnostics of geological environment, testing for vulnerability of buildings and structures, embankments under railways and highways, dams and dikes. Seismological studies find application even in such areas of research as hydrology. For example, a study of seismic noise conducted along the riverbed made it possible to draw a conclusion about important role of transportation of the pebble along the riverbed and the effect on the processes of river bed erosion [Burtin et al., 2008].

Despite the low level of seismicity in the East Baltic Region, seismological studies can be used to solve such applied problems as vulnerability assessment of soils, buildings, and structures.

The method is gaining popularity of studying the horizontal to vertical spectra ratio (*HVSR*), also called the Nakamura method in honour of researcher who made the strongest contribution to the method development. A great advantage of the method is the possibility of using seismic noise to estimate the resonant frequencies of the upper part of the section, usually represented by Quaternary sediments. The subject of the study is ambient seismic noise, which allows one to apply the *HVSR* method in any territory, including aseismic regions.

Thus, the seismological method originally intended to solve the classical problems of seismology-earthquake monitoring, seismic hazard assessment and warning of earthquakes, is increasingly used in a number of applied problems. In this chapter we will discuss both traditional methods of seismology and nonstandard methods for solving applied problems in conditions of low seismicity.

5.1. Seismic zoning and microzoning

Seismic zoning (SZ) is a direction seismological studies, the purpose of which is to divide the territory into regions with varying degrees of intensity of the expected earthquakes. SZ uses data on historical earthquakes, instrumental observations of tectonic earthquakes, geological, tectonic and geophysical maps, as well as data on movements of the Earth's crust (neotectonic and modern movements).

Outcomes of seismic zoning serve as a basis for more detailed studies of seismic hazard, namely for detailed seismic zoning (DSZ) and seismic microzoning (SMZ), aimed to refine the parameters of seismic impacts on sites for the construction of buildings, structures, as well as the existing facilities, if necessary.

SMZ is the final part of the entire complex of seismological studies and has practical, applied significance. But before directly carrying out SMZ, it is necessary to have a basis,

i.e. to obtain parameters of seismic actions for ground conditions identified with the bedrocks. According to recommendations of *Eurocode-8*, the seismic effect is expressed in the value of the reference peak ground acceleration a_{gR} on soil of type A. Soils of type A include hard rocks or hard rock-like geological formations, also a weaker subsurface layer not thicker than 5 m. For type A soil, the shear wave velocity $v_{S,30} > 800$ м/с [Eurocode 8, 2005]. a_{gR} is chosen for each seismic source (SSZ) corresponds to a certain return period T_{NCR}. Parameter a_{gR} is taken from the SSZ map.

Thus, before proceeding with SMZ, it is first necessary to perform a general seismic hazard assessment and obtain the parameter a_{gR}. Therefore, we start with consideration of issues related to the conduct of studies on general seismic zoning (GSZ). In this context, the main principles of GSZ will be given, as well as examples of studies in the East Baltic Region.

5.1.1. Main provisions of general seismic zoning

General seismic zoning (GSZ) precedes the performance of SMR for individual sites. Therefore, the scope of the study at GSZ and SMZ is different. For large territories, throughout the country and big regions, scales 1:2500000, 1:1000000 are used. In some cases, when SMZ is carried out for highly responsible facilities, such as nuclear power plants, hydroelectric power stations, transport structures (bridges, tunnels, gas and oil pipelines, offshore platforms for extraction of hydrocarbons, hazardous chemical production facilities, facilities of military-industrial complex), it may be preceded by a detailed seismic zoning – DSZ. Its difference from GSZ is that, for example, the features of focal zones of earthquakes that can affect the seismic vibrations are studied in more detail in case of DSZ. The most characteristic scale of DSZ is 1:1500000.

The main tasks of the GSZ and DSZ are to assess the seismic hazard or seismic risk in a given territory. Seismic hazard is a natural phenomenon, such as a shaking caused by an earthquake. Seismic hazard is the probability that an earthquake will occur in a given area, during a certain time window, with the intensity of the Earth's surface movement exceeding the given threshold.

Seismic hazard analysis should distinguish between two important methods: deterministic seismic hazard analysis (DSHA) and probabilistic seismic hazard analysis (PSHA) for assessment of the seismic risk.

Regardless of the method of seismic hazard analysis, a set of some universal data is used, which need to be characterized. These data include the catalogue of earthquakes, seismic source zone (SSZ), which are distinguished on the basis of seismotectonic map analysis, the unification of earthquake magnitudes, the seismic intensity damping law and other parameters.

To distinguish SSZ, seismotectonic provinces and individual active tectonic faults, the seismotectonic zoning is carried out, which involves the preparation of a model of regionalization of seismic sources, i.e. identification of *earthquake source*. Seismotectonic zoning is based on a complex of available geological, geophysical, tectonic, geodetic and seismological data.

The seismotectonic zoning maps can show the epicentres of historical and modern earthquakes, velocities of neotectonic and modern movements of the Earth's crust characterizing the intensity of tectonic movements, geophysical parameters characterizing the potential energy (geothermal anomalies, anomalies of the gravitational and magnetic fields), velocity of seismic waves in the Earth's crust, geological parameters (thickness of the Earth's crust, depth of crystalline basement etc.) – in a word, a complex is used of geological and geophysical, tectonic and seismic parameters that are appropriate for characterization of seismic potential.

An important part of studies on seismic zoning is the unification (homogenization) of earthquake magnitudes. As a rule, earthquake catalogues contain earthquakes with different types of magnitudes. For historical earthquakes, only the tremor intensity is usually known. It can also be expressed in different macroseismic scales. Therefore, bringing different magnitude scales to the "common denominator" needs the homogenization of magnitudes.

Seismicity is the main but not the only criterion for seismogenic zones to be distinguished. In areas with a low level of seismicity, such as the East Baltic Region, geological and geophysical parameters play a key role.

In the territory of the East European Platform, studies were conducted to find the correlation between various geological and geophysical parameters with seismicity for differentiating the seismically quiet territory of the ancient platform according to the degree of its modern geodynamic activity [Юдахин и др., 2003]. In this case, seismicity was considered as the main, classifying attribute of geodynamic activity. In particular, the following geological and geophysical parameters were considered: 1) magnetic field anomalies $(\Delta T)_a$; 2) height of topographical terrain (H_{ter}); 3) terrain of Mohorovicic surface (H_M); 4) dismemberment of the Earth's crust (H_{dismem}); 5) density differentiation of mantle and crustal blocks (ρ_{mcd}); 6) deep anomalies of gravity (Δg_{deep}); 7) characteristic of geological and geophysical formations by petrographic density (ρ_{ptg}); 8) mixed derivative of geodetic potential (latitudinal gradient from derivative of geodetic potential with respect to longitude) ($T_{\varphi\lambda}$); 9) anomalies of vertical gradient of gravitation's force (T_{rr}); 10) anomalies of heat flow (Q); 11) geothermal gradient ($gradQ$); 12) velocity gradient of vertical recent movements ($gradN_a$); 13) boundary velocity of longitudinal seismic waves on Moho surface (V_r); 14) seismic activity ($A10$).

Within the framework of these studies [Юдахин и др., 2003], as targets (reference elements) of the study there were selected the sources of weak earthquakes with a magnitude $M \geq 3.0$ for the East European Platform. The obtained results were considered as a complex geological and geophysical basis for the tasks of seismic zoning of seismically quiet territories. Table 17 shows the average values of geological and geophysical parameters for the Belarusian-Baltic Region in comparison with the Kola-Karelian Region, as well as the correlation coefficients of geological and geophysical parameters with the classification characteristic – seismicity for the East European Platform in comparison with the regions of Crimea-Caucasus-Kopet Dagh and Central Asia. For seismically active regions, the classification criterion was earthquakes with magnitude $M \geq 6.0$.

High information content of geological and geophysical features in conditions of low seismicity of the East European Platform belongs to the geothermal gradient

Table 17.

Correlation ratios of geological and geophysical parameters with classification criterion – seismicity and average values for EEP

Parameter	Average values for the Belarusian-Baltic region	Mean values for the Kola-Karelian region	Eastern European Platform	Crimea-Caucasus-Kopet Dag	Central Asia
$(\Delta T)_a$	0.3	0.15	0.07	–0.11	–0.06
grad Q	25	11	0.86	0.52	0.68
Q	1.1	0.9	–0.80	0.52	0.85
H_M	40	35	0.43	0.19	0.53
H_{dismem}	2	2	–0.73	0.22	0.32
ρ_{mcd}	0.5	0.5	0.51	0.28	–0.89
Δg_{deep}	-	-	–0.48	0.46	0.33
ρ_{ptg}	2.4	2.7	0.73	–0.30	0.01
$T_{\varphi\lambda}$	–0.06	–0.16	–0.12	0.23	–0.08
T_{rr}	–0.40	–0.30	0.77	–0.08	–0.79
H_{ter}	0.10	0.10	0.42	0.22	0.66
grad N_a	0.05	0.04	0.22	0.72	0.58
$A10$	0	2	0.11	0.62	0.47
V_r	8.1	8.1	–0.28	–0.21	–0.44

grad Q, heat flow Q, anomalies of vertical gradient of gravity pull T_{rr}, dismemberment of the Earth's crust H_{dismem} and characterization of geological-geophysical formations by petrographic density ρ_{ptg}. Range of correlation ratios: – 0.80 to + 0.86.

For seismically active regions of Central Asia, the highest informativity was noted for the density differentiation of mantle and crustal blocks ρ_{mcd}, heat flow Q, anomalies of vertical gradient of gravity pull T_{rr}, geothermal gradient *grad Q*, height of topographical terrain H_{ter}. For seismically active region Crimea-Caucasus-Kopet Dag, the higher informativity was noted for the velocity gradient of vertical recent movements *grad* N_a and seismic activity $A10$. Seismic activity $A10$ features the seismicity level for earthquakes of class $K_0 = 10$, т.е. earthquakes with seismic energy $E = 10^{10}$ Joules. Such seismic energy approximately corresponds to the seismic effect that arose from explosion of atomic bomb dropped on Hiroshima [Riznichenko, 1985].

Applicability of these promising geological and geophysical features in studies assessing the seismic hazard of a particular region depends on the exploration maturity of this region, information available in necessary scope, level of seismicity. For example, the parameter of seismic activity $A10$ is difficult to be applied in the East Baltic Region since there are very few earthquakes with such energy. Information on the depth of occurrence of the Moho discontinuity is limited to data obtained only by two profiles of the DSS. For EBR, information is available on the heat flow, but the small scale of

the heat flow charts (1:5 000 000) does not allow to confidently use this geological and geophysical feature for GSZ.

At the same time, such parameters as the dismemberment of the Earth's crust and anomalies of vertical gradient of gravity pull can be available in EER for use as promising geological and geophysical features. New geological-geophysical and seismological methods in the future can provide valuable information from the standpoint of revealing new classification features of seismicity in seismically quiet territory.

In practice of seismic hazard research, two main seismic hazard assessment methods are used: DSHA (Deterministic Seismic Hazard Analysis) and PSHA (Probabilistic Seismic Hazard Analysis).

5.1.2. Deterministic analysis of seismic hazard

Deterministic method *DSHA* (Figure 115) is usually applied for selection of the most unfavourable cases where the maximum values of seismic parameters are considered: maximum magnitude, minimum depth of the earthquake origin, lowest epicentral distance etc. It is advisable to perform the deterministic parameter estimates for two cases of earthquakes: 1) maximum possible magnitude from the main seismogenic zones at minimum distance from centre of the source to the investigated site and 2) earthquakes of diffuse background seismicity, directly under the investigated site [Алешин, 2010].

Deterministic assessments of epicentral intensity I and the maximum acceleration A_{max} should be close to the ultimate, probabilistic assessments of those parameters with respect to large return periods, for instance, T = 10 000 years.

The first step to be taken in the DSHA procedure is the identification of seismogenic structures, active tectonic faults, or individual parts of a fault that can act as earthquake sources. Are allocated also seismotectonic provinces, i.e. regions where seismic hazard can exist but no active tectonic faults or seismogenic structures have been identified, are also highlighted.

The next step is the determination of the maximum possible earthquake (MPE), the maximum credible earthquake (MCE) and the maximum historic earthquake (MHE).

For the most part, they are based on empirical correlations between the magnitudes of earthquake and sizes of tectonic faults and between motion parameters (vertical or horizontal displacements) and magnitudes. For the assessment of the maximum possible earthquake (MPE), various methods can be applied. For example, the correlation between magnitudes and vertical displacements, or, between the fault length and vertical displacements has been obtained [Стром, Никонов, 1999] with respect to $M > 5$ magnitude earthquakes and the tectonic fault length $L > 1$ km (Figure 116].

The next stage is the assessment of the ground motion (amplitude) intensity attenuation law subject depending on magnitude. In general, the expression for amplitude attenuation can be presented in the form, as follows:

$$A(f,t) = A_0 e^{-\pi f k} e^{\frac{-\pi f t}{Q(f)}} \tag{37}$$

where – A_0 – initial amplitude; $A(t)$ – the amplitude of wave after crossing the way over a time; f – frequency (Hz); $Q(f)$ – frequency dependent factor, or seismic quality factor.

1. Sources ➔	2. Controlling earthquake ➔
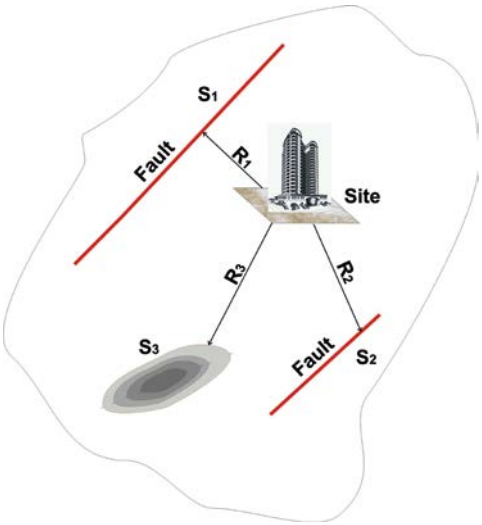	Fixed distance R Fixed magnitude M
3. Ground motion ➔	4. Hazard at site
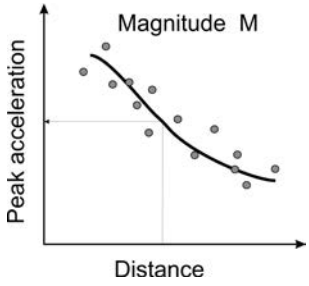	The danger of an earthquake in this site is characterized by a peak value of the ground acceleration PGA = 0.15g, which is caused by an earthquake with a magnitude M = 5.4 on a tectonic fault remote from the site under study at a distance R_1 = 5 km.

Figure 115. Sequence of DSHA steps to be carried out

Legend: S_1, S_2, S_3 – seismic sources; R_1, R_2, R_3 – epicentre distances

The following two factors impact the ground motion intensity attenuation: 1) (geometric) scattering and 2) anelastic attenuation. Geometric scattering occurs due to energy re-distribution in process of the energy dissipation. Absorption takes place due to heat loss or the so-called seismic absorption or intrinsic Q. $Q(f)$ is inversely proportional to attenuation, and it quantifies the impact from inelastic attenuation on seismic wavelet). Wavelet is a mathematical function which makes it possible to analyze various frequency components of data. Geometric scattering $G(\Delta, h)$ depends on the wave type, epicenter distance, and hypocenter depth. Generally, it may be presented as:

$$G(\Delta, h) = r^{-\beta} \tag{38}$$

where $r = \sqrt{(\Delta^2 + h^2)}$ – hypocentre distance; β – the constant.

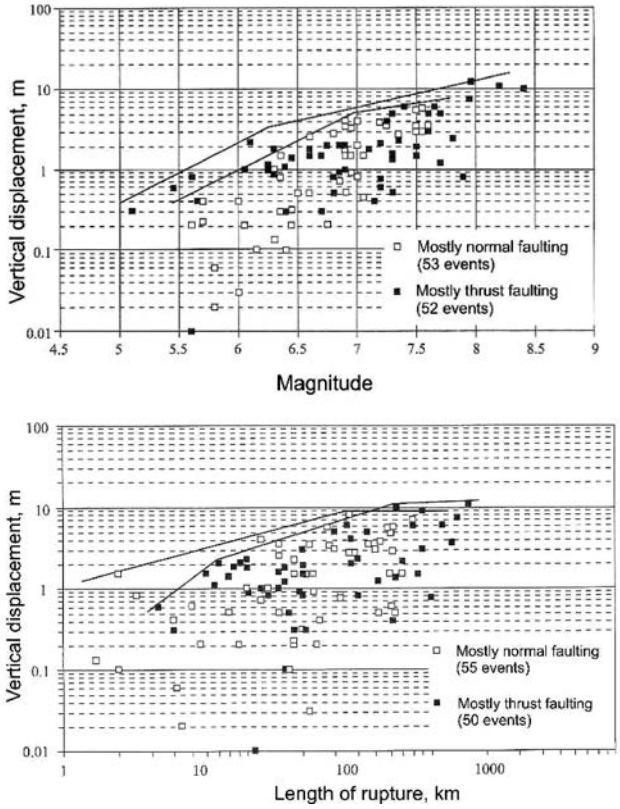

Figure 116. Ultimate values of the maximum vertical displacements, which depend from magnitude (left) and surface fault length (right) [Стром, Никонов, 1999]

Constant β for body P-wave and for shear S-wave, within the near-field zone, can be set to1. With respect to surface waves and large distances, $\beta = 0.5$. The most typical values are: $k = 0.05$ and $Q(f) = Q_0 f^a = 100 f^{0,8}$.

The above-stated set of the main parameters is necessary to carry out the deterministic seismic hazard analysis.

5.1.3. The probabilistic seismic hazard analysis

The purpose of PSHA is a quantitative estimation, or, the assessment of the probability of exceeding various levels of ground motion in the study area, by taking into account all possible earthquakes from the corresponding source areas. The PSHA procedure for natural seismicity was proposed by Cornell [Cornell, 1968] and was later developed by McGuire [McGuire, 2004]. Subsequently, a more comprehensive and detailed definition of PSHA was given in the special recommendations from the Senior Seismic Hazard Analysis Committee [SSHAC].

One of the important PSHA parameters is the assessment of the annual norm λ, which characterizes a certain intensity measure of the ground motion, exceeding the preset amplitude x on the given territory:

$$\lambda(IM > x) = \sum_{i=1}^{n_{sources}} \lambda(M_i > m_{min}) \times \int_{m_{min}}^{m_{max}} \int_0^{r_{max}} P(IM > x|m,r) f_{M_i,R_i}(m,r) dr dm \quad (39)$$

where, $n_{sources}$ – the number of earthquake sources considered; M_i and R_i – the magnitude and the source distance.

The expression $f_{Mi,Ri}(m, r)$ is the probability-density function for the magnitude and the source distance i; $\lambda(M_i > m_{min})$ – the annual norm of earthquake occurrence in the source i with the magnitude higher than m_{min}, i.e., with the minimal magnitude of interest. The members of the equation (39) $\lambda(M_i > m_{min})$ and $f_{M_i,R_i}(m, r)$ reflect part of the source characteristics in calculating. The probability that m- magnitude earthquake can cause ground motion with intensity higher than x, $P(IM > x|m, r)$ at a distance r, is part of the characteristic in the analysis of the danger of ground motion. The PSHA method is applied if some alternative versions of the assessment of the main parameters specifying seismic hazard are available. Those are: maps of the areas of earthquake origins (SSZ), seismic energy attenuation models, and the laws of distribution of magnitudes or maximal vibration intensity.

The *PSHA* procedures allow one to take uncertainty into account, if the main initial parameters are not known precisely – i.e., the earthquake source mechanism, the dimensions and spatial position of SSZ, the return period of strong earthquakes, and soil behavior at strong earthquakes. With *PSHA*, the degree of credibility of quantitative estimation of seismic hazard is assessed. Despite the existing various methods for *PSHA* analysis, a certain set of probabilistic computations is available for assessing the degree of uncertainty in earthquake focus positions, the repeatability and the intensity of seismic impacts. Normally, seismic hazard (exceedance curves) are plotted, where the average annual repeatability of exceeding the threshold value of the ground motion selected parameter is seen. Based on that, the probability of exceeding a preset selected parameter of ground motion is calculated. Uncertainties inherent in seismic hazard models and parameters are included into hazard analysis by using logic trees.

The flowchart of *PSHA* analysis may be presented, as follows (Fig 117):

Similar to DSHA, the PSHA process implies the specification of seismic source positions; the magnitudes in the parametric earthquake catalogue are set up to a unique standardized value, like for instance, to moment magnitude M_w. In process of practical PSHA operation, it seems expedient to divide the objective and the subjective factors when assessing the seismic hazard. The objective factors are associated with randomness of a seismic process – like the formation of a tectonic fault and seismic wave propagation. Subjective (human) factors are associated with lack of knowledge on the seismicity of a specific region. Such an uncertainty makes one consider several models of seismic setting. This problem is solved with the aid of using logic-tree method. The logic-tree method was first proposed in 1985 [Youngs, Coppersmith, 1985] to take into account the objectivity and the subjectivity of seismic process knowledge.

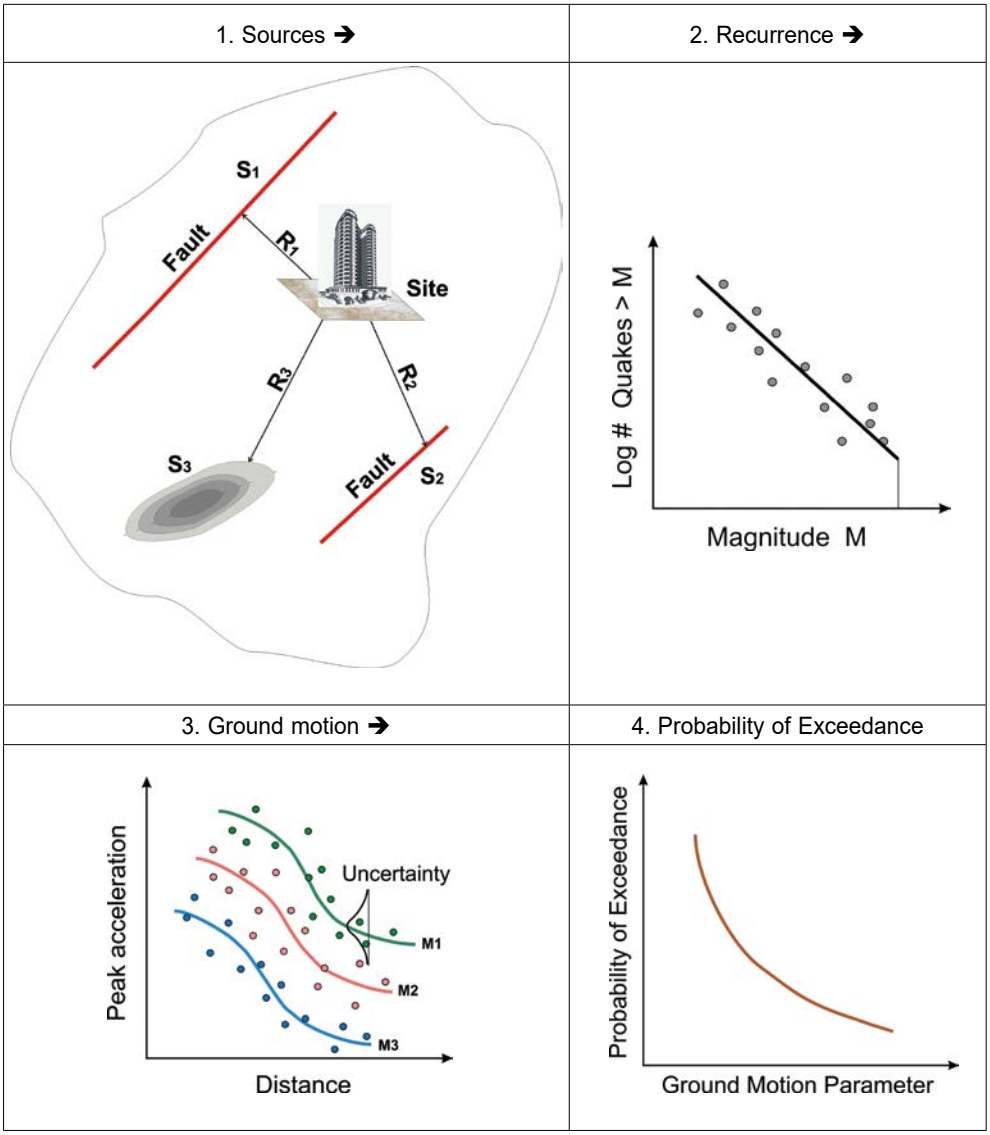

Figure 117. The PSHA work flow

Legend: S_1, S_2, S_3 – seismic sources; R_1, R_2, R_3 – epicentral distances

Logic "tree" is a graphic presentation of cause-effect relationship, with the "tree" consisting of logical entities connected by arrows, based on logical necessity and logical sufficiency. The logical entities are assigned weight factors, which should be understood as a relative probability of the correct selection.

A logical tree consists of branches converging to nodes. The sum of the weights of all the elements of the branches stemming from one node is equal to unity. A typical logical tree for taking several models into account may consist of 5 levels (nodes).

The first level is Catalog M uncertainty models. The second level is Catalog-completeness models. The third level is mb (Lg) to M conversion uncertainty models. The fourth level is Maximum magnitude (M_{max}) models. The fifth level is Ground motion models.

An example of a logic tree is shown in Figure 118.

The result outputs of PSHA are the estimates of *Peak Ground Acceleration* (PGA) of the ground motion within a definite *T* period, or, the assessment of response spectra based on acceleration (SA). Those estimates simulate the unidirectional oscillatory system's response to the external seismic impact.

Probabilistic analysis is normally carried out with respect to the mean type of grounds. According to *Eurocode 8* recommendations [Eurocode 8, 2005] accepted in EU countries as a reference document, 7 types of soil conditions have been specified (A, B, C, D, E, S_1, S_2). The main characteristics of soils for evaluating the spectral response are the velocities of flexural, shear waves $v_{S,30}$ (m/s), the standard penetration test value N_{SPT} (blow/30cm) and the shear strength c_u (kPa). One of the main characteristics of a section is the shear wave velocity $v_{S,30}$. Seismic wave velocities can be determined based on various seismic methods, in particular, based on the Seismic reflection method and the Seismic refraction method for shallow depths of at least 30 m. The soil type can be determined by using the Standard Penetration Test method *(SPT).* The difference between *DSHA* and *PSHA* can by illustrated by an example of the description of seismic hazard.

If seismic hazard is determined by using *DSHA* method, the following assessment can be given: "*The earthquake danger on the site under study is characterized by peak ground acceleration PGA = 0.25g induced by a 6.0 magnitude- earthquake on the tectonic fault lying at a distance of 15 km from the site*".

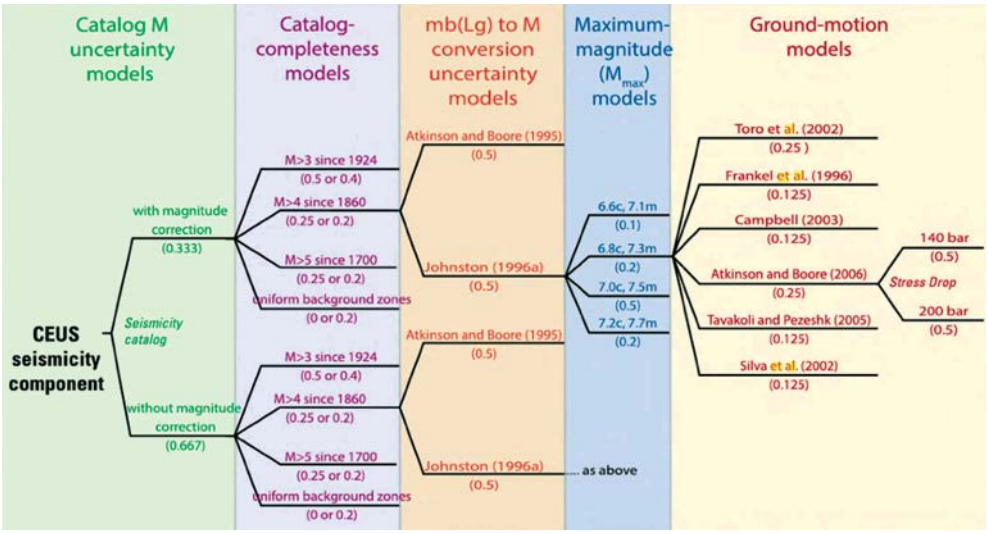

Figure 118. Logic tree for seismicity-derived hazard component in the central and eastern United States (CEUS) [Petersen et al., 2012]

If seismic hazard is determined by using *PSHA* method, the estimate may be formulated, as follows: "*The earthquake danger on the site under study is characterized by peak ground acceleration PGA = 0.25g with the 2% probability of exceedance of that value within a 50-year period*".

When carrying out seismic zoning investigations, two different kinds of analysis can be used, namely, the analysis of seismic hazard and that of seismic risk.

Seismic hazard characterizes potentially dangerous natural phenomena, associated with an earthquake. This is directly the earthquake-induced shocks affecting soil, buildings, and structures, the phenomenon of the Earth's surface rupture along the tectonic fault, water-saturated soil liquefaction due to a weakening of bonds between soil particles (sands, ooze), etc. Seismic risk assesses the probability of occurrence of damage associated with seismic hazard. The damage is associated with human losses, social implications, and economic consequences.

5.1.4. Review of seismic zoning results in the East Baltic Region

This section examines the results of seismic zoning for the entire East-Baltic region, or its individual parts. These assessments are based on international global, regional or national projects since the 1990s.

5.1.4.1. Seismic zoning of Belarus and the Baltic States

For the first time ever, a seismic zoning project for the East Baltic Region was implemented by Institute of Geophysics and Geochemistry under the Academy of Sciences of Belarus. In 1995, seismic hazard assessment with respect to Belarus and the Baltic States was carried out according to the All-Union program 0.74.03 [Гарецкий & Боборыкин, 1989]. The seismic zoning map for Belarus and the Baltic States is shown in Figure 119.

Within the framework of preliminary investigations, a seismotectonic map was prepared, which enabled one to assess the seismotectonic potential of the respective source zones: the Osmussaare, the West Estonian, the two Central Estonian, the Narva, the Kurzeme, the Riga, the East Latvian, the Daugavpils, the Kaliningrad – Lithuanian, the Vilnius, and the Oshmyany Zones [Айзберг и др., 1997].

The parameters of source zones of the East Baltic region are shown in Table 18.

To a certain extent, the research findings have confirmed the accuracy of some estimates for the Kaliningrad – Lithuanian seismogenic area (KLSA) [Safronov et al., 2005]. In particular, the epicenter of the first Kaliningrad earthquake in September 21, 2004 (11.05 UTC) is associated with the first KLSA zonule that had been highlighted within the framework of the seismic zoning project for Belarus and the Baltic States.

5.1.4.2. Seismic zoning of Latvia – 1998

In 1998, Geological Survey of Latvia acting jointly with the seismology department of the Crimea branch of Subbotin Institute of Geophysics under the National Academy of Sciences of the Ukraine, had implemented the project of seismic zoning of Latvia

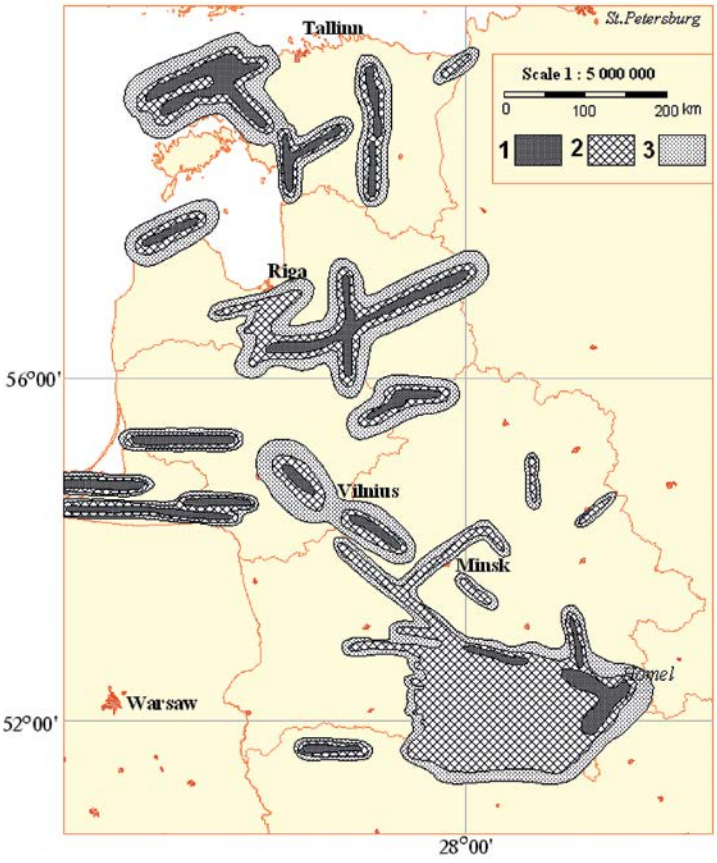

Figure 119. Seismic source zone according to seismic zoning studies for Belarus and the Baltic States [Айзберг и др., 1997]

Denotation of intensity degree of tremors: 1 – VII; 2 – VI; 3 – V

Table 18.

Parameters of seismic source zones of the East Baltic Region according to seismic zoning results for Belarus and the Baltic States [Айзберг и др., 1997]

N	Names of seismic source zones	Subzones	M_{max}	H, км	I_0	Note
1	Osmussaar		4.7	10.0	VI	
2	Western-Estonian		4.5	5.0	VI	
3	Central-Estonian	Northern	4.0	5.0	VI	
4	Central-Estonian	South	4.0	5.0	VI	
5	Narva		3.5	5.0	V	
6	Kurzeme		4.5	8.0	VI	

7	Riga	7.1	3.5	5.0		Consists of 3 subzones
		7.2	3.5	5.0		
		7.3	4.5	10.0		
8	East-Latvian		4.5	8.0		
9	Daugavpils		4.5	8.0	VI	
10	Kaliningrad-Lithuanian	Northern	4.0	5.0		Consists of 3 subzones
		Central	4.0	5.0		
		South	4.0	5.0		
11	Vilnius		4.9	10.0		
12	Oshmyany		4.5	5.0		

[Safronovs & Ņikuļins, 1999]. As a methodological foundation, the deterministic method (DSHA) was used.

As a preliminary stage of the project, a seismotectonic map of Latvia based on geological, geophysical, and seismological data was plotted. In particular, the tectonic and the geological map of Latvia was used as well as the tectonic and the neo-tectonic map of the Baltic Region and some other map documents that didn't have any reliable topographic snapping. This was associated with some peculiar features of the time (i.e., the time before 1991) – specifically, by information protection for security considerations.

The earthquake catalogue covered the territory by far larger than the territory of Latvia: φ = 51°N – 60°N and λ = 18°E – 34°E. This was explained by the fact that the seismogenic areas did not have any "national frontiers" and could be located on the adjacent territories. 189 earthquakes were detected inside the above-stated Baltic Region. The assessments of the maximum possible earthquake magnitudes have shown that maximum magnitudes may reach 5.1–5.4 [Nikulins, 1998]. The basis for assessing seismic hazard was the map of seismic sources' zones (Figure 120).

One of the specific features of the project was the usage of the Earth's crust seismotectonic potential assessment results.

Seismotectonic potential depended on Earth's crust classification, which was developed based on a number of geologic and geophysical features – such as heat flow, crustal thickness, terrain height, and the depth of the consolidated basement. The authors of the idea [Reisner et al., 1986] believe that the above-enumerated parameters characterize the current state and the structure of the Earth's crust, directly associated with seismic process. Seismotectonic potential is indirectly related to the maximum possible earthquake magnitude M_{max} that can be realized in the specific cell of the Earth's crust pertaining to a definite tectonic type.

An analysis of the Earth's crust classification was carried out with respect to neo-tectonic activity areas of Europe and Central Asia, and partly of platform territories. High detail level of the Earth's crust classification was achieved due to smoothing of the data describing the above-stated parameters – within the limits of elementary cells of the size 20' × 30'.

Therefore, if a cell of the Earth's crust on the territory under study (the East Baltic Region) was characterized by a set of parameters close to those of the Earth crust's cell located in the regions with a known earthquake magnitude, then the cell under study was assigned a corresponding seismotectonic potential expressed in magnitude units. If two maximum magnitude values were known for a specific cell of the Earth's crust (the real earthquake magnitude and the magnitude specified based on the classification of the Earth's crust – the cell was assigned the highest of the two magnitude values in question.

The main outcome of the project was the map of general seismic zoning of Latvia on a scale 1:1000000. As a result of the research conducted, 17 seismic zones were singled out, which consist of three different types: the confident, the potential, and the seismotectonic zones (Table 19).

Confident seismic zones (CSZ) are the ones whose abnormality is confirmed by a set of geologic, geophysical, and seismological features. In this zone, the sources of earthquakes have already appeared and can appear in the future.

Potential seismic zones (PSZ) are the zones dated as active disjunctive dislocations, which are defined on the basis of a complex of geologic-geophysical signs. Near these active dislocations one or several earthquakes are located, which could be recorded by instrumental method.

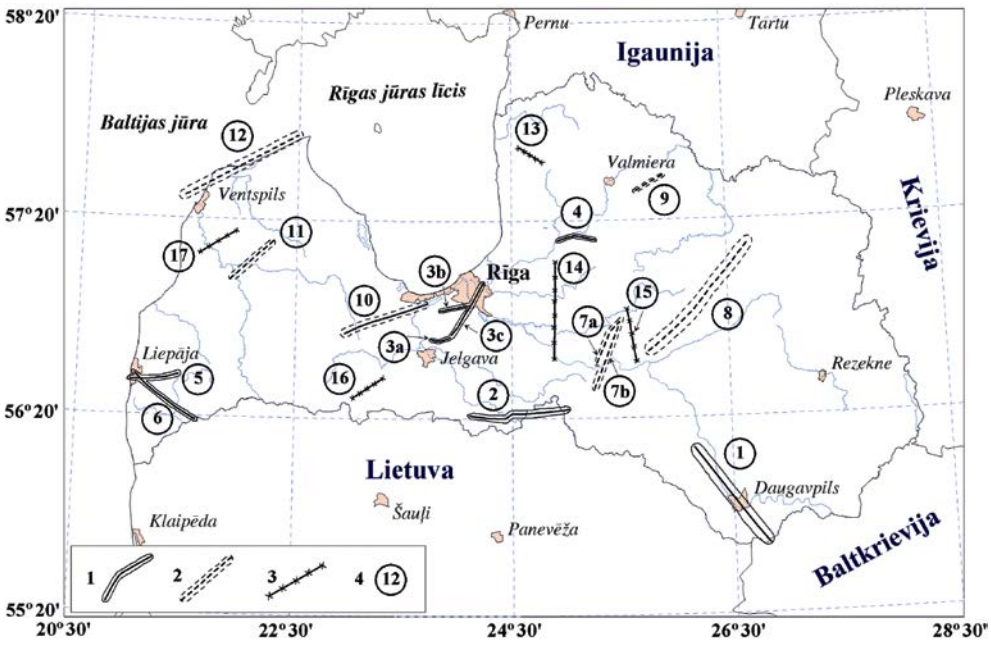

Figure 120. Map of seismogenic zones of Latvia [Ņikuļins, 2007_t]

Legend: 1 – confident seismic zones (CSZ); 2 – potential seismic zones (PSZ); 3 – seismotectonic zones (STZ); 4 – seismogenic zone numbers

Table 19.

Parameters of seismic sources zones and seismic shaking areas
[Safronov & Nikulin, 1999]

N	Name of seismic sources zones	Type of area	M_{max}	H_{min}, km	I_0	Area of epicentral intensity (km²)	
						S_6	S_7
1	Daugavpils	SSA	4.7	10	VII	1600	570
2	Bauska	SSA	4.1	5	VII	900	270
3	Jelgava	SSA	3.5	5	VI	~ 30	-
	Pārdaugava	SSA	3.6	5	VI	~ 20	-
	Riga region	SSA	4.1	7.5	VI	~ 160	-
4	Sigulda region	SSA	4.0	5	VI	50	-
5	Liepāja – Saldus region	SSA	3.9	7	VI	120	-
6	North-Western Žemaitijas	SSA	3.7	6	VI	150	-
7	Aizkraukle – 1	PSA	4.5	10	VI	780	-
	Aizkraukle – 2	PSA	4.5	10	VI		
8	Gulbene	PSA	4.8	13	VI	1700	-
9	Valmiera	PSA	3.6	5	VI	20	-
10	Sloka	PSA	4.2	8	VI	430	-
11	Usmas	PSA	4.1	8	VI	120	-
12	Irbe – Pērnavas	PSA	4.5	10	VI	990	-
13	Svētupe	STA	3.5	5	VI	50	-
14	The West Baltic	STA	4.5	11	VI	490	-
15	The East Baltic	STA	4.0	7.5	VI	~ 120	-
16	Dobele	STA	3.8	6	VI	100	-
17	Piltene	STA	3.9	7	≤ VI	~ 9	-

Seismotectonic zones (STA) are passive tectonic disjunctive dislocation. Near these dislocations, earthquake sources are located, which maybe are genetically associated with them.

The map of seismic sources zones was based on assessing the intensity of concussions, using the equation of macroseismic field [Шебалин, 1975] with world average constants.

$$I = 1.5M - 3.5lgR + 3.0 \qquad (40)$$

where I – the intensity of concussions (MSK-64 macroseismic scale); M – magnitude; $R = \sqrt{(D^2 + H^2)}$; R – hipocentral distance (km); D – epicentral distance (km); H – earthquake focal depth (km).

As a result, for a map of intensity of concussions was obtained intensity of concussions in grades of the MSK-64 scale (Figure 121).

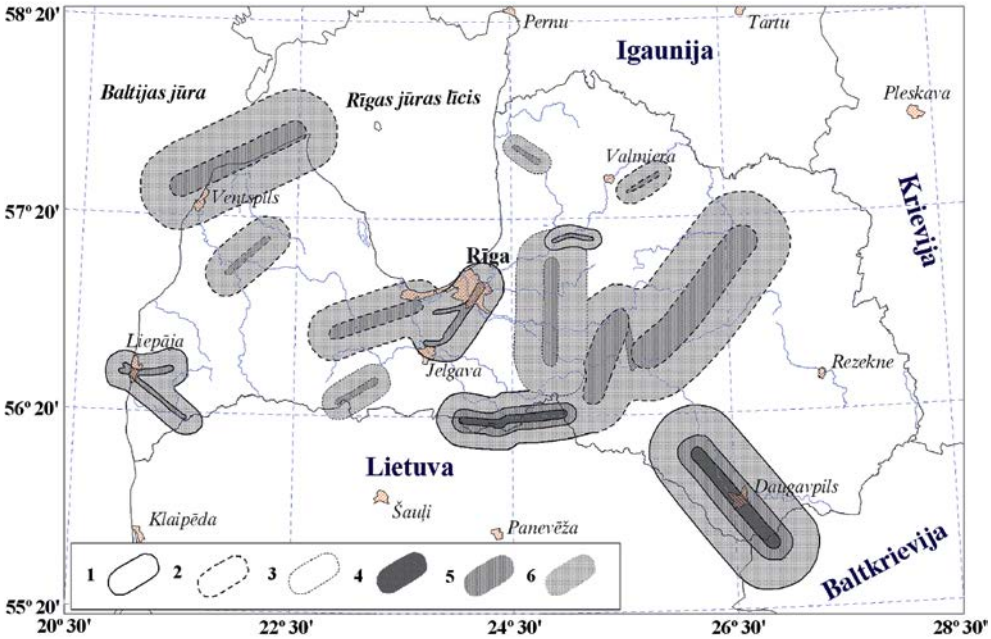

Figure 121. Map of general seismic zoning of Latvia (LVSR-98) [Ņikuļins, 2007_t]

Legend: 1 – confident seismic zones borders; 2 – potential seismic zones borders; 3 – borders of possible seismotectonic zones ; 4 – seismic intensity VII grade of MSK-64 scale; 5 – seismic intensity VI grade of MSK-64 scale; seismic intensity V grade of MSK-64 scale.

5.1.4.3. Seismic zoning of Latvia – 2007

After the EU regulatory document Eurocode-8 [Eurocode-8, 2005] was adopted in Latvia, bringing assessments of seismic hazard in line with Eurocode-8 recommendations has become necessary. The promoter of the new project for seismic hazard assessment in Latvia was the Ministry of Economy. The earthquake catalogue was based on data describing 123 historical and present-day earthquakes that took place within the area of the Baltic Region (φ = 54.0°N – 60.0°N; λ = 18.0°E – 30.0°E) from 1302 to 2007.

The principal sources of seismological data were: *FENCAT* catalogue for Nordic countries of Europe [FENCAT_*i*], some materials on historical earthquakes from B. Doss [Doss,1898; Doss,1905; Doss,1909; Doss,1910; Doss,1911], the materials from Boborykin [Авотиня и др., 1988; Боборыкин и др., 1993], Nikonov [Nikonov & Sildvee, 1986; Nikonov, 1992; Nilonov & Sildvee, 1991], the data base of the Bergen University *SWISWEB* [SWISWEB_*i*] and other sources of information [Nikulins, 2007_*upm*].

Since the earthquake statistics of Latvia was very scarce, the geological and geophysical and deformation parameters were vital for the highlighting of seismogenic areas.

The seismotectonic analysis took into account such geological and geophysical parameters as: 1) the configuration of tectonic faults in the Caledonian structural

Table 20.

Geological, geophysical and deformation parameters of seismogenic zones of Latvia [Nikulins, 2007_upm]

Name of seismogenic zones	Faults in the Caledonian complex	Faults in the crystalline basement	Deep fractures	Isostatic anomalies	Lineaments	Neotectonic movements, ΣA,м)	Vertical movements, mm/year	The number of earthquakes
Ventspils – Irbe	+	+			+	120	1.8	4
Liepāja	+	+	+	+	+	100	1.1	2
Jelgava – Kuršeņi	+	+	+	+	+	80	2.0	1
Riga – Valmiera	+	+	+	+	+	100	2.0	11
Aizkraukle	+	+	+	+	+	40	0.5	7
Bauska	+	+	+		+	50	1.2	1
Daugavpils		+	+		+	20	1.1	1
Madona		+				20	0.2	2

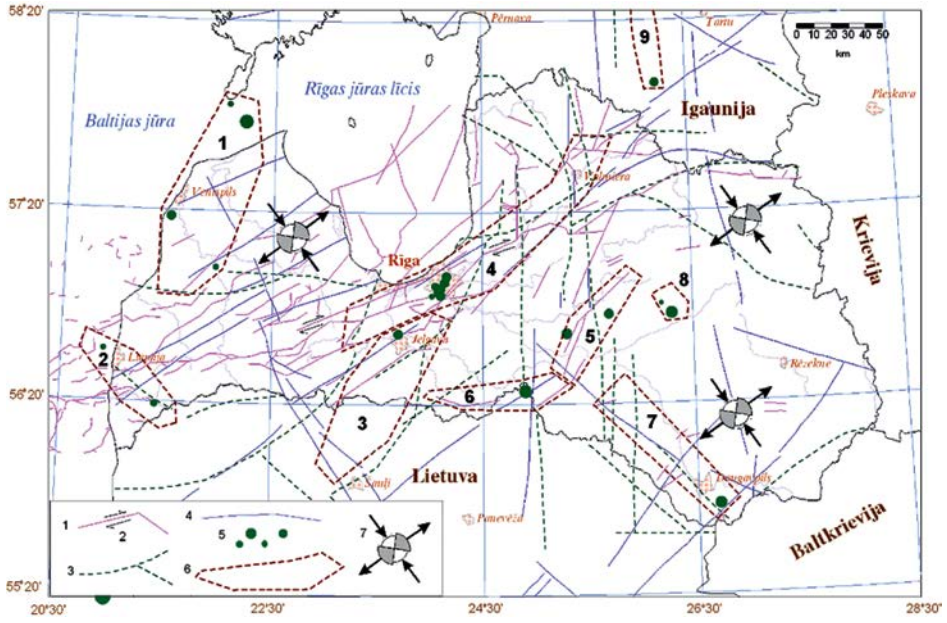

Figure 122. Seismotectonic map of Latvia showing faults in sedimentary cover, deep-seated crust fractures, and seismogenic zones [Ņikuļins, 2007_upm]

Legend: 1 – tectonic faults in the Caledonian structural complex of sedimentary cover [Brangulis & Kaņevs, 2002]; 2 – directions of motions along the faults; 3 – deep-seated tectonic faults in the Earth's crust (according to gravimetric and magnetometric data), which do not manifest themselves within the sedimentary mantle; 4 – lineaments according to space images data [Суеўизdис и dр., 1980]; 5 – epicentres of tectonic earthquakes; 6 – seismogenic zones (the figures inside the areas designate the sequence number of the area); 7 – stress ellipse with the direction of the compression axes and axes of tension

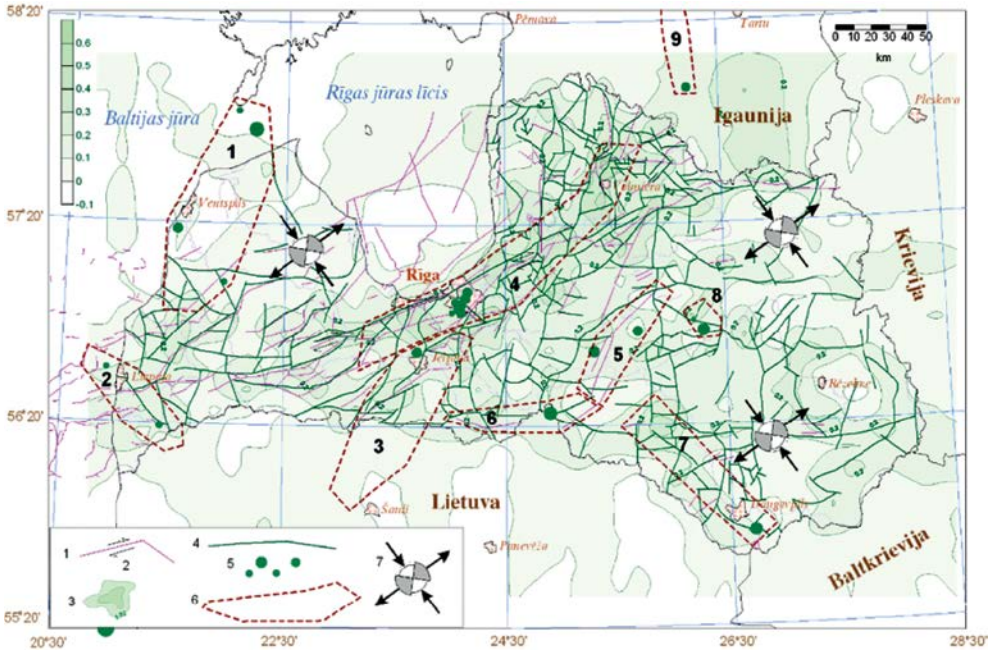

Figure 123. Seismotectonic map of Latvia showing faults in the crystalline basement, tectonic faults contour density, and seismogenic zones [Ņikuļins, 2007_*upm*]

Legend: 1 – tectonic faults in the Caledonian structural complex of sedimentary cover [Brangulis & Kaņevs, 2002]; 2 – movement directions along the faults; 3 – boundary density contours of geological and formation zones in the crystalline basement (as according to gravimetric and magnetometric data), which do not manifest themselves within the sedimentary mantle; 4 – boundaries between the geological and formational zones [Vetrennikovs, 1997_upm]; 5 – epicentres of tectonic earthquakes; 6 – seismogenic zones (the figures inside the areas designate the sequence number of the area); 7 – stress ellipse with the direction of the compression and the tension axes. Top left: the color scale shows the density of boundaries of geological and formational zones in the crystalline basement

complex of the sedimentary cover [Brangulis & Kaņevs, 2002]; 2) configuration of deep tectonic faults of the Earth's crust according to gravimetric and magnetometric data [Апирубите, 1980_*upm*]; 3) configuration of the boundaries of structural-formational complexes in a crystalline basement [Vetrenņikovs, 1997f]; 4) lineaments according to space image data [Сувейздис и др., 1980]; 5) epicentres of tectonic earthquakes [Никулин, 2007]; 6) contours of the density of tectonic faults in the crystalline basement (according to gravimetric and magnetometric data) [Ņikuļins V., 2007_*upm*]; 7) crustal thickness [Ņikuļins V., 1998_*upm*]; 8) isostatic equilibrium disturbance index [Nikulin V., 1997; Nikulin V., 1999; Никулин В.Г., 2008b]; 9) contours of the total amplitudes of neo-tectonic motions [Garetsky et al., 1999]; 10) the velocity of modern vertical motions [Ковалевский и др., 1966_*upm*].

The following criteria were accepted as the main classification criteria of seismicity (Table 20): 1) the existence of tectonic faults in the Caledonian structural complex within

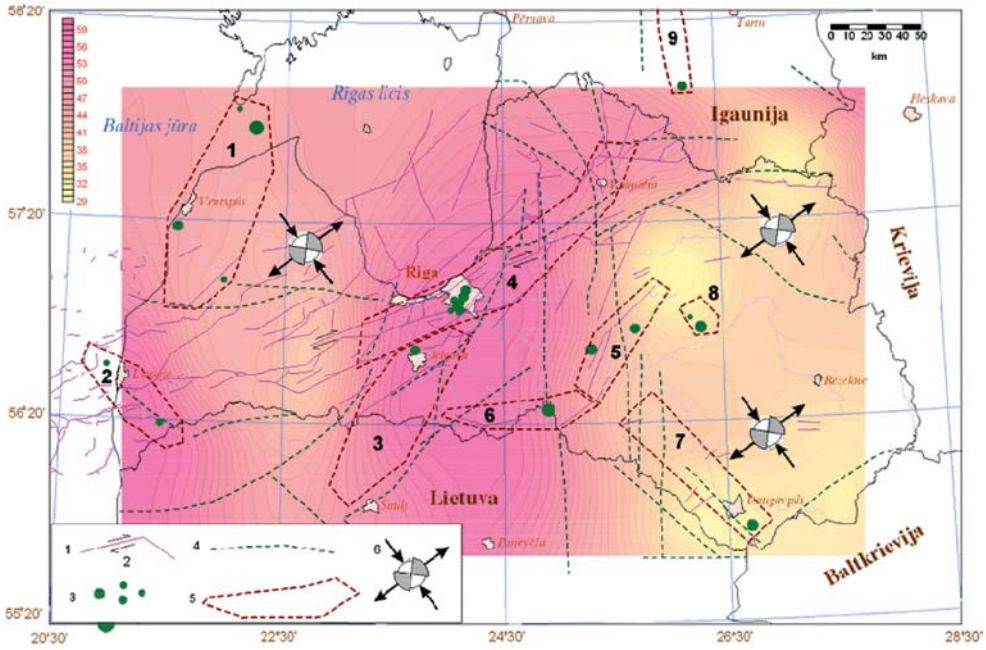

Figure 124. Seismotectonic map of Latvia showing faults in sedimentary cover, deep-seated faults, crustal thickness, and seismogenic zones [Ņikuļins, 2007_ upm]

Legend: 1 – tectonic faults in the Caledonian structural complex of the sedimentary cover [Brangulis & Kaņevs, 2002]; 2 – movement directions along the faults; 3 – epicentres of tectonic earthquakes; 4 – deep-seated faults in the Earth's crust; 5 – seismogenic zones (the digits inside the zones designate the sequence number of the zone); 6 – stress ellipse with the direction of the compression and the tension axes. Top left: the color scale shows crustal depth

the seismogenic area; 2) the existence of tectonic faults on the crystalline basement within the seismogenic zone; 3) the existence of deep-seated (abyssal) faults within the seismogenic zone; 4) the existence of isostatic anomalies of the Earth's crust within the seismogenic zone; 5) the existence of lineaments within the seismogenic zone; 6) the intensity of neo-tectonic crustal motions inside the seismogenic zone; 7) the intensity of the present-day vertical crustal motions within the boundaries of the seismogenic zone; 8) the number of earthquakes within the seismogenic zone.

The series of seismotectonic maps that served as a basis for seismic zoning of Latvia carried out in 2007 is presented in Figures 122–127.

Unlike the General Seismic Zoning (GSZ) of Latvia as of 1998, geological maps in the seismic zoning studies of 2007 were furnished with a reliable common topographic control base – LKS-92. Moreover, as a result of a new interpretation of the tectonic structure of Latvia, tectonic maps of the Caledonian and Hercynian complex and the crystalline basement were prepared separately [Brangulis & Kaņevs, 2002]. In particular, according to a new interpretation for confirmation of the tectonic structure

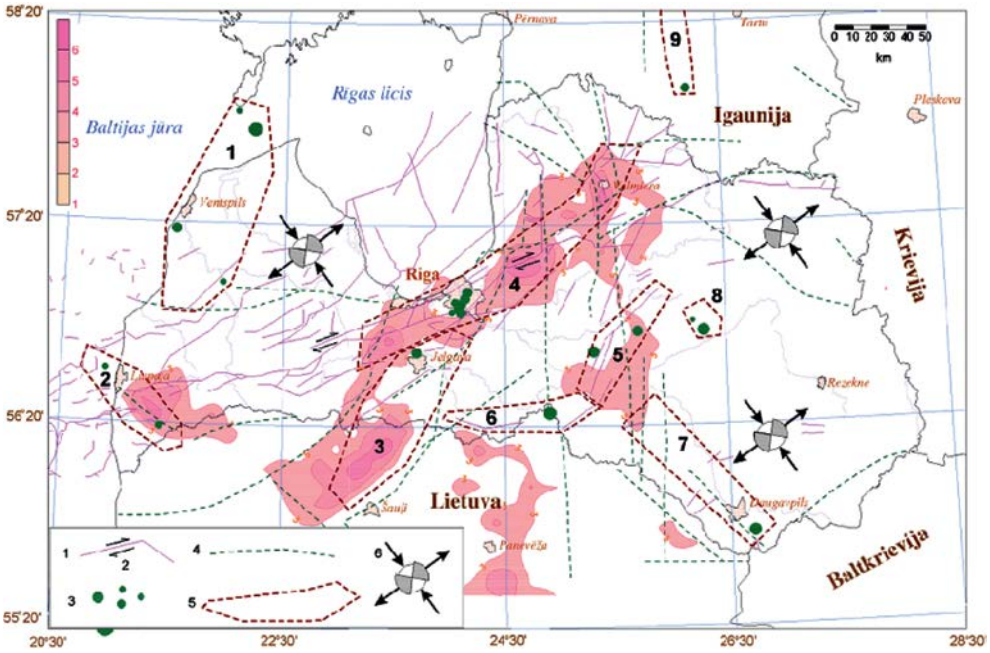

Figure 125. Seismotectonic map of Latvia showing faults in sedimentary cover, deep-seated faults, crustal thickness, and seismogenic zones [Ņikuļins, 2007_ upm]

Legend: 1 – tectonic faults in the Caledonian structural complex of the sedimentary cover [Brangulis & Kaņevs, 2002]; 2 – movement directions along the faults; 3 – epicentres of tectonic earthquakes; 4 – deep-seated faults in the Earth's crust; 5 – seismogenic zones (the figures inside the zones designate the sequence number of the zone); 6 – stress ellipse with the direction of the compression and the tension axes. Top left: the color scale shows the index of violation of isostatic equilibrium

of Latvia in the new version, the location of some tectonic faults (the Piebalga and Aizkraukle ones) was corrected, while other faults (the Madona, the Daugavpils) were not found].

It was exactly the Caledonian structural complex developed anywhere on the territory of Latvia and in the Baltic Sea that was of a special interest. The complex embraces the Supra-Baltic terrigenous deposits, Lower Cambrian deposits, Lower- and middle Cambrian terrigenous rocks, clay and carbonaceous rocks, terrigenous and carbonaceous formations of (Euro-Paleozoic) Ordovician and Silurian systems, and the Gargzhdaysky series of Lower Devonian rocks [Брангулис и др., 1984]. The thickness of the Caledonian structural complex varies from 200 to 1000 m.

The structural geometry of the Caledonian complex duplicates the terrain of the crystalline basement. The tectonic faults of the basement and the Caledonian structural complex practically coincide. The Caledonian structural complex turned out to be more preferable as against the Hercynian structural complex, because in it a lot of tectonic faults were found [Brangulis & Kaņevs, 2002].

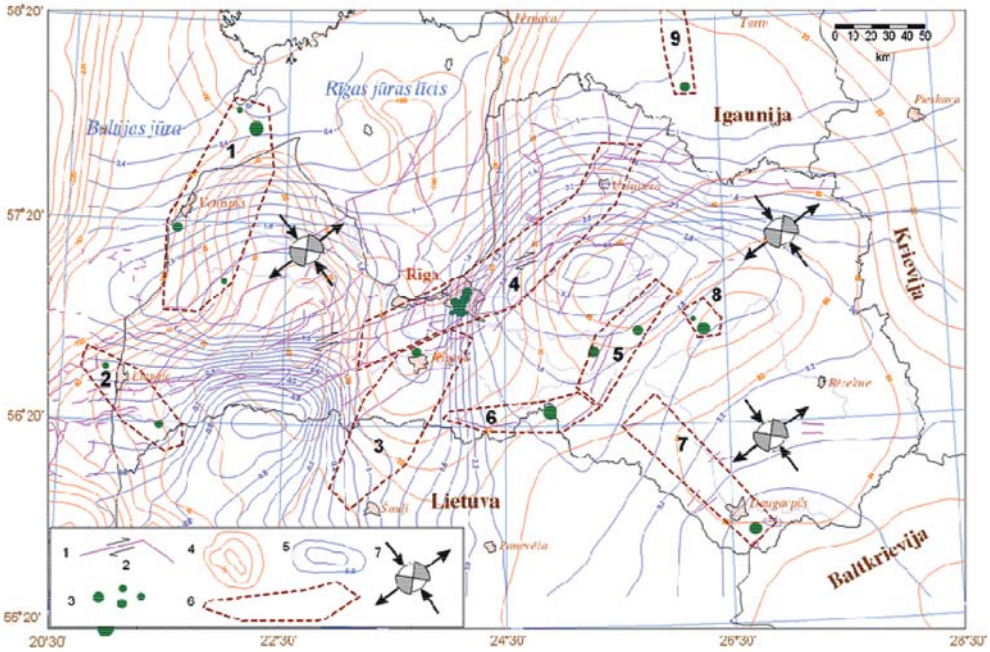

Figure 126. Seismotectonic map of Latvia showing faults in sedimentary cover, amplitudes of resulting neo-tectonic motions, present-day vertical motions, and seismogenic zones [Ņikuļins, 2007_ upm]

Legend: 1 – tectonic faults in the Caledonian structural complex of the sedimentary cover [Brangulis & Kaņevs, 2002]; 2 – movement directions along the faults; 3 – epicentres of tectonic earthquakes; 4 – contours of resulting amplitudes of neo-tectonic motions, in metres [Garetsky et al., 1999]; 5) velocity of the present-day vertical motions, mm/year [Ковалевский и др., 1966_upm]; 6) seismogenic zones (the figures inside the areas designate the sequence number of the zone); 7 – stress ellipse with the direction of the compression and the tension axes

The deep-seated tectonic faults were necessary to characterize the divisibility of the Earth's crust. They have been obtained, based on the interpretation of gravimetric and magnetometric data [Апирубите, 1980_*upm*].

One of the efficient methods for the investigation of a deep structure of a territory is lineament analysis. Lineaments are linear and arc-shaped elements of terrain, associated with deep-seated faults of the Earth's crust. The lineaments coincidence with tectonic faults can be regarded as an index attesting to the present-day activation of deep-seated tectonic structures.

Therefore, a lineament structure has always been considered as one of the classification criteria of seismicity.

The strain ellipse presented was determined based on the predominant regional stress oriented from north-west to south-east, i.e., along the movement direction from North Atlantic Ridge.

The contours of geological and formational zones boundary densities reflect the divisibility of the crystalline basement. Those boundaries are identical to tectonic faults

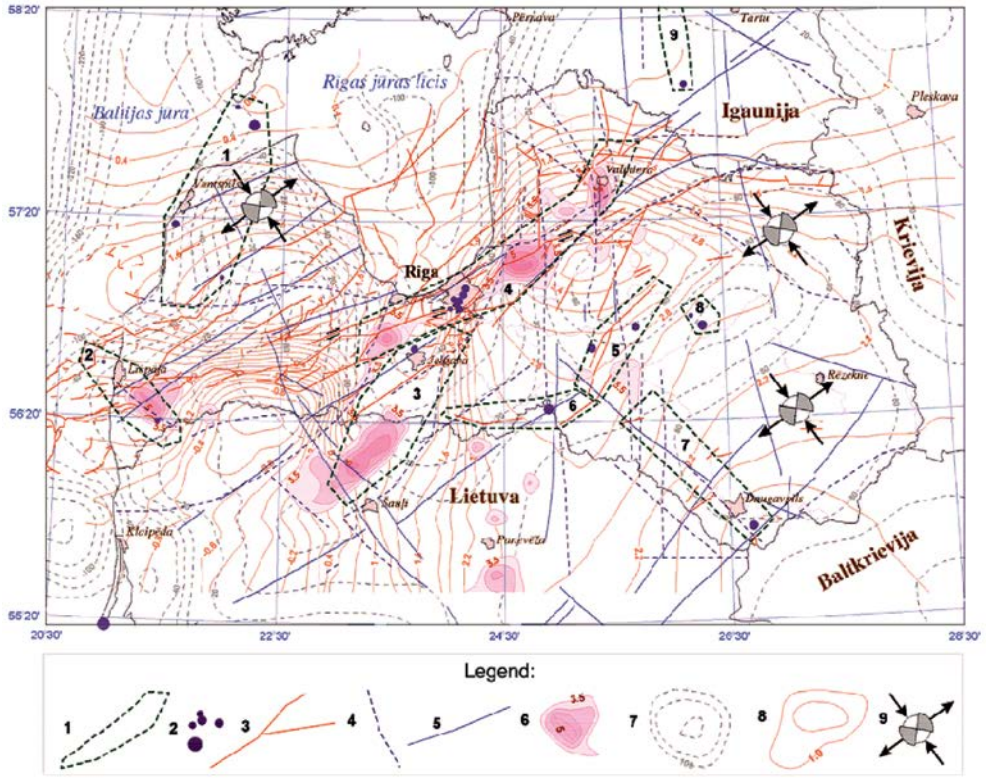

Figure 127. Generalized seismotectonic map of Latvia with classification criteria for seismicity, earthquake epicentres, and contours of seismogenic zones [Nikulins, 2007_*upm*]

Legend: 1 – contours of seismogenic zones; 2 – earthquakes epicentres; 3 – tectonic faults in the Caledonian structural complex; 4 – deep-seated tectonic faults; 5 – linear active zones; 6 – isostatic anomalies; 7 – amplitudes of neotectonic movements; 8 – the present-day vertical crustal movements (mm/year); 9 – the tectonic stress ellipse

in individual cases only, whereas in most cases, they are boundaries between various geological and formational complexes of the crystalline basement [Ветренников, 1991].

The subdivision of complexes by the types of their formational appurtenance was based on such criteria as structural position, the character of geological record, the internal structure, material and mineral composition, textural and structural features, the major and the minor chemical elements distribution within rocks and minerals, petrophysical rock properties, and the typical facies of metamorphism [Vetrenņikovs, 1997_*upm*] Gravimetric and magnitometric data was the main source materials for carrying out the geological and formational zoning.

As the main characteristics of the crustal dynamics, the resulting amplitudes of neo-tectonic motions ΣA_{neotec} [Garetsky et al., 1999] and the speed of the present-day vertical motions V_{ver} [Kovalevsky et al, 1966_f] were used. Values ΣA_{neotec} are defined for

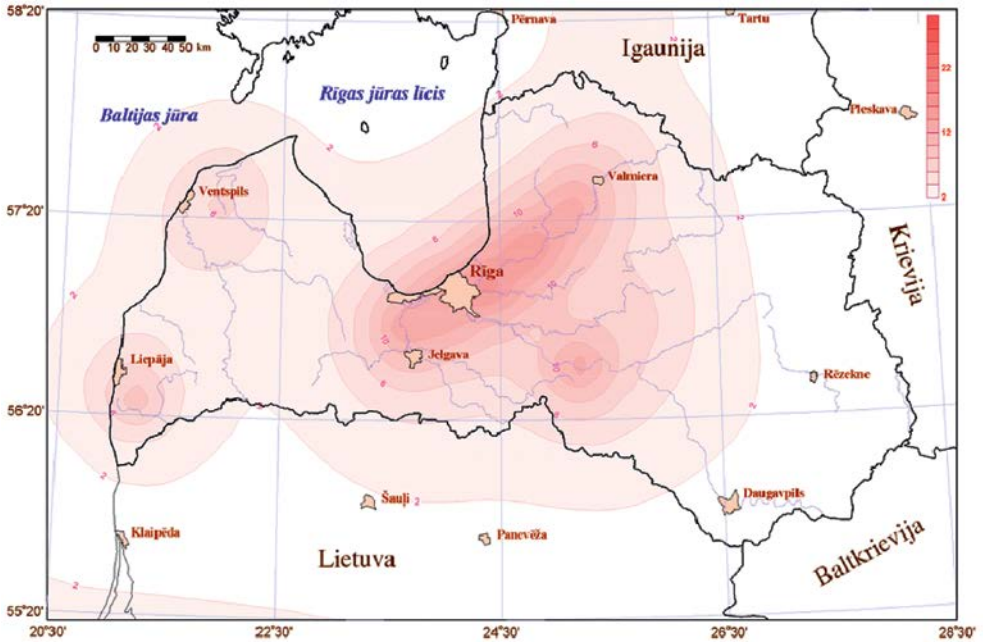

Figure 128. The map of horizontal peak accelerations agR of "stiff" ground (PGA), with the 10% probability of exceedance of the predicted seismic intensity (in cm/sec²) within a 50-year period [Ņikuļins, 2007_*f*]

the neo-tectonic period, which began from Rupelian age 35 million years ago. V_{ver} are determined based on repeated geodetic measurements on leveling profiles, performed within the period from 1935 to 1965.

A generalized seismotectonic map with the main classification criteria of seismicity is shown in Figure 127. In particular, it shows contours of seismogenic zones, epicenters of earthquakes, tectonic faults in the Caledonian structural complex, deep-seated tectonic faults in the Earth's crust, linear active zones identified by the results of interpretation of space images, isostatic anomalies at the crustal boundary level – the Moho discontinuity, the amplitudes of neo-tectonic movements, starting from Rupelian age (35 million years ago), and the present-day crustal movements; moreover, an ellipse of tectonic stresses is shown on the map, wherein the compression axis corresponds to the pressure from the North Atlantic Ridge.

As a result of the investigations carried out in 2007, 8 (eight) seismogenic areas were singled out with respect to the territory of Latvia, namely: Ventspils – Irbe, Liepāja, Jelgava – Kuršenai, Riga – Valmiera, Aizkraukle, Bauska, Daugavpils, and Madona.

The map of horizontal peak accelerations of "stiff" ground (PGA) with the 10% probability of exceedance of the predicted seismic intensity (in cm/sec²) within a 50-year period, is shown in Figure 128.

As the conclusive results of seismic zoning of 2007, the maps of horizontal peak accelerations (PGA) of "stiff" ground were plotted – with the 10%, 5%, 1% and

0.5% probability of exceedance of the predicted seismic intensity within a 50-year period. The corresponding *return periods* (*recurrence intervals*) are 475, 975, 4975 and 9975 years. The "stiff" ground in this case corresponds to the top of Devonian sediments, which are spread across the entire territory of Latvia and which underlie the Quaternary deposits.

5.1.4.4. GSHAP International Project

From 1992 to 1999, the GSHAP international project (*Global Seismic Hazard Assessment Program*) was implemented [*http://www.gfz-potsdam.de/en/section/seismic-hazard-and-stress-field/projects/previous-projects/probabilistic-seismic-hazard assessments/gshap/*]. The project scope was the development of seismic risk maps on all the continents including Europe. Within the framework of the project, seismic risk was assessed with respect to Region 3, too – namely, with respect to Northern Eurasia (Region 7) and Central, North, and Northwest Europe (Region 3) (Figures 129–132).

Results of the working group of Northern Eurasia

The concept that the Northern Eurasia included structural and structural-dynamic models (for genesis) and deterministic-probabilistic models (for the form).

The catalogue covered the earthquakes dating back to 10 thousand years B.C. to December, 1995. Unfortunately, the catalogue included only $M \geq 4.5$-earthquakes. For that reason, some important earthquakes that took place in EBR were not included into the catalogue. Among those ones, in particular, the following earthquakes can be mentioned: the Bauska earthquake of 1616, the earthquakes that took place in the Vyrtsyarv Lake neighborhood, those in Estonia etc. – despite the fact that all of those earthquakes were perceived by the local people.

Three question pools were considered additionally: 1) the modern geodynamics; 2) regional seismicity; 3) strong motions. The concept of the Northern Eurasia group was a two-stage procedure that included the development of a model of seismic source zones and a model of seismic effects.

At the final stage, the ground shaking level and seismic hazard were assessed within the definite time period. The following parameters were considered in the model of seismic source zones: maximum earthquake magnitude, magnitude-frequency dependence in the Region, lineaments, domains, and potential earthquake sources. In the seismic effect model, the following parameters were considered: maximal intensity, attenuation at strong motions, and correlation between the parameters of ground's strong motion response. At the final stage, the assessment of ground shaking (tremor rate) and of the probability of seismic hazard within a specific time span.

As it follows from the research findings obtained by the Northern Asia Group, three types of seismic source areas were highlighted on the territory of the East Baltic Region [Ulomov et al., 1999] (Figure 129). In the north-eastern zone (the north-eastern Estonia), earthquake magnitude may reach 4.0 ± 0.2, while in the eastern zone (the major part of Estonia and Latvia and the north-eastern part of Lithuania) it may reach –5.0, and in the western zone (the western part of Latvia and the major part of Lithuania –4.5.

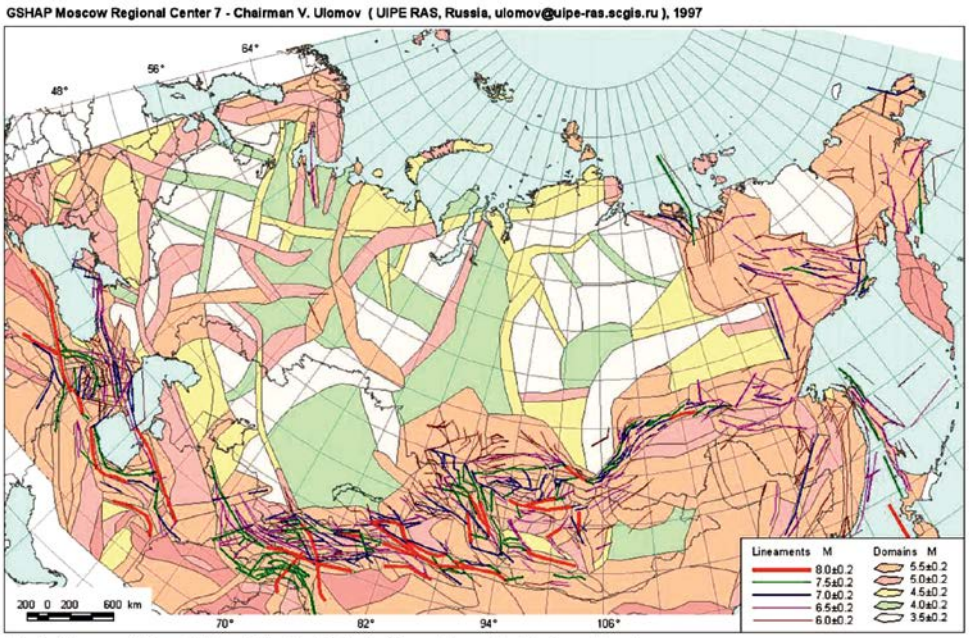

Fig. 7 : Lineament-Domain-Focal Model of Seismic Source Zones for Northern Eurasia

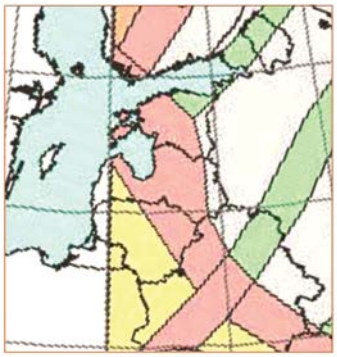

Figure 129. The lineament-domain-focal model for seismic source zones in the Northern Eurasia [Ulomov et al., 1999]

Accordingly, ground motion peak acceleration values (PGA) have the value of 0.2–0.4 m/sec^2 [Ulomov et al., 1999] (the left side of Figure130) within the limits of a single zone having sub-meridional strike in the direction of Pärnu, Valmiera, Cēsis, Pļaviņas, Jēkabpils, and Jodupe (the right side of Figure 130).

Results of the working group of Central, North, and Northwest Europe (Region 3)

The working group of Central, North and Northern Europe, to which Region 3 belonged, was engaged in the zoning of central, northern and north-western Europe. The group was facing a difficult task of harmonizing the individual results obtained in different European countries. One of the main stages in this respect was ensuring homogenization and unification of magnitude. As a single equivalent, the moment magnitude M_w was used. This is due to the fact that historical earthquakes were determined, based on macroseismic

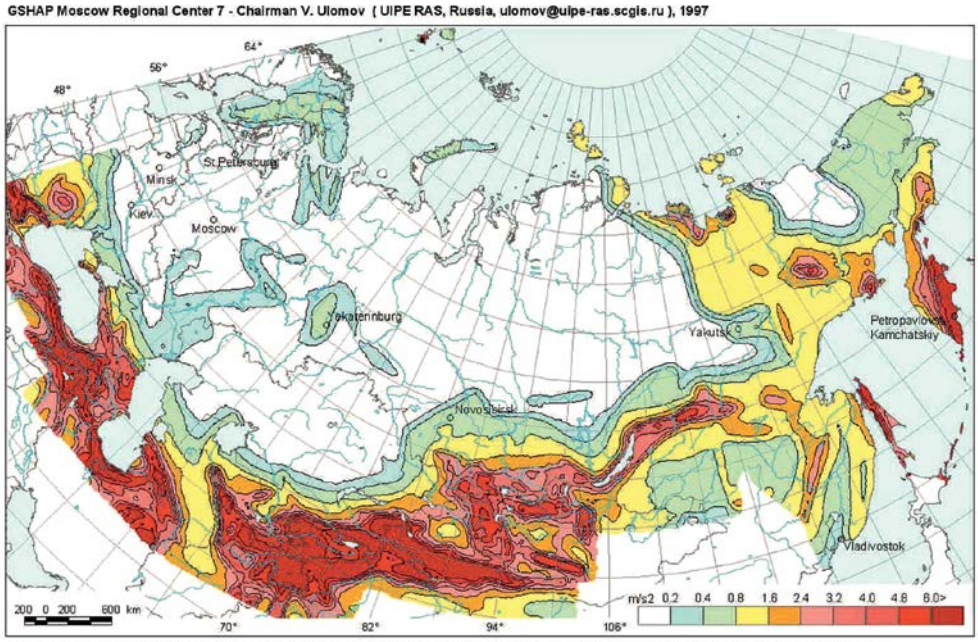

Fig. 10 : Peak Ground Acceleration (m/s2) Map with 10% Probability of Exceedance in 50 Years for Northern Eurasia

Figure 130. Ground peak acceleration map (m/sec²) with the 10% probability of exceedance within a 50-year period – for Northern Eurasia [Ulomov et al., 1999]

data (shock intensity, tremor area), while the magnitude proper of an earthquake could be determined based on instrumental data (seismograms). Precisely because of the use of different magnitude scales, there arose a need for homogenization.

The moment magnitude M_w is related to the seismic moment M_0 through a known correlation. Therefore, a transition from macroseismic magnitudes or shock perceptibility areas (for historical earthquakes) and from the local magnitude M_L, (for instrumentallyregistered earthquakes) to the seismic moment M_0 was carried out. The formula for earthquakes with the intensity not lower than III was used:

$$\log(M_0) = 25.87 - 2.92\log(A_{III}) + 0.45\log(A_{III})^2 \quad (41)$$

where, A_{III} – isoseismic area with point III intensity.

To recalculate the local magnitude M_L into seismic moment M_0, the following correlation was used:

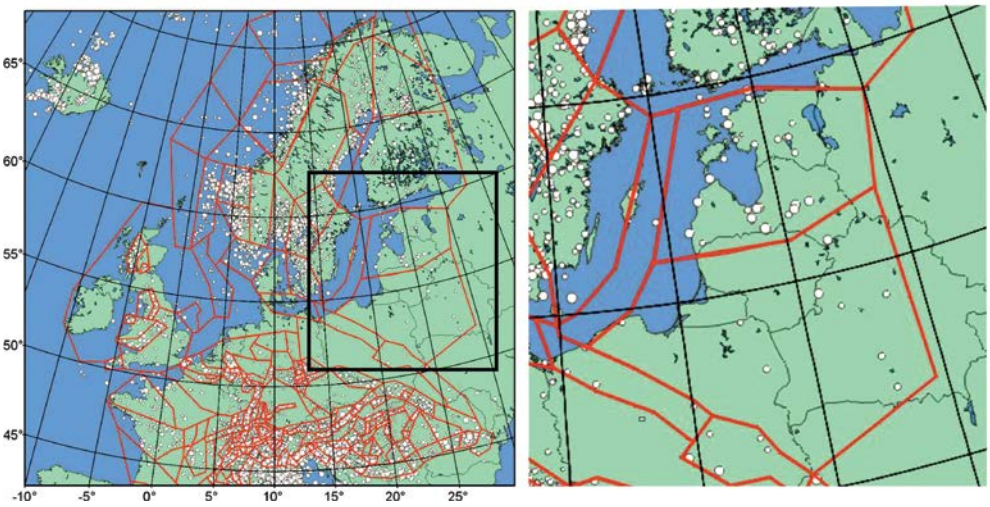

Figure 131. The GSHAP project seismic source map for Region 3 and tracing of the map for East Baltic Region (right)

$$\log(M_0) = 18.6 + 0.2M_L + 0.13M_L^2 \quad (42)$$

To calculate seismic hazard, 196 seismic source zones were used. Two seismic source regions were singled out on the territory of East Baltic Region. One more, narrow region of seismic source was located in the central part of the Baltic Sea (Figure 131). Seismic source regions were specified based on the distribution of seismicity and seismotectonic criteria.

The magnitude-frequency correlation was determined with respect to each seismic source region. If lack of data was observed within a region, the dependence on the adjacent, larger regions with similar tectonic characteristics was used. The results of calculation of Peak ground horizontal (PGH) acceleration are presented in Figure 132.

Seismic hazard was assessed in terms of stochastic observations. This probabilistic assessment means that, within 50 years, accelerations (m/sec^2) will not exceed the values shown on the map with the 90% probability. Consequently, the earthquake return period will constitute 475 years. This means that an earthquake with the shock level reaching the values shown on the map will take place in 475 years' time with the 100% probability.

When singling out earthquake source zones (SSZ), the value of relative peak acceleration a_{gR} on *A*-type grounds is indicated. *A*-type grounds include, in particular, rock materials or some geological formations similar to rock material, including a thinner near-surface layer not exceeding 5 cm. Shear wave velocity $v_{s,30} > 800$ m/sec [Eurocode 8, 2005].The estimated seismic impact a_{gR} is selected for each SSZ and is expressed in terms of the reference seismic impact associated with a reference probability of exceedance P_{NCR} within 50 years or within reference return period T_{NCR}, taking into account the importance factor γ_I as well [Eurocode 8, 2005]. The recommended parameters are of the values as follows: $P_{NCR} = 10\%$, $T_{NCR} = 475$ years. They correspond to reference seismic

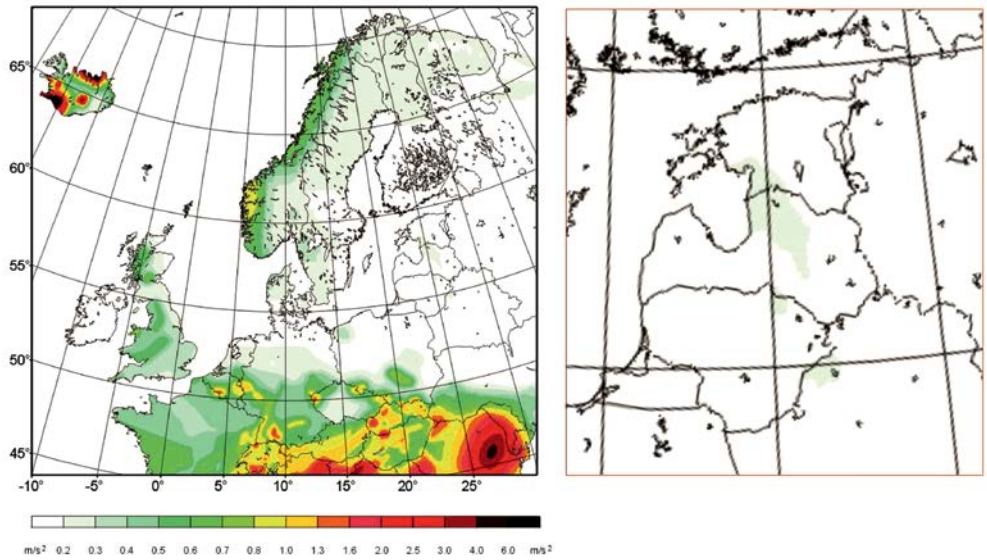

Figure 132. Map of Peak ground horizontal acceleration with the 10% probability of exceedance of stiff ground tremor within 50 years

action for the no-collapse requirement. The P_R probability of exceedance of a definite level of seismic impact is associated with the mean return time T_R of that seismic impact level – according to the expression, as follows:

$$T_R = -T_L/\ln(1 - P_R) \tag{43}$$

Thus, with respect to the given T_L value, seismic impact can be equivalently preset - either by using the mean return period T_R, or through the probability of exceedance P_R within T_L years. The seismic zoning results obtained from 1992 to 1997 within the GSHAP program have shown that peak tremors with the accelerations of 0.2– 0.3 (0.4) m/sec^2 may be expected on the territory of the East Baltic Region with the probability exceeding 10% (Figure 132).

In a generalized survey dedicated to regionalization of Fennoscandia and the adjacent territories [Wahlstrom & Grunthal, 2001], a number of models are generalized up until 1998. As a result of comparison between the model developed within the framework of GHSAP project (A) and other models (B, C) it can be seen (Figure 133) that the regionalization of the East Baltic Region did not change essentially.

The version of a seismic sources model as of 1998 (F) developed for GSHAP project contains 31 seismic source zones (SSZ). In EBR, the East Baltic zone boundary passed close to the Latvian-Lithuanian border. The regionalization model B contains 21 SSZ and it was based mainly on seismicity distribution. Model C contains 31 SSZ located in Sweden, Finland, and Denmark and additionally 21 SSZ for Norway and the near-shore zone territory.

Model B based on seismicity distribution seems to be less realistic. The "appendix" of the East-Baltic SSZ, directed towards eastern Lithuania, is mainly based on seismic shocks of 1908. As shown in Chapter 3, seismic shocks in 1908 in the territory of the

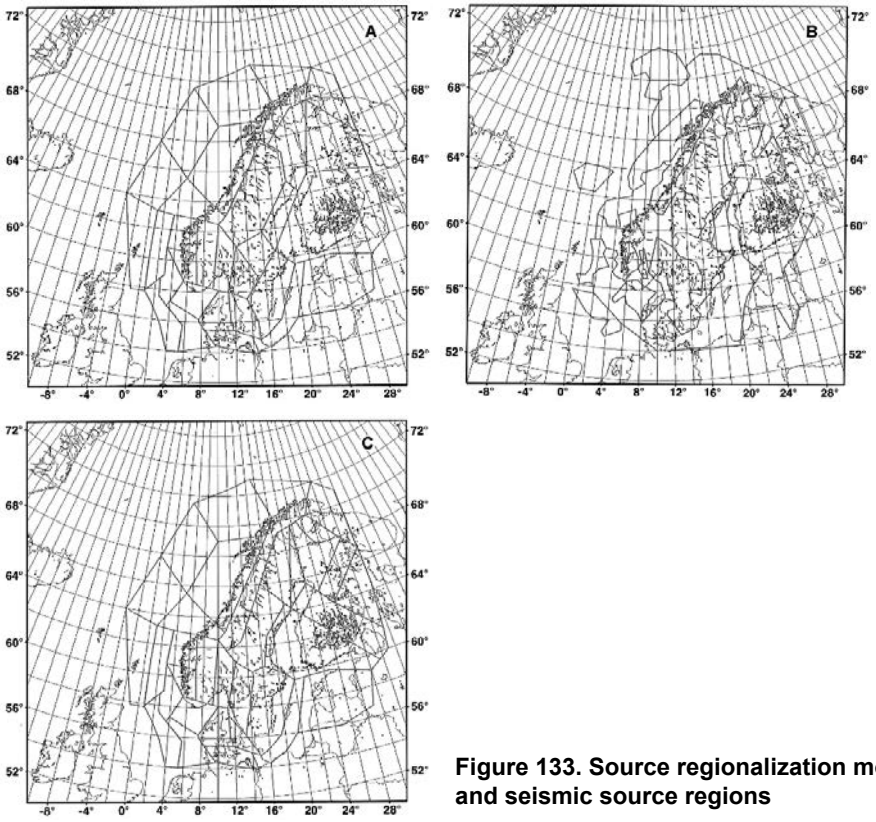

Figure 133. Source regionalization models and seismic source regions

EBR were most likely associated with cryogenic shocks. These seismic phenomena of a non-tectonic nature cannot be taken into account when assessing the seismic hazard based on tectonic phenomena.

5.1.4.5. Assessment of seismic hazard in the Baltic Region

Seismic source zones were assessed within the framework of specification of initial seismicity for seismic hazard assessment of the Ignalina NPP (Figure 134). To this end, the research of seismic potential of the East Baltic Region was conducted in 2007 [Pacesa & Sliaupa, 2007]. Methodologically, a probabilistic approach, i.e., the PSHA method, was chosen.

Seven seismic sources were identified in the Baltic sedimentary basin on the basis of seismological and geological information. These sources include: Leba, East Baltic Sea, Kaliningrad, West Estonian, East Baltic North, Latvian, and East Baltic South. The Ignalina NPP is located within the last seismic source. The law of seismic energy attenuation is based on the equations of Ambraseys et al. [Ambraseys et al., 2005]. The earthquake catalogue is prepared on the basis of compilation of historical data and some rare instrumental data.

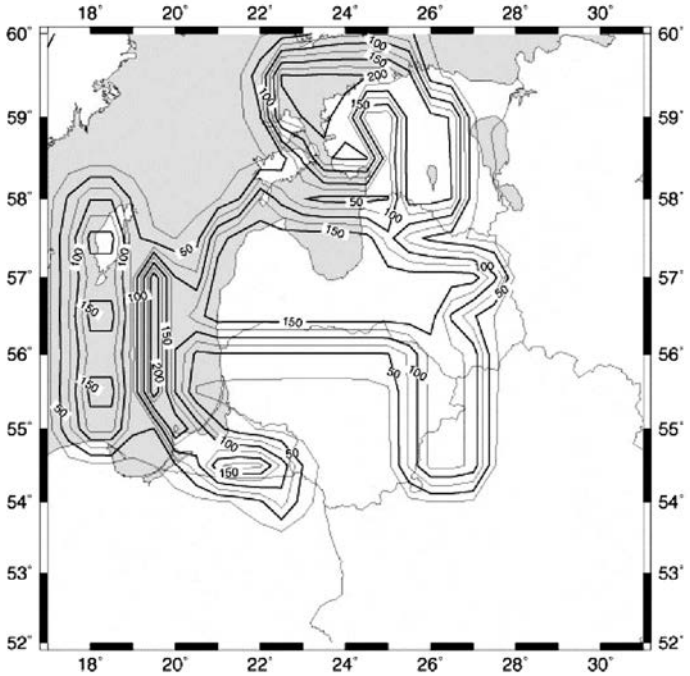

Figure 134. Map of seismic hazard for the Baltic Region in PGA units, with the probability of exceedance $^{10-4}$ [Pacesa & Sliaupa, 2007]

The magnitude of historical earthquakes was calculated on the basis of the equation for the Western Carpathian region. The parameter b in the equation reflecting the correlation between the number of earthquakes and the magnitude was taken as equal to 0.63, whereas for the territory of Finland, for example, b = 0.59. PGA (Peak Ground Acceleration) was calculated for the probability of exceedance of 10-4, which is a typical norm for seismic risk assessment under the terms of SL-2. As a result, it was found that the Ignalina nuclear power plant is located on the territory where PGA = 0.13 g.

For the territory of Latvia, PGA = 0.166 g, while for the Osmussare area in Estonia, PGA = 0.2g and for the Kaliningrad Region PGA = 0.17 g. The territories of Lithuania are characterized by low seismic hazard.

However, the PGA assessment results obtained in process of the research are not associated with any specific types of ground.

5.1.5. The basic concepts of seismic microzoning

Seismic microzoning is an important step in reducing the risk of earthquakes. It requires a multidisciplinary approach and a definite contribution from such fields of Earth sciences as geology, seismology, geophysics, geotechnics, and structural engineering.

General seismic zoning (GSZ) creates a basis enabling one to carry out seismic microzoning (SMZ) on individual areas. If survey areas are located on a territory where GSZ has already been carried out, then the base parameter a_{gR} i.e., the value of relative peak ground acceleration of *A*-type – is already known for them [Eurocode 8, 2005].

SMZ is the assessment of a soil layer's response induced by earthquakes (explosions) affecting the Earth's surface. SMZ is a multi-disciplinary study area, calling for contribution from geology, seismology, geophysics, geotechnical and structural engineering. SMZ is applied with respect to urban agglomeration and the territories where essential structures are located – like nuclear power plants, underground railroads, bridges, engineering lines and utilities (gas and oil pipelines), dams, power transmission lines, and important main traffic arteries.

SMZ maps have been plotted for many large cities worldwide. They allow one to better understand the earthquake vulnerability of urban structure. SMZ maps are the final stage of seismic hazard assessment, preceded by GSZ or DSZ investigations.

According to recommendations from Technical Committee on Earthquake Geotechnical Engineering of the International Society of Soil Mechanics and Foundation Engineering [Bhattacharjee et al., 2011], the scope of investigation at different forms of seismic zoning can be presented in the following sequence: 1) General Seismic Zonation (GSZ) on a scale from 1:50 000 to 1:1 000 000; 2) Detailed Seismic Zonation (DSZ) on a scale from 1:10 000 to 1:100 000; 3) Rigorous Zonation (RZ) on a scale from 1:5 000 to 1:25 000. The micro-zoning scale depends on the availability of the source data and on the required detail of investigations. The general spider diagram reflecting the interrelations between seismic zoning (SZ) and seismic microzoning (SMZ) procedures can be presented as is shown in Figure 135 [A General Framework for Seismic Microzonation Studies_*si*].

The most important SMZ parameters are: peak ground acceleration values, frequency-dependent spectral acceleration, elastic response spectrum, soil properties, etc.

As a rule, the depth of geological deposits considered in seismic microzoning, is confined by 30 m of the near-surface section. The near-surface section is normally represented by grounds characterized by lower velocities of shear waves and lower densities. In most cases, the near-surface section corresponds to quaternary deposits. On the contrary, the underlying half-space is most frequently represented by more dense layers which are characterized by higher flexural wave velocities and higher densities. Local geologic setting essentially affects ground motion characteristics.

A typical example of the effect exercised by local geological setting on the epicenter intensity of is the case of the Kaliningrad earthquakes that were perceived on the adjacent territories of Lithuania and Latvia. According to macroseismic studies [Nikulin, 2005; Никулин, 2008a], the epicenter intensity in the Nigrand *volost* (district) (Kalni settlement and Saldus city) in Latvia, which is remotely located 200– 220 km from the foci of the Kaliningrad earthquakes, was estimated at V-V ½ grade on the EMS-98 scale. On the territory of Lithuania located closer to the epicenter of the earthquake, the epicenter intensity reached only 3–4 or 4 grade on the EMS-98 scale (Figure 60).

Non-linear attenuation of seismic energy caused by local geological engineering conditions may be associated with the fact that, with respect to a lower-density layer,

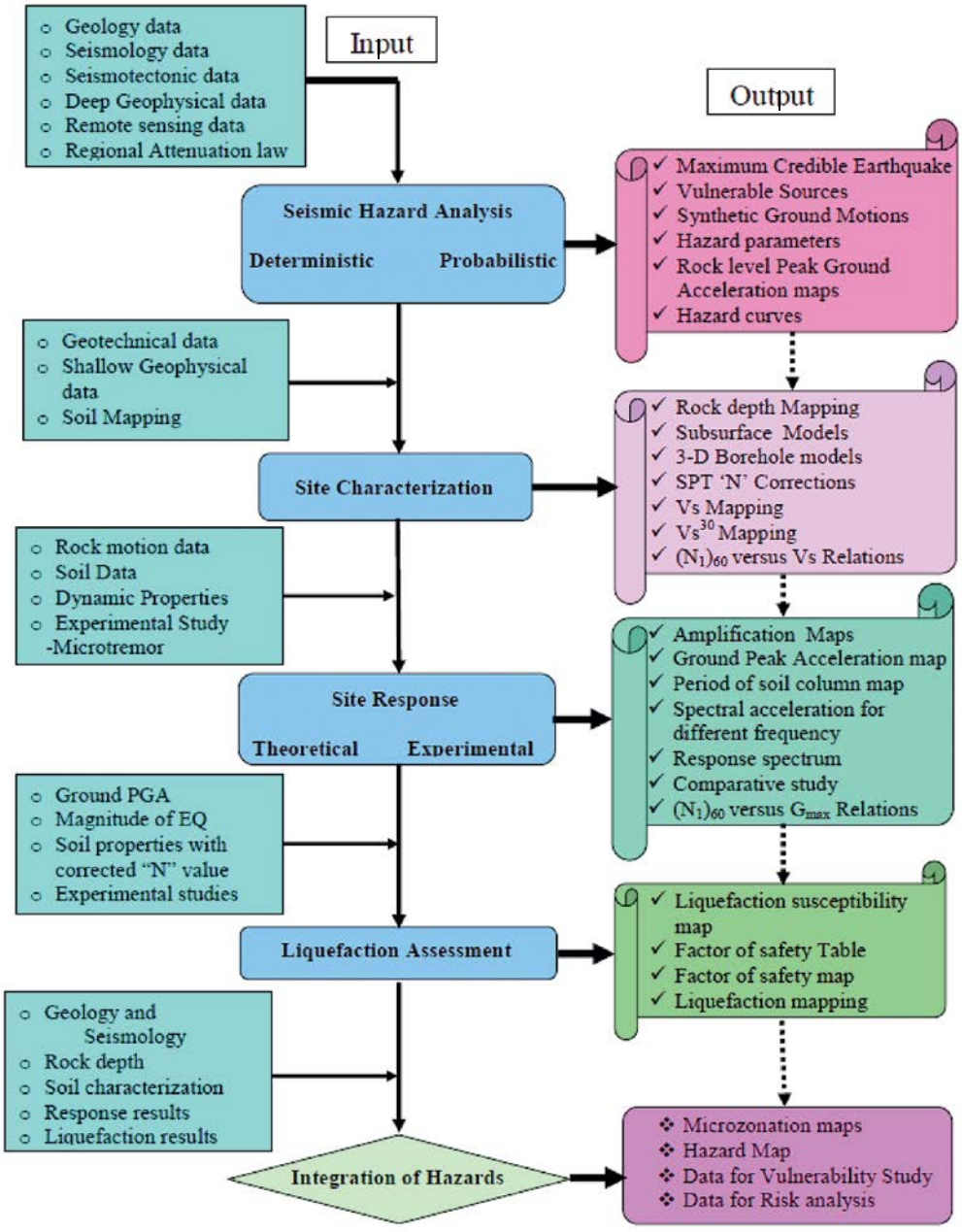

Figure 135. The general diagram reflecting the interrelations between seismic zoning and seismic microzoning procedures [A General Framework for Seismic Microzonation Studies_*si*]

a higher particles oscillation velocity is required to ensure observation of the law of conservation of energy. The amplification factor plays an important role in engineering seismology. This issue will be considered in the chapter dedicated to the horizontal-vertical spectral ratio (HVSR).

The ground motion induced by earthquake effect at a given point on the Earth's surface is characterized by the elastic ground acceleration response spectrum, or elastic response spectrum. This is the fundamental characteristic to be used in seismic microzoning. At a ground motion, both the horizontal and the vertical elastic response spectrum should be taken into account.

For horizontal components of seismic impact, the elastic response spectrum $S_e(T)$ is specified by the following expressions which hold true for individual sections of the spectrum [Eurocode 8, 2005]:

$$0 \le T \le T_B \qquad S_e(T) = a_g \cdot S \cdot [1 + (T/T_B) \cdot (\eta \cdot 2.5 - 1)] \tag{44}$$

$$T_B \le T \le T_C \qquad S_e(T) = a_g \cdot S \cdot \eta \cdot 2.5 \tag{45}$$

$$T_C \le T \le T_D \qquad S_e(T) = a_g \cdot S \cdot \eta \cdot 2.5 \cdot [T_C/T] \tag{46}$$

$$T_D \le T \le 4s \qquad S_e(T) = a_g \cdot S \cdot \eta \cdot 2.5 \cdot [(T_C \cdot T_D/T^2] \tag{47}$$

where, $S_e(T)$ – the elastic response spectrum; T – the vibration period of a linear single-degree-of-freedom system; a_g – the design ground acceleration on type A ground ($a_g = \gamma_I \cdot a_{gR}$); T_B – the lower limit of the period of the constant spectral acceleration branch; T_C – the upper limit of the period of the constant spectral acceleration branch; T_D – the value defining the beginning of the constant displacement response range of the spectrum; S – the soil factor; η – the damping correction factor with a reference value $\eta = 1$ for 5% of viscous damping; γ_I – the building importance factor. The importance factor depends on the importance class. There are 4 (four) such classes established [Eurocode 8, 2005]. With respect to a conventional building, $\gamma_I = 1.0$ (II importance class). The recommended values of γ_I for I, III and IV classes of importance are equal to 0.8, 1.2 and 1.4.

Elastic response spectrum $S_e(T)$ is shown (Figure 136) for the $M_S < 5.5$ magnitude earthquakes. In the East Baltic Region, the maximum magnitude value of the Kaliningrad earthquake was $M_w = 5.2$ or $M_S = 5.03$ – according to the formula elaborated for stable continental regions [Hanks & Kanamori, 1979]. The diagram applies to the case where A-type ground is vibrating with a horizontal acceleration $a_g = 10$ cm/sec^2.

The attenuation correction factor η in formulas 44–47 can be determined by the formula, as follows:

$$\eta = \sqrt{(10/(5 + \xi)} \ge 0.55 \tag{48}$$

where, ξ – viscous damping coefficient of structure expressed in percentage.

The elastic response spectrum can be obtained by a simple transformation of the elastic acceleration response:

$$S_{De}(T) = S_e(\mathrm{T})[T/2\pi]^2 \tag{49}$$

Math expression 49 can be applicable to vibration period $T < 4.0$ sec. For structures with $T > 4.0$, elastic response spectrum is formulated in a more complicated way.

The elastic response spectrum of vertical component $S_{ve}(T)$ (Figure 137) is specified by the following formulas:

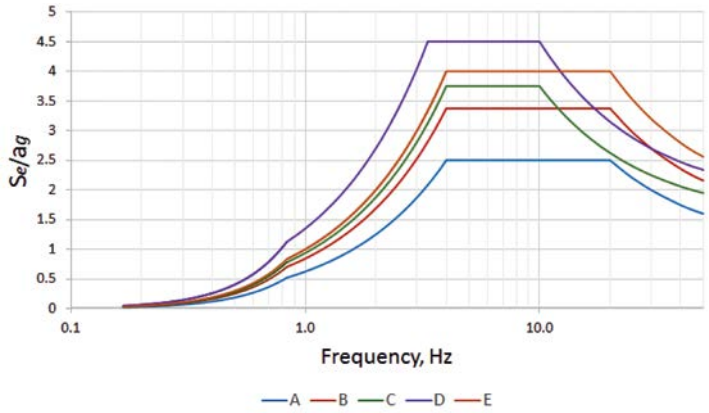

Figure 136. Normalized spectra of horizontal elastic response S_e/a_g with respect to grounds of A, B, C, D, and E-types – given that M_S < 5.5 (type 2) and the 5% attenuation [Eurocode 8, 2005]

$$0 \le T \le T_B \qquad S_{ve}(T) = a_{vg} \cdot [1 + (T/T_B) \cdot (\eta \cdot 3.0 - 1)] \tag{50}$$

$$T_B \le T \le T_C \qquad S_{ve}(T) = a_{vg} \cdot \eta \cdot 3.0 \tag{51}$$

$$T_C \le T \le T_D \qquad S_{ve}(T) = a_{vg} \cdot \eta \cdot 3.0 \cdot [T_C/T] \tag{52}$$

$$T_D \le T \le 4s \qquad S_{ve}(T) = a_{vg} \cdot \eta \cdot 3.0 \cdot [(T_C \cdot T_D/T^2] \tag{53}$$

The elastic response spectrum of the vertical component $S_{ve}(T)$ is shown in Figure 137. This graphic illustrates the case where the estimated vertical acceleration a_g = 4.5 cm/sec^2 takes place on any type of ground.

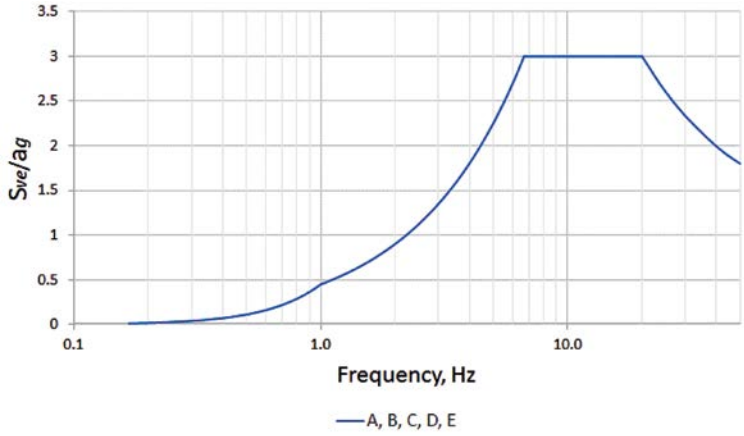

Figure 137. Normalized spectra of vertical elastic response S_{ve}/a_g for grounds of all types – i.e., A, B, C, D, E given that M_S < 5.5 (type 2) and that the attenuation = 5% [Eurocode 8, 2005]

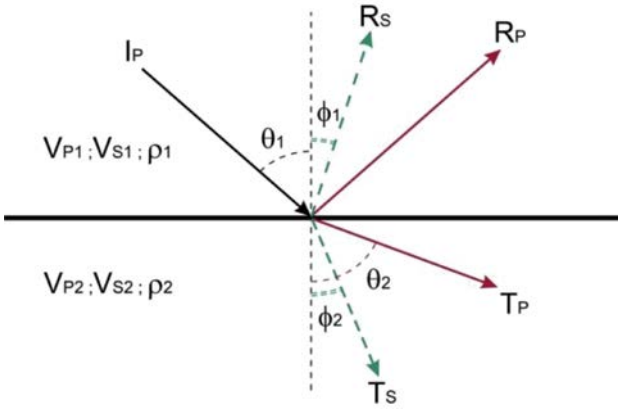

Figure 138. The body wave IP incidence on a discontinuity between two mediums at an angle θ1 and types of reflected (RP and RS) and refracted (TP and TS) waves spreaded in mediums 1 and 2.

Legend: IP – P body wave incident on discontinuity; RP – reflected body wave P propagating within medium 1; RS – refracted shear wave S propagating within medium 1; TP – refracted body wave P propagating within medium 2; TS – refracted shear wave S, propagating within medium 2

Therefore, unlike the elastic response spectrum of the horizontal component $S_e(T)$, the ground factor S is missing in the elastic response spectrum of the vertical component $S_{ve}(T)$ and coefficient 3.0 is used instead of coefficient 2.5.

SMZ procedure implies that the ground seismic response is associated with physical and mechanical properties of the ground. Among physical and mechanical properties of ground, the so-called seismic impedance and the water content (water saturation) of grounds are quite essential.

To specify seismic impedance, the transformation processes of body seismic wave $P(PP_i)$ incidence upon a discontinuity between two mediums at an angle θ_1 (Figure 138), must be taken into consideration.

The upper medium 1 is characterized by density ρ_1, body wave velocity V_{P1} and shear wave velocity V_{S1}. The lower half-space – i.e., medium 2 is characterized by the density ρ_2, body wave velocity V_{P2} and shear wave velocity V_{S2}. Please note that the angle of incidence I_p of body wave θ_1 is equal to the angle of reflection of body wave R_P.

Seismic waves energy distribution on the discontinuity is described by *Zoeppritz* equation. It consists of 4 (four) equation and is presented in the following form:

$$\begin{bmatrix} R_P \\ R_S \\ T_P \\ T_S \end{bmatrix} = \begin{bmatrix} -\sin\theta_1 & -\cos\phi_1 & \sin\theta_2 & \cos\phi_2 \\ \cos\theta_1 & -\sin\phi_1 & \cos\theta_2 & -\sin\phi_2 \\ \sin 2\theta_1 & \frac{V_{P1}}{V_{S1}}\cos 2\phi_1 & \frac{\rho_2 V_{S2}^2 V_{P1}}{\rho_1 V_{S1}^2 V_{P2}}\cos 2\phi_1 & \frac{\rho_2 V_{S2} V_{P1}}{\rho_1 V_{S1}^2}\cos 2\phi_2 \\ -\cos 2\phi_1 & \frac{V_{S1}}{V_{P1}}\sin 2\phi_1 & \frac{\rho_2 V_{P2}}{\rho_1 V_{P1}}\cos 2\phi_2 & \frac{\rho_2 V_{S2}}{\rho_1 V_{P1}}\sin 2\phi_2 \end{bmatrix}^{-1} \begin{bmatrix} \sin\theta_1 \\ \cos\theta_1 \\ \sin 2\theta_1 \\ \cos 2\phi_1 \end{bmatrix} \quad (54)$$

where R_P, R_S, T_P, T_S – the reflected P and S-waves and the refracted P and S-waves, accordingly; θ_1 – the angle of incidence of P-wave; ϕ_1 – the angle of reflection of S-wave; θ_2 – the angle of refraction of P-wave; ϕ_2 – the angle of refraction of S-wave.

Seismic impedance is included into formula 55 and is expressed by the multiplication of density by velocity. If the upper layer thickness consists of several layers, then, the average weighted seismic impedance of the layer pack is determined according to the formula, as follows:

$$\rho V_{1s} = \Sigma(\rho_i V_{si}) h_i / \Sigma h_i \quad (55)$$

where h_i – depth of *i-th* layer within the layer pack; $\rho_i V_{si}$ – seismic impedance of *i*-th layer within the layer pack.

The water content (water saturation) of grounds enhances the seismic impact. Medvedev [Медведев, 1962] had proposed a formula expressing the tremor increment subject to ground water level *h*:

$$\Delta I = \exp(-0.04h^2) \quad (56)$$

However, the increment depends on the ground type. That is why some reference documents [PCH-60-86, 1986] recommend taking into consideration the correction associated with the ground type. In the case of dispersion ground, humidity has a notable effect on the velocity of longitudinal waves V_P. A study of this phenomenon [Кригер и др., 1994] has shown the existence of a few moisture categories in grounds – namely, gravity moisture, capillary moisture, film moisture, loosely coupled and firmly bound moisture.

Each moisture category affects the speed V_p and elastic modules in a different way. For example, the humidity of sand is mainly due to gravitational water, the moisture of clays is associated with the bound film and absorbed water; with respect to loam and sandy loam, all moisture categories of are of great importance. It was found that, at defined values of moisture content in clays, loam, sandy loam and fine-grained sands, a rather sharp decrease in V_p is observed (Figure 140).

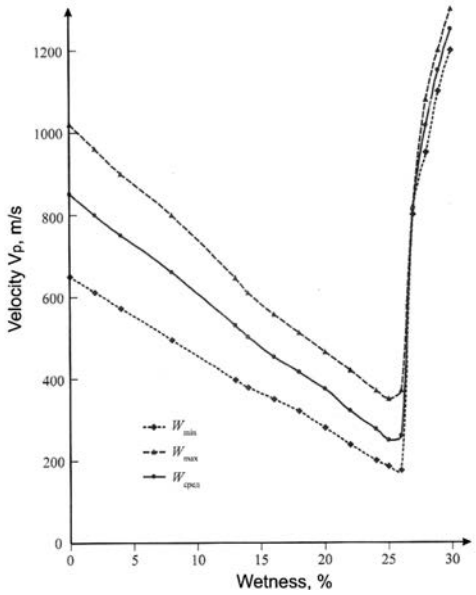

Figure 139. Body wave velocity dependence on dispersion ground humidity [Кригер и др., 1994]

The moisture interval, wherein a sudden increase in the velocity of the body (longitudinal) wave V_p is obseved, has been called *"a paradoxical moisture interval"* [Кригер и др., 1994]. Depending on the amount of water and moisture categories, there may be several moisture thresholds in the dispersed soil. When passing through these moisture values, the seismic properties of soils are changing abruptly [Алешин, 2010].

5.1.6. Examples of seismic microzoning in the East Baltic Region

Generally, the East Baltic Region is characterized by a low level of seismic hazard. For instance, according to seismic risk assessment results obtained in 2007, Latvia pertains to the territories with a very low seismicity. This means that PGA on stiff (hard) grounds (Pre-Quaternary deposits) may exceed 10–13 cm/sec^2 with the 10% probability within 50 years – in Sigulda, Riga, Olaine, Cēsis, and in the neighborhood of those cities [Ņikuļins, 2011].

According to [Eurocode 8, 2005], on areas characterized by low seismicity level, the calculated acceleration of A-type ground does not exceed 0.08 g (0.78 m/sec^2); in other words, the entire seismic response $a_{gR}S$ is not higher than 0.1 g (0.98 m/sec^2). In the case of very low seismicity, the calculated acceleration of A-type ground, i.e., a_{gR} is not higher than 0.05 g (0.49 m/sec^2). In other words, the entire seismic response $a_{gR}S$ is not above 0.05 g (0.49 m/sec^2).

However, the low level of seismic impacts on A-type hard grounds does not guarantee the complete safety of buildings, engineering facilities, and environmentally hazardous facilities located on loose and water-bearing grounds. This is due to the unfavorable physical and mechanical properties of the soils in the East-Baltic region.

5.1.6.1. The Salaspils nuclear-power reactor site

For the first time, seismic microzoning was conducted in Latvia on the territory of the Salaspils research studies nuclear reactor. From 1990 to 1991, the Industrial and Research Institute for Engineering Surveying in Construction carried out complex geological-geophysical and seismological studies on the seismic microzoning of the reactor site. Taking into account the importance of the facility, SMZ studies were preceded by a preliminary research conducted with the aim of specifying the initial seismicity of the area more in detail.

The expected maximum epicenter intensity (MCE – the maximum credible earthquake) on the Salaspils reactor site, with respect to II category grounds, was assessed as 7.3 on the MSK-64 scale [Севастьянов, 1991_*upm*]. Such a seismic impact could have been induced by the Liepaja – Riga – Pskov seismogenic area. Those assessments were based on the correlation between the length of seismogenic fault and the earthquake magnitude. The magnitudes assessed this way were used in the macroseismic field equation derived for the Russian Platform [Savich & Suvilova, 1988]. The high intensity level was mostly associated with the reactor site proximity to the Liepaja – Riga – Pskov seismogenic area (4 km).

The maximum computed earthquake magnitude is equal to 4.5. The physical and mechanical properties of the grounds were obtained based on the analysis and generalization of research materials of various years, and according to the stratigraphic test well data obtained in 1990.

The upper part of sedimentary cover (up to 10–15 m) is represented by soft loam soils characterized by average velocities of shear *S*-waves $\overline{v}_S^{0-15}$ = 400 – 550 m/sec.

The augmentation of seismic activity on the reactor site (a direct task of seismic microzoning) was assessed based on the seismic impedance comparison method, by using the following formula:

$$\Delta J = 1.67 \cdot \lg(v_0\rho_0 / v_i\rho_i) + e^{-0.04 \cdot h^2} + \Delta J_{res} \quad (57)$$

where ΔJ – general increment of seismic intensity in points of MSK-64 scale; $1.67 \cdot \lg(v_0\rho_0 / v_i\rho_i)$– the part of increment associated with the difference between seismic impedance values of the reference ground ($v_0\rho_0$) and on investigated area ($v_i\rho_i$); $e^{-0.04 \cdot h^2}$ – the part of increment associated with water saturation of the 10 m-thick layer; ΔJ_{res} – the part of increment associated with the resonance properties of the sedimentary cover with the thickness from 10 up to 100–200 m, located over bedrock (i.e., given that there exists a strong refracting boundary within the geologic medium).

The seismic conditions (seismic impedance of the grounds) on the site differ insignificantly. Deviations of seismic intensity from the "average" level are insignificant. Soil conditions are assigned to the II soil category as according to seismic properties. The augmentation of seismic intensity on the site, including the reactor, is absent ($\Delta J = 0$). As a result, the total intensity of the maximum estimated earthquake J_MEE = VII points. Deepening the basement of the reactor structure to 12 m allows one to reduce the seismic intensity due to an increase in the seismic impedance of the base soils. Amplitude-frequency characteristics (horizontal component) of the medium in the central part of the Salaspils nuclear reactor site is depicted in Figure 140.

The maximum value of spectral level for the horizontal component is 8.8 Hz (Figure 140). The Earth model consists of 5 layers located on a rock half-space. The accepted

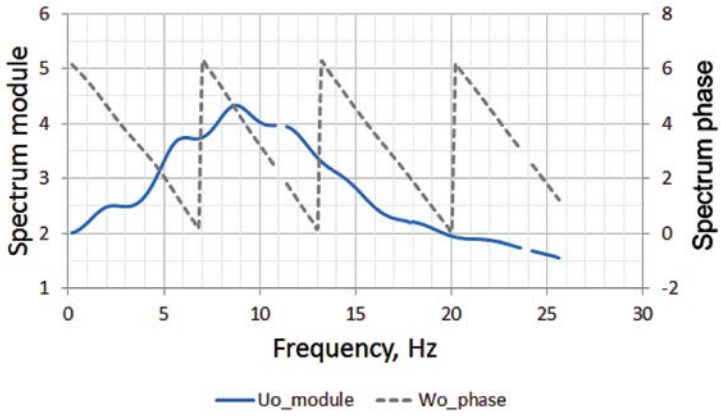

Figure 140. Amplitude-frequency characteristics (horizontal component) of the medium in the central part of the Salaspils nuclear reactor site

seismic intensity on the site corresponds to 190 cm/sec^2 for MEE (the maximum estimated earthquake) and 99 cm/sec^2 for PE (projected earthquake).

In the Russian terminology these types of estimates of an earthquake correspond to the following characteristics. Projected earthquake (PE) is an earthquake of a given seismicity with an average repeatability of once every 500 years. The maximum estimated earthquake (MEE) is an especially powerful earthquake with an average frequency of once every 5,000 years; usually exceeds by two times the intensity of PE with similar spectral characteristics.

5.1.6.2. Seismic zoning of Kaliningrad

After the Kaliningrad earthquakes of 2004, the O.Schmidt Institute of Physics of the Earth under the Russian Academy of Sciences (RAS), seismic microzoning of the territory of Kaliningrad was carried out in 2007–2008. The seismic microzoning studies were preceded by some works on a detailed seismic zoning. The research efforts included, in particular, seismological observations, paleo-seismologic studies of geologic exposures, trenching, archival research, plotting source zonation (SZ) maps, the determination of maximum possible earthquakes magnitudes, their depths, and specification of other parameters. In order to study seismic-geological characteristics, seismic sections on individual areas were studied, based on the propagation of shear waves in the Earth strata – down to depths of the order of 30 m; anomalous sections with low-velocity layers were identified, a set of seismic microzoning maps was plotted at a scale of 1: 25000, and frequency characteristics of seismic oscillations of soil strata were determined with respect to the main types of soil. As parameters of "medium" soils in accordance with the recommendations [PCH 60-86, 1987], the density ρ_{ave} = 1.8 G / cm3 and the velocity of shear waves v_S = 300 m/sec were adopted.

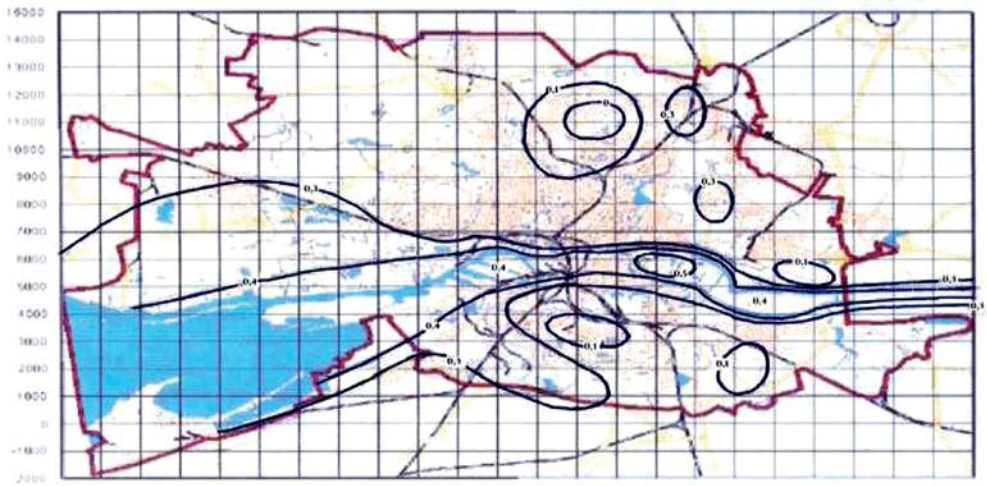

Figure 141. Map of seismic intensity augmentation on the territory of Kaliningrad, taking into account the 10 m thick layer of sedimentary deposit [Алешин и др., 2014]

According to RF reference documents and the general seismic zoning map OSR-97-V (OCP-97-B) relating to significant industrial engineering facilities, the territory of the Kaliningrad Region was attributed to the area, where seismic impact is not expected to exceed 5. Nevertheless, a 6.5-magnitude earthquake on the MSK-64 scale took place there in epicenter area. In 2007–2008, a complex of seismological, seismotectonic, and geological geophysical studies was carried out by the Institute of Earth Physics under the Russian Academy of Sciences, and detailed assessments of the seismic hazard of Kaliningrad and its environs were obtained. In particular, the Bakalinsk SSZ was singled out, for which the maximum magnitude is M_{max} and the depth of the focus is h = 15 [Алешин и др., 2014].

The generalization of data on the wells of Kaliningrad showed that the city's territory can be divided into the moraine (uplifted) and the flood plain (lowered) parts. With the exception of the artificial layer of soil, the density of the moraine part of the city is within the range from 1.9 to 2.2 t/m^3, and the velocities of flexural (transverse) waves vary from 320 to 400 m/s^2. The deposits of the moraine part are represented by loam, sandy loam, clay, sand, and marl. In the floodplain areas of the Pregol River, along with sandy-argillaceous strata analogous to the moraine soil, anomalous engineering geological sections are also found, which include weak soils, such as peat or flowing ooze. For the flood plain, ρ_{flo} varies from 1.2 to 2.2 t/m^3, and v_{flo} varies from 90 to 400 m/sec^2. Anomalous parameters characterize the peat deposits with ρ_{peat} = 1.1 t/m^3 and v_{peat} = 90 m/sec$^{2.}$

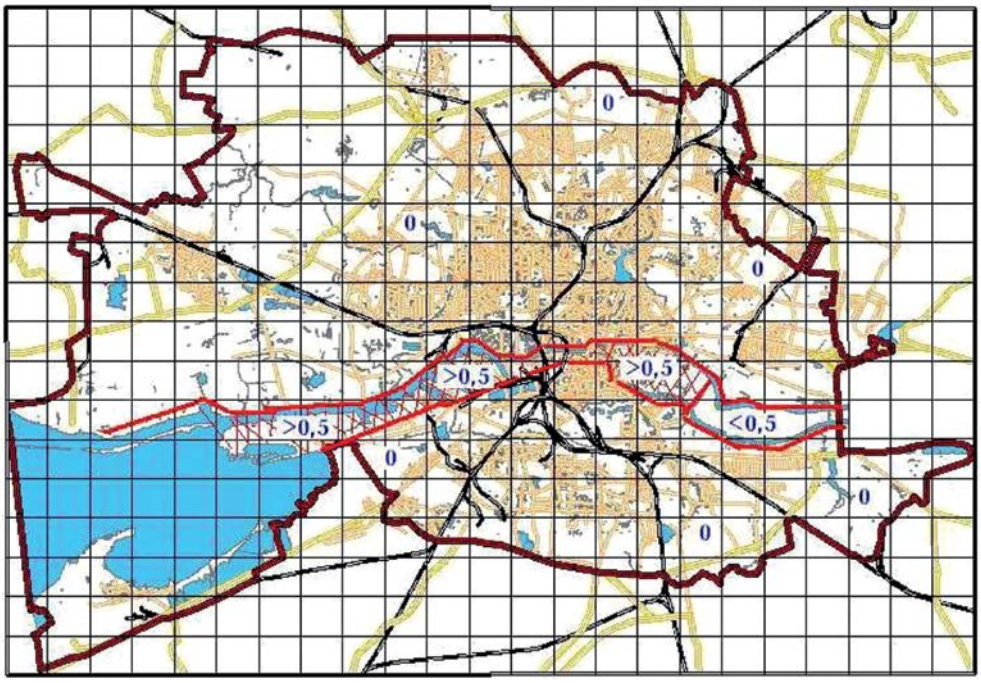

Figure 142. Map of seismic intensity augmentation on the territory of Kaliningrad, taking into account the 30 m thick layer of sedimentary deposit [Алешин и др., 2014]

Taking into account the 10 meter thickness of sedimentary deposits, in the flood plain part of the Pregol River, the augmentation of seismic intensity ΔJ in the floodplain part of the Pregol river is equal to 0.4–0.5 points of MSK-64 scale. In other, local areas, $\Delta J < 0.3$ points of MSK-64 scale (Figure 141). Taking into account the 30 meter thickness of sedimentary deposits, the augmentation of seismic intensity ΔJ in the floodplain part of the Pregol River = 0.5 points of MSK-64 scale (Figure 142).

5.2. The applied approach used in seismology for East Baltic Region research

The primary task of seismological methods is to study the earthquake nature, make forecast of seismic parameters to ensure protection of structures against seismic waves or some other seismic source-induced impact. Depending on the type of a seismic wave, the epicenter intensity may vary significantly. Since earthquake-induced seismic waves are propagating through the depths of the Earth, seismology was used to study the deep, inner structure of the Earth. These research areas are related to ensuring safety of people and structures, as well as obtaining new scientific knowledge about our planet. However, the application of seismology extends further, thranscending the classical methods described above.

As regards the applied research area, a note should be made, first of all, of the significance of seismology associated with seismic microzoning of construction sites used for designed or already existing structures.

SMZ is intended to assess the influence of soil properties upon seismic vibrations recorded on sites where specific structures are located, or, on the agglomeration areas.

During the past decade, the SMZ role in the East Baltic Region (EBR) has increased significantly. First, notwithstanding the low level of seismic activity in EBR after the Kaliningrad earthquakes took place in 2004, SMZ promotion started to progress largely due to economic feasibility thereof. The costs of remedial actions required to eliminate earthquake sequences can far exceed the costs of preventive measures aimed at the identification of parts of urban infrastructure, which are most vulnerable to seismic impact. Secondly, the development of nuclear power engineering dictates the necessity of conduction of seismological surveys both at the design stage and at the stage of operation. Therefore, seismic zoning and microzoning are no longer deemed "exotic" directions of research and are gradually spread on the territory of the East Baltic Region.

Is the importance of seismology confined to the above-stated lines of research in the East Baltic Region, or maybe there exist some opportunities for its practical application as well? Answering this question, two points should be noted.

The low level of natural seismicity in East Baltic Region means that natural seismic phenomena rarely affect buildings and structures and have low magnitude values – except for some rare cases like the 4.7 magnitude – Osmussaare earthquake (in Estonia) and the 5.2 magnitude – Kaliningrad earthquake of 2004.

Human-induced seismic phenomena sometimes may adversely impact buildings and structures. An example is an accident that took place in Mezhciems, a district of Riga

City, on July 29, 2014. As a result of pile driving jobs performed on a construction site located at a distance 120 m from a high-rise apartment building, the roof structure of the house was deformed. Strong vibration was enhanced by a few unfavorable factors – precipitation and ground moistening, soft soil existing in the accident area, and the proximity of the Olaine-Inčukalns tectonic fault to the above-mentioned residential building (about 100 m) [Nikulins, 2017a].

Soil conditions are an unfavorable seismic-geological factor affecting seismic vibration intensity generated both by strong seismic sources and human-induced vibration caused by rail trains, trams, and load-carrying vehicles in cities or on the corresponding trunk railroads and highways. Ground conditions in EBR are characterized by non-consolidated, characteristic water-encroached grounds lying on more dense deposits like Devonian dolomites, for example. As a rule, seismic wave propagation velocities in bottom set beds by far exceed those velocities surficial ground.

In this case, seismic impedance ratio $\rho_1 V_1 / \rho_2 V_2$ between grounds ($\rho_1 V_1$) and rock materials ($\rho_2 V_2$) is of importance. Seismic impedance is the multiplication of deposit density ρ by seismic wave propagation velocity V. A great difference between the seismic impedance values of ground materials and those of the underlying rocks lays the groundwork for vibrational enhancement as a result of resonance phenomena. The second condition for resonance enhancement should be the equality between ¼ of a wavelength and the thickness of loose coating (Figure 143).

This condition can also be satisfied, since frequencies from 1 Hz and higher are present mostly in the spectra of human-induced signals and, partly – in those of ambient seismic noise (ASN). Exactly at these frequencies, the occurrence of resonant enhancement of the earth covers is possible, taking into account the insignificant thickness of the covers and a small velocity of shear waves V_S.

For example, a survey carried out in Kaliningrad (Russia) showed [Paseka et al., 2014] that the thickness of the upper, most unconsolidated layer represented by peat

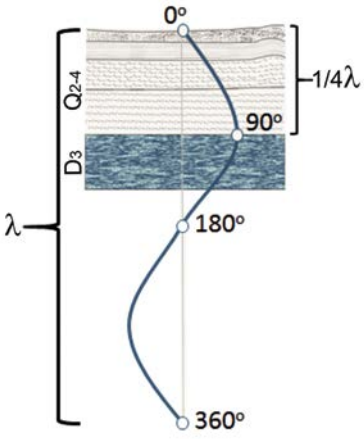

Figure 143. Condition for the earth cover resonance occurrence under the impact of seismic waves

and peat-bearing sediments does not exceed 20–25 m, and the shear waves propagation velocities do not exceed 150 m/sec^2. Dense rocks (the so-called technical foundation) are located at depths of 60–70 m. The shear wave velocities within them are $V_S \geq 750$ m/ sec^2. For the intermediate layer, V_S = 150 - 500 m/sec^2. An additional unfavorable factor in Kaliningrad is the groundwater level which is mainly located at a depth of 0.4 to 3.3 m. The response spectra estimated for the two soil-thickness models showed that the maxima of spectral acceleration are within the range 4–5.5 Hz [Aleshin et al., 2014]. This is exactly the frequencies at which the amplification of the soil thickness vibrations is possible due to resonant phenomena.

Vibrations generated by man-made sources of various origins (like transport and pile driving) and by ambient seismic noise (ASN) may enhance due to resonant phenomena taking place in grounds, and may have a detrimental effect on buildings and structures. ASN consists of the natural (ASN_{NTR}) and the man-made (ASN_{MMD}) components.

Ambient seismic noise – microseism – lies within the frequency range about lower than 1 Hz, whereas the human-induced seismic noise – micro tremor – lies within the frequency range higher than 1 Hz. The frequency 1 Hz is not the absolutely large

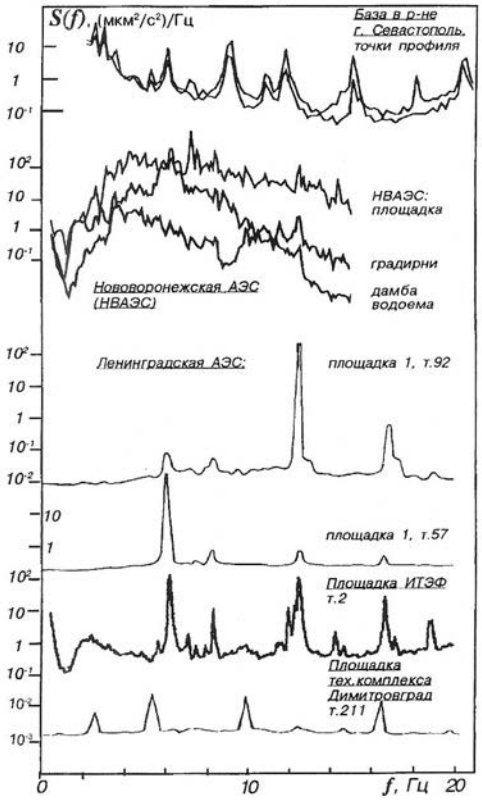

Figure 144. Characteristics of human-induced seismic sources of mechanical vibrations: power spectra of seismic noises on sites for industrial facilities [Юдахин & Капустян, 2004]

velocity contrast of the above-mentioned types of seismic noise. Close to that frequency, the frequency bands of the natural and the human-induced seismic noise may overlap. The natural and the human-induced components of ASN may affect buildings and structures differently. Large periods of microseisms may coincide with natural cycles of vibration of high-rise buildings and structures (2–9 sec) and individual crustal blocks (50–65 sec), whereas the high-frequency micro tremor may affect smaller-size facilities like earth cover, house footings, structure elements, etc.

It should be noted that the human-induced noise generated by motor traffic is actually ceaseless – at least, during the entire business-day period.

This repeated exposure takes place for years and dozens of years. Moreover, some individual manmade facilities (NPP, HPP, and combined heat and power-supply plants (CHPSP) may generate signals within definite frequency bands. An example here is the investigations carried out in the neighborhood of nuclear power plants and production facilities [Yudakhin & Kapustyan, 2004].

Spectral peaks are most distinctly observed, if we observe the site of the Leningrad NPP (site 1, points 92 and 57 on Figure 144), the site of Institute of Theoretical and Experimental Physics (ITEP) (point 2) and the production complex site in Dimitrovgrad (PCD) (point 211). As regards the Leningrad NPP, the peaks are located at the frequencies ~ 12.5 and 6 Hz, and for ITEP – at the frequencies ~ 6.2, 12.4 and 16.4 Hz and for PCD – at the frequencies ~ 2.5, 5.5, 10 and 16.5 Hz [Юдахин & Капустян, 2004].

Therefore, despite the low seismic activity in the East Baltic Region, some definite prerequisites still exist there for the augmentation of human-induced seismic impact from transport (like motor and rail traffic, industrial enterprises, power facilities, and ASN. These prerequisites are: inundated (water-encroached) grounds and the large difference in seismic impedance between grounds and the underlying rocks). Since this impact is of a continuous, cyclic nature, there exists a probability for the fatigue effects occurrence in foundations and engineering materials.

Apart from the adverse effect exercised by seismic signals on buildings and structures, seismic signals can be useful for the assessment of dynamic parameters of grounds, and may be used in other types of applied research to which this chapter is dedicated.

5.2.1. Structural monitoring

Seismic micro zoning provides information on seismic properties of a site where buildings, structures, and other facilities are located. The major facilities that are in need of protection against seismic impact are buildings and structures proper, bridges, high-speed railways, masts, elevated water tanks, wind turbines, and other facilities that can be located on the site. Buildings and structures are physical bodies of fixed dimensions and these have natural frequency of oscillations. Seismic energy excitation within a structure depends on several factors, as follows: 1) the earthquake source (ES), 2) the properties of geologic environment lying on the way of seismic waves propagation from the source to the structure proper (ES-SP), 3) the properties of seismic geological setting on the local site beneath the structure proper (PLS), 4) soil-structure interaction

effects – SSIE. The sum of the first three factors leads to the occurrence of a "free-field" ground motion. The structure response to the "free-field" ground motion depends on the fourth factor – SSIE. In particular, the acceleration inside a structure is caused by the flexibility of the foundation whereon the structure sits, and by the differences between the foundation and "free-field" movements.

With the growth and development of urbanized areas, the construction of large energy complexes, the storage of radioactive and toxic materials, the development of transport communications and complex transport systems, the responsibility for the technical condition and proper control of the reliability of operated structures and systems increases. Systematic monitoring or periodic diagnostics of the technical condition of structures and systems can fix deviations in the properties of the structure material or geometric form from the standard; moreover, monitoring and diagnostics allow one to identify the damaged sites. An important element of this control is the so-called monitoring of the state of structures and systems, or Structural Heals Monitoring (SHM). SHM is a relatively new direction in engineering research, developing over the past 10–20 years. Structural monitoring is an experimental part of the dynamics of structures.

A keen interest in *SHM* monitoring has essentially increased with the development of major construction projects – such as large dams, cable-stayed bridges, oil platforms, and offshore platforms. Besides, *SHM* targets of research can be telecommunication and television relay towers, elevated water tanks, and high-rise buildings. A peculiar feature of SHM is that high-rise buildings, sophisticated engineering facilities, and other objects are individual as a rule; consequently, no uniform testing procedure exists with respect to them. As a rule, SHM is aimed at a long-term evaluation of a building or structure condition, and the comparison of obtained characteristics with reference standards. Reference standards can be obtained right after the commissioning of the respective building or structure.

SHM monitoring is expedient if associated with the solution of the following problems: [Ross & Matthews, 1995; Mita, 1999]:

1. The existing objects (structures) change verification;
2. Assessing the safety and efficiency of facilities impacted by external works;
3. Monitoring in process of demolition work;
4. Monitoring of facilities subject to a long movement or material degradation;
5. Feedback provision to improve the subsequent design, based on the gained experience;
6. Fatigue assessment of structure materials;
7. Testing new construction methods and new building structures;
8. Assessment of structural reliability after an earthquake;
9. assessment of material efficiency upgrading when construction deadlines are cut down, and the growing need in the structure servicing;
10. Servicing facilities created on the basis of design philosophy.

The SHM method began with the simplest, but, at the same time, important tasks – namely, visual surveys and the assessment of structure condition. At the same time, the targets of research were such phenomena as cracking, flaking, and deformation. Over

time, SHM became less subjective, since new ways of measuring, storage, managing, integrating and interpreting the results were introduced. As a result of a holistic, systematic approach, there appeared much more opportunities for interpretation. SHM has evolved into a continuous system identifying a physical or parametric model of a structure by using time-dependent data [Brownjohn, 2017].

An example of a monitoring and warning system is shown in Figure 145. The facility examined is located in a seismically hazardous area.

The purpose of a monitoring system is to assess building's response to seismic impacts both before and after earthquakes. As regards a warning system, it allows quick asessment of the security of the building and taking the corresponding steps aimed at the building's renovation.

It goes without saying that, in the context of low seismicity, there is no need to develop a warning system at all. However, the monitoring system is, essentially, a universal one. To carry out SHM, both the passive and the active methods may be used. The passive method is based on the detection of a structure's response to ambient perturbations – without any actuation of a sounding signal. The source in this case may be urban, human-induced noise associated, first of all, with rail or motor traffic. The active method implies the usage of artificial excitation. Normally, passive methods can be easily implemented. They can be used in SHM to ensure detection of global deteriorations. Generally, however, active methods are more precise in localizing the damaged section.

From the standpoint of engineering control of buildings and structures, the main tasks of SHM are the detection of damages and the determination of the characteristics of engineering structures. The parameters under study make it possible to assess the vulnerability of engineering structures. The time supervision of engineering facilities

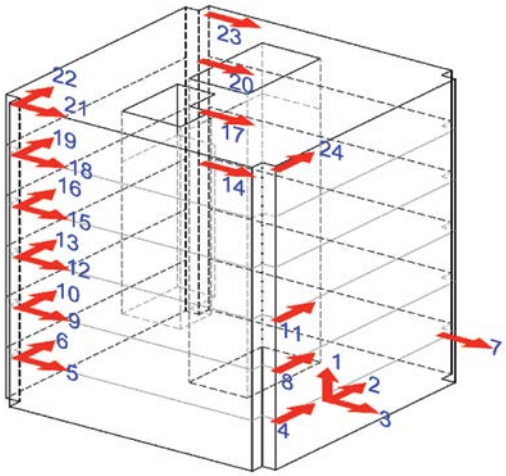

Figure 145. Structural monitoring scheme of a 5-storey building of health-care center in Memphis, Tennessee [Ulusoy et al., 2012]

involves the use of periodic selective measurements of dynamic response by using a sensor system, obtaining characteristics sensitive to damage inflicted on structures, statistical analysis of these characteristics to determine the current state of the structures, informing the user about the nascent damage to the structure, and estimating the useful life of the structure.

The updating of structural monitoring is based on three main prerequisites: 1) the occurrence of new building materials and technologies, 1) the inevitable ageing and degradation of the existing structures, and 3) the enhancement of human-induced, dynamic, and cyclic loading directed to structures.

New construction materials and technologies made it possible to implement the most ambitious, large-scale plans to create high-rise buildings and large engineering structures with complex engineering and technical solutions. Large-scale structures also pose more rigorous requirements to organization of building safety and controlling the parameters of physical and mechanical properties of materials and the geometry of structures. The damage that can arise due to insufficient attention to the safety of high-rise buildings and engineering facilities can substantially exceed the costs of measures of organizing the building safety (namely, systematic monitoring, periodic expert assessments of the physical and mechanical parameters of materials and geometry of structures).

Thanks to the appearance of new building materials and construction technologies, the volumes and rates of construction of buildings were increased. The East Baltic region can serve as an example. In Riga, the capital of Latvia, there is 29 high-rise objects of various purposes, the height of which exceeds 60 m. Of these, 15 objects have been built over the last 15 years – such as the Riga TV Tower (368.5 m), Z-Towers (123 m), Sun Stone (123) m), and Panorama Plaza II (114 m), Panorama Plaza I (99 m).

Quite a number of high-rise buildings are located in the capitals of Estonia and Lithuania. There are 22 objects in Tallinn, the height of which exceeds 52 m. Among them, there are such modern buildings as Swissotel Tallinn (117 m), Tornimae Maja (117 m), and Radisson Blu Hotel (104.8 m). In Vilnius and other Lithuanian cities, 11 objects have been built, whose height exceeds 77 m. Among them are such modern buildings as the Europa Tower in Vilnius (148 m), Pilsotas (112 m) in Klaipeda, Helios City Tower *A* in Vilnius (96 m), Europa Square Apartments in Vilnius (95 m) etc.

High-rise buildings have sufficiently large natural periods of vibrations (structural periods). The fundamental periods of vibrations can be assessed, for example, based on the recommendations of the standard from *American Society of Civil Engineering* [ASCE/SEI 7-05, 2006]:

$$T_a = C_t h_n^x \tag{58}$$

where, h_n is the height in feet *(ft)* above the foundation, to the highest level of the structure; x and C_t are the coefficients.

The dependence of the fundamental mode frequency on the height and material of buildings and structures is given in Figure 146. The logarithmic dependence of the building height (in meters) on the fundamental mode frequency is shown with respect to: 1) steel frames with resistance to the moment of motion (Steel); 2) Concrete frames with resistance to the momentum (Concrete); 3) eccentrically-fixed steel frameworks (Eccentricity); 4) all other structural systems (Other systems).

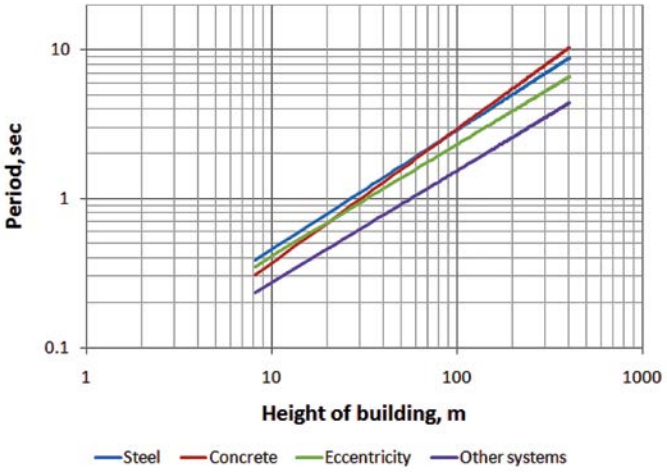

Figure 146. Fundamental mode oscillations dependence on building height and material

The fundamental frequency of the natural period of vibrations of the Riga TV tower is about 8.2 sec. (0.122 Hz), while that of Panorama Plaza I is about 2.9 sec. (0.345 Hz). The natural vibrations of the other above-mentioned high-rise buildings in Riga lie within the interval between the stated values.

As a result of the use of structures, the inevitable ageing and degradation of them takes place eventually. The building materials used for construction may change their properties with the loss of their strength characteristics. Most frequently, it takes place due to corrosion processes within metallic structures and fatigue processes in the material.

Fatigue processes develop under the influence of a dynamic load, resulting in the formation of fatigue cracks. A prolonged cyclic, vibrational action is a prerequisite for the occurrence of fatigue cracks in solid materials. The fatigue cracks propagation can lead to damage.

The fatigue phenomenon occurring under the influence of cyclic loads was first discovered by Wilhelm Albert [Schultz, 1996].

The term "*fatigue*" was first introduced directly in 1839 – after a reduction in the strength of steel structures under the impact of cyclic stresses was observed. Later, the fatigue phenomenon was also investigated on concrete-fabricated objects, starting from 1900. The process of fatigue cracks occurrence is observed within concrete items at a repeated compressive and a repeated flexural loading. However, this phenomenon is also encountered at reversed flexural loading and repeated tensile loading [Lloyd et al., 2007]. Accounting for the occurrence and development of fatigue cracks within concrete is especially important if the respective structures are located near sources of cyclic loading.

Since concrete has become a modern building material relatively recently (approximately, from the middle of the XIX century), and reinforced concrete – even

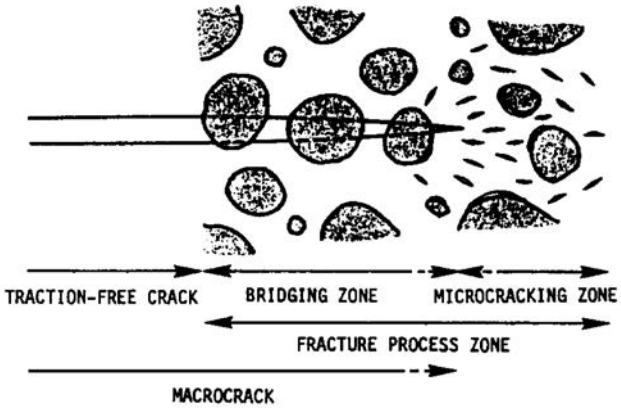

Figure 147. Schematic illustration of the area of crack formation process [Horii et al., 1992]

later, the study of their physical mechanical properties was delayed in time. The present-day studies of fracture mechanics of quasi-brittle materials such as concrete, rock, and ceramics, have shown that destruction occurs in a certain zone. This cracking zone is located at the head of the crack, which consists of a microcracking zone and a bridging zone. A schematic illustration of these processes is shown in Figure 147.

Microcracks occur within the microcrack zone where microcracks mostly propagate. The junction zone is part of the macrocrack zone, along which, stress is transferred by way of aggregate or fibre reinforcement. The role of the junction and the microcrack-occurrence zone can be different in different materials. The importance of using instrumental and analytical methods to predict the destruction phenomena within brittle and disordered materials, and to identify and simulate the destruction mechanism – becomes obvious.

The essential factors of the dynamic load are the traffic flow-induced vibration and the weather impact on buildings and structures (wind, precipitation). The transport component of the dynamic load is especially relevant for urban agglomerations. Buildings and structures located along transport communications with intensive traffic are also subject to an anthropogenic, dynamic load. The traffic flow intensity is continuously increasing. For example, according to data from LLC "Latvijas Valsts ceļi" [LVA, 2015_*si*] covering the period from 2012 to 2015, the motor rally on Latvian state roads grew by 17%, including freight transportation volume that increased by 15.7%. Freight transport along with rail transport and the trams movement in cities is the most intensive factor of anthropogenic, vibrational loading on soils and structures.

Apart from the modern high-rise buildings and structures, there are many old and ancient architectural monuments in the East-Baltic region, which are valuable from historical, architectural, and cultural point of view. These buildings have been standing for several dozens and hundreds of years. During this time, the building materials could significantly change their physical and mechanical characteristics under the influence of static load and the ever-increasing dynamic load. The condition of these buildings is

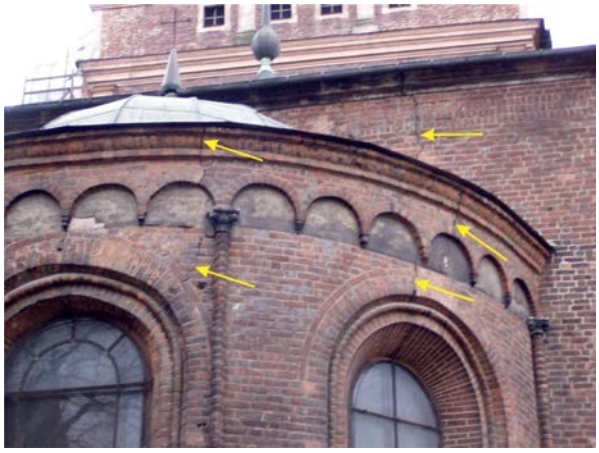

Figure 148. Cracks on the Riga Dome Cathedral

frequently a matter of concern. For example, cracks were seen on the walls of the Riga Dome Cathedral (Figure 148).

The Riga Dome Cathedral is the largest and one of the oldest religious buildings in Latvia and the entire Baltic region. Laying the foundation for the Riga Dome Cathedral dates back to the reign of Bishop Albert – it took place on July 25, 1211. In 2001, funds were allocated for the repair and preservation of the Dome Cathedral portal. Nevertheless, after the completion of the project it was discovered that the Cathedral suffered more severely from structural instability. Cracks were found in basements and lateral aisles. Due to these problems, some parts of the church are closed to visitors since 2004. The World Monuments Fund in 2006 included the Riga Dome Cathedral in the list of monuments of universal importance [https://www.wmf.org/project/riga-cathedral].

Additional funding from *Kress Foundation* was provided to carry out structural monitoring by the Riga Technical University – with the view of solving the Dome Cathedral instability problems.

According to State Control data as of November 20, 2015, the total number of monuments on file in Latvia was 8848. Out of this number, 5310 monuments are nationally significant, and 3538 are topical [*Valsts Kontrole* (State Control), 2016_*si*].

A number of significant problems arise with respect to the ageing and wear of bridges.

The condition analysis of 928 bridges erected on motor roads of Latvia has shown that 720 bridges have damaged waterproofing compounds and carriageway items, while 175 bridges have their load-carrying structures damaged, and prompt repair is acutely necessary to stop the progressing damage and a possible reduction of load-carrying ability of the bridges under study [Highways of Latvia].

SHM based on measurement of vibration can solve direct and return problems. At the solution of a direct task dynamic characteristics are defined. At the solution of the return task, the known dynamic characteristics are used for definition of characteristics of damages.

5.2.2. Structural analysis

Structural monitoring is the experimental part of structural dynamics research. The theoretical part of structure dynamics research is structural analysis. Structural analysis is necessary to simulate the behavior of a physical structure under applied forces. The correlation of model analytical calculations with experimental results makes it possible to identify structural variations or changes in material properties.

The impact may be both static and dynamic one. The principal criterion of type of action is the acceleration magnitude. Therefore, the dynamic and the static analysis should be distinguished. Static load is either constant or it changes very slowly as against natural frequency of the structure under study, whereas the dynamic load is changing rapidly.

For that reason, if a dynamic load is applied, the structural response should be calculated at every instant.

Dynamic analysis is a type of structural analysis considering structural behaviour under dynamic load. Dynamic analysis can be used to look for dynamic movements and for modal analysis.

Modal analysis allows one to determine the frequency and shape of oscillations, which depend on the design model of the structure, to get an idea of the relationship between the frequency response functions and their individual modal parameters. Knowledge of the frequencies and vibration modes makes it possible to foresee a thorough picture of constrained vibrations, optimize the analysis process, identify the unfavorable values of the frequencies of periodic loads or the duration of impulse (transit) loads, doing all that more purposefully, – and to conduct the measurement process with a greater accuracy.

Structural analysis allows one to analyze both the time-controlled deterministic processes changing according to a definite law, and stochastic processes changing at random (stochastically) and characterized by stochastic values. For example, ambient seismic noise refers to stochastic processes. A typical example of a dynamic load is cyclic loads that have a certain frequency, period, and intensity. The response of a system (structure) to a cyclic load can be accompanied by damping of the oscillations, stable oscillations without

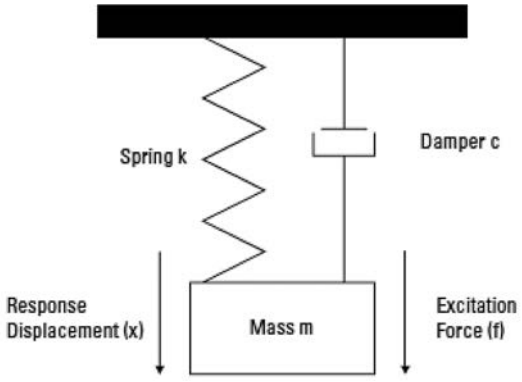

Figure 149. Discrete parameters of the simplest SDOF model

damping, or excitation, i.e. an increase in the amplitude of the oscillations over time. Using the total mass and rigidity of structural bonds, different periods of oscillation of the structure are calculated, from which the structure can resonate in a natural way.

Structural analysis is based on the finite element method – FEM, which is a computational (numerical) method of solving problems in the field of engineering and mathematical physics. FEM is intended to solve partial differential equations, as well as integral equations in problems of applied physics. The essence of the method lies in the fact that the domain in which the solution of differential equations is sought is split into a finite number of elements. Subsequently, a certain type of approximating function is selected in each area. The coefficients of approximating functions are determined and a system of linear, algebraic equations is compiled. The number of equations depends on the number of nodes, and is proportional to the number of elements. Despite the fact that real structures are complex systems with multiple degrees of freedom (MDOF) and have some degree of nonlinearity, they can be represented as a superposition of simple, linear models with a single degree of freedom (SDOF). This approximation makes the MDOF models easier to understand.

An idealized *SDOF* system can be represented in the form of a mass, spring, damper, or excitation (Figure 149) [Agilent Technologies, 2000].

Mass, spring, and dumper describe a physical system. The kinetic and the potential energy within the system are stored in mass and in spring, respectively. The energy enters the system through excitation and dissipates through damping. The elements of an idealized physical system can be described by the motion equation, as follows:

$$m\ddot{x} + c\dot{x} + kx = f(t) \tag{59}$$

where, m – mass, x – displacement, c, k – coefficients.

$$\omega_n^2 = k/m \tag{60}$$

$$2\zeta\omega_n = c/m \tag{61}$$

$$\zeta = c/\sqrt{2km} \tag{62}$$

where, ω_n – natural frequency (rad/s), ζ – attenuation.

This equation connects the action of mass, stiffness, and damping, and makes it possible to calculate the natural frequency and the vibrations damping factor of the system. The complex routes of the equation for solving the SDOF system without excitation look as follows:

$$s_{1,2} = -\sigma + j\omega_d \tag{63}$$

where, σ – damping rate, ω_d – damped natural frequency.

The attenuation factor can also be presented as percent of critical damping, i.e., such a damping where the system has no vibrations at all. This percent ratio is more frequently used in modal analysis. As regards structural dynamics, only the < 1 damping case is of interest. In that case, the excited structure vibrations will attenuate slowly (Figure 150).

Frequency-phase response of a non-excited *SDOF* system looks, as follows (Figure 151).

The actual MDOF structures with n degrees of freedom are approximated by the system with interrelated simplest *SDOF* structures, i.e., structures with one degree of freedom (Figure 152).

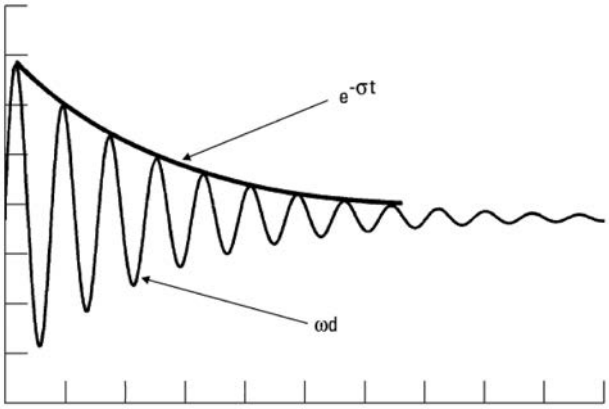

Figure 150. Impulse response with damping for SDOF system

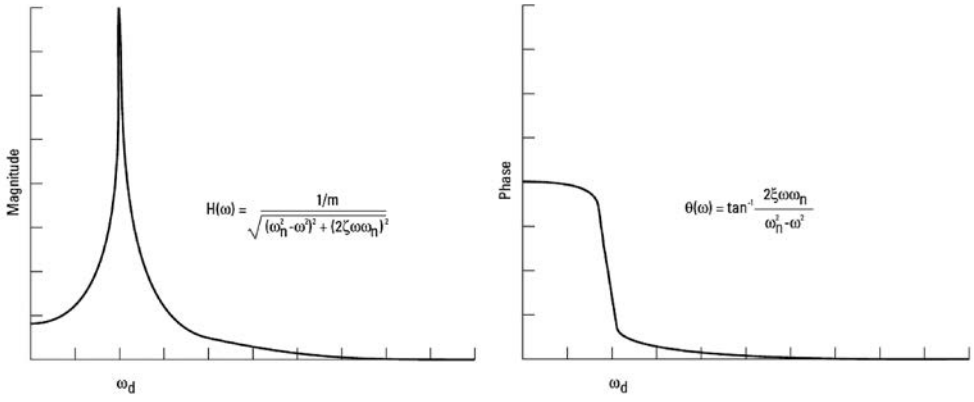

Figure 151. Frequency-phase response of SDOF system without external excitation

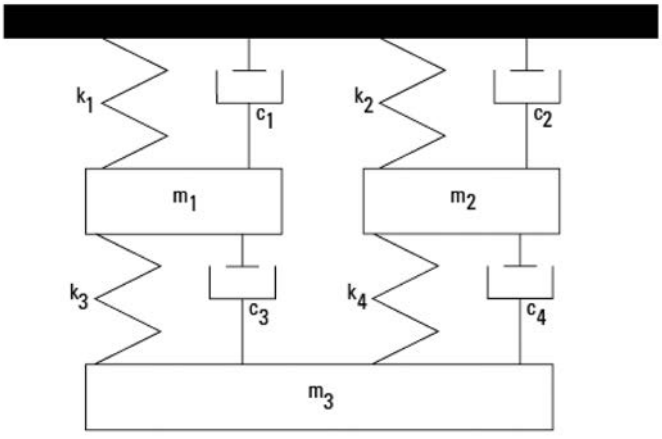

Figure 152. Discrete parameters of MDOF model

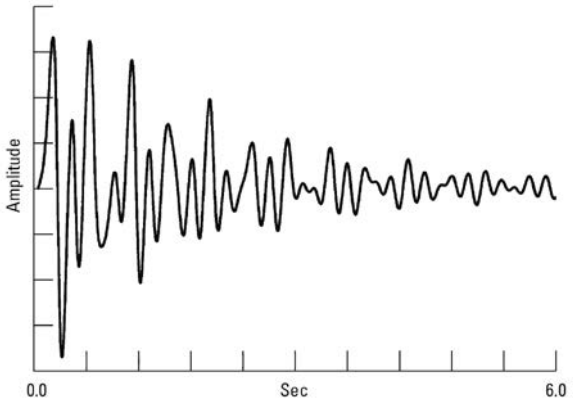

Figure 153. Impulse response with a free damping of MDOF system

In this case, the motion equation is expressed in matrix form, where

$$[m]\{\ddot{x}\} + [c]\{\dot{x}\} + [k]\{x\} = \{f(t)\} \tag{64}$$

$\{\phi\}_r$, $r = 1$, n modes

Solution of equation (64) for MDOF system also yields modal parameters (roots of equation) of the system. However, in that case, a displacement vector called mode shape $\{\phi\}_r$ exists with respect to every separate frequency and damping. The vibration response of the system without any exciting force is shown in Figure 153.

The structure motion equation describing the case of exciting force yields the frequency characteristics of the MDOF system as shown in Figure 154. In the case of MDOF, weighting factor is normally called a modal participation factor, which is the excitation and the mode form function for the degrees of freedom at the input and output of the system.

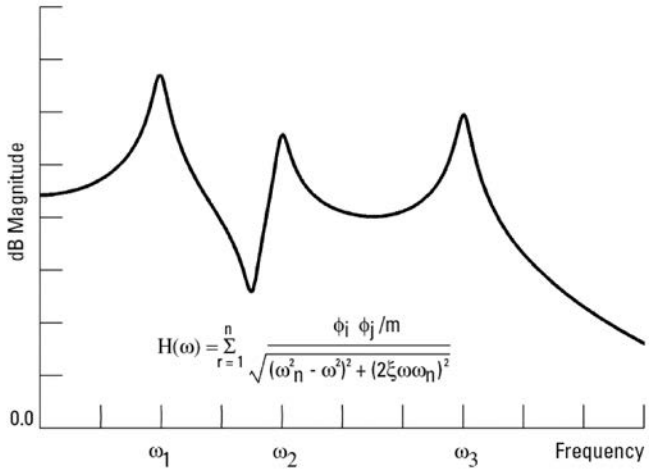

Figure 154. Frequency response of MDOF system with three degrees of freedom

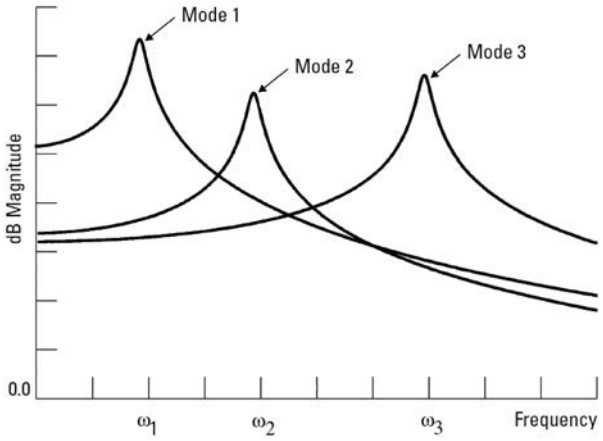

Figure 155. Frequency response of MDOF system with three degrees of freedom, with individual modal contributions

In the case of MDOF system, participation factor is also introduced, which specifies the quantitative contribution made by each mode (SDOF) into general response at a definite point. In particular, an example with three degrees of freedom in the form of individual modal contributions is shown in Figure 155.

Hence, structural analysis is the necessary supplement to structural monitoring. Structural analysis makes it possible to compare experimental results with model results, optimize the structural monitoring system, and recognize areas subject to deformation.

5.2.3. Summary of results of structural analysis

The issues of identifying damage areas of various structures with the aid of the procedures of modal analysis were highlighted in a review carried out by Richardson [Richardson & Mannan, 1993; Doebling et al., 1996_*upm* and other].

The main attention was paid to monitoring the integrity of nuclear power plants, large structures, rotating machines and offshore platforms. All these objects, somehow or other, experience a prolonged impact of mechanical vibration generated by various sources such as turbines, generators, sea waves, and transport microseisms. Many of these sources function in a cyclic vibration mode, which is a prerequisite for the development of fatigue processes of materials in structures subject to this kind of vibration.

Modal analysis makes it possible to localize the section subject to deformation. Modal frequencies may serve as deformation indices, since a change in structure properties induces a change in vibration frequencies. As a result of frequency analysis, damages can be identified.

For example, in a study of offshore platforms [Lolland & Dodds, 1976] it was found that changes in resonant frequencies by 3% were caused by changes in the mass on decks and by changes in the tide level. Changes in frequency from 10% to 15% were

observed, when the platform itself changed; moreover, that could be caused by some structural changes in the vicinity of the waterline. Thus, it was concluded that changes in the response spectrum can be used to control the structure integrity.

As far as composite materials are concerned, frequency shift can be an indicator of damage [Cawley & Adams, 1979]. These authors considered the correlations between frequency shifts for several models. A grid of possible points of damage was specified and an error was determined that linked a change in the frequency shift with a local decrease in rigidity. Several pairs of modes were considered for each potential damage site. The pair giving the most minimal error indicated the location of the fault. However, the method does not take into account the possibility of multiple damages. Particular attention in this research is paid to the anisotropic behavior of composite materials.

Modeling the effect of rupture of various modules (units) of an offshore platform on the structural response [Coppolino & Rubin, 1980] has shown that, subject to the fault location, resonant frequencies vary from 1% to 2%, which indicates a damage.

A crack occurring and propagating in the structure may either be open or open or close periodically. A research of such a crack behavior has shown [Ismail et al., 1990] that a frequency reduction caused by an opening and closing crack is less than the frequency reduction caused by an open crack. This crack's property may be error source. Frequency variation may be influenced by such factors as preload and residual stress and not only the crack size and location.

With the occurrence of damage, resonant frequencies decrease, and this reduction by an order of magnitude exceeds the standard deviation of measurement [Osegueda et al., 1992]. To ensure the correct monitoring of resonant frequencies, the mode form associated with those frequencies should be identified.

Based on numerical and experimental results, Fox [Fox, 1992] has shown that changes in resonant frequencies are a bad indicator of damage with respect to a slotted girder.

After damage was developed, resonant frequencies increased a little for some modes of vibrations. The author believes that those damages were associated with some inaccuracies of the methods used for the assessment of resonant frequencies.

A study of the minimum crack size that can be detected by using the frequency shift method showed that the minimum detectable size is 10% of the girder depth [Man et al., 1994].

[Brincker et al., 1995]. An attempt to use two fault indicators (showing the presence of a crack) has shown that the degree of confidence can be increased by scaling the measured modal frequency with the aid of standard deviation.

With a low standard deviation, frequency changes become a more important indicator. An analogous importance factor is specified for the mode with measured damping correlation. The unified importance indicator is specified by summing up the frequency and damping importance factors for several measured modes. The importance factor turned out to be a sensitive indicator of structural damage; however, this indicator cannot be used to localize a breakdown. The authors of the study believe that knowledge of the input signal is not essential for the fault detection with the aid of that method.

5.2.4. An example of modal analysis of 5-storey building design

Modal analysis is an important part of structural analysis. By using the finite elements method, the behavior of various structures under static and dynamic loads can be predicted; moreover, it becomes possible to take into account geometric nonlinearity and inelasticity of structure materials.

As an example, let us consider the modal analysis of a 5-storey building whose design consists of 8 building frames and 4 compartments. The frame width is 4.5 m. The compartment width is 3.0 m. The building length is 36 m, the width – 12 m and the height – 15m. The nominal lateral shear load is 100.0 KN in the direction of *X* axis. The overall view of the structure is presented in Figure 156.

As a result of the assessment of natural vibrations of the structure, the following modal frequencies have been obtained: 1) 2.90 Hz; 2) 3.44 Hz; 3) 3.56 Hz; 4) 8.68 Hz; 5) 10.40 Hz; 6) 10.72 Hz; 7) 14.35 Hz; 8) 17.62 Hz; 9) 19.34 Hz; 10) 22.91 Hz.

The shapes of the deformation envelope are depicted in Figure 158. The effective modal masses calculation results are shown in Table 21.

The analysis of the first 10 modes makes it possible to make a comprehensive assessment of the distribution of modal masses at translational movements progressing in the direction *X(Ux)* and *Y (Uy),* and for the rotational movement around *Z(Rz)* axis. In these cases, the general effective modal mass of the model exceeds 90%. As regards the other components *Uz*, *Rx* and *Ry,* a larger number of modes must be calculated.

According to the analysis of the natural frequencies of the structure (Figure 156):

- Mode 1 corresponds to the translational-rotational motion of the structure along *Y* and *X* axes, respectively, with a vast predominance (by about 36 times) of the effective masses involved in the translational movement;
- Mode 2 corresponds to the translational-rotational motion of the structure along *Y* and *X* axes, respectively, with a vast predominance (by about 8 times) of the effective masses involved in the translational movement;

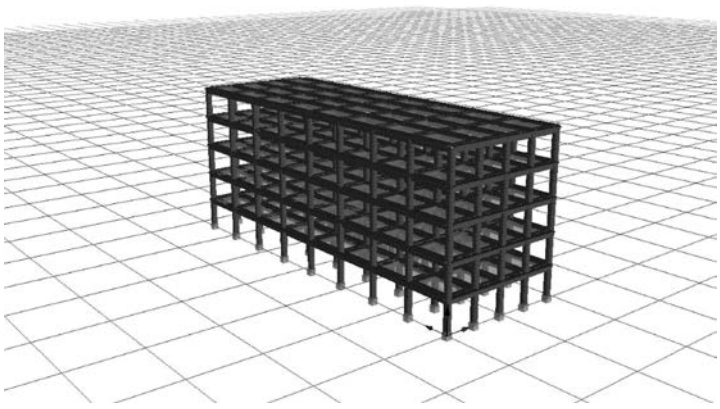

Figure 156. Overall view of a 5-storey building design

Legend: the reference axes are of the colors as follows: X – red; Y – green; Z – blue

Table 21.

The percentage of effective modal masses under individual modes with respect to the structure shown in Figure 156

Мода	*f*, Hz	Ux	Uy	Uz	Rx	Ry	Rz
1	2.899	0.0000	85.8143	0.0000	2.354	0.0000	0.0000
2	3.442	84.5855	0.0000	0.0000	0.0000	10.9306	0.0000
3	3.559	0.0000	0.0000	0.0000	0.0000	0.0000	84.8748
4	8.685	0.0000	9.5895	0.0000	9.4500	0.0000	0.0000
5	10.397	10.4980	0.0000	0.0000	0.0000	40.0000	0.0000
6	10.727	0.0000	0.0000	0.0000	0.0000	0.0000	10.2631
7	14.347	0.0000	3.1171	0.0000	0.6532	0.0000	0.0000
8	17.622	3.2809	0.0000	0.0000	0.0000	2.5071	0.0000
9	19.337	0.0000	1.1847	0.0000	1.0253	0.0000	0.0000
10	22.908	0.0000	0.2941	0.0000	0.05503	0.0000	0.0000

- Mode 3 corresponds to the rotational movement of the structure along *Z* axis. This mode has the largest participation factor, which exceeds the participation factor of the most active modes (6, 2, and 1) by 2.9–5.7 times.
- Mode 4 corresponds to the compound translational-rotational motion along *Y* and *X* axes, respectively;
- Mode 5 corresponds to the compound translational-rotational movement along *Y* and *X* axes, respectively, with the predominance or rotation;
- Mode 6 corresponds to the structure rotational movement along Z axis – similarly to Mode 3 but with a lower modal mass;
- Mode 7 corresponds to the compound translational-rotational movement along *Y* and *X* axes, respectively – similarly to Mode 4 but with a far lower modal mass;
- Mode 8 corresponds to the compound translational-rotational movement along *Y* and *X* axes, respectively – similarly to Mode 4 but with a far lower modal mass;
- Mode 9 corresponds to the compound translational-rotational movement along *Y* and *X* axes, respectively – similarly to Mode 5 but with a far lower modal mass;
- Mode 10 corresponds to the compound translational-rotational movement along *Y* and *X* axes, respectively – similarly to Mode 5 but with a far lower modal mass.

Envelopes of the 10 first modes of natural oscillations are presented with respect to the structural components from *n111* to *n116*. These components correspond to the structural nodes located on the rib closest to the viewer, shown in Figure 151, on floors 1 to 6. The total number of those structural components is 270. As a result of the modal analysis, mode envelopes can be presented for each rib of the structure (6 nodes) or in other, arbitrary directions.

Each point (node) is characterized by 6 components of the movement: X, Y, Z and RX, RY, RZ. The first three components of the movement in the nodes characterize the translational movement, while the second three components of the movement in the

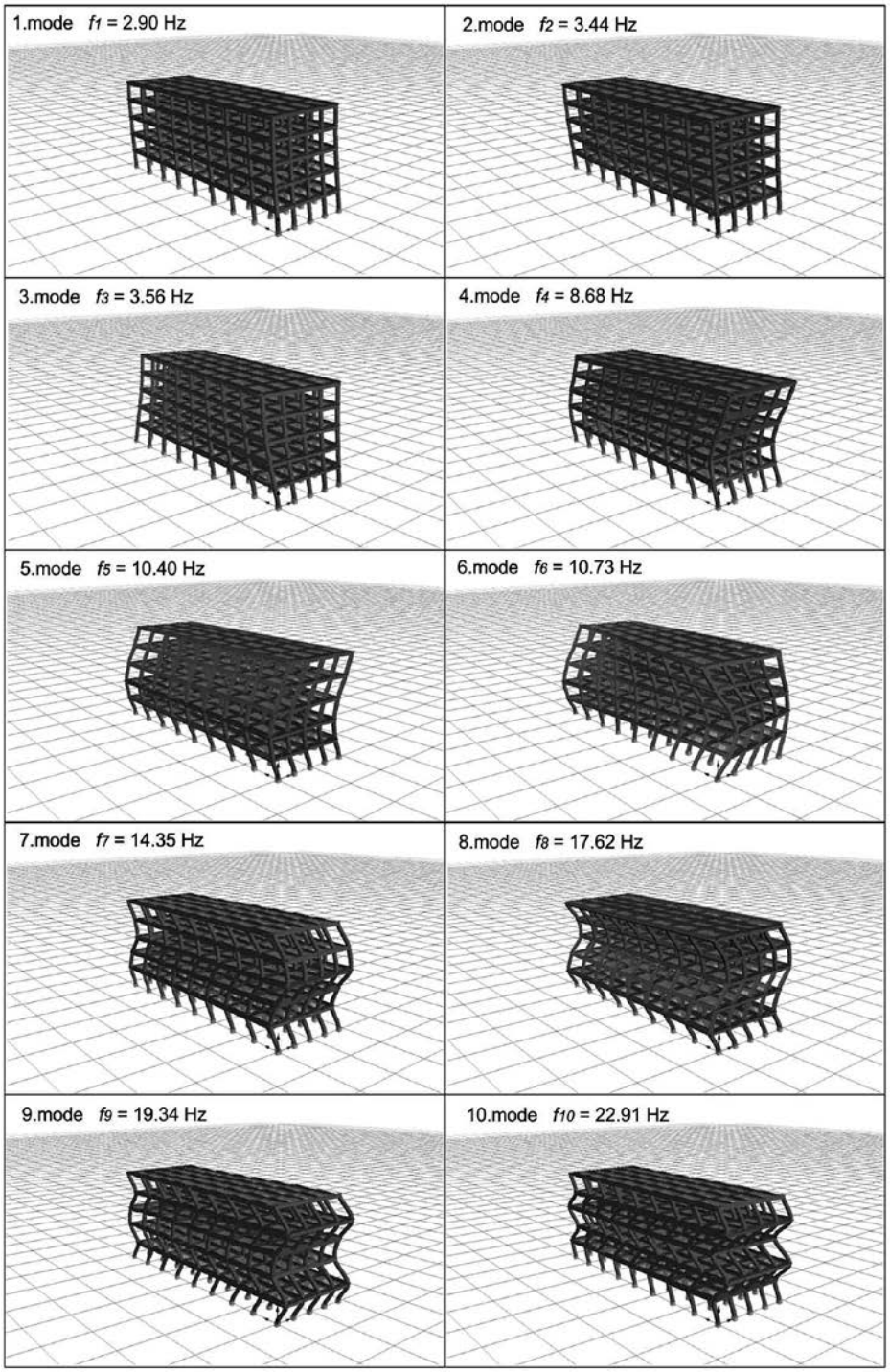

Figure 157. Envelope shapes according to the results of modal analysis of a 5-storey building

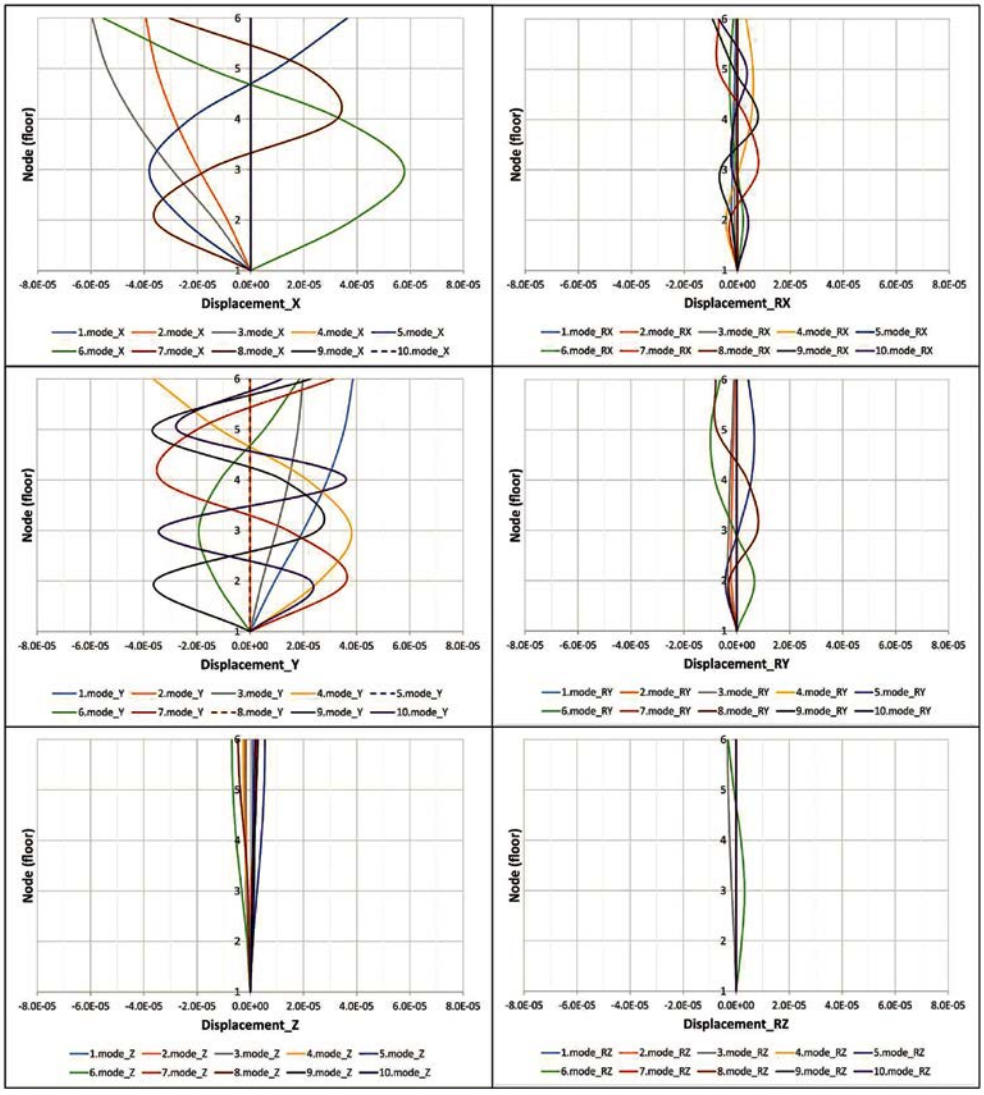

Figure 158. Envelopes of the first 10 modes for structural components (nodes) n111 – n116, located on the nearest rib on floors 1–6 (Figure 156)

nodes characterize the rotational motion. In Figure 158, the bias scale is chosen to be the same for all directions of translational and rotational movement, which makes it possible to compare the displacement amplitudes.

It is obvious that the largest shift amplitudes along *X* axis are typical for Modes 3 and 6. The largest modal masses correspond to those amplitudes. Both of those modes correspond to the rotational movement along *Z* axis.

The largest shift amplitudes along *Y* axis are typical to Modes 1, 4, 7, 9 and 10. Mode 1 is the Eigen tone. The largest modal mass is typical to Modes 1, 2 and 3.

All the other movements: the translational movement along *Z* axis and the rotational ones along each axis *RX*, *RY*, and *RZ* do not exceed the shift equal to $1 \cdot 10^{-5}$ nominal units.

5.2.5. HVSR method in earthquake engineering.

Since the early 1970s, seismological methods using seismic noise for the assessment of seismic properties of soils and dynamic response of structures were actively developed. In this respect, the method of Horizontal to Vertical Spectral Ratio (HVSR) is the most advanced one. Actually, this method makes it possible to assess the Quasi-Transfer Spectra function (QTS) of the near-surface section – the sedimentary cover which is represented, as a rule, by loose (unconsolidated) quaternary deposits with low propagation velocities of longitudinal and transverse waves.

The method was proposed in 1971 by Nogoshi & Igarashi [Nogoshi & Igarashi, 1971]. After that, the method was successfully tested in many regions of the world where sedimentary rocks are present – both in seismically active and in aseismic regions. The successful approbation became possible thanks primarily to the research of Yutaka Nakamura [Nakamura, 1989] and his successors. Advantage of a method consists in it. Initially, the method was applied to solve problems of engineering seismology, such as the assessment of dynamic properties of soil lying under railroad embankments [Nakamura, 1997], as well as the vulnerability assessment of buildings and structures, including historical monuments [Gallipoli et al., 2004; Nakamura, 2008]. The method is used in seismic micro-zoning to estimate the prevailing frequencies and resonance amplitudes of the [Zaharia et al., 2008]. At present, the method is applied for solving a wide range of problems: investigation of sedimentary basins, faults, cavities and, finally, for monitoring buildings and structures. Apart from the fact that the *HVSR* method is suitable for application practically in any regions (both seismic and aseismic ones), characterized by the existence of a sedimentary cover, the method is an operational, economically feasible, and environmentally friendly tool – especially in the context of agglomerations.

At one observation point, record of conventional microseisms is made during a few dozens of minutes. The recommended duration of seismic noise record depends on the lower frequency used in studies; anyway, the record duration as a rule does not exceed 30 minutes. The method makes it possible to use strong signals induced by earthquakes, as well. But, taking into account that earthquakes are a very rare occurrence in aseismic regions such as the East Baltic Region, it is expedient to use exactly seismic noise. It is commonly known that seismic noise is a superposition of vibrations generated both by natural processes (microseisms) and the human-induced seismic noise proper (micro-tremor). The natural processes are associated mostly with Rayleigh and Love surface waves, whereas the human-induced activities are characterized mostly by body wave generation.

Although a consensus among researchers has been reached as to the applicability of the HVSR method, nevertheless, in terms of a clear theoretical explanation of the observed phenomena, different points of view still exist. [Mucciarelli & Gallipoli, 2001]. The consensus among seismologists and geophysicists seems to be expressed by the following statement: "*The Nakamura technique is capable of predicting the resonance*

frequency of ground, but it does not allow for a correct evaluation of the Earth's motion gain". The implication of the sentence is that the capabilities of the method in question have been acknowledged, and they are mentioned in many publications. The main discussions mainly took place in explaining the peak frequencies of H/V spectral relations.

Nogoshi and Igarashi [Nogoshi & Igarashi, 1971] have shown the correlation between the HVSR ratio and the Rayleigh wave ellipticity curve. This allowed them to conclude that microtremor consisted predominantly of Rayleigh wave. In a number of theoretical investigations [Lachet & Bard, 1994; Konno & Ohmachi, 1998; Bard et al., 2004_*si*] was assumed that peak values of H/V spectral ratio can be explained by the fundamental mode of Rayleigh waves. From the standpoint of Nakamura [Nakamura, 2008], if we take such an approach for the truth, the microtremor should be regarded as the one consisting of Rayleigh waves only. However, Nakamura himself held some other view. He asserted [Nakamura, 2008] that, with a closer look at the examples given by Nogoshi and Igarashi [Nogoshi & Igarashi, 1971] one can see clearly that, at the peak frequency of *H/V*, the Rayleigh wave energy is very low and even close to zero. The Rayleigh wave has the maximum energy of its own – but at a frequency close to the peak frequency of the H/V spectral ratio. Therefore, he believed that the peak of the H/V spectral ratio cannot be explained by the energy of the Rayleigh waves. Nakamura explains the peak frequency of the H/V ratio by the vertically incident *SH* wave [Nakamura, 1989].

It should be noted that the existing contradiction between researchers on the explanation of the origin of the H/V spectral peak may be due to the fact that different types of waves can prevail in different parts of the seismic noise spectrum. For example, in a review study [Bonnefoy-Claudet et al., 2006] it is pointed out that a consensus between researchers has been achieved in the issue of the formation of ambient seismic noise. At the same time, however, a clear-cut classification of all sources of seismic noise is quite a challenging problem.

Since the H/V method of spectral relations uses ambient seismic noise (ASN), a brief characteristic of ASN and its individual components is given below. In particular, the characteristic applies to natural seismic noises, i.e., microseisms (MCS) and human-induced seismic noises – microtremor (MCR). A conventional border between the above-mentioned ASN types can be the frequency of 1 Hz. However, the higher frequencies of MCS and the lower frequencies of MCR may overlap.

At frequencies higher than 1 Hz, seismic noise displays daily and weekly variations; this attests to its association with human-induced activities. Table 22 contains a list of various types of sources generating seismic noise.

At lower frequencies (from 0.005 to 0.3 Hz), a change in seismic noise correlates with natural processes (oceanic, meteorological etc.) The terms "microseisms" refers to ocean waves generating seismic signals within two frequency bands.

Those are, first of all, ocean gravity waves within the frequency range from 0.04 to 0.17 Hz (with the period 25 – 5.9 sec), which are known as primary microseisms – PM).

Secondly, this is a higher-frequency band of double ocean waves acting within the frequency range from 0.08 to 0.34 Hz (12.5–2.9 seconds), which are known as double-frequency microseisms (DF) [Traer et al., 2012]. Ocean waves approaching the coasts generate surface waves within three frequency bands: 1) the main microseisms PM

Table 22.

Generalized frequency parameters of ambient seismic noise

	Gutenberg (1958)	Asten (1978, 1984)
Oceanic waves striking along the coasts	0.05–0.1 Hz	0.5–1.2 Hz
Monsoon/Large scale meteorological perturbation	0.1–0.25 Hz	0.16–0.5 Hz
Cyclones over the oceans	0.3–1 Hz	0.5–3 Hz
Local scale meteorological conditions	1.4–5 Hz	
Volcanic tremor	2–10 Hz	
Urban	1–100 Hz	1.4–30 Hz

resulting from direct pressure on the seabed; 2) standing waves resulting from the interaction between the approaching and the reflected waves, i.e., microseisms of double frequency DF; 3) the infra-gravitational wave interaction, i.e. the Earth's seismic hum, transformed into a swell-transformed infragravity wave interactions.

Thus, the ambient seismic noise consisting of a natural (low-frequency) and human-induced (high-frequency) components can be the target of research for solving applied problems in the East-Baltic region.

5.2.6. Bases of HVSR spectral ratio method

When the method was at the fledging stage, records of strong motions in various areas of Japan were used to analyze the horizontal/vertical HVSR spectral ratio.

On a soft ground, the horizontal movement amplitudes by far exceed those of vertical movements. On the other hand, as far as hard rock deposits are concerned, the horizontal and the vertical movements are very much alike – both in terms of the maximum value and the wave shape [Nakamura, 2008].

Let us consider the fundamental concepts of HVSR method, which is also called the *Nakamura* method.

The geological section (Figure 159) is represented by a foundation and a sedimentary basin, along the edges of which, some exposures of rock deposits at point A are observed. At points A, B and C, microtremor consists of a superposition of Rayleigh waves and other types of seismic waves. The horizontal and vertical spectra of H_f, V_f on the surface of sediment pool soil at point B can be represented in the following form:

$$H_f = A_h * H_b + H_s \quad (65)$$

$$V_f = A_v * V_b + V_s \quad (66)$$

$$T_h = H_f / H_b \quad (67)$$

$$T_v = V_f / V_b \quad (68)$$

where, A_h and A_v – gain ratios (coefficients) (i.e., the amplifications of horizontal and vertical movements from vertically-incident body wave (for point B); H_b and V_b– spectra of horizontal and vertical movements in the basement under the sedimentary basin at point C or, on the outcrops, on the surface, and at point A; H_s and V_s – Rayleigh

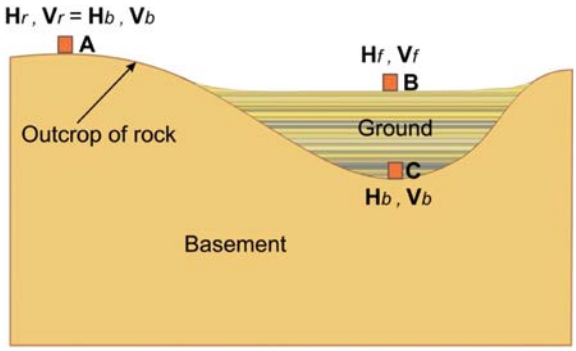

Figure 159. A typical geologic cross-section of a sedimentary basin and hard rock deposits exposure area

Designations: and horizontal and vertical spectra on rock exposures at A point; and – horizontal and vertical spectra on rock deposit on the bottom of basin – at C point; and – horizontal and vertical spectra on the surface of sedimentary deposits, at B point

wave spectra in horizontal and vertical directions; T_h and T_v – gain ratios (coefficients) of horizontal and vertical movements of the sedimentary soil surface, based on seismic motions on rock outcrops at point A near the basin. The P-waves velocities are normally 3–4 times higher than those of S-waves.

Within the sedimentary layer, near the frequency range where the horizontal component has a large gain, the vertical component cannot be enhanced ($A_v = 1$). In the absence of effects from Rayleigh waves, vertical spectra on the sole and the top of sedimentary cover are equal: $V_f \cong V_b$. Otherwise, when $V_f \gg V_b$, then the influence of surface waves takes place [Nakamura, 2000]. Thus, the ratio V_f/V_b between the vertical spectra on the roof V_f and the bottom V_b of the sedimentary mantle, according to Nakamura, is an indicator of the impact from Rayleigh waves. When estimating the effect of Rayleigh waves, horizontal amplification can be represented as:

$$T_h^* = \frac{T_h}{T_v} = \frac{\frac{H_f}{V_f}}{\frac{H_b}{V_b}} = \frac{QTS}{\frac{H_b}{V_b}} = \frac{\left[A_h + \frac{H_S}{H_b}\right]}{\left[A_v + \frac{V_S}{V_b}\right]} \tag{69}$$

where

$$QTS = \frac{H_f}{V_f} = \frac{A_h * H_b + H_S}{A_v * V_b + V_S} = \frac{H_b}{V_b} \cdot \frac{\left[A_h + \frac{H_S}{H_b}\right]}{\left[A_v + \frac{V_S}{V_b}\right]} \tag{70}$$

In the equation (69 and 70), $H_b/V_b \cong 1$.). The expressions H_s/H_b and $\frac{V_s}{V_b}$ are related

to the energy source of Rayleigh waves [Nakamura, 2000]. If there is no influence from Rayleigh waves, then $QTS = A_h/A_v$. According to Nakamura, if the number of Rayleigh waves is large, the second term in the above equations dominates, and $QTS = H_s/V_s$, while the lowest peak frequency of the ratio H_s/V_s is almost equal to the lowest natural frequency F_0 of the horizontal gain factor A_h. Within F_0 the vertical movement gain factor $A_v = 1$. QTS shows a stable peak at frequency F_0. QTS represents the natural frequency of the first order

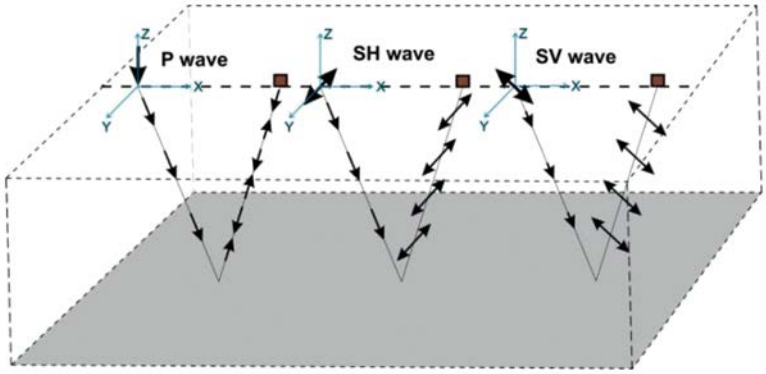

Figure 160. Diagram of P, SH and SV-waves distribution within a ground layer

due to multiple reflections of the SH wave in the surface layer of the soil (Figure 160) and contributes to the gain factor, regardless of the degree of influence of the Rayleigh waves.

Figure 160 shows the main types of seismic waves being excited at the top of the layer. For P-waves, particles of the medium oscillate along the wave propagation path, whereas, for SP- and SH-waves, particles of the medium oscillate at the right angle to the propagation path. For SV-waves, at the same time, particles oscillate in the vertical plane which is perpendicular to the propagation path, and with respect to SH-waves, they oscillate in the horizontal plane perpendicular to the propagation path.

QTS is associated with multiple reflections of S –waves, and it justifies its title as a quasi-transmissional spectrum. At the same time, the depth of the basement (rock deposits) should be taken into account when *QTS* is considered. The frequency F_0 is associated with QTS:

$$F_0 = C_s/4h \tag{71}$$

For this frequency, the A gain ratio is connected with seismic rigidity. Seismic rigidity characterizes the reflectivity of the interface between the corresponding layers. In the case of a two-layered model (Figure 161), reflection coefficient can be represented in the form of the following expression:

$$R = \frac{I_1 - I_2}{I_1 + I_2} = \frac{\rho_1 V_1 - \rho_2 V_2}{\rho_1 V_1 + \rho_2 V_2} \tag{72}$$

where ρ_1 and ρ_2 – the geological rock density in the upper (near-surface) layer and the lower half-space; V_1 and V_1 the propagation velocity of seismic wave in the upper layer and the lower half-space.

Should the hard rock and the near-surface layer densities be equal, then,

$$A_0 = C_b/C_s \tag{73}$$

where, C_b and C_S are S-wave velocities in rock material (basement) and sedimentary deposits.

The hard rock depth is specified as:

$$h = C_b/(4A_0 \cdot F_0) \tag{74}$$

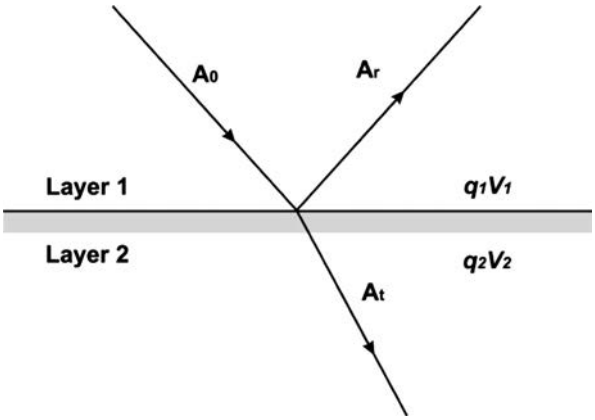

Figure 161. Scheme of converting an incident wave to the boundary of a two-layer model

Formula (74) are of prime importance in *HVSR* method. It make it possible to assess the depth of hard rock (the basement) over which sedimentary deposits lie. The greater the difference in seismic rigidity, the larger the peak amplitude at F_0 frequency.

An important parameter proposed by *Nakamura* [Nakamura, 1997] is the so-called *vulnerability index*. In buildings and structures, damage to the elements of the structure can occur if seismic action (a short-term one, like an earthquake or explosion, or a long-term one – like cyclic, repeated vibration) exceeds the permissible strain limits.

The shearing of the surface soil γ may be the most dangerous. Ishihara [Ishihara, 1978] noted that starting from $\gamma \cong 1000 \times 10^{-6}$ the soil begins to exhibit a nonlinear character, i.e. deformations occur beyond the Hooke's law. When $\gamma > 10000 \times 10^{-6}$, huge deformations and even destruction of buildings and structures occur. In general, the dependence of the dynamic properties of the soil on deformations is presented in Table 23.

Schematic diagram of shear deformation of soil is presented in Figure 162.

The average shearing γ of surface soil γ can be assessed according to the formula, as follows:

$$\gamma = A_g \times d/H \tag{75}$$

where, A_g – gain ratio; H – top layer thickness; d – seismic displacement of ground bottom site.

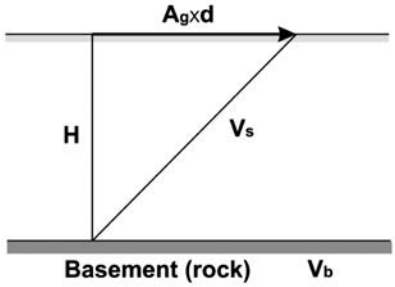

Figure 162. Surface soil deformation

Table 23.

Variation of soil dynamic properties with strains [Ishihara & Ansal, 1982]

Magnitude of strain	10^{-6}	10^{-5}	10^{-4}	10^{-3}	10^{-2}	10^{-1}
Phenomena	Wave propagation, Vibration			Crack, Differential Settlement		Slide, Compaction, Liquefaction
Mechanical characteristics	Elastic			Elastic-Plastic		Failure

Ishihara K., Ansal A.M., 1982. Dynamic behavior of soils, soil amplification and soil-structure interaction. Earthquake risk reduction in the Balkan region. UNDP Project Executed by UNESCO in Association with Undro (Rep/79/014). Final Report. Working group D. p. 185.

Assuming that S-wave velocities in the basement (the lower half-space) and in the surface layer are equal to v_p and v_S respectively, we shall express the dominant frequency F_g of the ground surface, as follows:

$$F_g = v_b/(4A_g \times H) \tag{76}$$

The rock bed acceleration α_b can be expressed, as follows:

$$\alpha_b = (2\pi F_g)^2 \times d \tag{77}$$

In this case, deformation γ can be expressed through F_g, A_g and v_b in the form, as follows:

$$\gamma = (A_g \cdot \frac{\alpha_b}{(2\pi F_g)^2} \cdot (4A_g \cdot F_g/v_b) = (A_g{}^2/F_g) \cdot (\frac{\alpha_b}{\pi^2 v_b}) = \mathrm{c} \cdot K_g \cdot \alpha_b \tag{78}$$

If we express the dynamic force efficiency through static force, as follows:

$$\gamma_e = K_g(e) \times \alpha_b \tag{79}$$

The respective vulnerability index will be of the following value:

$$K_g(e) = e \times (\frac{A_g{}^2}{F_g})/(\pi^2 v_b)/100 \tag{80}$$

The velocity in rock formations v_b is almost constant over a large area. If we assume that $v_b \cong 600$ m/sec and the dynamic load is approximately 60% of the static load [Nakamura, 1997], then

$$K_g(e) \cong A_g^2/F_g \tag{81}$$

The vulnerability index K_g characterizes the measured point. It shows how large is the probability of deformation at the preset point, and is useful for identifying "weak spots" of the ground.

5.2.7. Ground seismic properties assessment results in the East Baltic Region

With the aim of approbation of the HVSR method in the context of the East-Baltic region, studies were carried out to assess seismic properties of soils at the locations of seismic stations included into the *GEOFON* international network with center at *GFZ Potsdam*.

In the course of the studies, seismic noise records were used as well as those of earthquakes and industrial explosions; records were made at the stations included into the BAVSEN network – namely, MEF, RAF, MTSE, VSU, SLIT, SUW, PBUR, and PABE (Figure 6.5).

The stations are located in different geological environment: on the Baltic Shield (MEF and RAF), the southern slope of the Baltic Shield (MTSE and VSU), the Baltic Syneclise (SLIT, PBUR and PABE), and on the boundary between border the Baltic Syneclise and Mazuro-Belorussian Anteclise (SUW). Whereas a sedimentary cover is practically absent on the Baltic shield, than, in the southward direction, the thickness of the sedimentary cover with respect to stations located within the Baltic syneclise (SLIT, PABE, PBUR) increases from 10 to 130 m.

Seismic sensors STS-2 were located at a depth of 0 to 6.5 m. An important advantage of these studies was that unified, standard equipment sets were used at all stations of the GEOFON network. Broadband sensors Streckeisen STS-2 and analogue-digital converters PS6-SC were mainly used. Records of channels HHZ, HHN, HHE with a sampling frequency of 100 Hz were used. The BSD and PUL stations that are part of the BAVSEN network were not used because they did not have any similar registration channels. To process the measurement results, the *Geopsy* software program was used. This program makes it possible to evaluate the ratio of the HVSR spectra. The results obtained within the framework of the international *SESAME* project [Bard et al., 2004_*si*] were used as a basis for methodological guidelines.

Windows for analysis were selected automatically. The length of each window reached 25 seconds. About 70 windows were used to calculate the average values. Random, transient processes were excluded from seismic noise. The frequency range occupied the band from 0.2 to 15 Hz. To smooth the data, the Konno-Ohmachi method was used [Konno & Ohmachi, 1998].

In each window, the horizontal spectrum has been calculated by way of the union of horizontal components (N-S and E-W) and by using the root-mean-square estimation method – according to the formula, as follows:

$$H = \sqrt{(H_{EW}^2 + H_{NS}^2)/2} \tag{82}$$

Seismic noise records were used at the stations of the BAVSEN network during night time in August 2015. This allowed one to minimize the impact of human-induced seismic noise – tremor. Duration of records reached 30 minutes. Due to some technical problems, the number of records at seismic stations varied from 23 to 27. The HVSR analysis was performed within in the range of 0.2 to 10 Hz, i.e. within the range of engineering seismology, which takes into account the natural resonant frequencies of buildings and structures.

The HVSR parameters of ambient seismic noise for BAVSEN stations are shown in Table 24. The generalized HVSR charts for ambient seismic noise and seismic events, as well as standard deviations for ambient seismic noise, are shown in Figure 163.

The HVSR spectral ratios vary depending on the geological setting For stations located on the Baltic Shield (MEF and RAF), the HVSR curves have an almost flat characteristic (Figure 7.33) with a gradual increase towards higher frequencies. The HVSR level for

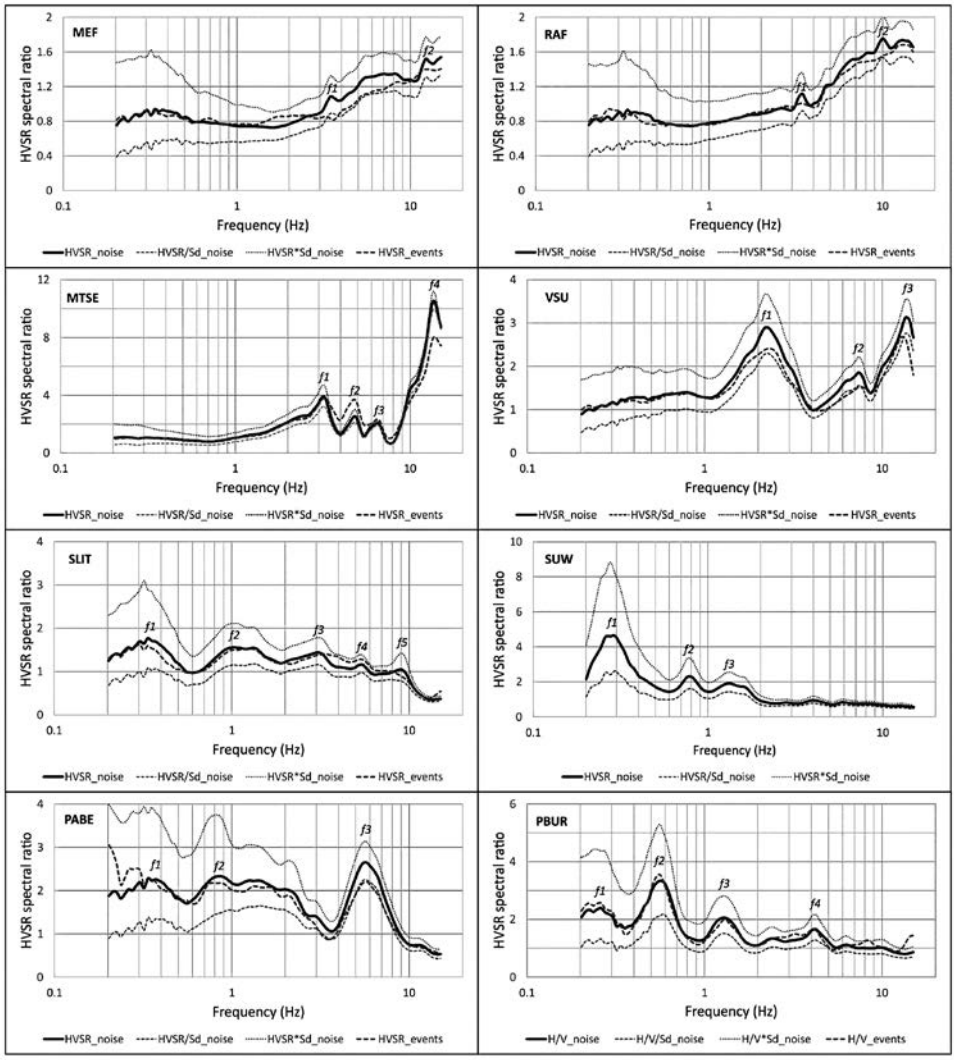

Figure 163. Horizontal to vertical spectral ratios (HVSRs) for stations of the BAVSEN network.

*Notes: HVSR_noise – the generalized curve of the HVSR for ambient seismic noise; HVSR/Sd_noise and HVSR/V*Sd noise – the HVSRcurve divided and multiplied by the standard deviation Sd; HVSR_events – the generalized curve of the HVSR for seismic events(earthquakes, explosions and other man-made events); f_1 ... f_5 – frequencies of HVSR peaks pointed in Table 24 for relevant seismic stations."*

MEF and RAF stations does not exceed 1.52–1.75 for frequencies of the order of 10 Hz and higher. Therefore, there are no clear-cut spectral peaks [Nikulins, 2017c].

The SUW station role in the location of seismic events in the East-Baltic region was insignificant. Therefore, for this station, only the HVSR spectral ratios of seismic noise are given.

For SLIT station, the level of spectral peaks of seismic noise at frequencies $f_1 - f_5$ does not exceed 2. For other stations, the spectral peak levels $f_1 - f_n$ varied from 1.66 to 10.52 (Table 24).

In accordance with the methodological recommendations of the *SESAME* project [Bard et al., 2004], frequencies above 0.4 Hz (f_0 > 10 /window length) correspond to the criterion of a confident spectral peak. Therefore, the frequencies 0.34 Hz (SLIT),

Table 24.

HVSR seismic noise parameters for the BAVSEN network stations

Station	*Par.*	f_1	f_2	f_3	f_4	f_5	*Station*	*Par.*	f_1	f_2	f_3	f_4	f_5
MEF	*f*, Hz	3.46	12.25	-	-	-	*SLIT*	*f*, Hz	0.34	1.03	3.12	5.45	9.04
	σ_f	0.14	0.79					σ_f	0.03	0.10	0.36	0.18	0.56
	A_{HVSR}	1.08	1.52	-	-	-		A_{HVSR}	1.77	1.56	1.43	1.16	1.05
	$\sigma_A(f)$	1.22	1.52					$\sigma_A(f)$	1.63	1.35	1.24	1.20	1.36
RAF	*f*, Hz	3.46	10.01	-	-	-	*SUW*	*f*, Hz	0.29	0.76	1.35	-	-
	σ_f	0.10	0.65					σ_f	0.02	0.02	0.07		
	A_{HVSR}	1.11	1.75	-	-	-		A_{HVSR}	4.62	2.28	1.90	-	-
	$\sigma_A(f)$	1.21	1.15					$\sigma_A(f)$	1.77	1.46	1.34		
MTSE	*f*, Hz	3.24	4.87	6.61	13.54	-	*PABE*	*f*, Hz	0.34	0.84	5.73	-	-
	σ_f	0.00	0.00	0.32	0.65			σ_f	0.04	0.17	0.18		
	A_{HVSR}	3.87	2.52	2.00	10.52	-		A_{HVSR}	2.28	2.33	2.65	-	-
	$\sigma_A(f)$	1.21	1.19	1.08	1.06			$\sigma_A(f)$	1.66	1.60	1.18		
VSU	*f*, Hz	2.19	7.38	13.56	-	-	*PBUR*	*f*, Hz	0.26	0.56	1.26	4.23	-
	σ_f	0.07	0.12	0.33				σ_f	0.02	0.02	0.06	0.11	
	A_{HVSR}	2.89	1.86	3.13	-	-		A_{HVSR}	2.39	3.33	2.05	1.66	-
	$\sigma_A(f)$	1.27	1.20	1.13				$\sigma_A(f)$	1.82	1.59	1.36	1.30	

f_i – frequency of an HVSR peak, A_{HVSR} – amplitude of a peak at frequency f, $\sigma_A(f)$ – standard deviation for the amplification factor A_{HVSR}, σ_f – standard deviation of the frequency of an HVSR peak, the dash '–' means there are no peaks."

0.29 Hz (SUW), 0.34 Hz (PABE) and 0.26 Hz (PBUR) do not meet these requirements. Therefore, in these studies, spectral peaks for the range 0.4–10.0 Hz were analyzed.

There were 22 frequencies only, which had met the criterion for a real spectral peak. However, neither of those frequencies meets the criterion for a clear-cut peak. Only three frequencies have a significant level of H/V spectral relations and, therefore, are of a practical interest. These frequencies are the following: f_1 = 2.19 Hz (VSU), f_3 = 5.73 Hz (PABE) and f_2 = 0.56 Hz (PBUR).

The HVSR peak amplitudes for seismic noises are generally higher than those for seismic events. The standard deviations of peak amplitudes and *HVSR* frequencies for seismic noise are predominantly smaller than for seismic events. Within the frequency range from 0.4 to 10 Hz, the standard deviations of spectral peaks frequency σ_f for seismic noise vary from 0.00 for the MTSE station to 0.65 for the RAF station. The MTSE station is characterized by the fact that the spectral peaks f_1 = 3.24 Hz and f_2 = 4.87Hz are stable in time (σ_f = 0.00). Standard deviations in the amplitude of the spectral peaks $\sigma_A(f)$ for seismic noise vary from 1.08 at the MTSE station (for = 6.61 Hz) to 1.59 at the PBUR station (for $\sigma_A(f)$ = 0.56Hz).

It should be noted that the assessment of HVSR amplitudes and spectral peak frequencies based on seismic event records relies on a low statistical representativeness. Thus, for the RAF, MTSE and VSU stations, 23 seismic event records were used, 16 records for the MEF station, 13 records for the SLIT station, and only 6 records – for the PABE and PBUR stations. All seismic events were localized through using the BAVSEN network. These events occurred between July 2 and 22, 2016. Epicenters of most seismic events are located in northeastern Estonia. Other epicenters of seismic events are located in the area of Pskov Lake and the north-west of Russia, and in the coastal part of Sweden and Finland. With a high probability, all these seismic events are associated with human-induced explosions. Only two seismic events have an obscure genesis. The epicenters of these events are located on the border of Moldova and Ukraine, and in the Black Sea.

Therefore, as regards those studies, more reliable *HVSR* results are based on the analysis of seismic noises.

Since the observations were made at night, this made it possible to minimize human-induced seismic noise (tremor). Therefore, the share of seismic noise associated with natural processes – i.e., microseisms – increases. Microseisms should mostly consist of Rayleigh and Love surface waves.

As noted above, a significant level of spectral ratios was recorded at three stations only. At the VSU station, the spectral ratio level reached the maximum A_{HVSR} = 2.89 at the frequency f_1 = 2.19 Hz. This attests to a high level of seismic impedance. To interpret the above-mentioned spectral peak, an elliptic curve (ellipticity) simulation was performed (Figure 164).

Ellipticity criteria was used in many investigations for spectral peak interpretation [Nogoshi & Igarashi, 1971; Lachet & Bard, 1994; Malischewsky et al., 2010]. Theoretical ellipticity makes it possible to identify the impact from Rayleigh surface waves. Ellipticity is the amplitude ratio between horizontal and vertical movements of a particle in the Rayleigh wave plane. For ellipticity assessment, a three-layer model of the medium underlying the Vasula station was used.

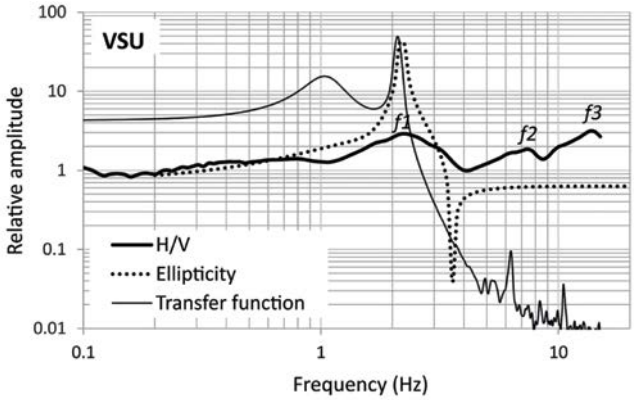

Figure 164. Spectral ratio curve H/V, ellipticity and transfer function for the station Vasula [Nikulins, 2017c]

Note: the frequency parameters f_1... f_3 of HVSR spectral ratios for VSU station are shown in Table 24

The simulation results have shown that the peak amplitude of the ellipticity curve of the Rayleigh wave fundamental mode practically coincides with the frequency of the resonance peak f_1 = 2.19 Hz at the Vasula station (Figure 164). In addition, the transfer function for the vertical component is also shown in Figure 164; its peak amplitude is also located close to the above-mentioned *HVSR* and ellipticity peak amplitudes. To simulate the transfer function, the Berlage pulse was used as the input signal. In accordance with the views of some researchers [Корчинский, 1971], the motions of the surface are most accurately described when using the *Berlage* pulse.

Since the *HVSR* spectral peak at frequency f_1 = 2.19 Hz is in good agreement with the *Rayleigh* wave ellipticity, we can assume that, with respect to the Vasula station, this spectral peak is associated with the Rayleigh wave.

The assessment of vulnerability index K_g is of a great practical interest. Nakamura [Nakamura, 2008] considers K_g = 20 to be a boundary value, above which deformations occur. As an example, he shows the effect from the Loma Prieta earthquake that took place in 1989 in California. The moment magnitude reached 6.9 and the focal depth reached 19 km. The coastal part was damaged to a large extent. From the opposite side of the hills, no damage was observed.

The assessments show that, with respect to two stations (SUW and PBUR) and three frequencies (f_{1_SUW} = 0.29 Hz, f_{1_PBUR} = 0.26 Hz and f_{2_PBUR} = 0.56 Hz) K_g reaches or exceeds the value 20 (K_{g1_SUW} =73.6, K_{g1_PBUR} = 22.0 and K_{g2_PBUR} = 20.0). It is commonly known that, if deformation level exceeds $\gamma = 10^{-4}$, the soil surface starts to exhibit non-linear properties, while in the case of deformation $\gamma = 10^{-2}$, landslides, soil compaction, and soil liquefaction may occur, as a result of which, the building may be destroyed (see Table 78) [Ishihara, 1978].

Let us assess ground deformation according to the formula 78, for the geological conditions typical for the stations Suwalki (Poland) and Paburge (Lithuania) – as if an

earthquake similar to the Kaliningrad earthquake of M_W = 5.2 magnitude, took place there. The maximum epicentral intensity during the second shock of the Kaliningrad earthquake (13:32 GMT) reached VI ½ points on the MSK-64 scale [Nikonov et al., 2005]. According to the national standard of the Russian Federation [GOST R 57546-2017, 2017], with such an epicentral intensity, the acceleration in the epicentral zone reaches the value α_{PGA} = 70 cm/ sec^2. Thus, for the above values of the vulnerability index K_g, the γ deformations will reach levels from 0.002 to 0.0087 (for shear wave velocities V_S in the range from 600 to 800 m/sec). Such levels are typical to the non-linear behavior of the geomaterial and imply the possibility of the occurrence of cracks and sediments in the ground.

The above-stated frequencies and the corresponding deformation levels pose threat to buildings and structure with a height varying from 55 to 115 m [Nikulins, 2017c].

As regards the method of *HVSR* spectral ratio, the possibility of assessment of non-consolidated, quaternary deposits is of practical interest. To date, such investigations are widely used [Ibs-von Seht & Wohlenberg 1999; Parolai et al., 2002; Mokhberi et al, 2013]. In these studies, a functional relationship between the frequency of spectral peaks and the thickness of unconsolidated deposits is assessed. This connection is usually considered in the form of a power series function.

$$h = a \cdot f^b \tag{83}$$

where, a and b – constants; f – peak frequencies for H/V spectral ratio.

To study the correlation between the peak frequency f of the H/V spectral ratios and the thickness of the unconsolidated layer, only limited data was used in the East Baltic region. The data is based on measurements taken at 6 points (seismic stations) sitting on sediments. With respect to 4 stations (VSU, SLIT, PABE, PBUR), the thickness values of unconsolidated deposits are more reliable than for the other two stations (SUW, MTSE). Therefore, two functional dependencies were obtained (Figure 165).

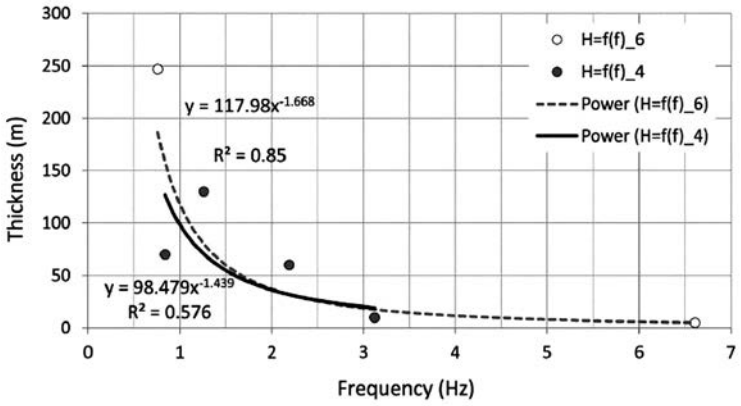

Figure 165. Correlation between HVSR peak frequencies based on ambient seismic noise and thickness of quaternary deposits

$H = f(f)_6$ and $H = f(f)_4$ – values to assess the quaternary deposits thickness/frequency ratio – for 4 and 6 observation points, accordingly. Power ($H = f(f)_6$ and power ($H = f(f)_4$ – the power function curve, for 6 and 4 observation points (stations), respectively.

The following functional relationships were obtained for the 6 (formula 84) and the 4 (formula 85) observation points (stations):

$$h = 118.0 \cdot f_0^{-1.67} \tag{84}$$

$$h = 98.5 \cdot f_0^{-1.44} \tag{85}$$

In both cases, correlation coefficients are high enough – 0.92 and 0.76, respectively.

Comparison with similar parameters of the relationship between spectral peaks and the power of unconsolidated deposits for Germany [Ibs-von Seht & Wohlenberg, 1999; Parolaietal, 2002] shows that *a* and *b* coefficients in expression (7.70) are close to these coefficients characterizing the East-Baltic region. For instance, for the Aachen area, $a = 96$ and $b = -1.388$, and for Cologne $a = 108$, and $b = -1.551$. For Iran [Mokhberi et al., 2013], these coefficients differ more significantly from the corresponding coefficients for the East-Baltic region. For example, for the Bushehra area, $a = 29.86$ and $b = -0.63$, while for the South Pars area $a = 128$ and $b = -1.15$.

5.2.8. Applied methods of seismology and their application prospects in the East Baltic Region

This chapter will give you a brief description of applied seismological methods and analyze the prospects of their application in the East Baltic Region. Since the EBR seismicity is low, tectonic earthquakes are a rare occurrence and their magnitude are insignificant, ambient seismic noise (ASN) comes to the fore and becomes the main target of research.

ASN consists of the natural component – microseisms and the human-induced component – microtremor. These constituent parts of *ASN* extend over various sections of the frequency range. Although 1 Hz-frequency is accepted as a conventional interface between those two components, microseism and micro tremor may still have an overlap region. Microseisms and microtremor affect material objects differently. Microseisms are characterized by a considerable wavelength comparable to crustal blocks, high-rise buildings and structures, whereas the wavelength of micro tremor is small and is comparable with smaller-size objects like earth covers, basements, and various small objects. Stemming from the "areas of responsibility" of the individual components of ambient seismic noise, we shall consider the areas wherein those components may be used to solve various applied problems in the East Baltic Region.

5.2.8.1 Monitoring of ambient seismic noise to control landslide processes

Sometimes, monitoring of physical and mechanical properties of geologic setting is quite necessary – for example, if landslide processes are developing. A soil slip is a hazardous geological phenomenon, which occurs due to rock formations' shifting downslope under gravity action or as affected by an additional load caused by slope underwashing, water saturation, seismic shocks, and other processes. Landslide occurs on the slopes of river valleys and ravines, on sea shores, and in some other cases. One of the factors promoting the landslide development is the alternation of water-resistant rocks and

water-bearing formations located at the slopes of valleys and ravines. Due to soil wetting by rainwater, the soil mass becomes heavier and it starts moving more actively, while the adhesion power of soils and rocks on slopes is insufficient to hold back the soil mass. Slip processes are known to take place in the East Baltic Region. For example, ravine networks are quite developed in the valleys of many rivers of Latvia: Venta, Abava, Daugava, Gauja etc. In the Daugava river valley, erosion processes develop inside the ravines, and the connection between ravine parameters and landslide processes is identified [Kukemilks & Saks, 2013]. In 2002, two major landslides took place around the Turaida medieval castle in the valley of Daugava River. The landslides blocked the regional road traffic Sigulda – Turaida and posed a threat of damage to a historical monument – the Turaida Castle, which was built in 1214. Thus, the need to control the development of landslide processes in EBR is quite relevant, and it can be sought in the future.

The basic physics for studying landslide processes with the aid of ASN ASN (ambient seismic noise) method are changes in physical and mechanical properties of soil mass, associated with the dynamic process of landslide development.

ASN monitoring makes it possible to check a change of V velocity within the material. A change in V velocity and especially the velocity of shear waves V_S is an indirect sign of a change in the density or stiffness of the soil mass. Reduction in the stiffness of landslide material can invoke a drop of the parameter dV/V to in the process of landslide development.

The velocity change mechanism depicted above was observed in process of a landslide monitoring in the vicinity of a Swiss mountain ski resort – *Les Diablerets* (Figure 166). The landslide monitoring was under way within a 4-year period (from March 2010 to July, 2014). The monitoring data was processed according to the respective developed technique [Larose et al., 2015]. The frequency range 8 – 14 Hz was selected, which was associated with surface waves penetrating into the slip layer subject to deformation – to the depth from a few meters to 15 m.

Variations of relative velocity dV/V had been obtained due to the correlation of continuous record received by two vertical seismic sensors installed on the landslide. The seismic sensors are located at the ends of the red horizontal arrow shown on Figure 166 c. The results of relative velocity variations dV/V were compared to weekly amount of precipitation (the right scale on Figure 166 a). It was found that the background fluctuations (those inside the horizontal dark yellow lines on Figure 166 *a*) may reach ± 2% dV/V.

The background fluctuations are associated with some environmental changes like temperature, freezing and thawing cycles, the snow cover and its melting. In autumn 2011, a precipitation anomaly was observed within a month's time and a velocity was reduce from +2% to -2%. In other words, hydro-meteorological processes can induce dV/V fluctuations, which do not go beyond the limits of background effects anyway.

In addition, based on the results of spectral analysis of velocity reduction and standard analysis of surface waves, it became possible to determine the location of the slip change at the base of the layer. In other words, changes in rigidity occurred in the layer located at a depth of 9–11 m. The major event was taking place from July 15 to August 19, 2010 when the velocity reduction went beyond the limits of background values and dropped

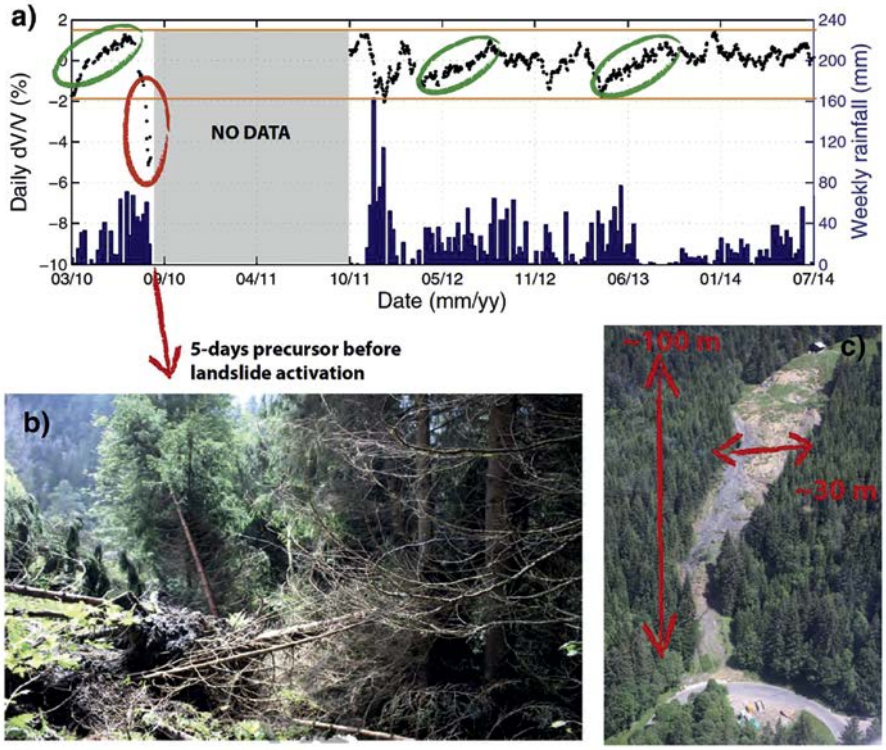

Figure 166. Landslide in the vicinity of Swiss mountain ski resort Les Diablerets [Larose et al, 2015]

Legend: a) variation of relative velocity observed within a 4-year period; b) soil slip collapse of 2010; c) soil slip position before the event of 2010

from -2% to -7% [Larose et al., 2015]. As a result of reduction in rigidity, a sink of the slope took place, whereas the creeping process followed subsequently – from August, 20 to August, 22. Therefore, a forerunner exceeding the limits of the background level sprung up five days prior to the landslide (creeping) event.

One of the important findings of the studies [Larose et al., 2015] is that, despite heavy rains and fluctuations in the groundwater level fluctuations, a 4% velocity change (from 2% to -2%) was recorded only late in the autumn of 2011; however, the change was within the limits of background values.

This attests to the fact that the data obtained by groundwater studies cannot be used as the only criterion for the forecasting of soil slip activity. ASN makes it possible to control tiny changes in the subsurface.

In this respect, a promising parameter is changes in relative velocity dV/V of seismic waves, or changes in resonant frequencies of geological structures. The background fluctuations of velocity change dV/V are, most probably, within the limits from 2% to -2%. Variations dV/V exceeding those limits should be interpreted as internal changes – such as changes in rheology.

5.2.8.2. Relationship between soil-borne radon emanation and ambient seismic noise

A topical problem of environmental safety is the control of radon airborne concentration. Radon R^{222} is an inert gas adversely affecting human health. The half-life time of radon is 3.824 days only. According to UN statistics, from 3% to 14% of all the lung cancer cases worldwide are associated with human exposure to this radioactive gas. The airborne concentration of radon depends of geologic setting. Granites with a high content of uranium are an active, radon-generating source. Sedimentary cover is a screen for radon penetration onto the surface. In the context of sedimentary cover, a high concentration of radon may be observed in tectonic fault areas. This fact is confirmed by a number of studies carried out within the boundaries of East European Platform [Спивак & *Шувалов*, 2008; Spivak et al., 2009; Матвеев и др., 2012].

Due to its high permeability, a fault is a channel for underground fluids migration. Deep-seated structures within sedimentary cover manifest themselves as narrow enough areas of excessive fissuring and fluid permeability, and as anomalies of geophysical fields and gradient morphological features [Anisimova & Koronovsky, 2007; Nikolaev et al., 2002; Юдахин и др., 2003; Горбунова и др., 2002].

The radon registration results have shown (Figure 167) that the absolute intensity of gas emanations in the fracture zones is usually 3–6 times higher than in the middle sections of structural blocks [Матвеев и др., 2012; Spivak et al., 2009].

The profile Medvinovichi – Baranovichi – Krasnaya Sloboda is located in Western Belarus and it extends from north-west to south-east – from the Belorussian anteclise to Pripyat Trough.

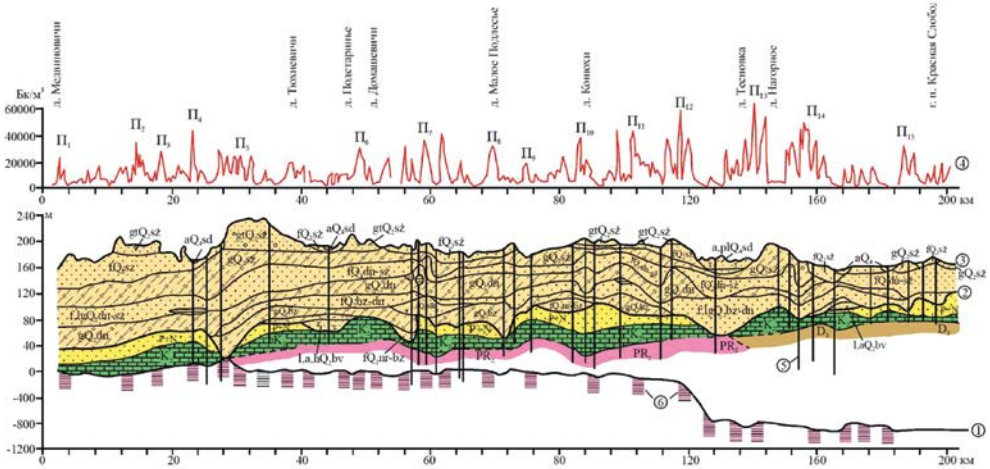

Figure 167. Distribution of radon concentrations in the subsurface layer along the Medvinovichi – Krasnaya Sloboda profile (Belarus) [Matveev et al., 2012]

Legend: 1 – the basement surface; 2 – Pre-Quaternary bedrock surface; 3 – the Earth surface; 4 – radon concentration in soil air; 5 – wells; 6 – the basement dislocations with a break of continuity; П1–П15 – abnormal radon concentration

The measurement interval used on the profile was 100–250 m. The background values of radon concentration were about 10,000 (20,000) Bq/m^3, while the anomalous values varied within the range 20,000 to 50,000 – 55,000 Bq/m^3. It was found that most of the 15 identified anomalies are associated with geological rocks characterized by the smallest content of uranium. There are no direct dependencies of elevated radon concentrations in the composition and bedding depth of foundation rocks. Although the association of anomalies with some genetic types of the upper part of Quaternary deposits is certain, it is not always clearly expressed anyway. Radon anomalies are most closely associated with rupture anomalies. It is exactly in these zones that active current geodynamic processes are the main factor contributing to the formation of elevated radon concentrations [Матвеев и др., 2012].]

Underground gas flows in the fault zones exceed the background values substantially, which is clearly illustrated by the example of the Prioksky section of Nelidovo-Ryazan tectonic structure (Figure 168). The underground gas flow level and the concentration of gases on surface sections reflect the permeability degree of migration channels – i.e., faults [Спивак & Шувалов, 2011].

Moreover, radon is an indicator of geodynamic activity. In the area of tectonic faults, an increased content of radon may be expected even on platforms. In addition, the

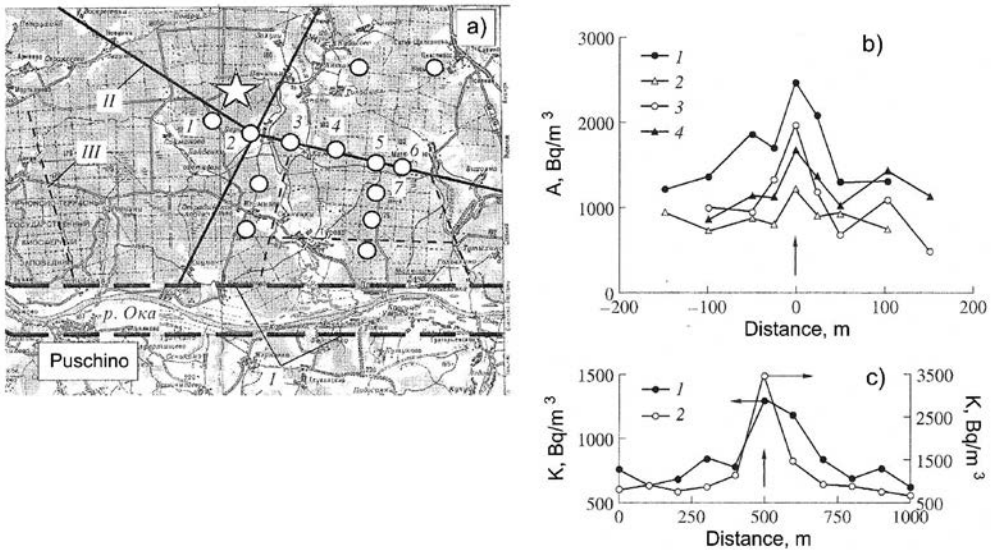

Figure 168. Volumetric activity of radon in subsoil atmosphere along the traces crossing a second-order tectonic dislocation (fault) [Спивак и др., 2009]

Legend: a) the scheme of observation area for the Prioksko-Tersky section of the Nelidovo-Ryazan tectonic structure: II and III – tectonic faults of II and III order, respectively; 1–7 – record points; the asterisk denotes the "Mikhnevo" observatory. The volumetric activity of radon in subsoil atmosphere along the traces crossing a second-order tectonic fault: b) points 3–6 correspond to curves 1–4; c) points 6 and 5 correspond to points 1 and 2. The vertical arrows designate the position of the tectonic fault

radon concentration is affected by meteorological conditions. Rain, snow, and frosty weather obstruct the access of radon into the air. On the contrary however, such factors as an increase in temperature and in wind speed, favor the ingress of radon into the air. Thus, meteorological factors make it difficult to estimate radon concentration accurately by special detectors and slow down the measurement process.

Seismologic measurements can render a substantial aid when the identification of fault zones with an elevated radon concentration should be carried out. This becomes possible as a result of the fact that, as a result of laboratory measurements, the impact of certain vibration frequencies on the radon flux from samples was determined. The subject of research was the ratio of the radon flux from the surface of granite sample Q to the initial flow Q_0, which was measured in the absence of vibrations. Figure 169 demonstrates, how the vibration influence increases the radon flux from the rock sample significantly. Regardless of the Q_0 value, the maximum flux was observed at a vibration frequency of about 16 Hz [Spivak et al., 2009].

Another, less pronounced maximum of the ratio $Q/Q_0(f)$ was observed at a frequency of about 32 Hz with respect to the sample with Q_0 – 375 particles/sec. A comparison between variations in the volumetric activity of subsoil radon and the amplitude variations of micro seismic background and individual quasi-harmonic oscillations of different frequencies under natural conditions – showed a high correlation between the radon exhalation levels (the correlation coefficient is about 0.9) and the relative amplitude of quasiharmonic oscillations at a characteristic frequency of 16.6 Hz [Спивак и др., 2009; Spivak et al., 2009].

Thus, on the basis of the revealed correlation between the activity of subsoil radon and microseisms, the surrounding seismic noise – in particular, frequencies close to 16 Hz, can be used as diagnostic signs of an increased radon exhalation in tectonic fault zones. Seismic noise measurements are less susceptible to atmospheric conditions and more operational than the direct measurements of radon concentration by radiation

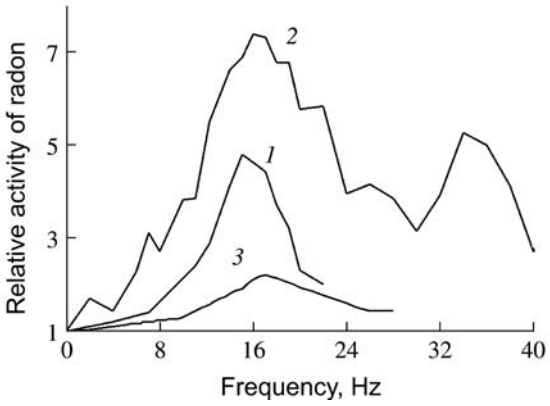

Figure 169. Relative radon flux from a granite sample depending on vibration frequency at different initial flux Q_0 rate (particles/sec): 1 – 200; 2 – 375; 3 – 75 [Spivak et al., 2009]

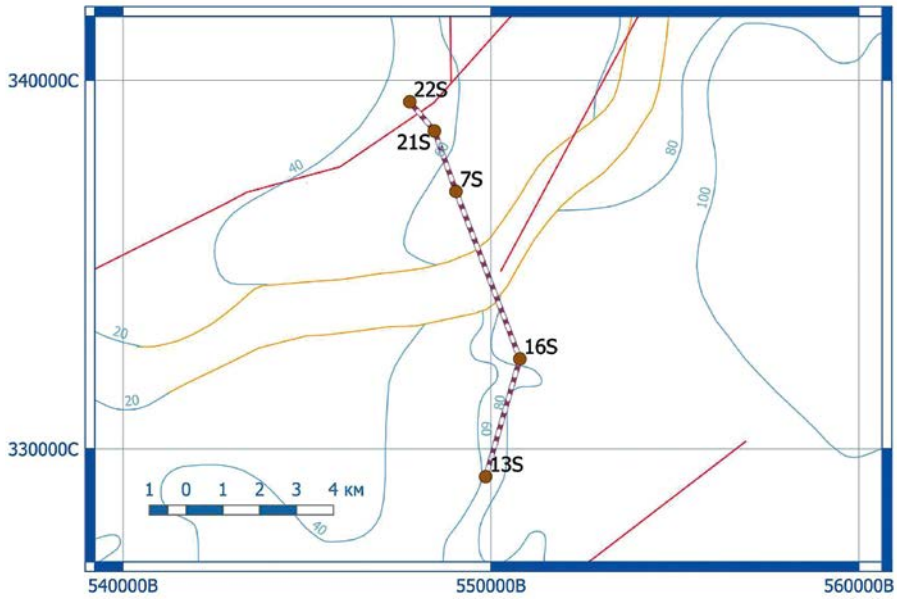

Figure 170. *Rn*^{222} measurement profile scheme at the Inčukalns – Vangaži section
Legend: red lines – tectonic faults; yellow lines – river valleys; blue lines – structural contours of rock deposits

detectors. On the profile sections where spectral peaks at frequencies close to 16.6 Hz will be detected, control measurements of the activity of subsoil radon should be carried out to confirm the increased radon concentration.

Within the framework of a test survey, radon concentration measurements were carried out in Latvia on three pilot sites: Inčukalns – Vangaži, the Riga suburbs, and Talsi – Valdemārpils [Gilucis, 2014_*upm*]. The tectonic faults of the Caledonian structural complex are located only within the limits of some of those sections. In particular, the Olaine – Inčukalns and the Turaida tectonic faults are located in the area of the Inčukalns – Vangaži section (Figure 170).

Within the 1 km-long profile section – i.e., between the measurement points 22S and 21S – the Olaine-Inčukalns, a tectonic fault is located. An abnormal concentration of *Rn*^{222} is observed at the observation point 21S (Figure 171). This observation point is located at 1.4 km distance only from the tectonic node which lies to the north of that point. Therefore, we can assume that the anomaly recorded at point 21S is associated with the Olaine-Inčukalns tectonic fault.

Taking into account the existing signs of the fault activation [Ņikuļins, 2017a], we can state one more evidence confirming this conclusion The seismological method application for ambient seismic noise measurement in the tectonic faults location area will make it possible to specify the locations covered by seismic noise spectrum of the frequency $f = 16.6 \pm 0.2$ Hz. It is advisable to carry out radon concentration measurement in those sections in the future. Firstly, such studies will make it possible to identify areas

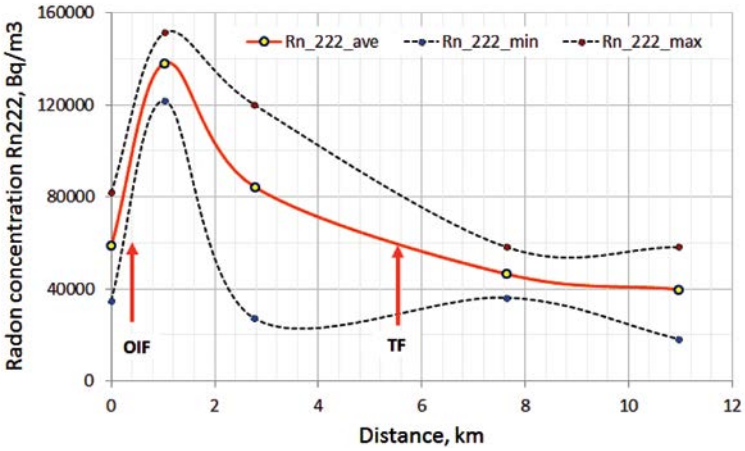

Figure 171. Changes in Rn^{222} concentration level at the Inčukalns – Vangaži section

Legend: OIF – Olaine-Inčukalns fault; TF – Turaida fault

of high concentration of radioactive gas – radon, which is dangerous for human health and life; secondly, the studies of that kind will enable determining geodynamic hazard-prone areas, where it is inappropriate to build any residential buildings and important economic facilities.

5.2.8.3. Assessment of dynamic parameters of soil lying under traffic arteries

A relevant practical task is to assess the parameters of soil ballast under traffic arteries – such as railways and motor roads. The main functions of ground ballast are: distribution of load from cross-sleepers, damping of dynamic load, increasing the lateral resistance, and the provision of free drainage conditions. However, in the process of operation of railways and motor roads, soil deterioration occurs under the roadway liner over time.

When designing a rail track, it is necessary to choose the most favorable option from several possible ones. The specific location of the rail tracks is influenced by such factors as geological structure, topography, the possibility of slips, soil density, and groundwater level. The design routes can be explored by using geophysical, geological, and geotechnical methods. Geophysical methods, in particular, seismic ones, are used to calculate the dynamic properties of soils and to estimate the velocity of compression and shear waves. Velocities are are key parameters in predicting the soil response to dynamic loads.

The simplest method for the assessment of an embankment under railway is to assess the vulnerability index K_g (Formula 106). With respect to railway trunks, this method has been proposed and further developed by Nakamura [Nakamura, 1997]. The embankment proper can be considered as a local, additional surface layer with the vulnerability index of its own. Ideally, the first measurement runs should be carried out after the completion of railway construction, or after the railway repair. Then,

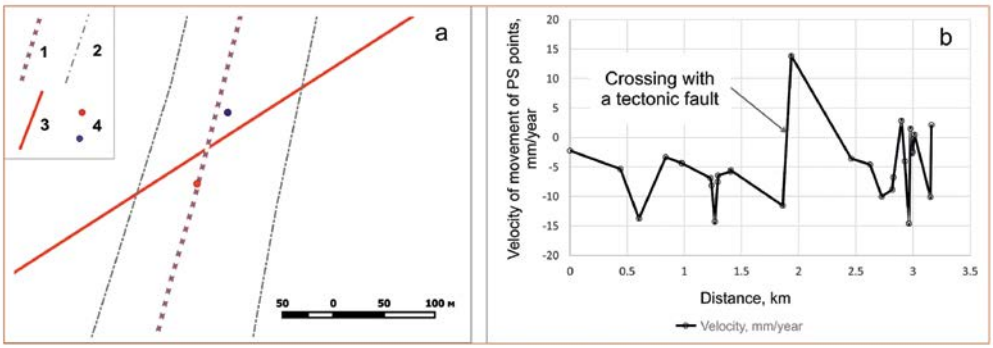

Figure 172. Abnormal velocities of movement of points of sounding of PS on the site of the railroad which is crossed by a tectonic fault [Ņikuļins, et al., 2016].

Legend: a – scheme of railway crossing by a tectonic fault: 1 – the railway, 2 – the contours of polygon of geological hazard polygon, 3 – the tectonic fault, 4 – the red point PS (V_{PS} = –11.6 mm/year), 5 – the blue point PS (V_{PS} = +13.8 mm/year); b – curvevelocity of movement PS points

the following measurement runs will make it possible to specify the nature and the magnitude of K_g change after the earthquake.

At the same time, such assessments can provide useful information on the railway embankment condition at sections where slow crustal motions are taking place. As an example, let us consider the situation on a railway section in the Riga suburbs (Figure 172a). Within the framework of the *PanGeo* project, the sounding locations travelling speed velocities V_{PS} were estimated. At the PS point of the railroad section between Tiraine and Gaismas, opposite movement velocities V_{PS} took place [Ņikuļins u.c., 2016]. Those points are located at different sides of an unnamed tectonic fault crossing the railway (Figure 172b). With regard to the territory of Riga, the background values of V_{PS} = ± 1.5 mm/year. The overall annual travel speed of the two fault edges in the opposite directions reaches 25.4 mm/year.

At such a movement velocity of the opposite fault edges, the railway bed can be damaged. An assessment of the dynamic properties of the ballast under the railway could clear up the matter of development of deformation. Should that be the case, it would be expedient to apply the vulnerability index assessment method.

CONCLUSION

At present, the subject of seismicity of the East Baltic Region, as well as the seismological survey issues have become relevant due to several reasons.

Firstly, it became obvious after the Kaliningrad earthquakes of 2004 that, although the East Baltic Region is among the territories with a low seismicity level, there is still a possibility that strong earthquakes may occur therein, causing substantial material damage to buildings and structures, and posing hazard to human health and even human life. Secondly, EBR features unfavorable soil conditions – namely, the upper layer of soft and water-saturated soil lies on hard rocks, which are predominantly represented by Devonian deposits. Under certain soft soil thickness/seismic wave length ratios, resonance phenomena occur which enhance seismic oscillations.

Thirdly, hydraulic power and nuclear power engineering are currently gaining pace on the territory of the East Baltic Region. This demands higher standards – not only in terms of selection of construction sites but in terms of the follow-up control as well, including, in particular, seismic monitoring of energy facilities in process of their operation. As regards nuclear power stations (NPS), the corresponding instructions from IAEA are applicable, prescribing the way of selecting the construction site and the monitoring mode during operation. Such a precedent already exists in EBR in the form of the local system of seismic monitoring around the Ignalina NPS. It is also expedient to develop a similar system in other power facilities location areas – in particular, in the area of the Pļaviņas HPP. This is related to the currently existing complicated geodynamic situation.

Fourthly, over recent decades, certain prerequisites have arisen for the development of a seismological direction based on the study of specific features of ambient seismic noise (ASN). Such prospects have arisen due to the appearance of high-sensitivity sensors with low internal noises and the leading-edge time service (GPS), the creation of compact systems of seismological observations (seismic array), the increase in the capabilities of computer-based technology, the development of methodology (ASN correlation, the study of coda waves, development of data collection systems, and the improved data processing).

Thanks to the implementation of those prerequisites, the study of ASN characteristics makes it possible to detect subtle changes in the parameters of the geologic environment located directly under the Earth's surface, and to identify small-power seismic sources among the ambient noise, – thereby, shaping a new environmental trend in seismology.

The East Baltic Region is located within the boundaries of Fennoscandia, which, apart from Sarmatia and Volga-Uralia, is one of the three constituent parts of the East European Platform (EEP). A typical feature of the formation of Palaeoproterozoic and juvenile Earth's crust between the Baltic and the Ukrainian shields were accretionary processes, which resulted in the formation of terrains as geologic features (bodies) confined by faults and having a considerable extension.

Paleo reefs are of prime importance in platform geodynamics. Within the limits of EEP, the Paleo-reef system extends from north-east to south-west. The Polotsk-Kurzeme belt of faults crosses the EEP from west to east. The deep-seated geologic framework shows that the thickness of the Earth's crust varies from 30–35 km to 42–47 km when passing through the Teisseyre-Tornquist zone – from the Paleozoic West European Platform to the Precambrian East European Platform.

The maximum thickness of the Earth's crust in the East Baltic Region – 64 km – has been stated in the central part of Latvia. A deep seismic sounding carried out within the Baltic Sea waters had identified a depression at a depth of 45 km, which is interpreted as an ancient rift zone. A simulation of a disequilibrium of isostatic balance at the level of Moho discontinuity, which was carried out along the deep seismic sounding profile Sovetsk-Riga-Kohtla-Jarve, made it possible to get an idea of the isostatic index behavior and its connection with geologic geophysical, neo-tectonic, and geodetic parameters, and to make a reliable assessment of the dominating processes of the Earth's crust development.

In the Ierikˌi region, where the maximum ascentional velocity of the Earth's crust was recorded, an excessive depth of the Moho discontinuity is fixed, which is interpreted as disequilibrium of isostatic balance, while the elevation of the Earth's crust should be regarded as a compensation for this disequilibrium.

Thus, despite the fact that the EBR is located on the territory of an ancient platform, the geological-tectonic and geodynamic situation on the EBR territory do not seem absolutely favorable, and require a comprehensive and systematic attention and control.

The EBR seismicity review covers a long historic period – from written records of seismological phenomena to plotting maps of seismic hazard and carrying out seismic monitoring with the use of the BAVSEN virtual seismic stations network.

Analysis of seismic-tectonic conditions as prerequisites of seismicity was carried out with respect to the stable continental crust as a whole, as well as for the well-studied North American platform and the East European Platform (EEP). Such a comparison made it possible to find some analogies in the association of seismicity with certain structural elements of the Earth's crust of the EEP. The analogies imply that the most part of intra-plate earthquakes are associated with rift crust, whereas the other part of earthquakes characterizes dispersed seismicity. The analogies also concern the impact on both platforms from the glacial sheets of the Northern Hemisphere, the disequilibrium of isostatic balance, the subsequent re-establishing of the balance, and its effect on seismicity. At present, the processes of re-establishing isostatic equilibrium have lost their dominant impact on seismicity, which currently is mostly associated with the pressure exercised from the Northern Atlantic ridge.

The analysis of seismic conditions has shown that the depth of the seismically active layer on EEP varies from 0 to 68 km, while the maximum magnitude value is assessed as 6.1–6.3 – depending on the source of information (the Russian or the Finnish catalogues). The EEP seismicity is mostly concentrated on the Baltic Shield. The earthquake-prone areas are the coast of the Gulf of Bothnia, as well as the south-west of Sweden. The main horizontal tectonic strains are oriented from the NW to SE and are caused by pressure from the North Atlantic ridge.

The EBR seismicity, exactly like the EEP general seismicity on the whole, is unevenly distributed in space and time. This is associated with the fact that the EEP with its Precambrian crust was considered to be an aseismic region where the earthquake phenomenon is quite a rare occurrence. Therefore, instrumental observations started to gain pace practically since the 1950s. So statistical representativeness of earthquake is scarce enough.

The distribution of earthquake foci in the East Baltic Region shows that several seismic foci are associated with the Polotsk-Kurzeme belt of faults. Relative concentration of earthquake foci is stated in Estonia – particularly on the west coast of the country (the Osmussaare Island) and the area of the Vyrtsyarv Lake. The foci of the Irbene, the Liepaja, the Ventspils, and the Kaliningrad earthquakes are associated with the coastal part of the Baltic Sea. Generally, the littoral area of the Baltic Sea is characterized by a higher seismicity as against the inland part of the EBR.

Among the historical earthquakes that took place in EBR, the intraplate earthquakes of Bauska and Koknese can be highlighted. Certain geological tectonic prerequisites have been brought to light to explain the Koknese earthquakes. Analysis of distribution of winter temperatures has shown that the earthquakes of 1908 are associated with cryoseisms. This point of view was already given by Professor A. Nikonov, based on the EEP earthquake studies. Such phenomena occur at winter temperature jumps that had taken place in December, 1908 in EBR.

Strong earthquakes took place in EBR in 1976 and 2004 on the Osmussaare Island in Estonia and the Kaliningrad Region in Russia. The Kaliningrad earthquake as of September 21, 2004 (13:32 GMT) had the largest magnitude 5.2 among all the known earthquakes that took place in EBR.

The first two Kaliningrad earthquakes were the only ones for which solutions of the focal mechanism were found. They showed that, in the earthquake foci, there was right lateral strike slip on a WNW-ESE near-vertical fault of orientation almost parallel to the Tornquist-Teisseyre Zone. Detailed parameters of the foci of the first two Kaliningrad earthquakes are given in chapter 3.3.2. At the same time, there was a certain discrepancy in the determination of the epicenters of the Kaliningrad earthquakes based on seismic monitoring data and macroseismic studies. This is a prerequisite for further studies of the characteristics of the focal zones of strong earthquakes that took place in EBR.

Much of the work is devoted to the human-induced seismicity in the EBR. Most of the sources of human-induced seismicity are associated with explosions occurring in the continental part and in industrial quarries; much fewer explosions occur in the water area of the Baltic Sea. Magnitudes of mass explosions, as a rule, do not exceed 2.4–2.6, but in most cases they are much smaller. Baltic Virtual Seismic Network *BAVSEN* is formed by broadband seismic stations, which are located at great distances from each other.

Thus, this makes it difficult to isolate signals generated by weak seismic events against a background of seismic noise, and further complicates their identification. The methods of identifying tectonic earthquakes do not give an unambiguous answer to the question of the genesis of seismic event. To a large extent, this is due to the limited number of records of regional earthquakes that took place in EBR. Nevertheless, this work outlines some methods that can be used in further studies directed at identifying

the genesis of seismic events. The local BAVSEN network's capability of identifying a nuclear explosion on the Korean peninsula has been demonstrated.

The fifth chapter is dedicated to applied methods of seismology. Within the framework of this section, results of seismic zoning carried out on EBR territory are presented. They cover both the results of the projects, wherein the EBR was only a small constituent part (like for example, the GSHAP project or the results of seismic zoning carried out prior to 1991) and the results of research conducted directly with respect to the EBR territory or its individual parts (Latvia). The results showed that the maximum epicentral intensity on the EBR territory may reach VI–VII on the EMS-98 scale or its earlier analogue – the MSK-64 scale.

Unlike the research conducted prior to 1991 which had applied deterministic methods, the later research relies preferably on the probabilistic methods for the assessment of seismic hazard.

The modern insight into the seismic hazard and the use of probabilistic methods for the assessment thereof is based on the methodological recommendations of Eurocode-8. The assessments of seismic hazard for the territory of Latvia are expressed in Peak Ground Acceleration values. The assessment results showed that shocks with the acceleration of 10–13 cm/sec^2 may occur on hard ground (Pre-Quaternary deposits) in a some of populated localities of Latvia (Sigulda, Riga, Olaine, Aizkraukle, Ainaži, Cēsis) and their environs with a probability exceeding 10% within the time period of 50 years.

As regards seismic microzoning results (SMR), they are more important from a practical standpoint. On the territory of EBR, SMR was carried out in two cases. For the first time ever, SMR using the seismic intensity augmentation method was carried out on the site of the Salaspils nuclear reactor under the Academy of Sciences of Latvia in Salaspils.

Lack of augmentation of seismic intensity on the site was stated, including the reactor proper.

It turned out that the resulting maximal intensity of the expected earthquake was VII on the MSK-64 scale. Deepening the basement of the reactor structure to the depth of 12 m makes it possible to lower the seismic intensity at the expense of increasing the seismic rigidity of the underlying rock.

The seismic zoning of the Kaliningrad city was carried out after the earthquakes of 2004 took place. Within the Kaliningrad city limits, the maximum augmentation of seismic intensity, taking into account the 30 m thick upper part of sedimentary deposits, reached 0.5 points and was associated with the flood plain part of Pregol River.

From the practical standpoint, the significance of the work is connected with the systematization and the applicability analysis of the applied methods for seismic surveys – with respect to territories characterized by low seismic activity, to which EBR refers to. At the same time, the main target of research is ambient seismic noise (ASN), which is present everywhere. From the viewpoint of environmental standards, the ASN investigation method is a non-destructive, environmentally-friendly method where no seismic wave generation is required. This fact is especially topical in the context of urban agglomerations.

The study of dynamic characteristic of soils by applying the HVSR spectral ratio-based method is an important real-world application when investigating soil properties on construction sites intended building various facilities.

With respect to buildings, structures, ballast under railway embankments, highways, and other objects bearing signs of deformation, the HVSR method allows to obtain vulnerability assessments, which can characterize the reliability of a structure, road or other object, and the prospects for its further use. The *HVSR* method makes it possible to assess the thickness of loose (unconsolidated) quaternary deposits on mineral deposits and also in cases where one has to delineate the area of a productive layer, lying most closely to the Earth surface. For a number of seismic stations operating in EBR, parameters of spectral peaks and frequencies were specified. A preliminary assessment of the correlation between the resonance frequencies and the thickness of loose quaternary deposits is obtained. This assessment is of great practical importance for the rough analysis, but it needs additional, original statistics. Among the methods considered, it is necessary to highlight the structural monitoring of buildings and structures, which complements its design method of structural analysis and especially modal analysis. For structural monitoring, both the active (seismic source) and the passive (ASN) method can be used. The expediency of structural monitoring of high-rise buildings and structures, located within urban agglomerations, is based on the fact that it is exactly urban environment that is associated with a high probability of the presence of human-induced seismic sources, such as traffic, especially railways, operating boiler houses, thermal power stations, vibration from machines and mechanisms, pile driving in soil, powerful transformers, etc. These sources can have a cyclic effect on objects and cause fatigue in structural materials. Due to that, relatively small, but systematic and prolonged cycling may lead to violations of material integrity and the occurrence and propagation of cracks in buildings and structures. An additional disadvantage is soil conditions, which may adversely affect buildings and structures.

Some of the equally important practical methods, which are briefly described in this work are ASN monitoring to control landslide processes that take place, especially in river valleys of the EBR, localization of weak seismic sources due to using time correlation of signals recorded at least by two sensors, and using *ASN* parameters (16.6 Hz frequency) as diagnostic signs of elevated radon concentration. These methods, based on the ASN analysis, relate to the field of ecological seismology, which has been developed over the past two decades. It is exactly these methods that can be effective for solving a number of environmental problems existing on the EBR territory.

Thus, seismological methods are already currently used in territories with a low level of seismicity – particularly in EBR. So far, this has concerned seismic zoning and seismic microzoning. It is to be hoped that new applied methods in the field of environmental safety, structural monitoring and analysis of dynamic properties of soils will also be in demand in the East-Baltic region in the near future.

List of publications

Adams J., Basham P.W., 1989. Seismicity and seismotectonics of Canada's eastern margin and craton. Earthquakes at North-Atlantic Passive Margins: Neotectonics and Postglacial rebound. / Edd. Gregersen S., Basham P.W. pp. 355–370.

Agilent Technologies, 2000. The Fundamental Modal Testing. Application Note 243–3.

Ahjos T., Saari J., Pentilla E., Korhonen H., 1984. Earthquakes and seismic hazard in Finland. Engineering Geology, v. 20, N 1/2, 1–12.

Aki K. and Richards P.G., 1980. *Quantitative seismology*. Freeman, San Francisco, Vol. I and II, 932 pp.

Allamehzadeh M., Mokhtari M., 2003. Prediction of Aftershocks Distribution Using Self-Organizing Feature Maps (SOFM) and Its Application on the Birjand-Ghaen and Izmit Earthquakes. Journal of Seismology and Earthquake Engineering (JSEE), 5, 1–15.

Albini P., Musson R.M.W., Gomez Capera A.A., Locati M., Rovida A., Stucchi M., Vigano D., 2013. Global Historical Earthquake Archive and Catalogue (1000–1903). GEM Technical Report 2013-01. 202 pp.

Ambraseys N.N., Douglan J., Sarma S.K., Smit P.M., 2005. Equations for the estimation of strong ground motion from shallow crustal earthquakes using data from Europe and the Middle East: horizontal peak ground acceleration and spectral acceleration. Bulletin of Earthquake Engineering 3, 1–53.

Ananyin I.V., Bulin N.N., Klaasman E.R., 1980. *The Osmussaar earthquake of October 25, 1976*. Землетрясения в СССР в 1976 году. М., Наука, 91–97.

Anderson E.M., 1951. The dynamics of faulting and dyke formation with application to Britain, 2nd ed., Edinburgh, Oliver and Boyd.

Anisimova O.V., Koronovsky N.V., 2007. Lineaments in the central part of the Moscow syneclise and their relations to faults in the basement. Geotectonics 41 (4), 315–332.

Arai N, Yoshida Y., 2004. Discrimination by short-period seismograms. International Institute of Seismology and Earthquake Engineering, Building Research Institute (IISEE), Lecture Note, Global Course, Tsukuba, 10 pp.

ASCE/SEI 7-05, 2006. *Minimum Design Loads for Buildings and Other Structures*. American Society of Civil Engineers. 419 pp.

Assinovskaya Б.А., Nikonov **A.A., 1998**. Felt earthquakes of the XXth century in the Eastern Baltic shield. / XXVI General Assembly of the European Seismological Commision: Abstracts. Tel Aviv, Israel, p. 10.

Asten M.W., 1978. *Geological control of the three-component spectra of Rayleigh-wave microseisms*. Bulletin of the Seismological Society of America 68 (6), 1623–1636.

Asten M.W. & Henstridge J.D., 1984. *Arrays estimators and the use of microseisms for reconnaissance of sedimentary basins*. Geophysics 49 (11), 1828–1837.

Astiz L., Earle P., Shearer P., 1996. Global stacking of broadband seismograms. Seismol. Res. Lett., 67, 8 - 18.

Anisimova O.V., Koronovsky N.V., 2007. Lineaments in the central part of the Moscow syneclise and their relations to faults in the basement. Geotectonics 41 (4), 315–332.

Basham P.W., Adams J., 1983. Earthquakes on the continental margin of eastern Canada: need future large events be confined to the locations of large historical events? USGS Open File Report 83-843, pp. 456–467.

Bennet T.J., Murphy J.R., 1986. Analysis of seismic discrimination capabilities using regional data from western United States events. Bull. Seism. Soc. Am., 76, 1069–1086.

Bogdanova S. V., 1993. *Segments of the East European Craton*. In: Gee, D. G. & Beckholmen M. (eds) EUROPROBE in Jablonna 1991. European Science Foundation–Polish Academy of Sciences, 33–38.

Bogdanova S.V., Pashkevich I.K., Gorbatschev R. & Orluk M., 1996. *Riphean rifting and major Palaeoproterozoic boundaries in the East European Craton: geology and geophysics*. Tectonophysics, 268, 1–22. Русского географического общества, СПб., 582 с.

Bogdanova S. V., Gorbatschev R. & Garetsky R. G., 2005. *The East European Craton*. In: Selley R. C., Cocks L. R. & Plimer I. R. (eds) Encyclopedia of Geology, 2. Elsevier, Amsterdam, 34–49.

Bogdanova S., Gorbatschev R., Grad M., Janik T., Guterh A., Kozlovskaya E., Motuza G., Skridlaite G., Starostenko V., TaranL. & EUROBRIDGE and POLONAISE working groups, 2006a. *EUROBRIDGE: new insight into the geodynamic evolution of the East European Craton*. European Lithosphere Dynamics. Gee D.D. & Stephenson R.A. (eds), Geological Society, London, Memoirs, 32, 599 0 625.

Bogdanova S., Kozlovskaya E., Janik T., Taran L. & Yliniemi J. 2006b. *EUROBRIDGE: origin and geodynamic significance of the highvelocity lower crust in the Fennoscandia–Sarmatia suture zone*. Bulletin of the Geological Society of Finland, Special Issue, 1, 17.

Bonnefoy-Claudet S., Cotton F., Bard P-Y., 2006. *The nature of noise wavefield and its applications for site effects studies.* A literature review. Earth-Science Reviews, 79, 205–227.

Borman P., Bergman E.A., Engdahl E.R., King R., Baumbach M., Bock G., Grosser H., Choy G., Boatwright J.L., Wielandt E., Asch G., Trnkoczy A., Hanka W., Holcomb L.G., Nigbor R.L., Havskov J., Ottemoller L., Schweitzer J., Fyen J., Mykkeltveit S., Kvaerna T., Dost B., Zednik J., Willeman R.J., Klinge K., Wendt S., Musson R.M.W., Wassermann J., Kruger F., Bribach J., Teupser Ch., Wylegalla K., Storchak D., Udias A., Zurn W., Zivcic M., Ravnik J., Peterson C., 2002. New Manual of Seismological Observatory Practice. (NMSOP). Volume 1,Potsdam, Boulder : GeoForschungsZentrum Potsdam, IASPEI.

Bracewell R.N., 1978. The Fourier Transfornation and its Applications (2nd edn.). McGraw-Hill, New York. 444 p.

Brangulis A.J., Kanev S., 2002. Latvijas tektonika.p. 50.

Brincker R., Anderson P., Kirkegaard P.H., and Ulfkjaer J.P., 1995. Damage Detection in Laboratory Concrete Beams. Proc. of the 13th International Modal Analysis Conference, 1, 668–674.

Brownjohn J.M.W., 2007. *Structural heath monitoring of civil infrastructure*. Philosophical transactions of the Royal Society A, 365, 589–622.

Brune J.N., Oliver J., 1959. The seismic noise of the Earth's surface, *BSSA*, 49, 349–353.

Bulin N.K., Afanaseyeva N.A., Volkov A.V., 1980. *Aftershocks in the Estonia earthquake of 1976 and deep structure of the epicentral zone*. Seismicity and recent movements of the Earth's crust in the Eastern Baltics, Apatity, 24–39.

Bulletin of International Seismological Centre, 1976. Newbury, R6, 13, 1LZ. Berkshire, UK, 84 p.

Bungum H., Alsaker A., Kvamme L. B., Hansen R. A., 1991. Seismicity and seismotectonics of Norway and nearby continental shelf areas, J. Geophys. Res., 96, 2249–2265.

Byrtin A., Bollinger L.,Vergne J., Cattin R., Nabelek J.L., 2008. Spectralanalysisofseismic noise induced by rivers: A new tool to monitor spatiotemporal changes in stream hydrodynamics. Journal of Geophysical Research, 113, B05301, pp. 1–14.

Carder D.S., 1945. Seismic investigations in the Boulder Dam area, 1940–1944, and the influence of reservoir loading on earthquake activity. Bull. Seismol. Soc. Am. 35, 175–192.

Cawley P., Adams R.D., 1979. *The Locations of Defects in Structures from Measurements of Natural Frequencies*. Journal of Strain Analysis, 14 (2), 49–57.

Charney F.A., Easterling W.S., Harris J.R., Klingner R.E., Martin J.R., Pryor S., Symans M.D., 2007. Instructional Material Complementing FEMA 451, Design Example.NEHRP Recommended Provisions for New Buildings and Other Structures: Training and Instructional Metarials. 2097 p.

Coppersmith K. J., Johnston A. C., and Arabasz W. J., 1987. Methods for assessing maximum earthquakes for central and eastern United States, E.P.R.I. Research Project 2556-12, Working Report, Electric Power Research Institute, Palo Alto, CA.

Coppolino R.N. & Rubin S., 1980. Detectability of Structural Failures in Offshore Platforms by ambient Vibration Monitoring. Proc. 12th Annual Offshore Tech. Conf., 4, 101–110.

Cornell C.A., 1968. Engineering Seismic Risk Analysis.Bulletin of the Seismological Society of America, vol. 58, N 5, 1583–1606.

CTBTO Preparatory Commission, 2003. *International monitoring system* (map).

David M.Lucas, 1813. Preussische Chronik. Funfter Band. Konigsberg, 246 p.

Dewey J. W., 1988. Midplate seismicity exterior to former rift-basins.Seismol. Res. Lett., 59, pp. 213–218.

Dišlere S., 2010. Sufozijas procesu norises likumsakarības Daugavas ielejā pie Pļaviņu HES. Latvijas Universitātes 68. zinātniskā konference. Ģeoloģija. 294–295.

Dietz R. S., 1961. Continent and Ocean Basin Evolution by Spreading of the Sea Floor. *Nature,* 190 (4779),pp. 854–857.

Doss B., 1898. Ubersicht und Natur der in Ostseeprovinzen vorgekommen Erdbeben. Korrespondezblatt des Naturforschen – Vereinz zu Riga. XL, pp. 145–162.

Doss B., 1905. Über ein unbeachtet gebleibenes Beben in Estland. Korrespondenzblatt der Naturforschen – Vereins zu Riga. XL VIII, s. 121–138.

Doss B., 1909. *Die historisch beglaubigten Einsturzbeben und seismish-akustishen phonomene der russischen Ostseeprovinzen*. Beitrage tuz Geophysik. Leipzig, B.X, H.1, S. 1–124.

Doss B., 1910. Die Erdstösse in der Ostseeprovinzen im Dezember 1908 und Anfang 1909. Korrespondenzblatt der Naturforschen – Vereins zu Riga. LIII, s. 73–107.

Doss B., 1911. Über die Erdstösse in den Ostseeprovinzen in den Jahren 1908 und 1909 sowie einige frühere, bisher unbekannt gebliebeneErdstösse ebendaselbst. Riga, Polyrechnikum.

Dynamique d'une experience spatiale: analyses et verification, 1994. J.M. Defise. 3 eme Congres National Berge de Mecanique Theorique et Appliquee, 253–256. Universite de Liege.

Eurocode 8, 2005. Design of structures for earthquake resistance – Part 1: General rules – Seismic action and rules for buildings.

Ellerbrock P., 1997. DC-XA Structural Health Monitoring Fiber-optic Based Strain Measurement System, Proceedings of the SPIE, 3044: 207–218.

Ellsworth W., 2013. Injection-Induced Earthquakes. Science. Vol. 341, 6142.

EN 1998-1: 2004 (E). Eurocode 8 – Design of structures for earthquake resistance – Part 1: General rules – Seismic action and rules for buildings.

Engdahl E.R., Vander Hilst. R. and Buland R., 1998. Global teleseismic earthquake relocation with improved travel times and procedures for depth determination, Bull. Seism. Soc. Am. **88**, 722–743.

FEMA 451, 2007. *Instructional Material Complementing FEMA 451, Design Examples.*

Foulger G.R., Wilson M., Gluyas J., Julian B.R., Davies R., 2017. A Global Review of Human-Induced Eartquakes.

Fox C.H.J., 1992. The Location of Defects in Structures: A Comparison of the Use of Natural Frequency and Mode Shape Data. Proc. of the 10th International Modal Analysis Conference, 522–528.

Garetsky R., Levkov E., Schwab G., Karabanov A., Aizberg R., Garbar D., Kockel F., Ludwig A.O., Lukke-Andersen H., Ostaficzuk S., Palienko V., Sim L., Sliaupa A., Sokolowski J., Stackebrandt W., 1999. *Main Neogeodynamic features of the Baltic Sea depression and adjacent areas*. Technika poszukiwan geologicznych. Geosynoptyka i geotermia. №.1 (195), 17–27.

Gallipoli, M. R., Mucciarelli, M., Castro, R. R., Monachesi, G. & Contri, P. 2004. *Structure, soil-structure response and effects of damage based on observations of horizontal-tovertical spectral ratios of microtremors*. Soil Dynamics and Earthquake Engineering, **24**, 487–495.

Gasiūnienė V. E. 1998. *Lietuvos kietosios naudingosios iškasenos*[Lithuanian Solid Mineral Resources]. Lietuvos geologijostarnyba. 61 p.

Girard A., 1985. Réponse des structures à un environnment basse-fréquence," Note Technique no. 116, CNES.

Girard A., Roy N.A., 1997. Modal effective parameters in structural dynamics. Revue Europeenne des elements finis, v. 6, N 2, 233–254.

Gorbatschev R. & Bogdanova S., 1993. *Frontiers in the Baltic Shield*. Precambrian Research, 64, 3–22.

Gorbatschev R., Bogdanova S., 1993. *The Baltic Shield and the Precambrian basement along the Tornquist Zone*. In: Gee, D. G. & Beckholmen M. (eds) EUROPROBE in Jablonna. European Science Foundation–Polish Academy of Sciences, 73–79.

Grad M., Tiira T., Working group "Crustal Structure Maps of Europe", 2009. *The Moho depth map of the European Plate*. Geophys. J. Int., 176, 279–292.

Gregersen S., Korhonen H., Husebye E.S., 1991. *Fennoscandian dynamics: Present-day earthquake activity*. Tectonophysics, TECTO 03052, 1–12.

Gregersen S., 1992. Crustal stress regime in Fennoscandia from focal mechanisms, J. Geophys. Res., 97, 11821–11827.

Gregersen S., Wiejacz P., Debski W., Domanski B., Assinovskaya B., Guterh B., Mantyniemi P., Nikulin V.G., Pacesa A., Puura V., Aronov A.G., Aronova T.I., Grunthal G., Husebye E.S., Sliaupa S., 2007. *The exceptional earthquakes in Kaliningrad district, Russiaon September 21, 2004*. Physics of the Earth Plabetary Interiors 164, 63–74.

Gregersen S., Voss P., 2009. Stress change over short geological time: case of Scandinavia over 9000 years since the Ice Age, in: Paleoseismology: Historical and prehistorical records of earthquake ground effects for seismic hazard assessment, edited by: Reicherter, K., Michetti, A. M., and Silva Barroso, P. G., Geological Society of London, Special Publications, 316, 173–178.

Grunthal G., Bosse C., Camelbeeck T., De Crook T., Garial J.-C., Gregersen S., Guterh B., Halldorsson P., Labak P., Lindholm C., Lenhardt W., Mantyniemi P., Mayer-Rosa D., Musson R.M.W., Schenk V., Schenkova Z., Sleiko D., Verbeiren R., Wahlstrom R., Zabukovec B., Ziros T., 1999. Seismic hazard assessment for Central, North and Northwest Europe: GSHAP Region 3, Annals of geophysics, 42 (6), 999–1011.

Gupta H.K., 2002. A review of recent studies of triggered earthquakes by artificial water reservoir with special emphasis on earthquakes in Koyna, India. / Earth-Science Review 58, 279–310.

Gutenberg B., Richter C. F., 1936. On seismic waves (third paper). GerlandsBeiträgezurGeophysik, 47, 73–131.

Gutenberg B., Richter C. F., 1944. Frequency of earthquakes in California, Bull. Seismol. Soc. Am. 34, 185–188.

Gutenberg B., 1945a. Amplitudes of surface waves and magnitudes of shallow earthquakes. Bull. Seism. Soc. Am., 35, 3–12.

Gutenberg, B., 1945b. Amplitudes of P, PP, and S and magnitude of shallow earthquakes. Bull. Seism. Soc. Am., 35, 57–69.

Gutenberg B., 1945c. Magnitude determination of deep-focus earthquakes. Bull. Seim. Soc.Am., 35, 117–130.

Gutenberg B., Richter C. F., 1954. Seismicity of the Earth and Associated Phenomena, Second ed., Princeton University Press, Princeton.

Gutenberg B., Richter C. F., 1956a. Magnitude and energy of earthquakes. Annali di Geofisica, 9, 1, 1–15.

Gutenberg B., Richter C. F., 1956b. Earthquake magnitude, intensity, energy and acceleration. Bull. Seism. Soc. Am., 46, 105–145.

Gutenberg B., 1958. *Microseisms*. Advances in Geiphysics 5, 53–92.

Hanks T.C., Kanamori H., 1979. A moment magnitude scale. J. Geophys. Res. 84, 2,348–2,350.

Havskov J., Ottemoller L., 2009. ProcessingEarthquakeData. 303 p.

Heinloo O., 2006. Seismographs constructed after prince B.Galitzin and prof. J.Wilip. Современные методы обработки и интерпретации сейсмологических данных. Материалы Международной сейсмологической школы, посвященной 100-летию открытия сейсмических станций «Пулково» и «Екатеринбург». ГС РАС &ИФЗ, Обнинск, 144–155.

Hinze W.J., Bralie L.W., 1988. Geophysical aspects of the craton: U.S. Sedimentary cover – North American craton: U.S. pp. 5–24 (514 pp.).

Horii H., Shin H.C., Pallewatta T.M., 1992. *Mechanism of Fatigue Crack Growth in Concrete*. Cement & Concrete Composities 14, 83–89.

Huber J.E., Fleck N.A. and Ashby M.F., 1997. "The Selection of Mechanical Actuators based on Performance Indices." Proceedings of the Royal Society of London, 2185–2205.

Hough S.E., Morgan P., 2015. A Century of Induced earthquakes in Oklahoma? Bulletin of the Seismological Society of America, vol. 105, N 6, pp. 1–8.

IAEA Safety Standards, 2009. *Evaluation of Seismic safety for Existing Nuclear Installations*. Safety Guide, No. NS-G-2.13. IAEA International Atomic Energy Agency. 83 pp.

Ibs-von Seht M. & Wohlenberg J. 1999. *Microtremor measurements used to map thickness of soft sediments*. Bulletin of the Seismological Society of America, **89**, 250–259.

Imbert J.F., Mamode A., 1978. La masse effective un concept important pour la caracterisation dynamique des structures avec excitation de la base. Mecanique, materiaux, electricite, 342–354.

Ishihara K., 1978. *Introduction to Dynamic Soil Mechanism* (in Japanese).

Ismail F., Ibrahim A., Martin H.R., 1990. Identification of Fatigue Cracks from Vibration Testing. Journal of Sound and Vibration, 140, 305–317.

Johnston A.C., SchweigE.S., 1996. The enigma of the New Madrid earthquakes of 1811–1812. Annu. Rev. Earth Planet. Sci., 24, 339–384.

Johnston A. C., Coppersmith K. J., Kanter L.R., Cornell C.A., 1994. The earthquakes of stable continental regions: assessment of large earthquake potential, TR-102261, Vol. 1–5, ed. Schneider, J.F., Electric Power Research Institute (EPRI), Palo Alto, CA.

Jost M. L. and Herrmann R. B., 1989. A student's guide to and review of moment tensors. Seismological Research Letters, 60, 37–57.

Kabir M.Z., Hojatkashani A., 2013. *Experimental examination of impact and CFRP retrofitted RC berams under monotonic and high-cycle fatigue loading*. Advanced Design and Manufacturing Technology, v. 6, N 3, 63–70.

Kanamori H., 1983. Magnitude scale and quantification of earthquakes. Tectonophysics, 93, 185–199.

Kabir M.Z., Hojatkashani A., 2013. Experimantal Examination of Intact and CFRP Retrofitted RC Beams under Monotonic and High-Cycle Ragigue Loadings. Int. J. Advanced Design and Manufacturing Technology, v. 6, N 3, 63–70.

Karnik V., Kondorskaya N. V., Riznichenko Yu. V., Savarensky Ye. F., Soloviev S. L., Shebalin N. V., Vanek J., Zatopek A., 1962. Standardisation of the earthquake magnitude scales. StudiaGeophysicaetGeodaetica, 6, 41–48.

Kedar S., Longuet-Higgins M., Webb F., Graham N., Clayton R., Cathleen J., 2008. The origin of geep ocean microseisms in the North Atlantic Ocean. Proc. R. Soc A., 464, 777–793.

Keilis-Borok V. I., 1959. On the estimation of displacement in an earthquake source and of source dimension. Ann. Geofis., 12, 205–214.

Kessler S.S., Spearing S.M., xxxx. Design of a piezoelectric-based structural health monitoring system for damage detection in composite materials. Department of Aeronautics and Astronautics Massachusetts Institute of Technology Cambridge, MA 02139, USA.

Kessler S.S., Spearing S.M., 2002. In-situ sensor-based damage detection of composite materials for structural health monitoring. Department of Aeronautics and Astronautics, Massachusetts Institute of Technology, Cambridge, MA 02139, USA.

Khain V. E. & Leonov Y. G. (eds), 1996. *International Tectonic Map of Europe and Adjacent Areas*, Scale 1:5 000 000. IUGS–UNESCO–CGMW, Paris.

Kikuchi M., Kanamori H., 1991. Inversion of complex body waves - III, Bull. Seism. Soc. Am., 81, 2335–2350.

Kim W.-Y., Wahlstrom R., Uski M., 1989. Regional spectral scaling relations of source parameters for earthquakes in the Baltic Shield. Tectonophysics, 166, 1–3, 151–161.

Kim W-Y., Simpson D.W., Richards P., 1993. Discrimination of Earthquakes and Explosions in the Eastern United States Using Regional high-Frequency Data. Geophysical Research Letters 20(14), 1507–1510.

King P.B., (compiler), 1969. Tectonic map of North America, U.S. Geol. Surv. Map, scale 1:5000000.

Kohonen T., 2012. Self-Organization and Associative memory. Springer Series in Information Sciences. 312 pp.

Konno, K. & Ohmachi, T. 1998. *Ground-motion characteristics estimated from spectral ratio between horizontal and vertical components of microtremor*. Bulletin of the Seismological Society of America, **88**, 228–241.

Korhonen H., Ahjos T., 1984. *Catalogue of historical earthquakes in Fennoscandian area*. Proceedings of the Simposium between Imatra Voima Oy and the USSR Ac. Sci. on Fennoscandian seismicity. M., 1–18.

Kondorskaya N.V., Shebalin N.V., 1982. *New catalog of strong earthquakes in the USSR from ancient times through 1977*. Department of commerse. National oceanic and atmospheric administration. USA, 499 p.

Kondorskaya N.V., Nikonov A.A., Ananyin I.V., Dolgopolov D.V., Korhonen H., Arhe K., Sildvee H.H., 1988. Osmussaar earthquake in the East Baltics of 1976. Recent seismological investigation in Europe. Proceedings of the XIX General Assembly of the European Seismological Commission. M., "Nauka", 376–387.

Kondorskaya N.V. & Ulomov V.I., 1995. Special catalogue of earthquakes of the Northern Eurasia (SECNE). 144 pp.

Kukemilks K., Saks T., 2013. Landslides and gully slope erosion on the banks of the Gauja River between the towns of Sigulda and Ligatne. Estonian Journal of Earth Sciences, 62, 4, 231–243.

Lachet C. & Bard P.Y., 1994. *Numerical and Theoretical Investigations on the Possibilities and Limitations of Nakamura's Technique*, J. Phys. Earth,42, 377–397.

Lahtinen A., 1984. *Seismotectonic studies for Liovisa power plant region*. Proceedings of the Symposium between Imatran Voima Oy and the USSR Ac. Sci, on Fennoscandian seismicity. M., 1–18.

Larose E., Carriere S., Voisin C., Bottelin P., Bailett L., Gueguen P., Walter F., Jongmans D., Guillier B., Garambois S., Gimbert F., Massey C., 2015. Environment seismology: What can we learn on earth surface processes with ambient noise? Journal of Applied Geophysics, 116, 62–74.

Lee H., Shum C. K., Guo J., Yi Y., Braun A., Wu P., Kuo C. Y., Schmidt H., Wang H. 2007. Laurentia glacial isostatic adjustment: Constraints from Satellite data and modeling. IUGG Perugia, Italy.

Levret A., Mohammadioun B., 1984. Determination of seismic reference motion for nuclear sites in France. Engineering Geology, 20, 25–38.

Lighthill M.J., 1962. Introduction to Fourier Analysis and Generalised Funktions. Cambridge Univ. Press, Cambridge. 79 p.

Lindholm C. D., Bungum H., Hicks E., Villagran M., 2000. Crustal stress and tectonics in Norwegian regions determined from earthquake focal mechanisms, Geol. Soc. London, 167, 429–439.

Lloyd J.P., Loff J.L., Kesler C.E., 2007. Fatigue of concrete. Engineering experiment station University of Illinois. Bulletin 499.

Loland O. & Dodds J.C., 1976. Experience in Developing and Operating Integrity Monitoring System in North Sea. In Proc. of the 8th Annual Offshore Technology Conference, 313–319.

Malagnini L.,Herrmann R. B., Koch K., 2000. Regional ground motion scaling inCentral Europe. Bull. Seism. Soc. Am. 90, 1052–1061.

Malischewsky P. G., Zaslavsky Y., Gorstein M., Pinsky V., Tran T. T., Scherbaum F. & Estrella H. F. 2010. *Some new theoretical considerations about the ellipticity of Rayleigh waves in the light of site-effect studies in Israel and Mexico*. Geofísica Internacional, **49**, 141–152.

Man X.T., McClure L.M., Wang Z., Finch R.D., Robin P.Y., and Jansen B.H., 1994. Slot Depth Resolution in Vibration Signature Monitoring of Beams Using Frequency Shift. Journal of the Acoustic Society of America, 95(4), 2029–2037.

Mancelius G., 1619. Meditatio theologistoricophysica de terrae motv. Das ist: Kurtze vnnd ernste / jedoch wolgemeinte Christliche Erjnnerung von dem Erdbeben / welches im Jahr nach Christi Geburt 1616. den 20 Junij nach dem Alten / vnd den 30 nach dem Newen Calender / Morgens frü zwischen sieben vnd acht Vhren / an etlichen örtern im Fürstenthumb Sengallen gewesen. Aus Göttlicher heiliger Schrifft / bewerten Historien / vnd der Naturkunst / woher ein Erdbeben gemeiniglish entstehe / was es bedeute / vnd wie man den gedreweten Straffen vorbeugen möge. Gestellet durch Georgivm Mancelivm, Diener des Worts Gottes zum Wallhofe. Zu Riga / bey Nicolaum Mollinum / Im 1619 Jahr.

Marantidis C., Van Way C. B. and Kudva J. N., 1994. Acoustic emission Sensing in an On-board Smart Structural Health Monitoring System for Military Aircraft, Proceedings of the SPIE Conference on Smart Structures and Integrated Systems, 2191: 258–264.

Massonnat G., Roland J-P., 1997. Characterization and modelling of a surprising process: increasing permeability induced by the recovery of a naturally fractured reservoir (LacqProfond, France). *Bulletin du Centre de Recherches Elf Exploration Production*. France. Vol. 21, N 2, 347–363.

McGuire R.K., 2004. Seismic Hazard and Risk Analysis. Earthquake Engineering Research Institute, Berkeley, California.

Mindel A., 1994. Geological background of the present regional uplift anomaly in Estonia. Proc. Estonian Acad. Sci., 43, 2, 69–80.

Ministru kabineta noteikumi Nr. 341, 2003. *Noteikumi par pieļaujamiem vibrācijas lielumiem dzīvojamo un publisko ēku telpās.*. Latvijas Vēstnesis, 96 (2861), 27.06.2003.

Minster J.B., Jordan T.H., 1978. Present-Day Plate Motions. J. Geophys. Res., 83, 5331–5354.

Mita A., 1999. Emerging needs in Japan for health monitoring technologies in civil and building structures. In Proc. 2nd Int. workshop on structural heath monitoring. Stanford University.

Mokhberi M., Davoodi M., Haghshenas E. & Jafari K. 2013. *Experimental evaluation of the H/V spectral ratio capabilities in estimating the subsurface layer characteristics*. Iranian Journal of Science and Technology, Transactions of Civil Engineering, **37**(N C+), 457–468.

Morner N.A., 1979. The Fennoscandian uplift and Late Cenozoic geodynamics: geological evidence. GeoJournal 33, 287 – 318.

Moskvina A.G., Shebalin N.V., 1961. A study of seismic noise and calculation of the optimum seismograph constants. Ceskoslovenska Akad. Ved Studia Geophys. Et Geod., v.5, N 3, 227–230.

Mucciarelli M., Gallipoli M.R., 2001. *A critical review of 10 years of microtremor HVSR technique*. Bolletino di Geofisica Teorica ed Applicata, vol. 42, N 3 - 4, 255–266.

Muir Wood R., Woo G., 1987. The historical seismicity of the Norwegian continental shelf, ELOCS Earthquake loading on the Norwegian continental shelf, Report 2-1 (Norwegian Geotechnical Institute, Oslo, Norway), pp. 118.

Muir Wood R., 1989. *Extraordinary deglaciation reverse faulting in northern Fennoscandia*. In: S.Gregersen and P.W.Basham (Editors), Earthquakes at North-Atlantic Passive Margins: Neotectonics and Postglacial Rebound. Kluwer, Dordrecht, 143–174.

Nakamura, Y. 1997. *Seismic vulnerability indices for ground and structures using microtremor*. In World Congress on RailwayResearch, Florence, pp. 1–7.

Nakamura, Y. 1989. *A method for dynamic characteristic estimation of subsurface using microtremor on the ground surface*. Quarterly Report of Railway TechnicalResearch Institute, **30**, 25–33.

Nakamura Y., 1997. Seismic vulnerability indices for ground and structures using microtremor. In World Congress on Railway Research, Florence, pp.1–7.

Nakamura, Y. 2000. *Clear identification of fundamental idea of Nakamura's technique and its applications*. In The 12th World Conference on Earthquake Engineering, Auckland, New Zealand, pp. 1–8.

Nakamura, Y. 2008. *On the H/V spectrum*. In The 14th World Conference on Earthquake Engineering, Beijing, China, pp. 1–10.

Nikolaev V.G., Garetskii R.G., Aizberg R.E., Kovkhuto A.M., 2002. Faults of the Moscow syneclise. Geotectonics36 (6),463–468.

Nikonov A., Sildvee H., 1986. Seismic and tectonic activity of Estonian territory. *7th International symposium and Recent Crustal Movements of the Earth*. Abstracts. Tallin, p. 99.

Nikonov A.A, Sildvee H., 1991. *Historical earthquakes in Estonia and their seismotectonic position*. Geophysica, 27, 1–2, 79–93.

Nikonov A.A., 1992. *Distribution of maximum observed tremors and zones of possible occurrence of earthquakes in Estonia*. Izvestiya, Earth Physics, 28, N 5, 430–434.

Nikonov A.A., 2002. The Osmussaar earthquake of October 25, 1976: macroseismic analysis, seismotectonics, and focal mechanism. Izvestiya Physics of the Solid Earth, v. 38, N 8, 690–703.

Nikonov A.A., Aptikaev F.F., Aleshin A.S., Assinovskaya B.A., Pogrebchenko V.V., Ponomareva O.N., 2005. *Kaliningrad earthquake of September 21, 2004, Macroseismic data for near and mesoseismal zones*. Kaliningrad earthquake September 21, 2004. Workshop materials. Tartu, 26–29.

Nikonov A.A., 2007. *Approach to parametrization of tectonic earthquakes within the Kaliningrad district, Russia, by macroseismic data*. Seismicity and seismological observations of the Baltic Sea region and adjacent territories. International Workshop, Vilnius, 57–59.

Nikonov A.A., 2011. The Narva Earthquake on January 28, 1881, in the Eastern Part of the Gulf of finland. Seismic Instruments, 2011, vol. 47, N 4, pp. 337–345.

Nikulin V., 1997. *Preliminary results of isostatic conditions estimation of Earth crust in Latvia*. Lithuanian Institute of Geology,Eurobridge Workshop, Abstracts, Vilnius, 56–58.

Nikulins V., 1998. Dažu Baltijas reģiona seismisko parametru novērtējums. Latvijas ģeoloģisko vēstis, 4, 29–35.

Nikulin V., 1999. *Correlation between isostatic anomalies and neotectonic movements in Latvia.* Tehnika Poszukiwan Geologicznuch. Geosynoptyka i Geotermia. Krakow, 1 (195), 68–76.

Nikulin V., 2005. *Estimation of seismic effects in Latvia from the Kaliningrad earthquake of September 21, 2004*. Kaliningrad earthquake September 21, 2004. Workshop Materials. Tartu, 30–31.

Nikulin V., 2007. *Regional features of seismotectonics and deformation of Earth crust of the Baltic region*. International Workshop "Seismicity and seismological observations of the Baltic Sea region and adjacent territories". Vilnius, 63–65.

Nikulin V., 2011. *Assessment of the seismic hazard in Latvia. Versionof 2007 year*. RTU zinātniskie raksti. Materiālzinātne un lietišķā ķīnija. Serija 1, sējums 24, 110–115.

Ņikuļins V., Segliņš V., Konšins G., 2016. Persistent Scatterer Interferometry tālizpētes metodes pielietošana Rīgas un Liepājas ģeoloģiskās bīstamības novērtēšanā un rezultātu praktiskā nozīme. Latvijas Universitātes 74. zinātniskā konference. Ģeogrāfija, Ģeoloģija un Vides zinātne, Referātu tēzes, Rīga, 328–330.

Ņikuļins V., 2017a. Olaines-Inčukalna-Berģu lūzumu zonas seismotektoniskās aktivitātes pazīmes. Lietišķi ģeoloģiskie pētījumi. Tēžu krājums. Latvijas Universitāte 75. zinātniskā konference. 26–28.

Nikulins V., 2017b. *Estonian earthquake 12 November 2016 and its seismotectonic position*. Lietiski geokogiskie petijumi. Latvijas Universutates 75. zinātniska konference. 29–31.

Nikulins V., 2017c. *Seismic properties of soil in the Eastern Baltic Sea Region based on the horizontal to vertical spectral ratio method*. Estonian Journal of Earth Sciences, 66, 109–117.

Nirmalendran S., Horii H., 1992. *Analytical modeling of microcracking and bridging in fracture of quasi-brittle materials*. Journal of the Mechanics and Physics of Solids 40(2), 863–886.

Nogoshi, M. & Igarashi, T. 1971. *On the amplitude characteristicsof microtremor – Part 2*. Journal of the SeismologicalSociety of Japan, **24**, 26–40 [in Japanese, withEnglish abstract].

Noteikumi par Latvijas būvnormatīvu LBN 005-99, 2000. *Inženierizpētes noteikumi būvniecībā*. Ministru kabineta noteikumi Nr. 168, 02.05.2000 (prot. Nr. 20 11.). Latvijas Vēstnesis, 164/165 (2075/2076), 06.05.2000.

Olesen O., Blikra L.H., Braathen A., Dehls J. F., Olsen L., Rise L., Roberts D., Riis F., Faleide J. I., Anda, E., 2004. Neotectonic deformation in Norway and its implications: a review, Norwegian J. Geol., 84, 3–34.

Osegueda R.A., Dsouza P.D., Qiang Y., 1992. Damage Evaluation of Offshore Structures Using Resonant Frequency Shifts. Serviceability of Petroleum, Process, and Power Equipment, ASME PVP 239/MPC 33, 31–37.

Ostrovsky A.A., Flueh E.R., Luosto U., 1994. *Deep seismic structure of the Earth's crust along the Baltic Sea profile*. Tectonophysics 233, 279–292.

Ottemöller L., Voss P., Havskov J., 2016. SEISAN earthquake analysis software for Windoes, Solaris, Linux and Macosx. Version 10.5. Manual. 526 pp.

PačesaA. & ŠliaupaS., 2007. *Application of the probabilistic approach in assessment of the seismic hazard of the Baltic region*. Seismicity and seismological observations of the Baltic Sea region and adjacent territories. International Workshop, Vilnius, 69–70.

Parolai S., Bormann P. & Milkereit C. 2002. *New relationship between Vs, thickness of sediments, and resonance frequency calculated by the H/V ratio of seismic noise for the Cologne area (Germany)*. Bulletin of the SeismologicalSociety of America, **92**, 2521–2527.

Paulson A., Zhong S., Wahr J., 2007. Inference of mantle viscosity from GRACE and relative sea level data. Geophys. J. Int., 171, 497–508.

Peter, 1997. Peter iz Duisburga. Khronika zemli Prusskoi (Peter from Duisburg. Chronic of the Prussia Land). M., Ladomir, 384 p. (In Russian).

Petersen M.D., Frankel A.D., Harmsen S.C., Mueller C.S., Boyd O.S., Luco N., Wheeler R.L., Rukstales K.S., Haller K.M., 2012. The 2008 U.S. Geological Survey national seismic hazard models and maps for the central and eastern United states. Recent Advances in North American Paleoseismology and Neotectonics East of the Rockies. Edited by Cox R.T., Tuttle M.P., Boyd O.S., Locat J., Geological Society of America. 275 pp.

Pino N.A., Piatanesi A., Valensise G., Boschi E., 2009. The 28 December 1908 Messina Straits Earthquake (Mw 7.1): A Great Earthquake throughout a Century of Seismology. Seismological Research Letters, v. 80, N 2, 243–259.

Plesseria J.Y., Rochus P., Defise J.M., 2000. *Effective modal masses. 5 Congres National de Mecanique Theorique et Appliruee*. Louvain-la-Neuve, 1–4.

Ponomareva O.N., 2005. Kaliningrad earthquake of September 21, 2004, macroseismic data for near and mesoseismal zones. Kaliningrad earthquake September 21, 2004. Workshop materials. Tartu, 26–29.

Rees D., Chiu W. K. And Jones R., 1992. A Numerical Study of Crack Monitoring in Patched Structures Using a Piezo Sensor, Smart Materials and Structures, 1(3): 202–205.

Richardson M.H. & Mannan M.A., 1993. Correlating Minute Structural Faults with Changes in Modal Parameters. Proc. of the 11th International Modal Analysis Conference, 893–898.

Ross R.M. & Matthews S.L., 1995. *In-service structural monitoring - a state of the art review*. Structural Engineering, 73, 23–31.

Sadigh K., Chang C.-Y., Egan J.A., Makdisi F., Youngs R.R., 1997. Attenuation Relationship for Shallow Crustal Earthquakes Based on California Strong Motion Data. Seismological Research Letters, vol. 68, 1, 180–189.

Safronovs O.N., Ņikuļins V.G., 1999. Latvijas vispārīgā seismiskā rajonēšana. Latvijas ģeoloģijas vēstis, 6, 30 - 35.

Schulte S.M., Mooney W.D., 2005. An updated g;obal earthquake catalogue for stabule continental reģions: reassessing the correlation with ancient rifts. Geophys. J. Int., 161, 707–721.

Schutz W., 1996. *A history of fatigue*. Engineering Fracture Mechanics. 54 (2): 263–300.

Shearer P., 2009. Introduction to Seismology. Second Ed. Cambridge University Press.

Sildvee H., 1988. *Võrtsjärvemaavärin (AnearthquakeunderLakeVortsjarv)*. EestiLoodus, 1, 26–31 (in Estonian, summary in English).

Simpson D.W., Leith W.S., Schols C.H., 1988. Two types of reservoir induced seismicity. Bulletin seism. Soc. Am., 78 (6), 2025–2040.

Slunga R., 1979. *Source mechanism of a Baltic earthquake inferred from surface-wave recordings*. Bull. Seism. Soc. Amer., v. 69, N 6, 1931–1964.

Special Earthquake Catalogue of Northern Eurasia from ancient times through 1995, 1996. Eds. N.V.Kondorskaya, V.I.Ulomov. /www.scgis.ru System of data bases. JIPE RAS.

Spivak A.A., Kozhukhov S.A., Sukhorukov M.V., Kharlamov V.A., 2009. Radon emanation as an indicator of the intensity of intergeospheric interactions at the Earth's crust atmosphere interface. Izvestiya, Physics of the Solid Earth 45 (2), 118–133.

SSHAC (Senior Seismic Hazard Analysis Committee). Recommendations for Probabilistic Seismic Hazard Analysis: Guidance on Uncertainty and Use of Experts, US Nuclear Regulatory Commission report CR-6372, Washington DC

Stein S., Wyssession M., 2003. Introduction to seismology, earthquakesandearthstructure. BlackwellPublishing, 498 pp.

Sviridov N.I., 1981. *Disturbance in a layer structure of a sedimentary cover of the Baltic Sea bottom*. Geotectonica, 4, 31–43.

Talwani P., 1997. Onthenatureofreservoir-inducedseismicity.Pureappl.Geophys., 150, 473–492.

Traer J., Gerstoft P., Bromirski P.D., Shearer P.M., 2012. Microseisms and hum from ocean surface gravity waves. Journal of Geophysical Research, v. 117, B11307, 1–16.

Ulomov V.I. and the GSHAP Region 7 Working Group, 1999. Seismic hazard of Northern Eurasia. Annalidi Geofisica, v. 42, N 6, 1023–1038.

Ulusoy H.S., Kalkan E., Fletcher J.P.B., Friberg P., Leith W.K., Banga K., 2012. Design and Implementation of A Structural Health Monitoring and Alerting System for Hospital Buildings in the United States. 15 World Conference on Earthquake Engineering. 1–10.

Utheim T., Havskov J., Natvik Y., 2001. SeisLogdataacquisitionsystem. Seismological Research Letters. 72 (1), pp. 77–79.

Vassiliou M.S., Kanamori H., 1982. The energy release in earthquakes. Bull. Seismol. Soc. Am., 72, 371–387.

Wahlström, R. & Grünthal, G., 2001. Probabilistic seismic hazard assessment (horizontal PGA) for Fennoscandia using the logic tree approach for regionalization and nonregionalization models. Seismological Research Letters 72 (1), 33–45.

Wieland M., Griesser L., Kuendig C., 2000. *Seismic early warning system for a nuclear power plant*. 12th World Conference on Earthquake Engineering, Auckland, New Zeland, 1781, 8 pp.

Wu P. & Johnston P., 2000. Can deglaciation trigger earthquakes in N. America? Geophysical Research Letters, v. 27, N 9, 1323–1326.

York E., Oliver J.E., 1976. Cretaceous and Cenozoic faulting in eastern North America. Geological Society of America Bulletin 87, 1105–1114.

Youngs R.R., Coppersmith K.J., 1985. Implications of faults slip rates and earthquake recurrence models to probabilistic seismic hazard estimates. Bull. Seismol. Soc. Am., v. 75, 939–964.

Zaharia, B., Radulian, M., Popa, M., Grecu, B., Bala, A. & Tataru, D. 2008. *Estimation of the local response using the Nakamura method for the Bucharest area*. Romanian Report in Physics, **60**, 131–144.

Zoback M.L., 1992. First- and second-order patterns of stress in the lithosphere: The World Stress Map project. J. Geophys. Res., 97, 11,703-11,728.

Айзберг Р.Е., Аронов А.Г., Гарецкий Р.Г., Карабанов А.К., Сафронов О.Н., 1997. Сейсмотектоника Беларуси и Прибалтики. Літасфера, 7, 5–18.

Аксаментова Н.В., 2004. Структурно-вещественные комплексы и тектоническое районирование кристаллического фундамента Русской плиты. Бюллетень МОИП. Отделение геологии, т. 79, вып. 1, 3–13.

Алешин А.С., 2010. Сейсмическое микрорайонирование особо-ответсвенных объектов. СветочПлюс, М., 303 с.

Алешин А.С., Аносов Г.И., Бессараб Ф.С., Дробиз М.В., Дементьев Ю.В., Погребченко В.В., Рогаль Л.А., Скворцов А.Г., Царев А.М., Чугаевич В.Я., 2014. Сейсмическое микрорайонирование территории г. Калининграда. Инженерные изыскания, N 9 –10, 68–79.

Ананьин И.В., 1968. Связь сейсмичности Русской платформы с современными тектоническими движениями. Современные движения земной коры. М., 3, 282 – 295.

Ананьин И.В., 1977. Сейсмичность Северного Кавказа. М., Наука, 148 стр.

Анкудинов С.А., Брио Х.С., Садов А.С., 1991. Глубинное строение земной коры на территории Прибалтики по данным сейсморазведочных работ ГСЗ. Белорусскийсейсмологическийбюллетень, 1, 111–117.

Аптикаев С.Ф., Мирмович Э.Г., Рузайкин А.И., 2012. Реальная сейсмическая активность Восточно-Европейской платформы как основа ее прогнозирования.

Аранович З.И., Кирнос Д.П., Токмаков В.А., Фремд В.М., Харин Д.А., Шнирман Г.Л., Ярошевич М.И., 1974. II Основные типы сейсмометрических приборов. Аппаратура и методика сейсмометрических наблюдений в СССР. М., Наука, 43–115.

Артемьев М.Е., 1975. *Изостазия территории СССР*. Наука, М., 215 стр.

Асминг В.Э., Кременецкая Е.О., Виноградов Ю.А., Евтюгина З.А., 2010. Использование критериев идентификации взрывов и землетрясений для уточнения оценки сейсмической опасности региона. Вестник МГТУ, т. 13, N 4/2, 998–1007.

Авотиня И.Я., Боборыкин А.М., Емельянов А.П., Сильдвээ Х.Х., 1988. Каталог исторических землетрясений Белоруссии и Прибалтики. Сейсмологический бюллетень сейсмических станций «Минск» (Плещеницы) и «Нарочь» за 1984 год. Академия наук Белорусской ССР, Институт геохимии и геофизики, Минск, 126–137.

Аптикаев С.Ф., Мирмович Э.Г., Зузайкин А.И., 2012. *Реальная сейсмическая активность Восточно-Европейской платформы как основа ее прогнозирования*. Научные и образовательные проблемы гражданской защиты, 2, 12–21.

Баум Ф.А., Орленко Л.П., Станюкович К.П., Челышев В.П., Шехтер Б.И., 1975. Физика взрыва. Наука, Москва, 704 с.

Боборыкин А.М., 1988. Зоны возможных очагов землетрясений (ВОЗ) Беларуссии и Прибалтики по литературным источникам и инструментальным наблюдениям. Сейсмологический бюллетень сейсмических станций «Минск» (Плещеницы) и «Нарочь» за 1985 год. 115–121.

Боборыкин А.М., Гарецкий Р.Г., Емельянов А.П., Сильдвээ Х.Х., Сувейздис П.И., 1993. *Землетрясения Беларуси и Прибалтики*. Современное состояние сейсмических наблюдений и их обобщений (Методические работы ЕССН), 4, 29–39.

Брангулис А.П., Страуме Я.А., Бендруп Л.П., Биргер А.Я., Биркис А.П., Брио Х.С., Гаврилова А.В., Мейронс З.В., Юшкевичс В.В., 1984. Геология Латвийской ССР. Гл. ред. Мисанс Я.П. "Зинатне", Рига, 214 с.

Брангулис А.П.. Страуме Я.А., Бендруп Л.П., Биргер А.Я., Биркис А.П., Брио Х.С., Гаврилова А.В., Мейронс З.В., Юшкевичс В.В., 1984. Геология Латвийской ССР. Объяснительная записка к геологическим картам Латвийской ССР масштаба 1:500000. Рига, Зинатне, 214 с.

Буш В.А., Ермаков Ю.Н., Уйманова Л.Н., 2000. Геодинамическая модель формирования позднеархейских – раннепротерозойских структур Воронежского массива. Геотектоника, № 4, 14–24.

Ветренников В.В., 1991. Железтсто-кремнистые формации докембрия Латвии. Рига, Зинатне, 180 с.

Вяхер Р.М., 1983. *Тектоника фосфоритно-сланцевого бассейна Северо-Восточной Эстонии*. Автореферат канд. дис. Минск.

Гарецкий Р.Г., Боборыкин А.М., 1989. О Сейсмотектоническом районировании запада СССР. Сейсмологический бюллетень сейсмических станций «Минск» (Плещеницы), «Гомель» и «Нарочь» за 1986 год. АН Белорусской ССР, ОНТИ, Минск, 150–155.

Гарецкий Р.Г., Айзберг Р.Е., Сафронов О.Н. и др., 1997. Общее сейсмическое районирование Беларусско-Прибалтийского региона. Доклады АН Беларуси, т.41, N4, с. 98–103.

Гарецкий Р.Г., 2007. Особенности тектоники и геодинамики Восточно-Европейской платформы. Літасфера, 2 (27), 3–13.

Горбунова Э.М., Иванченко Г.Н., СпивакА.А., 2002. Выбор объекта для проведения комплексных исследований геодинамических и геофизических аномалий взонах влияния тектонических структур. Нестационарные процессы в верхних и нижних геосферах Земли. М.:ИДГ РАН, с. 114–129.

ГОСТ Р 57546-2017, 2017. *Землетрясения. Шкала сейсмической интенсивности*. Национальный стандарт Российской Федерации. 33 с.

Гурвич И.И., 1970. Сейсмическая разведка. Недра.

Добровольский И.П., 2004. *Прогноз тектонического землетрясения: опрделение места и энергии землетрясения по данным сейсмического просвечивания*. ФизикаЗемли, 12, 31–41.

Жарков В.Н., 1978. Внутреннее строение Земли и планет. М., Наука, 191 стр.

Казаков С.В., Омельченко В.Д., Рыбалко С.И., 1994. Геофизические исследования и сейсмотектоника района размещения Чернобыльской АЭС. 64 с.

Капустян Н.К., 2000. Техногенная эрозия литосферы плата за прогресс. II, Наука в России, М., 2, 15–23.

Каратаев Г.И., Гирин Р.Е., Данкевич И.В. и др., 1993. Геофизические модели земной коры Белорусско-Прибалтийского района. Навука і техника, Минск, 188 с.

Кохонен Т., 2008. Самоорганизующиеся карты. М.: БИНОМ. Лаборатория знаний, 655 с.

Корчинский Н.П., 1971. Сейсмостойкое строительство зданий. Высшая школа, Москва, 320 с.

Костров Б.В., 1975.*Механика очага тектонического землетрясения*. М.: Наука, 176 с. – 23.

Кригер Н.И., Кожевников А.Д., Миндель И.Г., 1994. Сейсмические свойства дисперсных пород (сейсмолитоэкологический подход). М., Инжэко, 196 с.

Литосфера Центральной и Восточной Европы, 1989. Наукова думка, Киев, 188 с.

Литвиненко И.В., Анкудинов С.А., Дворецкая Л.М и др., 1982. Глубинный сейсмический разрез земной коры Приладожья и юго-западной Карелии. Методика геофизических исследований Балтийского щита и его склонов. Л., Зап. ЛГИ, т. XCII, 3–29.

Маловичко А.А., Габсатарова И.П., Чепкунас Л.С., Старовойт О.Е., 2007. Инструментальные сейсмологические наблюдения на Восточно-Европейской платформе (глава 1). / Ред. Шаров Н.В., Маловичко А.А., Щукин Ю.К. Землетрясения и микросейсмичность в задачах современной геодинамики Восточно-Европейской платформы. Книга 1, стр. 14–66.

Матвеев А.В., Нечипоренко Л.А., Лосич В.В., Иваненко А.П., 2012. Концентрация радона в почвенном воздухе на смежных площадях Белорусской антеклизы и Припятского прогиба (Беларусь). Природопользование, 21, 68–74.

Медведев С.В., 1962. Инженерная сейсмология. М., Стройиздат, 284 с.

Муратов М.В., 1979. Раннепротерозойский (афебский) этап развития древних платформ и его роль в истории их формирования. Геотектоника, N 2, 3–28.

Мушкетов И.В., Орлов А.П., 1893. *Каталог землетрясений Российской империи*. Записки Русского географического общества, СПб., 582 с.

Мячкин В.И., Долбилкина Н.А., Максимов О.А. и др., 1975. *Аппаратура и методика работ по просвечиванию очаговых зон землетрясений*. Физика очага землетрясения. Ред. Садовский М.А., М.: Наука, 160–164.

Мячкин В.И., 1978. *Процессы подготовки землетрясений*. М.: Наука, 232 с.

Никонов А.А., 1995. Нетектонические землетрясения Восточно-Европейской платформы. Природа, 10, 26–38.

Никонов А.А., 1996. Проблема выделения нетектонических землетрясений на Восточно-Европейской платформе в оценке сейсмической опасности. Недра Поволжья и Прикаспия. Спец. выпуск, 13, 42–49.

Никонов А.А., Аптикаев Ф.Ф., Алешин А.С., Погребченко В.В., Эртелева О.О., Ассиновская Б.А., 2005. *Обследование последствий землетрясения 21 сентября 2004 года в Калининградской области*. Элекгоннный научно-информационный журнал, 1 (23), 1–18.

Никонов А.А., 2006. О механизме очага Калининградского землетрясения 21 сентября 2004 года. Доклады Академии наук, т. 407, N 1, 102–105.

Никонов А.А., 2009. *Исторические землетрясения района Юго-Восточной Балтики: проблемы и решения*. Сейсмотектоника плит древних платформ в области четвертичного оледенения. Под ред. Р.Г. Гарецкого, С.А. Несмеянова. М., 138–221.

Никонов А.А., 2010. *Морозобойные сотрясения как особый класс сейсмических явлений (по материалам Восточно-Европейской платформы)*. ФизикаЗемли, 3, 79–96.

Никонов А.А., 2013. *Новый этап познания сейсмичности Восточно-Европейской платформы и ее обрамления*. Доклады Академии Наук, том 450, N 4, 465–469.

Никулин В.Г., 2007. Сейсмичность территории стран Балтии. Землетрясения и микросейсмичность в задачах современной геодинамики Восточно-Европейской платформы. Ред. Шаров Н.В., Маловичко А.А., Щукин Ю.К. 364–368.

Никулин В.Г., 2008a. *Калининградские землетрясения 2004 года и их проявление на территории Латвии*. Отв. ред. А.В.Николаев, Калининградское землетрясение 21 сентября 2004 года. 104–109.

Никулин В.Г., 2008b. *Проявление сейсмотектонических процессов в Латвии*. Материалы 14 ой международной конференции «Связь поверхностных структур Земной коры с глубинными». Петрозаводск, Россия, часть 2, 81–84.

Никулин В.Г., 2011. Сейсмические сотрясения 22 ноября 2010 года в Риге и Рижском районе. Актуальные вопросы мониторинга геологической среды и безопасности урбанизированных территорий. Тезисы докладов 1-й международной конференции. Балтийский Федеральный Университет им. И. Канта, Калининград, 49–52.

Никулин В.Г., 2014. Зоны геологической опасности для Лиепаи и Риги на основе результатов дистанционного зондирования методом Persistent Scatterer Interferometry. Sabiedrība un kultūra, Rakstu krājums, Liepājas Universitāte, XVI, 432–439.

Пасека О.Н., Аносов Г.И., Дементьев Ю.В., Зиновьев В.Н., Чугвевич В.Я., 2014. Особенности изучения грунтов оснований фундаментов сооружений на острове Октябрьский г. Калининграда. International Journal Geotechnics, N 5–6, 4–12.

Павловский Е.В., 1965. Происхождение и развитие древних платформ. Вопросы сравнительной тектоники древних платформ. М., Наука, 7–14.

Побул Э.А., Сильдвээ Х.Х., 1975. *О блоковом строении кристаллического фундамента Эстонии*. Современныедвижениятерриторииприбалтики. Тарту, 64–73.

Подъяпольский Г.С., Физика упругих волн. Справочник геофизика. Сейсморазведка. Ред. Гурвич И.И., Номоконов В.П., т. 4, 749 с.

Пуура В.А., 1979. *Об унаследованности дифференцированных тектонических движений на южном склоне Балтийского щита*. Проблемы унаследованности тектонических структур в Прибалтике и Белоруссии. Таллинн, 13–19.

Рейснер Г.И., Рейснер М.Г., 1986. Современные эндогенные режимы. ДАН СССР, т. 291, N 6, 1336–1339.

РезановИ.А., 1974. *Земнаякора*. Наука, М, 159 стр.

Ризничено Ю.В., Артамонов А.М., 1975. Развитие энергетической модели сейсмичности. Известия АН СССР. Физика Земли. 12, 41–45.

Ризниченко Ю.В., 1985. Проблемы сейсмологии. Избранные труды. Москва, Наука, 408 с.

РСН-60-86, 1986. Республиканские строительные нормы. М., Стройиздат.

РСН-60-86, 1987. Инженерные изыскания для строительства. Сейсмическое микрорайонирование. Нормы производства. М., Госстройиздат, 18 с.

Рустанович Д.Н., 1967. Сейсмичность территории Туркменской ССР и Ашхабадское землетрясение 1948 года. Наука, 96 с.

Савич А.И., Сувилова А.В., 1988. Современное состояние проблемы оценки сейсмической опасности участков строительства крупных энергетических сооружений. Сборникнаучсныхтрудов. Гидропроект, вып. 130, 7–18.

Савович М.К., 2005. *Динамический расчет каркасных зданий*. 31 с.

Садовский М.А., Писаренко В.Ф., 1991. Сейсмический процесс в блоковой среде. Москва, Наука, 96 с.

Сафронов О.Н., Никулин В.Г., Аронова Т.И., 2005. Сейсмотектоника и возможности прогноза сейсмической опасности в Белорусско-Балтийском регионе. Геофизический-журнал, Киев, 27, 3, 491–494.

Спивак А.А., Шувалов В.В., 2008. Вариации фильтрационных свойств тектонических нарушений в результате твердого прилива. Локальныеи глобальные проявления воздействий на геосферы. М.: ГЕОС, 2008. С. 30–42.

Спивак А.А., Кожухов С.А., Сухоруков М.В., Харламов В.А., 2009. Эманации радона как индикатор интенсивности межгеосферных взаимодействий на границе земная кора – атмосфера. Физика Земли, 2, 34–48.

Спивак А.А., Кожухов С.А., Сухоруков М.В., Харламов В.А., 2009. Эманация радона как индикатор интенсивности межгеосферных взаимодействий на границе земная кора – атмосфера. Физика Земли, 2, 34–48.

Страхов В.Н., Старостенко В.И., Харитонов О.М. идр., 1997. Сейсмические явления в районе Чернобыльской АЭС. Геофизический журнал, т.19, N 3, 3–15 с.

Стром А.Л., Никонов А.А., 1999. Распределение смещений вдоль сейсмогенных разрывов и учет неравномерности подвижек при палеосейсмологических исследованиях. Вулканология и сейсмология, 6, 47–59.

Сувейздис П.И., Брангулис А.П., Пуура В.А., 1980. Структурно-формационная карта республик Советской Прибалтики. Масштаб 1:500 000. ЛитНИГРИ.

Сухоруков М.В., 2016. Геофизические связи эманации почвенного радона с колебанием среды и атмесферным электрическим полем. Успехи современной науки, т. 11, N 12, 98–104.

ТеркотД., ШубертДж., 1985. Геодинамика. Геологические приложения физики сплошных сред. Мир, Москва, 1 часть, 374 с.

Туулинг И.И., 1990. *Структура Прибалтийского бассейна горючих сланцев и фосфоритов*. Автореферат канд. дис. Минск.

Уломов В.И., Шумилина Л.С., 1999. Проблемы сейсмического районирования территории России. Всероссийский НИИ проблем научно-технического прогресса и информации в строительстве. М., ВНИИНТПИ госстроя России, 56 с.

Файтельсон А.Ш., 1973. *Архимедоворавновесиеземнойкоры*. Ред. Артемьев М.Е., Изостазия. Наука, Москва, 44–49.

Хаттон Л., Уэрдингтон М., Мейкин Дж., 1989. Обработка сейсмических данных. Мир, М., 215.

Хотько Ж.П., 1974. Глубинное строение территории Беларуси и Прибалтики по данным геофизики. Минск, 92 с.

Шаров Н.В., Никонов А.А., Французова В.И., Щукин Ю.К., Сыстра Ю.Й., 2005. Нетектонические землетрясения 2003 - 2004 годов в Северной карелии и Онежской губе Архангельской области. Материалы 11 международной научной конференции «Строение, динамика и минералогические процессы в литосфере». Сыктывкар, 390–392.

Шебалин Н. В., 1975. Об оценке сейсмической интенсив- ности. В кн.: Сейсмическая шкала и методы из- мерения сейсмической интенсивности. Москва, Наука, 87–109.

Юдахин Ф.Н., Щукин Ю.К., Макаров В.И., 2003. Глубинное строение и современные геодинамические процессы в литосфере Восточно-Европейской платформы. Отв. Редактор Н.П.Лаверов. РАН, Екатеринбург, 299 стр.

Юдахин Ф.Н., Капустян Н.К., 2004. Микросейсмические наблюдения. Цикл лекций. Материалы всероссийской конференции с международным участием «Геодинамика и геологические изменения в окружающей среде северных регионов». Архангельск, том II, 1–66.

Яновская Т.Б., 2014. К истории Российской сейсмологии. Вопросы геофизики. Вып. 47, 32–41.

Internet Sources

A General Framework for Seismic Microzonation Studies_*si* http://nidm.gov.in/easindia2014/err/pdf/earthquake/seismic_microzonation.pdf

Bard P.-Y. et al., 2004. *Guidelines for the Implementation of the H/V Spectral Ratio Technique on Ambient Vibrations. Measurements, Processing and Interpretation*. Grenoble, 62 pp. Available at: http://sesame.geopsy.org/Papers/HV_User_Guidelines.pdf [accessed 20 February 2017].

Clayton L., Attig J.W., Mickelson D.M., Johnson M.D., Syverson K.M., 2006_*si*. Glaciation of Wisconsin. Educational Series 36, 4 p. Available at http://www.geology.wisc.edu/~davem/abstracts/06-1.pdf [accessed 20 February 2017].

Чернобыльский форум, 2006_ *si*. Наследие Чернобыля: медицинские, экологические и социально-экономические последствия и рекомендации правительствам Беларуси, Российской федерации и украины. 58 с. Available at file:///D:/res/2017/lat_seis_liet/ref/objects/chernobyl_digest_report_RUS.pdf [accessed 20 February 2017].

FENCAT_*si*. *Available at* http://www.seismo.helsinki.fi/english/bulletins/catalog_northeurope.html [accessed 20 February 2017].

Freaky 'frost quakes' boom and shake frozen Midwest towns_*si*. Available at http://www.latimes.com/nation/nationnow/la-na-nn-frost-quakes-cryoseism-20140206-story.html [accessed 20 February 2017].

Frost Quake_*si*. Available at http://frostquake.org/ [accessed 20 February 2017].

Growth of Continents_*si*. Available at http://geologylearn.blogspot.com/2015/11/the-proterozoic-earth-in-transition.html [accessed 20 February 2017].

Highways of Latvia_*si*. Available at http://rus.tvnet.lv/hi_tech/nauka/114992-avtomobilnye_dorogi_latvii_ustarevshie_i_neukhozhennye [accessed 20 February 2017].

IRIS Earthquake Browser_*si*. Available at *http://ds.iris.edu/ieb/index.html?format=text&nodata=404&starttime=1970-01-01&endtime=2025-01-01&minmag=0&maxmag=10&mindepth=0&maxdepth=900&orderby=time-desc&limit=1000&maxlat=88.71&minlat=-88.71&maxlon=180.00&minlon=-180.00&zm=1&mt=ter* [accessed 20 February 2017].

Jet Propulsion Laboratory, California Institute of Technology_*si*. Available at https://sideshow.jpl.nasa.gov/post/series.html [accessed 20 February 2017].

Lapinskis, 2008_*si*. Jūras krasti un klimata mainība. Available at http://www.lza.lv/images/stories/Pasakumi/Juras%20Krasti_%20Janis%20Lapinskis.pdf [accessed 20 February 2017].

Latvijas Valsts autoceļu, 2015_*si*. Latvijas Valsts autoceļu statistika. Available at http://lvceli.lv/wp-content/uploads/2015/08/Valsts-autocelu-tikls-Statistika-State-Road-Network-Statistics-2015.pdf [accessed 20 February 2017].

Lowman P., Yates J, 2002_*si*. Digital map of tectonic activity of the Earth. NASA Goddard Space Flight Center. Available at *https://visibleearth.nasa.gov/view.php?id=88415* [accessed 20 February 2017].

Messina earthquake and tsunami of 1908_*si*. Available at https://www.britannica.com/event/Messina-earthquake-and-tsunami-of-1908 [accessed 20 February 2017].

NASA, DTAM project team, 1998_si. Preliminary determination of epicentres 358214 events, 1963 – 1998. Available at http://denali.gsfc.nasa.gov/dtam/seismic/ ; https://commons.wikimedia.org/wiki/File:Quake_epicenters_1963-98.png [accessed 20 February 2017].

National Geographic, Waterfall_*si*. **Available at https://www.nationalgeographic.org/encyclopedia/waterfall/** [accessed 20 February 2017].

Никонов А.А., 2015*i*. **Землетрясение в Калининграде - неудивительная неожидканность. Available at http://geo.1september.ru/article.php?ID=200403805** [accessed 20 February 2017].

North Korea explosion_*si*. Available at https://earthquake.usgs.gov/earthquakes/eventpage/us2000aert#executive [accessed 20 February 2017].

Northern California Earthquake Data Center & BerkeleySeismological Laboratory_*si*. Available at http://www.ncedc.org/anss/catalog-search.html [accessed 20 February 2017].

Reuter, 2011_*si*. TEPCO shares hit new low, eyes on government. Available at http://www.reuters.com/article/us-japan-tepco-idUSTRE7350NI20110406 [accessed 20 February 2017].

Строение Восточно-Европейской платформы. Авлакогены. Осадочный чехол_*si*. Available at http://atlantic.ginras.ru/education/russia/lecture_04.pdf [accessed 20 February 2017].

SWISWEB_*si*. Available at http://www.uib.no/fg/geodyn/57638/earthquake-data [accessed 20 February 2017].

Уломов В.И., 2013_*si*. Сейсмическое районирование территории России. Available at http://seismos-u.ifz.ru/personal/zoning.htm [accessed 20 February 2017].

Valsts kontrole, 2016__*si*. Available at http://www.lrvk.gov.lv/uploads/reviziju-zinojumi/2015/2.4.1-15_2015/vkontrole_pieminekli_05_08_2016-ru.pdf [accessed 20 February 2017].

Vigil J.F., 1997_*si*. A cross section illustrating the main types of plates boundaries. Illustration by Jose F. Vigil from This Dynamic Planet – a wall map produced jointly by the U.S. Geological Survey, the Smithsonian Institution, and the U.S. Naval Research Laboratory. Available at *https://pubs.usgs.gov/gip/earthq1/plate.html* [accessed 20 February 2017].

Wikimedia.NASA/Goddard Space Flight Center, 2002_*si*. Digital tectonic activity map of the Earth. Tectonism and Volcanism of the Last one million years. Available at *https://upload.wikimedia.org/wikipedia/commons/b/b4/Plate_tectonics_map.gif* [accessed 20 February 2017].

Wikimedia commons. Atlas of the World/Geological, 2005_*si*. Геологические провинции мира. Available at *https://commons.wikimedia.org/wiki/File:World_geologic_provinces.jpg* [accessed 20 February 2017].

Wikimedia.NASA/Goddard Space Flight Center, 2002_*si*. Digital tectonic activity map of the Earth. Tectonism and Volcanism of the Last one million years. Available at *https://upload.wikimedia.org/wikipedia/commons/b/b4/Plate_tectonics_map.gif* [accessed 20 February 2017].

Unpublished materials

Аболтыньш О.П., 1969_*ирт*. Современные движения в районе водохранилища Плявиньской ГЭС. Министерство геологии СССР. ВНИИМОРГЕО. 107 стр.

Аболтыньш О.П., 1971_*ирт*. Изучение современных движений на опытном полигоне по данным повторного высокоточного нивелирования с целью подтверждения их колебательного характера. Министерство геологии СССР. ВНИИМОРГЕО. 94 стр.

Апирубите Р.А., 1980_*ирт*. Анализ размещения и глубинности разломов земной коры Прибалтики по геофизическим данным. Отчет. Вильнюс.

Бебриш Э.В., Веремейчик Р.А., Кучеренко В.И. и др., 1985_*ирт*. Отчет о проведении поисковых работ для захоронения промстоков, не поддающихся очистке в Елгавском, Бауском, Стучкинском и Екабпилском районах за 1981 – 1985 гг. Valsts ģeoloģijas fonds.

Bhattacharjee et al., 2011_*ирт*. Geotechnical_Geophysical Investigations for Seismic Microzonation Studies of Urban Centres in India. Technical report. National Disaster management Authority Government of India. 175 p.

Doebling S.W., Farrar C.R., Prime M.B., Shevitz D.W., 1996_*ирт*. Damage Identification and Health Monitoring of Structural and Mechanical Systems from Changes in Their Vibration Characteristics: A Literature Review. Los Alamos, National Laboratory, LA-13070-MS.

Gilucis A., 2014_*ирт*. Sākotnējais radona novērtējums Latvijas teritorijā. Starpziņojums. SIA "Geo Consultants", 97 lpp.

Ковалевский М.И., Берзинь Л.Э., Спрингис Е.Н., 1966_*ирт*. Выяснение закономерностей современных и новейших движений земной коры на территории Латвийской ССР. Отчет. Рига.

Lagerback R., 1988_*ирт*. *Postglacial faulting and paleoseismicity in the Lansjarv area, northern Sweden*. Swed. Nucl. Fuel Waste Manage. Co. Tech. Rep. No. 88–25.

Озолиня Н.К., Ковригин В.П., 1986_*ирт*. Отчет по теме «Обобщение физических свойств горных пород по территории Латвийской ССР» за 1984 – 1986 годы. 1 том, 144 стр.

Никулин В.Г., 1991_*ирт*. Геолого-экономическое обоснование сейсмического мониторинга Латвии. Отчет по договору N 209 – 91. ГНПО «Моринжгеология», Научно-исследовательский институт морской геологии и геофизики (НИИМоргео), Рига, 137 с.

Ņikuļins V., 1998_*ирт*. Latvijas seismiskās rajonēšanas. Pārskats. Valsts ģeoloģijas dienests. Latvijas ģeoloģijas fonds, Rīga, 44 lpp.

Ņikuļins V., 2007_*ирт*. Pārskats par darba rezultātiem varbūtējais seismiskās iedarbības un apstākļu novērtējums uz ēkām, atbilstoši Eirostandarta 8 prasībām, nacionālā pielikuma projekta LVS EN 199801: 2004 sagatavošana un priekšlikumi grozījumiem būvnormatīvā LBN-005-01 "Inženierizpētes noteikumi būvniecībā". 43 lpp.

Risk Management Solution, Inc., 2008_*ирт*. The 1908 Messina earthquake: 100-year retrospective.

Садов А.С., Пензина В.Н., 1986_*ирт*. Отчет: Изучение глубинного строения земной коры (региональные сейсморазведочные работы ГСЗ) по геотраверсу г. Советск – г. Рига – г. Кохтла-Ярве. ПГО «Севзапгеология» Калининградская комплексная геофизическая экспедиция. 1 том, 208 стр.

Севастьянов В.Б., 1991_*ирт*. Отчет «Сейсмическое микрорайонирование площадки института Физики АН ЛР». Госкомархстрой, ПНИИС, том 1, 152 с.

Шарак К.А. & Смирнов В.М., 1972_*ирт*. Геолого-экономическая оценка местных карбонатных пород в качестве заполнителей бетона и облицовочно-декоративного камня. ВНИИМОРГЕО. 205 стр.

Slunga R. & Norrman P., 1984_*upm*. *Seismicity of southern Sweden*. FOA Report, C2 C 20543-T1, Stockholm, 106 pp.

Vetrenņikovs V., 1997_*upm*. Latvijas kristāliskā pamatklintājastratigrāfijas, tektonikas un metaloģenijas izpēte (1993.-1996.g.). Valsts ģeoloģijas dienests.Фонды LVĢMC.

Zazimko A. and Sokurenko L., 1994_*upm*. *Geothermal resources of Latvia*. Contract No JOU2 - CT920115/H. Regional maps (Scale 1: 500 000). Latvia. Riga.

Theses

Капустян Н.К., 2002_*t*. Сейсмический мониторинг воздействий техногенных вибраций на земную кору. Автореферат диссертации на соискание ученой стапени доктора физико-математических наук. УДК 550.34. Москва, 28 с.

Ņikuļins V., 2007_*t*. Latvijas seismotektoniskie apstākļi un seismiskā bīstamība. Promocijas darba kopsavilkums. Latvijas Universitāte. 163 lpp. Available at https://dspace.lu.lv/dspace/bitstream/handle/7/4865/36137-Valerijs_Nikulins_2008.pdf?sequence=1&isAllowed=y [accessed 20 February 2017].

Paulson, A., 2006_*t*. Inference of the Earth's mantle viscosity from post-glacial rebound, PhD. thesis, University of Colorado. Available at https://commons.wikimedia.org/wiki/File:PGR_Paulson2007_Rate_of_Lithospheric_Uplift_due_to_PGR.png [accessed 20 February 2017].

Туулинг И.И., 1990_*t*. *Структура Прибалтийского бассейна горючих сланцев и фосфоритов*. Автореферат канд. дис. Минск.

Annex

Earthquakes in the East-Baltic region from 1302 (1303) up to 2017 (φ = 53.9°N – 59.7°N; λ = 19.4°E – 29.6°E).

Type	Date	Time	Latitude	Longitude	H, km
TEQ	1302(1303)/08/15	10:30 ± 2 h	55 ± 0.5	20 ± 1.0	15 (10–20)
TEQ	1302(1303)/08/15	10:30 ± 2 h	55 ± 0.5	20 ± 1.0	15 (10–20)
TEQ	1302(1303)/08/15	10:30 ± 2 h	55 ± 0.5	20 ± 1.0	15 (10–20)
TEQ	1302(1303)/12/01	14 ± 6 h	55.3 ± 0.3	21.0 ± 0.5	10 (5–20)
TEQ	1328		55.1 ± 0.3	23.5 ± 0.5	10 (6–18)
TEQ	1616/06/30	05:30	56.4	24.2	5
TEQ	1670/02/01	22	58.4	24.5	8
P-KST	1783/03/		56.9	23.4	
TEQ	1785/10/31	00	57.3	21.5	
TEQ	1807/02/23	01	56.9	24.1	
TEQ	1821/02/20		56.65 ± 0.01	25.40 ± 0.01	
TEQ	1821/02/21	4	56.64 ± 0.01	25.41 ± 0.01	
TEQ	1821/02/21	7	56.64 ± 0.01	25.41 ± 0.01	13
TEQ	1821/02/23	23	56.59 0.01	25.51 ± 0.01	
TEQ	1823/02/05	22	58	26.2	7
TEQ	1827/09/28	9	59	23.5	14
TEQ	1844/01/12	22	58.6	23.7	6

Mag	Mag Type	Intensity	Epi	SRC 1	Other SRC
4.5 ± 0.5		VI–VII ± 0.5	RUS	NIK-1	
4.3 ± 0.5		V–VI ± 0.5	RUS	NIK-1	
3.8 ± 0.5		V–VI ± 1.0	RUS	NIK-1	
5.0 ± 0.5		VII ± 0.5	RUS	NIK-1	
5.0 ± 0.5		VII ± 0.5	LIT	NIK-1	
4.1		VII	LAT	DOS	BOB, KOND & ULO
3.9		VI	EST	MUS & ORL	DOS, NIK-1 & SIL
			LAT	DOS	BOB, FENCAT
3.5		V	LAT	DOS	BOB, FENCAT
2.9		IV	LAT	DOS	BOB, FENCAT
		VI–VII	LAT	DOS	BOB, NIK-2
			LAT	DOS	BOB, NIK-2
4.5		VII	LAT	DOS	BOB, KOND & ULO, FENCAT, NIK-2
			LAT	DOS	BOB, NIK-2
3.9		VI +	EST	MUS & ORL	DOS, NIK-1 & SIL, FENCAT
4		V	EST	DOS	NIK-1 & SIL, FENCAT
2.5		IV	EST	DOS	BOB, NIK-1 & SIL, FENCAT

Type	Date	Time	Latitude	Longitude	H, km
TEQ	1853/02/04	23:45	56.8	25.7	
TEQ	1853/02/05		56.8	25.7	
TEQ	1853/03/26	01:30	59.5	24.7	5
TEQ	1853/12/29		56.96 ± 0.05	24.14 ± 0.1	
TEQ	1854/01/05		56.96 ± 0.05	24.14 ± 0.1	
TEQ	1857/05/18	11	57.7	22.2	10
TEQ	1858/01/15	11:10	59.3	22.6	8
TEQ	1869/02/15	00	59.5	24.7	6
TEQ	1870/02/06	02:45	56.9	24.1	0
TEQ	1870/02/06	03:20	56.9	24.1	0
TEQ	1877/10/16	02:25	59.0	23.5	10
TEQ	1877/10/16	02:25	59.0	23.5	10
TEQ	1881/01/28	11:15	59.4	28.2	5
TEQ	1887/12/22		54.2	28.5	
TEQ	1896/09/20	13	56.7	23.7	
P-TEQ	1909/01/31	07:15	56.9	24	
P-TEQ	1909/02/12	12:01	56.6	20.9	
TEQ	1909/06/02	08:30	58.4	25.6	7
TEQ	1910/05/21	03	56.6	24	
TEQ	1912/04/08	13:30	59.7	25	5

Mag	Mag Type	Intensity	Epi	SRC 1	Other SRC
3.5		V	LAT	DOS	BOB, FENCAT
2.9		IV	LAT	DOS	BOB, FENCAT
1.2		III	EST	DOS	NIK-1 & SIL, FENCAT
3.5		V	LAT	DOS	BOB, FENCAT, NIK-2
2.9		IV	LAT	DOS	BOB, FENCAT, NIK-2
4.5		VII	LAT	DOS	BOB, FENCAT, KOND & ULO
3		V	BALT – SEA	MUS & ORL	DOS, BOB, FENCAT
2.5		IV	EST	DOS	NIK-1 & SIL, FENCAT
3.5		V	LAT	DOS	BOB, FENCAT
2.9		IV	LAT	DOS	BOB, FENCAT
3.0		IV	EST	DOS	NIK-1 & SIL, FENCAT
3.5		V	EST	DOS	NIK-1 & SIL, FENCAT
2.0		V +	EST – RUS	MUS & ORL	DOS, NIK-1& SIL, FENCAT
3.7		V–VI	BEL	PAN	BOB, FENCAT
3.5		V	LAT	DOS	BOB, FENCAT
		V	LAT	DOS	BOB
		VI	LAT	DOS	BOB
1.8		III	EST	SIL, FENCAT	
		VI	LAT	DOS	BOB
2		III	BALT – SEA	DOS	NIK-1 & SIL, FENCAT

Type	Date	Time	Latitude	Longitude	H, km
TEQ	1912/04/08	20:15	59.7	25	5
TEQ	1912/06/15		59.7	25	6
TEQ	1931/07/12	22	59.4	25.3	5
TEQ	1976/10/25	08:39:45	59.26	23.39	10
TEQ	1976/10/25	08:49	59.3	23.5	
TEQ	1976/10/25	09:07	59.3	23.5	
TEQ	1976/11/08	10:17:07	59.33	23.47	
TEQ	1976/11/22	12:14:42.5	59.3	23.5	13
TEQ	1979/07/24	16:02:46.4	55.45	19.7	
TEQ	1980/01/09	01:24:52.4	58.91	22.99	
TEQ	1981/06/22	19:27:37.7	59.45	22.66	7
TEQ	1982/06/02	07:58:17.7	57.04	21.94	
TEQ	1987/04/08	19:21	58.4	26.1	7
TEQ	1988/04/29	15:36:52	56.97	19.53	1
TEQ	1988/04/29	15:41:22.7	56.32	21.4	7
TEQ	2004/09/21	11:05:01.6 ± 1.4 *	54.924 ± 0.021 *	20.120 ± 0.050 *	16 ± 9.3 *
TEQ	2004/09/21	13:32:31 ± 1.3 *	54.876 ± 0.021 *	20.120 ± 0.055 *	20 ± 10.1 *
TEQ	2004/09/21	13:32:36	54.88	19.91	5

Mag	Mag Type	Intensity	Epi	SRC 1	Other SRC
1.6		II +	BALT - SEA	DOS	NIK-1 & SIL, FENCAT
2		III +	BALT - SEA	DOS	NIK-1 & SIL, FENCAT
2.5		IV +	EST	NIK-1 & SLI, FENCAT	
4.7	M_B	VI +	EST	KOND & NIK-1 & ANA & DOL & KOR & ARH & SIL	
3.5		IV +	EST	KOND & NIK-1 & ANA & DOL & KOR & ARH & SIL	
3		III +	EST	KOND & NIK-1 & ANA & DOL & KOR & ARH & SIL	
3.5		IV +	EST	KOND & NIK-1 & ANA & DOL & KOR & ARH & SIL	
2.5		III	EST	KOND & NIK-1 & ANA & DOL & KOR & ARH & SIL	
2.7	M_L		BALT - SEA	HEL	
2.4	M_L		EST	HEL	
2.6	M_L	III	BALT - SEA	HEL	
2.3	M_L		LAT	HEL	
3.5		IV	EST	SIL	
3.3	M_C		BALT - SEA	BER	
3.2	M_C		LAT	BER	
5.04 *	M_W	VI ± 0.5 **	RUS	IGF (PROB) instrumental * NIK-1 macroseismic **	
5.22 *	M_W	VI–VII ± 0.5 **	RUS	IGF (PROB) instrumental * NIK-1 macroseismic **	
2.2	M_S	IV–V ± 0.5	RUS	NIK-1	

Type	Date	Time	Latitude	Longitude	H, km
TEQ	2004/09/21	19:30 ± 30	54.9	20.05	7
TEQ	2004/09/21	21:30 ± 5	55.0	20.0	8
TEQ	2004/09/22	00 ± 5	54.55	20.10	5
TEQ	2004/09/22	02 ± 2	55.0	20.0	5
P-TEQ	2010/11/22	12	56.89 ± 0.08	24.09 ± 0.10	
TEQ	2013/02/04	20:17:54.2	58.921	23.522	4.4
P-TEQ	2015/06/12	08:18:26	55.517	21.398	2.6
TEQ	2016/11/12	02:48:52.8	58.304	26.193	1.4
TEQ	2017/03/22	03:00:27.5	59.34	24.356	4.0
TEQ	2017/07/15	08:01:50.5	59.047	22.956	12.2

Mag	Mag Type	Intensity	Epi	SRC 1	Other SRC
2.3 ± 0.5	M_S	IV ± 0.5	RUS	NIK-1	
2.5 ± 0.5	M_S	IV ± 0.5	RUS	NIK-1	
2.3 ± 0.5	M_S	IV–V ± 0.5	RUS	NIK-1	
1.8 ± 0.5	M_S	III–IV ± 0.5	RUS	NIK-1	
		II + ± 0.5	LAT	NIK-2	
1.0	M_L	Felt	EST	HEL	
0.8	M_L		LIT	NIK-2	
1.8	M_L		EST	HEL	
1.2	M_L		EST	HEL	
2.1	M_L		EST	HEL	

Designation: Type – type of seismic event; TEQ – tectonic earthquake; P-KST – probable karst event; P-TEQ – probable tectonic earthquake; H, km – focal depth; Mag – magnitude; Mag Type - type of magnitude; I_0 – epicentral intensity (MSK-64 or EMS-98); Epi - epicenter position; RUS – Russia; LIT – Lithuania; LAT – Latvia; EST – Estonia; BALT-SEA – Baltic Sea; BEL – Belorussia; EST-RUS-Border of Estonia and Russia; SRC 1 – primary source; Other SRC – Other sources that were taken into account in determining different the parameters of a seismic event (epicenter location, origin time, intensity, magnitude, focal depth); NIK-1 & SIL – Nikonov & Sildvee, 1986, 1991; Nikonov, 1992, 2002, 2007; 2011; Nikonov et al., 2005; Никонов, 2009; DOS – Doss B., 1898, 1905, 1909, 1910, 1911; BOB – Авотиня и др., 1988, Боборыкин, 1988, Боборыкин и др., 1993; MUS & ORL – Мушкетов И.В. & Орлов А.П., 1893; KOND & NIK-1 & ANA & DOL & KOR & ARH & SIL – Kondorskaya et al., 1988; KOND & ULO – Kondorskaya N.V. & Ulomov V.I., 1995; PAN – Panasenko 1977, 1979; FENCAT – Insitute of Seismology at the University of Helsinki, Catalog of earthquakes in Northern Europe 1375 -; NIK-2 – Nikulins V., this publication, Никулин В.Г., 2011; HEL – Insitute of Seismology at the University of Helsinki; BER – University of Bergen; IGF – Institute of Geophysics, Polish Academy of Sciences; PROB - Probabilistic Location Method; M_B – magnitude determined by body waves; M_L – local magnitude; M_C – magnitude determined by duration of code of waves; M_W – magnitude determined by seismic moment; M_S – magnitude determined by surface waves.

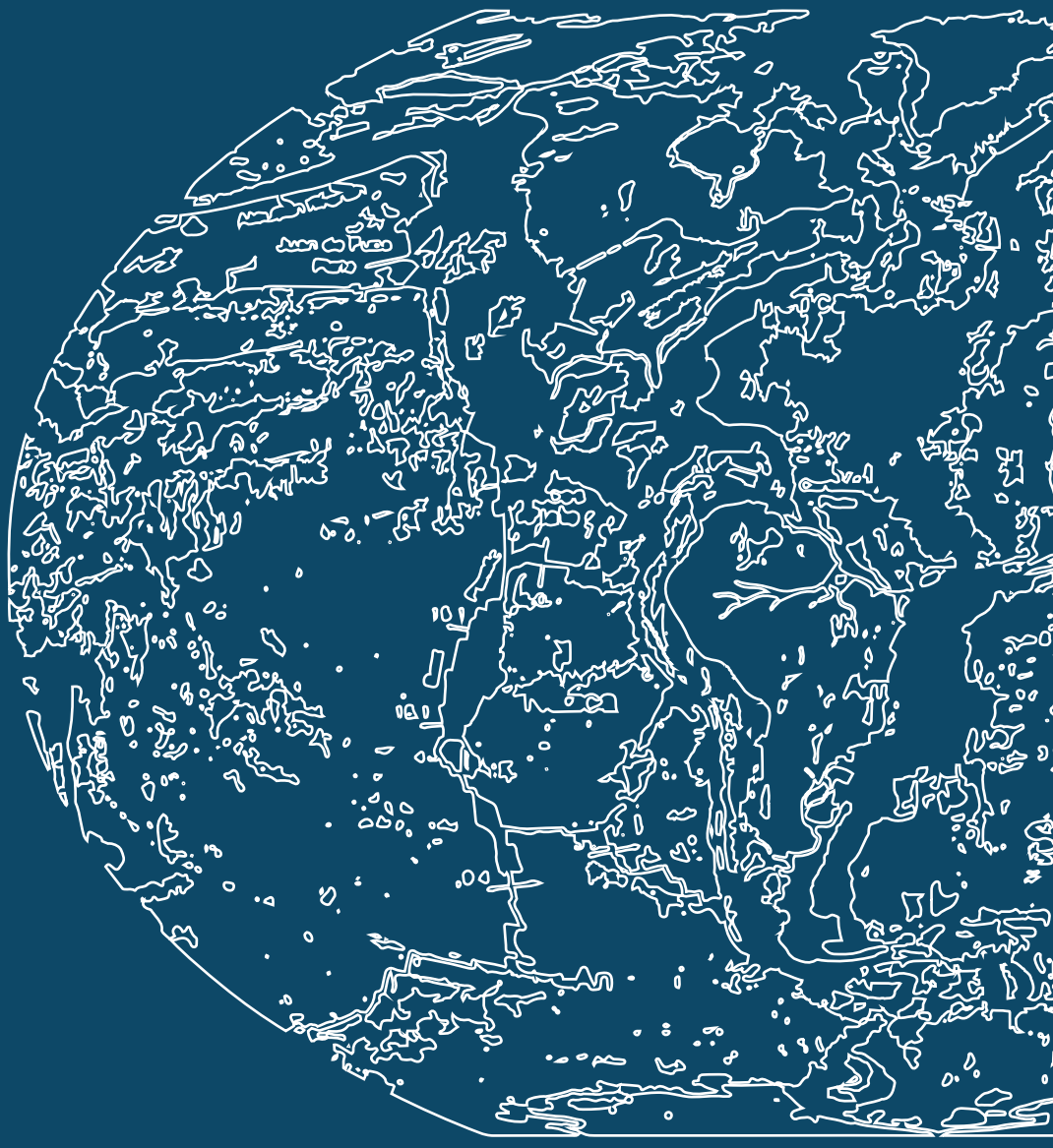

ISBN 978-9934-18-300-3

LATVIJAS UNIVERSITATE
ANNO 1919